

University of Alberta

Selection of DNA Aptamers Against Live Bacterial Cells

by

Camille Hamula

A thesis submitted to the Faculty of Graduate Studies and Research
in partial fulfillment of the requirements for the degree of

Doctor of Philosophy

Medical Sciences - Laboratory Medicine and Pathology

©Camille Hamula
Fall 2010
Edmonton, Alberta

Permission is hereby granted to the University of Alberta Libraries to reproduce single copies of this thesis and to lend or sell such copies for private, scholarly or scientific research purposes only. Where the thesis is converted to, or otherwise made available in digital form, the University of Alberta will advise potential users of the thesis of these terms.

The author reserves all other publication and other rights in association with the copyright in the thesis and, except as herein before provided, neither the thesis nor any substantial portion thereof may be printed or otherwise reproduced in any material form whatsoever without the author's prior written permission.



Library and Archives
Canada

Published Heritage
Branch

395 Wellington Street
Ottawa ON K1A 0N4
Canada

Bibliothèque et
Archives Canada

Direction du
Patrimoine de l'édition

395, rue Wellington
Ottawa ON K1A 0N4
Canada

Your file *Votre référence*
ISBN: 978-0-494-81320-1
Our file *Notre référence*
ISBN: 978-0-494-81320-1

NOTICE:

The author has granted a non-exclusive license allowing Library and Archives Canada to reproduce, publish, archive, preserve, conserve, communicate to the public by telecommunication or on the Internet, loan, distribute and sell theses worldwide, for commercial or non-commercial purposes, in microform, paper, electronic and/or any other formats.

The author retains copyright ownership and moral rights in this thesis. Neither the thesis nor substantial extracts from it may be printed or otherwise reproduced without the author's permission.

In compliance with the Canadian Privacy Act some supporting forms may have been removed from this thesis.

While these forms may be included in the document page count, their removal does not represent any loss of content from the thesis.

AVIS:

L'auteur a accordé une licence non exclusive permettant à la Bibliothèque et Archives Canada de reproduire, publier, archiver, sauvegarder, conserver, transmettre au public par télécommunication ou par l'Internet, prêter, distribuer et vendre des thèses partout dans le monde, à des fins commerciales ou autres, sur support microforme, papier, électronique et/ou autres formats.

L'auteur conserve la propriété du droit d'auteur et des droits moraux qui protègent cette thèse. Ni la thèse ni des extraits substantiels de celle-ci ne doivent être imprimés ou autrement reproduits sans son autorisation.

Conformément à la loi canadienne sur la protection de la vie privée, quelques formulaires secondaires ont été enlevés de cette thèse.

Bien que ces formulaires aient inclus dans la pagination, il n'y aura aucun contenu manquant.


Canada

Examining Committee

Dr. X. Chris Le, Department of Laboratory Medicine and Pathology, University of Alberta

Dr. Xing-Fang Li, Department of Laboratory Medicine and Pathology, University of Alberta

Dr. Jeff Fuller, Department of Laboratory Medicine and Pathology, University of Alberta

Dr. Chris Cairo, Department of Chemistry, University of Alberta

Dr. Greg Tyrrell, Department of Laboratory Medicine and Pathology, University of Alberta

Dr. Yi Lu, Departments of Chemistry, Biochemistry, and Materials Science and Engineering, University of Illinois at Urbana-Champaign, Urbana, Illinois, USA.

Abstract

This thesis focuses on selection and characterization of DNA aptamers that bind live bacterial cells. Aptamers are short, synthetic, single-stranded nucleic acid molecules created via iterative rounds of *in vitro* selection known as Systematic Evolution of Ligands by Exponential Enrichment (SELEX). They possess a variety of advantages over antibodies including increased stability, ease of synthesis, ease of chemical modification, and low variability.

To eliminate the need of purifying or identifying target molecules from the cell surface, a novel bacterial cell-SELEX technique using whole, live bacterial cells as targets was developed. Live *Lactobacillus acidophilus* cells in suspension were used to demonstrate proof-of-principle. After 8 rounds of selection, aptamer pools showing high affinity and selective binding for *L. acidophilus* cells were cloned. Twenty-seven aptamers were sequenced and characterized. A binding dissociation constant (K_d) value as low as 1.2 nM, and selective binding to *L. acidophilus* over other common microorganisms suggests that the new technique is successful in selecting specific, high affinity aptamers.

The bacterial cell-SELEX technique was extended to a mixture of the 10 most prevalent pathogenic invasive Group A Streptococcus (GAS) M types in Canada. Aptamer pools with high affinity and selectivity were obtained after 8–20 rounds of selection. A total of 102 aptamers from 5 different pools were sequenced and subjected to structural prediction. Further characterization revealed many of the aptamers to be species specific and have high affinity, with K_d values in the low nanomolar range. An aptamer specific for the M11 GAS cells was

isolated. Separate sets of bacterial cell-SELEX using GAS cells and different types of DNA denaturation and starting library size yielded some of the same high affinity sequences. Identification of different GAS M-types is clinically important, but appropriate methods are lacking. These aptamers can be used in affinity assays for surveillance of invasive *Streptococcus* species.

Acknowledgements

I would like to thank everyone involved in the birth of this thesis.

Foremost, I would like to thank my supervisor Dr. Chris Le. In addition to providing me the opportunity to work in his lab, he has offered endless amounts of guidance and encouragement. He always believed in my abilities, even when I did not. He is a wonderful mentor and I will miss working for him.

I am also grateful to Dr. Xing-Fang Li for her invaluable support, and the many coffees she has bought me over the years. She has always been a great source of advice and insight.

My excellent doctoral supervisory committee comprised of Drs. Xing-Fang Li, Chris Cairo, Jeff Fuller, and Greg Tyrrell also deserves a big thank you. Many an idea began with our stimulating discussions. Drs. Tyrrell and Fuller have also helped me a great deal with my future career plans.

I would like to thank both Katerina Carastathis and Dianne Sergy to listening to my numerous questions and always providing a friendly, thoughtful answer. They have also patiently facilitated the proper execution of many a last-minute request up to and including the printing and submission of this thesis.

The AET Division has been a great place to work. I would like to thank my coworkers both past and present for their expertise and more importantly their friendship. They are too numerous to mention but I am grateful to them all. I would particularly like to thank Alevtina Goulko, Hongquan Zhang, Leluo Guan, Jessica Boyd, Anthony McKnight-Whitford, Emily Chan, Kim MacDonald, and Birget Moe.

Finally, I could not have finished my PhD without the backing of my family and husband. I would like to thank my superb parents and sister for all their love, encouragement, and support. They have been instrumental at pulling me out of the lab or away from the computer at times when I need a break. They also listen to all of my complaints without complaining themselves (at least not to my face). I thank my dear husband Matt for the same and for his great sense of humour. After a long day in the lab, he can always be counted on to make me smile. He was there to help me relax in the days prior to both my candidacy and defense, and was invaluable in proofreading this thesis. Most importantly, he is always willing to listen and understand.

Table of Contents

<u>Chapter 1: Introduction and literature review</u>	1
1.0 Nucleic acids	1
1.1 Aptamers and SELEX	2
1.2 Variation in SELEX protocols	6
1.2.1 Libraries	6
1.2.2 Presentation of target.....	8
1.2.3 Partitioning of aptamer-target complexes	10
1.2.4 Screening of aptamer pools during selection/monitoring progress of SELEX	14
1.3 Aptamers in assay formats traditionally dominated by antibodies	15
1.3.1 ELISA-like assays	16
1.3.2 Aptamer blotting	17
1.3.3 Affinity Chromatography	18
1.3.4 Aptamer affinity capillary electrophoresis	19
1.3.5 Aptamer arrays	20
1.4 SELEX targets	23
1.4.1 Purified bacterial and viral target molecules.....	24
1.4.2 Complex targets.....	26
1.5 Uses of aptamers derived against cell surface molecules	29
1.5.1 Aptamer-based post-SELEX target elucidation	29
1.5.2 Flow cytometry	31
1.5.3 Whole cell and virus aptamer sensors	33
1.5.4 Cell labeling and imaging	37
1.5.5 Aptamers with therapeutic potential against pathogens.....	39
1.5.6 Aptamer-targeted delivery of therapeutics	40
1.7 Rationale and scope of thesis	42
1.6 References	46
<u>Chapter 2: Bacterial cell-SELEX proof-of-principle</u>	- 66 -
2.1 Introduction	- 66 -
2.2 Experimental	- 68 -
2.2.1 Reagents	- 68 -

2.2.2 PCR amplification and gel electrophoresis.	- 69 -
2.2.3 Aptamer selection.....	- 70 -
2.2.4 Flow cytometric analysis.....	- 71 -
2.2.5 Slide-binding assays and electron microscopy.....	- 71 -
2.2.6 Flow injection coupled with fluorescence detection.	- 73 -
2.2.7 Cloning, sequencing, and structural analysis of aptamers.	- 74 -
2.3 Results	- 75 -
2.3.1 Selection of DNA aptamers against live <i>Lactobacillus acidophilus</i>	- 75 -
2.3.2 Binding Affinity and Selectivity of Aptamer Pools Following Each Round of Selection.	- 77 -
2.3.3 Cloning and sequence analysis of aptamer pools.....	- 85 -
2.3.4 Binding of individual aptamer sequences to target cells.....	- 86 -
2.3.5 Binding of aptamer hemag1P to <i>L. acidophilus</i>	- 91 -
2.4 References	- 99 -
Chapter 3: Bacterial cell-SELEX against Group A Streptococcus	- 100 -
3.1 Introduction	- 100 -
3.2 Experimental	- 103 -
3.2.1 Reagents	- 103 -
3.2.2 PCR amplification and gel electrophoresis.	- 105 -
3.2.3 Aptamer selection.....	- 105 -
3.2.4 Flow cytometric analysis of aptamer pool and individual aptamer binding.....	- 107 -
3.2.5 Cloning, sequencing and structural analysis of aptamers.	- 108 -
3.2.6 Crude pepsin extract preparation, PAGE, and mass spectrometry.	- 109 -
3.3 Results.	- 110 -
3.3.1 Aptamer selection.....	- 110 -
3.3.2 Binding Affinity and Selectivity of Aptamer Pools Following Each Round of Selection.	- 115 -
3.3.3 SDS-PAGE and mass spectrometry analysis of <i>S.pyogenes</i> surface protein expression.	- 120 -
3.3.4 Cloning and sequence analysis of aptamer pools.....	- 121 -
3.3.5 Binding of individual aptamer sequences to target cell mixture.....	- 122 -
3.3.6 Binding of aptamers to specific M-types.	- 129 -
3.3.7 Binding of high affinity aptamers to <i>S.pyogenes</i>	- 134 -
3.3.8 Selectivity of high affinity aptamers for <i>S.pyogenes</i>	- 142 -

3.4 References	- 146 -
Chapter 4: Modified bacterial cell-SELEX against Group A Streptococcus	- 147 -
4.1 Introduction	- 147 -
4.2 Experimental	- 148 -
4.2.1 Reagents	- 148 -
4.2.2. PCR amplification and gel electrophoresis.	- 150 -
4.2.3. Denaturing gel electrophoresis and gel purification.	- 151 -
4.2.4. Aptamer selection.....	- 151 -
4.2.5. Counterselection.....	- 155 -
4.2.6. Flow cytometric analysis.....	- 155 -
4.2.7. Cloning, sequencing, and structural analysis of aptamers.	- 156 -
4.3 Results	- 157 -
4.3.1 Aptamer selection.....	- 157 -
4.3.2 Counterselection.....	- 162 -
4.3.3 Binding Affinity and Selectivity of Aptamer Pools Following Each Round of Selection.	- 165 -
4.3.4 Cloning and sequence analysis of aptamer pools.....	- 167 -
4.3.5 Binding of individual aptamer sequences to target cell mixture.....	- 171 -
4.3.6 Binding of aptamers to specific M-types.	- 176 -
4.3.7 Binding of high affinity aptamers to <i>S.pyogenes</i>	- 180 -
4.3.8 Selectivity of high affinity aptamers for <i>S.pyogenes</i>	- 185 -
4.4 References	- 188 -
Chapter 5: Post-SELEX target molecule elucidation	- 189 -
5.1 Introduction	- 189 -
5.2 Experimental	- 193 -
5.2.1 Flow cytometry.	- 193 -
5.2.2 S-layer protein purification.	- 193 -
5.2.3 Capillary electrophoresis.....	- 193 -
5.2.4 Aptamer-magnetic bead pulldowns.....	- 194 -
5.2.5 Crude pepsin extract preparation, PAGE, and mass spectrometry.	- 195 -
5.2.6 Mass spectrometric identification of proteins.	- 196 -
5.2.7 Western blotting analysis of aptamer pool target binding to crude pepsin and whole cell extracts.....	- 196 -
5.3 Results	- 198 -
5.3.1 Putative target molecule of hemag1P.	- 198 -

5.3.2 Identification of a putative target of GAS aptamer pools.	211 -
5.3.3 Removal of aptamer sequences from PVDF membrane.	218 -
5.4 References	220 -
Chapter 6: Comparison of aptamer pools from different sets of SELEX	221 -
6.1 Introduction	221 -
6.2 Reagents	222 -
6.2.1 Lacto heat pool.	222 -
6.2.2 Lacto mag pool.	222 -
6.2.3 GAS 15A and 20A pools.....	223 -
6.2.4 GAS 13B pool.	223 -
6.2.5 GAS 8D and 8E pools.	223 -
6.3 Results	224 -
6.3.1 Amplification of DNA from different SELEX fractions.	224 -
6.3.2 Evolution of aptamer pool binding to target cells with increasing SELEX rounds.....	226 -
6.3.3 Aptamer pool sequence characteristics.	230 -
6.3.4 Free energy distribution of each aptamer pool.....	230 -
6.3.5 Secondary structural motif distribution of each aptamer pool.	240 -
6.3.6 Sequences and secondary structures common to multiple aptamer pools.	243 -
6.3.7 Screening of individual sequences tested from each aptamer pool against target cells.	249 -
6.3.8 Screening of sequences from <i>S.pyogenes</i> aptamer pools against different M-types.....	255 -
6.3.9 Binding affinities of sequences from different aptamer pools for target cells.....	262 -
6.3.10 Selectivities of sequences from each aptamer pool for target cells.....	269 -
6.3.11 Sequences with highest target cell affinity and selectivity from each aptamer pool.....	274 -
6.3.12 Comparison of library binding across all experiments.....	276 -
6.4 References	278 -
Chapter 7: Conclusions and Synthesis	279 -
7.1 Introduction	279 -
7.2 Advancement of Knowledge	281 -
7.3 Conclusions	287 -
7.4 Future Work	288 -
7.5 References	291 -

List of Figures

Figure 1.1. Schematic of Systematic Evolution of Ligands via Exponential Enrichment (SELEX).....	4
Figure 1.2. Schematic of Cell-SELEX developed by the Tan Group.....	29
Figure 2.1. Schematic showing the main steps for the selection of aptamers against live bacterial cells.	67
Figure 2.2. Native PAGE of PCR-amplified oligonucleotide fractions after the first round of SELEX using heat denaturation.....	76
Figure 2.3. Typical flow cytometry outputs following each round of selection, showing increase in gated fluorescence intensity above background (boxed area) following incubation with round 8 aptamer pool.....	77
Figure 2.4. Increase in percent gated fluorescence intensity of <i>L. acidophilus</i> 4356 cells incubated with fluorescently-labeled aptamer pools after increasing SELEX rounds.....	79
Figure 2.5. Change in heat-denatured aptamer pool binding to <i>L.acidophilus</i> 4356 cells, as indicated by percent gated fluorescence intensity above background, with removal of BSA and tRNA from incubation mixture.....	80
Figure 2.6. Change in aptamer pool binding with time after flow cytometry sample preparation.....	81
Figure 2.7. Binding of the highest binding aptamer pools (rounds 7HEAT and 8SS) to different types of cells.....	82
Figure 2.8. Scanning Electron Microscopy (SEM) close-up of <i>L.acidophilus</i> 4356 cells used for slide-binding assay.....	83

Figure 2.9. Slide-binding assay showing binding of <i>L. acidophilus</i> 4356 cells to microscope slides coated with heat denatured aptamer pools after each round of SELEX (round number labeled on each picture).....	84
Figure 2.10. Total number of <i>L.acidophilus</i> 4356 cells binding to slides coated with aptamer pools.....	85
Figure 2.11. Sequences derived via cloning of aptamer pools which show increased binding affinity to <i>L. acidophilus</i> 4356, 4357, and 4355 cells and minimal binding to other cells when screened via flow cytometry.....	87
Figure 2.12. Most energetically favorable predicted secondary structures of some selected aptamer sequences.....	89
Figure 2.13. Predicted secondary structure of aptamer hemag1P.....	90
Figure 2.14. Binding characteristics of aptamer hemag1P as determined via flow cytometry.....	92
Figure 2.15. Binding characteristics of aptamer hemag1P as determined via flow cytometry.....	93
Figure 2.16. Figure 2.16. Binding characteristics of aptamer hemag1P with and without the inclusion of a pre-heating step.....	94
Figure 2.17. Binding characteristics of aptamer SSH1P as determined via flow injection coupled to fluorescence detection both with (a) and without (b, c) filtration.....	97
Figure 2.18. Flow injection with fluorescence detection analysis of aptamer removal from pools with increasing rounds of selection.....	98
Figure 3.1. The <i>S. pyogenes</i> M protein.....	102

Figure 3.2. Molecules present on the <i>S. pyogenes</i> cell surface.....	103
Figure 3.3. Schematic of SELEX approach against <i>S. pyogenes</i> isolates.....	111
Figure 3.4. Native PAGE of PCR-amplified oligonucleotide fractions after the first round of SELEX A/B.....	114
Figure 3.5. Increase in percent gated fluorescence intensity of <i>S. pyogenes</i> cells incubated with fluorescently-labeled aptamer pools after increasing SELEX rounds.....	116
Figure 3.6. Binding of SELEX 20A aptamer pool to two separate logarithmic phase cultures of each M-type.....	118
Figure 3.7. Binding of SELEX 20A aptamer pool to each M-type using two separate incubations of the same logarithmic phase culture.....	119
Figure 3.8. Binding of SELEX 20A aptamer pool to two separate stationary phase cultures of each M-type.....	120
Figure 3.9. SDS-PAGE gels of crude pepsin extracts from duplicate cultures of M-types M1, M2, M3, M4, M6, M11, M12, M28, M77, and M89.....	124
Figure 3.10. Screening of sequences from SELEX 15A, 20A, and 13B aptamer pools against a mixture of 10 <i>S. pyogenes</i> M-types used as a SELEX target.....	125
Figure 3.11. Predicted structures of aptamer sequences with high affinity for <i>S. pyogenes</i>.....	128
Figure 3.12. Binding of high affinity aptamer sequences to the 10 different <i>S. pyogenes</i> M-types used for SELEX.....	131
Figure 3.13. Binding of medium affinity aptamer sequences to the 10 different <i>S. pyogenes</i> M-types used for SELEX.....	132

Figure 3.14. Binding of low affinity aptamer sequences to the 10 different <i>S. pyogenes</i> M-types used for SELEX.....	133
Figure 3.15. Binding of high affinity aptamer sequences to a mixture of <i>S. pyogenes</i> M-types not used as targets during selection.....	134
Figure 3.16. Binding of aptamers 20A1P and 20A1 to the mixture of <i>S. pyogenes</i> cells used in SELEX.....	137
Figure 3.17. Binding of aptamers 20A8P and 20A8 to the mixture of <i>S. pyogenes</i> cells used in SELEX.....	138
Figure 3.18. Binding of aptamers 20A9P and 20A9 to the mixture of <i>S. pyogenes</i> cells used in SELEX.....	139
Figure 3.19. Binding of aptamers 20A12P and 20A14P to the mixture of <i>S. pyogenes</i> cells used in SELEX.....	140
Figure 3.20. Binding of aptamers 20A24P and 15A3P to the mixture of <i>S. pyogenes</i> cells used in SELEX.....	141
Figure 3.21. Binding of randomized oligonucleotide library to the mixture of <i>S. pyogenes</i> cells used in SELEX.....	142
Figure 3.22. Selectivity of high affinity aptamer sequences for <i>S.pyogenes</i>.....	145
Figure 4.1. Denaturing PAGE of fractions collected and amplified after round 1 of SELEX D.....	160
Figure 4.2. Native PAGE of fractions collected and amplified after round 1 of SELEX E.....	161

Figure 4.3. PAGE gel showing amplification of library with increasing PCR cycle number.....	162
Figure 4.4. Native PAGE of supernatant and wash fractions collected and amplified after round 3 (counterselection) of SELEX D and E.....	164
Figure 4.5. Typical flow cytometry outputs from screening of aptamer pools following each round of selection, showing increase in gated fluorescence intensity above background (boxed area) following incubation with round 7D aptamer pool.....	165
Figure 4.6. Change in percent gated fluorescence intensity of <i>S. pyogenes</i> cells incubated with fluorescently-labeled aptamer pools after increasing SELEX D and E rounds.....	167
Figure 4.7. Common secondary structural motifs DE1 (a) and DE2 (b).....	169
Figure 4.8. Screening of sequences from SELEX 8D aptamer pools.....	173
Figure 4.9. Screening of sequences from SELEX 8E aptamer pools.....	174
Figure 4.10. Predicted structures of aptamer sequences with high affinity for <i>S.pyogenes</i>.....	175
Figure 4.11. Binding of low affinity sequences from SELEX D and E to different M-types of the <i>S. pyogenes</i> target mixture.....	178
Figure 4.12. Binding of high affinity sequences from SELEX D to different M-types of the <i>S. pyogenes</i> target mixture.....	179
..	
Figure 4.13. Binding of high affinity aptamer sequences to a mixture of <i>S. pyogenes</i> M-types not used as targets during selection.....	180
Figure 4.14. Binding of aptamers 8D cells 1 and 8D cells 1P to the mixture of <i>S. pyogenes</i> cells used in SELEX.....	183

Figure 4.15. Binding of aptamers 8D cells 9 and 8D cells 9P to the mixture of <i>S. pyogenes</i> cells used in SELEX.....	184
Figure 4.16. Binding of randomized oligonucleotide library to the mixture of <i>S. pyogenes</i> cells used in SELEX.....	185
Figure 4.17. Screening of high affinity aptamers against non-target cells.....	188
Figure 5.1. Schematic of aptamer blotting procedure of Noma et al. 2006.....	191
Figure 5.2. Principle of affinity CE-LIF separation of free (unbound) DNA from DNA-protein complexes (Figure 2 from Pavski and Le 2001).....	192
Figure 5.3. Binding of aptamer hemag1P to <i>Lactobacillus sp.</i> without an S-layer.....	199
Figure 5.4. SDS-PAGE of S-protein purified via LiCl extraction.....	201
Figure 5.5. Capillary electrophoresis of fluorescently-labeled hemag1P incubated with BSA or with S-layer protein.....	202
Figure 5.6a. CE-LIF chromatograms showing increased formation of complex peaks in incubations containing increasing amounts of S-protein and fixed amounts of hemag1P.....	203
Figure 5.6b. CE-LIF chromatograms showing increased formation of complex peaks in incubations containing increasing amounts of S-protein and fixed amounts of hemag1P.....	204
Figure 5.6c. CE-LIF chromatograms showing increased formation of complex peaks in incubations containing increasing amounts of S-protein and fixed amounts of hemag1P.....	205
Figure 5.7. Irregular complex peak formation seen after CE-LIF of incubations containing high S-layer protein concentrations (5 μM).....	206

Figure 5.8. Change in unbound DNA peak intensity with increasing S-layer protein concentration.....	208
Figure 5.9. Change in unbound DNA peak intensity with increasing S-layer protein concentration.....	209
Figure 5.10. SDS-PAGE of eluates from aptamer-coated magnetic bead pulldowns.....	210
Figure 5.11. Blot of different amounts of lysozyme detected with a fixed amount of anti-lysozyme aptamer (180 nM).....	212
Figure 5.12. Aptamer blot of PE pepsin cell surface extracts using randomized oligonucleotide library (270 nM) and fixed amount of total protein per lane.....	214
Figure 5.13. Aptamer blot of WC insoluble fractions using randomized oligonucleotide library (270 nM) and fixed amount of total protein per lane.....	215
Figure 5.14. Aptamer blots of WC insoluble fractions using fixed amount of aptamer pool (270 nM) and fixed amount of total protein per lane.....	216
Figure 5.15. Aptamer blots of PE pepsin cell surface extracts using fixed amount of aptamer pool (270 nM) and fixed amount of total protein per lane.....	217
Figure 5.16. PAGE gel of aptamer sequences amplified from 100 KDa bands on a PVDF membrane.....	219
Figure 6.1. Typical fluorescence histograms from flow cytometry analysis of aptamer pool binding for (a) Lacto heat and (b) GAS B SELEX.....	227
Figure 6.2. Comparison of change in gated fluorescence intensity over background with increasing cycle number for different sets of SELEX.....	229

Figure 6.3. Free energy distribution of sequences from the Lacto mag (beads) aptamer pool, both without and with primers (P).....	233
Figure 6.4. Free energy distribution of sequences from the Lacto heat aptamer pool, both without and with primers (P).....	234
Figure 6.5. Free energy distribution of sequences from the GAS 15A aptamer pool, both without and with primers (P).....	235
Figure 6.6. Free energy distribution of sequences from the GAS 20A aptamer pool, both without and with primers (P).....	236
Figure 6.7. Free energy distribution of sequences from the GAS 13B aptamer pool, both without and with primers (P).....	237
Figure 6.8. Free energy distribution of sequences from the GAS 8D aptamer pool, both without and with primers (P).....	238
Figure 6.9. Free energy distribution of sequences from the GAS 8E aptamer pool, both without and with primers (P).....	239
Figure 6.10. Secondary structure motifs repeated between unique sequences both with and without primers from Lacto heat and mag pools.....	246
Figure 6.11. Secondary structure motifs repeated between unique sequences both with and without primers from different GAS A and B aptamer pools (15A, 20A, 13B).....	247
Figure 6.12. Secondary structure motifs shared between unique sequences from all <i>S.pyogenes</i> aptamer pools (13B, 15A, 20A, 8D, 8E).....	248
Figure 6.13. Secondary structure motifs shared between unique sequences from <i>S. pyogenes</i> and <i>L.acidophilus</i> aptamer pools.....	249

Figure 6.14. Affinities of different sequences for target cells as determined via flow cytometry, grouped by aptamer pool.....	252
Figure 6.15. Affinities of sequences cloned from the heat-eluted (CA) and cell-bound (Cells) fractions of aptamer pool 8D, determined via flow cyotmetry.....	253
Figure 6.16. Binding of aptamer pool 13B sequences 13B 5 and 13B 8 to each of the 10 <i>S. pyogenes</i> M-types used in SELEX B.....	258
Figure 6.17. Binding of aptamer pool 15A sequences 15A3, 15A 3P, and 15A 15 to each of the 10 <i>S. pyogenes</i> M-types used in SELEX A.....	259
Figure 6.18. Binding of aptamer pool 20A sequences 20A8 and 20A8P to each of the 10 <i>S. pyogenes</i> M-types used in SELEX A.....	260
Figure 6.19. Binding of aptamer pool 8D sequences 8D cells 1, 8D cells 1P, 8D cells 9, and 8D cells 9P to each of the 10 <i>S. pyogenes</i> M-types used in SELEX D.....	261
Figure 6.20. Binding of aptamer pool 8E sequences 8E CA20, 8E CA 20P, and 8E cells 1P to each of the 10 <i>S. pyogenes</i> M-types used in SELEX E.....	262
Figure 6.21. Binding curves for all high affinity aptamers tested and <i>S. pyogenes</i> target cell mixture.....	265
Figure 6.22. Binding curves for all high affinity aptamers tested and <i>S. pyogenes</i> target cell mixture.....	266
Figure 6.23. Binding of fluorescently-labeled randomized library to mixture of <i>S. pyogenes</i> cells.....	268
Figure 6.24. Selectivity of aptamer sequences from Lacto mag and heat pools for target cells <i>L.acidophilus</i> 4356.....	271

Figure 6.25. Affinity of aptamer sequences from 15A, 20A, and 8D pools for non-target cells.....	272
Figure 6.26. Affinity of aptamer sequences from 15A, 20A and 8D pools for a mixture of non-target <i>S. pyogenes</i> M-types.....	273
Figure 6.27. Binding of fluorescently-labeled randomized oligonucleotide library to each different target M-type of <i>S. pyogenes</i>.....	277

List of Tables

Table 1. Purified pathogen molecules targeted by SELEX.....	25
Table 2. Whole mammalian cell SELEX targets.....	27
Table 3. Whole bacterial cell and viral particle SELEX targets.....	28
Table 4. Screened aptamer sequences with (hemag1P, mag2P, and hemag3P) and without (hemag 1, mag1, and hemag3) primers.....	88
Table 5. Varying amounts of BSA, tRNA, DNA, and cells used in SELEX incubations.....	113
Table 6. Screened aptamer sequences with (hemag1P, mag2P, and hemag3P) and without (hemag 1, mag1, and hemag3) primers.....	126
Table 7. Binding dissociation constants (Kd) and theoretical maximum binding (Bmax) of high affinity aptamer sequences for a mixture of 10 different <i>S. pyogenes</i> M-types used in SELEX.....	136
Table 8. List of all species, isolates and strains used to test selectivity of aptamers to <i>S. pyogenes</i>.....	144
Table 9. Summary of conditions used in GAS SELEX D and E.....	154
Table 10. Screened SELEX 8D aptamer pool sequences with (CA cells 6P, CA 17P, cells 1P, cells 9P, cells 20P) and without (CA cells 6, CA 17, cells 1, cells 9, cells 20) primers.....	170
Table 11. Screened SELEX 8E aptamer pool sequences with (CA cells 4P, CA 9P, CA 20P, cells 1P) and without (CA 4, CA 20) primers.....	171

Table 12. Binding dissociation constants (Kd) and theoretical maximum binding (Bmax) of high affinity SELEX D aptamer sequences for a mixture of 10 different <i>S. pyogenes</i> M-types used in SELEX.....	182
Table 13. List of all species, isolates and strains used to test selectivity of aptamers to <i>S. pyogenes</i>.....	187
Table 14. Mean free energies of likely predicted secondary structures of sequences cloned from different aptamer pools.....	231
Table 15. Mean free energies of predicted secondary structures of aptamer sequences cloned from CA (heat-eluted), cell-bound (cell), or pooled (CA cells) fractions in SELEX D and E.....	232
Table 16. Distribution of different types of predicted secondary structures within aptamer pools for sequences both with and without primers.....	242
Table 17. Sequences shared between different aptamer pools.....	245
Table 18. Summary of high affinity sequences ($\geq 30\%$ gated fluorescence) from each aptamer pool.....	254
Table 19. Binding dissociation constants (Kds) of aptamer sequences evolved from all sets of SELEX (Lacto SELEX heat and mag, GAS SELEX A, B, D, E).....	267
Table 20. Theoretical maximum binding (Bmax) values of aptamers derived from all sets of SELEX (Lacto SELEX, SELEX A,B,D,E).....	267
Table 21. Sequences with highest target cell affinity and selectivity.....	275

List of Abbreviations

B_{\max} = theoretical maximum binding

CA = heat-eluted cell aptamer

Cells fraction = aptamers that could not be released via heat elution

ELISA = Enzyme-linked immunosorbent assay

ELONA = Enzyme-linked oligonucleotide assay

GAS = Group A Streptococcus

GBS = Group B Streptococcus

iGAS = invasive Group A Streptococcus

IC_{50} = Half maximal inhibitory concentration

K_d = Binding dissociation constant

PCR = Polymerase Chain Reaction

PDGF = Platelet-derived growth factor

PSMA = Prostate-specific membrane antigen

QD = quantum dot

qPCR = quantitative or real-time PCR

SELEX = Systematic Evolution of Ligands via Exponential Enrichment

S_0 = supernatant

ssDNA/ssRNA = single-stranded deoxyribonucleic acid/single-stranded
ribonucleic acid

VEGF = Vascular Endothelial Growth Factor

W = wash

Chapter 1*

Introduction and Literature Review

1.0 Nucleic Acids

Deoxyribonucleic acid (DNA) and ribonucleic acid (RNA) are macromolecules comprised of nucleotides that encode the genetic information inside a cell. Each nucleotide consists of a nitrogenous organic base, a pentameric sugar (ribose or deoxyribose), and one to three phosphate groups. There are four organic bases present in either DNA or RNA; adenine, cytosine, guanine, and either thymine (DNA) or uracil (RNA). Nucleotide monomers are strung together via formation of phosphodiester bonds, to form variable length polymers. The portion of a nucleic acid sequence that codes for a protein is known as a gene; amino acids are translated from triplicate nucleotide sequences (codons) in messenger RNA molecules transcribed from genes.

The integral role of DNA and RNA in gene and protein expression and regulation frequently overshadows the inherent sequence and conformational complexity of these biopolymers. The native secondary structure of DNA within the cell is in the form of a double-stranded helix. The major structural difference between RNA and DNA is the presence of an additional hydroxyl moiety on the pentose ring of RNA. This confers some additional flexibility to RNA molecules;

* A portion of this section has been published as C. Hamula, J. Guthrie, H. Zhang, X.-F. Li, and X.C. Le. 2006. *Trends in Analytical Chemistry* 25: 581.

however both DNA and RNA are capable of forming a variety of functional tertiary and secondary structures. These include transfer RNAs, ribosomal RNAs, and pseudoknots. Many of these structures bind tightly to other molecules. Some folded RNAs are even catalytically active, and are known as *ribozymes*. The first naturally-occurring RNAs discovered to have catalytic activity include the RNA portion of RNase (215) and the *Tetrahymena thermophila* group 1 intron (1, 2), which catalyze transesterification and hydrolysis reactions, respectively.

Nucleic acid structures can have functions outside of the cell.

Complementary DNA or RNA probes are used in Southern and Northern blotting, and as primers for PCR amplification. Engineered nucleic acid molecules including DNA plasmids and bacteriophages are used as vectors in molecular cloning. Populations of nucleic acid molecules can be placed under selective pressure to enrich for specific structures. Sol Spiegelman et al. evolved a population of RNA molecules *in vitro* using a polymerase with a high error rate to mutate the sequences (3). Mutants were selected on the ability of a given RNA to act as a template for itself during amplification. It was this application of the principles of Darwinian evolution to a population of RNA *in vitro* that paved the way for the selective engineering of nucleic acid molecules known as aptamers.

1.1 Aptamers and SELEX

The term *aptamer* was coined from the Greek “aptus,” meaning “to fit.” Aptamers are short, synthetic nucleic acid molecules capable of binding to a target molecule with high affinity and selectivity. Some aptamers inhibit the activities of the molecules to which they bind; others are enzymatically active and

are known as *aptazymes*. Aptamer affinities and selectivities are comparable to or better than those of antibodies, with binding dissociation constants for aptamer-target complexes frequently in the micromolar to picomolar range. Aptamers are developed via an iterative combinatorial chemistry technique called Systematic Evolution of Ligands via Exponential Enrichment (SELEX). Conventional SELEX procedures involve binding a random nucleic acid library to a purified target molecule, separating the bound and unbound nucleic acids, and amplifying the bound nucleic acids by the polymerase chain reaction (PCR) for use in the next round of selection. The random nucleic acid library typically contains 40-100 nt single-stranded sequences with a randomized stretch of nucleotides in the center and fixed primer sequences on either end. An incredibly large number of unique sequences are present in the library; usually on the order of 10^{15} or 10^{16} . SELEX employs similar principles as the directed evolution experiments of Spiegelman, and can be used to evolve aptamers that bind virtually any target molecule. Typically, 8–15 rounds of SELEX are carried out in order to generate a pool of aptamers with sequences enabling the highest binding affinity for the target. These aptamers can then be cloned and sequenced. **Figure 1.1** describes the underlying premise of most SELEX procedures.

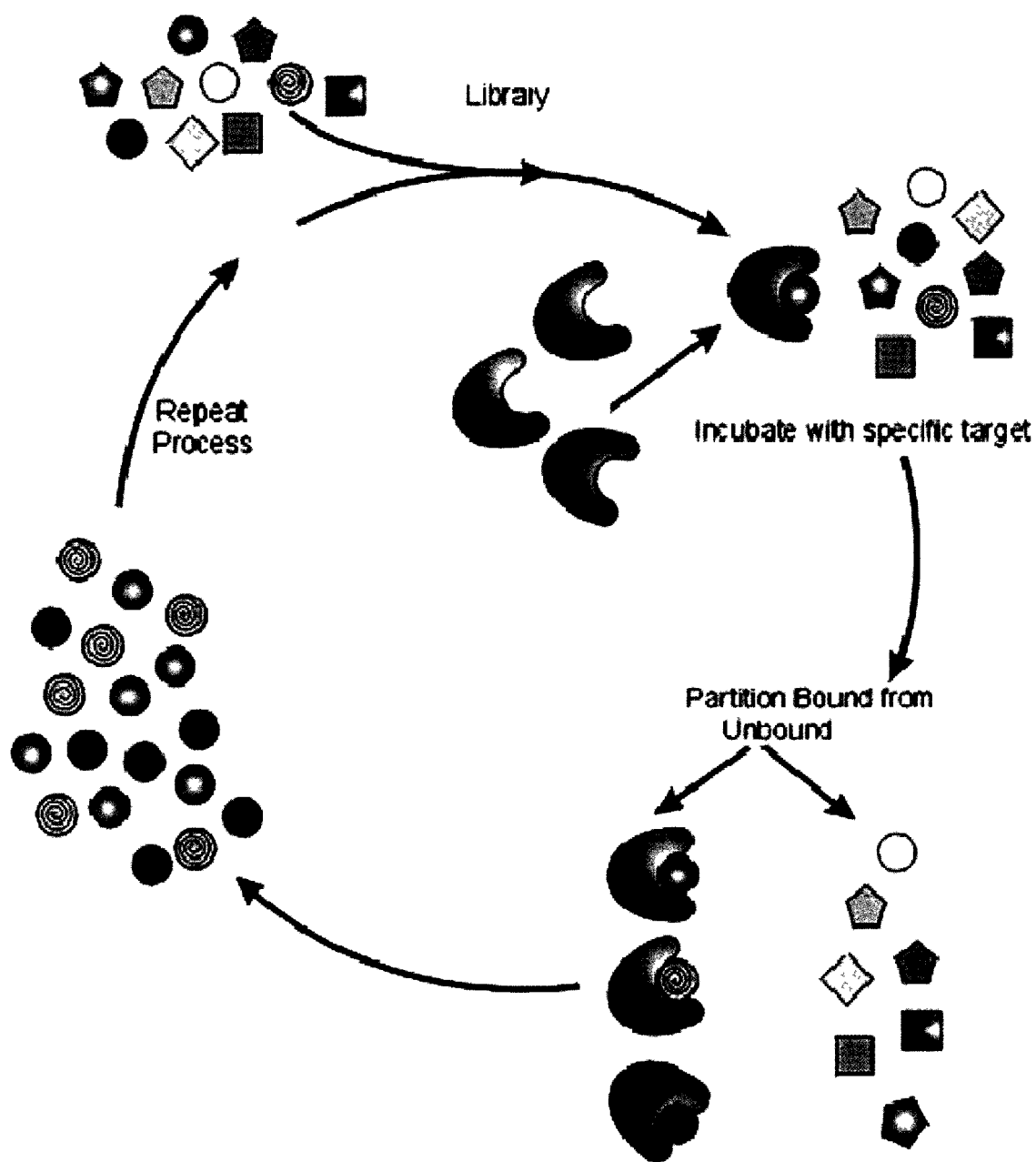


Figure 1.1. Schematic of Systematic Evolution of Ligands via Exponential Enrichment (SELEX) (4).

The very first aptamers were developed separately by two groups in 1990; Ellington and Szostak developed RNA aptamers against organic dye molecules and Tuerk and Gold developed RNA aptamers against the protein T4 DNA Polymerase (5, 6). Both studies relied on purified target molecules. The organic dyes were attached to an affinity column, through which the RNA molecules were passed. Sequences with high affinity for the dyes were retained and subsequently eluted by decreasing salt concentration. The resultant RNA aptamers specific for organic dyes had K_{ds} in the micromolar range. Conversely, aptamers against the T4 DNAP were selected by repeatedly incubating the protein and RNA together, then separating the proteins on a nitrocellulose filter and washing the filter to remove weakly bound RNAs. The K_{ds} of the aptamers for wildtype T4 DNAP were in the nanomolar range.

DNA, like RNA, has the capacity to bind a target molecule. The first single-stranded DNA aptamers were developed against organic dyes and the protein thrombin (7, 8). Ellington and Szostak successfully selected DNA aptamers with a similar methodology and the same six organic dyes as for the RNA aptamers. Notably, there were no sequence similarities between the DNA aptamers and the RNA aptamers for the same target. To obtain ssDNA aptamers that bind thrombin, Bock et al. passed a DNA library with a 60 nt randomized region over thrombin immobilized on an agarose column. The resultant aptamers bound thrombin with K_{ds} in the nanomolar range and some of them also inhibited thrombin-catalyzed fibrin clot formation.

1.2 Variation in SELEX Protocols

1.2.1 Libraries

A typical SELEX library consists of single-stranded RNA or DNA, in which a central region of randomized sequence is flanked on either side by fixed primer sequences for PCR and/or qPCR amplification. The first SELEX procedures used randomized single-stranded RNA libraries, in which the random sequence region was 100 nucleotides (nt) (5) or 8 nt (6) in length, respectively. Since then, many other SELEX procedures have been carried out using randomized ssRNA or ssDNA libraries, typically containing 10^{13} to 10^{15} different randomized sequences (9). Although any length of randomized region may be used to provide 4^n theoretical random sequences, in reality, synthetic limitations prevent most libraries from containing greater than 10^{16} random sequences. For example, for a library to contain one molecule each of 10^{16} random sequences, a minimum of 1.67 nmole nucleic acids (or 0.4 mg of nucleic acids containing 40 nt random region and two 20 nt primer regions, ~25 kDa) is required. Therefore, in practice, randomized regions of 30–60 nt are most common (9). DNA libraries are particularly useful for applications requiring increased aptamer stability, such as biosensing, environmental monitoring, and therapy. However in many cases, RNA libraries yield aptamers with higher binding affinities than DNA libraries due to the ability of RNA to take on a wider variety of conformations than DNA.

Several SELEX techniques have been developed that use modified randomized ssRNA or ssDNA libraries. Photocrosslinking procedures use ssDNA libraries substituted with fluorophore-modified nucleotides such as 5'-

bromodeoxyuridineUTP or 5-iodouracil (10, 11). Upon irradiation with a laser, these nucleotides facilitate crosslinking of an aptamer to the target.

Non-randomized or partially-randomized nucleic acid libraries can also be used. Structurally-constrained libraries are one example, in which randomized regions or nucleotide positions are incorporated along with motifs able to form a particular secondary structure. Libraries of sequences known to form pseudoknots, stem-loops, hairpins or G-quartet structures have been used to select aptamers against various antibodies, HIV-1 Rev, and Hepatitis C RNA Polymerase (12-16). Doped libraries yield improved versions of previously selected aptamers and can be used to determine which nucleotides in the sequence are essential and which are mutable. In a doped library, a known successful aptamer sequence is partially randomized at all or some positions (17). During synthesis of the library a small amount (1–30%) of the other 3 nucleotides is added at each doped position so that the library resembles the initial sequence to a variable extent (18). Doped libraries have been successfully used to select aptamers against the ribonuclease colicin E3, HIV-reverse transcriptase, phororeactive peptides, and cell-surface displayed recombinant protein (19-21). In recent years, primer-free SELEX has gained increasing popularity in which aptamer size is minimized by using adaptors to amplify the DNA (22). This technique minimizes the interference of the primers in secondary structure formation and non-specific binding.

Genomic SELEX procedures make use of ssDNA or ssRNA libraries derived from the genome of an organism of interest to probe for genome

sequences that interact with a specified target (22-25). Deep sequencing of genomic SELEX aptamer pools can map resultant sequences to regions in the genome of interest. This approach was used by Lorenz et al. to study RNA sequence motifs that bind to the *E. coli* regulatory protein Hfq and are potentially part of regulatory RNAs (26). In addition, the smaller size of genomic libraries as compared to randomized libraries increases the likelihood of isolating high affinity natural binders (27). Currently, there are *Escherichia coli*, *Drosophila melanogaster*, *Saccharomyces cerevisiae*, bacteriophage fd, and human genomic DNA libraries that are able to be transcribed into RNA or amplified by PCR (22, 23, 28-30). In all other respects, genomic SELEX is similar to conventional SELEX. Unfortunately, genomic SELEX tends to be biased towards strong or highly abundant interactions and yield many interactions that may not be important *in vivo*. Many genomic SELEX procedures have yielded aptamers with relatively low binding affinities and high K_d values in the micromolar range in as few as 5 rounds of selection (24). The non-primer SELEX technique of Wen and Gray can improve genomic aptamer binding affinity, generating a 23-fold increase in affinity over aptamers selected with a fixed primer-containing genomic library (22).

1.2.2 Presentation of target

During the incubation step of SELEX, target molecules are either incubated with library in free solution, or are bound to some sort of solid support. This dichotomy is reflected in the first two SELEX experiments, in which either target was bound to an affinity column (5) or both aptamers and target were

incubated in free solution (6). The solid support can be a column, slide, plate, chip, or beads. Recently, SELEX was carried out directly on paraffin-embedded carcinoma tissue slices (31).

Dissolving target in free solution is preferable; binding target molecules to a solid support has a number of drawbacks. The first of these is that fixing a target molecule to a solid support prevents the conjugation side of the molecule from interacting with the library, hence limiting the evolution of high-affinity aptamers. Conjugation of target molecules or nucleic acids to a support can also limit conformational flexibility. The presence of linker molecules used to bind targets to supports may also contribute to the cross reaction of non-specific binders. Also, a high amount of non-specific binding of the library to the solid surface can take place. Columns are difficult to prepare and maintain, and when using them it can be difficult to elute the strongest binding sequences. The end result is that use of solid supports usually decreases the efficiency of SELEX and the binding affinities of the resultant aptamers. The SELEX techniques that result in the highest affinity aptamers, with subnanomolar and picomolar K_d values, all have incubation steps wherein target and library are both in free solution (10, 32-34).

Typically during SELEX, the same target is used in each round. Exception is made for procedures where the goal is to affect aptamer selectivity. Counter-selection is performed to select certain aptamer sequences and to exclude those that do not bind to the molecule of interest. During counter-selection, the target is switched with an undesirable molecule for one selection round, and the nucleic acid sequences binding the undesirable molecule are removed from the pool prior

to the next round of selection with the desired target. This increases the selectivity of the aptamers for the target of interest. The approach can also be carried out against the solid surface to which a target is fixed during selection, to decrease non-specific binders. The result is an increase in aptamer binding affinity for the desired target in cases where the target is bound to a solid surface. However, this adds complexity to and decreases the efficiency of the procedure. Counter-selection is often applied to complex targets such as whole cells, usually once or twice during the course of selection but sometimes in alternate rounds. Cells that do not express a target molecule or a closely-related non-target cell type are used to remove aptamer sequences that are not specific for the cell surface molecule or cell type of interest.

Another instance in which the target molecule is switched during selection is the ToggleSELEX technique (34). ToggleSELEX is used to select aptamers that are species cross-reactive. White et al. carried out alternating rounds of selection with human or porcine thrombin as a target; the final aptamers had high affinity for thrombin of both species, with K_d values of 1–4 nM for human and < 1 nM for porcine thrombin. These aptamers were also able to inhibit thrombin-mediated plasma clot formation and platelet activation in both human and porcine samples.

1.2.3 Partitioning of aptamer-target complexes

Most vital in determining SELEX efficiency and key in resultant aptamer characteristics is the method via which aptamer-target complexes are separated from free target and unbound nucleic acids. The more traditional methods are columns or nitrocellulose membranes to separate aptamer-target complexes (5, 6,

24, 25, 34, 35). Nitsche et al. bound heat-inactivated Vaccinia virus particles to an affinity column and used the column itself as a means of partitioning DNA aptamer complexes and selecting aptamers specific to Vaccinia in one step (36). Randomized library was run through the column; it was washed multiple times and then physically segmented. The amount of DNA retained in each segment was analyzed via qPCR. Segments containing DNA were identified and the aptamer pools were eluted and amplified. However, these techniques have low separation efficiencies and often require large amounts of target and library in the initial incubation. Aptamers resulting from using nitrocellulose membranes and columns as separation techniques have K_d values from the nanomolar range to as high as 600 μM .

Improvements in separation efficiency are demonstrated when target is attached to magnetic beads as a separation matrix (37). Use of magnetic beads requires less target, and yields aptamers with high binding affinity (K_d of 57–85 nM). Furthermore, these aptamers can potentially be used to check the surface occupancy of the beads and as linkers to join other molecules to the beads. However, it is important to note that using magnetic beads to purify ssDNA from dsDNA can result in detachment of covalently-bound streptavidin from the beads if alkaline denaturation is used (38). In addition, magnetic beads can induce aggregation of whole cells during cell-SELEX (38). Coupling magnetic bead separation with qPCR has been successful in selecting aptamers against murine prion protein (39). The target mouse PrP was attached to the beads and the beads were incubated with DNA; after washing aptamer-protein complexes were eluted.

A single-step SELEX method was developed by Fan et al. and relies on the interaction of a target with dsDNA aptamers and magnetic bead separation (40). Three separate dsDNA libraries comprising 10^{15} molecules were combined and incubated with target; the three libraries had randomized inserts of 30,40, and 50 bp. Upon target binding, the DNA aptamers are rendered single-stranded. A capture aptamer with attached to a magnetic bead is then introduced to the mixture to remove the complimentary target-bound DNA sequences for PCR amplification and cloning. This technique was used to select aptamers against *Bacillus anthracis* and *Bacillus thuringensis* spores, botulinum neurotoxin, MS-2 bacteriophage, and ovalbumin.

Photocross-linking is another method of partitioning aptamer-target protein complexes. Jensen et al. (10) first described this technique in developing ssRNA aptamers against HIV-1 Rev protein, and it has also been used by Golden et al. (11) to create ssDNA aptamers against recombinant basic human fibroblastic growth factor (bFGF). Briefly, a nucleic acid library substituted with a fluorophore such as 5-iodouracil or 5-bromodeoxyuridine is incubated with target. The libraries are then irradiated by 308 nm excimer laser light in the presence of target, which facilitates covalent cross-linking of the aptamer to the target. Both studies also used PAGE to partition the aptamer-target complexes.

Aptamers obtained via cross-linking have high binding affinities and pM K_d values. They are also highly specific for their target. Photocross-linking has been recently applied to create microarray chips of ssDNA aptamers capable of detecting 17 different proteins simultaneously in a complex sample matrix with

detection limits below 10 fM for interleukin-6, vascular endothelial growth factor, and endostatin (41). A third of the aptamers exhibited high affinity for their target analytes, enabling a pM detection limit, and proteins could be measured in serum. A limitation of the photocross-linking technique is that it may not be successful against small molecule targets because small targets may not offer functional groups for cross-linking.

The application of capillary electrophoresis to SELEX has resulted in vast improvement of selection efficiency and aptamer affinity for protein targets (42). Capillary electrophoresis (CE) separates target-aptamer complexes from the unbound library in free solution. Because of the high separation efficiency and low non-specific binding of CE, CE-SELEX takes only 2–4 rounds of selection to generate ssDNA aptamers with extremely high target affinities (32, 42-44). Berezovski et al. were able to isolate nanomolar-level affinity DNA aptamers against proteins after a single round (33). CE-SELEX is less laborious than other methods and takes only 1 to 3 days to complete whereas most SELEX takes weeks to months. Typical K_d values of aptamers obtained via CE-SELEX are in the low nM range but have been as low as 180 pM. These aptamers also show high selectivity for their target proteins, binding unrelated or structurally-related but different proteins with K_d values several orders of magnitude higher than the desired target. Throughout CE-SELEX, the heterogeneity of the aptamer pool remains high resulting in a larger number of unique high affinity aptamers following selection (45). Unlike photocross-linking, CE-SELEX has been successfully applied to small targets; Mendonsa and Bowser applied it to create

aptamers to Neuropeptide Y, which is smaller than the DNA used for selection (44).

CE-SELEX techniques have a major drawback in that CE has a nL injection volume, meaning that a limited amount of DNA library can be injected at a time without overloading the column. Hence, this means that a lower number of possible DNA sequences can be used for selection, typically 10^{13} rather than the 10^{14-15} typical of conventional SELEX (32). In addition, some limitations are placed on target size since the target must be large enough to shift mobility of the aptamer upon complexation. The smallest target molecule for which an aptamer was successfully selected via CE-SELEX is Neuropeptide Y, which is 36 amino acids in length. The resultant aptamer had a K_d of 300 nM (44).

1.2.4 Screening of aptamer pools during selection/monitoring progress of SELEX

Methods to assess whether an aptamer pool is increasing in affinity and selectivity for a target vary widely. Typically the aptamer pool is labeled, incubated with target molecules or cells, and the resultant target-aptamer complexes are quantitated. Conversely, the amount of remaining unbound aptamer can also be measured. Some caution must be exercised when carrying out aptamer pool screening since most methods do not distinguish between specific binding and non-specific adhesion. Proper controls, including testing against similar non-target molecules or cells, are necessary. Randomized library or scrambled sequence controls should also be carried out. The most common screening technique is nitrocellulose filter-binding assays with radiolabeled or

fluorescently-labeled aptamer pools. Other common techniques include direct fluorescence or absorbance measurement, qPCR, microscopy, dot or western blots, and flow cytometry for monitoring whole cells and beads. Flow cytometry is a common method for cell typing and sorting. Cells are passed through a flow cell individually, and each is irradiated with a laser. Forward and side-scattered light intensity are measured. Hence, cells bound to a fluorescent probe or dye can be differentiated from those that are not and separated from the population through application of an electric field.

1.3 Aptamers in Assay Formats Traditionally Dominated by Antibodies

Aptamers possess key advantages over antibodies, due mainly to their increased temperature stability and ease of production. They have a longer shelf-life, low variability between batches, do not rely on animals for their production, are fast to produce, and can be synthesized against a complex target without prior knowledge of a specific target molecule or without purifying a known target molecule. Aptamers also offer ease of chemical modification and can easily be created against toxic or non-immunogenic targets. Hence, aptamers have proven useful in a variety of bioanalytical assays and array devices which conventionally use antibodies.

1.3.1 ELISA-like assays

Enzyme-linked immunosorbent assays (ELISAs) come in direct and sandwich formats. In direct format, a target molecule immobilized on a solid support is the capture reagent. An enzyme or fluorophore-labeled antibody probe is used to detect the target. Conversely, introduced sample containing the target molecule competes with the capture reagent for labeled probe. In a sandwich assay, a capture antibody is immobilized on a solid surface. Upon target binding a secondary detection antibody attached to an enzyme or fluorophore is added. The secondary antibody binds to a different epitope on the target molecule than the capture reagent. Aptamers can easily take the place of the one or both ELISA antibodies, provided that in sandwich format capture and detection aptamers bind separate epitopes on the target molecule.

The first enzyme-linked oligonucleotide assay (ELONA) was developed by Drolet et al. using a nuclease-stabilized oligonucleotide aptamer to detect human vascular endothelial growth factor (VEGF) in serum (46). The capture reagent was an anti-VEGF antibody attached to a microtiter plate; the aptamer was fluorescently-labeled and acted as the detection reagent. Similar sandwich and direct assays measure bile acids, Tenascin C, and human IgE (47-49). Several direct assays have been developed to measure bacterial antigens. Aptamers selected against *Francisella tularensis* antigen were tested in a aptamer-linked immunosorbent assay for binding to microtitre-plate wells coated with antigens from other bacterial species (50). Another direct assay involved screening a

ssDNA aptamer population specific for *Leishmania infantum* histone H2A protein using purified recombinant H2A-coated microtitre plate wells (51).

1.3.2 Aptamer blotting

Using an aptamer in place of a primary antibody in western blotting is also feasible. Proteins are electrophoresed on a gel and electrophoretically transferred to a membrane, or directly spotted on a membrane. Often a blocking step using either skim milk or BSA is introduced. The membrane is then incubated with a labeled aptamer following a blocking step. A secondary antibody against the aptamer label is then used to visualize the aptamer-target molecule complexes on the membrane. The two main goals of aptamer blotting are either 1) target molecule elucidation or 2) aptamer selection.

The first group to use aptamer blotting transferred proteins to a nitrocellulose membrane, incubated the membrane with a fluorescently-labeled randomized DNA library, and cut out individual protein bands to isolate bound aptamers (52). This approach successfully isolated target-specific aptamers in one step. They then used aptamer blotting to select aptamers against mouse prion protein PrP in 4 SELEX rounds (53). Blotting has subsequently been used to select aptamers against vascular endothelial growth factor (VEGF) and insulin (54) (55). Recent work has demonstrated the successful use of quantum dots (QDs) as aptamer labels for blotting (56). Aptamer-QDs eliminate the need for a secondary antibody due to their intrinsic fluorescence, and allow multiplex detection of different proteins on the same membrane (54). Aptamer-QDs

decrease the number and length of incubation steps required, while maintaining a sensitivity and selectivity similar or superior to antibody labels.

1.3.3 Affinity chromatography

In a few cases, aptamers have been used to replace antibodies as ligands in affinity purifications. Aptamers offer more flexible attachment chemistry, smaller size and hence greater attachment density, and less harsh elution options over antibodies. Most aptamer chromatography methods employ either packed columns or capillary electrochromatography (CEC) in which a capillary is coated with aptamers and used as a stationary phase. The first such study used DNA aptamers immobilized to a column to purify a recombinant human L-selectin-Ig fusion protein from Chinese Hamster Ovary cell medium (57). The aptamers were immobilized via biotin-streptavidin interaction and the column was connected to an HPLC system. Since the study by Romig et al., aptamers have successfully been used as ligands for affinity purification of other molecules including thrombin, Hepatitis C virus RNA polymerase and replicase, flavin mononucleotides, amino acids, and yeast telomerase (58-65). In a novel methodology, Zhao et al. used DNA aptamer-modified monolithic columns to separate cytochrome c and thrombin from both a protein mixture and spiked serum, and to preconcentrate thrombin (66, 67). Monolithic columns consist of a single, rigid porous structure that is synthesized *in situ*, and possess advantages over packed columns including ease of synthesis, lower pressure, higher loading volume, and gentle elution via changing ionic strength.

Separation of closely related proteins such as isomers and enantiomers is also possible via aptamer chromatography. Bovine milk proteins including casein and lactalbumin α and β isoforms were separated on a fused silica capillary coated with DNA aptamers on the inner surface (68, 69). This group employed the same technique to successfully separate albumin proteins from different species (70). RNA aptamer affinity chromatography has been used for chiral separation of adenosine, vasopressin, various amino acids and polypeptides (4, 71-77). Thorough reviews of aptamer chromatography applications have been published (45, 75, 78).

1.3.4 Aptamer affinity capillary electrophoresis

In addition to acting as a method of aptamer selection capillary electrophoresis (CE) can be harnessed to detect and separate target molecules via aptamer affinity interactions. Aptamer-target molecule complexes migrate at a different rate down the capillary than free aptamer; fluorescent labeling of the aptamer enables visualization of unbound and bound aptamer peaks on a chromatogram. German et al. first used a fluorescently-labeled DNA aptamer and laser-induced fluorescence (LIF) detection to detect IgE with a picomolar detection limit (79). Affinity CE separations have been carried out for HIV-1 reverse transcriptase, thrombin, ricin, arginine, antithrombin III, and hemin (75, 79-84).

Variations on basic affinity CE allow for a wide range of applications. Most separations require pre-column incubation of the aptamer and target; Ruta et al. have developed a novel competitive affinity CE assay for D-arginine using

labeled target and on-column mixing of aptamer-arginine with labeled arginine (77). Aptamer-protein fractions can be collected from the capillary and PCR amplified for ultrasensitive detection of proteins down to the femtomolar level (85). Multiple proteins and protein isomers can be simultaneously analysed via tunable aptamer capillary electrophoresis, which modulates the length of the aptamer while taking into account the size of the protein in order to modify the electrophoretic mobilities of the protein-aptamer complexes and separate them (86). This approach has been successfully used to separate a mixture of HIV-1 RT, thrombin, PDGF, and IgE as well as different isomers of PDGF (87).

Most aptamer affinity CE is carried out using capillary zone electrophoresis but there are exceptions. Recently, detection of thrombin was carried out by conducting CE in either buffer or gel on a glass microchip (88, 89). Aptamer-modified micellar electrokinetic CE (MEKCE) has been successful in separating enantiomers of adenosine monophosphate using an enantiomer-specific aptamer (90). In MEKCE, nonionic micelles act as a stationary phase in the capillary. Free aptamers tagged with a hydrophobic moiety (for example, cholesterol) are retained in the micelles where they interact with subsequently-injected target analytes and retain them. Very recent work has used MEKCE for multiplex analyte detection (91).

1.3.5 Aptamer arrays

Typically, antibody arrays are used to discover novel biomarkers and diagnose disease via the detection of certain illness-associated proteins in biological samples. Antibody arrays mostly use labeled secondary antibodies for

visualization of target binding. Replacing the antibodies in such arrays with aptamers is an attractive option; the decreased lability of nucleic acids means that such arrays can be stored for long periods of time and are potentially reusable. In addition, aptamers are easy to modify and hence flexible in their attachment and detection chemistries. Finally, aptamers typically have lower cross-reactivities than antibodies hence lowering the likelihood of false positive results.

Increasingly large multiplex aptamer arrays are being synthesized via *in situ* DNA synthesis or non-contact printing of nanoliter volumes. The maximum size of such arrays can reach hundreds of thousands of features. One recent study used a 44,000 feature array to scan the sequence space of a DNA aptamer for optimum IgE-binding (92).

Photoaptamer arrays have excellent detection limits, in the femtomolar range and picomolar range. These arrays consist of aptamers modified with photoreactive crosslinking groups that form a covalent linkage with target proteins upon irradiation. Golden et al. designed the first photoaptamer array (11). Arrays subsequently constructed based on these principles could simultaneously detect 17 different proteins in serum including bFGF, interleukin-6, VEGF, and endostatin (41). Photoaptamer technology and photoaptamer arrays are current intellectual property of SomaLogic Inc., a company founded by SELEX co-discoverer Larry Gold. SomaLogic is currently designing and automating photoaptamer arrays for simultaneous sensitive, specific analysis of thousands of proteins (93).

Non-crosslinking aptamers have also been successfully integrated into arrays. Quantification of target proteins via a conventional aptamer array was first demonstrated by the Ellington group with antilysozyme RNA aptamers (94). The array demonstrated specific, sensitive, dose-dependent detection of lysozyme with a picomolar detection limit. Similar arrays have been developed for detection of IgE and cancer-related proteins (95). Ellington et al. then developed a multiplex aptamer array consisting of biotinylated DNA and RNA aptamers against multiple protein targets thrombin, IgE, lysozyme and ricin (96). The proteins were labeled with Cy3 and simultaneously incubated with the array. Detection limits were found to be in the picomolar range for lysozyme and nanomolar range for the remaining proteins.

Unfortunately, dye conjugation to proteins is not always possible and can bias aptamer binding. Label-free protein detection avoids these problems. Aptamer-protein-target or aptamer-protein-aptamer sandwich assays require labeling of the aptamers and not the target. Detection is typically via a labeled secondary probe. Alternative array formats also permit label-free detection. For example, an electronic-tongue sensor (ETS) array was developed to detect the toxin ricin (97). This array format consists of a flow cell containing a silicon chip with small micromachined wells through which fluid can pass. The wells hold microspheres coated with immobilized aptamers, enabling the development of sandwich assays and detection of unlabeled ricin. Biotinylated aptamers attached to the microspheres are the capture reagents, and fluorescently-labeled aptamers

are the detection reagents. Wells can be visualized under a fluorescent microscope and fluorescence intensity measured.

1.4 SELEX targets

One beneficial feature of aptamers is that they can be created against a myriad of different target molecules. The target molecule is specified by the experimenter. The first SELEX procedures targeted organic dye molecules (5) and the protein T4 DNA Polymerase (6). Since then, a small molecules, proteins, and complex targets have been used.

The majority of SELEX procedures are still carried out against purified target molecules. The number of targets in the literature grow each year and are too numerous to mention. Small molecule targets include representatives from both organic and inorganic worlds. A comprehensive review by Stoltenburg et al. lists small molecule targets including heavy metals, nucleotides, drugs, amino acids, carbohydrates, peptides, antibiotics, cofactors, toxins, and growth factors (98). The smallest molecule targeted to date is ethanolamine, comprised of a C₂ chain with two functional groups (99). The DNA aptamer targeting ethanolamine binds with nanomolar affinity. However, aptamers against small targets frequently have lower affinities than those against larger targets such as proteins. Typical small molecule-aptamer dissociation constants are in the micromolar range, while for larger targets a nanomolar to picomolar binding dissociation constant is common.

Purified proteins make ideal SELEX targets since they possess surfaces rich in potential aptamer “epitopes” and positively-charged amino acid residues.

Some of the earliest protein targets of SELEX include thrombin, IgE, interferon gamma, HIV-1 reverse transcriptase, streptavidin, lysozyme, and prion protein (98). Many of these aptamers are still used along with their target proteins as model systems for development of novel aptasensors, particularly the anti-thrombin aptamers. Some aptamers inhibit their protein target's action and are potentially useful therapeutics.

1.4.1 Purified bacterial and viral target molecules

It is common for aptamers targeting pathogens to be created using purified bacterial or viral molecules during SELEX. Various purified pathogen targets have been used and are summarized in **Table 1**; most are protein.

Table 1. Purified pathogen molecules targeted by SELEX.

Target Molecule	References
<u>HIV-1</u> Integrase	(100)
Reverse Transcriptase	(32, 101-103)
Nucleocapsid protein	(104, 105)
Tat protein	(106)
R5 SV glycoprotein (gp120)	(107-108)
Drug-resistant Reverse Transcriptase	(109)
<u>Hepatitis C virus</u> RdRp	(110)
NS3	(111)
NS3 helicase	(112)
3'X tail	(113)
NS3 protease	(114, 115)
NS5B RNA Polymerase	(116)
IRES (internal ribosome entry site)	(117)
<u>Influenza virus</u> H5N1 HA protein	(118)
<u>SARS Coronavirus</u> NTPase, Helicase	(119, 120)
<u>Apple stem pitting virus</u> coat proteins	(121)
<u>Foot and Mouth Disease virus</u> VP1 protein	(122)
<u>Prion proteins</u> PrP ^{sc}	(123)
PrP ^{sc} fibrils	(124)
rPrP ^{sc}	(125)
rPrP ^c	(126)
mammalian prion proteins	(39)
<u>Escherichia coli</u> Release factor 1	(127)
Core RNA Polymerase	(128)
Lipopolysaccharide O111: B4	(129)
<u>Mycobacterium</u> <i>M. avium</i> sub.paratuberculosis MAP0105c gene product	(130)
<i>M. tuberculosis</i> MPT64 protein	(131)
<u>Francisella tularensis</u> protein lysate	(50)
<u>Campylobacter jejuni</u> Surface extract	(132)
<u>Salmonella enterica</u> serovar Typhi Type IVB pilus	(133)
Outer membrane proteins	(134)
<u>Leishmania infantum</u> H2 Antigen	(51)
<u>Burkholderia pseudomallei</u> BipD/BopE/BPSL2748	(135)
<u>Ustilago maydis (corn pathogen)</u> RNA-binding protein Rrm4	(136)
<u>Venezuelan equine encephalitis virus</u> Capsid protein	(137)
<u>Bacterial toxins</u> Staphylococcal enterotoxin B, Cholera toxin	(138)
Botulinum neurotoxin	(40, 139)

1.4.2 Complex targets

In recent years, an increasing number of complex targets have been used consisting of non-purified targets and multiple targets during a single selection. The first studies of complex targets employed red blood cell membrane fragments (35) and *Torpedo californica* electroplax membrane preparations (140). Since then, whole live cells have become increasingly common targets, in particular mammalian cancer cells. SELEX against whole cells is named cell-SELEX; a protocol for mammalian cells that has recently been published can be seen in **Figure 1.2** (141, 142). Briefly, cells are incubated in solution with a randomized nucleic acid library, and cell-bound nucleic acids are separated from unbound via centrifugation. Cells are then washed, and bound nucleic acids eluted and PCR amplified either for use in the next round of selection or cloning and sequencing. Aptamer pools obtained after each round can be subjected to screening for increased target cell binding affinity. Rounds of positive selection against target cells are alternated with rounds of negative selection against non-target cells in which the cell-bound aptamers are discarded. The idea of alternating rounds of counterselection and SELEX against complex targets was first introduced by Wang et al. as means of creating aptamers able to distinguish differentiated from undifferentiated PC12 cells (143). A summary of whole mammalian cell targets is presented in **Table 2** while **Table 3** presents all whole bacterial and parasite cell and viral particle targets to date.

Table 2. Whole mammalian cell SELEX targets.

Target	References
U251 glioblastoma cell line	(48)
YPEN-1 endothelial cells	(144)
NGF-differentiated pheochromocytoma PC12 cell line	(143)
PC12 cells expressing recombinant MEN2A mutant of RET receptor	(145)
Human prostate cancer cells expressing prostate-specific membrane antigen (PSMA)	(146)
Chinese Hamster Ovary (CHO) cells expressing recombinant transforming growth factor- β type III receptor (TGF β RIII)	(21)
Adult mesenchymal stem cells	(147)
CCRF-CEM lymphoblastic leukemia cells	(148)
Burkitt's lymphoma cell line (Ramos cells)	(149)
Mouse liver hepatoma cell line (MEAR cells)	(150, 151)
Small lung cancer cell line NCI-H69	(152, 153)
Neoplastic breast cancer tissue sections in paraffin	(31)
U87MG human glioma cell line	(154)
Acute myeloid leukemia (HL60) cells	(141)
Vaccinia-infected A549 cells	(155)

Table 3. Whole pathogen cell and particle SELEX targets.

Pathogen	References
Rous Sarcoma Virus particles	(133, 156)
<i>Bacillus anthracis</i> spores	(40, 157, 158)
Live African Trypanosomes	(159)
<i>Trypanoma cruzi</i>	(160)
<i>Bacillus thuringiensis</i> spores	(40, 161)
Human Influenza virus particles	(162-164)
Vaccinia virus particles	(36)
<i>Mycobacterium tuberculosis</i>	(165)
<i>Lactobacillus acidophilus</i>	(166)
<i>Escherichia coli</i> DH5 α	(167)
MS-2 Bacteriophage particles	(40)
Mammalian cells expressing Hepatitis C E2 envelope glycoprotein	(152)
Vaccinia-infected A549 cells	(155)
<i>Staphylococcus aureus</i>	(168)
<i>Streptococcus pyogenes</i>	Hamula et al. 2010

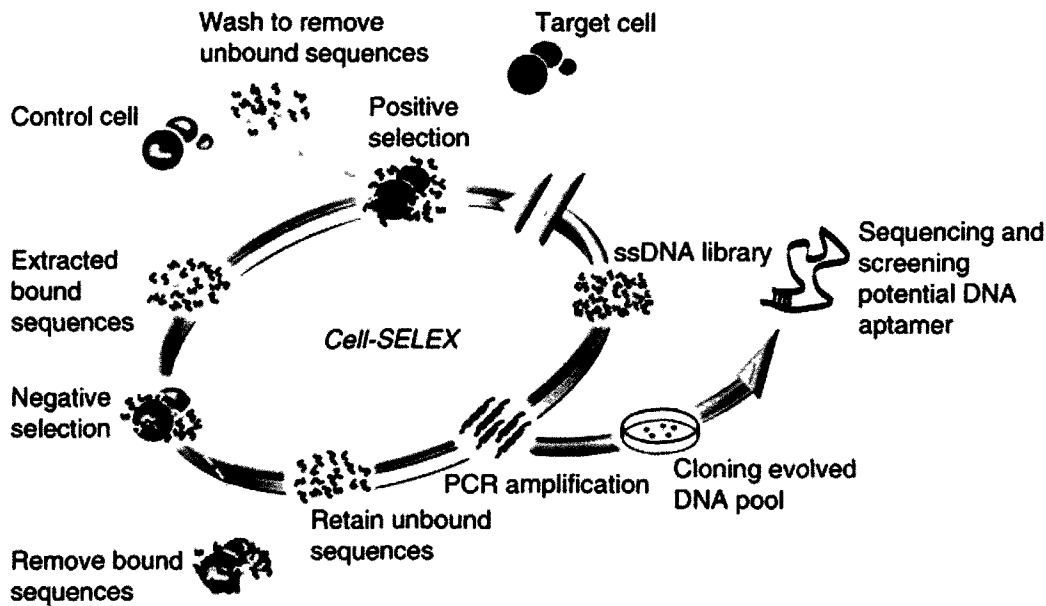


Figure 1.2. Schematic of Cell-SELEX developed by the Tan Group (169).

1.5 Uses of Aptamers Derived Against Cell Surface Molecules

1.5.1 Aptamer-based post-SELEX target elucidation

One of the major advantages of using whole cell targets is that a specific target molecule does not need to be identified or purified ahead of time. The resultant cell-SELEX aptamers will bind to the cell surface and can be used post-SELEX to purify or identify their respective target molecules. Some of the earliest SELEX procedures with whole cell targets involved post-SELEX target purification and identification. Aptamers against cell surface molecules can be conjugated to magnetic beads and the beads used to pull the target out of a cell lysate or crude membrane preparation via either affinity interaction or photocross-linking. The resultant protein(s) or aptamer-protein complexes can be eluted from

the magnetic beads, electrophoresed, and identified via mass spectrometry (35, 144).

Aptamers have been used to discover important cell surface biomarkers. Blank et al. identified the target of a high affinity aptamer to YPEN-1 endothelial cells as the rat homologue of mouse *pigpen*, a protein associated with angiogenesis (144). Similarly, the protein Tenascin-C was identified as the target of a DNA aptamer derived via cell-SELEX against U251 glioblastoma cells (48). Tenascin-C is thought to function in oncogenesis and its expression is upregulated on tumour cells. Aptamers derived against the surfaces of whole African Trypanosomes (159) were used to identify continuously expressed proteins in the variant surface coat of *Trypanosoma brucei* including a 42 kDa protein in the flagellar attachment zone (170) and a variant surface glycoprotein (171). Berezovski et al. report aptamer-mediated discovery of a marker that differentiates mature from immature dendritic cells (172). The group of Weihong Tan, at the University of Florida, has also used aptamers evolved against whole cancer cells as a means for novel cell surface biomarker discovery. A comprehensive review of their work has recently been published (169). They have used the aptamer sgc8 against T-cell acute lymphoblastic leukemia CCRF-CEM cells to identify the receptor protein tyrosine kinase (PTK7), a colon carcinoma kinase, as its target (150, 173). They identified the target of aptamer TD05 against Ramos cells as Immunoglobulin mu heavy chain, a protein known to be associated with development of Burkitt's lymphoma (149). Our group has potentially

identified the target of a *Lactobacillus acidophilus* specific DNA aptamer as the S-layer protein (166).

1.5.2 Flow cytometry

Aptamers are useful probes for flow cytometric identification and collection of cells expressing a target molecule of interest. Aptamers have been found to be equally efficient as antibodies in serving this function (174). The first flow cytometry study to use aptamers detected mouse T-cells expressing human recombinant CD4 (175). Since then, flow cytometry has been used both to evaluate target recognition by an aptamer pool and to isolate cell populations expressing a target. A recent review article published an overview of some flow cytometry applications of aptamers (176). One early study used aptamers to isolate a glioblastoma cell population expressing a tumour marker (216). Aptamers have been used for flow cytometric sorting of mesenchymal stem cells from bone marrow (217). They have also been used for determination via flow cytometry of aptamer pool target binding affinity to *L. acidophilus* (166), *M. tuberculosis* (165), and various cancer cell lines including leukemia cells and Burkitt's lymphoma cells (148, 149, 151, 177, 178).

Aptamers can be used alone or as a group for cell typing. Recently, flow cytometry was used to screen aptamers that are specific for vaccinia-virus infected A549 cells (155). A total of 8 selected aptamers were used together as a panel in flow cytometric analysis. These aptamers were proven to be useful probes for the identification of vaccinia infection in a variety of cell lines. The aptamers also generated distinct intensities and patterns of binding dependent on

the strain of vaccinia. Panels of aptamers selected against Ramos lymphoma cells were used to identify cancerous cells spiked into healthy bone marrow aspirates (179). Cancerous cells were identified based on a distinct pattern of multiple aptamer binding. Closely-related cell lines gave their own distinct aptamer patterns. This same group used a panel of 6 aptamers evolved against different tissue culture cells to identify specific types of cancer cells in patient samples (177). Cancer types identified included lymphoma, and T-cell leukemia. Another study selected aptamers against whole *Staphylococcus aureus* cells and used a fluorescently-labeled panel of 5 high affinity aptamers to differentiate different *S. aureus* strains (168). The aptamers were shown to bind different cell surface targets using a competitive flow cytometry experiment; 5 aptamers combined rather than individually was superior at detecting bacteria in pyogenic fluid.

Fluorescence-activated cell sorting (FACS) has been integrated into SELEX to select aptamer sequences against live Burkitt's lymphoma (Ramos) cells (180). This method is superior to centrifugation-based methods in that dead cells are sorted out rather than included in the cell mixture. Composite cell mixtures containing both live and dead cells were incubated with fluorescently-labeled ssDNA library, subjected to flow cytometry, and live cells were sorted from dead cells. After 10 rounds of selection, sequences with high affinity for live cells were obtained. One resultant aptamer could differentiate cancerous from non-cancerous B cells.

Other recent advances in the field of aptamer cytomics involve conjugation of aptamers to nanomaterials. Conjugation of aptamers to fluorescent

nanoparticles allows for increased fluorescence intensity over regular fluorescent labels when cells are analyzed via flow cytometry, and hence increased sensitivity of detection. Aptamer-modified magnetic nanoparticles have been used to collect CCRF-CEM leukemia cells from whole blood samples, with fluorescently-labeled aptamer nanoparticles being simultaneously used for detection (181). This technology has been extended to other cell types including Burkitt's lymphoma (Ramos) and non-Hodgkins lymphoma (Toledo) cells (182). Similarly, aptamers conjugated to nanorods were used in flow cytometric detection of cancer cells (183). Using fluorescent nanorods as aptamer scaffolds for flow cytometry can increase the binding affinity of aptamers derived from cell-SELEX. Up to 80 aptamers can be conjugated to a single rod; the assembly of the aptamers on the nanorod surface increases their binding affinity up to 26-fold for the target cells. In addition, the fluorescence intensity of aptamers conjugated to fluorescent nanorods is 300-fold greater than fluorophore-conjugated aptamers.

1.5.3 Whole cell and virus aptamer sensors

Several excellent extensive reviews have been recently published on aptamers as biosensors (184, 185). All biosensors are composed of a biological molecular recognition element (MRE) and a signal transduction element (STE). A classical biosensor functions to transduce target binding by the MRE into a readable output. The term *aptasensor* applies to biosensors in which an aptamer is used as a MRE and/or STE. Early aptasensors involved using aptamers as MREs and either attaching the aptamer directly to a STE or labeling it with a molecule

that allows the aptamer itself to function as a STE. In some cases, the conformational change induced by aptamer-target binding is the STE (218).

A variety of novel aptasensors for whole cells have been developed. In the simplest form, aptamers can be conjugated to a fluorophore and then used to label cells expressing a target molecule on their surface. Aptamers bound to a cell surface can also be detected via proximity ligation and subsequent PCR amplification (186). Two aptamers that bind in close proximity to each other can be ligated to yield a unique amplicon. This method is particularly useful for detection of specific cell surface molecules. Pai and Ellington used two different aptamers specific for PSMA expressing cells; the method is sensitive enough to detect 10 cells in a complex sample.

Aptamer-nanoparticle conjugates have also been used in cancer cell detection. The assembly of the aptamer-gold nanoparticle conjugates on a cell surface causes a change in the nanoparticle absorption spectra, translating into a dark purple colour visible to the naked eye. A colorimetric assay using aptamer-conjugated gold nanoparticles was able to detect leukemia and lymphoma cells (187). An aptamer-nanoparticle strip biosensor was developed for detection of B-cell lymphoma (Ramos) cells (188). A pair of aptamers generated against Ramos cells via cell-SELEX was labeled with either gold nanoparticles or biotin. The biotinylated aptamer is attached to the test zone of a strip in a lateral flow device. Ramos cells interact with aptamer-NPs to form red complexes which migrate down the strip and are captured in the test zone where they form a red band. The

device detected as few as 800 cells in 15 minutes in complex matrices including blood.

The earliest aptasensor for bacterial detection was an electro-chemiluminescence sandwich system (157). DNA aptamers with high affinity for anthrax spores were conjugated to magnetic beads or to biotin. The magnetic bead-aptamer conjugates acted as capture reagents and the biotinylated aptamers as reporters for detection of as few as 10 spores with linear dynamic range of 10^6 . This same group designed a similar assay by conjugating aptamers to magnetic beads or QDs for detection of *Bacillus thuringiensis* spores and *Campylobacter jejuni* (132, 161). In the *C. jejuni* assay, capture aptamer-magnetic bead conjugates could be adhered to the surface of a cuvette via a magnet. Unlike the previous sensors for spores, this sensor detected both live and heat-killed cells at levels as low as 2.5 cfu in complex food matrices. The assay was also portable; fluorescence could be measured via benchtop or hand-held fluorometer.

A FRET-based approach was used to detect *E. coli* using aptamers evolved against *E. coli* outer membrane proteins (OMPs) (189). *E. coli* cells labeled with a quencher molecule were complexed to fluorescently-labeled aptamers and attached to a plate; introduced unlabeled bacteria competing with quencher-labeled bacteria for aptamers generated a signal. A DNA capture element (DCE) sensing system based on fluorescence quenching was also developed by this group for both aptamer selection and sensing of *B. thuringiensis*, *B. anthracis* spores, botulinum neurotoxin and MS-2 bacteriophage (40). Magnetic beads are attached to a dual fluorescently-labeled and quencher-labeled

dsDNA aptamer; upon interaction of the aptamer with a target cell the dsDNA is denatured into ssDNA. This dissociates the quencher and generates a fluorescent signal. The magnetic bead-aptamer-target cell complexes can be then be purified out of solution and re-detected with a complimentary DNA probe attached to a quencher.

Aptamers do not need to be fluorescently-labeled for use in pathogen detection; there are a variety of alternative methods that can be used. One of these is PCR amplification. Antibody-coated magnetic beads were used to collect *Escherichia coli* from complex samples with detection via PCR amplification of an *E. coli* specific aptamer (190). Similarly, aptamers against *Salmonella typhimurium* OMPs were conjugated to magnetic beads for collection of *S. typhimurium* from chicken carcass rinse samples and subsequent quantitative PCR detection (134). The assay had a detection limit of 10–100 cfu per mL of rinsate.

Another detection method used in pathogen sensors is electrochemical, which has recently been applied to the design of a probe for *Salmonella typhi* in complex food samples (191). A single-walled carbon nanotube (SWCNT) layer is deposited on a glass rod electrode. The layer is coated with an aptamer specific for *S. typhi* type IV pili. Conformational changes induced by target cell binding to the aptamers results a charge change in the SWCNTs and a subsequent change in potential recorded by the electrode. This system is sensitive and could detect below 1 cfu per mL of sample. The probe is rapid, portable, and label-free. The electrodes are also reusable after reconstitution in buffer.

In addition to whole bacterial and cancer cells, aptasensors have been created for viral particles. Virus aptasensors have been designed for both Foot and Mouth Disease (FMD) virus and Hepatitis C Virus (HCV). A FRET-based assay was developed for detection of a peptide from FMD using fluorescently-labeled polyclonal aptamers and a quencher-labeled FMD peptide (122). Binding of the FMD peptide to the aptamer resulted in a “lights-off” response that could measure FMD peptide at nanomolar levels. The peptide-bound aptamers could also be fixed to a solid support for a competitive assay with introduced analyte resulting in a “lights-on” response. Novel aptasensors developed for unlabeled Hepatitis C virus particles (HCV) include a chip-based diagnostic sensor using aptamers against HCV core protein for detection of HCV in infected patient sera (192, 193). A novel resonance sensor using nanomechanical microcantilevers was also designed to detect HCV helicase at levels as low as 100 pg/mL (193). RNA aptamers specific to HCV helicase are attached to the cantilever surface; aptamer-target binding induces stress on the cantilever surface and a dynamic response change that can be measured.

1.5.4 Cell labeling and imaging

Aptamers can be labeled and used in microscopy for detection of target cells. In fact, fluorescence microscopy is recommended as a confirmatory method to use in addition to flow cytometry or fluorescence measurement for aptamer-based cell typing (194). Some of the earliest cell-SELEX procedures visualized aptamer binding to the target cell surface (157, 159). Aptamers specific for *Trypanosoma cruzi* were used as probes to fluorescently-label the parasite surface

(159). Microscopy with fluorescently-labeled aptamers has since been extensively used in studies of cancer cell SELEX (144, 181, 182). Aptamers can also be conjugated to nanomaterials for cell labeling and microscopic visualization, an approach taken with CdSe and CdTe nanocrystals for specific targeting of cells expressing PSMA (195). Aptamers have also been labeled with fluorescent nanoparticles for detection of cancer cells and confocal microscopy imaging (181, 182, 196).

There are instances where the target cell/aptamer interaction cannot be microscopically visualized. For example, Bruno and Kiel were able to detect aptamer-coated magnetic beads binding to spores using a modified avidin method but could not visualize the interaction under the microscope (157). This is most likely due to the hindrance from the spacing of the aptamers on the beads and the size of both the beads and the spores.

A variety of new aptamer-based cell imaging methods are emerging. Multicolour fluorescent imaging is possible using aptamer-conjugated quantum dots (197). Quantum dots have broad adsorption and very narrow emission spectra; they can use a single absorption source and still produce multiple colours. Another method uses aptamer-functionalized superoxide magnetic nanoparticles as contrast agents in magnetic resonance imaging (MRI) of adenosine (198). A cobalt-ferrite aptamer-functionalized nanoparticle targeting nucleolin has been used for MRI tracking of cancer cells after injection into mice (199). This conjugate was specific for cancer cells and could also be used for confocal and radionuclide imaging.

1.5.5 Aptamers with therapeutic potential against pathogens

Not only do aptamers bind a target with high affinity and have the potential to be catalytically active, many also act as inhibitors of their target molecules. This fact has obvious therapeutic ramifications. Aptamers have been used to inhibit both intracellular and cell surface targets but the majority of therapeutic aptamers are against extracellular proteins including antibodies, chemokines, cytokines, and cell surface molecules. A number of inhibitory aptamers have been isolated for pathogens. Aptamers specific for whole *Trypanosoma cruzi* inhibit its invasion of monkey kidney cells (160). These aptamers bind to parasite receptors for host cell proteins and are each specific for a given receptor as they are selected via competitive displacement. Similarly, an aptamer against Hepatitis C Virus (HCV) envelope glycoprotein E2 blocks binding of the protein to immune cells and invasion of hepatocytes by HCV (152). Aptamer sequences that bind to the HCV IRES and inhibit translation of the viral genome have also been discovered (117). Aptamers that prevent dsDNA unwinding during viral replication have also been isolated against severe acute respiratory syndrome (SARS) coronavirus NTPase/Helicase (120). Anti-lipopolysaccharide (LPS) aptamers have demonstrated *in vivo* antibacterial effects when coupled to human C1qrs (200). C1qrs is the first component of the complement cascade, and attachment to the anti-LPS aptamer (and subsequent target binding) mimics the fixation of complement to bacterial cells. When the C1qrs-aptamer complexes are applied to *E. coli* cells in diluted human serum, they significantly reduced plate colony counts.

1.5.6 Aptamer-targeted delivery of therapeutics

Aptamers that bind cell surface molecules can be conjugated to drugs and used as vectors for targeted therapy. This approach has been applied to mammalian cancer cell lines. Aptamers have been used as escorts for the toxin gelonin, not only targeting it to prostate tumour cells expressing PSMA but also facilitating its uptake via endocytosis (201). Aptamer-functionalized liposomes have also been created for cell specific drug delivery (202). The anticancer drug cisplatin was encapsulated in an aptamer-conjugated liposome specific for cells expressing nucleolin on their surface (202). Similar studies have been carried out with the drug Doxorubicin; Dox-aptamer conjugates have an IC_{50} value comparable to that of free Dox but are specific for target cells (183).

Nanoparticles encapsulated with anticancer drugs can also be conjugated to aptamers. Nanoparticles are attractive chemotherapeutic agents since they deliver a constant dose of chemotherapy over an extended period of time. Nanoparticles encapsulated with docetaxel were conjugated to aptamers specific for PSMA and used to reduce tumour size in LNCaP cell xenograft mice (203-205). Targeted release of cisplatin to LNCaP prostate tumour cells was achieved using aptamer functionalized platinum prodrug-PLGA-PEG nanoparticles (206). Aptamers have also been radiolabeled and conjugated to phototherapy agents for targeting cancer cells (149, 207).

One of the most promising methods of aptamer-targeted therapy is the use of aptamers for siRNA delivery. RNA interference is a cellular mechanism wherein short RNAs (siRNAs) mediate degradation of specific mRNAs thus

inhibiting gene expression. The first such study engineered siRNA-aptamer chimeras made entirely of RNA for targeting of survival genes in PSMA expressing cells (208). Direct injection of the chimeras into tumours in a mouse xenograft prostate cancer model resulted in tumour regression. A subsequent study by the same group introduced a variety of stabilizing chemical modifications to the chimeras for more flexible *in vivo* use and found the modified chimeras to induce tumour regression after systemic (intravenous) administration to mice (209). Another group used aptamers coupled to siRNAs via modified streptavidin bridges for targeting of PSMA expressing cells (210).

The Tan group has introduced some new technologies for aptamer-mediated cancer-cell targeting based on conjugation of aptamers to nanomaterials (169). They have focused on developing aptamer conjugates for intracellular delivery, targeted chemotherapy, and targeted phototherapy. Included among these are aptamer-conjugated nanorods (183) and aptamer-micelle nanostructures (211). The aptamer nanorod conjugates were specific for CCRF-CEM T cell leukemia cells and can be used for phototherapy due to the excellent broad absorption characteristics of the nanorods. The aptamer-micelle structures are created via attachment of a lipid tail to the aptamers; formation of micelles increased the binding affinity of even low affinity aptamers. An *in vitro* microfluidic blood tumour model was created employing cancer cells attached to a flow chamber surface, and the aptamer micelles demonstrated selective cancer cell recognition in a human blood matrix.

1.7 Rationale and Scope of Thesis

Aptamers possess many advantages over antibodies including increased temperature stability, low variability between batches, and ease of synthesis. They can be evolved against virtually any target, including those that are non-immunogenic or toxic. Their similarity to antibodies makes them easily integrated into existing antibody-based technologies such as affinity chromatography, microarrays and ELISAs. In addition, a variety of unique aptasensor technologies exist due to the ease of aptamer modification, engineering, and labeling. Aptamers that inhibit the activity of their target molecules can be used as novel therapeutics.

Development of a novel SELEX technique capable of generating aptamers against whole, live bacterial cells eliminates the need to purify a specific cell surface target molecule ahead of time and then affix that purified molecule to a solid support. Instead, an aptamer can be developed and used to elucidate its specific cell surface target molecule post-selection. Aptamers generated against live bacterial pathogens are potentially useful for diagnosis of bacterial infections, detection of bacteria in the environment and in food, and as therapeutics against bacterial pathogens. Despite the myriad benefits of generating aptamers against cell surface targets, very little work has been done on using cell-SELEX to generate aptamers against bacterial cells. When this work was started, cell-SELEX had never been applied to live bacterial cells. Since then, we have applied it to *L. acidophilus* and *Streptococcus pyogenes* and it has also been applied to *Mycobacterium tuberculosis*, *Escherichia coli* DH5 α , and *Staphylococcus aureus*.

Group A streptococcus (GAS) is implicated in a variety of diseases, including streptococcal pharyngitis, necrotizing fasciitis, scarlet fever, toxic shock syndrome (TSS), invasive systemic infections and endocarditis. One of the major virulence factors of invasive GAS (iGAS) isolates is the M protein which is present on the surface of the bacteria. This protein can also be utilized as a typing tool for understanding the epidemiology of iGAS disease. Epidemiological surveillance of GAS clinical isolates is important for outbreak management as well as vaccine development and implementation. Different M-types are often but not always associated with different invasive infections. For example, the M-types M1 and M3 are more often associated with invasive infections than other M-types (212, 213). Conventionally, GAS is M-typed via precipitin or latex agglutination methods, which involve screening bacterial surface extracts against different M-protein specific reference polyclonal antisera or antibodies conjugated to latex beads. More recently, sequencing of the *emm* gene that codes for M-protein is replacing antibody-based typing methods as the gold standard (214) and has expanded the repertoire of GAS *emm* types worldwide. In addition, due to the complexity of these methods, the M typing of GAS isolates has tended to be centralized in laboratories specializing in GAS characterization. Both these methods are laborious and have low-throughput as each requires comparison of a bacterial isolate to a myriad of reference strains or databases. The protein-based serotyping system of GAS makes it an ideal aptamer target. Aptamers specific for the GAS cell surface, in particular M protein, could replace antisera and

sequencing for surveillance of clinical isolates and enable reliable point-of-care *S.pyogenes* detection.

A novel cell-based SELEX technique can be developed using live bacteria in solution to select aptamers that bind with high affinity and selectivity to bacterial cell surface molecules, without prior knowledge of a specific target. This cell-based SELEX technique can be applied against a variety of bacterial cells, both pathogenic and non-pathogenic, to develop aptamers against a variety of molecules, including proteins and carbohydrates. Aptamers developed with the bacterial cell SELEX technique can be used post-selection to elucidate specific cell surface target molecules. The aptamers developed via bacterial cell SELEX can be applied towards development of bacterial typing, diagnostic, and detection technologies. Specifically, the aptamers can be used for M-typing GAS.

This thesis consists of 7 chapters. **Chapter 1** reviews the current literature on different SELEX methods and aptamer-based technologies with a focus on cell-SELEX and different applications of aptamers targeting bacterial and mammalian cell surface molecules. **Chapter 2** describes a novel cell-SELEX method for selection of ssDNA aptamers against whole, live *Lactobacillus acidophilus* cells. These non-pathogenic cells were chosen as a target to demonstrate proof-of-principle, and the resultant SELEX technique generated a specific, high affinity aptamer Hemag1P that binds *L. acidophilus* with nanomolar Kd values. **Chapter 3** describes the application of our bacterial cell-SELEX to a pathogenic target, *Streptococcus pyogenes*. Aptamers were generated that were

S. pyogenes specific but not M-type specific. In addition, many rounds of selection were needed to generate these aptamers; high affinity aptamer pools did not evolve until up to 20 rounds of SELEX against *S. pyogenes* whereas only 7 rounds were necessary with *L. acidophilus* as a target. These problems necessitated the development of a modified bacterial cell-SELEX technique as detailed in **Chapter 4**. This modified technique incorporates gel purification of ssDNA, a much larger starting library size, and counterselection steps. It was successful in generating *S. pyogenes* specific aptamers in as short as 8 rounds of selection, and an M11 specific sequence. **Chapter 5** describes attempts at post-SELEX target molecule elucidation for both *S. pyogenes* and *L. acidophilus* targets. The presumptive target of aptamer hemag1P is identified as the S-layer protein. Detailed comparison of aptamer pool characteristics from the different types of bacterial cell-SELEX is given in **Chapter 6**. There is some sequence overlap between the resultant aptamer pools of the two different bacterial cell-SELEX methodologies used against *S. pyogenes*. It was also discovered that SELEX with a large starting library, counterselection steps, and gel purification of ssDNA was more efficient at generating high affinity aptamers. **Chapter 7** is a summary of the conclusions and implications from this research, as well as a discussion of future research directions.

1.6 References

1. Gardiner K, Pace NR. RNase P of bacillus subtilis has a RNA component. *J Biol Chem.* 1980 Aug 25;255(16):7507-9.
2. Guerrier-Takada C, Gardiner K, Marsh T, Pace N, Altman S. The RNA moiety of ribonuclease P is the catalytic subunit of the enzyme. *Cell.* 1983 Dec;35(3 Pt 2):849-57.
3. Saffhill R, Schneider-Bernloehr H, Orgel LE, Spiegelman S. In vitro selection of bacteriophage Q-beta ribonucleic acid variants resistant to ethidium bromide. *J Mol Biol.* 1970 Aug;51(3):531-9.
4. Nimjee S.M., Rusconi C.P., Sullenger B.A. *Annu. Rev. Med.* 2005 56: 555.
5. Ellington AD, Szostak JW. In vitro selection of RNA molecules that bind specific ligands. *Nature.* 1990 Aug 30;346(6287):818-22.
6. Tuerk C, Gold L. Systematic evolution of ligands by exponential enrichment: RNA ligands to bacteriophage T4 DNA polymerase. *Science.* 1990 Aug 3;249(4968):505-10.
7. Ellington AD, Szostak JW. Selection in vitro of single-stranded DNA molecules that fold into specific ligand-binding structures. *Nature.* 1992 Feb 27;355(6363):850-2.
8. Bock LC, Griffin LC, Latham JA, Vermaas EH, Toole JJ. Selection of single-stranded DNA molecules that bind and inhibit human thrombin. *Nature.* 1992 Feb 6;355(6360):564-6.
9. Osborne SE, Ellington AD. Nucleic acid selection and the challenge of combinatorial chemistry. *Chem Rev.* 1997 Apr 1;97(2):349-70.
10. Jensen KB, Atkinson BL, Willis MC, Koch TH, Gold L. Using in vitro selection to direct the covalent attachment of human immunodeficiency virus type 1 rev protein to high-affinity RNA ligands. *Proc Natl Acad Sci U S A.* 1995 Dec 19;92(26):12220-4.
11. Golden MC, Collins BD, Willis MC, Koch TH. Diagnostic potential of PhotoSELEX-evolved ssDNA aptamers. *J Biotechnol.* 2000 Aug 25;81(2-3):167-78.
12. Hamm J. Characterisation of antibody-binding RNAs selected from structurally constrained libraries. *Nucleic Acids Res.* 1996 Jun 15;24(12):2220-7.

13. Hamm J, Huber J, Luhrmann R. Anti-idiotypic RNA selected with an anti-nuclear export signal antibody is actively transported in oocytes and inhibits rev- and cap-dependent RNA export. *Proc Natl Acad Sci U S A*. 1997 Nov 25;94(24):12839-44.
14. Tsai DE, Kenan DJ, Keene JD. In vitro selection of an RNA epitope immunologically cross-reactive with a peptide. *Proc Natl Acad Sci U S A*. 1992 Oct 1;89(19):8864-8.
15. Giver L, Bartel DP, Zapp ML, Green MR, Ellington AD. Selection and design of high-affinity RNA ligands for HIV-1 rev. *Gene*. 1993 Dec 27;137(1):19-24.
16. Biroccio A, Hamm J, Incitti I, De Francesco R, Tomei L. Selection of RNA aptamers that are specific and high-affinity ligands of the hepatitis C virus RNA-dependent RNA polymerase. *J Virol*. 2002 Apr;76(8):3688-96.
17. Knight R, Yarus M. Analyzing partially randomized nucleic acid pools: Straight dope on doping. *Nucleic Acids Res*. 2003 Mar 15;31(6):e30.
18. Kulbachinskiy AV. Methods for selection of aptamers to protein targets. *Biochemistry (Mosc)*. 2007 Dec;72(13):1505-18.
19. Hirao I, Harada Y, Nojima T, Osawa Y, Masaki H, Yokoyama S. In vitro selection of RNA aptamers that bind to colicin E3 and structurally resemble the decoding site of 16S ribosomal RNA. *Biochemistry*. 2004 Mar 23;43(11):3214-21.
20. Hayashi G, Hagihara M, Nakatani K. RNA aptamers that reversibly bind photoresponsive azobenzene-containing peptides. *Chemistry*. 2009;15(2):424-32.
21. Ohuchi SP, Ohtsu T, Nakamura Y. Selection of RNA aptamers against recombinant transforming growth factor-beta type III receptor displayed on cell surface. *Biochimie*. 2006 Jul;88(7):897-904.
22. Wen JD, Gray DM. Selection of genomic sequences that bind tightly to the gene 5 protein: Primer-free genomic SELEX. *Nucleic Acids Res*. 2004 Dec 15;32(22):e182.
23. Singer BS, Shtatland T, Brown D, Gold L. Libraries for genomic SELEX. *Nucleic Acids Res*. 1997 Feb 15;25(4):781-6.
24. Shtatland T, Gill SC, Javornik BE, Johansson HE, Singer BS, Uhlenbeck OC, et al. Interactions of escherichia coli RNA with bacteriophage MS2 coat protein: Genomic SELEX. *Nucleic Acids Res*. 2000 Nov 1;28(21):E93.

25. Shimada T, Fujita N, Maeda M, Ishihama A. Systematic search for the cr-binding promoters using genomic SELEX system. *Genes Cells*. 2005 Sep;10(9):907-18.
26. Lorenz C, Gesell T, Zimmermann B, Schoeberl U, Bilusic I, Rajkowitsch L, et al. Genomic SELEX for hfq-binding RNAs identifies genomic aptamers predominantly in antisense transcripts. *Nucleic Acids Res*. 2010 Jun 1;38(11):3794-808.
27. Zimmermann B, Gesell T, Chen D, Lorenz C, Schroeder R. Monitoring genomic sequences during SELEX using high-throughput sequencing: Neutral SELEX. *PLoS One*. 2010 Feb 11;5(2):e9169.
28. Kim S, Shi H, Lee DK, Lis JT. Specific SR protein-dependent splicing substrates identified through genomic SELEX. *Nucleic Acids Res*. 2003 Apr 1;31(7):1955-61.
29. Ogasawara H, Hasegawa A, Kanda E, Miki T, Yamamoto K, Ishihama A. Genomic SELEX search for target promoters under the control of the PhoQP-RstBA signal relay cascade. *J Bacteriol*. 2007 Jul;189(13):4791-9.
30. Watrin M, Von Pelchrzim F, Dausse E, Schroeder R, Toulme JJ. In vitro selection of RNA aptamers derived from a genomic human library against the TAR RNA element of HIV-1. *Biochemistry*. 2009 Jul 7;48(26):6278-84.
31. Li S, Xu H, Ding H, Huang Y, Cao X, Yang G, et al. Identification of an aptamer targeting hnRNP A1 by tissue slide-based SELEX. *J Pathol*. 2009 Jul;218(3):327-36.
32. Mosing RK, Mendonsa SD, Bowser MT. Capillary electrophoresis-SELEX selection of aptamers with affinity for HIV-1 reverse transcriptase. *Anal Chem*. 2005 Oct 1;77(19):6107-12.
33. Berezovski M, Drabovich A, Krylova SM, Musheev M, Okhonin V, Petrov A, et al. Nonequilibrium capillary electrophoresis of equilibrium mixtures: A universal tool for development of aptamers. *J Am Chem Soc*. 2005 Mar 9;127(9):3165-71.
34. White R, Rusconi C, Scardino E, Wolberg A, Lawson J, Hoffman M, et al. Generation of species cross-reactive aptamers using "toggle" SELEX. *Mol Ther*. 2001 Dec;4(6):567-73.
35. Morris KN, Jensen KB, Julin CM, Weil M, Gold L. High affinity ligands from in vitro selection: Complex targets. *Proc Natl Acad Sci U S A*. 1998 Mar 17;95(6):2902-7.

36. Nitsche A, Kurth A, Dunkhorst A, Panke O, Sielaff H, Junge W, et al. One-step selection of vaccinia virus-binding DNA aptamers by MonoLEX. *BMC Biotechnol.* 2007 Aug 15;7:48.
37. Stoltenburg R, Reinemann C, Strehlitz B. FluMag-SELEX as an advantageous method for DNA aptamer selection. *Anal Bioanal Chem.* 2005 Sep;383(1):83-91.
38. Paul A, Avci-Adali M, Ziemer G, Wendel HP. Streptavidin-coated magnetic beads for DNA strand separation implicate a multitude of problems during cell-SELEX. *Oligonucleotides.* 2009 Sep;19(3):243-54.
39. Bibby DF, Gill AC, Kirby L, Farquhar CF, Bruce ME, Garson JA. Application of a novel in vitro selection technique to isolate and characterise high affinity DNA aptamers binding mammalian prion proteins. *J Virol Methods.* 2008 Jul;151(1):107-15.
40. Fan M, McBurnett SR, Andrews CJ, Allman AM, Bruno JG, Kiel JL. Aptamer selection express: A novel method for rapid single-step selection and sensing of aptamers. *J Biomol Tech.* 2008 Dec;19(5):311-9.
41. Bock C, Coleman M, Collins B, Davis J, Foulds G, Gold L, et al. Photoaptamer arrays applied to multiplexed proteomic analysis. *Proteomics.* 2004 Mar;4(3):609-18.
42. Mendonsa SD, Bowser MT. In vitro evolution of functional DNA using capillary electrophoresis. *J Am Chem Soc.* 2004 Jan 14;126(1):20-1.
43. Mendonsa SD, Bowser MT. In vitro selection of high-affinity DNA ligands for human IgE using capillary electrophoresis. *Anal Chem.* 2004 Sep 15;76(18):5387-92.
44. Mendonsa SD, Bowser MT. In vitro selection of aptamers with affinity for neuropeptide Y using capillary electrophoresis. *J Am Chem Soc.* 2005 Jul 6;127(26):9382-3.
45. Mosing RK, Bowser MT. Microfluidic selection and applications of aptamers. *J Sep Sci.* 2007 Jul;30(10):1420-6.
46. Drolet DW, Moon-McDermott L, Romig TS. An enzyme-linked oligonucleotide assay. *Nat Biotechnol.* 1996 Aug;14(8):1021-5.
47. Kato T, Yano K, Ikebukuro K, Karube I. Bioassay of bile acids using an enzyme-linked DNA aptamer. *Analyst.* 2000 Aug;125(8):1371-3.

48. Daniels DA, Chen H, Hicke BJ, Swiderek KM, Gold L. A tenascin-C aptamer identified by tumor cell SELEX: Systematic evolution of ligands by exponential enrichment. *Proc Natl Acad Sci U S A*. 2003 Dec 23;100(26):15416-21.
49. Papamichael KI, Kreuzer MP, Guilbault GG. Viability of allergy (IgE) detection using an alternative aptamer receptor and electrochemical means. *Sensors Actuators B: Chem*. 2007 1/30;121(1):178-86.
50. Vivekananda J, Kiel JL. Anti-francisella tularensis DNA aptamers detect tularemia antigen from different subspecies by aptamer-linked immobilized sorbent assay. *Lab Invest*. 2006 Jun;86(6):610-8.
51. Ramos E, Pineiro D, Soto M, Abanades DR, Martin ME, Salinas M, et al. A DNA aptamer population specifically detects leishmania infantum H2A antigen. *Lab Invest*. 2007 May;87(5):409-16.
52. Noma T, Ikebukuro K, Sode K, Ohkubo T, Sakasegawa Y, Hachiya N, et al. Screening of DNA aptamers against multiple proteins in tissue. *Nucleic Acids Symp Ser (Oxf)*. 2005;(49)(49):357-8.
53. Ogasawara D, Hasegawa H, Kaneko K, Sode K, Ikebukuro K. Screening of DNA aptamer against mouse prion protein by competitive selection. *Prion*. 2007 Oct;1(4):248-54.
54. Hasegawa H, Sode K, Ikebukuro K. Selection of DNA aptamers against VEGF165 using a protein competitor and the aptamer blotting method. *Biotechnol Lett*. 2008 May;30(5):829-34.
55. Yoshida W, Mochizuki E, Takase M, Hasegawa H, Morita Y, Yamazaki H, et al. Selection of DNA aptamers against insulin and construction of an aptameric enzyme subunit for insulin sensing. *Biosens Bioelectron*. 2009 Jan 1;24(5):1116-20.
56. Shin S, Kim IH, Kang W, Yang JK, Hah SS. An alternative to western blot analysis using RNA aptamer-functionalized quantum dots. *Bioorg Med Chem Lett*. 2010 Jun 1;20(11):3322-5.
57. Romig TS, Bell C, Drolet DW. Aptamer affinity chromatography: Combinatorial chemistry applied to protein purification. *J Chromatogr B Biomed Sci Appl*. 1999 Aug 20;731(2):275-84.
58. Connor AC, McGown LB. Aptamer stationary phase for protein capture in affinity capillary chromatography. *J Chromatogr A*. 2006 Apr 14;1111(2):115-9.

59. Cho JS, Lee YJ, Shin KS, Jeong S, Park J, Lee SW. In vitro selection of specific RNA aptamers for the NFAT DNA binding domain. *Mol Cells*. 2004 Aug 31;18(1):17-23.
60. Chung WJ, Kim MS, Cho S, Park SS, Kim JH, Kim YK, et al. Microaffinity purification of proteins based on photolytic elution: Toward an efficient microbead affinity chromatography on a chip. *Electrophoresis*. 2005 Feb;26(3):694-702.
61. Deng Q, Watson CJ, Kennedy RT. Aptamer affinity chromatography for rapid assay of adenosine in microdialysis samples collected in vivo. *J Chromatogr A*. 2003 Jul 11;1005(1-2):123-30.
62. Clark SL, Remcho VT. Electrochromatographic retention studies on a flavin-binding RNA aptamer sorbent. *Anal Chem*. 2003 Nov 1;75(21):5692-6.
63. Kotia RB, Li L, McGown LB. Separation of nontarget compounds by DNA aptamers. *Anal Chem*. 2000 Feb 15;72(4):827-31.
64. Charles JA, McGown LB. Separation of trp-arg and arg-trp using G-quartet-forming DNA oligonucleotides in open-tubular capillary electrochromatography. *Electrophoresis*. 2002 Jun;23(11):1599-604.
65. Shcherbakova DM, Sokolov KA, Zvereva MI, Dontsova OA. Telomerase from yeast *saccharomyces cerevisiae* is active in vitro as a monomer. *Biochemistry (Mosc)*. 2009 Jul;74(7):749-55.
66. Zhao Q, Li XF, Le XC. Aptamer-modified monolithic capillary chromatography for protein separation and detection. *Anal Chem*. 2008 May 15;80(10):3915-20.
67. Zhao Q, Li XF, Shao Y, Le XC. Aptamer-based affinity chromatographic assays for thrombin. *Anal Chem*. 2008 Oct 1;80(19):7586-93.
68. Rehder MA, McGown LB. Open-tubular capillary electrochromatography of bovine beta-lactoglobulin variants A and B using an aptamer stationary phase. *Electrophoresis*. 2001 Oct;22(17):3759-64.
69. Rehder-Silinski MA, McGown LB. Capillary electrochromatographic separation of bovine milk proteins using a G-quartet DNA stationary phase. *J Chromatogr A*. 2003 Aug 8;1008(2):233-45.
70. Dick LW, Jr, McGown LB. Aptamer-enhanced laser desorption/ionization for affinity mass spectrometry. *Anal Chem*. 2004 Jun 1;76(11):3037-41.

71. Michaud M, Jourdan E, Ravelet C, Villet A, Ravel A, Grosset C, et al. Immobilized DNA aptamers as target-specific chiral stationary phases for resolution of nucleoside and amino acid derivative enantiomers. *Anal Chem.* 2004 Feb 15;76(4):1015-20.
72. Michaud M, Jourdan E, Villet A, Ravel A, Grosset C, Peyrin E. A DNA aptamer as a new target-specific chiral selector for HPLC. *J Am Chem Soc.* 2003 Jul 16;125(28):8672-9.
73. Ravelet C, Boulkedid R, Ravel A, Grosset C, Villet A, Fize J, et al. A L-RNA aptamer chiral stationary phase for the resolution of target and related compounds. *J Chromatogr A.* 2005 May 27;1076(1-2):62-70.
74. Ruta J, Ravelet C, Grosset C, Fize J, Ravel A, Villet A, et al. Enantiomeric separation using an l-RNA aptamer as chiral additive in partial-filling capillary electrophoresis. *Anal Chem.* 2006 May 1;78(9):3032-9.
75. Ruta J, Ravelet C, Baussanne I, Decout JL, Peyrin E. Aptamer-based enantioselective competitive binding assay for the trace enantiomer detection. *Anal Chem.* 2007 Jun 15;79(12):4716-9.
76. Ruta J, Grosset C, Ravelet C, Fize J, Villet A, Ravel A, et al. Chiral resolution of histidine using an anti-D-histidine L-RNA aptamer microbore column. *J Chromatogr B Analyt Technol Biomed Life Sci.* 2007 Jan 15;845(2):186-90.
77. Ruta J, Ravelet C, Desire J, Decout JL, Peyrin E. Covalently bonded DNA aptamer chiral stationary phase for the chromatographic resolution of adenosine. *Anal Bioanal Chem.* 2008 Feb;390(4):1051-7.
78. Peyrin E. Nucleic acid aptamer molecular recognition principles and application in liquid chromatography and capillary electrophoresis. *J Sep Sci.* 2009 May;32(10):1531-6.
79. German I, Buchanan DD, Kennedy RT. Aptamers as ligands in affinity probe capillary electrophoresis. *Anal Chem.* 1998 Nov 1;70(21):4540-5.
80. Pavski V, Le XC. Detection of human immunodeficiency virus type 1 reverse transcriptase using aptamers as probes in affinity capillary electrophoresis. *Anal Chem.* 2001 Dec 15;73(24):6070-6.
81. Buchanan DD, Jameson EE, Perlette J, Malik A, Kennedy RT. Effect of buffer, electric field, and separation time on detection of aptamer-ligand complexes for affinity probe capillary electrophoresis. *Electrophoresis.* 2003 May;24(9):1375-82.

82. Huang CC, Cao Z, Chang HT, Tan W. Protein-protein interaction studies based on molecular aptamers by affinity capillary electrophoresis. *Anal Chem.* 2004 Dec 1;76(23):6973-81.
83. Haes AJ, Giordano BC, Collins GE. Aptamer-based detection and quantitative analysis of ricin using affinity probe capillary electrophoresis. *Anal Chem.* 2006 Jun 1;78(11):3758-64.
84. Li T, Li B, Dong S. Aptamer-based label-free method for hemin recognition and DNA assay by capillary electrophoresis with chemiluminescence detection. *Anal Bioanal Chem.* 2007 Oct;389(3):887-93.
85. Zhang H, Wang Z, Li XF, Le XC. Ultrasensitive detection of proteins by amplification of affinity aptamers. *Angew Chem Int Ed Engl.* 2006 Feb 27;45(10):1576-80.
86. Zhang H, Li XF, Le XC. Tunable aptamer capillary electrophoresis and its application to protein analysis. *J Am Chem Soc.* 2008 Jan 9;130(1):34-5.
87. Zhang H, Li XF, Le XC. Differentiation and detection of PDGF isomers and their receptors by tunable aptamer capillary electrophoresis. *Anal Chem.* 2009 Sep 15;81(18):7795-800.
88. Gong M, Nikcevic I, Wehmeyer KR, Limbach PA, Heineman WR. Protein-aptamer binding studies using microchip affinity capillary electrophoresis. *Electrophoresis.* 2008 Apr;29(7):1415-22.
89. Obubuafo A, Balamurugan S, Shadpour H, Spivak D, McCarley RL, Soper SA. Poly(methyl methacrylate) microchip affinity capillary gel electrophoresis of aptamer-protein complexes for the analysis of thrombin in plasma. *Electrophoresis.* 2008 Aug;29(16):3436-45.
90. Ruta J, Perrier S, Ravelet C, Roy B, Perigaud C, Peyrin E. Aptamer-modified micellar electrokinetic chromatography for the enantioseparation of nucleotides. *Anal Chem.* 2009 Feb 1;81(3):1169-76.
91. Zhu Z, Ravelet C, Perrier S, Guieu V, Roy B, Perigaud C, et al. Multiplexed detection of small analytes by structure-switching aptamer-based capillary electrophoresis. *Anal Chem.* 2010 Jun 1;82(11):4613-20.
92. Katilius E, Flores C, Woodbury NW. Exploring the sequence space of a DNA aptamer using microarrays. *Nucleic Acids Res.* 2007;35(22):7626-35.
93. Keeney TR, Bock C, Gold L, Kraemer S, Lollo B, Nikrad M, et al. Automation of the SomaLogic proteomics assay: A platform for biomarker

- discovery. *Journal of the Association for Laboratory Automation*. 2009 12;14(6):360-6.
94. Collett JR, Cho EJ, Lee JF, Levy M, Hood AJ, Wan C, et al. Functional RNA microarrays for high-throughput screening of antiprotein aptamers. *Anal Biochem*. 2005 Mar 1;338(1):113-23.
95. Stadtherr K, Wolf H, Lindner P. An aptamer-based protein biochip. *Anal Chem*. 2005 Jun 1;77(11):3437-43.
96. Cho EJ, Collett JR, Szafranska AE, Ellington AD. Optimization of aptamer microarray technology for multiple protein targets. *Anal Chim Acta*. 2006 Mar 30;564(1):82-90.
97. Kirby R, Cho EJ, Gehrke B, Bayer T, Park YS, Neikirk DP, et al. Aptamer-based sensor arrays for the detection and quantitation of proteins. *Anal Chem*. 2004 Jul 15;76(14):4066-75.
98. Stoltenburg R, Reinemann C, Strehlitz B. SELEX--a (r)evolutionary method to generate high-affinity nucleic acid ligands. *Biomol Eng*. 2007 Oct;24(4):381-403.
99. Mann D, Reinemann C, Stoltenburg R, Strehlitz B. In vitro selection of DNA aptamers binding ethanolamine. *Biochem Biophys Res Commun*. 2005 Dec 30;338(4):1928-34.
100. Allen P, Collins B, Brown D, Hostomsky Z, Gold L. A specific RNA structural motif mediates high affinity binding by the HIV-1 nucleocapsid protein (NCp7). *Virology*. 1996 Nov 15;225(2):306-15.
101. Tuerk C, MacDougall S, Gold L. RNA pseudoknots that inhibit human immunodeficiency virus type 1 reverse transcriptase. *Proc Natl Acad Sci U S A*. 1992 Aug 1;89(15):6988-92.
102. Schneider D, Tuerk C, Gold L. Selection of high affinity RNA ligands to the bacteriophage R17 coat protein. *J Mol Biol*. 1992 Dec 5;228(3):862-9.
103. DeStefano JJ, Cristofaro JV. Selection of primer-template sequences that bind human immunodeficiency virus reverse transcriptase with high affinity. *Nucleic Acids Res*. 2006 Jan 5;34(1):130-9.
104. Kim SJ, Kim MY, Lee JH, You JC, Jeong S. Selection and stabilization of the RNA aptamers against the human immunodeficiency virus type-1 nucleocapsid protein. *Biochem Biophys Res Commun*. 2002 Mar 8;291(4):925-31.

105. Jeong YY, Kim SH, Jang SI, You JC. Examination of specific binding activity of aptamer RNAs to the HIV-NC by using a cell-based in vivo assay for protein-RNA interaction. *BMB Rep.* 2008 Jul 31;41(7):511-5.
106. Yamamoto R, Baba T, Kumar PK. Molecular beacon aptamer fluoresces in the presence of tat protein of HIV-1. *Genes Cells.* 2000 May;5(5):389-96.
107. Khati M, Schuman M, Ibrahim J, Sattentau Q, Gordon S, James W. Neutralization of infectivity of diverse R5 clinical isolates of human immunodeficiency virus type 1 by gp120-binding 2'F-RNA aptamers. *J Virol.* 2003 Dec;77(23):12692-8.
108. Cohen C, Forzan M, Sproat B, Pantophlet R, McGowan I, Burton D, et al. An aptamer that neutralizes R5 strains of HIV-1 binds to core residues of gp120 in the CCR5 binding site. *Virology.* 2008 Nov 10;381(1):46-54.
109. Li N, Wang Y, Pothukuchy A, Syrett A, Husain N, Gopalakrishna S, et al. Aptamers that recognize drug-resistant HIV-1 reverse transcriptase. *Nucleic Acids Res.* 2008 Dec;36(21):6739-51.
110. Jones LA, Clancy LE, Rawlinson WD, White PA. High-affinity aptamers to subtype 3a hepatitis C virus polymerase display genotypic selectivity. *Antimicrob Agents Chemother.* 2006 Sep;50(9):3019-27.
111. Kumar PK, Machida K, Urvil PT, Kakiuchi N, Vishnuvardhan D, Shimotohno K, et al. Isolation of RNA aptamers specific to the NS3 protein of hepatitis C virus from a pool of completely random RNA. *Virology.* 1997 Oct 27;237(2):270-82.
112. Hwang B, Cho JS, Yeo HJ, Kim JH, Chung KM, Han K, et al. Isolation of specific and high-affinity RNA aptamers against NS3 helicase domain of hepatitis C virus. *RNA.* 2004 Aug;10(8):1277-90.
113. Fukuda K, Toyokawa Y, Kikuchi K, Konno K, Ishihara R, Fukazawa C, et al. Isolation of RNA aptamers specific for the 3' X tail of HCV. *Nucleic Acids Symp Ser (Oxf).* 2008;(52)(52):205-6.
114. Fukuda K, Vishnuvardhan D, Sekiya S, Hwang J, Kakiuchi N, Taira K, et al. Isolation and characterization of RNA aptamers specific for the hepatitis C virus nonstructural protein 3 protease. *Eur J Biochem.* 2000 Jun;267(12):3685-94.
115. Fukuda K, Umehara T, Sekiya S, Kunio K, Hasegawa T, Nishikawa S. An RNA ligand inhibits hepatitis C virus NS3 protease and helicase activities. *Biochem Biophys Res Commun.* 2004 Dec 17;325(3):670-5.

116. Biroccio A, Hamm J, Incitti I, De Francesco R, Tomei L. Selection of RNA aptamers that are specific and high-affinity ligands of the hepatitis C virus RNA-dependent RNA polymerase. *J Virol.* 2002 Apr;76(8):3688-96.
117. Kikuchi K, Umehara T, Nishikawa F, Fukuda K, Hasegawa T, Nishikawa S. Increased inhibitory ability of conjugated RNA aptamers against the HCV IRES. *Biochem Biophys Res Commun.* 2009 Aug 14;386(1):118-23.
118. Cheng C, Dong J, Yao L, Chen A, Jia R, Huan L, et al. Potent inhibition of human influenza H5N1 virus by oligonucleotides derived by SELEX. *Biochem Biophys Res Commun.* 2008 Feb 15;366(3):670-4.
119. Ahn DG, Jeon IJ, Kim JD, Song MS, Han SR, Lee SW, et al. RNA aptamer-based sensitive detection of SARS coronavirus nucleocapsid protein. *Analyst.* 2009 Sep;134(9):1896-901.
120. Jang KJ, Lee NR, Yeo WS, Jeong YJ, Kim DE. Isolation of inhibitory RNA aptamers against severe acute respiratory syndrome (SARS) coronavirus NTPase/Helicase. *Biochem Biophys Res Commun.* 2008 Feb 15;366(3):738-44.
121. Lautner G, Balogh Z, Bardocz V, Meszaros T, Gyurcsanyi RE. Aptamer-based biochips for label-free detection of plant virus coat proteins by SPR imaging. *Analyst.* 2010 May 26;135(5):918-26.
122. Bruno JG, Carrillo MP, Phillips T. Development of DNA aptamers to a foot-and-mouth disease peptide for competitive FRET-based detection. *J Biomol Tech.* 2008 Apr;19(2):109-15.
123. Proske D, Gilch S, Wopfner F, Schatzl HM, Winnacker EL, Famulok M. Prion-protein-specific aptamer reduces PrP^{Sc} formation. *Chembiochem.* 2002 Aug 2;3(8):717-25.
124. Rhie A, Kirby L, Sayer N, Wellesley R, Disterer P, Sylvester I, et al. Characterization of 2'-fluoro-RNA aptamers that bind preferentially to disease-associated conformations of prion protein and inhibit conversion. *J Biol Chem.* 2003 Oct 10;278(41):39697-705.
125. Weiss S, Proske D, Neumann M, Groschup MH, Kretzschmar HA, Famulok M, et al. RNA aptamers specifically interact with the prion protein PrP. *J Virol.* 1997 Nov;71(11):8790-7.
126. Takemura K, Wang P, Vorberg I, Surewicz W, Priola SA, Kanthasamy A, et al. DNA aptamers that bind to PrP(C) and not PrP(sc) show sequence and structure selectivity. *Exp Biol Med (Maywood).* 2006 Feb;231(2):204-14.

127. Sando S, Ogawa A, Nishi T, Hayami M, Aoyama Y. In vitro selection of RNA aptamer against escherichia coli release factor 1. *Bioorg Med Chem Lett*. 2007 Mar 1;17(5):1216-20.
128. Kulbachinskiy A, Feklistov A, Krasheninnikov I, Goldfarb A, Nikiforov V. Aptamers to escherichia coli core RNA polymerase that sense its interaction with rifampicin, sigma-subunit and GreB. *Eur J Biochem*. 2004 Dec;271(23-24):4921-31.
129. Bruno JG, Carrillo MP, Phillips T. In vitro antibacterial effects of antilipoplysaccharide DNA aptamer-C1qrs complexes. *Folia Microbiol (Praha)*. 2008;53(4):295-302.
130. Bannantine JP, Radosevich TJ, Stabel JR, Sreevatsan S, Kapur V, Paustian ML. Development and characterization of monoclonal antibodies and aptamers against major antigens of mycobacterium avium subsp. paratuberculosis. *Clin Vaccine Immunol*. 2007 May;14(5):518-26.
131. Qin L, Zheng R, Ma Z, Feng Y, Liu Z, Yang H, et al. The selection and application of ssDNA aptamers against MPT64 protein in mycobacterium tuberculosis. *Clin Chem Lab Med*. 2009;47(4):405-11.
132. Bruno JG, Phillips T, Carrillo MP, Crowell R. Plastic-adherent DNA aptamer-magnetic bead and quantum dot sandwich assay for campylobacter detection. *J Fluoresc*. 2009 May;19(3):427-35.
133. Pan Q, Zhang XL, Wu HY, He PW, Wang F, Zhang MS, et al. Aptamers that preferentially bind type IVB pili and inhibit human monocytic-cell invasion by salmonella enterica serovar typhi. *Antimicrob Agents Chemother*. 2005 Oct;49(10):4052-60.
134. Joshi R, Janagama H, Dwivedi HP, Senthil Kumar TM, Jaykus LA, Schefers J, et al. Selection, characterization, and application of DNA aptamers for the capture and detection of salmonella enterica serovars. *Mol Cell Probes*. 2009 Feb;23(1):20-8.
135. Gnanam AJ, Hall B, Shen X, Piasecki S, Vernados A, Galyov EE, et al. Development of aptamers specific for potential diagnostic targets in burkholderia pseudomallei. *Trans R Soc Trop Med Hyg*. 2008 Dec;102 Suppl 1:S55-7.
136. Konig J, Julius C, Baumann S, Homann M, Goring HU, Feldbrugge M. Combining SELEX and the yeast three-hybrid system for in vivo selection and classification of RNA aptamers. *RNA*. 2007 Apr;13(4):614-22.

137. Kang J, Lee MS, Watowich SJ, Gorenstein DG. Combinatorial selection of a RNA thioaptamer that binds to venezuelan equine encephalitis virus capsid protein. *FEBS Lett.* 2007 May 29;581(13):2497-502.
138. Bruno JG, Kiel JL. Use of magnetic beads in selection and detection of biotoxin aptamers by electrochemiluminescence and enzymatic methods. *BioTechniques.* 2002 Jan;32(1):178,80, 182-3.
139. Tok JB, Fischer NO. Single microbead SELEX for efficient ssDNA aptamer generation against botulinum neurotoxin. *Chem Commun (Camb).* 2008 Apr 28;(16)(16):1883-5.
140. Ulrich H, Ippolito JE, Pagan OR, Eterovic VA, Hann RM, Shi H, et al. In vitro selection of RNA molecules that displace cocaine from the membrane-bound nicotinic acetylcholine receptor. *Proc Natl Acad Sci U S A.* 1998 Nov 24;95(24):14051-6.
141. Sefah K, Tang ZW, Shangguan DH, Chen H, Lopez-Colon D, Li Y, et al. Molecular recognition of acute myeloid leukemia using aptamers. *Leukemia.* 2009 Feb;23(2):235-44.
142. Sefah K, Shangguan D, Xiong X, O'Donoghue MB, Tan W. Development of DNA aptamers using cell-SELEX. *Nat Protoc.* 2010;5(6):1169-85.
143. Wang C, Zhang M, Yang G, Zhang D, Ding H, Wang H, et al. Single-stranded DNA aptamers that bind differentiated but not parental cells: Subtractive systematic evolution of ligands by exponential enrichment. *J Biotechnol.* 2003 Apr 10;102(1):15-22.
144. Blank M, Weinschenk T, Priemer M, Schluesener H. Systematic evolution of a DNA aptamer binding to rat brain tumor microvessels. selective targeting of endothelial regulatory protein pigpen. *J Biol Chem.* 2001 May 11;276(19):16464-8.
145. Cerchia L, Duconge F, Pestourie C, Boulay J, Aissouni Y, Gombert K, et al. Neutralizing aptamers from whole-cell SELEX inhibit the RET receptor tyrosine kinase. *PLoS Biol.* 2005 Apr;3(4):e123.
146. Lupold SE, Hicke BJ, Lin Y, Coffey DS. Identification and characterization of nuclease-stabilized RNA molecules that bind human prostate cancer cells via the prostate-specific membrane antigen. *Cancer Res.* 2002 Jul 15;62(14):4029-33.
147. Guo KT, SchAfer R, Paul A, Gerber A, Ziemer G, Wendel HP. A new technique for the isolation and surface immobilization of mesenchymal stem cells from whole bone marrow using high-specific DNA aptamers. *Stem Cells.* 2006 Oct;24(10):2220-31.

148. Shangguan D, Li Y, Tang Z, Cao ZC, Chen HW, Mallikaratchy P, et al. Aptamers evolved from live cells as effective molecular probes for cancer study. *Proc Natl Acad Sci U S A*. 2006 Aug 8;103(32):11838-43.
149. Mallikaratchy P, Tang Z, Kwame S, Meng L, Shangguan D, Tan W. Aptamer directly evolved from live cells recognizes membrane bound immunoglobulin heavy mu chain in burkitt's lymphoma cells. *Mol Cell Proteomics*. 2007 Dec;6(12):2230-8.
150. Shangguan D, Cao Z, Meng L, Mallikaratchy P, Sefah K, Wang H, et al. Cell-specific aptamer probes for membrane protein elucidation in cancer cells. *J Proteome Res*. 2008 May;7(5):2133-9.
151. Shangguan D, Meng L, Cao ZC, Xiao Z, Fang X, Li Y, et al. Identification of liver cancer-specific aptamers using whole live cells. *Anal Chem*. 2008 Feb 1;80(3):721-8.
152. Chen F, Hu Y, Li D, Chen H, Zhang XL. CS-SELEX generates high-affinity ssDNA aptamers as molecular probes for hepatitis C virus envelope glycoprotein E2. *PLoS One*. 2009 Dec 3;4(12):e8142.
153. Chen HW, Medley CD, Sefah K, Shangguan D, Tang Z, Meng L, et al. Molecular recognition of small-cell lung cancer cells using aptamers. *ChemMedChem*. 2008 Jun;3(6):991-1001.
154. Cerchia L, Esposito CL, Jacobs AH, Tavitian B, de Franciscis V. Differential SELEX in human glioma cell lines. *PLoS One*. 2009 Nov 24;4(11):e7971.
155. Tang Z, Parekh P, Turner P, Moyer RW, Tan W. Generating aptamers for recognition of virus-infected cells. *Clin Chem*. 2009 Apr;55(4):813-22.
156. Pan W, Craven RC, Qiu Q, Wilson CB, Wills JW, Golovine S, et al. Isolation of virus-neutralizing RNAs from a large pool of random sequences. *Proc Natl Acad Sci U S A*. 1995 Dec 5;92(25):11509-13.
157. Bruno JG, Kiel JL. In vitro selection of DNA aptamers to anthrax spores with electrochemiluminescence detection. *Biosens Bioelectron*. 1999 May 31;14(5):457-64.
158. Zhen B, Song YJ, Guo ZB, Wang J, Zhang ML, Yu SY, et al. In vitro selection and affinity function of the aptamers to bacillus anthracis spores by SELEX. *Sheng Wu Hua Xue Yu Sheng Wu Wu Li Xue Bao (Shanghai)*. 2002 Sep;34(5):635-42.

159. Homann M, Goringer HU. Combinatorial selection of high affinity RNA ligands to live african trypanosomes. *Nucleic Acids Res.* 1999 May 1;27(9):2006-14.
160. Ulrich H, Magdesian MH, Alves MJ, Colli W. In vitro selection of RNA aptamers that bind to cell adhesion receptors of trypanosoma cruzi and inhibit cell invasion. *J Biol Chem.* 2002 Jun 7;277(23):20756-62.
161. Ikanovic M, Rudzinski WE, Bruno JG, Allman A, Carrillo MP, Dwarakanath S, et al. Fluorescence assay based on aptamer-quantum dot binding to bacillus thuringiensis spores. *J Fluoresc.* 2007 Mar;17(2):193-9.
162. Gopinath SC, Kawasaki K, Kumar PK. Selection of RNA-aptamer against human influenza B virus. *Nucleic Acids Symp Ser (Oxf).* 2005;(49)(49):85-6.
163. Gopinath SC, Misono TS, Kawasaki K, Mizuno T, Imai M, Odagiri T, et al. An RNA aptamer that distinguishes between closely related human influenza viruses and inhibits haemagglutinin-mediated membrane fusion. *J Gen Virol.* 2006 Mar;87(Pt 3):479-87.
164. Gopinath SC, Sakamaki Y, Kawasaki K, Kumar PK. An efficient RNA aptamer against human influenza B virus hemagglutinin. *J Biochem.* 2006 May;139(5):837-46.
165. Chen F, Zhou J, Luo F, Mohammed AB, Zhang XL. Aptamer from whole-bacterium SELEX as new therapeutic reagent against virulent mycobacterium tuberculosis. *Biochem Biophys Res Commun.* 2007 Jun 8;357(3):743-8.
166. Hamula CL, Zhang H, Guan LL, Li XF, Le XC. Selection of aptamers against live bacterial cells. *Anal Chem.* 2008 Oct 15;80(20):7812-9.
167. So HM, Park DW, Jeon EK, Kim YH, Kim BS, Lee CK, et al. Detection and titer estimation of escherichia coli using aptamer-functionalized single-walled carbon-nanotube field-effect transistors. *Small.* 2008 Feb;4(2):197-201.
168. Cao X, Li S, Chen L, Ding H, Xu H, Huang Y, et al. Combining use of a panel of ssDNA aptamers in the detection of staphylococcus aureus. *Nucleic Acids Res.* 2009 Aug;37(14):4621-8.
169. Fang X, Tan W. Aptamers generated from cell-SELEX for molecular medicine: A chemical biology approach. *Acc Chem Res.* 2010 Jan 19;43(1):48-57.
170. Homann M, Lorger M, Engstler M, Zacharias M, Goringer HU. Serum-stable RNA aptamers to an invariant surface domain of live african trypanosomes. *Comb Chem High Throughput Screen.* 2006 Aug;9(7):491-9.

171. Lorgner M, Engstler M, Homann M, Goring HU. Targeting the variable surface of african trypanosomes with variant surface glycoprotein-specific, serum-stable RNA aptamers. *Eukaryot Cell*. 2003 Feb;2(1):84-94.
172. Berezovski MV, Lechmann M, Musheev MU, Mak TW, Krylov SN. Aptamer-facilitated biomarker discovery (AptaBiD). *J Am Chem Soc*. 2008 Jul 16;130(28):9137-43.
173. Shangguan D, Li Y, Tang Z, Cao ZC, Chen HW, Mallikaratchy P, et al. Aptamers evolved from live cells as effective molecular probes for cancer study. *Proc Natl Acad Sci U S A*. 2006 Aug 8;103(32):11838-43.
174. Davis KA, Abrams B, Lin Y, Jayasena SD. Use of a high affinity DNA ligand in flow cytometry. *Nucleic Acids Res*. 1996 Feb 15;24(4):702-6.
175. Davis KA, Lin Y, Abrams B, Jayasena SD. Staining of cell surface human CD4 with 2'-F-pyrimidine-containing RNA aptamers for flow cytometry. *Nucleic Acids Res*. 1998 Sep 1;26(17):3915-24.
176. Ulrich H, Wrenger C. Disease-specific biomarker discovery by aptamers. *Cytometry A*. 2009 Sep;75(9):727-33.
177. Shangguan D, Cao ZC, Li Y, Tan W. Aptamers evolved from cultured cancer cells reveal molecular differences of cancer cells in patient samples. *Clin Chem*. 2007 Jun;53(6):1153-5.
178. Zhang J, Jia X, Lv XJ, Deng YL, Xie HY. Fluorescent quantum dot-labeled aptamer bioprobes specifically targeting mouse liver cancer cells. *Talanta*. 2010 Apr 15;81(1-2):505-9.
179. Tang Z, Shangguan D, Wang K, Shi H, Sefah K, Mallikratchy P, et al. Selection of aptamers for molecular recognition and characterization of cancer cells. *Anal Chem*. 2007 Jul 1;79(13):4900-7.
180. Raddatz MS, Dolf A, Endl E, Knolle P, Famulok M, Mayer G. Enrichment of cell-targeting and population-specific aptamers by fluorescence-activated cell sorting. *Angew Chem Int Ed Engl*. 2008;47(28):5190-3.
181. Herr JK, Smith JE, Medley CD, Shangguan D, Tan W. Aptamer-conjugated nanoparticles for selective collection and detection of cancer cells. *Anal Chem*. 2006 May 1;78(9):2918-24.
182. Smith JE, Medley CD, Tang Z, Shangguan D, Lofton C, Tan W. Aptamer-conjugated nanoparticles for the collection and detection of multiple cancer cells. *Anal Chem*. 2007 Apr 15;79(8):3075-82.

183. Huang YF, Sefah K, Bamrungsap S, Chang HT, Tan W. Selective photothermal therapy for mixed cancer cells using aptamer-conjugated nanorods. *Langmuir*. 2008 Oct 21;24(20):11860-5.
184. Song S, Wang L, Li J, Fan C, Zhao J. Aptamer-based biosensors. *TrAC Trends in Analytical Chemistry*. 2008 2;27(2):108-17.
185. Sefah K, Phillips JA, Xiong X, Meng L, Van Simaey D, Chen H, et al. Nucleic acid aptamers for biosensors and bio-analytical applications. *Analyst*. 2009 Sep;134(9):1765-75.
186. Pai SS, Ellington AD. Using RNA aptamers and the proximity ligation assay for the detection of cell surface antigens. *Methods Mol Biol*. 2009;504:385-98.
187. Medley CD, Smith JE, Tang Z, Wu Y, Bamrungsap S, Tan W. Gold nanoparticle-based colorimetric assay for the direct detection of cancerous cells. *Anal Chem*. 2008 Feb 15;80(4):1067-72.
188. Liu G, Mao X, Phillips JA, Xu H, Tan W, Zeng L. Aptamer-nanoparticle strip biosensor for sensitive detection of cancer cells. *Anal Chem*. 2009 Dec 15;81(24):10013-8.
189. Bruno JG, Carrillo MP, Phillips T, Andrews CJ. A novel screening method for competitive FRET-aptamers applied to *E. coli* assay development. *J Fluoresc*. 2010 May 5.
190. Lee HJ, Kim BC, Kim KW, Kim YK, Kim J, Oh MK. A sensitive method to detect *Escherichia coli* based on immunomagnetic separation and real-time PCR amplification of aptamers. *Biosens Bioelectron*. 2009 Aug 15;24(12):3550-5.
191. Zelada-Guillen GA, Riu J, Duzgun A, Rius FX. Immediate detection of living bacteria at ultralow concentrations using a carbon nanotube based potentiometric aptasensor. *Angew Chem Int Ed Engl*. 2009;48(40):7334-7.
192. Lee S, Kim YS, Jo M, Jin M, Lee DK, Kim S. Chip-based detection of hepatitis C virus using RNA aptamers that specifically bind to HCV core antigen. *Biochem Biophys Res Commun*. 2007 Jun 22;358(1):47-52.
193. Hwang KS, Lee SM, Eom K, Lee JH, Lee YS, Park JH, et al. Nanomechanical microcantilever operated in vibration modes with use of RNA aptamer as receptor molecules for label-free detection of HCV helicase. *Biosens Bioelectron*. 2007 Nov 30;23(4):459-65.
194. Li N, Ebright JN, Stovall GM, Chen X, Nguyen HH, Singh A, et al. Technical and biological issues relevant to cell typing with aptamers. *J Proteome Res*. 2009 May;8(5):2438-48.

195. Chu TC, Shieh F, Lavery LA, Levy M, Richards-Kortum R, Korgel BA, et al. Labeling tumor cells with fluorescent nanocrystal-aptamer bioconjugates. *Biosens Bioelectron.* 2006 Apr 15;21(10):1859-66.
196. Estevez MC, Huang YF, Kang H, O'Donoghue MB, Bamrungsap S, Yan J, et al. Nanoparticle-aptamer conjugates for cancer cell targeting and detection. *Methods Mol Biol.* 2010;624:235-48.
197. Ko MH, Kim S, Kang WJ, Lee JH, Kang H, Moon SH, et al. In vitro derby imaging of cancer biomarkers using quantum dots. *Small.* 2009 May;5(10):1207-12.
198. Yigit MV, Mazumdar D, Kim HK, Lee JH, Odintsov B, Lu Y. Smart "turn-on" magnetic resonance contrast agents based on aptamer-functionalized superparamagnetic iron oxide nanoparticles. *Chembiochem.* 2007 Sep 24;8(14):1675-8.
199. Hwang do W, Ko HY, Lee JH, Kang H, Ryu SH, Song IC, et al. A nucleolin-targeted multimodal nanoparticle imaging probe for tracking cancer cells using an aptamer. *J Nucl Med.* 2010 Jan;51(1):98-105.
200. Bruno JG. Aptamer-biotin-streptavidin-C1q complexes can trigger the classical complement pathway to kill cancer cells. *In Vitro Cell Dev Biol Anim.* 2009 Nov 14.
201. Chu TC, Marks JW,3rd, Lavery LA, Faulkner S, Rosenblum MG, Ellington AD, et al. Aptamer:Toxin conjugates that specifically target prostate tumor cells. *Cancer Res.* 2006 Jun 15;66(12):5989-92.
202. Cao Z, Tong R, Mishra A, Xu W, Wong GC, Cheng J, et al. Reversible cell-specific drug delivery with aptamer-functionalized liposomes. *Angew Chem Int Ed Engl.* 2009;48(35):6494-8.
203. Farokhzad OC, Jon S, Khademhosseini A, Tran TN, Lavan DA, Langer R. Nanoparticle-aptamer bioconjugates: A new approach for targeting prostate cancer cells. *Cancer Res.* 2004 Nov 1;64(21):7668-72.
204. Farokhzad OC, Cheng J, Teply BA, Sherifi I, Jon S, Kantoff PW, et al. Targeted nanoparticle-aptamer bioconjugates for cancer chemotherapy in vivo. *Proc Natl Acad Sci U S A.* 2006 Apr 18;103(16):6315-20.
205. Bagalkot V, Zhang L, Levy-Nissenbaum E, Jon S, Kantoff PW, Langer R, et al. Quantum dot-aptamer conjugates for synchronous cancer imaging, therapy, and sensing of drug delivery based on bi-fluorescence resonance energy transfer. *Nano Lett.* 2007 Oct;7(10):3065-70.

206. Dhar S, Gu FX, Langer R, Farokhzad OC, Lippard SJ. Targeted delivery of cisplatin to prostate cancer cells by aptamer functionalized pt(IV) prodrug-PLGA-PEG nanoparticles. *Proc Natl Acad Sci U S A*. 2008 Nov 11;105(45):17356-61.
207. Hicke BJ, Stephens AW, Gould T, Chang YF, Lynott CK, Heil J, et al. Tumor targeting by an aptamer. *J Nucl Med*. 2006 Apr;47(4):668-78.
208. McNamara JO, 2nd, Andrechek ER, Wang Y, Viles KD, Rempel RE, Gilboa E, et al. Cell type-specific delivery of siRNAs with aptamer-siRNA chimeras. *Nat Biotechnol*. 2006 Aug;24(8):1005-15.
209. Dassie JP, Liu XY, Thomas GS, Whitaker RM, Thiel KW, Stockdale KR, et al. Systemic administration of optimized aptamer-siRNA chimeras promotes regression of PSMA-expressing tumors. *Nat Biotechnol*. 2009 Sep;27(9):839-49.
210. Chu TC, Twu KY, Ellington AD, Levy M. Aptamer mediated siRNA delivery. *Nucleic Acids Res*. 2006 Jun 1;34(10):e73.
211. Wu Y, Sefah K, Liu H, Wang R, Tan W. DNA aptamer-micelle as an efficient detection/delivery vehicle toward cancer cells. *Proc Natl Acad Sci U S A*. 2010 Jan 5;107(1):5-10.
212. Vlamincx BJ, Mascini EM, Schellekens J, Schouls LM, Paauw A, Fluit AC, et al. Site-specific manifestations of invasive group a streptococcal disease: Type distribution and corresponding patterns of virulence determinants. *J Clin Microbiol*. 2003 Nov;41(11):4941-9.
213. Sharkawy A, Low DE, Saginur R, Gregson D, Schwartz B, Jessamine P, et al. Severe group a streptococcal soft-tissue infections in ontario: 1992-1996. *Clin Infect Dis*. 2002 Feb 15;34(4):454-60.
214. Beall B, Facklam R, Thompson T. Sequencing emm-specific PCR products for routine and accurate typing of group A streptococci. *J Clin Microbiol*. 1996 Apr;34(4):953-8.
215. Kruger K, Grabowski PJ, Zaug AJ, Sands J, Gottschling DE, Cech TR. Self-splicing RNA: Autoexcision and autocyclization of the ribosomal RNA intervening sequence of tetrahymena. *Cell*. 1982 Nov;31(1):147-57.
216. Blank M, Weinschenk T, Priemer M, Schluesener H. Systematic evolution of a DNA aptamer binding to rat brain tumor microvessels. selective targeting of endothelial regulatory protein pigpen. *J Biol Chem*. 2001 May 11;276(19):16464-8.
217. Guo KT, SchAfer R, Paul A, Gerber A, Ziemer G, Wendel HP. A new technique for the isolation and surface immobilization of mesenchymal stem cells

from whole bone marrow using high-specific DNA aptamers. *Stem Cells*. 2006 Oct;24(10):2220-31.

218. Ostatna V, Vaisocherova H, Homola J, Hianik T. Effect of the immobilisation of DNA aptamers on the detection of thrombin by means of surface plasmon resonance. *Anal Bioanal Chem*. 2008 Jul;391(5):1861-9.

Chapter 2*

Bacterial Cell-SELEX Proof-of-Principle

2.1 Introduction

Our technique for the selection of aptamers against live bacterial cells involves five main steps (**Figure 2.1**): (1) incubating DNA library with live bacterial cells, (2) separating the bound from the unbound DNA sequences via centrifugation (and washing the cells), (3) releasing the bound DNA from the cell surface, (4) amplifying the incubation supernatant, wash fractions, and bound DNA sequences, (5) characterizing the selected (bound) DNA for binding affinity and selectivity after each SELEX round, prior to cloning and sequencing at the end of all SELEX rounds (once sufficiently high affinity and selectivity is obtained). *Lactobacillus acidophilus* 4356 was chosen as a non-pathogenic target to demonstrate proof-of-principle. It is gram positive and hence lacks a negatively charged outer membrane to repel DNA. This species is an ideal target due to the high abundance of well-characterized molecules on its surface available for binding to DNA in the library.

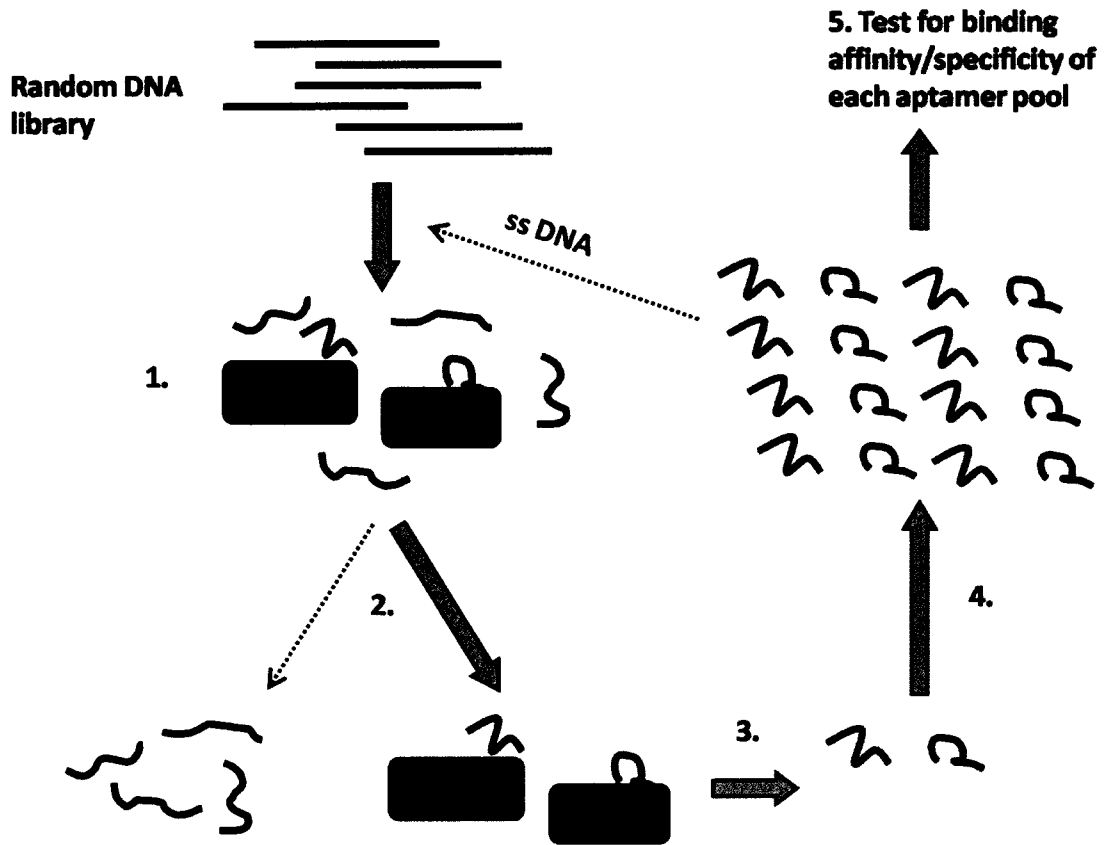


Figure 2.1. Schematic showing the main steps for the selection of aptamers against live bacterial cells. Step 1: Incubate a ssDNA library of 10^{15} random sequences with live bacterial cells. Step 2: Separate the DNA sequences bound to the cells from the unbound DNA sequences by centrifugation. Wash the cells three times to remove the weakly bound DNA sequences. Step 3: Release the bound DNA from the cell surface by heating and elution. Step 4: Amplify the DNA sequences eluted from the cells. Use this pool of DNA for the next round of selection starting from Step 1. Step 5: Test the binding of selected pool of DNA for the target cells prior to cloning and sequencing the selected DNA aptamers.

2.2 Experimental

2.2.1 Reagents

Bacterial strains and culture media. The *Lactobacillus acidophilus* strains ATCC 4355, 4356, and 4357, as well as *Streptococcus bovis*, *Escherichia coli*, and *Saccharomyces cerevisiae*, were obtained from the American Type Culture Collection (ATCC). All *L. acidophilus* strains were grown in MRS medium (BD Difco, Sparks, MD) under anaerobic conditions at 37 °C. *E. coli* and *S. bovis* were grown under aerobic conditions at 37 °C in Luria-Bertani (LB) and BBL Brain Heart Infusion (BHI) media, respectively (BD Difco). *S. cerevisiae* was grown aerobically at 30 °C in Yeast Peptone Dextrose (YPED) medium (BD Difco). All bacteria were harvested in their logarithmic phase of growth. *E. coli* DH5 α -T1^R cells (Invitrogen, Carlsbad, CA) were used for all transformations.

DNA library. An 80-nt oligonucleotide single-stranded DNA library consisting of a 40-nt randomized region flanked on both sides by 20-nt primer regions was used. The initial ssDNA library and the primers used to amplify it were obtained from Integrated DNA Technologies (Coralville, IA). DNA library or aptamer pools were rendered single-stranded in one of two ways: (i) via heat denaturation at 94 °C for 5 min and subsequent cooling at 0 °C for 10 min, or (ii) via purification of the forward strand using streptavidin-coated magnetic beads (Dynabeads; Invitrogen) and a biotinylated reverse primer.

2.2.2 PCR amplification and gel electrophoresis

The primers used to amplify the ssDNA library and subsequent aptamer pools have the following sequences:

Forward: 5'-AGCAGCACAGAGGTCAGATG-3'

Reverse: 5'-TTCACGGTAGCACGCATAGG-3'

The PCR conditions for amplification of the DNA library and subsequent aptamer pools during SELEX were 1X PCR reaction buffer, 2 mM MgCl₂, 0.4 μM of each primer, 0.2 mM dNTPs, 1 E.U. of Platinum Taq DNA Polymerase, and either 10 ng of DNA library or 39.5 μL of fraction supernatant (all reagents were obtained from Invitrogen). Thermocycling parameters were 94 °C for 5 min denaturation, followed by 20 cycles of denaturation at 94 °C for 30 s, annealing at 57 °C for 30 s, and extension at 72 °C for 20 s. A final extension step of 72 °C for 5 min was carried out following the last cycle (MJ Mini Gradient Thermocycler; Bio-Rad Laboratories, Hercules, CA). In order to amplify aptamer pools for binding assays, 1 μL of DMSO was added to the 50 μL reaction, and the annealing temperature was raised to 69 °C while all other conditions and reagents were kept the same. This change was to minimize the formation of misamplification products due to the increasing GC content of the evolving aptamer pools. After PCR, the reaction products were separated on 7.5% non-denaturing polyacrylamide gel electrophoresis (PAGE) in 1X TBE buffer (Bio-Rad Protean III) at 60-120 V. The gels were stained with ethidium bromide, and photographed under UV light. All PCR products were purified using Qiagen MinElute PCR Purification Kit (Qiagen, Valencia, CA).

2.2.3 Aptamer selection

L. acidophilus 4356 cells were grown overnight in liquid culture, and a sub-culture was grown the next morning until an OD₆₀₀ of 0.3 was obtained. Cells were pelleted at 5000x g and 4 °C, and then washed twice in 1X Binding Buffer (1X BB) (50 mM Tris-HCl (pH 7.4), 5 mM KCl, 100 mM NaCl, 1 mM MgCl₂) at room temperature. A total of 10⁸ cells were then incubated in binding buffer (600 μL for the initial round, 350 μL for subsequent rounds) for 45 min at room temperature with the ssDNA library (2 nmole initial round) or aptamer pool (100 pmole for subsequent rounds). An excess of tRNA and BSA (Invitrogen) were added to the incubation buffer (10-fold molar excess of each in the initial round, up to an 80-fold molar excess in the eighth round). Following incubation, the cells were centrifuged at 5000x g and 4 °C for 5 min, the supernatants were removed, and the cells were washed twice in 250 μL of 1x BB with 0.05% BSA (via resuspension and centrifugation) before a final resuspension in 100 μL of 1X PCR Reaction Buffer (Invitrogen). The cells were heated at 94 °C for 10 min and placed on ice for 10 min, in order to denature and elute cell-bound aptamers. The mixture was then centrifuged as described above and the supernatant isolated and designated as the cell-bound aptamer, or CA, fraction. All fractions collected were amplified by PCR and the PCR products of the CA fraction were used in the next round of selection. In between each incubation, washing, and elution steps, the re-suspended cell solution was transferred to a fresh microcentrifuge tube in order to eliminate aptamers bound to the tube wall. A total of 8 rounds of selection were performed using fresh aliquots of cells for each round. Negative controls

consisting of cells incubated with all medium components but without the oligonucleotide libraries were prepared for each round of selection.

2.2.4 Flow cytometric analysis

A FACScan flow cytometer with PowerMac G4 workstation and CellQuest software (Flow Cytometry Facility, Faculty of Medicine and Dentistry, University of Alberta) was used to assess the binding of the aptamer pool and individual aptamer sequences to different types of cells (*L. acidophilus* 4355, 4356, 4357, *E. coli* K12, *S. bovis*, *S. cerevisiae*). The aptamer pools were fluorescently labeled via PCR amplification with 5'-FAM modified primers (IDT), whereas the selected final individual aptamers were purchased with the fluorescent label (5'-FAM) attached (IDT). Aptamer pools were either heat denatured or rendered single-stranded via streptavidin-coated magnetic bead purification prior to incubation with target cells. The binding assays were carried out by incubating 100 pmole of fluorescently-labeled aptamer/aptamer pool with 10^7 cells for 45 min in binding buffer, and then washing the cells once in 1X BB with 0.05% BSA prior to resuspension in 1X BB for immediate flow cytometric analysis. Forward scatter, side scatter, and fluorescence intensity (FL1-H) were measured, and gated fluorescence intensity above background (cells with no aptamers added) was quantified.

2.2.5 Slide-binding assays and electron microscopy

Streptavidin-coated microscope slides (Xenopore Corp., Hawthorne, NJ) were incubated with denatured biotinylated aptamer pools. A 3 $\mu\text{g/mL}$ biotinylated aptamer pool solution in 1X SSC buffer was denatured at 94 °C for

10 min before being applied onto a 2-cm² surface area of each slide, saturating the streptavidin sites on the slide (maximum binding is 5 pmole biotin binding sites/cm² of slide). Slides were then incubated for 10 min at 37 °C and high humidity, and then left to air dry at room temperature. These slides, having aptamers immobilized on the surface, were stored at 4 °C when not in use. A negative control slide incubated with buffer alone was also prepared for each experiment.

To test the binding of cells to the immobilized aptamers on the slides, approximately 10⁶ *L. acidophilus* 4356 cells were suspended in 300 µL 1XBB and incubated over the 2 cm² surface area for 45 min at room temperature. The slides were each then washed 6 times in 1X BB, prior to fixation with 75% methanol and staining with crystal violet and Gram's iodine (Fisher Scientific Gram stain kit, Fair Lawn, NJ). Slides were then visualized at room temperature under 1000X magnification on a light microscope (Leica DMRXA Upright Microscope with Optronics MacroFire Digital Camera, Advanced Microscopy Facility, Department of Biological Sciences, University of Alberta). For each slide, a photograph was taken of 5 random fields of view, and the number of cells in 5 random fields was counted. The aptamer pools from each round of SELEX were tested using the same approach on duplicate slides and with the same number of cells. The total number of cells in each field was counted and totals from the 10 random fields were obtained for each aptamer pool.

Scanning electron microscopy (SEM) was used to confirm that the *L. acidophilus* 4356 cells had bound to the aptamer-immobilized slides

(Advanced Microscopy Facility, Biological Sciences, University of Alberta). The cells were prepared for SEM via fixation with a fresh mixture of one part 3% glutaraldehyde in 0.1 M phosphate buffer and two parts 2% (w/v) aqueous osmium tetroxide. The cells were then washed in 0.1 M phosphate buffer, desiccated, dehydrated with ethanol, and then treated with increasing amounts of HMDS (25–100%) prior to drying on a polycarbonate filter and gold-coating. The gold-coated samples were visualized the next day and photographed at 25000X on a Phillips XL SEM (Advanced Microscopy Facility, Biological Sciences, University of Alberta).

2.2.6 Flow injection coupled with fluorescence detection

To further confirm the specific binding of aptamers to their targets, the fluorescently-labeled aptamer (hemag1) was incubated with *L. acidophilus* 4356 cells in 1X BB, and the fluorescence was measured before and after the incubation and removal of the cells. From 10^5 to 10^9 cells were incubated with 0.25 or 0.5 pmole (0.5 or 1.0 nM) of aptamer for 45 min in 1X BB. Incubation times ranging from 10 to 120 min were also varied, using 5 pmole of aptamer. The mixture was then either centrifuged at 5000x g or filtered through a 0.22 μ m membrane to remove the cells. A 50 μ L aliquot of the supernatant or filtrate was injected into an Agilent 1100 HPLC system coupled to an Agilent 1100 series fluorescence detector to measure the remaining fluorescent aptamer. Fluorescence was detected at 520 nm with excitation at 495 nm. Peak areas were integrated and the concentrations of the remaining aptamers in the solution were measured against a standard calibration of 0 to 1 nM fluorescently-labeled aptamer. The

decrease of aptamer in the solution after incubation with the cells was a measure of the bound aptamer to the cells (which were removed by centrifugation or filtration). Negative control incubations of 10^5 to 10^9 cells in the absence of DNA were carried out, the cells were removed, and the fluorescence intensities of the negative control incubation supernatants were subtracted from the incubation supernatants containing fluorescently-labeled aptamers.

2.2.7 Cloning, sequencing, and structural analysis of aptamers

The highest affinity aptamer pools were chosen for sequencing analysis. Aptamer pools were cloned using a TOPO TA Cloning Kit for Sequencing (Invitrogen), transformed into *E. coli* DH5 α -T1^R cells (Invitrogen), and colonies containing the vector were selected via overnight incubation at 37 °C on LB plates containing 50 μ g/mL kanamycin. From each aptamer pool, 25 colonies were chosen for screening. The plasmid DNA was purified (Qiaex II gel extraction kit; Qiagen, Mississauga, ON) and analyzed for the presence of an 80 bp insert via digestion with 1 U of EcoR1 at 37 °C for 30 minutes, followed by 7.5% native PAGE. A total of 30 inserts were then sequenced (Molecular Biology Services Unit, Department of Biological Sciences, University of Alberta), yielding a total of 27 usable sequences. The secondary structure of each sequence was predicted using Oligoanalyzer 3.0 (IDT), with input conditions of room temperature (21 °C) and 1 mM MgCl₂.

2.3 Results

2.3.1 Selection of DNA aptamers against live *Lactobacillus acidophilus*

Two sets of SELEX, of 8 rounds each, were performed. Prior to incubation with the target cells, the double-stranded DNA aptamer pool was rendered single-stranded via either (i) heat denaturation in the first set of SELEX or (ii) streptavidin-bead purification in the second set of SELEX. Following the incubation of ssDNA library with the *L. acidophilus* cells, most of the DNA library/aptamer pool remained unbound in the supernatant as illustrated by the large number of PCR amplification products around 70–100 bp (**Figure 2.2, lane 4**). Only a small amount of DNA was present in the first 2 washes of the centrifuged cells (**lanes 6 and 9**). No DNA was amplified from the third wash fraction from any of the SELEX rounds. The amplification products of the heat-eluted cell aptamer (CA) fraction (**lane 13**) represented the DNA sequences strongly bound to the cells. No DNA was amplified from the wash or CA fractions of the negative control, which consisted of cells treated to the incubation, wash and heat elution procedures without the addition of library or aptamer pool DNA. The observation of a single 80-bp band on the gel after each round of selection and PCR amplification of the CA fraction suggested that the cells bound to a pool of aptamer sequences. The PCR products of the CA fraction were used in the next round of selection following purification. Gel photos from the remaining SELEX rounds can be found in the Appendix (**Figures A1-A9**).

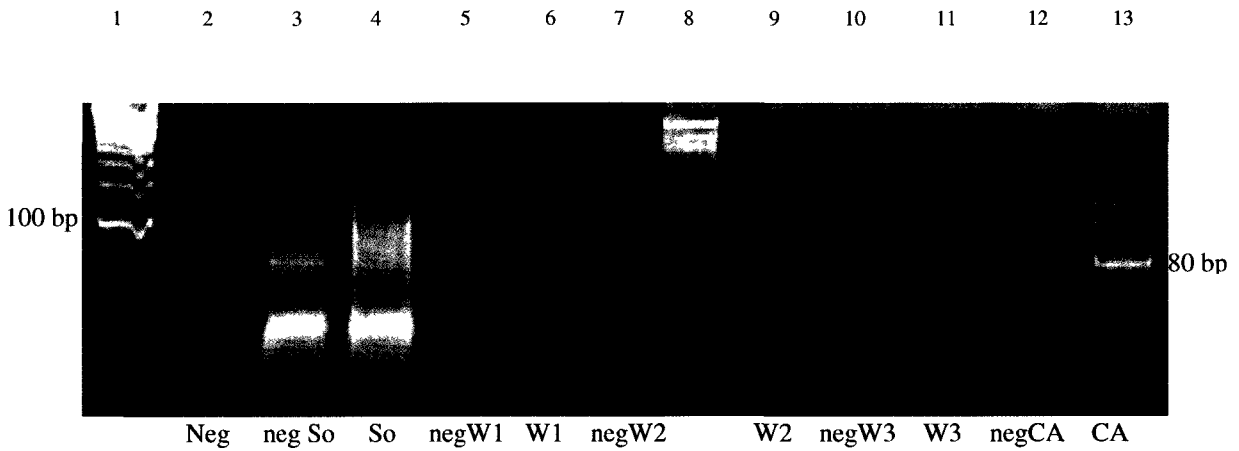


Figure 2.2. Native PAGE of PCR-amplified oligonucleotide fractions after the first round of SELEX using heat denaturation. A randomized, single-stranded DNA library was incubated with *L. acidophilus* cells in the presence of tRNA and BSA. Following incubation, the cells were centrifuged to remove the incubation supernatant (So) and repeatedly washed and centrifuged in binding buffer to remove DNA sequences that are non-specifically or weakly bound (W1, W2, W3). The cells were next heated at 94 °C, the suspension was centrifuged, and the supernatant was collected containing the heat-eluted cell aptamer fraction (CA). A SELEX negative control was carried out in which cells were incubated in the absence of DNA library (negSo), washed (negW1, negW2, negW3), and heat-eluted (negCA). The different fractions collected during SELEX (So, W1-W3, CA) and the parallel negative control were PCR amplified and analysed via PAGE. Lanes 1 and 8 on the gel contain the DNA ladder (100–2072 bp) and lane 2 contains the PCR negative control.

2.3.2 Binding Affinity and Selectivity of Aptamer Pools Following Each

Round of Selection

After each round of selection, the aptamer pools were assessed for binding affinity and selectivity to the target *L. acidophilus* 4356 cells using both flow cytometry (Figure 2.3) and microscopy.

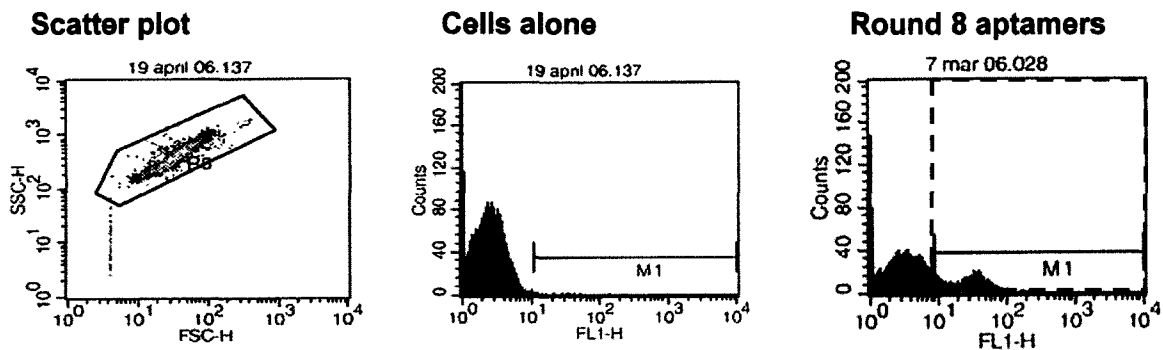


Figure 2.3. Typical flow cytometry outputs from screening of aptamer pools following each round of selection, showing increase in gated fluorescence intensity above background (dashed boxed area) following incubation with round 8 aptamer pool.

Flow cytometric analyses of incubation mixtures containing fluorescently-labeled aptamer pools and the target cells show that with increasing rounds of selection, the percent of cells with gated fluorescence above background increased to a maximum average of 67% at round 7 for the heat denatured aptamer pools and 49% at round 6 for the streptavidin-purified aptamer pools (Figure 2.4). This increase in the number of fluorescent cells is due to the increased binding of the fluorescent aptamers to the target cells. It thus appears that during SELEX, DNA rendered single-stranded via heat denaturation results

in the generation of aptamers that bind more efficiently to the target cells than DNA rendered single-stranded via streptavidin-coated magnetic bead purification. This may be due to the fact that in the streptavidin-purified pools, only the forward strand of the DNA is retained for incubation whereas in the heat denatured pools both forward and reverse strands are retained, effectively doubling the number of sequences available for selection. It is also possible that the streptavidin-coated magnetic bead purification procedure resulted in preferential retention of certain sequences and loss of others, or in non-specific loss of sequences due to the additional purification steps present when using magnetic beads versus heat. Increase in aptamer binding appears to level off after SELEX round 6 for both the heat-denatured and the streptavidin-purified aptamer pools (**Figure 2.4**). However, for the heat denatured pools, the 8th round of SELEX results in the loss of affinity aptamers for the bacterial cells. This de-selection may be due to a decrease in the aptamer pool complexity, inefficient partitioning of bound from unbound sequences during the 8th round selection process, or a combination of both. As a result, subsequent cloning of aptamer sequences was carried out from the round 7 heat-denatured aptamer pool and round 8 streptavidin-purified aptamer pools.

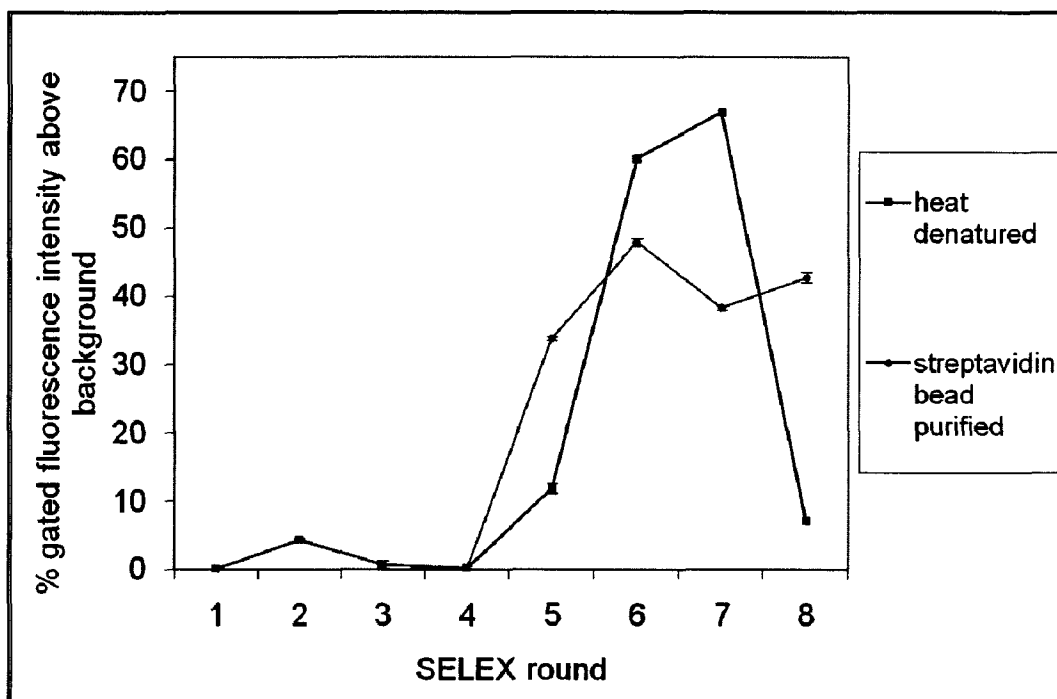


Figure 2.4. Increase in percent gated fluorescence intensity of *L. acidophilus* 4356 cells incubated with fluorescently-labeled aptamer pools after increasing SELEX rounds.

Controls carried out using fluorescent aptamer pools alone and buffer with BSA and tRNA alone did not yield any increase in gated fluorescence above background levels (data not shown). The absence of BSA and tRNA in the incubation buffer prior to flow cytometry analysis decreased both heat-denatured and streptavidin bead purified aptamer pool binding (**Figure 2.5**). This decrease in binding is most likely due to an increase in competition between DNA sequences for targets. Increasing the amount of time after incubation and washing at which the cell-aptamer solutions were analyzed via flow cytometry resulted in a maximum 9.7% decrease in maximum gated fluorescence above background. This decrease was constant up to 30 min post-incubation for the aptamer pool,

providing ample time for sample analysis without loss of aptamer pool binding or cell death (**Figure 2.6**).

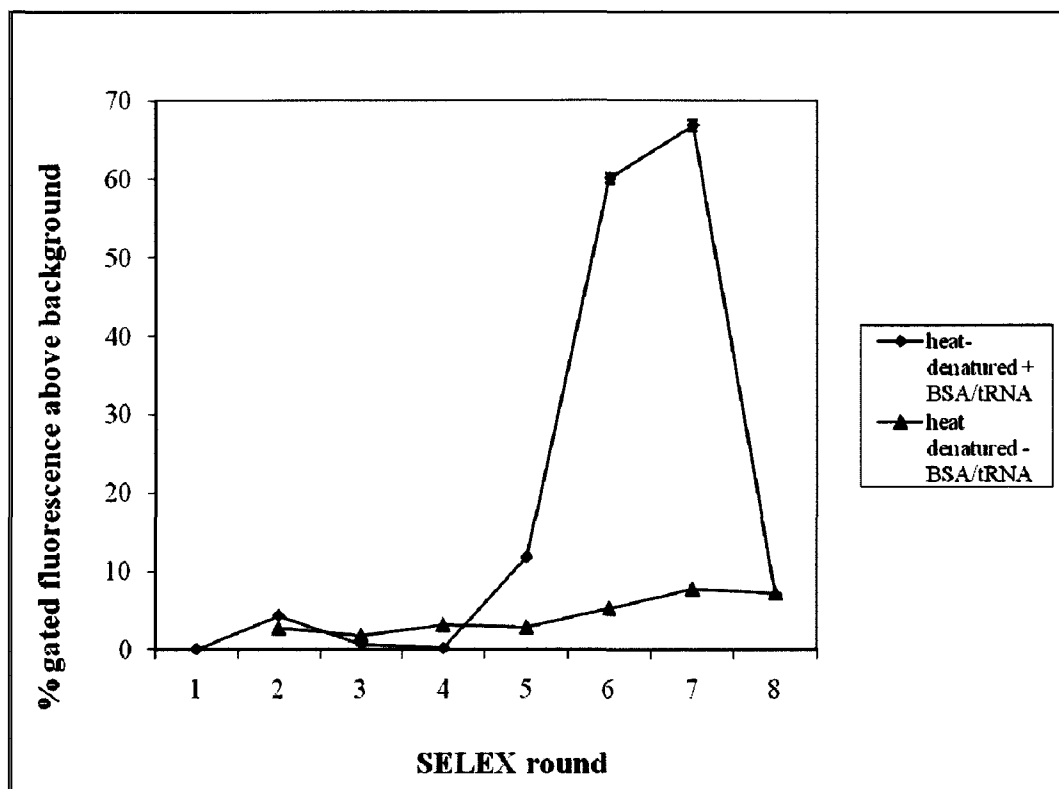


Figure 2.5. Change in heat-denatured aptamer pool binding to *L.acidophilus* 4356 cells, as indicated by percent gated fluorescence intensity above background, with removal of BSA and tRNA from incubation mixture.

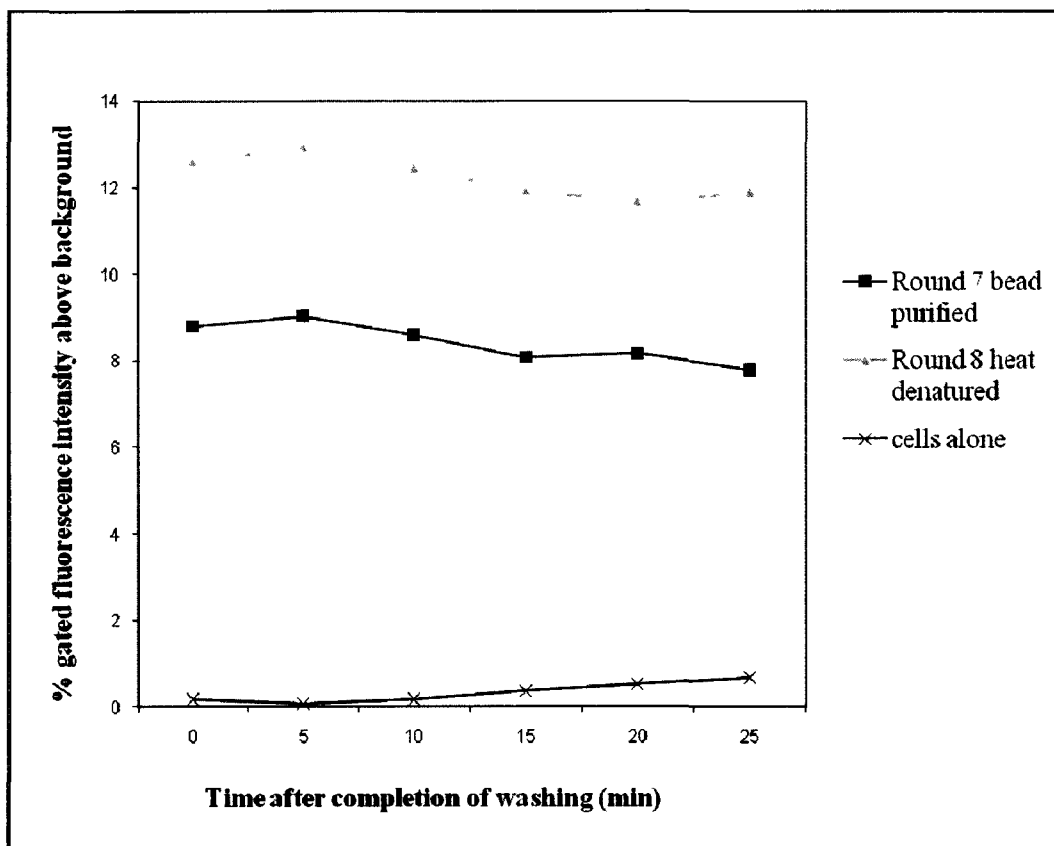


Figure 2.6. Change in aptamer pool binding with time after flow cytometry sample preparation.

Different bacterial species were used to test the selectivity of the aptamer pools. The increase in gated fluorescence intensity was less than 2% when the fluorescent aptamer pools were tested against *Streptococcus bovis*, *Escherichia coli* K12, and *Saccharomyces cerevisiae* (Figure 2.7). This indicates that the binding observed between the aptamers and *L. acidophilus* was target specific. Two additional strains of *L. acidophilus* were also tested, ATCC 4355 and 4357, which are rat and human isolates respectively (4356 is a human isolate). Minimal binding of the aptamer pool to the rat isolate strain 4355 was seen, but the aptamer pool bound strongly to the 4357 cells. Both strains 4356 and 4357 are

human isolates, are known to be highly genetically related, and they are covered in an S-layer comprised of similar S-proteins (1, 2). It is possible that the S-proteins on the cell surface are a molecular target of the selected aptamers.

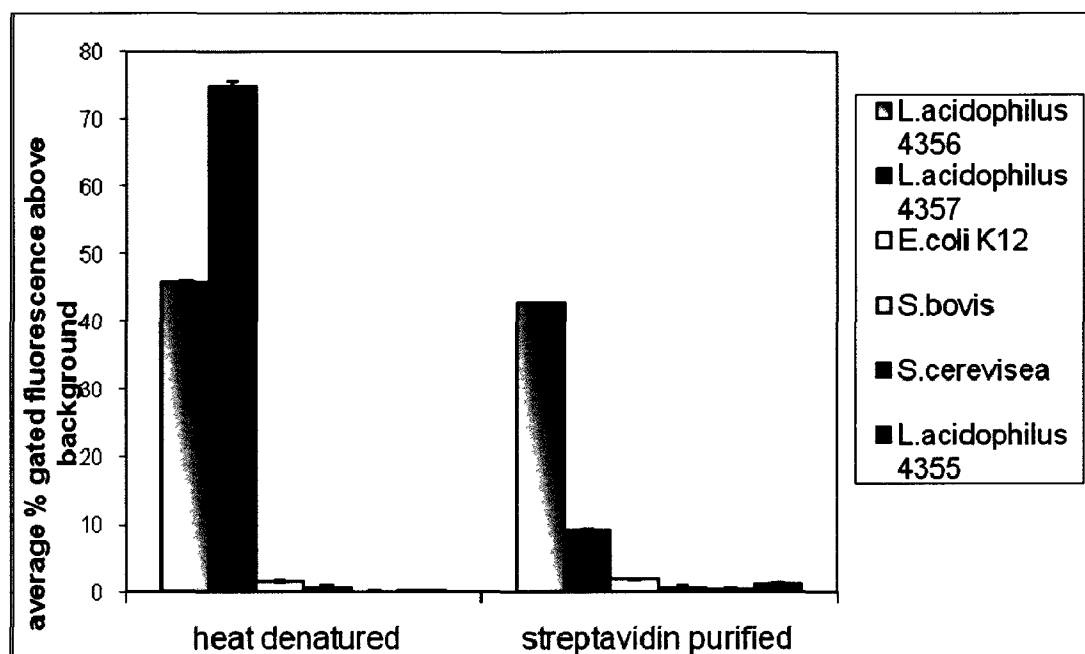


Figure 2.7. Binding of the highest binding aptamer pools to different types of cells.

To further confirm binding of the aptamer pool to the target cells, we developed a novel slide-binding assay using streptavidin-coated microscope slides and biotinylated aptamer pools. This idea is reminiscent of the previous work using aptamers to capture osteoblasts for the purpose of seeding bone growth after transplantation (69). *L. acidophilus* 4356 cells were incubated on the slides for 45 min, washed thoroughly, fixed with methanol, stained with crystal violet and viewed under a light microscope. Further scanning electron microscopy of the cells captured on the slides show their morphological similarity to those of the

Lactobacillus species (**Figure 2.8**). A series of photographs is shown in Figure 3 for slides coated with heat-denatured aptamer pools from SELEX rounds 1–8. As the round of SELEX after which the aptamer pool was isolated was increased, an increasing number of 4356 cells were found to bind to the slides for both heat denatured (**Figures 2.9, 2.10**) and streptavidin purified aptamer pools (**Figure 2.10**), indicative of increased binding affinity of the aptamers for the *L. acidophilus* cells. The ratio of cells bound/cm² to slides coated with heat-denatured round 7 aptamers versus uncoated slides is 61, and is 9 for round 7 heat-denatured aptamer pools versus round 1 heat-denatured aptamer pools. These results confirm those of flow cytometry, supporting the specific binding of the aptamer to the target cells. The key advantages of this slide-binding assay are that it allows visualization of bacterial cells, is rapid and inexpensive.

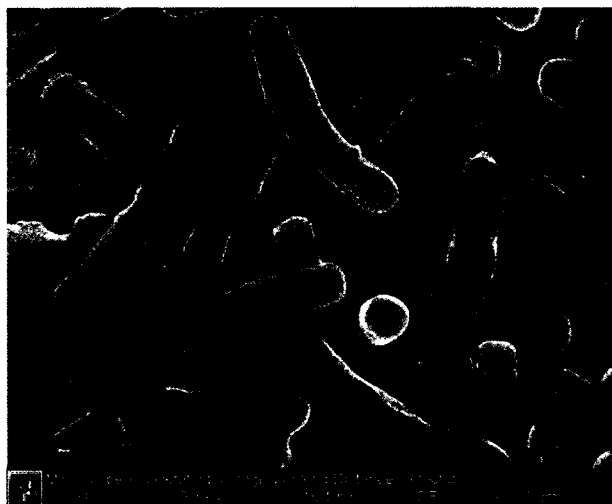


Figure 2.8. Scanning Electron Microscopy (SEM) close-up of *L. acidophilus* 4356 cells used for slide-binding assay.



Figure 2.9. Slide-binding assay showing binding of *L. acidophilus* 4356 cells to microscope slides coated with heat denatured aptamer pools after each round of SELEX (round number labeled on each picture). Aptamer pools obtained after each round of selection were biotinylated and attached to streptavidin-coated microscope slides. The slides were then incubated with *L. acidophilus* 4356 cells in binding buffer; cells were prepared via centrifugation at 5000xg and 4°C, washing twice in binding buffer. For each slide, approximately 10^6 cells were suspended in 300 μ L binding buffer and incubated over the 2 cm² surface area for 45 min at room temperature. The slides were each then washed 6 times in binding buffer, prior to fixation with 75% methanol and staining with crystal violet and Gram's iodine. Slides were then stored at room temperature until visualization under a light microscope at 1000X magnification. For each slide, the number of cells in 5 random fields was counted.

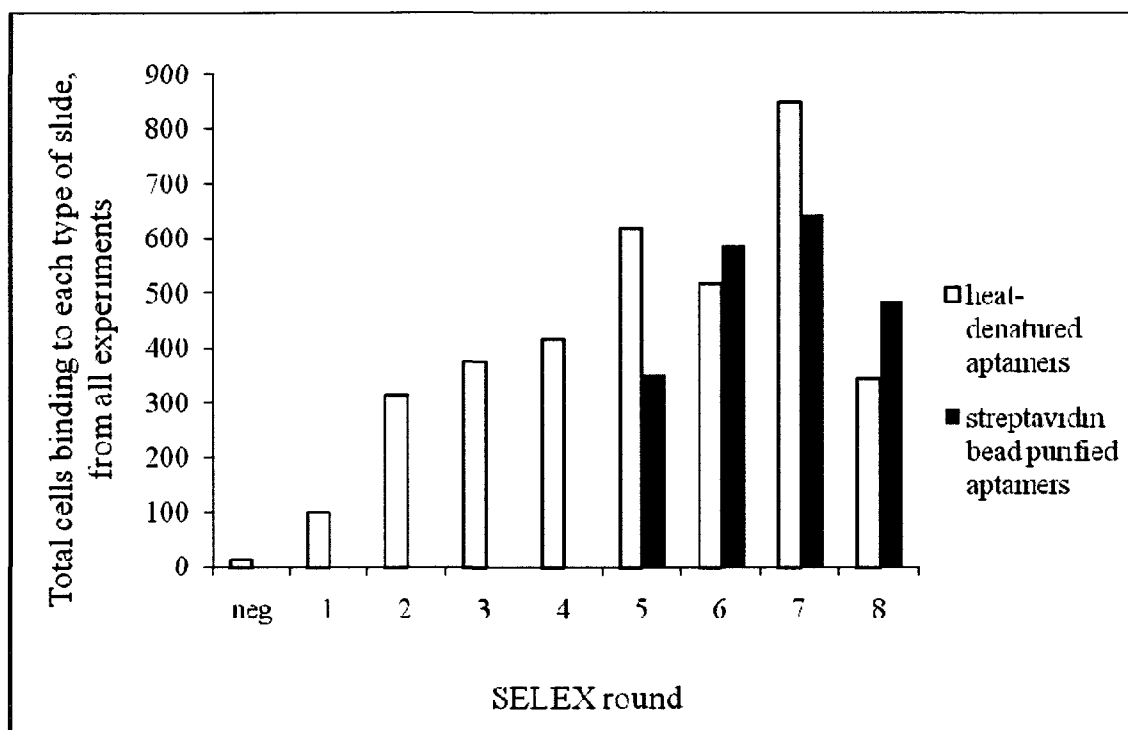


Figure 2.10. Total number of *L. acidophilus* 4356 cells binding to slides coated with aptamer pools. Each bar in the above graph represents totals from 10 separate microscope fields. The surface area of each field is 2 cm².

2.3.3 Cloning and sequence analysis of aptamer pools

Upon confirmation that aptamer pool binding was increasing with SELEX rounds, the heat-denatured (HE) and streptavidin-coated magnetic bead purified (MAG) aptamer pools were cloned and sequenced after the 7th and 8th rounds, respectively. These pools displayed the highest affinity for the target cells when screened via flow cytometry. A total of 27 sequences from both the streptavidin-magnetic bead purified and heat denatured aptamer pools were obtained (**Table 4**). Within this collection of sequences, there was one sequence that was repeated 6 times, 3 times in each pool. This sequence was named hemag1P. There were

several other sequences and sequence motifs that were repeated both within and between aptamer pools. Also, many of the sequences contained a high percentage of C and G bases, especially at their 5' and 3' ends, suggesting the presence of secondary structural motifs. All of the sequences obtained with and without primers are in Appendix **Table A1**.

2.3.4 Binding of individual aptamer sequences to target cells

Sequences representing a variety of secondary structures, as well as those sequences that were repeated within and between the aptamer pools, were selected for further screening. The sequences were screened both with and without primer sequences included, e.g., hemag1 and hemag1P. Each sequence was fluorescently labeled and tested via flow cytometry for binding to three separate strains of *L. acidophilus*: 4355, 4356, and 4357. Higher binding to the strains 4356 and 4357, rather than 4355, was seen with many of the sequences (**Figure 2.11**). This trend is similar to that seen with the aptamer pools (**Figure 2.7**). Binding of all the sequences was specific for *L. acidophilus* in that minimal or no binding was seen to *Escherichia coli*, *Streptococcus bovis*, or *Saccharomyces cerevisiae* (**Figure 2.11**). The most frequently repeated sequence with primers, hemag1P, exhibited by far the highest binding for both 4356 and 4357 cells. The secondary structure of each sequence, with and without primers, was predicted at room temperature and 1 mM MgCl₂ (**Figure 2.12**). The aptamer sequences can be classified into three broad categories of secondary structure: (i) tight hairpins, (ii) branched hairpins, and (iii) few or no hairpins.

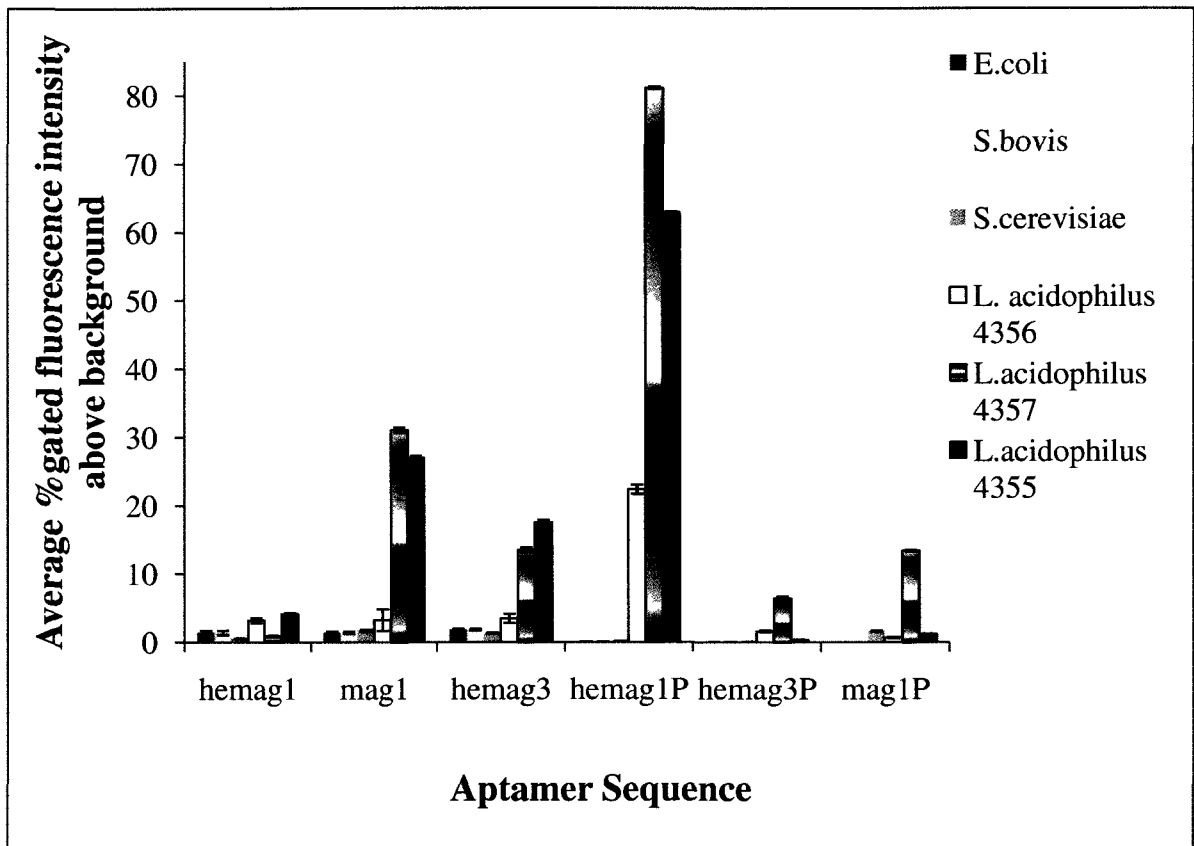


Figure 2.11. Sequences derived via cloning of aptamer pools that show increased binding affinity to *L. acidophilus* 4356, 4357, and 4355 cells and minimal binding to other cells when screened via flow cytometry. All aptamers were fluorescently-labeled with 5'-FAM. Incubations and centrifugation were carried out as in Figure 2. A ratio of 100 pmole of aptamer and 10^7 cells was used.

Table 4. Screened aptamer sequences with (hemag1P, mag2P, and hemag3P) and without (hemag 1, mag1, and hemag3) primers. Shown here are the aptamers of high affinity for *L. acidophilus* 4356 cells, selected from a total of 27 aptamers that were sequenced. The fluorescent label FAM is shown at the 5'-end. The underlined sequences are the primers.

Name	Sequence
hemag1	5'FAM/TAGCCCTTCAACATAGTAATATCTCTGCATTCTGTGATG-3'
mag1	5'FAM/TGAGCCCCACTAAAGTTGCAATCATGTCGTCAGCTTTGGG-3'
hemag3	5'FAM/CGTCGCGGC ATATTCCAGTGGAACGGTTACGATATGTTG-3'
hemag1P	5'FAM/ <u>AGCAGCACAGAGGTCAGATG</u> TAGCCCTTCAACATAGTAA TATCTCTGCATTCTGTGATG <u>CCTATGCGTGCTACCGTGAA</u> -3'
mag1P	5'FAM/ <u>AGCAGCACAGAGGTCAGATG</u> TGAGCCCCAGTAAAGTTGC AATCATGTCGTCAGCTTTGGG <u>CCTATGCGTGCTACCGTGAA</u> -3'
hemag3P	5'FAM/ <u>AGCAGCACAGAGGTCAGATG</u> TCGTCGCGGCATATTCCAG TGGAACGGTTACGATATGTTG <u>CCTATGCGTGCTACCGTGAA</u> -3'

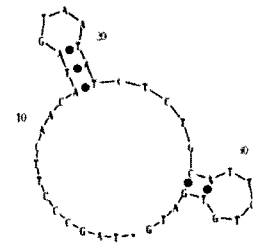
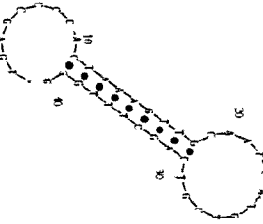
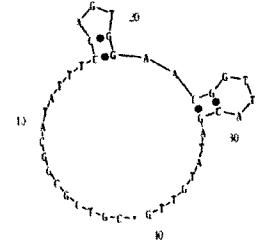
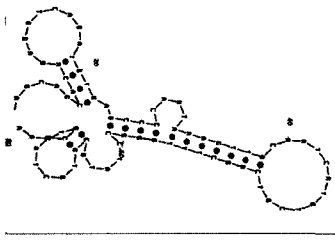
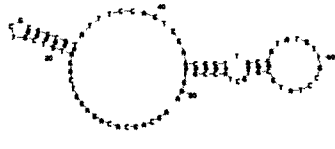
hemag1	
mag1	
hemag3	
mag1P	
hemag3P	

Figure 2.12. Most energetically favorable predicted secondary structures of some selected aptamer sequences.

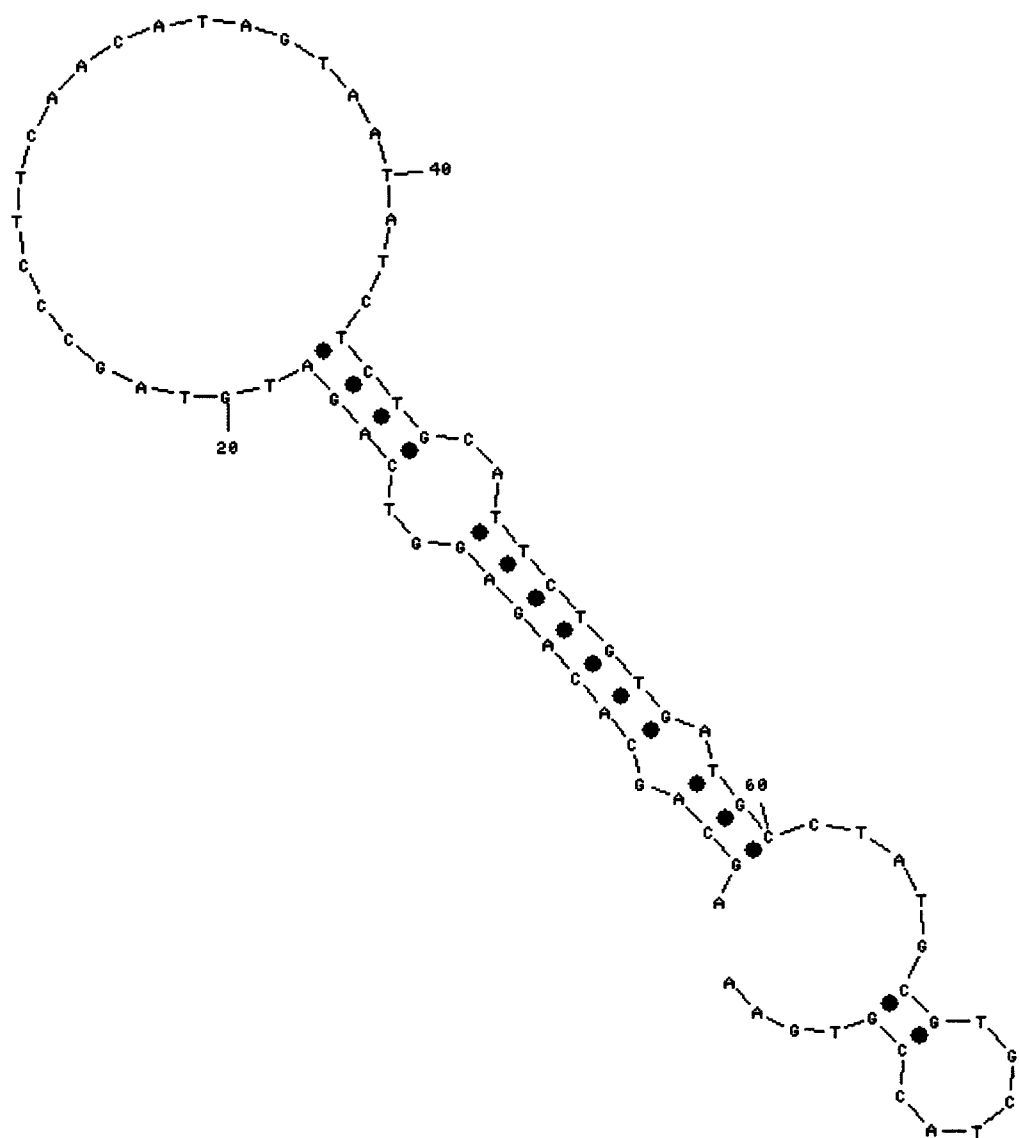


Figure 2.13. Predicted secondary structure of aptamer hemag1P. Structure was predicted at 21°C and 1 mM MgCl₂ using Oligoanalyzer 3.0 (IDT). Base-pairing interactions are represented by blue and red dots.

The most energetically favourable predicted secondary structure of aptamer hemag1P at room temperature and 1 mM MgCl₂ is shown in **Figure 2.13**. Inclusion of the primer sequences in hemag1P allows it to form a tight hairpin secondary structure whereas the shorter sequence hemag1 forms a more open structure (**Figures 2.12 and 2.13**). The hairpin secondary structure perhaps accounts for the superior binding of hemag1P to the target cells. Other sequences that demonstrated affinity for *L. acidophilus* also have predicted hairpin or branched structures (**Figure 2.12, Table 4**).

2.3.5 Binding of aptamer hemag1P to *L. acidophilus*

Binding of hemag1P to target 4356 cells was further examined via flow cytometry and flow injection coupled to fluorescence detection. The binding curve from flow cytometric analysis of fluorescently-labeled hemag1P and *L. acidophilus* 4356 cells (10⁷ cells) is shown in **Figure 2.14**. At first, aptamer concentrations in the incubation supernatant from 0 to 500 nM were tested, with the amount of aptamer binding found to level off at less than 100 nM (**Figure 2.15**). Subsequently, a lower concentration range (0–120 nM) was examined (**Figure 2.14**). The average gated fluorescence intensity above background was found to reach a maximum of 31.0% at a hemag1P concentration of 80 nM. Heating the single-stranded aptamers at 94 °C and then cooling at 0 °C prior to room temperature incubation had negligible effect on binding (**Figure 2.16**). The K_d of hemag1P was determined to be approximately 13 ± 3 nM based on the fit of the non-linear regression curve (GraphPad Prism 5).

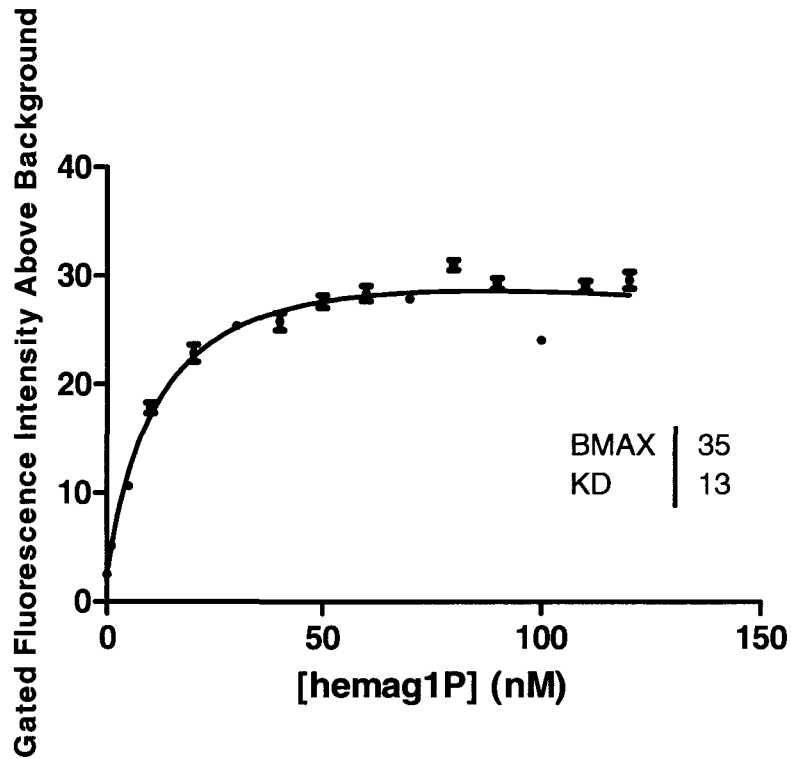


Figure 2.14. Binding characteristics of aptamer hemag1P as determined via flow cytometry. Various concentrations of aptamer hemag1P (x-axis) were incubated with 10^7 *L. acidophilus* 4356 cells in binding buffer for 45 min and analyzed via flow cytometry under the same conditions as in Figure 2. Error bars are standard error from 2 triplicate analyses.

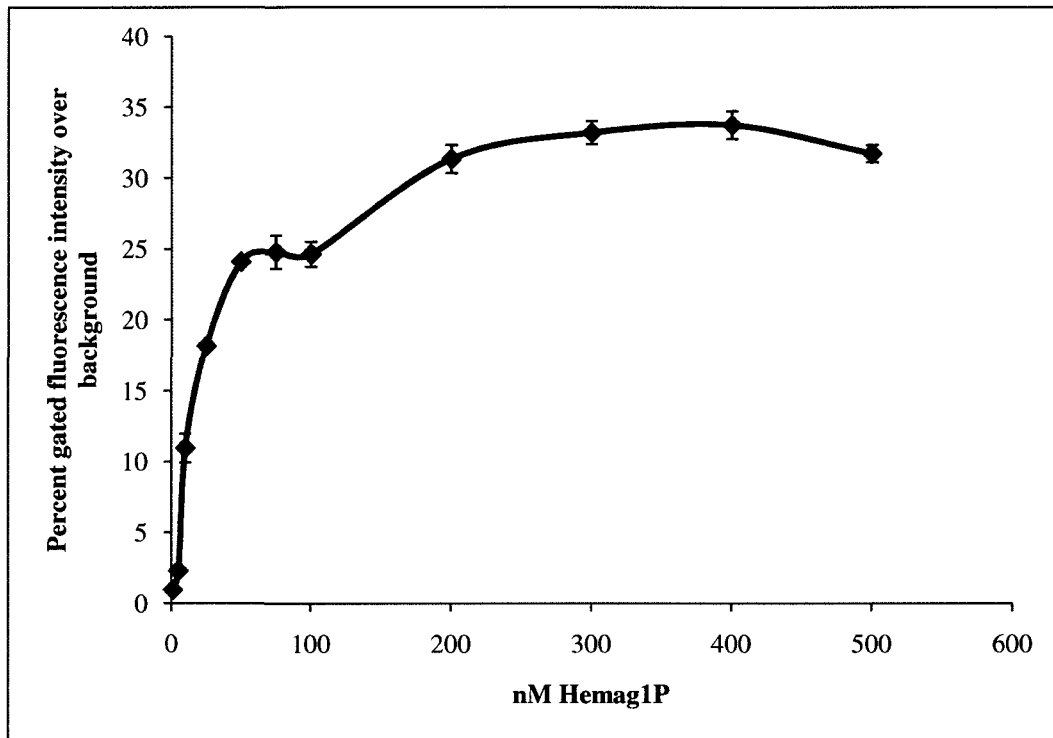


Figure 2.15. Binding characteristics of aptamer hemag1P as determined via flow cytometry. Various concentrations of aptamer hemag1P (x-axis) were incubated with 10^7 *L. acidophilus* 4356 cells in binding buffer for 45 min and analyzed via flow cytometry under the same conditions as in Figure 2. Error bars are standard error from 2 replicate analyses.

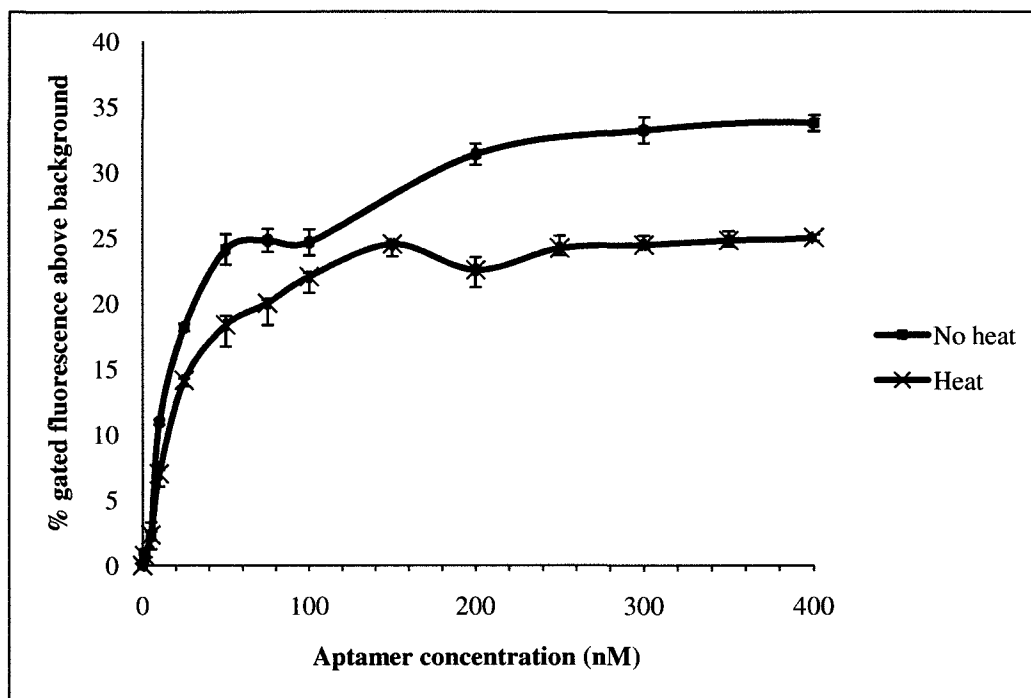
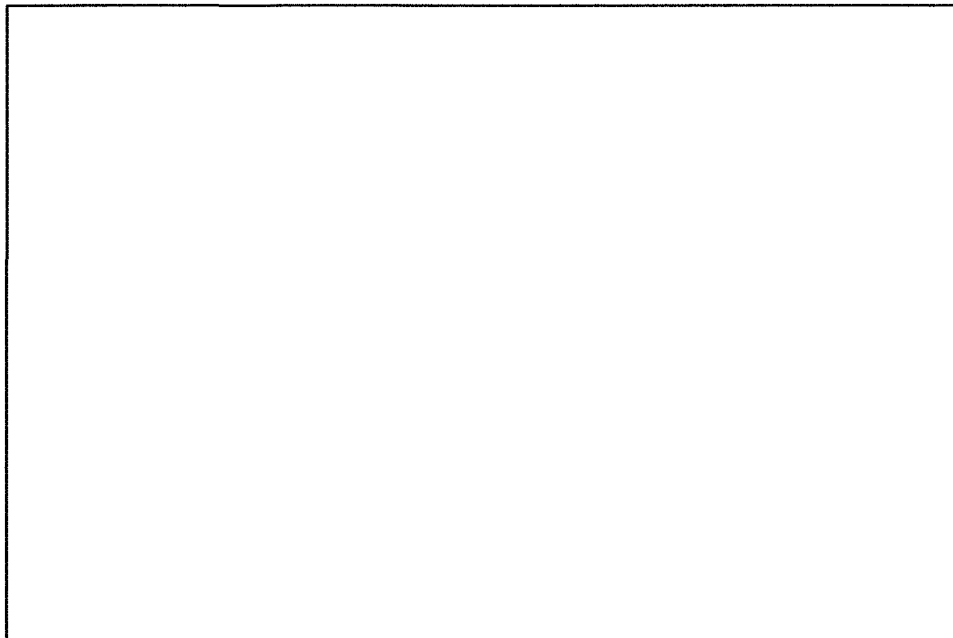


Figure 2.16. Binding characteristics of aptamer hemag1P with and without the inclusion of a pre-heating step. Pre-heating involved heating the aptamer at 94 °C for 10 minutes, then cooling at 0 °C for 10 minutes prior to incubation step. Flow cytometric analysis was carried out as in Figure 1.14 and Figure 1.15.

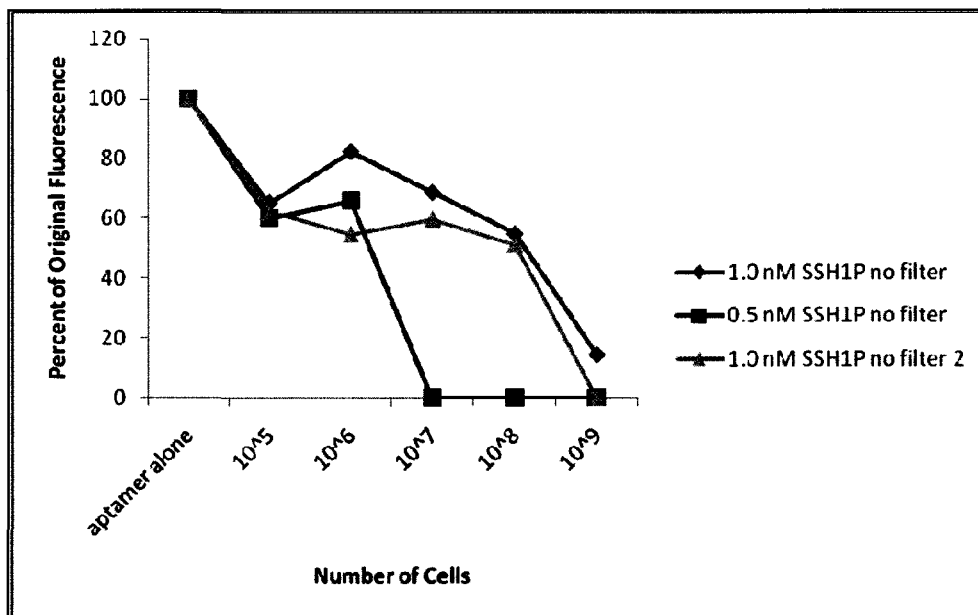
Analyses of fluorescent aptamers in supernatant before and after incubation with *L. acidophilus* 4356 indicate increased removal of hemag1P by increasing numbers of target cells (**Figure 2.17**). Separate experiments were carried out in which the supernatant was and was not passed through a 0.22 μM filter prior to analysis. The purpose of the filtration step was to remove any cells in the supernatant that may have dislodged from the pellet, and hence may interfere with the fluorescence measurement. The supernatants were then measured with a fluorescence detector, where the amount of fluorescence is proportional to the aptamer concentration of the sample. Increased aptamer

removal by the target cells is represented by a decrease in detectable supernatant fluorescence with increasing cell number, for both the filtered and unfiltered supernatants (**Figures 2.17a** and **2.17b**). An average of approximately 100% of 0.5 nM aptamer or 72% of the starting 1.0 nM aptamer was removed from the unfiltered supernatants by 10^9 cells. This corresponds to the binding of 150 ± 1 and 217 ± 22 aptamers/cell, respectively. Analysis of the filtered supernatant revealed that 84% of the 0.5 nM aptamer fluorescence was removed by 10^9 cells, corresponding to 126 ± 25 aptamer molecules/cell. These results complement the flow cytometry analysis, showing the binding of the fluorescently-labeled hemag1P aptamer to the *L. acidophilus* 4356 cells. These results also provide an estimate of the number of aptamer molecules binding to each cell (on average approximately 164 ± 47 aptamer molecules per cell). Aptamer removal by cells from aptamer pools was also found to increase with increasing SELEX round (**Figure 2.18**). This increase is indicative of increased aptamer binding affinity for the cells.

(a)



(b)



(c)

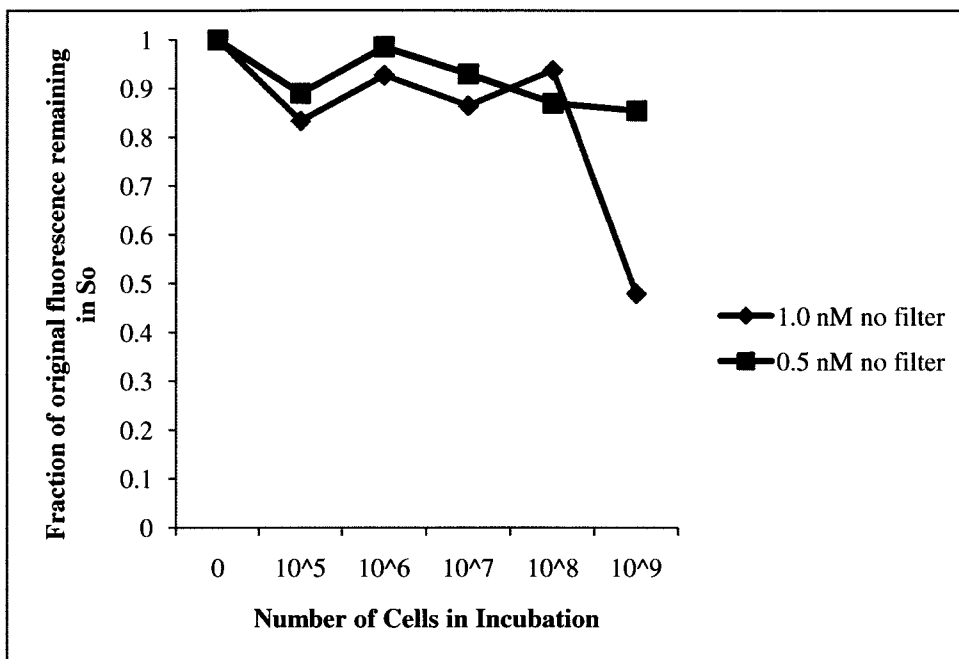


Figure 2.17. Binding characteristics of aptamer Hemag1P as determined via flow injection coupled to fluorescence detection both with (a) and without (b, c) filtration.

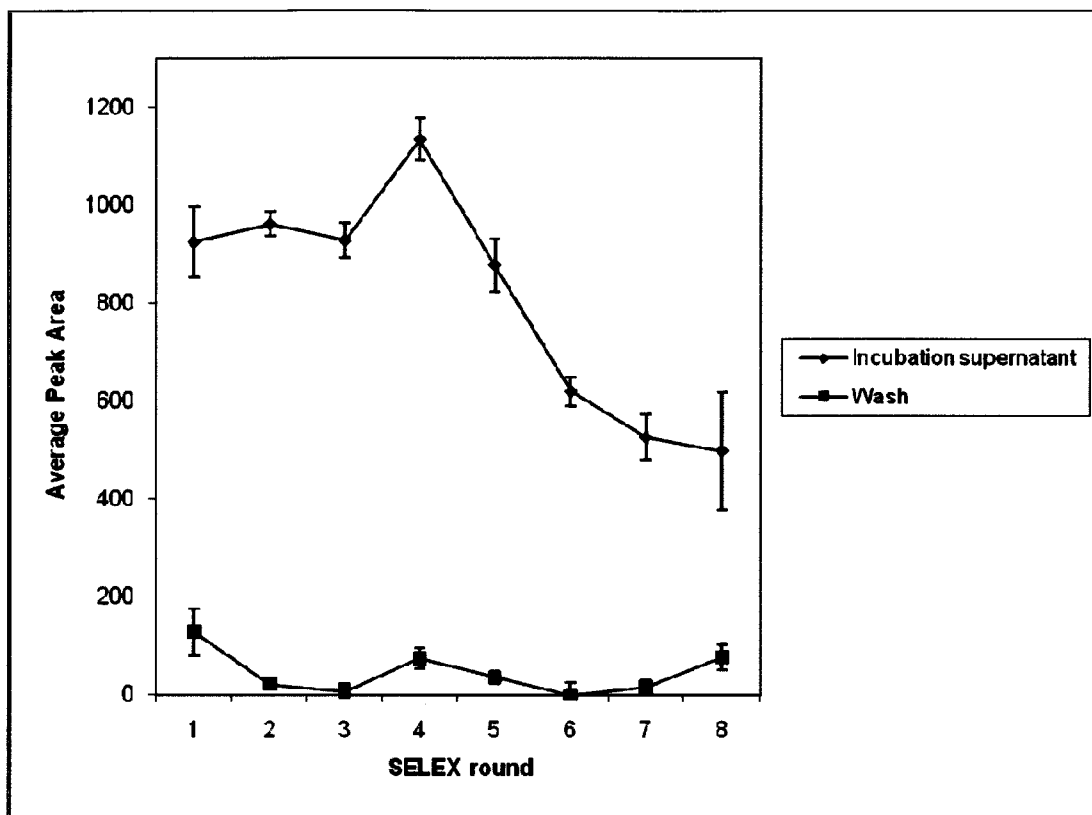


Figure 2.18. Flow injection with fluorescence detection analysis of aptamer removal from pools with increasing rounds of selection. A fixed number of cells (10^8) were incubated with 100 pmole of DNA from each aptamer pool from SELEX using heat denaturation. Aptamer pools were fluorescently labeled with 5'-FAM. Incubations were carried out as previously for SELEX and flow cytometry. The supernatant and first wash fractions were retained and analyzed.

2.4 References

1. Boot HJ, Kolen CP, Pouwels PH. Identification, cloning, and nucleotide sequence of a silent S-layer protein gene of *Lactobacillus acidophilus* ATCC 4356 which has extensive similarity with the S-layer protein gene of this species. *J Bacteriol.* 1995 Dec;177(24):7222-30.
2. Boot HJ, Pouwels PH. Expression, secretion and antigenic variation of bacterial S-layer proteins. *Mol Microbiol.* 1996 Sep;21(6):1117-23.

Chapter 3

Bacterial Cell-SELEX Against Group A Streptococcus

3.1 Introduction

Group A streptococcus (GAS) is implicated in a variety of diseases, including streptococcal pharyngitis, necrotizing fasciitis, scarlet fever, streptococcal toxic shock syndrome (STSS), invasive systemic infections, and endocarditis. Epidemiological surveillance of GAS clinical isolates is important for outbreak management as well as vaccine development and implementation. In addition, more reliable rapid identification of *S. pyogenes* in the clinic is needed. Current methodologies still require laboratory testing in the case of a negative result.

One of the major virulence factors of invasive GAS (iGAS) isolates is the M protein which is present on the surface of the bacteria. It is important to note that while the M protein is a critical virulence factor for GAS, this protein can also be utilized as a typing marker for understanding the epidemiology of iGAS disease. The M protein can be typed serologically or alternatively, GAS can be typed by sequencing of the gene that encodes the M protein, the *emm* gene. Currently, *emm* nomenclature extends from *emm1* to *emm124* with many *emm* types having minor variations in the nucleotide coding sequence resulting in *emm* subtypes for a particular *emm* type (1-4). Different M-types are often but not always associated with different invasive infections. For example, the M-types

M1 and M3 are more often associated with invasive infections than other M-types (5, 6). Conventionally, GAS is M-typed via precipitin or latex agglutination methods, which involve screening bacterial surface extracts against different M-protein specific reference polyclonal antisera or antibodies conjugated to latex beads (7). More recently, sequencing of the *emm* gene is replacing antibody-based typing methods as the gold standard (1) and has expanded the repertoire of GAS *emm* types worldwide. In addition, due to the complexity of these methods, the M typing of GAS isolates has tended to be centralized in laboratories specializing in GAS characterization. Both these methods are laborious and have low-throughput as each requires comparison of a bacterial isolate to a myriad of reference strains or databases.

The protein-based serotyping system of GAS makes it an ideal aptamer target. GAS also possesses a surface rich in other potential targets. **Figures 3.1** and **3.2** detail the GAS cell surface.

Chapter 2 describes the development of a novel cell SELEX technique against whole, live bacterial cells. The objective of this study is to extend this technique to GAS surveillance isolates and the development of aptamers useful in definitive identification of *S. pyogenes* in clinical samples and M-typing of clinical isolates.

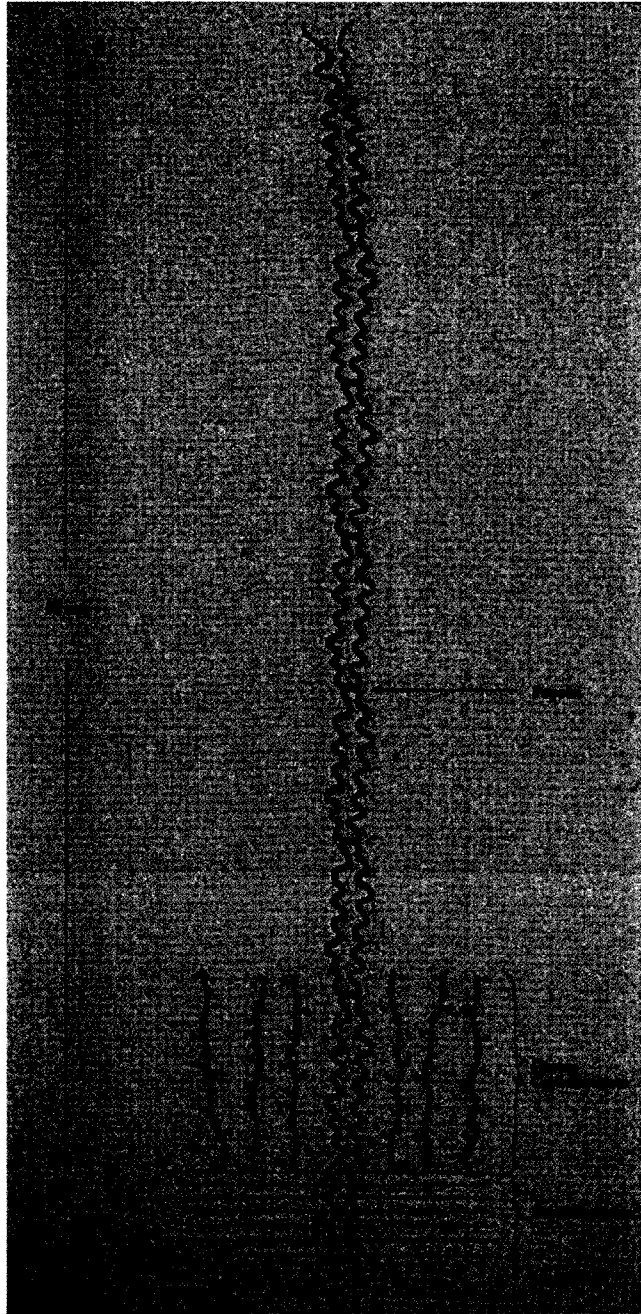


Figure 3.1. The *S.pyogenes* M protein (8).

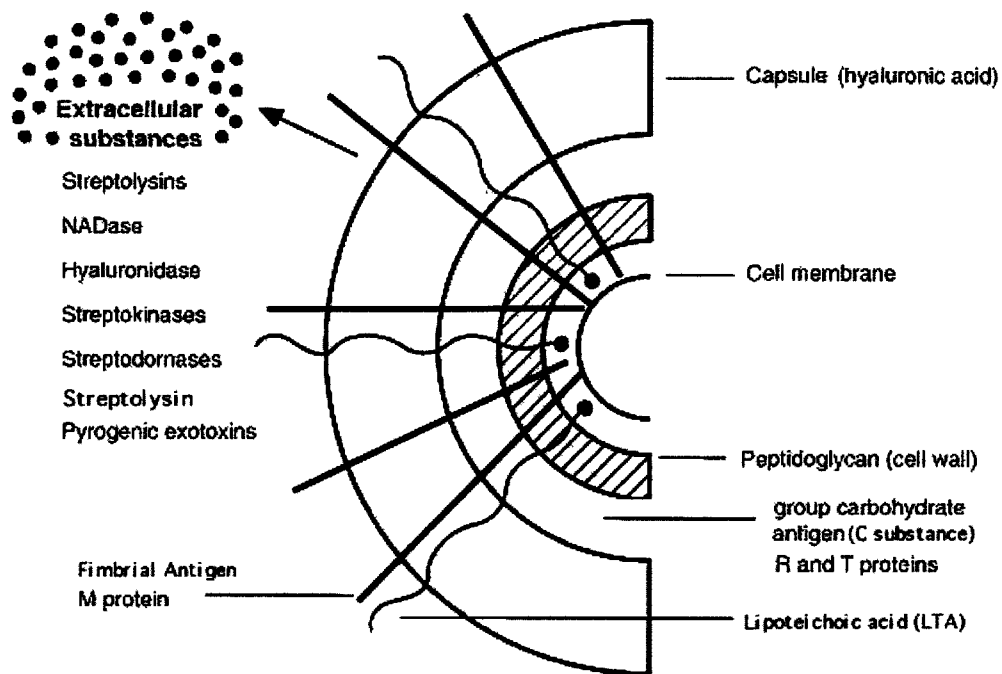


Figure 3.2. Molecules present on the *S. pyogenes* cell surface (9).

3.2 Experimental

3.2.1 Reagents

Bacterial strains and culture medium. *Streptococcus pyogenes* clinical isolates corresponding to M types M1, M2, M3, M4, M5, M6, M11, M12, M28, M41, M49, M59, M75, M77, M82, M83, M89, M91, M92, and M114 were obtained from the National Centre for Streptococcus (Provincial Laboratory, University of Alberta, Edmonton, AB). *S. pyogenes* isolates were streaked out on 5% defibrinated sheep's blood agar (Teknova, Hollister, CA) and single colonies were cultured in Todd-Hewitt Broth (Oxoid, Nepean, ON). *Streptococcus bovis* and *Escherichia coli* were obtained from the American Type Culture Collection

(ATCC) and were cultured in Brain Heart Infusion (BHI) (Teknova) and Luria-Bertani (LB) media (BD Difco, Sparks, MD), respectively. *Streptococcus pneumoniae* (serotypes 4,6B, 9V, 14, 18C, 19F, 23F, 19A, 5, and 6A), *Enterococcus* sp. (*E. sacchrolyticus*, *E. raffinosus*, *E. pseudoaerium*, *E. mundtii*, *E. malodoratus*, *E. hirap*, *E. gallinarium*, *E. faecium*, *E. faecalis*, *E. durans*, *E. cecorum*, *E. casseliflavus*, *E. avium*) and Group B *Streptococcus* strains (975R547 IV, JM9 VIII, 7271 VII, 975R390 VI, 965R400 Ia, 975R384 V, 12351 IV, 965R155 Ia, 975R938 II, 975R27 Ib, 975R331 IV, 955R2028 IV, 975R591 III, 975R138 II, 975R570 Ib, 975R104 VII, 9842 VI, 975R594 III) were also obtained from the National Centre for Streptococcus. *S. pneumoniae* and *Enterococcus* sp. were on 5% defibrinated sheep's blood agar and streaked out cultured in BHI broth and GBS isolates were cultured in TH broth. All bacteria were cultured overnight in aerobic conditions at 37 °C, and all liquid cultures were shaken at 200 rpm. *E. coli* DH5 α -T1^R cells (Invitrogen, Carlsbad, CA) were used for all transformations.

DNA library. An 80-nt oligonucleotide single-stranded DNA library consisting of a 40nt randomized region flanked on both sides by 20-nt primer regions was used. The initial ssDNA library and the primers used to amplify it were obtained from Integrated DNA Technologies (Coralville, IA). DNA library or aptamer pools were rendered single-stranded via heat denaturation at 94 °C for 10 min and subsequent cooling at 0 °C for 5 min.

3.2.2 PCR amplification and gel electrophoresis

The primers used to amplify the ssDNA library and subsequent aptamer pools have the following sequences:

Forward: 5'-AGCAGCACAGAGGTCAGATG-3'

Reverse: 5'-TTCACGGTAGCACGCATAGG-3'

The PCR conditions for amplification of the DNA aptamer pools during SELEX were 1X PCR reaction buffer, 2 mM MgCl₂, 0.4 μM of each primer, 0.2 mM dNTPs, 1 E.U. of Platinum Taq DNA Polymerase, and 39.5 μL of fraction supernatant (all reagents were from Invitrogen). Thermocycling parameters were 94 °C for 5 min denaturation, followed by 20 cycles of denaturation at 94 °C for 30 s, annealing at 57 °C for 30 s, and extension at 72 °C for 20 s. A final extension step of 72 °C for 5 min was carried out following the last cycle (MJ Mini Gradient Thermocycler, Bio-Rad Laboratories, Hercules, CA). After PCR, the reaction products were separated on 7.5% non-denaturing polyacrylamide gel electrophoresis (PAGE) in 1X TBE buffer (Bio-Rad Protean III) at 60–120 V. The gels were stained with ethidium bromide, and photographed under UV light. All PCR products were purified using Qiagen MinElute PCR Purification Kit (Qiagen Inc., Valencia, CA).

3.2.3 Aptamer selection

SELEX was carried out using a procedure modified from Hamula et al. (2008). Single colonies of 10 different *S. pyogenes* M-types (M1, M2, M3, M4, M6, M11, M12, M28, M77, and M89) were grown overnight in separate liquid cultures. The cells were then sub-cultured to a second set of tubes (with a 1:100

inoculum to media ratio) and were harvested upon reaching logarithmic phase (minimum OD₆₀₀ of 0.3). Aliquots containing the same number of cells from each culture were combined only once growth was complete. Cell mixtures were centrifuged at 6000x g and 4 °C for 10 minutes to remove media and to remove wash supernatants. Two separate sets of SELEX were carried out: SELEX A, in which conditions were the same as in Hamula et al. 2008, and SELEX B in which the DNA:cell ratio was altered in favour of increased competition between DNA sequences for target cells. The varying incubation conditions of both SELEX sets are summarized in **Table 4**. Both SELEX A and B were initiated with ssDNA library (2 nmole initial round). The aptamer pools used for incubation in SELEX B were decreased from 100 pmole for round 2 to 75 pmole for rounds 3 through 7, and then increased to 100 pmole again for rounds 9 through 11. The final two rounds of SELEX B, rounds 12 and 13, were carried out with 175 pmole of DNA. A total of 10⁸ cells, containing an equal number of cells of each M-type (10⁷), were used for each round of selection in SELEX A. For SELEX B, the total number of cells was decreased from 10⁸ to 10⁵ over rounds 5 to 8 and maintained at 10⁵ for rounds 9–13. An excess of tRNA and BSA (Invitrogen) were added to the incubation buffer (20-fold molar excess of each in the initial round, up to a maximum 400-fold molar excess in rounds 20) and 0.05% w/v BSA was added to the wash buffer. All washes and incubations were carried out in 1X Binding Buffer (1X BB) (50 mM Tris-HCl (pH 7.4), 5 mM KCl, 100 mM NaCl, 1 mM MgCl₂) at room temperature for 45 minutes. An initial incubation volume of 0.5 mL was used for round one, and this was decreased to 0.25 mL for subsequent

rounds; 4 washes were carried out for each round of SELEX A until round 8 at which the number of washes was decreased to 3 in order to increase the yield after amplification. Three washes were carried out for rounds 3–13 of SELEX B; 4 washes were done in rounds 1 and 2. A total of 20 rounds of SELEX A and 13 rounds of SELEX B were completed.

3.2.4 Flow cytometric analysis of aptamer pool and individual aptamer binding

A FACScan flow cytometer with PowerMac G4 workstation and CellQuest software (Flow Cytometry Facility, Faculty of Medicine and Dentistry, University of Alberta) was used to assess the binding of the aptamer pool and individual aptamer sequences to different types of cells (*S. pyogenes*, *Enterococcus* sp., *S. pneumoniae*, *S. agalactiae*, *E. coli* DH5a, *S. bovis*). The aptamer pools were fluorescently-labeled via PCR amplification with 5'-FAM modified primers (IDT), whereas the individual aptamer sequences were purchased with the fluorescent label (5'-FAM) attached (IDT). Aptamer pools were heat denatured prior to incubation with bacterial cells. The binding assays were carried out by incubating 200 pmole of fluorescently-labeled aptamer/aptamer pool with 10^8 cells for 45 min, as in the SELEX process, and then washing the cells once in 1X BB prior to resuspension in 1X BB for immediate flow cytometric analysis. In cases where mixtures of cells were used an equal number of each cell type was combined to a total of 10^8 cells for screenings and 10^9 cells for binding curves. Forward scatter, side scatter, and fluorescence intensity (FL1-H) were measured, and gated fluorescence intensity

above background (cells with no aptamers added) was quantified. Fluorescently-labeled ssDNA library was used as a control for non-specific binding in each experiment. Binding curves were run to estimate K_d s by varying aptamer concentrations (0–150 nM incubation) with a fixed number of cells (10^9). GraphPad Prism 5.0 software was used to predict K_d values. All cultures used for flow cytometric screening were harvested in stationary phase in order to minimize differences in cell surface molecule expression.

3.2.5 Cloning, sequencing and structural analysis of aptamers

The highest affinity aptamer pools measured via flow cytometry were chosen for sequencing analysis: pools 15A, 13B, and 20A. Aptamer pools were cloned using a TOPO TA Cloning Kit for Sequencing (Invitrogen), transformed into *E. coli* DH5 α -T1^R cells (Invitrogen), and colonies containing the vector were selected via overnight incubation at 37 °C on LB plates containing 50 μ g/mL kanamycin. From each aptamer pool, 20 colonies were chosen for screening. The plasmid DNA was purified (Qiaex II gel extraction kit; Qiagen, Mississauga, ON) and analyzed for the presence of an 80 bp insert via digestion with 1 U of EcoR1 at 37 °C for 30 minutes, followed by 7.5% native PAGE. A total of 60 inserts were then sequenced (Applied Genomics Center, Department of Medical Genetics, University of Alberta), yielding a total of 57 useable sequences. The secondary structure of each sequence was predicted using Oligoanalyzer 3.0 (IDT), with input conditions of room temperature (21 °C) and 1 mM MgCl₂. The most likely sequence was taken as that with the lowest predicted free energy of formation (ΔG) (kcal/mole).

3.2.6 Crude pepsin extract preparation, PAGE, and mass spectrometry

A protocol for extracting M proteins from the surface of *S.pyogenes* using pepsin was modified from Beachey et al., who found that optimal amounts of type-specific M protein were released after 20 minutes of digestion with 0.02 mg of pepsin per mL at pH 5.8 (10). A total of 40 mL of *S.pyogenes* culture was grown in TH broth for 16 hours. Cells were then sedimented and washed twice in ice-cold 0.02 M phosphate-buffered 0.9% NaCl (pH 7.4), then once in extraction buffer minus pepsin (0.9% NaCl adjusted to pH 5.8 with a mixture of 0.067 M Na₂HPO₄ and KH₂PO₄). Cells were resuspended in extracting medium containing 0.02 mg/mL of pepsin and incubated for 20 minutes at 37 °C. Pepsin digestion was halted by raising the pH to 7.5 via addition of 7.5% NaHCO₃ and the supernatant was removed following centrifugation at 10,000x g for 20 minutes. The supernatant was then passed through a 45 µM membrane filter and dialyzed against PBS (pH 7.4) then ddH₂O overnight at 4 °C, resulting in a crude pepsin extract for each of the 10 M-types used in SELEX.

Crude pepsin extracts were run on 7% native and SDS-PAGE gels as previously described (Laemmli). Total protein concentration was assayed using a Micro BCA Protein Kit (Pierce Protein Research Products, ThermoFisher Scientific) and 60 µg of total protein was loaded for each lane of the gel. Gels were run at 120 V and stained in BioSafe Coomassie (Bio-Rad, CA). Bands of interest were excised from the gels and analysed using tryptic digestion coupled with Liquid Chromatography Tandem Mass Spectrometry (LC/MS-MS) (Mass Spectrometry Facility, Department of Chemistry, University of Alberta,

Edmonton, AB). A Waters nanoAcquity UPLC System coupled to a Waters Q-TOF Premier Mass Spectrometer was used (Waters, Milford, MA).

3.3 Results

3.3.1 Aptamer selection

Aptamer selection was carried out using the protocol from Hamula et al. (2008) (**Chapter 2 Figure 2.1**) (11). A schematic of the approach taken in this set of selections is summarized in **Figure 3.3**. A mixture containing an equal number of cells from each of the 10 most prevalent *S. pyogenes* M-types in Canada was used as a target. A randomized ssDNA library is incubated with the cell mixture in order to select a pool of aptamers with increased affinity and selectivity for all the cells in the mixture. The advantage of this approach is that the M-type specific aptamers could be teased out of the aptamer pool via screening individual sequences, and if sequence diversity is too high the affinity and selectivity could be further enhanced via carrying out a second set of SELEX on the selected aptamer pool.

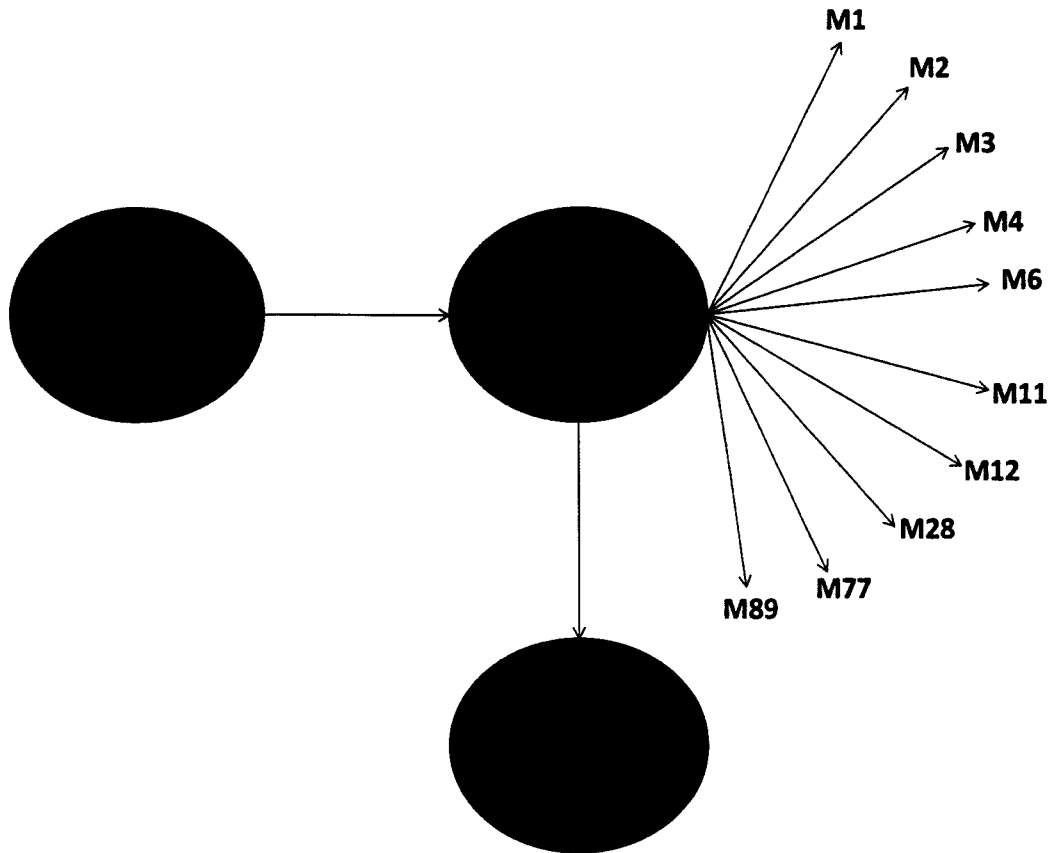


Figure 3.3. Schematic of SELEX approach against *S.pyogenes* isolates.

The different M-types were cultured separately prior to SELEX. The ratio of DNA to cells was maintained throughout selection (SELEX A) or steadily increased (SELEX B). A total of 20 rounds of SELEX A and 13 rounds of SELEX B were carried out. **Table 5** summarizes the amounts of DNA, cells and BSA/tRNA used in each round of selection. SELEX A is the same procedure as the Lactobacillus SELEX. In SELEX B, the competition between DNA sequences for a limited number of target cells was steadily increased by altering DNA: cell ratios in SELEX B. Practically, pellets containing fewer than 10^5 cells are difficult to handle without losing so the cell number was not decreased beyond this point.

In addition, PCR amplification of fewer than 50 pmole of DNA for the low cycle numbers used resulted in poor CA fraction yields. The use of increasing amounts of BSA/tRNA increases the competition between the desired target (cells) and non-targets (BSA molecules) for aptamer molecules. The tRNA is present to compete with the aptamer sequences for target binding sites. The end result is that SELEX B should have higher stringency than SELEX A. A total of 20 sets of SELEX A and 13 sets of SELEX B were performed.

The randomized DNA library was heat denatured prior to incubation with the GAS cell mixture. Fractions representing the incubation supernatant (So), washes (W), and eluted cell-bound aptamers (CA) were collected and amplified following incubation. As can be seen in **Figure 3.4**, the majority of the DNA is retained in the supernatant fraction. However, a substantial amount of DNA sticks to the cells even after the third wash (**Lane 9**). Hence, the number of washes was increased to four at which point no more DNA came off the cells (**Lane 11**). The aptamers were then heat eluted from the cells at high temperature in low salt (**Lane 13**). A negative control consisting of cells without added DNA library was run concurrently (**Lanes 2,4,6,8,10,12**).

Table 5. Varying amounts of BSA, tRNA, DNA, and cells used in SELEX incubations.

SELEX round	Molar Excess BSA/tRNA	DNA:cell ratio SELEX A	DNA:cell ratio SELEX B
1	20x	2000 pmole: 10^8 cells	2000 pmole: 10^8 cells
2	40x	100 pmole: 10^8 cells	100 pmole: 10^8 cells
3	60x	100 pmole: 10^8 cells	75 pmole: 10^8 cells
4	80x	100 pmole: 10^8 cells	75 pmole: 10^8 cells
5	100x	100 pmole: 10^8 cells	75 pmole: 5×10^7 cells
6	120x	100 pmole: 10^8 cells	75 pmole: 10^7 cells
7	140x	100 pmole: 10^8 cells	75 pmole: 5×10^6 cells
8	160x	100 pmole: 10^8 cells	100 pmole: 10^6 cells
9	180x	100 pmole: 10^8 cells	100 pmole: 10^6 cells
10	200x	100 pmole: 10^8 cells	100 pmole: 5×10^5 cells
11	220x	100 pmole: 10^8 cells	100 pmole: 5×10^5 cells
12	240x	100 pmole: 10^8 cells	125 pmole: 10^5 cells
13	260x	100 pmole: 10^8 cells	125 pmole: 10^5 cells
14	280x	100 pmole: 10^8 cells	N/A
15	300x	100 pmole: 10^8 cells	N/A
16	320x	100 pmole: 10^8 cells	N/A
17	340x	100 pmole: 10^8 cells	N/A
18	360x	100 pmole: 10^8 cells	N/A
19	380x	100 pmole: 10^8 cells	N/A
20	400x	100 pmole: 10^8 cells	N/A

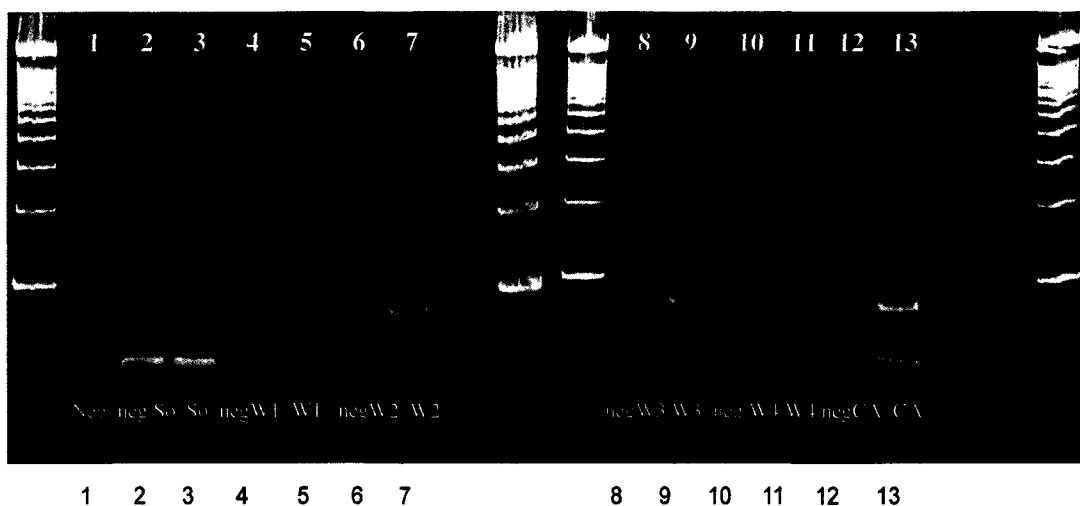


Figure 3.4. Native PAGE of PCR-amplified oligonucleotide fractions after the first round of SELEX A/B. A randomized, single-stranded DNA library was incubated with a mixture of 10 different M-types of *S. pyogenes* cells in the presence of tRNA and BSA. Following incubation, the cells were centrifuged to remove the incubation supernatant (So) and repeatedly washed and centrifuged in binding buffer to remove DNA sequences that are non-specifically or weakly bound (W1, W2, W3, W4). The cells were next heated at 94 °C, the suspension was centrifuged, and the supernatant was collected containing the heat-eluted cell aptamer fraction (CA). A SELEX negative control was carried out in which cells were incubated in the absence of DNA library (negSo), washed (negW1, negW2, negW3, neg W4), and heat-eluted (negCA). The different fractions collected during SELEX (So, W1-W4, CA) and the parallel negative control were PCR amplified and analysed via PAGE. Unlabelled lanes on the gel contain the DNA ladder (100–2072 bp) and lane 1 contains the PCR negative control.

The amplification products of the heat-eluted cell aptamer (CA) fraction (**lane 13**) represent the DNA sequences strongly bound to the cells. No DNA was amplified from the wash or CA fractions of the negative control, which consisted of cells treated to the incubation, wash and heat elution procedures without the addition of library or aptamer pool DNA. The observation of a single 80-bp band on the gel after each round of selection and PCR amplification of the CA fraction suggests that the cells were able to bind to a pool of aptamer sequences. The PCR products of the CA fraction were used in the next round of both SELEX A and SELEX B following purification. The remaining gel photos for SELEX 2A to 20A and SELEX 2B to 13B are in **Appendix A Figures A2 to A31**.

3.3.2 Binding affinity and selectivity of aptamer pools following each round of selection

After each round of selection, the aptamer pools were assessed for binding affinity and selectivity to the target *S. pyogenes* cells using flow cytometry (**Appendix Figure A10**). The aptamer pools (CA fractions) obtained after each round of selection were fluorescently-labeled and then used in flow cytometric assays to assess aptamer pool affinity for the *S. pyogenes* mixture as a whole and selectivity for each separate M-type. A fluorescently-labeled randomized oligonucleotide library was run during each experiment as a control to assess non-specific DNA adhesion to the cells.

Flow cytometric analyses of incubation mixtures containing fluorescently-labeled aptamer pools and the target cells show that with increasing rounds of selection, the percent of cells with fluorescence above library background

increased to a maximum average of 14% at round 15 for SELEX A aptamer pools and 21% at round 7 for SELEX B (Figure 3.5). The increase in the number of fluorescent cells is due to the increased binding of the fluorescent aptamers to the target cells. Controls carried out using fluorescent aptamer pools alone and buffer with BSA and tRNA alone did not yield any increase in gated fluorescence above background levels (data not shown).

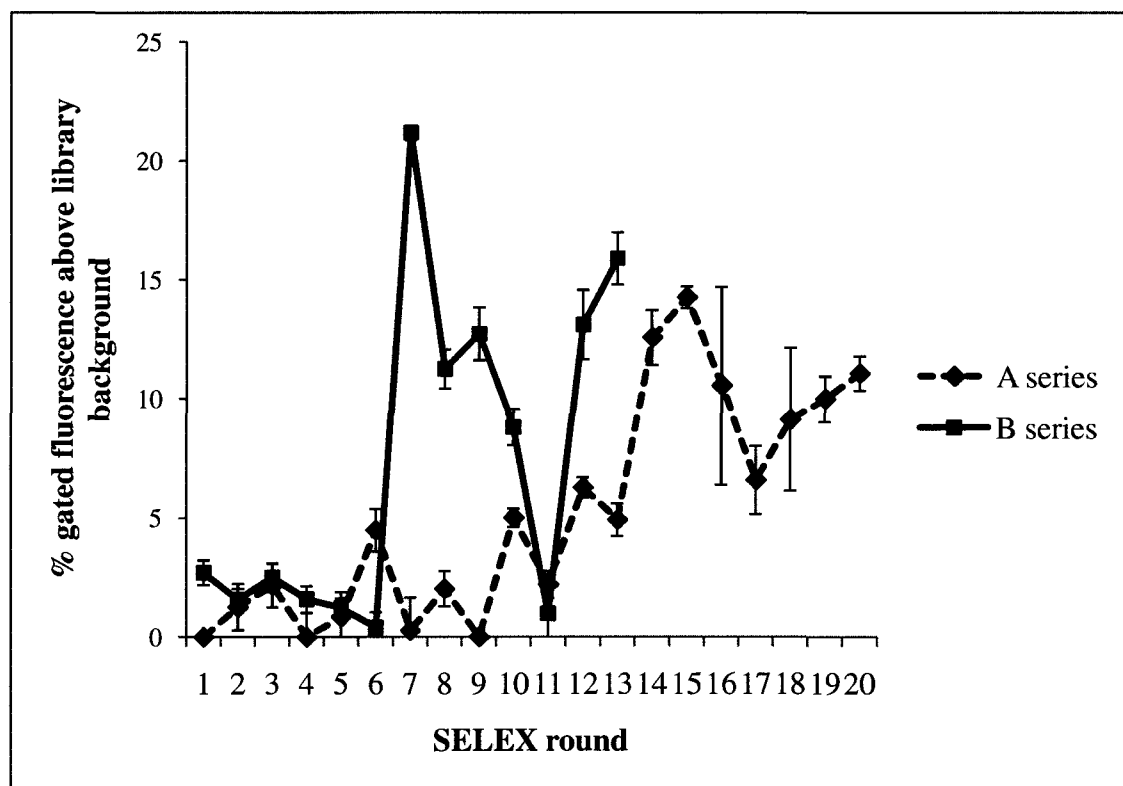


Figure 3.5. Percent gated fluorescence intensity of *S. pyogenes* cells incubated with fluorescently-labeled aptamer pools after increasing SELEX rounds.

For SELEX A, aptamer pool binding did not start to increase above background until round 10; whereas for SELEX B the increase was sooner, at round 7 (**Figure 3.5**). The maximum binding of the aptamer pool to the target mixture of *S. pyogenes* cells was substantially lower than the 67% maximum binding seen for the aptamer pools following selection against *Lactobacillus acidophilus* (**Figure 2.2**). This may partially be due to masking of evolving aptamer pool affinity by the high variability of aptamer pool binding to *S. pyogenes* seen over the course of both sets of selection. For SELEX B, the percent of cells with fluorescence above library background sharply decreased after round 7 and then increased to 16% at round 13 (**Figure 3.5**). A similar trend of lesser magnitude was seen with SELEX A, as the percent of cells with fluorescence above library decreased from 14% at round 15 to 7% at round 17 before increasing again to 11% at round 20 (**Figure 3.5**). A key source of variability in aptamer pool binding may be due to differences in expression of cell surface molecules between and within M-types. Since the SELEX target is a mixture of 10 different M-types, it is much more complex than a monoclonal population. Small day-to-day variations in the surface of each M-type may be additive, resulting in high overall variability. Differences in cell surface molecule expression are greatest when cells are grown in logarithmic phase (345) which is when they were harvested for selection. This argument is lent support by the results of separate screenings of the aptamer pools against each M-type (**Figures 3.6 to 3.8**). When duplicate incubations are set up using two separate colonies of each M-type, there is substantial variability in aptamer pool binding between the

incubations (**Figure 3.6**). This variability is minimal when duplicates from the same culture (**Figure 3.7**) or duplicates of two separate stationary phase cultures (**Figure 3.8**) are analyzed. Hence, screening aptamer pools against stationary phase cultures results in decreased variability of aptamer pool binding and is the procedure used for all remaining flow cytometry experiments.

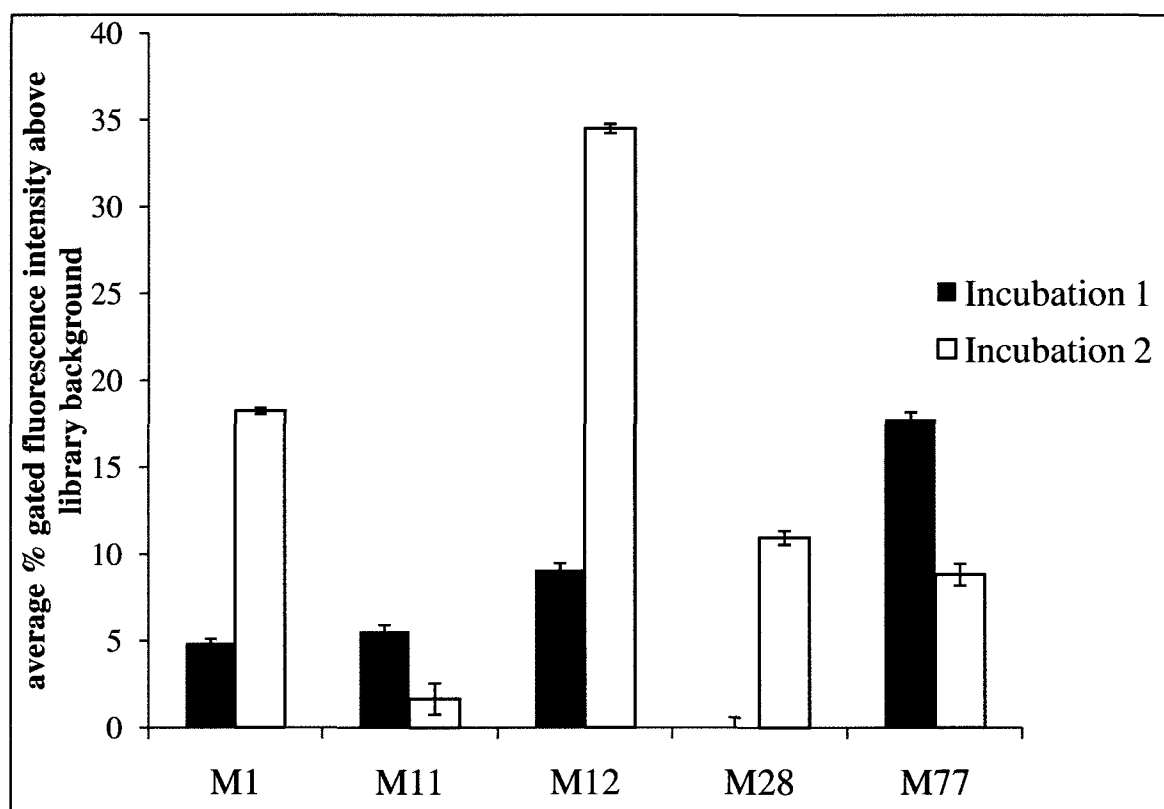


Figure 3.6. Binding of SELEX 20A aptamer pool to two separate logarithmic phase cultures of each M-type. Flow cytometric analysis was carried out as previously using 200 pmole of fluorescently-labeled aptamer pool and 10^8 total cells. Incubations 1 and 2 were both carried out simultaneously using two separate logarithmic phase cultures derived from two separate colonies of each M-type.

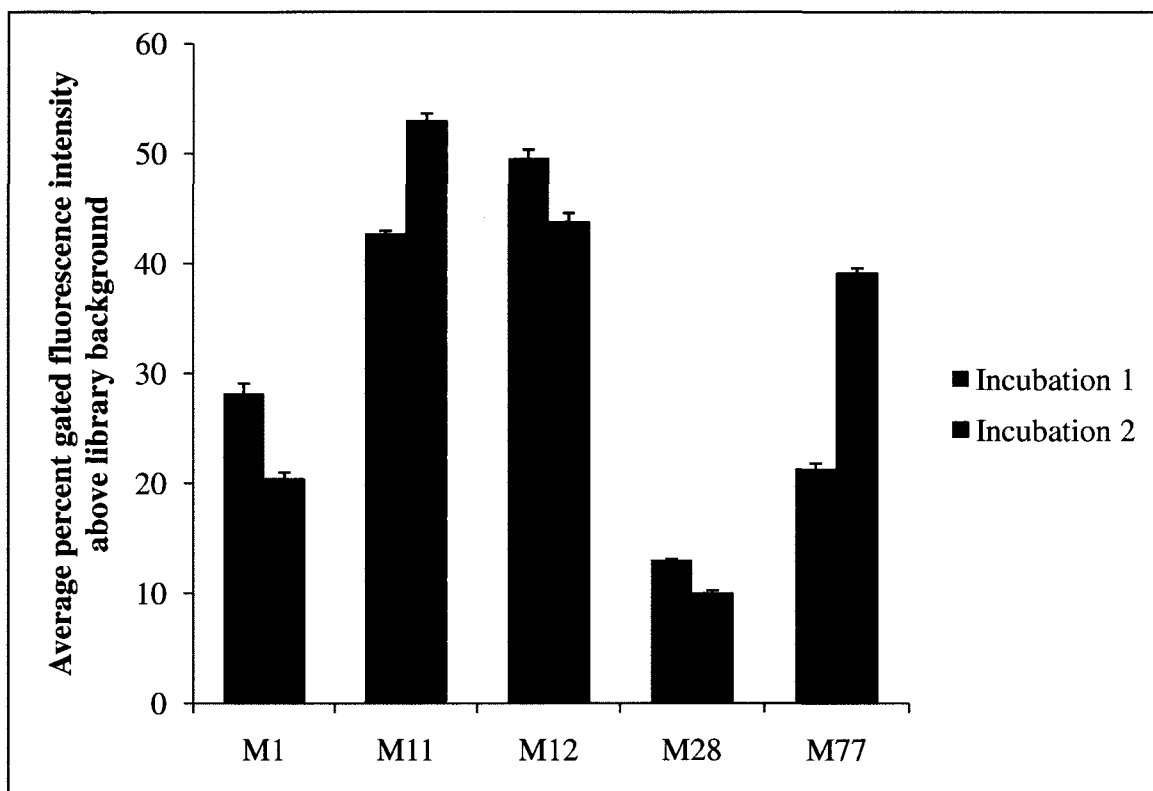


Figure 3.7. Binding of SELEX 20A aptamer pool to each M-type using two separate incubations of the same logarithmic phase culture. Flow cytometric analysis was carried out as previously using 200 pmole of fluorescently-labeled aptamer pool and 10^8 total cells. Incubations 1 and 2 were both carried out simultaneously using a single logarithmic phase cultures derived from one colony of each M-type.

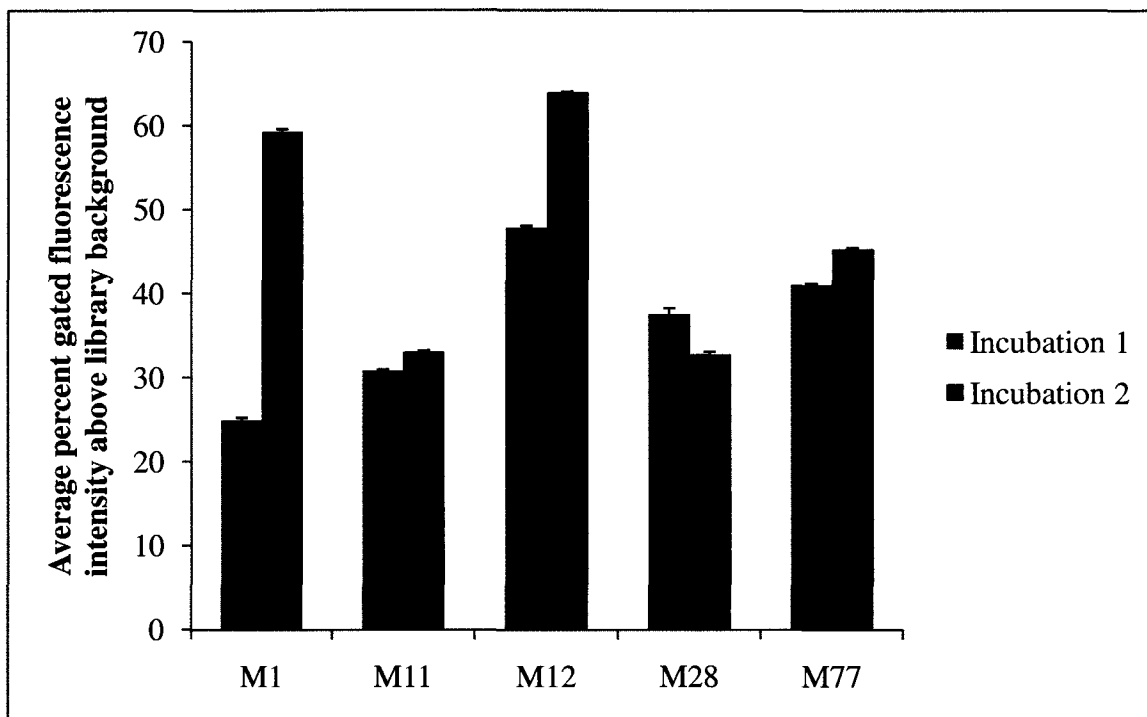


Figure 3.8. Binding of SELEX 20A aptamer pool to two separate stationary phase cultures of each M-type. Flow cytometric analysis was carried out as previously using 200 pmole of fluorescently-labeled aptamer pool and 10^8 total cells. Incubations 1 and 2 were both carried out simultaneously using two separate stationary phase cultures derived from two separate colonies of each M-type.

3.3.3 SDS-PAGE and mass spectrometry analysis of *S. pyogenes* surface protein expression

Duplicate logarithmic phase cultures of each of the 10 M-types used for selection were treated with pepsin to remove all surface proteins. Following dialysis each culture yielded a crude pepsin extract. The crude pepsin extracts were then run on SDS-PAGE gels and Coomassie stained yielding a unique surface protein profile for each culture. Bands were excised and identified via

mass spectrometry (**Figure 3.9**). The surface protein profiles of all the M-types are relatively similar. The main drawback of the pepsin extraction procedure is that pepsin comprises a large proportion of the total protein obtained, as can be seen in the gels (**Figure 3.9**). Despite the low sensitivity of this approach, several differences can be seen within and between the M-types. It seems as if only M1, M6 and M77 express the LPTXG anchored adhesin and putative adhesin (**bands 4 and 5**) at levels high enough to be seen on the gel. M77 and M1 are the only M-types expressing the Fc gamma receptor. There are also differences in the numbers of bands seen on the gel between two cultures of the same M-type. For example, the M1A crude extract contains bands 4 and 5 while the M1B extract does not. These results provide evidence that the variability of aptamer pool binding seen between monoclonal logarithmic phase cultures could be due to differences in surface molecule expression, particularly since the gels in **Figure 3.9** are of limited sensitivity.

3.3.4 Cloning and sequence analysis of aptamer pools

Upon confirmation that aptamer pool binding was increasing with SELEX rounds, the SELEX A and B aptamer pools were cloned and sequenced after the 15th and 20th rounds of SELEX A and the 13th round of SELEX B. These pools displayed the highest affinity for the target cells when screened via flow cytometry (**Figure 3.5**). A total of 57 sequences from the aptamer pools were obtained, 41 for SELEX A and 16 for SELEX B. Secondary structures were predicted using Oligoanalyzer 3.1 (Integrated DNA Technologies) for all the sequences. All sequences were analyzed both with and without primers. A

summary of the sequences, their most likely predicted secondary structures and corresponding lowest free energies of formation can be found in **Tables A2 to A4**. There is minimal repetition within this collection of sequences, and many sequences contain high GC content, indicative of potential formation of secondary structures. Within the 15A pool, sequences 15A 2 and 15A 15 are identical, as are sequences 15A 8, 16 and 17 (**Table A2**). Sequences 20A 6, 15, and 17 are identical, as is 15A 10 (**Tables A2, A3**). None of the sequences in aptamer pool 13B were repetitive (**Table A4**). Sequences were chosen for further screening based not only on their repetitiveness but also on predicted secondary structures and free energies of formation. Sequences with complex secondary structures, hairpin structures similar to hemag1P, and free energies of formation below -7 kcal/mole were all subjected to further screening.

3.3.5 Binding of individual aptamer sequences to target cell mixture

Aptamer sequences were synthesized to contain a fluorophore (FAM) on the 5' end. Each fluorescently-labeled aptamer was incubated with the target mixture of 10 *S. pyogenes* M-types used for selection. These incubations were washed and the cells were subjected to flow cytometry without elution of the aptamers from the cell surface. Results of these screenings are summarized in **Figure 3.10**. The aptamer sequences obtained after the 20th round of SELEX A seem to have the highest affinity for the cell mixture. A total of 9 sequences from that pool had greater than 50% gated fluorescence intensity above a randomized library control. These sequences are summarized in **Table 6**; their predicted secondary structures are in **Figure 3.11**. Sequences 20A 1, 20A 1P (with primers),

and 20A 8 were the highest binders with gated fluorescence above background values of around 72%. The highest binding sequence in the 15A pool is 15A 3P with a gated fluorescence above background of 48%. The 13B pool did not contain very many promising sequences; the highest gated fluorescence above background value for a sequence in that pool is 15% for 13B 5.

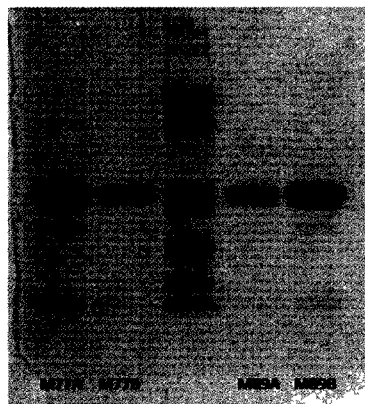
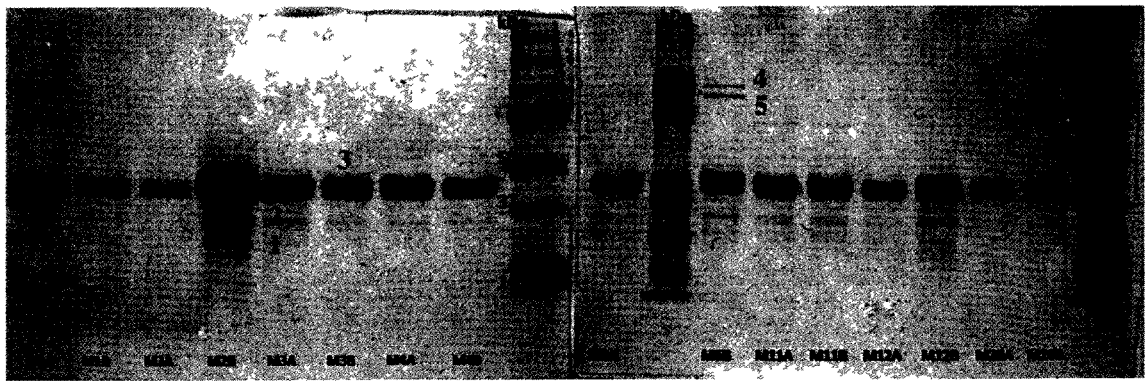


Figure 3.9. SDS-PAGE gels of crude pepsin extracts from duplicate cultures of M-types M1, M2, M3, M4, M6, M11, M12, M28, M77, and M89. The same amount of total protein was loaded of each crude pepsin extract, and 8% gels were run using previous methodology at 120V, and then Coomassie stained. Bands which were excised and identified via mass spectrometry are numbered on the gel and are as follows: 1) *S. pyogenes* fcrA8, 2) hypothetical bacterial protein, 3) pepsin doublet, 4) *S. pyogenes* LPTXG anchored adhesin, 5) *S. pyogenes* putative adhesin, 6) *S. pyogenes* Fc gamma receptor. The M-types of the corresponding cultures are indicated. A and B denote separate duplicate bacterial cultures. The unlabeled lanes contain protein standards; sizes in kDa are marked.

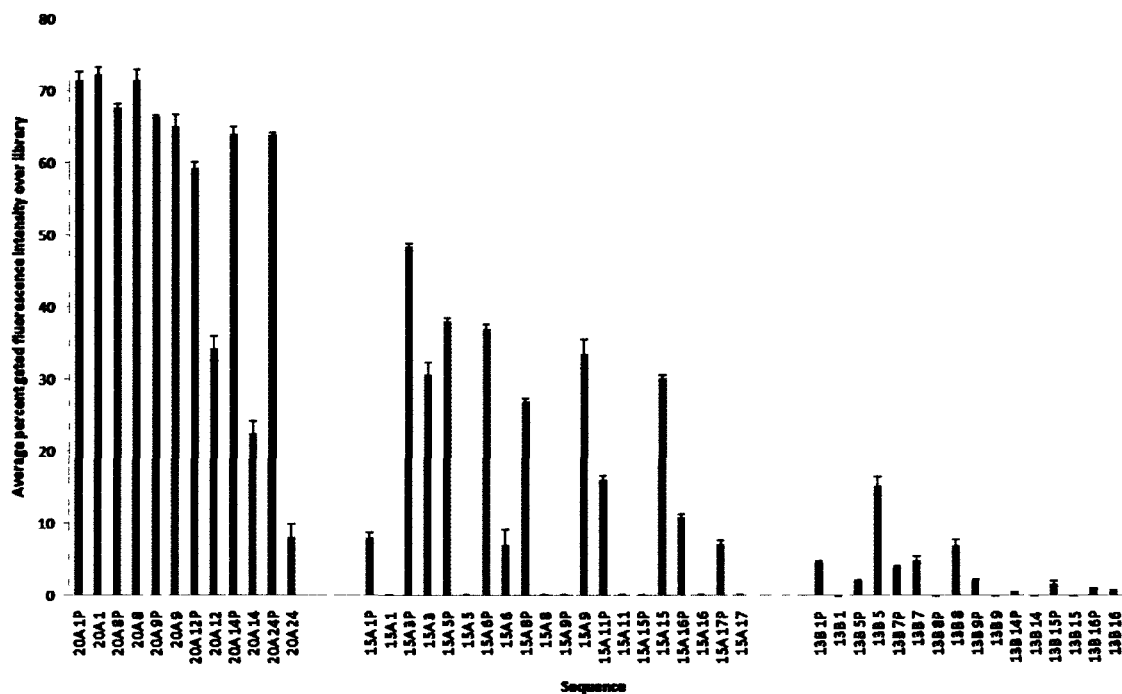
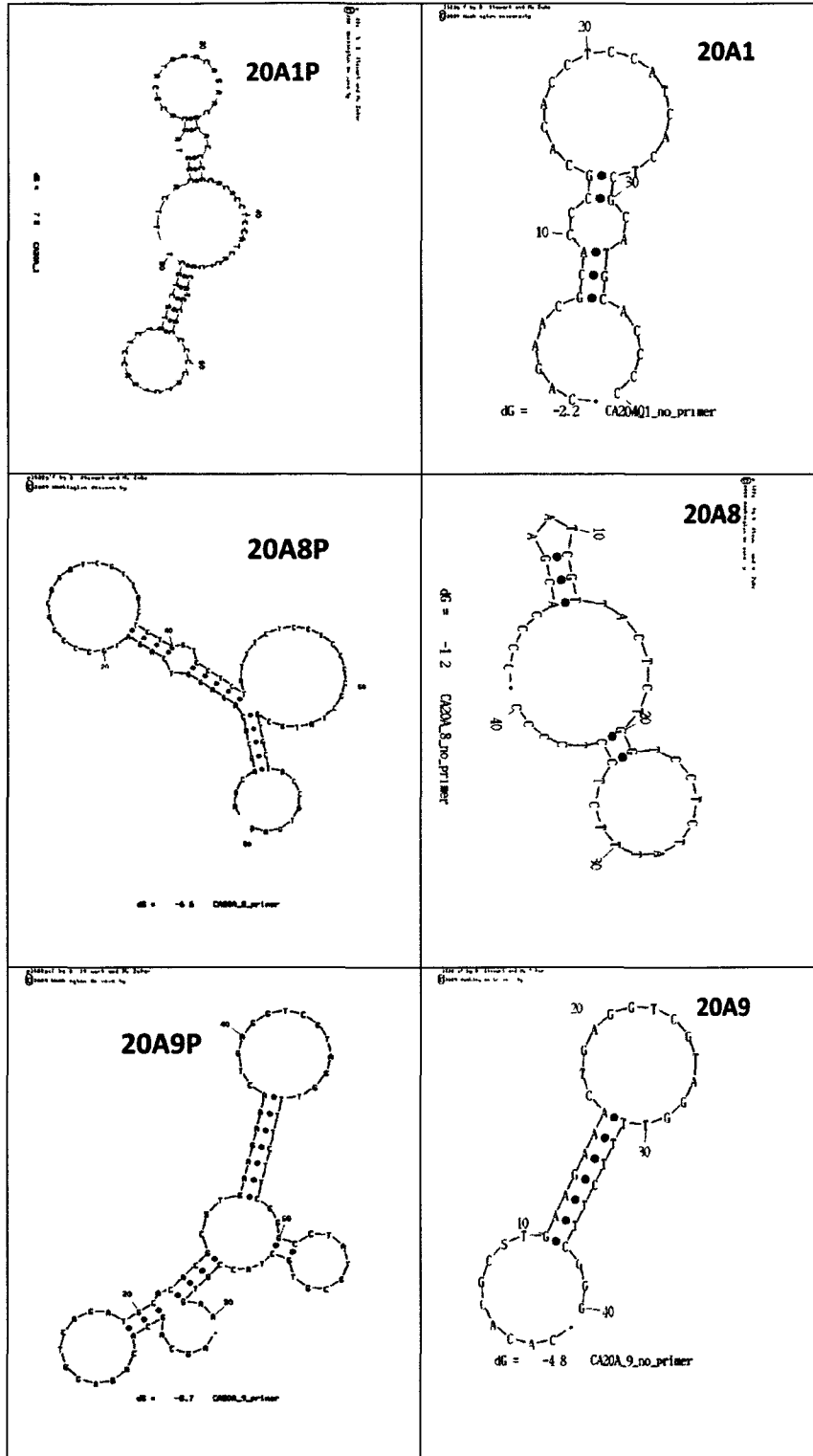


Figure 3.10. Screening of sequences from SELEX 15A, 20A, and 13B aptamer pools against a mixture of 10 *S. pyogenes* M-types used as a SELEX target. All aptamers were fluorescently-labeled with 5'-FAM. Incubations and centrifugation were carried out as in Section 3.2. A ratio of 200 pmole of aptamer and 10^8 cells was used.

Table 6. Screened aptamer sequences with and without primers. Shown here are the aptamers of high affinity for *S. pyogenes* cells, selected from a total of 57 aptamers that were sequenced. The fluorescent label FAM is shown at the 5'-end. The underlined sequences are the primers.

Name	Sequence
20A 1	5'FAM/ CAGAACGCACCCGCACACCTCCATCACTCGCATGCACCCC-3'
20A 1P	5'FAM/ <u>TTC ACG GTA GCA CGC ATA GG</u> CAGAACGCACCCGCACA CCTCCATCACTCG CATGCACCCC <u>CAT CTG ACC TCT GTG CTG CT</u> -3'
20A 8	5'FAM/ CCCACGAATCGTTACTCTGGTCCTCTATTTCTCCTCCC C-3'
20A 8P	5'FAM/ <u>AGC AGC ACA GAG GTC AGA TG</u> CCCACGAATCGTTACT CTGGTCCTCTATT TCT CCTCCCC <u>CCT ATG CGT GCT ACC GTG AA</u> -3'
20A 9	5'FAM/ CACACGCTGAAGAACTGAGGTCGTAGGTTTTCTTCGGG-3'
20A 9P	5'FAM/ <u>AGC AGC ACA GAG GTC AGA TG</u> CACACGCTGAAGAAAC TGAGGTCGTAGGTTTT CTTCGGG <u>CCT ATG CGT GCT ACC GTG AA</u> -3'
20A 12P	5'FAM/ <u>TTC ACG GTA GCA CGC ATA GG</u> GCCCGACACTCGTCCAC CCGATACC TCT CATGTGTCCC <u>CAT CTG ACC TCT GTG CTG CT</u> -3'
20A 14P	5'FAM/ <u>AGC AGC ACA GAG GTC AGA TG</u> GGCATGGGGAAGAGAAAG CGGGATAACTTCGTT ACCGGGC <u>CCT ATG CGT GCT ACC GTG AA</u> -3'
20A24P	5'-FAM/ <u>AGC AGC ACA GAG GTC AGA TG</u> GGG GGA AGA CAC AGA GAA AGG CCG GGG TGA AGT GTA GAG <u>GCCT ATG CGT GCT ACC GTG AA</u> -3'
15A 3P	5'FAM/ <u>TTC ACG GTA GCA CGC ATA GG</u> GACAGCAAGCCCAAGCTG GGTGTGCAAGGT GAG GAGTGGG <u>CAT CTG ACC TCT GTG CTG CT</u> -3'



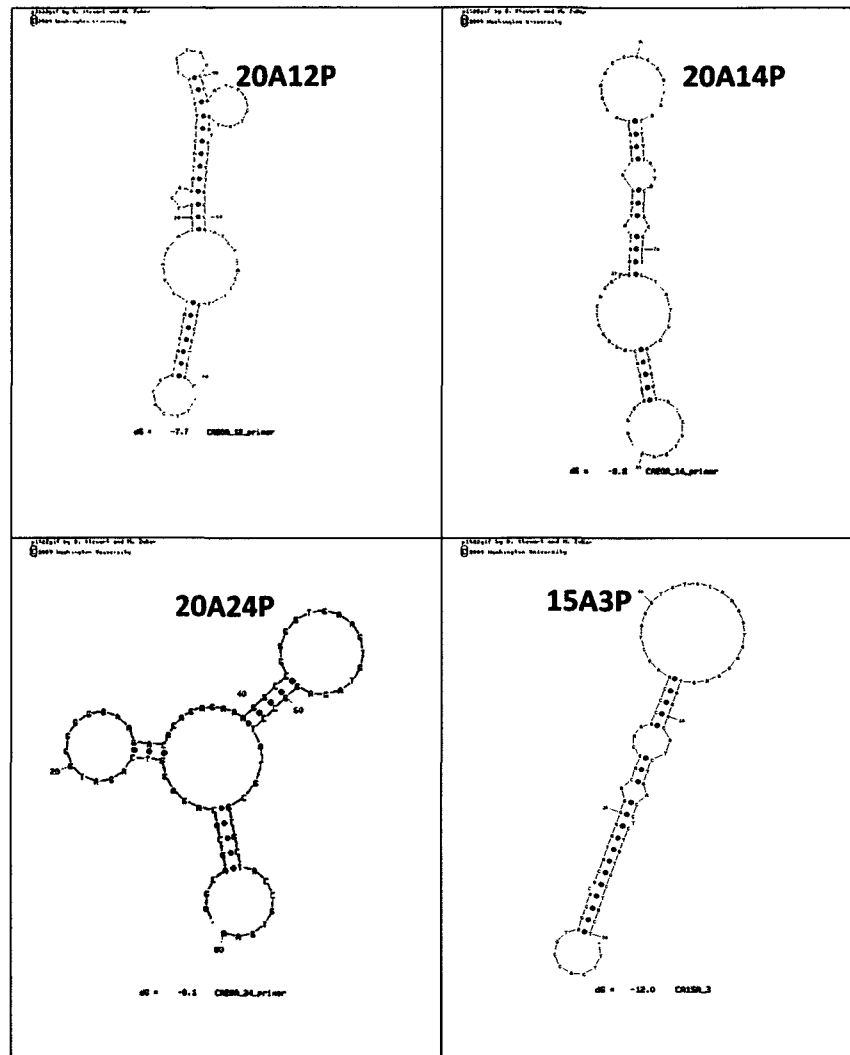


Figure 3.11. Predicted structures of aptamer sequences with high affinity for *S. pyogenes*.

The majority of the high affinity sequences have hairpin-like secondary structures (**Figure 3.11**). Sequences 20A1, 20A8, and 20A9 form hairpins both in the absence and presence of the primer sequences. The affinity of these three aptamers for the *S. pyogenes* mixture changes minimally upon inclusion or exclusion of primers in the sequence; it remained at 72% gated fluorescence intensity above library for both 20A1 and 20A1P, decreased from 72% for 20A8

to 68% for 20A8P, and increased from 65% for 20A9 to 66% for 20A9P (**Figure 3.10**). Inclusion of the primer sequences in 20A12P, 20A14P, and 15A3P allow them to form tighter hairpin secondary structures with more extensive base pairing, as opposed to hairpins containing more open structure when the primers are removed. It is reasonable to suggest that an extensive, tight hairpin secondary structure perhaps accounts for the superior binding of these three sequences to the target cells. However, not all non-hairpin sequences have low affinity for the target cells. Sequence 20A24P forms a branched structure with high affinity for the target cell mixture (gated fluorescence intensity above library of 64% in **Figure 3.10**); removal of the primers negates this affinity (8% in **Figure 2.10**). The sequence 20A24 forms a hairpin. Sequences with no or minimal affinity for the target cells tend to have minimal predicted secondary structures.

3.3.6 Binding of aptamers to specific M-types

Individual aptamer sequences were classified into three groups based on the results of screening against a mixture of 10 different *S. pyogenes* M-types (**Figure 3.10**): high, medium, and low affinity. Representative sequences from these three groups were then screened via flow cytometry against each M-type separately. The affinity of a given sequence for the *S. pyogenes* mixture seems to mirror its affinity for each M-type, with the high affinity sequences exhibiting high binding to most of the M-types and the low affinity sequences demonstrating minimal binding to each of the M-types (**Figures 3.12, 3.14**). Sequences 20A8 and 20A 8P have very similar affinities for a given M-type, with percent gated fluorescence above background above 50% for all M-types except M1; M-types

M2, M3, M6, M12, M77 and M89 have gated fluorescence above background greater than 70%. Binding of 20A24P is more variable but has greater than 50% gated fluorescence above background for M4, M6, M11, and M12 cells. It appears that all high affinity sequences bind poorly to M1 cells. Medium affinity sequences demonstrated binding for each M-type; for the most part this binding was lower than that of the high affinity sequences with the exception of M12 cells that had gated fluorescence intensity measurements above 70% for all the tested sequences (**Figure 3.13**). Binding of the medium affinity sequences was also more variable across M-types. However, M2, M3, M6, M77, and M89 all had at least one medium affinity sequence bind with a percent gated fluorescence above background measurement higher than 50%. Finally, the low affinity sequences bound poorly to all M-types; none of the aptamers yielded a percent gated fluorescence measurement above 40% and most were below 25% (**Figure 3.14**). Sequence 20A24 bound only to M-types M11 and M12, with percent gated fluorescence above background measurements of 26% and 27%, respectively. Hence, it appears as if the selection resulted in aptamer pools containing a mixture of sequences of similar affinity for all target M-types rather than a mixture of sequences with different affinities for different targets.

None of the aptamer sequences tested were M-type specific; they also bound *S. pyogenes* M-types other than the 10 used for SELEX. A cell mixture containing 10 M-types not used for selection was incubated with fluorescently-labeled aptamers and analyzed via flow cytometry (**Figure 3.15**). The M-types included in the mixture were M5, M41, M49, M59, M75, M82, M83, M91, M92,

and M114. However, binding to this mixture was quite low for all sequences tested, ranging from 23% for 20A8 to 1% for 20A9.

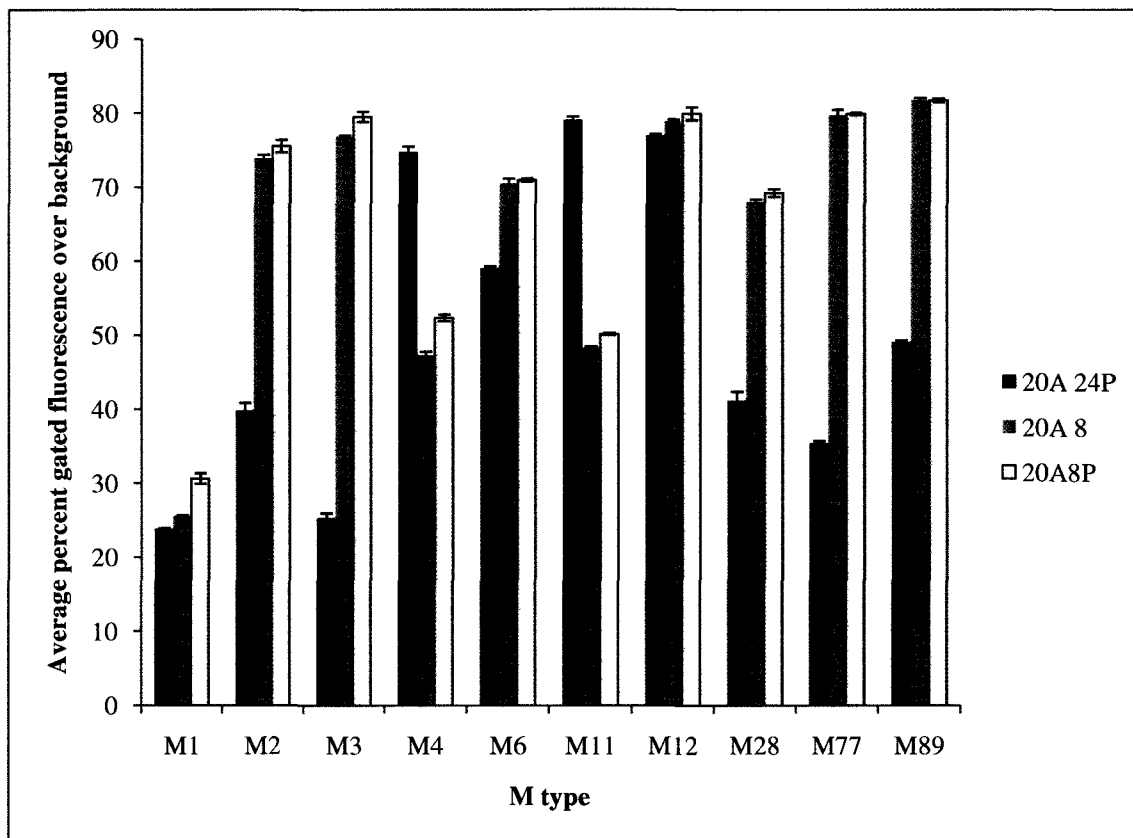


Figure 3.12. Binding of high affinity aptamer sequences to the 10 different *S. pyogenes* M-types used for SELEX. Aptamers were labeled with 5'-FAM, and 200 pmole of aptamers were incubated with 10^8 cells. Cells were then prepared for flow cytometry as previously.

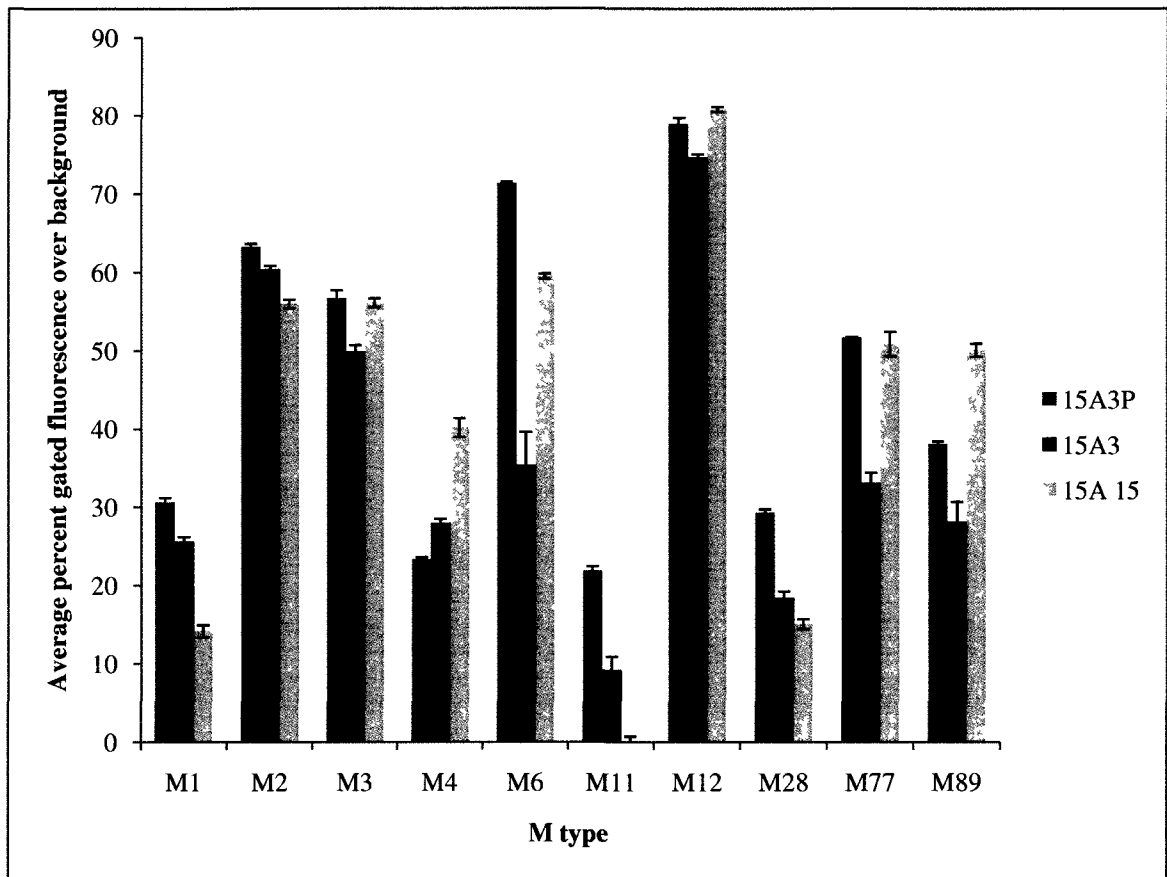


Figure 3.13. Binding of medium affinity aptamer sequences to the 10 different *S. pyogenes* M-types used for SELEX. Aptamers were labeled with 5'-FAM, and 200 pmole of aptamers were incubated with 10^8 cells. Cells were then prepared for flow cytometry as previously.

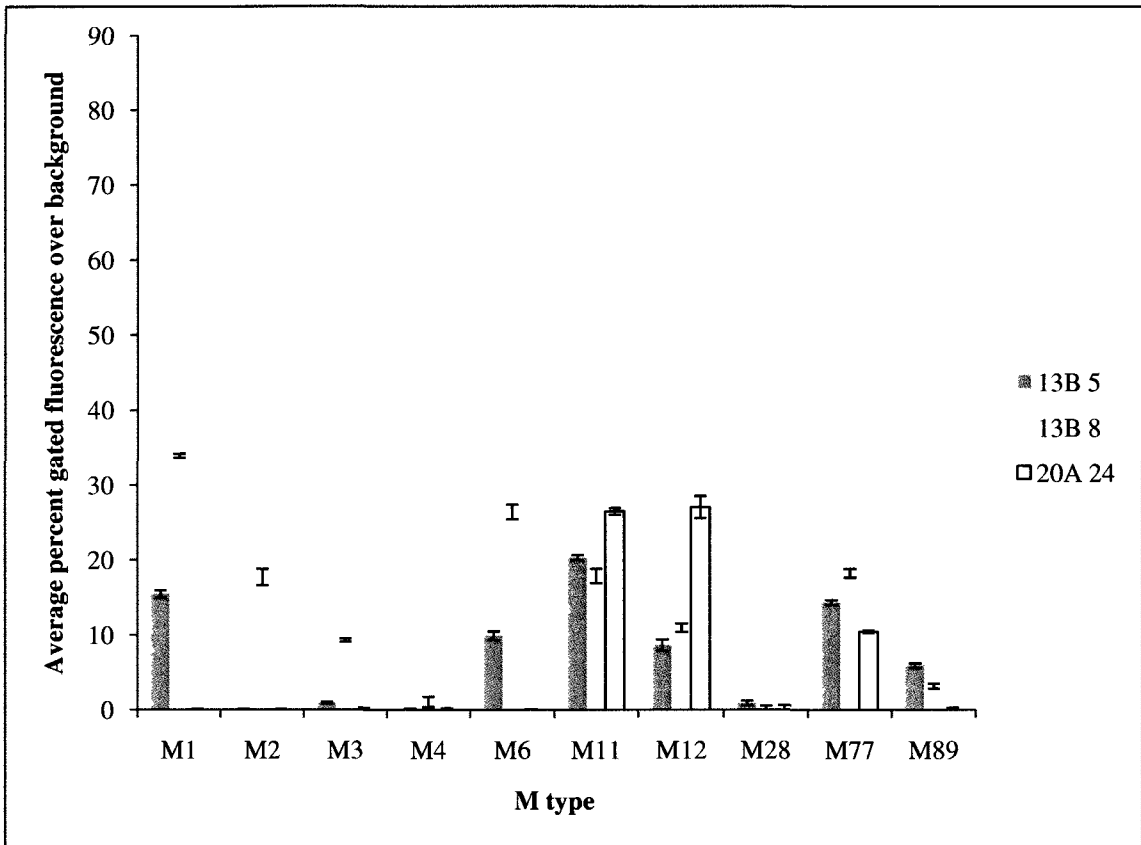


Figure 3.14. Binding of low affinity aptamer sequences to the 10 different *S. pyogenes* M-types used for SELEX. Aptamers were labeled with 5'-FAM, and 200 pmole of aptamers were incubated with 10^8 cells. Cells were then prepared for flow cytometry as previously.

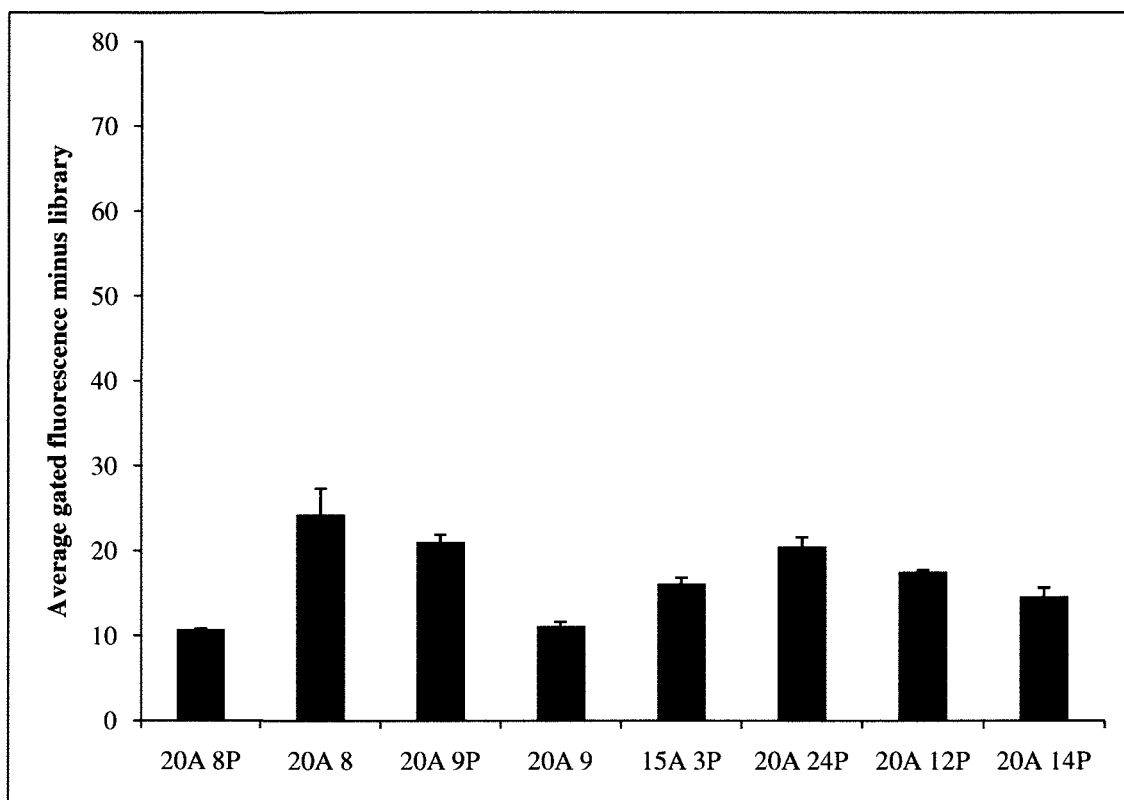


Figure 3.15. Binding of high affinity aptamer sequences to a mixture of *S. pyogenes* M-types not used as targets during selection. A total of 200 pmole of each fluorescently-labeled aptamer was incubated with a mixture of 10^8 total cells (M-types included were M5, M41, M49, M59, M75, M82, M83, M91, M92, and M114).

3.3.7 Binding of high affinity aptamers to *S. pyogenes*

The binding curves from flow cytometric analysis of fluorescently-labeled aptamers and the mixture of 10 different *S. pyogenes* M-types used for selection (10^8 cells) are shown in **Figures 3.16 to 3.20**. Aptamer concentrations in the incubation supernatant from 0 to 150 nM were tested, with the amount of aptamer binding found to level off at less than 60 nM for all sequences. Binding of a

fluorescently-labeled randomized oligonucleotide library to the *S. pyogenes* cell mixture was also examined over a concentration range of 0 to 150 nM (**Figure 3.21**). The single-stranded aptamers and library were heated at 94 °C and then cooled at 0 °C prior to incubation with the cells. The average gated fluorescence intensity increased linearly with library concentration and was found to reach a maximum of 23% at a library concentration of 150 nM. However, for all aptamer sequences tested, maximum percent gated fluorescence intensity reached a maximum and leveled off before or at an aptamer concentration of 50 nM. The maximum percent gated fluorescence intensity, and hence maximum binding, measured for each sequence is as follows: 1) 20A1: 69 ± 1 % at 120 nM; 2) 20A1P: 70 ± 0.3 % at 100 nM; 3) 20A8: 81 ± 1 % at 110 nM; 4) 82 ± 1 % at 60 nM; 5) 20A9: 80 ± 1 % at 140 nM; 6) 20A9P: 79 ± 1 % at 110 nM; 7) 20A12P: 75 ± 0.3 % at 100 nM; 8) 20A14P: 74 ± 1 % at 90 nM; 9) 20A24P: 79 ± 1 % at 130 nM; 10) 15A3P: 80 ± 1 % at 140 nM. Since the percent gated fluorescence intensity value increases with the number of cells bound to an aptamer and the number of target molecules (and hence aptamers) bound per cell, it seems that aptamer sequences 20A1, 20A1P, 20A12P and 20A14P bind to slightly fewer cells and/or fewer target molecules per cell than the remaining aptamer sequences tested.

The K_d of each aptamer was determined based on the fit of the non-linear regression curve assuming one site binding (GraphPad Prism 5). **Table 7** summarizes the K_d and B_{max} values of each aptamer tested. These values are also listed on **Figures 2.16 to 2.21**. Sequences 20A24P, 20A9P, 20A8, and 15A3P had

the highest affinities for the target cell mixture as all had K_d values below or equal to 10 nM ($K_d = 4.4 \pm 0.6$ nM for 20A8; 9.1 ± 0.6 nM for 20A9P; 9.1 ± 0.8 nM for 20A24P; and 9.6 ± 0.3 nM for 15A3P). Sequence 20A1 had the lowest affinity for the target cell mixture with a K_d of 31.1 ± 4.4 nM.

Table 7. Binding Dissociation constants (K_d) and theoretical maximum binding (B_{max}) of high affinity aptamer sequences for a mixture of 10 different *S. pyogenes* M-types used in SELEX.

Aptamer Sequence	K_d (nM)	SE (nM)	B_{max} (% gated)	SE (% gated)
20A1P	19.5	2.1	80.2	2.0
20A1	31.1	4.4	87.0	3.6
20A 8P	10.9	0.8	89.3	1.1
20A 8	4.4	0.6	85.5	1.1
20A 9P	9.1	0.6	85.8	0.8
20A 9	12.7	1.1	89.9	1.5
20A 12P	24.8	2.6	93.6	2.6
20A 14P	17.2	1.3	87.3	1.4
20A 24P	9.1	0.8	82.5	1.0
15A 3P	9.6	0.3	86.9	0.5

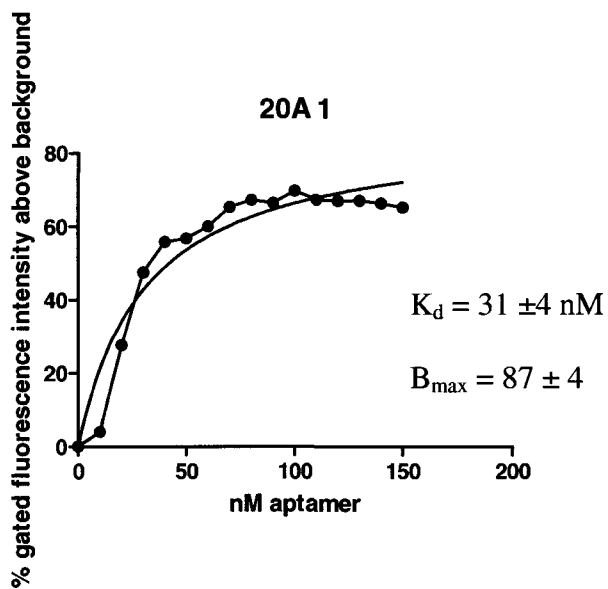
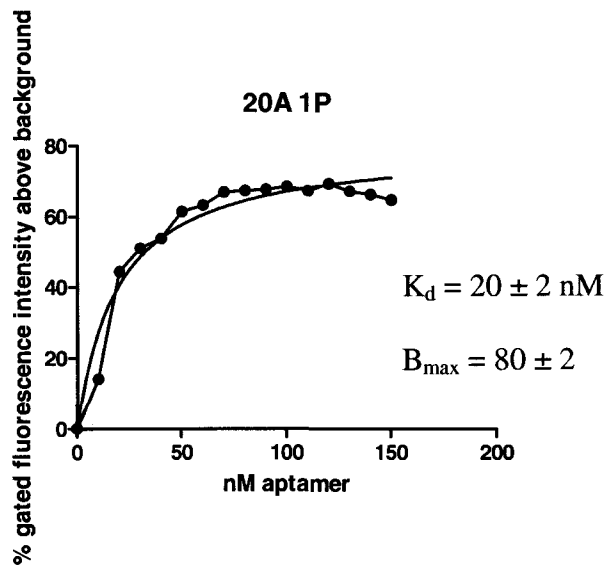


Figure 3.16. Binding of aptamers 20A1P and 20A1 to the mixture of *S. pyogenes* cells used in SELEX. Various concentrations of 5' FAM-labeled aptamer (x-axis) were incubated with a mixture of 10^8 *S. pyogenes* cells in binding buffer for 45 min and analyzed via flow cytometry. No washing steps were carried out.

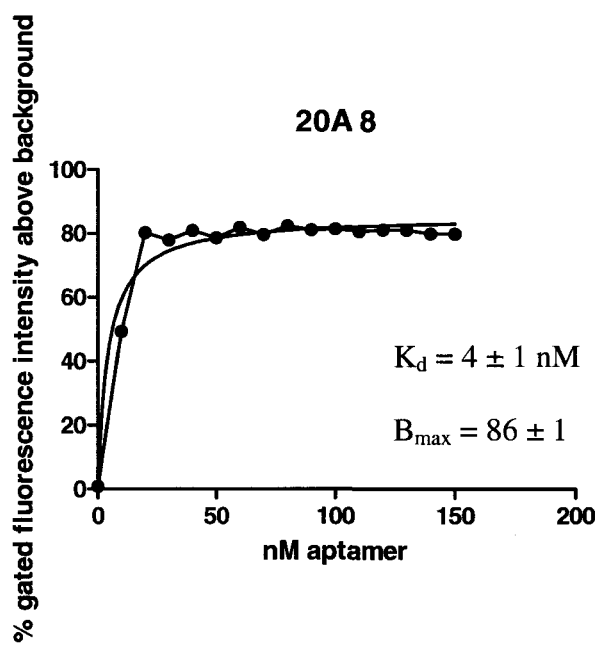
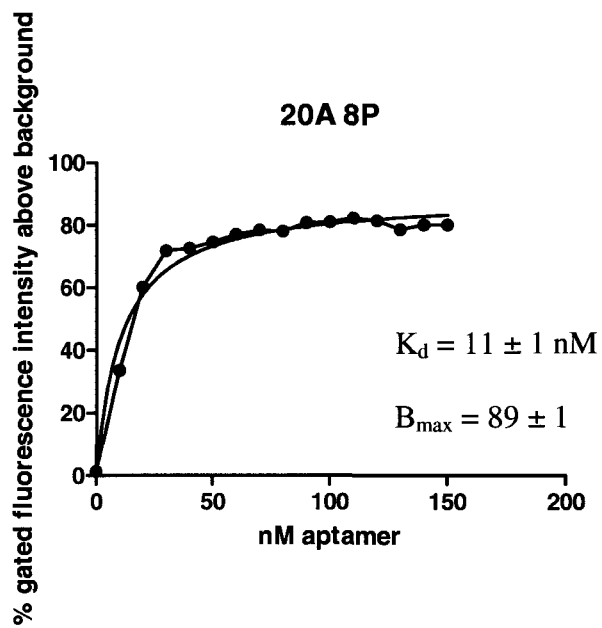


Figure 3.17. Binding of aptamers 20A8P and 20A8 to the mixture of *S. pyogenes* cells used in SELEX.

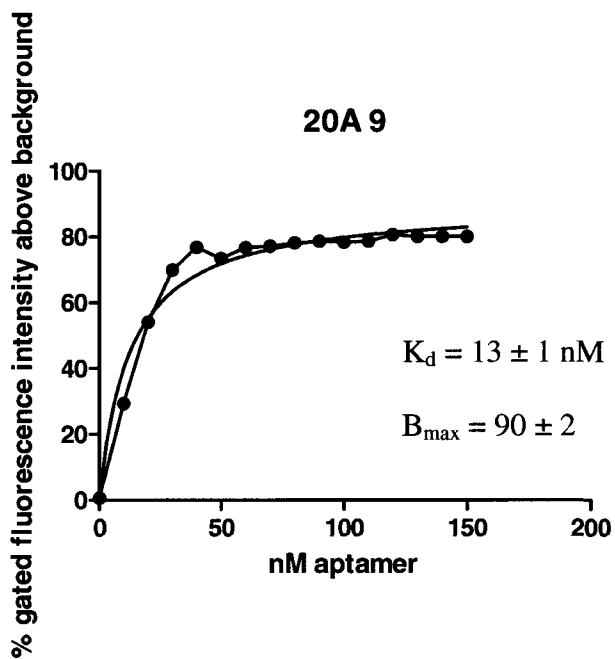
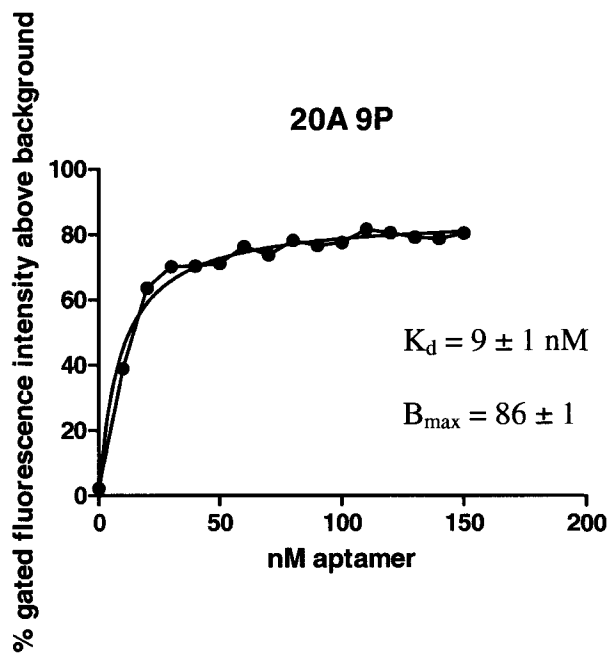


Figure 3.18. Binding of aptamers 20A9P and 20A9 to the mixture of *S. pyogenes* cells used in SELEX.

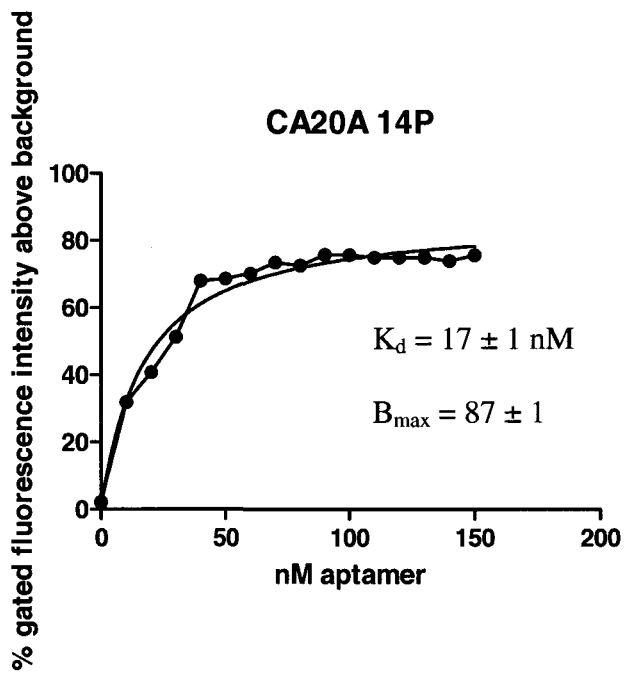
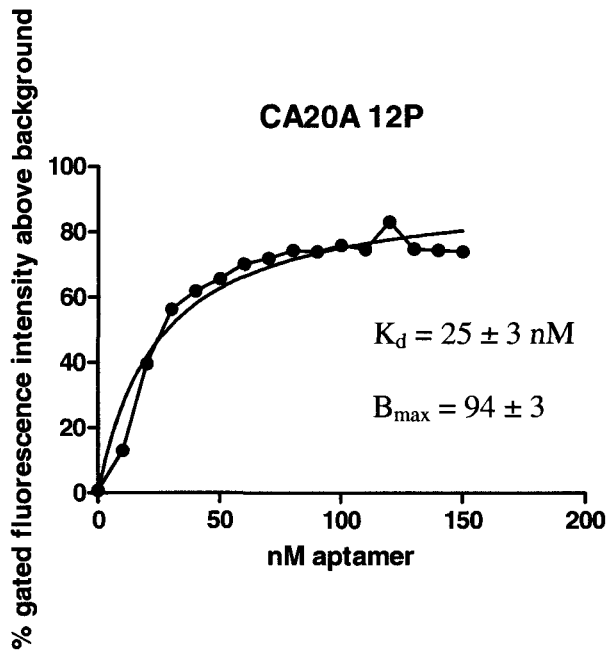


Figure 3.19. Binding of aptamers 20A12P and 20A14P to the mixture of *S. pyogenes* cells used in SELEX.

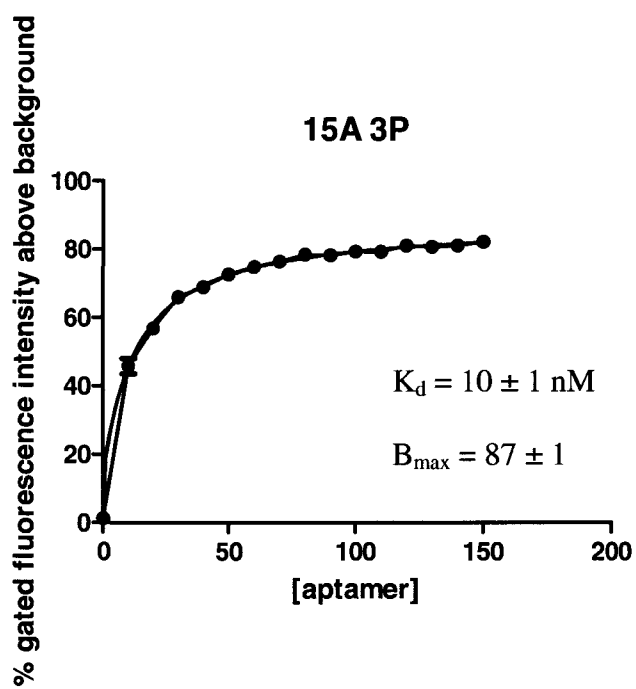
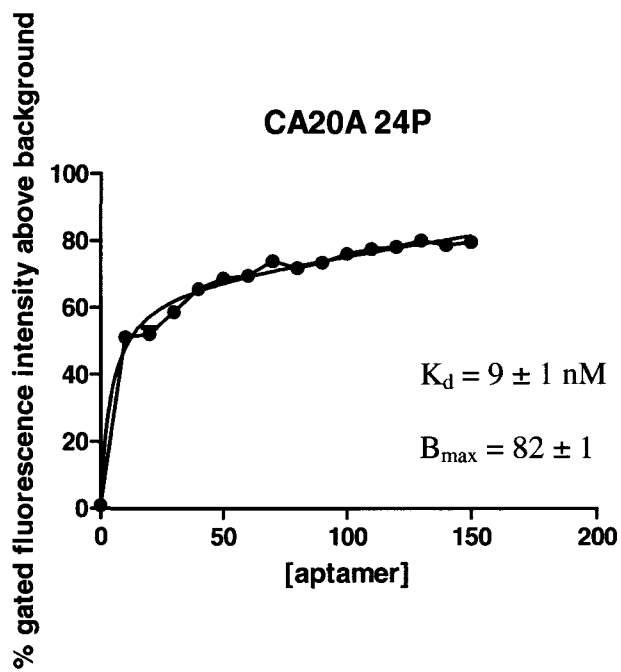


Figure 3.20. Binding of aptamers 20A24P and 15A3P to the mixture of *S. pyogenes* cells used in SELEX.

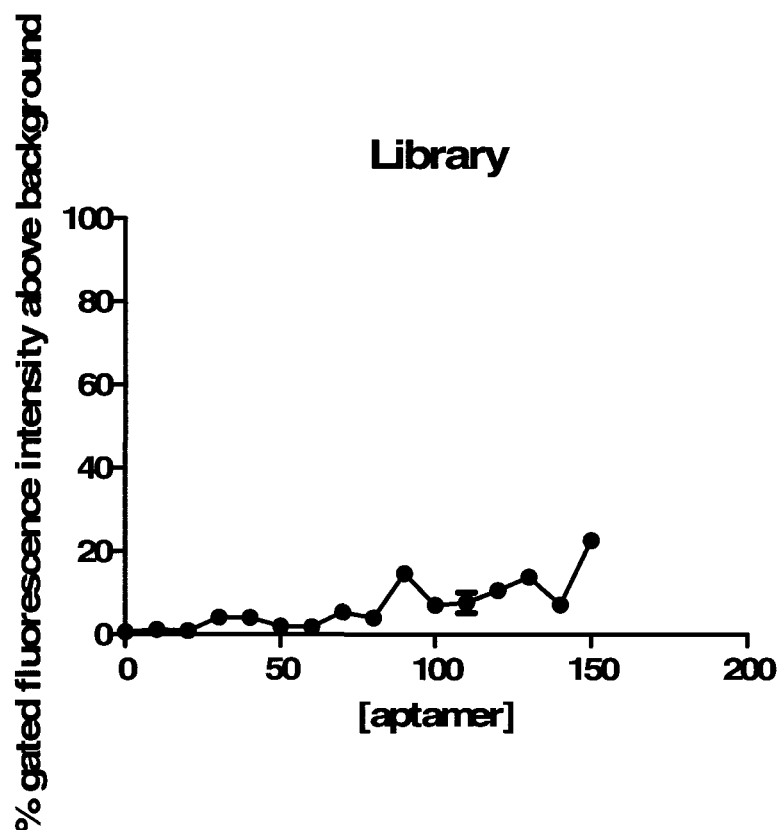


Figure 3.21. Binding of randomized oligonucleotide library to the mixture of *S. pyogenes* cells used in SELEX.

3.3.8 Selectivity of high affinity aptamers for *S. pyogenes*

Fluorescently-labeled aptamer sequences that demonstrated high affinity and low K_d s for the *S. pyogenes* M-types were tested against a variety of other bacteria including pathogens that could interfere with a diagnostic test. The aptamers chosen for testing were 20A8, 20A8P, 20A9, 20A9P, 15A3P, 20A24P, 20A12P and 20A14P. 20A1 and 20A1P were not chosen due to their higher K_d values and high variability of these predicted values (**Table 7**). Specifically, binding to other species of *Streptococcus* was tested using non-pathogenic

S. bovis, and the pathogens *S. pneumoniae* and *S. agalactiae* (Group B Streptococcus or GBS). *Escherichia coli* DH5 α was used to assess aptamer binding to a representative gram negative organism. Sequences were also screened against *Enterococcus* sp. since these are human flora and likely contaminants in diagnostic tests. For the *S. pneumoniae*, *S. agalactiae*, and *Enterococcus* isolates mixtures were prepared containing an equal number of cells from multiple isolates, as were the *S. pyogenes* mixtures used for selection. A summary of the isolates for each mixture is presented in **Table 8**.

None of the sequences bound strongly to any of the cells tested with the exception of 20A8, which seemed to have some affinity for the Group B Streptococcus (GBS) mixture (**Figure 3.22**). However, this affinity was low in comparison to the *S. pyogenes* target cell mixture. The percent gated fluorescence intensity above library background was 23% when 20A 8 was incubated with GBS cells and 72% when incubated with the original *S. pyogenes* target cell mixture (**Figure 3.10**), a three-fold difference which may or may not interfere in a diagnostic test. Inclusion of the primer sequences (20A8P) seems to negate GBS binding, bringing the percent gated fluorescence intensity above library background down to 1%. The same sequence (20A 8P) binding to the target GAS cells yielded 68% gated fluorescence above background (**Figure 3.10**). It can thus be concluded that the aptamer sequences tested are specific for *S. pyogenes*.

Table 8. List of all species, isolates and strains used to test selectivity of aptamers to *S. pyogenes*.

<i>Streptococcus agalactiae</i>	975R547 IV; JM9 VIII; 7271 VII; 975R390 VI; 965R400 Ia; 975R384 V; 12351 IV; 965R155 Ia; 975R938 II; 975R27 Ib; 975R331 IV; 955R2028 IV; 975R591; 975R138 II; 975R570 Ib; 975R104 VIII; 9842 VI; 975R594 III
<i>Streptococcus pneumoniae</i>	4; 6B; 9V; 14; 18C; 19F; 23F; 19A; 5; 6A
<i>Streptococcus bovis</i>	
<i>Enterococcus</i> sp.(ATCC #)	<i>E. saccharolyticus</i> (43076); <i>E. raffinosus</i> (49447); <i>E. pseudoarum</i> (49372); <i>E. mundtii</i> (43186); <i>E. malodoratus</i> (43197); <i>E. hirap</i> (8043); <i>E. gallinarium</i> (49573); <i>E. faecium</i> (19434); <i>E. faecalis</i> (19433); <i>E. durans</i> (19432); <i>E. cecorum</i> (43198); <i>E. casseliflavus</i> (25788); <i>E. avium</i> (14025)
<i>Escherichia coli</i>	DH5 α

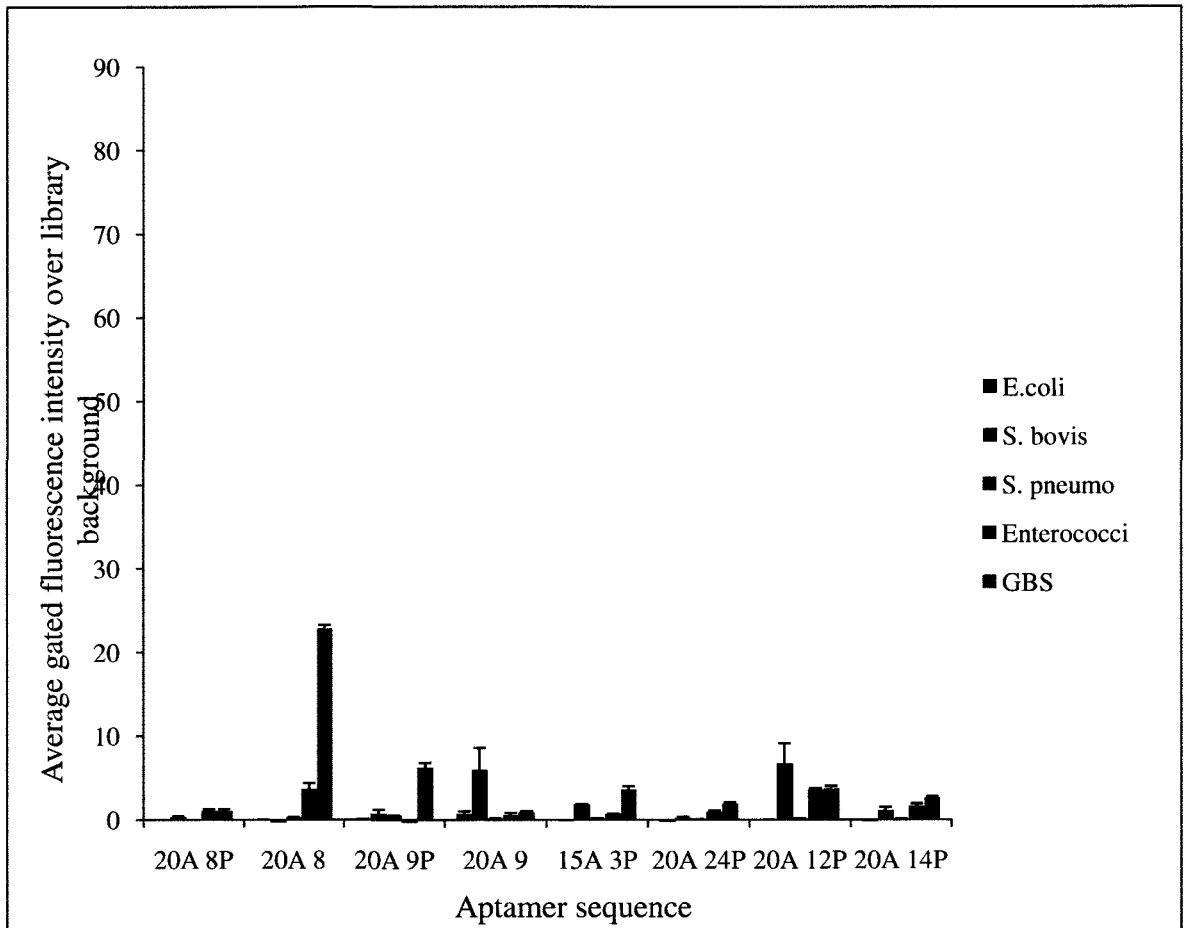


Figure 3.22. Selectivity of high affinity aptamer sequences for *S. pyogenes*. A total of 200 pmole of each aptamer was incubated with mixtures containing a total of 10^8 cells, and analyzed via flow cytometry as previously in Figure 3.10.

3.4 References

1. Beall B, Facklam R, Thompson T. Sequencing emm-specific PCR products for routine and accurate typing of group A streptococci. *J Clin Microbiol.* 1996 Apr;34(4):953-8.
2. Neal S, Beall B, Ekelund K, Henriques-Normark B, Jasir A, Johnson D, et al. International quality assurance study for characterization of streptococcus pyogenes. *J Clin Microbiol.* 2007 Apr;45(4):1175-9.
3. Beall B, Gherardi G, Lovgren M, Facklam RR, Forwick BA, Tyrrell GJ. Emm and sof gene sequence variation in relation to serological typing of opacity-factor-positive group A streptococci. *Microbiology.* 2000 May;146 (Pt 5)(Pt 5):1195-209.
4. Facklam R, Beall B, Efstratiou A, Fischetti V, Johnson D, Kaplan E, et al. Emm typing and validation of provisional M types for group A streptococci. *Emerg Infect Dis.* 1999 Mar-Apr;5(2):247-53.
5. Vlamincx BJ, Mascini EM, Schellekens J, Schouls LM, Paauw A, Fluit AC, et al. Site-specific manifestations of invasive group a streptococcal disease: Type distribution and corresponding patterns of virulence determinants. *J Clin Microbiol.* 2003 Nov;41(11):4941-9.
6. Sharkawy A, Low DE, Saginur R, Gregson D, Schwartz B, Jessamine P, et al. Severe group a streptococcal soft-tissue infections in ontario: 1992-1996. *Clin Infect Dis.* 2002 Feb 15;34(4):454-60.
7. Lancefield RC. A serological differentiation of human and other groups of hemolytic streptococci. *J Exp Med.* 1933 Mar 31;57(4):571-95.
8. Fischetti VA. Streptococcal M protein. *Scientific American.* 1991;264:58-65.
9. Baron S, editor. *Medical microbiology.* 4th ed. Galveston, Texas: The University of Texas Medical Branch; 1996.
10. Beachey EH, Stollerman GH, Chiang EY, Chiang TM, Seyer JM, Kang AH. Purification and properties of M protein extracted from group A streptococci with pepsin: Covalent structure of the amino terminal region of type 24 M antigen. *J Exp Med.* 1977 Jun 1;145(6):1469-83.
11. Hamula CL, Zhang H, Guan LL, Li XF, Le XC. Selection of aptamers against live bacterial cells. *Anal Chem.* 2008 Oct 15;80(20):7812-9.

Chapter 4

Modified Bacterial Cell-SELEX Against Group A

Streptococcus

4.1 Introduction

Our previous work has focused on developing aptamers that bind to cell surface molecules using the methodology in **Figure 2.1** (1). Two different types of cells, *L. acidophilus* and the pathogen *S. pyogenes*, were used as targets and aptamers with high affinity and selectivity were obtained. This methodology worked in only 7 SELEX cycles when *L. acidophilus* was used as a target, most likely due to the coating of the *L. acidophilus* cell surface with identical subunits of the same S-layer protein. However, 13 to 20 SELEX cycles were needed to generate a high affinity aptamer pool against *S. pyogenes* (**Figure 3.5**). The resultant aptamer pools were not M-type specific. Hence, changes were made to the existing protocol in order to improve it.

Downfalls of the previous methodology include a starting library diversity of only 10^{12} to 10^{13} different sequences and the use of heat denaturation or streptavidin-biotin mediated separation to render the library and aptamer pools single-stranded. Two sets of SELEX, GAS SELEX D and E, were carried out using modified protocols. Specifically, the amount of starting library, and hence the starting library diversity, was increased to either 10^{16} (SELEX D) or 10^{14}

(SELEX E). Also, the aptamer pools were rendered single-stranded via denaturing gel purification rather than heat denaturation in order to minimize the loss of sequence diversity due to reannealing. Furthermore, a counterselection step was introduced into SELEX D and E at round 3 with a non-pathogenic, non-target species of streptococcus, *S. bovis*. All other SELEX conditions were similar as in Hamula et al. (2008), except that the number of cells, incubation volumes, and incubation times were increased in proportion to the increased amount of DNA used in each round. This approach will enable us to compare the effect of increased library diversity versus increased copy number of each sequence and lower diversity. In addition, as with GAS SELEX A and B the M-type specific aptamers could be teased out of the aptamer pool by screening individual sequences, and if sequence diversity is too high the affinity and selectivity could be further enhanced by carrying out a second set of SELEX on the selected aptamer pool.

4.2 Experimental

4.2.1 Reagents

Bacterial strains and culture media. *Streptococcus pyogenes* clinical isolates corresponding to M types M1, M2, M3, M4, M5, M6, M11, M12, M28, M41, M49, M59, M75, M77, M82, M83, M89, M91, M92, and M114 were obtained from the National Centre for Streptococcus (Provincial Laboratory, Edmonton, AB). *S. pyogenes* isolates were streaked out on 5% defibrinated sheep's blood agar (Teknova, Hollister, CA) and single colonies were cultured in Todd-Hewitt

Broth (Oxoid, Nepean, ON). *Streptococcus bovis* and *Escherichia coli* were obtained from the American Type Culture Collection (ATCC) and were cultured in brain heart infusion (BHI) (Teknova) and Luria-Bertani (LB) media (BD Difco, Sparks, MD), respectively. *Streptococcus pneumoniae* (serotypes 4,6B, 9V, 14, 18C, 19F, 23F, 19A, 5, and 6A), *Enterococcus* sp. (*E. sacchrolyticus*, *E. raffinosus*, *E. pseudoaerium*, *E. mundtii*, *E. malodoratus*, *E. hirap*, *E. gallinarium*, *E. faecium*, *E. faecalis*, *E. durans*, *E. cecorum*, *E. casseliflavus*, *E. avium*) and Group B Streptococcus strains (975R547 IV, JM9 VIII, 7271 VII, 975R390 VI, 965R400 Ia, 975R384 V, 12351 IV, 965R155 Ia, 975R938 II, 975R27 Ib, 975R331 IV, 955R2028 IV, 975R591 III, 975R138 II, 975R570 Ib, 975R104 VII, 9842 VI, 975R594 III) were also obtained from the National Centre for Streptococcus. *S. pneumoniae* and *Enterococcus* sp. were on 5% defibrinated sheep's blood agar and streaked out cultured in BHI broth and GBS isolates were cultured in TH broth. All bacteria were cultured overnight in aerobic conditions at 37 °C, and all liquid cultures were shaken at 200 rpm. *E. coli* DH5 α -T1^R cells (Invitrogen, Carlsbad, CA) were used for all transformations.

DNA library. Two separate 80-nt oligonucleotide single-stranded DNA libraries consisting of a 40-nt randomized region flanked on both sides by 20-nt primer regions were used. The initial ssDNA library and the primers used to amplify it were obtained from Integrated DNA Technologies (Coralville, IA). SELEX set D was carried out using the single-stranded library containing a maximum of 10¹⁶ different sequences without amplification (as it arrived from IDT), while SELEX E was carried out using a second, PCR amplified library. The entire second

library was amplified for 3 cycles using the standard PCR conditions already described, and thus contained approximately 3–4 copies of the reverse strand of each of the original sequences. The total number of unique starting sequences used for SELEX E was about 10^{14} . Prior to incubation with target cells single-stranded oligonucleotides were treated via heat denaturation at 94 °C for 5 min and subsequent cooling at 0 °C for 10 min.

4.2.2. PCR amplification and gel electrophoresis

The forward primer contains a 5' polyA overlap of 20 adenine residues joined to the remaining primer sequence via a triethylene glycol spacer (IDT Spacer 9). The primers used to amplify the ssDNA library and subsequent aptamer pools have the following sequences:

Forward: 5'-A₂₀/5Sp9/AGCAGCACAGAGGTCAGATG-3'

5'-AGCAGCACAGAGGTCAGATG-3'

Reverse: 5'-TTCACGGTAGCACGCATAGG-3'

The PCR conditions for amplification of the DNA aptamer pools during SELEX were optimized after each round, in order to choose the highest cycle number at which misamplification products do not form. This cycle number was 3 for round 1, 7 for round 2, 7 for round 3 (counterselection round), 12 for round 4, and 20 for rounds 5–8. The amount of primers and nucleotides were increased compared to previous SELEX PCR conditions, in proportion to the increased amount of DNA being amplified. The standard PCR conditions were used for SELEX D and E: 1X PCR reaction buffer, 2 mM MgCl₂, 2.0 μM of each primer, 0.5 mM dNTPs, 1 E.U. of Platinum Taq DNA Polymerase, and 39.5 μL of

fraction supernatant (all reagents were from Invitrogen). Thermocycling parameters were 94 °C for 5 min denaturation, followed by up to 20 cycles of denaturation at 94 °C for 30 s, annealing at 57 °C for 30 s, and extension at 72 °C for 20 s. A final extension step of 72 °C for 5 min was carried out following the last cycle (MJ Mini Gradient Thermocycler; Bio-Rad Laboratories, Hercules, CA).

After PCR, the reaction products were visualized by separation on 7.5% non-denaturing polyacrylamide gel electrophoresis (PAGE) in 1X TBE buffer (Bio-Rad Protean III) at 60–120 V. The gels were stained with ethidium bromide, and photographed under UV light.

4.2.3. Denaturing gel electrophoresis and gel purification

DNA library or aptamer pools were rendered single-stranded via gel purification on a denaturing gel after amplification. Denaturing PAGE was carried out using 9% gels containing 8 M urea and 25% v/v formamide. After running the gel at 60–120 V and staining with ethidium bromide, the 100 nt forward strand could be distinguished from the 80 nt reverse strand, which was sliced from the gel. A Qiaex II Gel Extraction Kit (Qiagen) was used to purify the reverse strand from the slices. Upon purification single-stranded DNA was stored at -20 °C in 10 mM Tris-HCl pH 8.0.

4.2.4. Aptamer selection

Briefly, single colonies of the 10 most common *S. pyogenes* M-types (M1, M2, M3, M4, M6, M11, M12, M28, M77, and M89) were grown overnight in separate liquid cultures. The cells were then harvested the next morning in order

to decrease variability between M-types since surface molecule expression levels off in stationary phase. Aliquots containing the same number of cells from each culture were combined only once growth was complete. Cell mixtures were centrifuged at 6000x g and 4 °C for 10 minutes to remove media and to remove wash supernatants. Two separate sets of SELEX were carried out: SELEX D and SELEX E. The varying conditions of both SELEX sets are summarized in **Table 9**. Both SELEX D and E were initiated with ssDNA library (1 μmol initial round for SELEX D and SELEX E). The library used in SELEX E was only the reverse strand of the PCR-amplified initial library yet the same total amount of DNA (1 μmol) was used as in SELEX D. The aptamer pools used for incubation in SELEX D and E were decreased from 1 μmol for rounds 1 through 4, to 100 pmole for rounds 5 through 8. A total of 10⁹ cells, containing an equal number of cells of each M-type (10⁸), were used for each round of selection for both SELEX D and E. An excess of tRNA and BSA (Invitrogen) were added to the incubation buffer (20-fold molar excess of each in round 5, up to a maximum 60-fold molar excess in round 8) and 0.05% w/v BSA was added to the wash buffer in rounds 5 through 8. All washes and incubations were carried out in 1X Binding Buffer (1X BB) (50 mM Tris-HCl (pH 7.4), 5 mM KCl, 100 mM NaCl, 1 mM MgCl₂) at room temperature for 60 minutes. Incubation volumes for this set of selections were increased over previous sets (GAS SELEX A and B) and incubations were carried out under rotation in order to increase the likelihood of DNA and target cell contact. An initial incubation volume of 2 mL was used for round one, and this was decreased to 1 mL for round 2 and the counterselection round, 0.5 mL for

rounds 4 and 5, and 0.25 mL for rounds 6 to 8. A total of 3 washes were carried out for each round of SELEX D and E until round 5 at which the number of washes was increased to 4 in order to increase the stringency of the selection conditions. Aptamers were then eluted by heating the cells in 1X PCR Buffer (Invitrogen) at 94 °C for 5 minutes followed by 10 minutes on ice. The cells then centrifuged at 6,000x g and 4 °C for 10 minutes and the supernatant retained as the heat eluted (CA) fraction. The cell pellet was then resuspended in 1X PCR buffer and retained as the cell (Cells) fraction. A total of 8 rounds of SELEX D and 8 rounds of SELEX E were completed.

Table 9. Summary of conditions used in GAS SELEX D and E.

SELEX set	SELEX D	SELEX E
Initial starting library	Use entire IDT tube (10^{16} different sequences)	Amplify library and gel purify reverse strand (10^{14} different sequences)
Number of cells	10^9 Total cells 10^8 per M type	10^9 Total cells 10^8 per M type
Incubation	2 mL volume round 1 1 mL volume round 2 0.5 mL volume rounds 4, 5 0.25 mL volume rounds 6, 7, 8 1 hour at RT	2 mL volume 1 mL volume round 2 0.5 mL volume rounds 4, 5 0.25 mL volume rounds 6, 7, 8 1 hour at RT
Washes	Same as incubation volume	Same as incubation volume
CA fraction (heat-eluted)	500 μ L 1X PCR buffer 94°C for 5 minutes	500 μ L 1X PCR buffer 94°C for 5 minutes
Cell fraction	500 μ L 1X PCR buffer	500 μ L 1X PCR buffer
Number of PCR cycles	Optimize after each round until 20 cycles no longer produces misamplification	Optimize after each round until 20 cycles no longer produces misamplification

4.2.5. Counterselection

A counterselection step was carried out after 2 rounds of SELEX D and E against the *S. pyogenes* mixture. The purpose of the counterselection step is to remove sequences from the aptamer pools that are not specific for *S. pyogenes*. *S. bovis* liquid cultures were grown overnight in BHI broth at 37 °C and 200 rpm. Cells were harvested in the morning via centrifugation, and 10^9 cells were resuspended in 1X BB and incubated with 1 μ mole aptamer pool 2D or 2E in 1 mL final volume at room temperature for 60 minutes. Following incubation, the cells were treated as during SELEX, and the supernatant and three wash fractions were retained. The supernatant volume was 1 mL and each wash fraction was 1 mL. Aptamers from these fractions were ethanol precipitated, resuspended in 10 mM Tris pH 8.0, pooled, and then amplified under standard conditions using a polyA Sp9 forward primer and regular reverse primer. The 80-nt reverse strand of the resultant amplicons was gel purified as described previously.

4.2.6. Flow cytometric analysis

A FACScan flow cytometer with PowerMac G4 workstation and CellQuest software (Flow Cytometry Facility, Faculty of Medicine and Dentistry, University of Alberta) was used to assess the binding of the aptamer pool and individual aptamer sequences to different types of cells (*S. pyogenes*, *Enterococcus* sp., *S. pneumoniae*, *S. agalactiae*, *E. coli* DH5a, *S. bovis*). The aptamer pools were gel purified after fluorescent labeling via PCR amplification with 5'-FAM modified reverse primers (IDT) and the polyA-Sp9 forward primer, whereas the individual aptamer sequences were purchased with the fluorescent

label (5'-FAM) attached (IDT). Aptamer pools were heat denatured prior to incubation with bacterial cells. The binding assays were carried out by incubating 200 pmole of fluorescently-labeled aptamer/ aptamer pool with 10^8 cells for 45 min, as in the SELEX process, and then washing the cells once in 1X BB prior to resuspension in 1X BB for immediate flow cytometric analysis. In cases where mixtures of cells were used an equal number of each cell type was combined to a total of 10^8 cells for screenings and 10^9 cells for binding curves. Forward scatter, side scatter, and fluorescence intensity (FL1-H) were measured, and gated fluorescence intensity above background (cells with no aptamers added) was quantified. Fluorescently-labeled ssDNA library was used as a control for non-specific binding in each experiment. Binding curves were run to estimate K_d s by varying aptamer concentrations (0–150 nM incubation) with a fixed number of cells (10^9). GraphPad Prism 5.0 software was used to predict K_d values. All cultures used for flow cytometric screening were harvested in stationary phase in order to minimize differences in cell surface molecule expression.

4.2.7. Cloning, sequencing, and structural analysis of aptamers

The highest affinity aptamer pools measured via flow cytometry were chosen for sequencing analysis: pools 8D and 8E. Aptamer pools were cloned using a TOPO TA Cloning Kit for Sequencing (Invitrogen), transformed into *E. coli* DH5 α -T1^R cells (Invitrogen), and colonies containing the vector were selected via overnight incubation at 37 °C on LB plates containing 50 μ g/mL kanamycin. From each aptamer pool, 40 colonies were chosen for screening. The plasmid DNA was purified (Qiaex II gel extraction kit; Qiagen, Mississauga, ON) and analyzed for

the presence of an 80-bp insert via digestion with 1 U of EcoR1 at 37 °C for 30 minutes, followed by 7.5% native PAGE. A total of 80 inserts were then sequenced (Applied Genomics Center, Department of Medical Genetics, University of Alberta), yielding a total of 51 useable sequences. The secondary structure of each sequence both with and without primers was predicted using Oligoanalyzer 3.0 (IDT), with input conditions of room temperature (21°C) and 1 mM MgCl₂. The most likely sequence was taken as that with the lowest predicted free energy of formation (ΔG) (kcal/mole).

4.3 Results

4.3.1 Aptamer selection

A mixture containing an equal number of cells from each of the 10 most prevalent *S. pyogenes* M-types in Canada (148) was used as a target. A randomized ssDNA library is incubated with the cell mixture in order to select a pool of aptamers with increased affinity and selectivity for all the cells in the mixture. For SELEX D, an entire 1 μ mole library containing approximately 10^{16} unique sequences was used. For SELEX E, a second entire 1 μ mole library was PCR-amplified and the reverse strand was gel purified, leaving 3 to 4 copies of about 10^{14} unique sequences.

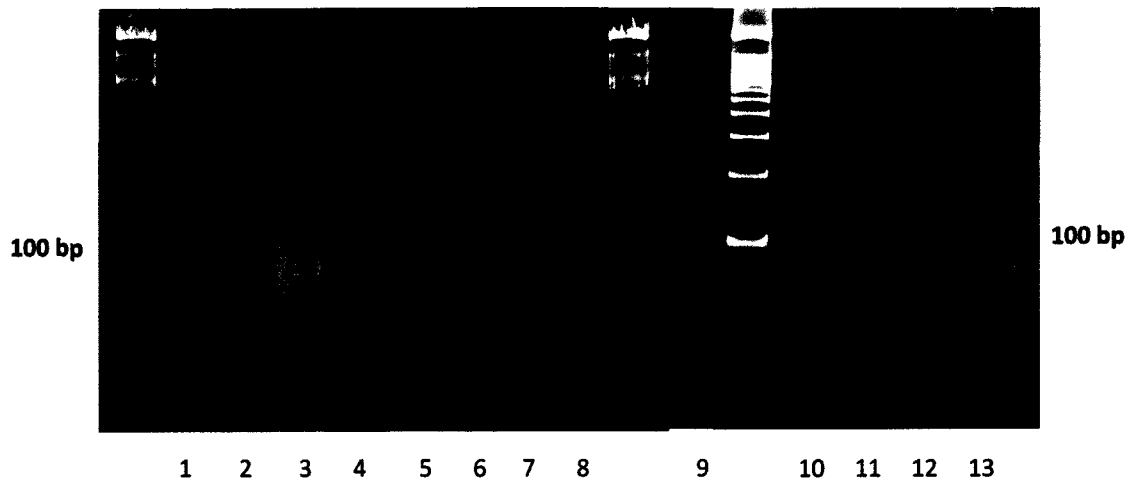
The different M-types were cultured separately prior to SELEX. A total of 8 rounds of SELEX D and 8 rounds of SELEX E were carried out. **Table 9** summarizes the amounts of DNA, cells and BSA/tRNA used in each round of selection. The amount of DNA used in each round of selection was maintained at

1 μ mole until later rounds (5-8) in order to minimize loss of potentially desirable aptamer sequences.

The randomized DNA libraries and aptamer pools were heated at 94 °C then cooled on ice prior to incubation with the GAS cell mixture. Fractions representing the incubation supernatant (So), washes (W), heat eluted aptamers (CA), and cell-bound aptamers (Cells) were collected and amplified following incubation. As can be seen in **Figure 4.1**, in SELEX D the majority of the DNA is retained in the supernatant fraction (**Lane 3**). A substantial amount of DNA sticks to the cells even after the second wash (**Lane 7**). Hence, the number of washes was increased to three at which point no more DNA comes off the cells (**Lane 9**). The aptamers were then heat eluted from the cells at high temperature in low salt (**Lane 11**). Cells pellets were resuspended in PCR buffer and any aptamer sequences that remained bound after elution were amplified (**Lane 13**). Since the fractions in **Figure 4.1** were run on a denaturing gel the separation of the 100 nt and 80 nt fragments can be seen, particularly in the CA and Cells fractions (**Lanes 11 and 13**). A negative control consisting of cells without added DNA library was run concurrently (**Lanes 2,4,6,8,10,12**). A native PAGE gel was run after amplification of the first round fractions of SELEX E (**Figure 4.2**). There are several key differences between the first round gels of SELEX E and SELEX D. During SELEX E, most of the DNA is retained in the supernatant (**Lane 3**) but the total amount of DNA amplified is lower than the supernatant of SELEX D. Also, DNA is still released from the cells after three washes in SELEX E but not SELEX D (**Figure 4.2 Lane 9**). The separation of the 100 nt and 80 nt bands is

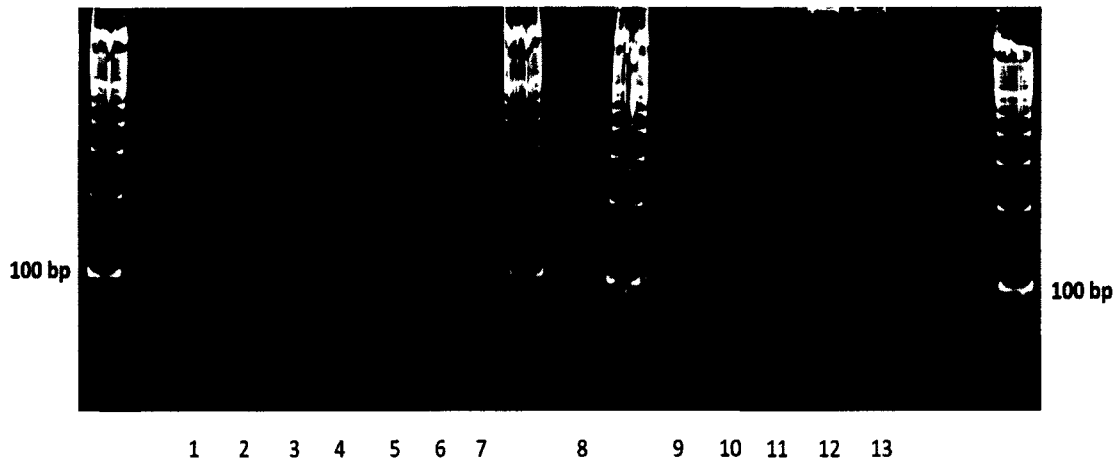
not seen in the SELEX E gels since they are native PAGE gels. For the rest of the SELEX rounds, collected fractions were run on native PAGE for the purpose of visualizing the results of PCR amplification of the various fractions (**Appendix Figures A41 to A47**). The CA and cell fractions were amplified separately and run on denaturing PAGE for the purpose of gel purifying single-stranded DNA for the next round of SELEX.

After each round of SELEX D and E, samples of the resultant aptamer pools were subjected to varying PCR cycle numbers in order to determine the highest cycle number at which misamplification does not occur. When a large number of different sequences are present, as in an oligonucleotide library, some of these sequences will inevitably bind to each other and form longer PCR amplicons. A set of test reactions was carried out prior to amplification of the majority of the CA and cell fraction for gel purification. The test reactions were carried out after each SELEX round until round 5, at which point the aptamer pool reached a low enough diversity that it could be amplified for 20 cycles without formation of misamplification products. The amplification of library with increasing cycle number is shown in **Figure 4.3**. Formation of misamplification products can be seen after round 3, so increasing the number of PCR cycles beyond this point will only result in decreased yield of the 80 bp band. Hence, the library was only amplified for 3 rounds prior to SELEX E.



1=neg control PCR; 2=neg So; 3= library So; 4=neg W1; 5=W1; 6=neg W2; 7=W2; 8=neg W3; 9=W3; 10=neg CA; 11=CA fraction; 12=neg cells; 13=cell fraction

Figure 4.1. Denaturing PAGE of fractions collected and amplified after round 1 of SELEX D. A randomized, single-stranded DNA library containing 10^{16} unique sequences was incubated with a mixture of 10 different M-types of *S. pyogenes* cells. Following incubation, the cells were centrifuged to remove the incubation supernatant (So) and repeatedly washed and centrifuged in binding buffer to remove DNA sequences that are non-specifically or weakly bound (W1, W2, W3). The cells were next heated at 94 °C, the suspension was centrifuged, and the supernatant was collected containing the heat-eluted cell aptamer fraction (CA). The cell pellet was resuspended in 1X PCR Buffer to comprise the Cell fraction. A SELEX negative control was carried out in which cells were incubated in the absence of DNA library (negSo), washed (negW1, negW2, negW3), and heat-eluted (negCA) then resuspended (neg cells). The different fractions collected during SELEX (So, W1-W3, CA) and the parallel negative control were PCR amplified and analysed via 9% denaturing PAGE. Unlabelled lanes on the gel contain the DNA ladder (100–2072 bp) and lane 1 contains the PCR negative control.



1=neg control PCR; 2=neg So; 3= library So; 4=neg W1; 5=W1; 6=neg W2; 7=W2; 8=neg W3; 9=W3; 10=neg CA; 11=CA fraction; 12=neg cells; 13=cell fraction

Figure 4.2. Native PAGE of fractions collected and amplified after round 1 of SELEX E. A randomized, single-stranded DNA library containing approximately 10^{14} unique sequences was incubated with a mixture of 10 different M-types of *S. pyogenes* cells. Following incubation, the cells were centrifuged to remove the incubation supernatant (So) and repeatedly washed and centrifuged in binding buffer to remove DNA sequences that are non-specifically or weakly bound (W1, W2, W3). The cells were next heated at 94 °C, the suspension was centrifuged, and the supernatant was collected containing the heat-eluted cell aptamer fraction (CA). The cell pellet was resuspended in 1X PCR Buffer to comprise the Cell fraction. A SELEX negative control was carried out in which cells were incubated in the absence of DNA library (negSo), washed (negW1, negW2, negW3), and heat-eluted (negCA) then resuspended (neg cells). The different fractions collected during SELEX (So, W1-W3, CA) and the parallel negative control were PCR amplified and analysed via 7.5% native PAGE. Unlabelled lanes on the gel contain the DNA ladder (100–2072 bp) and lane 1 contains the PCR negative control.

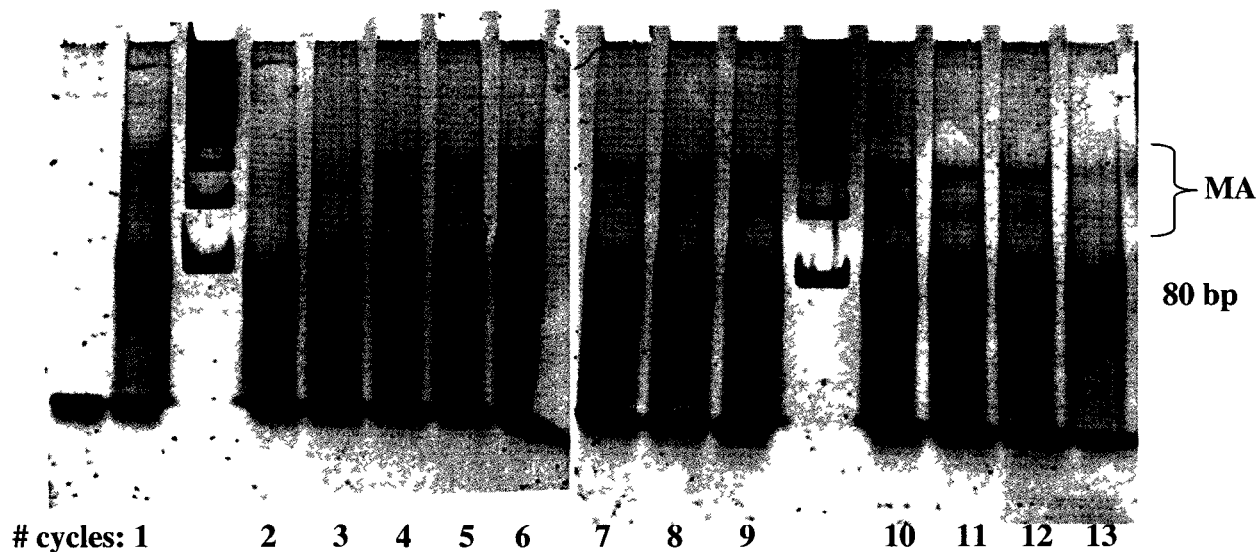
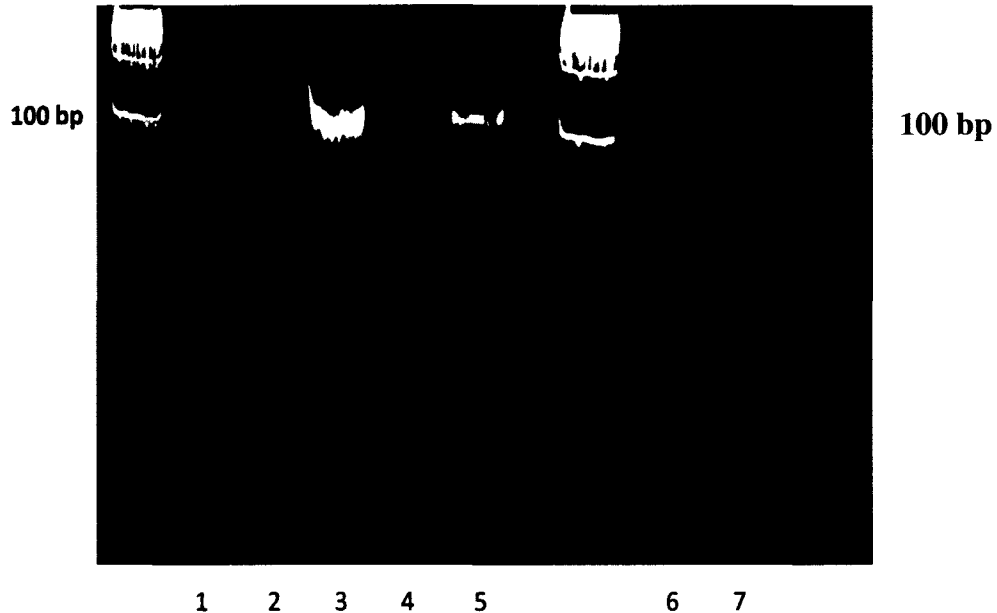


Figure 4.3. PAGE gel showing amplification of library with increasing PCR cycle number. Randomized oligonucleotide library was PCR-amplified under standard SELEX conditions and run on a 7.5% PAGE gel. PCR amplification was terminated after 1 to 13 cycles. Formation of misamplification products (MA) can be seen after 3 cycles.

4.3.2 Counterselection

A round of counterselection was performed after 2 rounds of SELEX D and E against the *S. pyogenes* mixture. This counterselection round was named SELEX 3D and 3E. For counterselection, *S. bovis* was used as a target in order to remove non-*S. pyogenes* specific sequences from the aptamer pools. The entire aptamer pools D and E (1 μ mole) were each incubated with 10^9 *S. bovis* cells under the same conditions as during SELEX. Following incubation, the supernatant and wash fractions were retained and amplified (**Figure 4.4**). The cells were washed three times but DNA was only amplified from the supernatant

fractions (**Lanes 3 and 5**) and the first wash fractions (**Lanes 6 and 7**). The majority of the DNA remained in the supernatant fractions. Following PCR supernatant and wash 1 fractions were pooled, concentrated via ethanol precipitation, and resuspended for use in the next round of SELEX D and E (round 4).



1=neg control PCR; 2=neg So 3D; 3= So 3D 4= neg So 3E; 5=So 3E; 6=W1 3D; 7=W1 3E;

Figure 4.4. Native PAGE of supernatant and wash fractions collected and amplified after round 3 (counterselection) of SELEX D and E. Aptamer pools 2D and 2E were incubated with 10^9 *S. bovis* cells. Following incubation, the cells were centrifuged to remove the incubation supernatant (So) and repeatedly washed and centrifuged in binding buffer to remove DNA sequences that are non-specifically or weakly bound (W1, W2, W3). A negative control was carried out in which cells were incubated (negSo) and washed negW1, negW2, negW3) in the absence of DNA library. The fractions were PCR amplified and analysed via 7.5% native PAGE. Unlabelled lanes on the gel contain the DNA ladder (100-2072 bp) and lane 1 contains the PCR negative control. Only the So and W1 fractions contained DNA, hence they are the only ones shown above.

4.3.3 Binding affinity and selectivity of aptamer pools following each round of selection

After each round of selection, the aptamer pools were assessed for binding affinity and selectivity to the target *S. pyogenes* cells using flow cytometry (Figure 4.5). The CA fractions and cell fractions obtained after each round of selection were pooled and then fluorescently-labeled and used in flow cytometric assays to assess aptamer pool affinity for the *S. pyogenes* mixture as a whole and selectivity for each separate M-type. A fluorescently-labeled randomized oligonucleotide library was run during each experiment as a control to assess non-specific DNA adhesion to the cells. The aptamer pools were rendered single-stranded via amplification with the polyA forward primer and a fluorescently-labeled reverse primer, and then gel purification of the reverse strand.

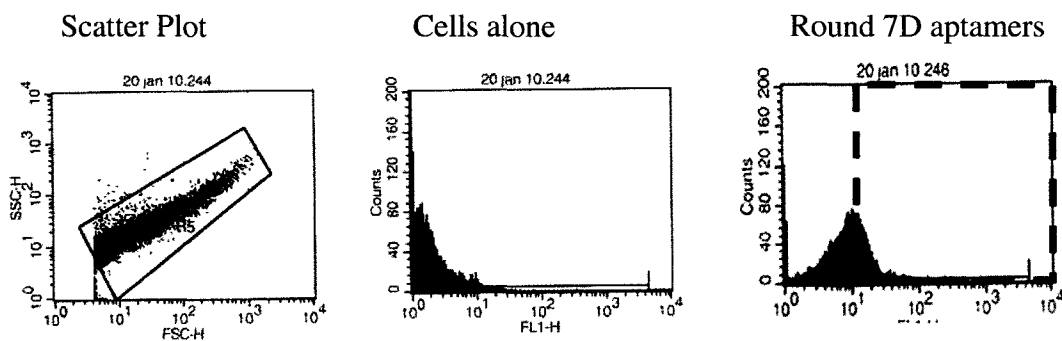


Figure 4.5. Typical flow cytometry outputs from screening of aptamer pools following each round of selection, showing increase in gated fluorescence intensity above background (dashed boxed area) following incubation with round 7D aptamer pool.

Flow cytometric analyses of incubation mixtures containing fluorescently-labeled aptamer pools from SELEX D and the target cells show that with increasing rounds of selection, the percent of cells with fluorescence above library background increased to a maximum average of 39 % at round 8 for SELEX D aptamer pools and 13% at round 7 for SELEX E (**Figure 4.6**). The increase in the number of fluorescent cells is due to the increased binding of the fluorescent aptamers to the target cells. Controls carried out using fluorescent aptamer pools alone and buffer with BSA and tRNA alone did not yield any increase in gated fluorescence above background levels (data not shown).

For SELEX D, aptamer pool binding did not start to increase above background until round 4; whereas for SELEX E the increase was sooner, after round 1 (**Figure 4.6**). However, for SELEX E binding did not increase significantly after counterselection (**round 3**), remaining at a similar level for rounds 4-8. For SELEX D, binding steadily increased after counterselection (**round 3**), decreasing in round 6 only to recover again in rounds 7 and 8. The maximum gated fluorescence intensity over library of 39% of the SELEX D aptamer pool to the target mixture of *S. pyogenes* cells was lower than the 67% maximum gated fluorescence intensity above background seen for the aptamer pools following selection against *Lactobacillus acidophilus* (**Figure 2.3**). However, it was higher than for GAS SELEX A and B, which had maximum binding above background values of 14% and 21%, respectively (**Figure 3.5**).

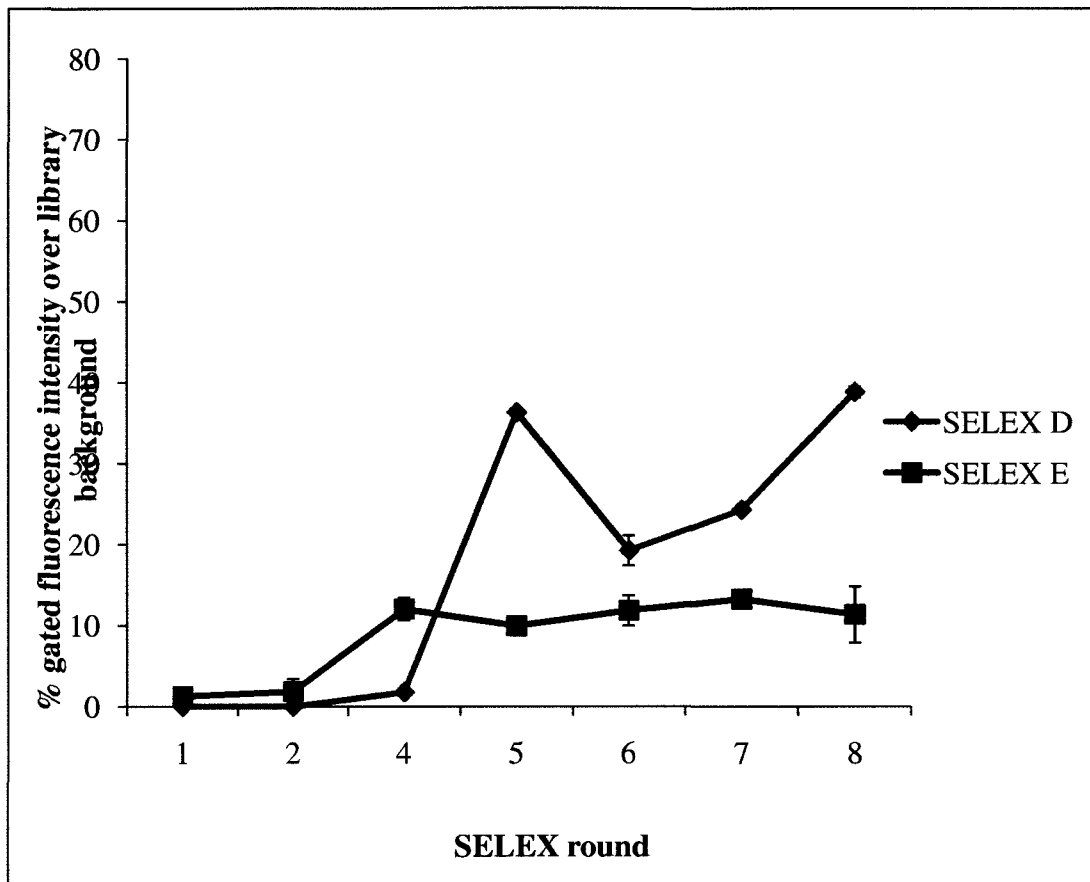


Figure 4.6. Change in percent gated fluorescence intensity of *S. pyogenes* cells incubated with fluorescently-labeled aptamer pools after increasing SELEX D and E rounds.

4.3.4 Cloning and sequence analysis of aptamer pools

Upon confirmation that aptamer pool binding was increasing with SELEX rounds, the SELEX D and E aptamer pools were cloned and sequenced after the 8th rounds. These pools displayed the highest affinity of later rounds for the target cells when screened via flow cytometry (**Figure 4.6**). A total of 51 sequences from the aptamer pools were obtained, 25 for SELEX D and 26 for SELEX E. Heat eluted (CA) and cell-bound (cells) fractions from round 8 were cloned

separately. Secondary structures were predicted using Oligoanalyzer 3.1 (Integrated DNA technologies) for all the sequences. All sequences were analyzed both with and without primers. A summary of all the sequences, their most likely predicted secondary structures and corresponding lowest free energies of formation can be found in **Appendix Tables A3.1 to A3.3**. There was a high amount of repetition within this collection of sequences, and many sequences contained high GC content, indicative of potential formation of secondary structures. Many of the secondary structures formed were similar even if the sequences were similar but not identical. Within this collection of sequences, there were two sequences, 8D cells 1 and 8D cells 9, that were highly repeated within and between the D and E aptamer pools. 8D cells 1 was repeated 13 times in the SELEX D pool, and 7 times in the SELEX E pool. 8D cells 9 was repeated 12 times in the SELEX D pool and 14 times in the SELEX E pool. These sequences can be found in **Table 9**. The sequences 8D cells 1 and 8D cells 9 formed similar secondary structures both with and without primers, both of which can be seen in **Figure 4.7**. Other sequences sharing these secondary structural motifs were often similar yet not identical. For example, 8D cells 9 and 8D cells 20 are two such sequences (**Table 9**). There were several other sequences and structural motifs that were repeated both within and between aptamer pools (**Tables A3.1 to A3.3**). Repetitive sequences or sequences with repetitive structural motifs, sequences with complex secondary structures, hairpin structures similar to hemag1P, and sequences with free energies of formation below -7 kcal/mole were all subjected to further screening. **Tables 10 and 11** summarize

the sequences chosen for screening. One sequence, 8D CA cells 6, was found within both the CA and cell fractions of aptamer pool 8D.

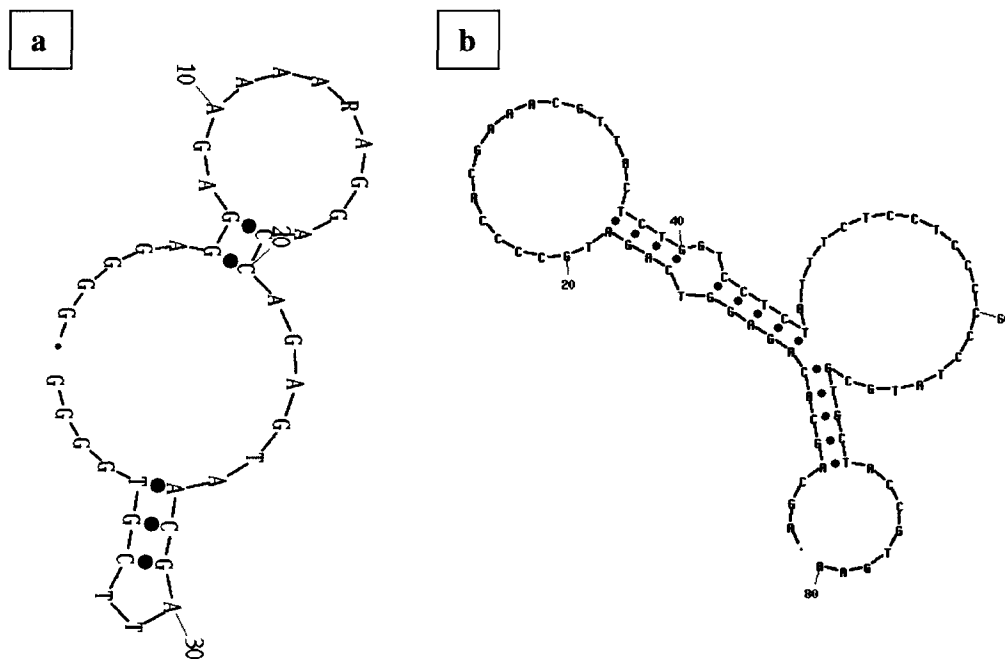


Figure 4.7. Common secondary structural motifs DE1 (a) and DE2 (b).

Table 10. Screened SELEX 8D aptamer pool sequences with (CA cells 6P, CA 17P, cells 1P, cells 9P, cells 20P) and without (CA cells 6, CA 17, cells 1, cells 9, cells 20) primers. Shown here are the aptamers selected from a total of 25 aptamers for which sequences were obtained. The fluorescent label FAM is shown at the 5'-end. The underlined sequences are the primers.

Name	Sequence
8D CA cells 6	5'FAM/GACGGGCGAGGAGGGGACCTCAAGTGGGTTTCGGTG-3'
8D CA cells 6P	5'FAM/ <u>AGCAGCACAGAGGTCAGATGGACGGGCGAGGAGGG</u> GACCTCAAGTGGGTTTCGGT <u>GCCTATGCTGCTACCGTGAA</u> -3'
8D CA 17	5'FAM/ GACGGTCTGAGGGAGGGGACCTCAAGTGGGTTTCGGTG-3'
8D CA 17P	5'FAM/ <u>AGCAGCACAGAGGTCAGATGGACGGTCTGAGGGAGG</u> GGACCTCAAGTGGGTTTCGGT <u>GCCTATGCGTGCTACCGTGAA</u> -3'
8D cells 1	5'FAM/ CCCCACGAATCGGTACTCTGGTCCTCTATTTCTCCTCCCC-3'
8D cells 1P	5'FAM/ <u>AGCAGCACAGAGGTCAGATGCCCCACGAATCGGTACTC</u> TGGTCCTCTATTTCTCCTCCCC <u>CCTATGCGTGCTACCGTGAA</u> -3'
8D cells 9	5'FAM/ GGGGAGGAGAAAAAGAGGACCAGAGTAACGATTCGTGGGG-3'
8D cells 9P	5'FAM/ <u>TTCACGGTAGCACGCATAGGGGGGAGGAGAAAAAGAGG</u> ACCAGAGTAACGATTCGTGGGG <u>CATCTGACCTCTGTGCTGCT</u> -3'
8D cells 20	5'FAM/ GGGGAGGAGAAATAGAGGACCAGAGTAACGATTCGTGGGG-3'
8D cells 20P	5'FAM/ <u>TTCACGGTAGCACGCATAGGGGGGAGGAGAAATAGAGGA</u> CCAGAGTAACGATTCGTGGGG <u>CATCTGACCTCTGTGCTGCT</u> -3'

Table 11. Screened SELEX 8E aptamer pool sequences with (CA cells 4P, CA 9P, CA 20P, cells 1P) and without (CA 4, CA 20) primers. Shown here are the aptamers selected from a total of 26 aptamers for which sequences were obtained. The fluorescent label FAM is shown at the 5'-end. The underlined sequences are the primers.

Name	Sequence
8E CA 4	5'FAM/ GGCACCAAGCAAAAATCGTAATGTTGGTGGTACACTTCGG-3'
8E CA 4P	5'FAM/ <u>TTCACGGTAGCACGCATAGGGGCACCAAGCAAAAATCGTA</u> ATGTTGGTGGTACACTTCGG <u>CATCTGACCTCTGTGCTGCT-3'</u>
8E CA 9P	5'FAM/ <u>AGCAGCACAGAGGTCAGATGCCTCACGAACGGTACTCTGGT</u> CCTCTATTTCTCCTCCCCCTATGCGTGCTACCGTGAA-3'
8E CA 20	5'FAM/ CACACACGGAACCCCGACAACATACATACGGTGAGGGTGG-3'
8E CA 20P	5'FAM/ <u>TTCACGGTAGCACGCATAGGCACACACGGAACCCCGACAAC</u> ATACATACGGTGAGGGTGGC <u>ATCTGACCTCTGTGCTGCT-3'</u>
8E cells 1P	5'FAM/ <u>TTCACGGTAGCACGCATAGGGGGGAGGAGAAAAGAGGACCA</u> GAGTAACGATTCGTGGGGC <u>ATCTGACCTCTGTGCTGCT-3'</u>

4.3.5 Binding of individual aptamer sequences to target cell mixture

Aptamer sequences were synthesized to contain a fluorophore (FAM) on the 5' end. Each fluorescently-labeled aptamer was incubated with the target mixture of 10 *S. pyogenes* M-types used for selection. These incubations were washed and the cells were subjected to flow cytometry without elution of the aptamers from the cell surface. Results of these screenings are summarized in **Figures 4.8 and 4.9**. As predicted from the aptamer pool binding profiles in

Figure 4.6, SELEX D seemed to produce more high affinity aptamers than SELEX E. None of the SELEX E sequences tested showed significant binding to the *S. pyogenes* mixture (**Figure 4.9**); neither did any of the SELEX D sequences found in the CA fraction (**Figure 4.8** 8D 6, 6P, CA 17, 17P). However, the aptamer sequences unique to the SELEX D cells fractions seem to have the highest affinity for the cell mixture (**Figure 4.8** 8D cells 9,9P, 20, 20P, 1, 1P). All 6 sequences unique to the SELEX D cell fraction pool had greater than 50% gated fluorescence intensity above a randomized library control. These sequences are summarized in **Table 10**; their predicted secondary structures are in **Figure 4.10**. Sequences 8D cells 1, 8D cells 1P (with primers), were the highest binders with gated fluorescence above background values of 75% and 71%, respectively. The second highest binding sequence was 8D cells 9P with a gated fluorescence above background of 65%. The 8D cells 9, 20, and 20P had percent gated fluorescence intensities above library of 55%, 55%, and 61% respectively.

The high affinity sequences all have very similar secondary structures (**Figure 4.10**). Sequences 8D cells 1, 9, and 20 have virtually identical secondary structures similar to sequence motif DE1 (**Figure 4.10**). The sequence 8D cells 1 has only 4 base-pairing interactions in its predicted secondary structure whereas 8D cells 9 and 20 have 5. In the presence of primers, 8D cells 9 and 20 form identical secondary structures. The 8D cells 1 form a different secondary structure when primers are included, similar to motif DE2 (**Figure 4.10**). The small differences in secondary structure of 8D cells 1 and 1P from the other sequences seems to account for their slightly higher binding to the target cell mixture over

the other sequences (**Figure 4.8**). The similarity of the predicted secondary structures of 8D cells 9 and 20 is hardly surprising due to their sequence similarity (**Table 10**). The affinity of these three aptamers for the *S. pyogenes* mixture changes minimally upon inclusion or exclusion of primers in the sequence; hence the target binding site must be in a central region of the sequence.

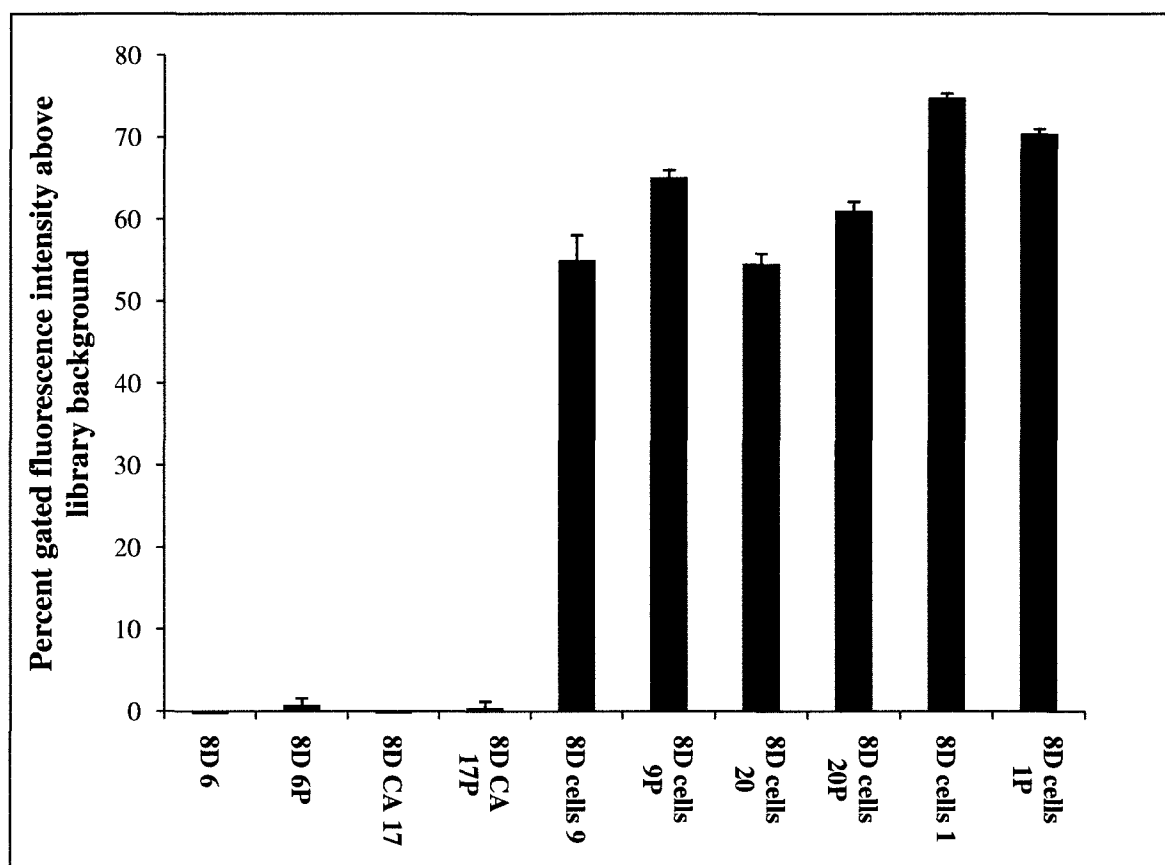


Figure 4.8. Screening of sequences from SELEX 8D aptamer pools. All aptamers were fluorescently-labeled with 5'-FAM. Aptamers were incubated with a mixture of the 10 most prevalent GAS M-types in Canada. Incubations and centrifugation were carried out as previously. A ratio of 200 pmole of aptamer and 10^8 total cells was used.

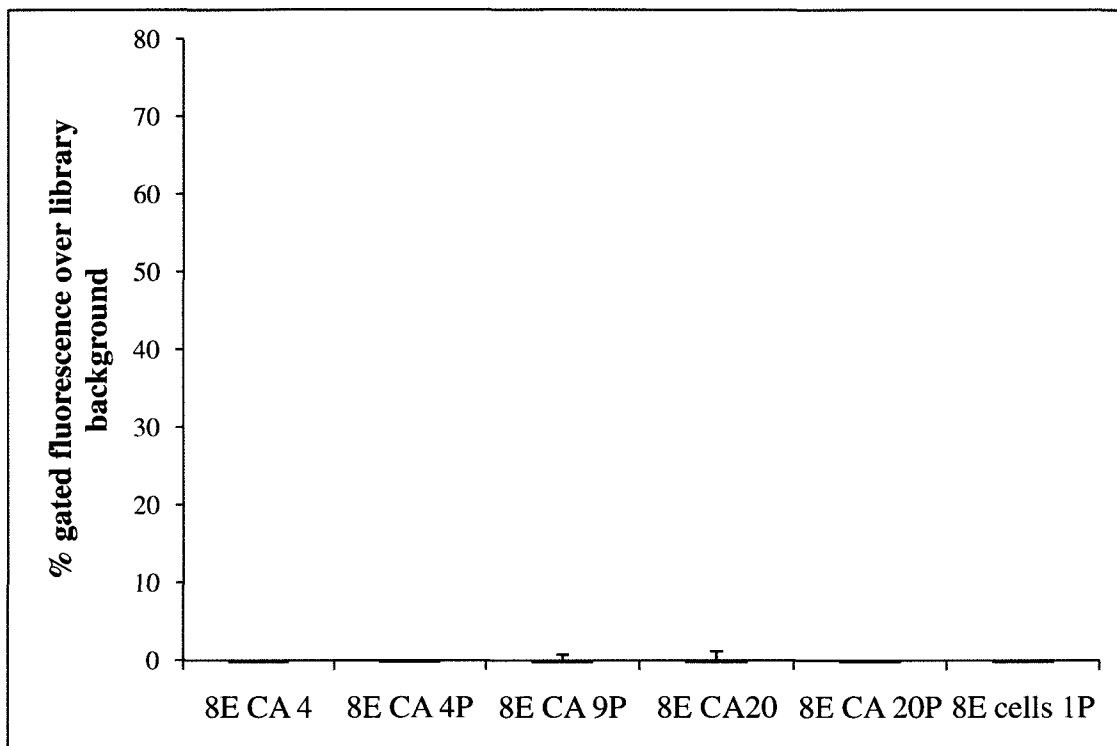


Figure 4.9. Screening of sequences from SELEX 8E aptamer pools. All aptamers were fluorescently-labeled with 5'-FAM. Incubations and centrifugation were carried out as previously. A ratio of 200 pmole of aptamer and 10^8 cells was used.

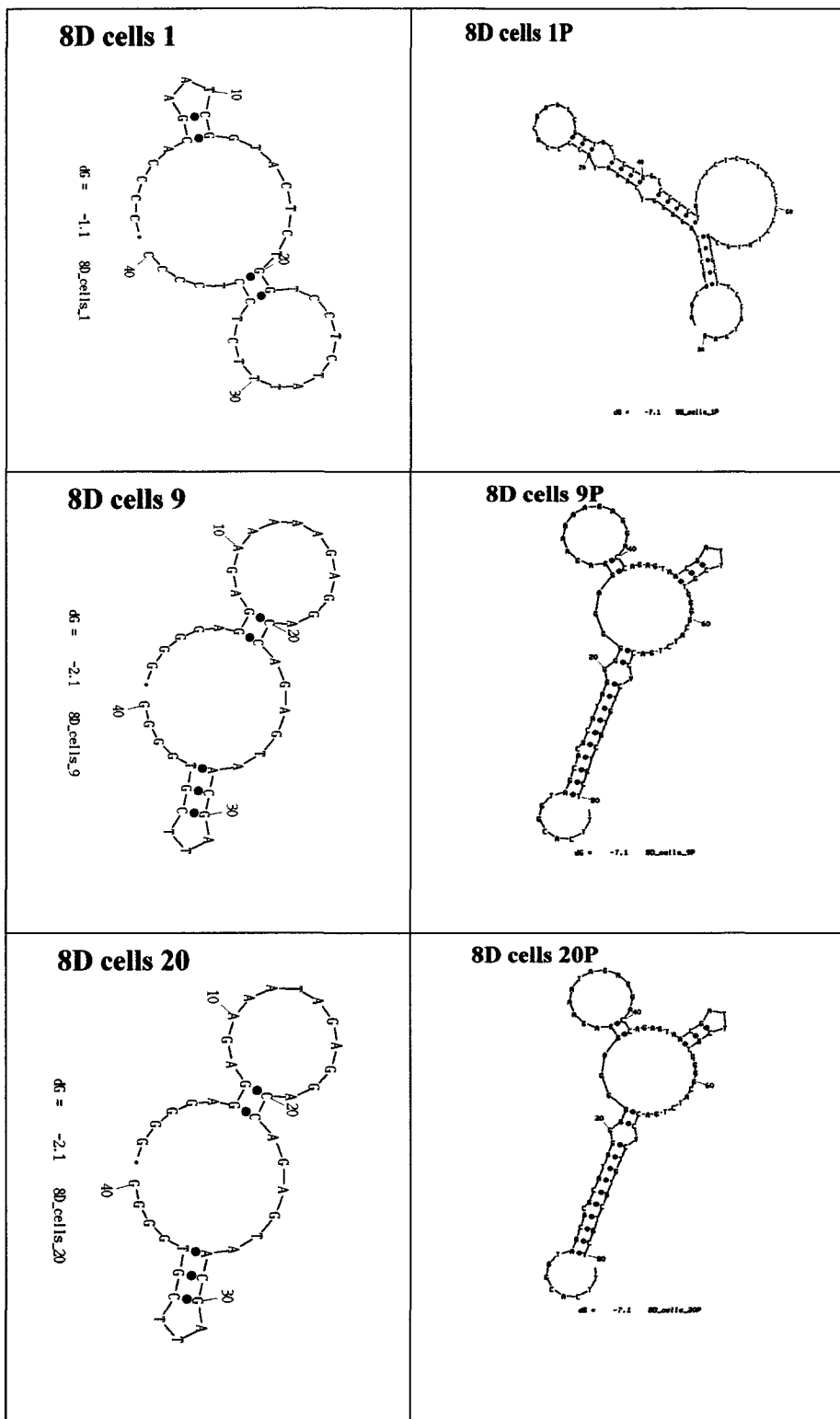


Figure 4.10. Predicted structures of aptamer sequences with high affinity for *S. pyogenes*.

4.3.6 Binding of aptamers to specific M-types

Individual aptamer sequences from both SELEX D and E could be classified into two groups based on the results of screening against a mixture of 10 different *S. pyogenes* M-types (**Figures 4.8 and 4.9**): high and low affinity. Representative sequences from these two groups were then screened via flow cytometry against each M-type separately. Sequences 8E CA 20, 8E CA 20P, and 8E cells 1P were chosen from the SELEX E pool. Since 8D cells 9 and 8D cells 20 are virtually identical sequences, 8D cells 9 and 8D cells 9P were chosen for further screening along with 8D cells 1 and 1P from the SELEX D pool. A fluorescently-labeled randomized oligonucleotide library was used as a negative control.

The selection resulted in aptamer pools containing a mixture of sequences with different affinities for different targets. The affinity of a given sequence for the *S. pyogenes* mixture did not always mirror its affinity for each M-type; for certain sequences it mirrors selectivity. The low affinity sequences tested are all specific for M11 cells; all exhibit binding to M11 cells only with percent gated fluorescence intensities below 20% (**Figure 4.11**). Sequences 8D cells 1 and 8D cells 1P have broad spectrum affinities for most M-types, with demonstrable binding to all M-types except M2 for 8D cells 1 and M1, M2, M3, and M4 for 8D cells 1P (**Figure 4.12**). The sequence 8D cells 9P also has broad-spectrum affinity for all M-types except M1 and M3 (**Figure 4.12**). The most surprising result is that the sequence 8D cells 9 appears to be specific for M11 cells, binding only to M11 cells with a percent gated fluorescence intensity above library background of

16 % (**Figure 4.1**). This result is surprising since 8D cells 9 has a relatively high affinity for the overall mixture (55% gated fluorescence intensity above background in **Figure 4.8**) but demonstrates only a medium range affinity for M11 cells and no affinity for other M-types. The addition of primers to the sequence 8D cells 9 seems to negate its selectivity, also resulting in higher affinity for the *S. pyogenes* mixture (65% gated fluorescence intensity above library background in **Figure 4.8**).

Since most of the high affinity aptamer sequences tested are not M-type specific, they are expected to bind *S. pyogenes* M-types other than the 10 used for SELEX. A cell mixture containing 10 M-types not used for selection was incubated with fluorescently-labeled aptamers and analyzed via flow cytometry (**Figure 4.13**). Sequences 8D cells 1, 8D cells 1P, 8D cells 9, and 8D cells 9P were tested. The M-types included in the mixture were M5, M41, M49, M59, M75, M82, M83, M91, M92, and M114. Binding to this mixture was lower than to the target mixture for all sequences tested, but was still significant ranging from 37% for 8D cells 1P to 21% for 8D cells 1. The aptamer sequence 8D cells 9 also bound to these other M-types with a percent gated fluorescence intensity of 30%; it proved not to be specific for M11 after all.

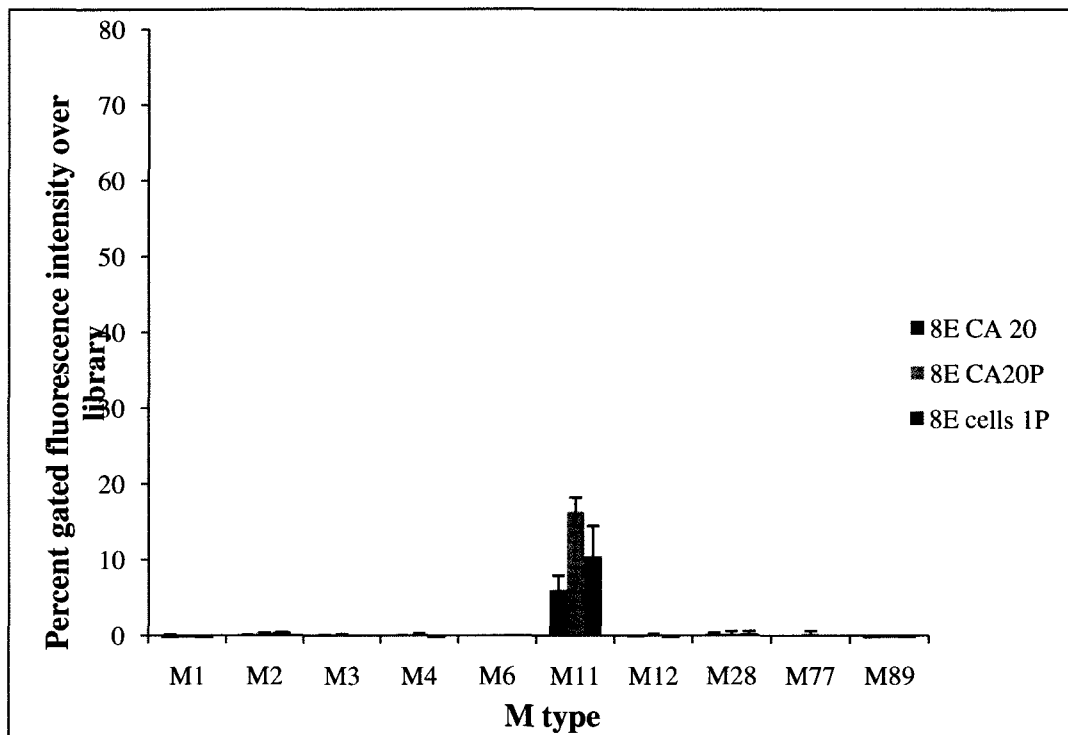


Figure 4.11. Binding of low affinity sequences from SELEX D and E to different M-types of the *S. pyogenes* target mixture. Aptamers were labeled with 5'-FAM, and 200 pmole of aptamers were incubated with 10^8 cells. Cells were then prepared for flow cytometry as previously.

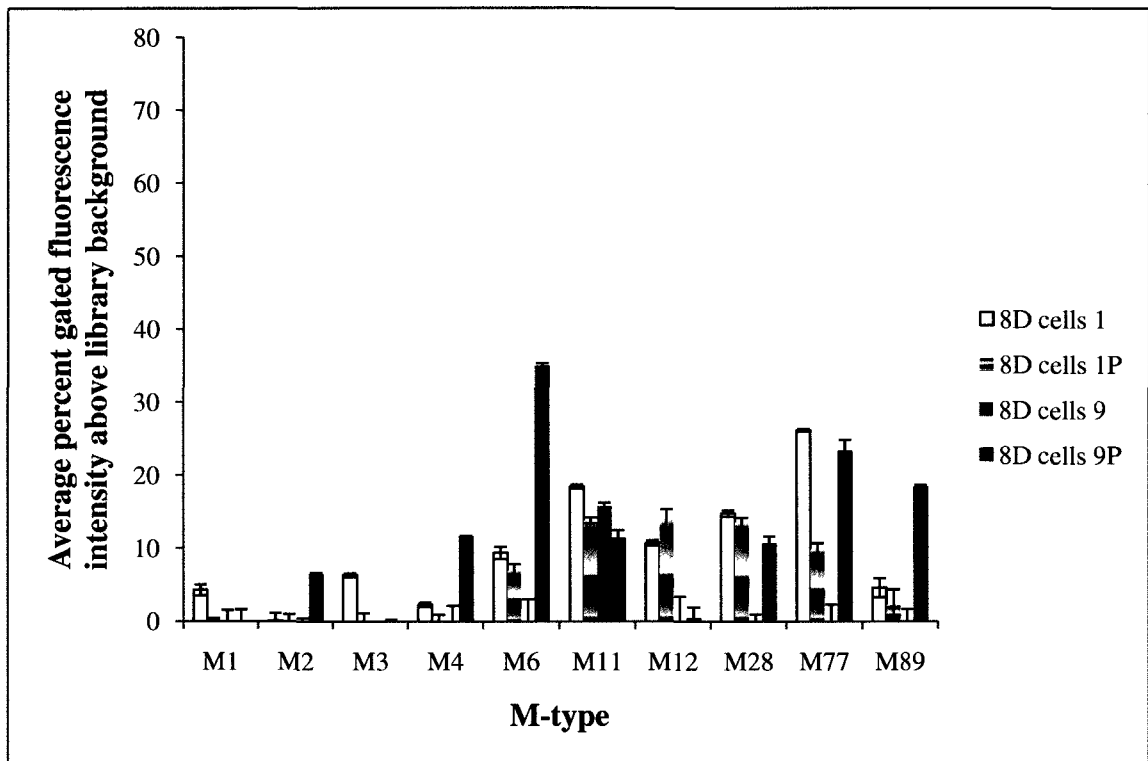


Figure 4.12. Binding of high affinity sequences from SELEX D to different M-types of the *S. pyogenes* target mixture. Aptamers were labeled with 5'-FAM, and 200 pmole of aptamers were incubated with 10^8 cells. Cells were then prepared for flow cytometry as previously.

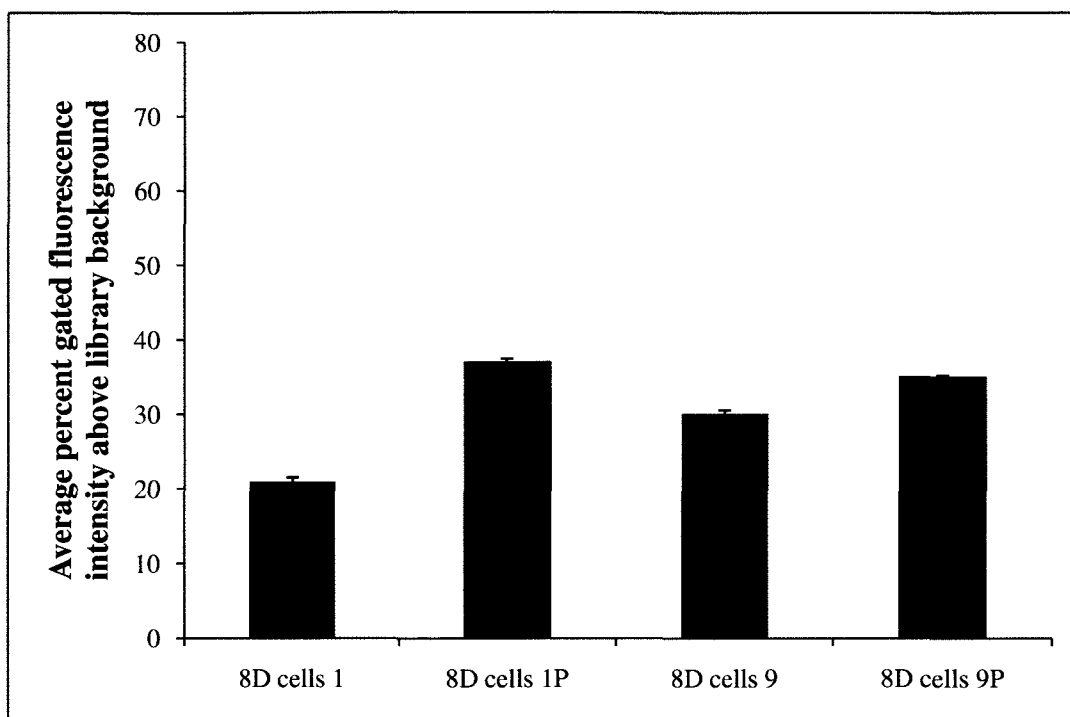


Figure 4.13. Binding of high affinity aptamer sequences to a mixture of *S. pyogenes* M-types not used as targets during selection. A total of 200 pmole of each fluorescently-labeled aptamer was incubated with a mixture of 10^8 total cells (M-types included were M5, M41, M49, M59, M75, M82, M83, M91, M92, and M114).

4.3.7 Binding of high affinity aptamers to *S. pyogenes*

Binding curves from flow cytometric analysis of fluorescently-labeled aptamers and the mixture of 10 different *S. pyogenes* M-types used for selection (10^9 cells) are shown in **Figures 4.14** and **4.15**. Aptamer concentrations in the incubation supernatant from 0 to 150 nM were tested, with the amount of aptamer binding found to level off at less than 40 nM for all sequences. Binding of a fluorescently-labeled randomized oligonucleotide library to the *S. pyogenes* cell

mixture was also examined over a concentration range of 0 to 150 nM (**Figure 4.16**). The single-stranded aptamers and library were heated at 94°C and then cooled at 0 °C prior to incubation with the cells. A cells only background control was used for these binding curves. The average gated fluorescence intensity increased linearly with library concentration and was found to reach a maximum of 57% at a library concentration of 150 nM. However, for all aptamer sequences tested, maximum percent gated fluorescence intensity above background followed an exponential curve, reaching a maximum and leveling off before or at an aptamer concentration of 40 nM.

The K_d and B_{max} of each aptamer was determined based on the fit of the non-linear regression curve (GraphPad Prism 5). **Table 12** summarizes the K_d and B_{max} values of each aptamer tested. These values are also listed on **Figures 4.14 to 4.16**. Sequences 8D cells 1P and 8D cells 9P had the highest affinities for the target cell mixture as all had K_d values below 10 nM ($K_d = 8.9 \pm 0.6$ nM for 8D cells 1P; 3.7 ± 0.5 nM for 8D cells 9P). Sequence 8D cells 9 had the lowest affinity for the target cell mixture with a K_d of 16.7 ± 3.1 nM.

The maximum percent gated fluorescence intensity, and hence maximum binding, measured for each sequence is as follows: 1) 8D cells 1: 75 ± 0.2 % at 125 nM; 2) 8D cells 1P: 73 ± 0.3 % at 150 nM; 3) 8D cells 9: 61 ± 0.1 % at 90 nM; 4) 8D cells 9P: 59 ± 1 % at 90 nM. Since the percent gated fluorescence intensity value increases with the number of cells bound to an aptamer and the number of target molecules (and hence aptamers) bound per cell, it seems that aptamer sequences 8D cells 9 and 8D cells 9P bind to slightly fewer cells and/or

fewer target molecules per cell than 8D cells 1 and 8D cells 1P. The calculated B_{\max} values (**Table 12**) agree with the conclusions reached by looking at the maximum percent gated fluorescence intensity above background values; 8D cells 9P had the lowest B_{\max} value of $69 \pm 1\%$ gated fluorescence above background.

Table 12. Binding dissociation constant (K_d) and theoretical maximum binding (B_{\max}) of high affinity SELEX D aptamer sequences for a mixture of 10 different *S. pyogenes* M-types used in SELEX.

Aptamer Sequence	K_d (nM)	SE (nM)	B_{\max} (% gated)	SE (% gated)
8D cells 1	13.8	2.4	90.9	3.3
8D cells 1P	8.9	0.6	84.2	1.0
8D cells 9	16.7	3.1	76.7	3.3
8D cells 9P	3.7	0.5	69.2	0.8

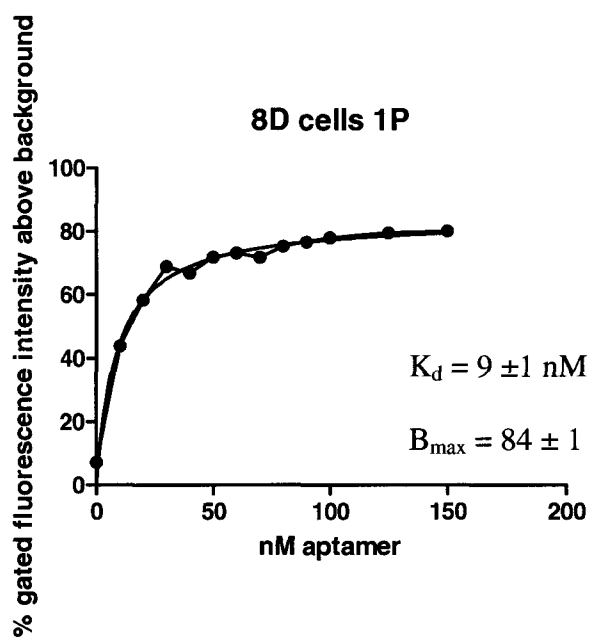
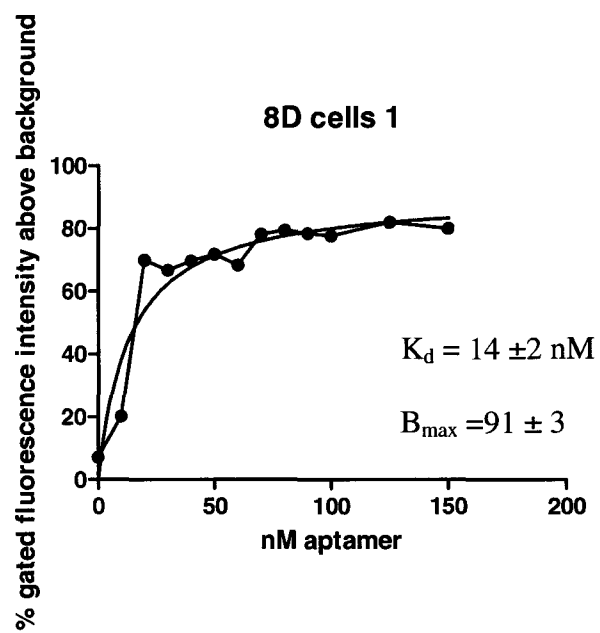


Figure 4.14. Binding of aptamers 8D cells 1 and 8D cells 1P to the mixture of *S. pyogenes* cells used in SELEX. Various concentrations of aptamer (x-axis) were incubated with a mixture of 10^9 *S. pyogenes* cells in binding buffer for 45 min and analyzed via flow cytometry under the same conditions as in **Figure 3.10**, except that no washing steps were carried out.

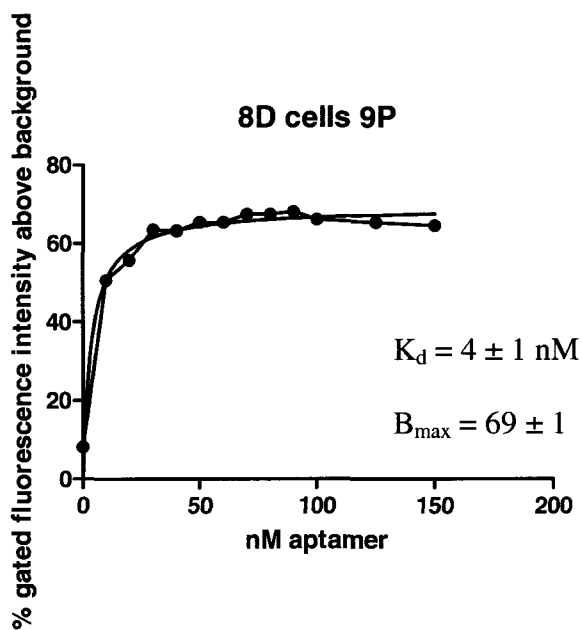
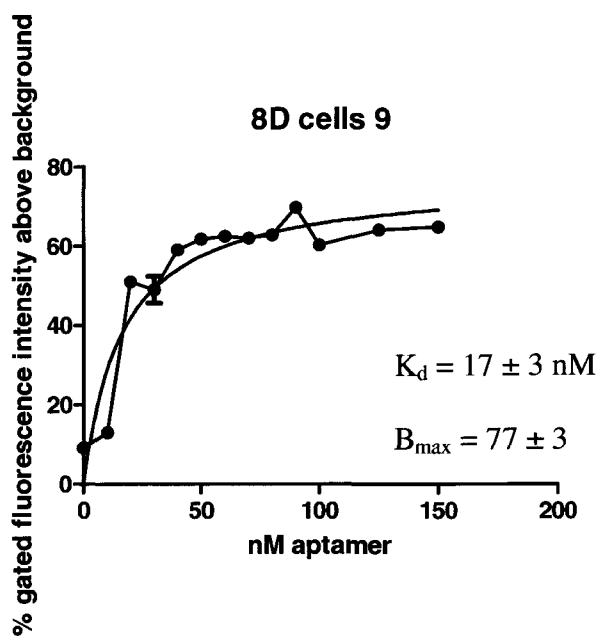


Figure 4.15. Binding of aptamers 8D cells 9 and 8D cells 9P to the mixture of *S. pyogenes* cells used in SELEX. Various concentrations of aptamer (x-axis) were incubated with a mixture of 10^9 *S. pyogenes* cells in binding buffer for 45 min and analyzed via flow cytometry under the same conditions as in **Figure 3.10**, except that no washing steps were carried out.

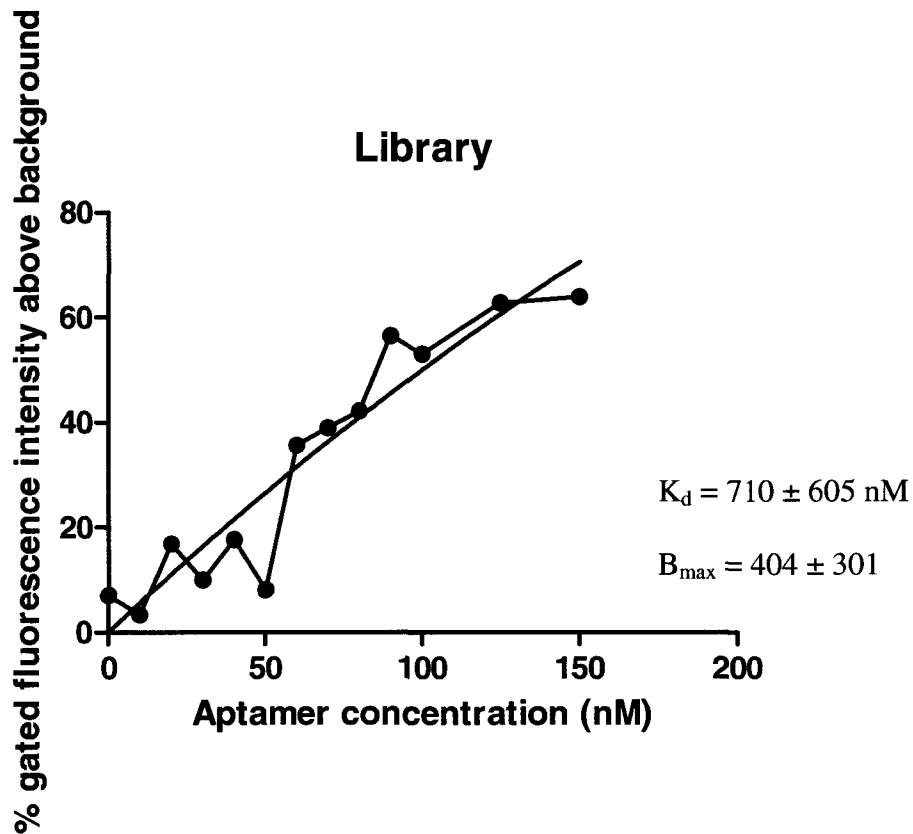


Figure 4.16. Binding of randomized oligonucleotide library to the mixture of *S. pyogenes* cells used in SELEX. Various concentrations of library (x-axis) were incubated with a mixture of 10^9 *S. pyogenes* cells in binding buffer for 45 min and analyzed via flow cytometry under the same conditions as in **Figure 3.10**, except that no washing steps were carried out.

4.3.8 Selectivity of high affinity aptamers for *S. pyogenes*

Fluorescently-labeled aptamer sequences 8D cells 1, 8D cells 1P, 8D cells 9, and 8D cells 9P were tested against a variety of other bacteria including pathogens that could interfere with a diagnostic test. Specifically, binding to other species of *Streptococcus* was tested using non-pathogenic *S. bovis*, and the

pathogens *S. pneumoniae* and *S. agalactiae* (Group B Streptococcus or GBS). *Escherichia coli* DH5a was used to assess aptamer binding to a representative gram negative organism. Sequences were also screened against *Enterococcus* sp. since these are human flora and likely contaminants in diagnostic tests. For the *S. pneumoniae*, *S. agalactiae*, and *Enterococcus* isolates mixtures were prepared containing an equal number of cells from multiple isolates, as were the *S. pyogenes* mixtures used for selection. A summary of the isolates for each mixture is presented in **Table 13**.

None of the sequences bound strongly to any of the cells tested with the exception of 8D cells 1P, which seemed to have some affinity for the Group B Streptococcus (GBS) mixture (**Figure 4.17**). However, this affinity was low in comparison to the *S. pyogenes* target cell mixture. The percent gated fluorescence intensity above library background was 22% when 8D cells 1P was incubated with GBS cells and 71% when incubated with the original *S. pyogenes* target cell mixture (**Figure 4.10**), a three-fold difference which may or may not interfere in a diagnostic test. Removal of the primer sequences seems to negate GBS binding, bringing the percent gated fluorescence intensity below the level of the library control (8D cells 1 in **Figure 4.17**). The 8D cells 9P and 8D cells 1 showed a small amount of binding to the *Enterococci* mixture (6 and 7 percent gated fluorescence intensity above background, respectively). The 8D cells 9 seems to be very specific for *S. pyogenes*; it did not bind to any of the other cell types tested (**Figure 4.17**). It can thus be concluded that the aptamer sequences tested are specific for *S. pyogenes*.

Table 13. List of all species, isolates and strains used to test selectivity of aptamers to *S. pyogenes*.

<i>Streptococcus agalactiae</i>	975R547 IV; JM9 VIII; 7271 VII; 975R390 VI; 965R400 Ia; 975R384 V; 12351 IV; 965R155 Ia; 975R938 II; 975R27 Ib; 975R331 IV; 955R2028 IV; 975R591; 975R138 II; 975R570 Ib; 975R104 VIII; 9842 VI; 975R594 III
<i>Streptococcus pneumoniae</i>	4; 6B; 9V; 14; 18C; 19F; 23F; 19A; 5; 6A
<i>Streptococcus bovis</i>	
<i>Enterococcus</i> sp. (ATCC #)	<i>E. saccharolyticus</i> (43076); <i>E. raffinosus</i> (49447); <i>E. pseudoaerium</i> (49372); <i>E. mundtii</i> (43186); <i>E. malodoratus</i> (43197); <i>E. hirap</i> (8043); <i>E. gallinarium</i> (49573); <i>E. faecium</i> (19434); <i>E. faecalis</i> (19433); <i>E. durans</i> (19432); <i>E. cecorum</i> (43198); <i>E. casseliflavus</i> (25788); <i>E. avium</i> (14025)
<i>Escherichia coli</i>	DH5 α

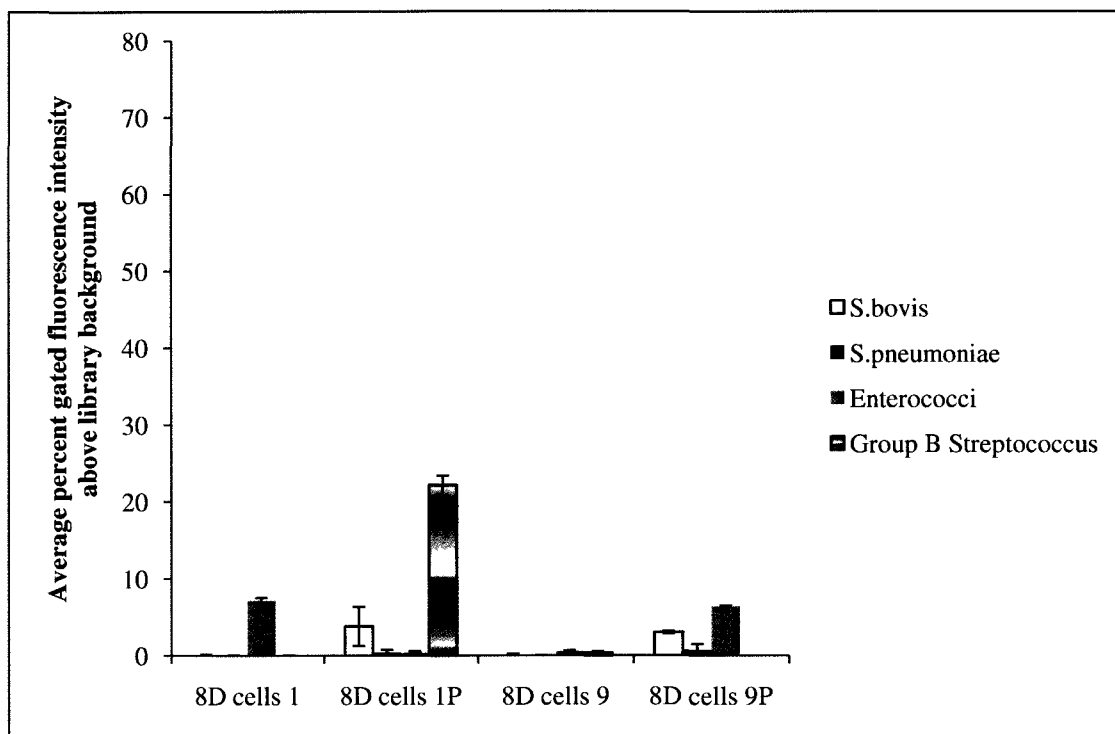


Figure 4.17. Screening of high affinity GAS aptamers against non-target cells.

4.4 References

1. Hamula CL, Zhang H, Guan LL, Li XF, Le XC. Selection of aptamers against live bacterial cells. *Anal Chem.* 2008 Oct 15;80(20):7812-9.

Chapter 5

Post-SELEX Target Molecule Elucidation

5.1 Introduction

Conventionally, a purified target molecule is used to select aptamers via SELEX. In cases where a complex target such as a whole cell is used, post-SELEX identification of the specific target molecule of a given aptamer or aptamer pool is necessary and challenging. Methods for rapid and high-throughput screening of aptamers can aid in this determination.

Aptamer blotting adapts the methodology of western blotting to aptamer screening, substituting aptamers in place of a primary antibody. Hence, it only detects non-covalent interactions of aptamers and target molecules. Noma et al. (2006) first used aptamer blotting to visualize the difference in binding selectivity of an oligonucleotide library before and after selection against chicken skeletal muscle (**Figure 5.1**) (1). Aptamers can not only replace antibodies in Western Blotting but can also be used in place of antibodies on magnetic beads in order to pull specific target molecules out of a complex solution such as a cell lysate.

Capillary electrophoresis (CE) is an ideal tool to quickly evolve libraries into aptamers. CE has primarily been used in development of rapid SELEX methods against purified protein target molecules, since it can be used to distinguish free DNA molecules from those bound to protein in a stable complex (**Figure 5.2**). In free-zone CE-LIF, an incubation mixture of fluorescently-labeled

aptamer and target molecule is run through the capillary and the fractions containing DNA-protein complexes are separated out. Free (unbound) aptamers in solution of varying lengths all have a similar mass-to-charge ratios and thus elute from the capillary at the same retention time. Aptamers bound to a protein molecule have different mass-to-charge ratios than free aptamers and elute at earlier retention times. Transient or weak protein binding by an aptamer results in a shift of the aptamer peak retention time without formation of a stable complex peak. Pavski and Le used this method in 2001 for detection of human HIV Reverse Transcriptase (RT) using fluorescently-labeled single-stranded aptamers as probes (2). This methodology can be harnessed in order to test an array of target molecules against a given aptamer sequence as a probe for post-SELEX target elucidation.

The aim of the research in this chapter is to use various techniques including aptamer blotting and free-zone affinity capillary electrophoresis for post-SELEX elucidation of specific aptamer target molecules on the bacterial cell surface. The aptamers studied are: 1) hemag1P specific for *Lactobacillus acidophilus* and 2) GAS SELEX aptamer pools 20A, 15A, and 13B, specific for a mixture of 10 different M-types of *Streptococcus pyogenes*.

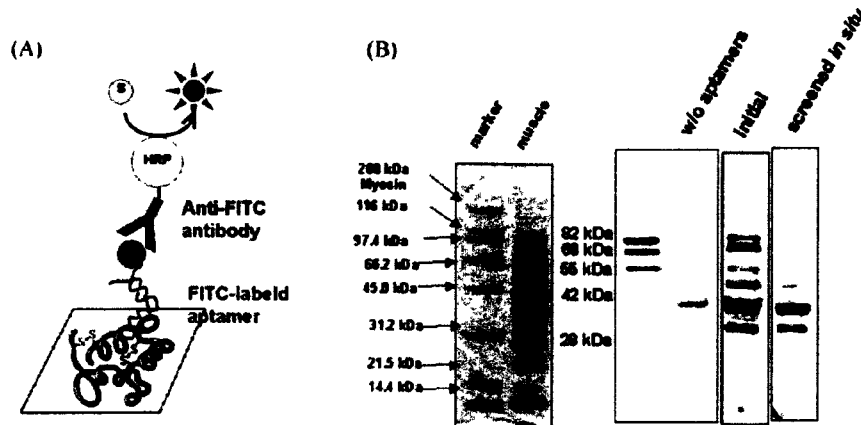


Fig. 1. Aptamer Blotting and comparison of the initial library with the screened library. (A) Method to assay affinity and specificity of the library by Aptamer Blotting. (B) Aptamer Blotting with the library before and after the screening.

Figure 5.1. Schematic of aptamer blotting procedure of Noma et al. 2006 (1).

(A) Aptamers are labeled with a fluorescent molecule (FITC) and incubated with proteins on a membrane. Anti-FITC antibodies conjugated to Horse-Radish Peroxidase (HRP) are used to bind the aptamers and visualize them via chemiluminescence. Biotin can be substituted for FITC and an anti-Biotin HRP secondary antibody used instead. (B) The results of blotting a muscle tissue extract with both randomized library (initial) and more specific aptamer pools (screened in situ) are shown.

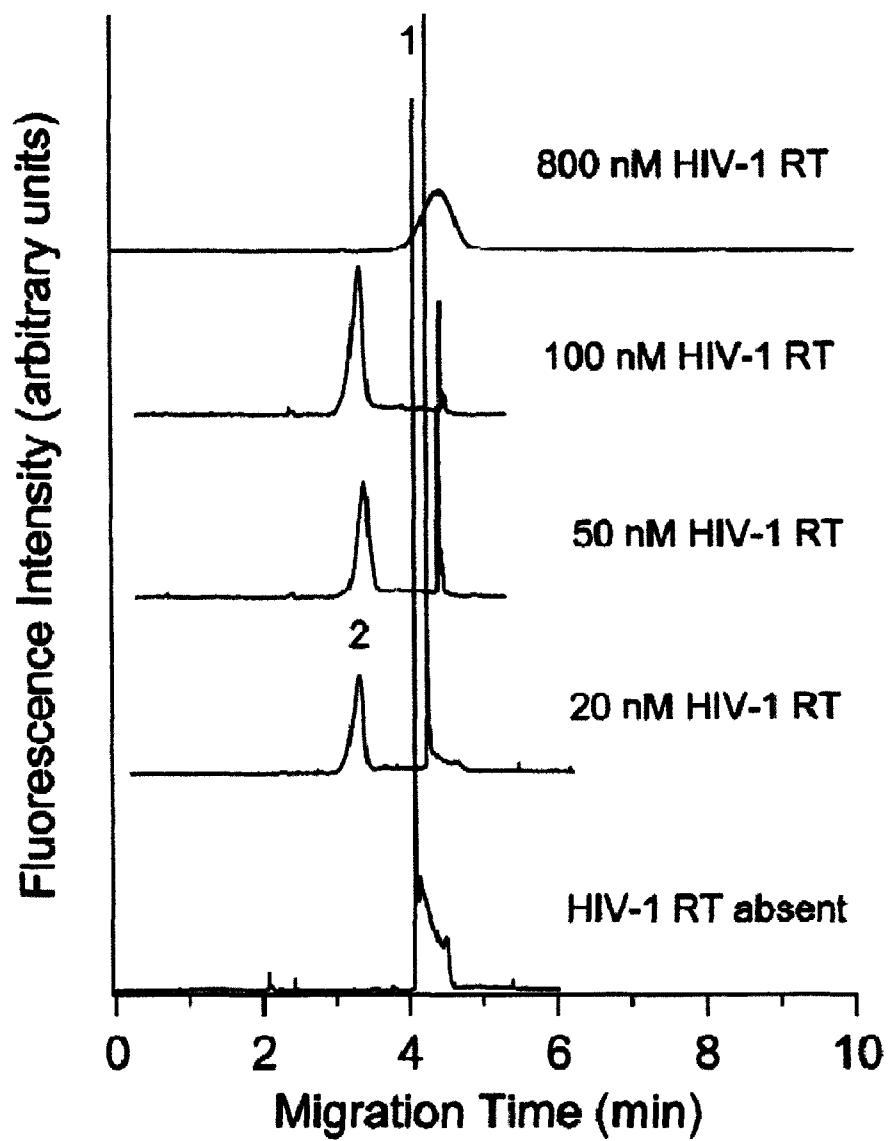


Figure 5.2. Principle of affinity CE-LIF separation of free (unbound) DNA from DNA-protein complexes (Figure 2 from Pavski and Le 2001 (2)). A fixed amount of aptamer (17 nM) is incubated with increasing amounts of target protein (HIV-RT). Free aptamer peak is 1, complex peak is 2.

5.2 Experimental

5.2.1 Flow cytometry

The binding assays were carried as described in Chapter 1 by incubating 100 pmole of 5'-FAM fluorescently-labeled aptamer hemag1P with 10^7 cells for 45 min in binding buffer, and then washing the cells once in 1X BB with 0.05% BSA prior to resuspension in 1X BB for immediate flow cytometric analysis. Forward scatter, side scatter, and fluorescence intensity (FL1-H) were measured, and gated fluorescence intensity above background (cells with no aptamers added) was quantified.

5.2.2 S-layer protein purification

The S-layer protein was purified from the surface of *L. acidophilus* 4356 using the LiCl extraction procedure of Lortal et al. (3) in which cells were incubated in 6M LiCl at 37 °C. Dialyzed extracts were freeze-dried, resuspended in 50 mM Tris (pH 7.4), and run on 8% SDS-PAGE gels to identify the presence of a 43 kDa band and assess the purity of the preparation. The 43 kDa band was then excised and analyzed via mass spectrometry to confirm its identity as the S-layer protein.

5.2.3 Capillary electrophoresis

Capillary electrophoresis with laser-induced fluorescence (CE-LIF) was carried out on mixtures of purified S-layer protein and fluorescently-labeled (5'-FAM) hemag1P or fluorescently-labeled randomized oligonucleotide library. For each mixture, the concentration of hemag1P was kept constant at 2.5, 5, or 10 nM

and the concentration of S-layer protein was varied from 0–5 μM . Fluorescein was included as an internal standard at a concentration of 7.5 nM. The mixtures were incubated in 1X BB without NaCl for 45 minutes. Light from an argon ion laser with an excitation wavelength of 488 nm was focused using a 10x microscope objective to a detection window near the end of the tip of the capillary, and the photomultiplier tube (PMT) value was recorded for fluorescence intensity.

5.2.4 Aptamer-magnetic bead pulldowns

Logarithmic-phase *L. acidophilus* 4356 cultures were pelleted at 1000x g for 5 minutes at 4 °C and resuspended in 10 cell volumes of ice-cold RIPA buffer (1% Triton-X 100, 0.5% deoxycholate, 150 mM NaCl, 1X CPI, 50 mM Tris-Cl pH 8.0). Lysates were prepared via sonication of cells for 30 seconds in ice-cold RIPA followed by centrifugation at 10,000x g for 10 minutes at 4 °C. The supernatants were removed and transferred to a clean tube. Both supernatant and pellet fractions were retained (the pellets were resuspended in RIPA), and the fractions were dialyzed overnight at 4 °C in a 10,000 MWCO cassette (Pierce) in 1X BB. Dynabeads M-280 Streptavidin (Invitrogen) were coated with either nothing, biotinylated randomized library, or biotinylated hemag1P. Coated magnetic beads were prepared as per manufacturer's instructions and resuspended in 1X BB. Incubations of beads with either lysate supernatant or lysate pellets were carried out in 1mL total volume and 1X BB for 45 minutes on ice. The beads were then washed 4 times in 1X BB, resuspended in SDS-PAGE loading buffer, and heated at 95 °C for 5 minutes in order to release and denature any

attached proteins. The beads were then removed from the sample, and the supernatants were run on a 12% SDS-PAGE gel with a 5% stacking gel at 90V for 60 minutes and stained with Bio-Rad Bio-Safe Coomassie.

5.2.5 Crude pepsin extract preparation, PAGE, and mass spectrometry

A protocol for extracting M proteins from the surface of *S. pyogenes* using pepsin was modified from Beachey et al. (4), who found that optimal amounts of type-specific M protein were released after 20 minutes of digestion with 0.02 mg of pepsin per mL at pH 5.8. A total of 40 mL of *S. pyogenes* culture was grown in TH broth for 16 hours. Cells were then sedimented and washed twice in ice-cold 0.02 M phosphate-buffered 0.9% NaCl (pH 7.4), then once in extraction buffer minus pepsin (0.9% NaCl adjusted to pH 5.8 with a mixture of 0.067 M Na₂HPO₄ and KH₂PO₄). Cells were resuspended in extracting medium containing 0.02 mg/mL of pepsin and incubated for 20 minutes at 37 °C. Pepsin digestion was halted by raising the pH to 7.5 via addition of 7.5% NaHCO₃ and the supernatant was removed following centrifugation at 10,000x g for 20 minutes. The supernatant was then passed through a 45 µM membrane filter and dialyzed against PBS (pH 7.4) then ddH₂O overnight at 4 °C, resulting in a crude pepsin extract for each of the 10 M-types used in SELEX.

Crude pepsin extracts were run on 7% native and SDS-PAGE gels as previously described (Laemmli). Total protein concentration was assayed using a Micro BCA Protein Kit (Pierce Protein Research Products, ThermoFisher Scientific) and 60 µg of total protein was loaded for each lane of the gel. Gels were run at 120 V and stained in BioSafe Coomassie (Bio-Rad, CA).

5.2.6 Mass spectrometric identification of proteins

Bands of interest were excised from the gels and analysed using tryptic digestion coupled with liquid chromatography tandem mass spectrometry (LC/MS-MS) (Mass Spectrometry Facility, Department of Chemistry, University of Alberta, Edmonton, AB). A Waters nanoAcquity UPLC System coupled to a Waters Q-TOF Premier Mass Spectrometer was used (Waters, Milford, MA). Peptide sequences were analyzed against the SRS/SwissProt database (EMBL-EBI) for identification.

5.2.7 Western blotting analysis of aptamer pool target binding to crude pepsin and whole cell extracts

Aptamer pool binding profiles were analysed via Western Blotting with the aptamer pool used in place of a primary antibody. Conditions for blotting were optimized using lysozyme and a biotinylated anti-lysozyme aptamer from IDT (5):

5'-/5BiodT/AT CTA CGA ATT CAT CAG GGC TAA AGA GTG CAG
AGT TAC TTA G-3'

The aptamers pools 13B, 15A and 20A were examined. SDS-PAGE gels of the crude pepsin extracts were run as described in **Chapter 3**. Whole cell extracts (WC extracts) for each M-type were also prepared via freeze-thawing, with soluble and insoluble fractions separated via centrifugation at 6000xg and 4 °C for 10 minutes. The soluble and insoluble WC fractions were then run as the pepsin fractions via SDS-PAGE. A set of biotinylated protein standards (Invitrogen) was also loaded on each gel. Gels were electrophoretically

transferred to PVDF membranes for 1 hour at 100V in 1X Tris-Glycine (TG) electrophoresis buffer (25 mM Tris pH 8.3, 192 mM glycine, 20% v/v methanol and 0.1% SDS). Following transfer membranes were dried, rehydrated in methanol, and blocked in 1X PBST (PBS containing 0.05% v/v Tween-20) containing 5% BSA for a minimum of 1 hour. A second blocking step in 1X PBST and 2.5% lysozyme for 1 hour was carried out for some of the blots. Blocked membranes were then incubated in 1X PBST containing 10 nM biotinylated aptamer pool or randomized library (IDT) for 1 hour at room temperature. A goat anti-biotin peroxidase was used as a secondary antibody (Sigma). A minimum of four 1X PBST rinses were carried out in between each incubation step. Membranes were visualized using X-ray film (Fuji) and a chemiluminescence kit (Pierce SuperSignal West Pico).

A procedure for removal of aptamer sequences from a PVDF membrane was carried out as described (1). The membranes were subjected to the same series of incubations as were carried out for western blotting, except for the incubation step with SuperSignal West Pico since chemiluminescence reagents inhibit amplification. An identical membrane was prepared and stained at the same time to enable identification and localization of bands of interest. Bands of interest were then excised from the unstained membrane and the slices were washed in 1X PBS, extracted with phenol and then ethanol precipitated. The DNA was resuspended in 1X PCR Reaction Buffer (Invitrogen) and amplified using the same set of conditions as were used for SELEX. PCR products were analyzed on a 7.5% PAGE gel as previously.

5.3 Results

5.3.1 Putative target molecule of hemag1P

The SELEX technique that has been presented in **Chapter 2** most likely favours the selection of aptamers that bind to abundant cell surface molecules. The high affinity of hemag1P for the target cells (nM K_d) supports this assertion, since aptamers selected against a single purified target typically possess lower K_ds than those selected against complex targets in which multiple target molecules are present. The estimated K_d of 13 ± 3 nM is comparable to K_ds of aptamers derived from purified protein targets (6-9). The most abundant surface structure on *L. acidophilus* 4356 is the evenly distributed S-layer comprised of 43 kDa S-proteins (10). The flow cytometry results (**Figure 2.10**) support this idea, since hemag1P binds only to cells with S-layers comprised of similar S-proteins (*L. acidophilus* 4355, 4356, and 4357) and not to other cells (*E. coli*, *S. bovis*, and *S. cerevisiae*). Further flow cytometric screening of hemag1P against *Lactobacillus* species both with (*L. acidophilus* 4356) and without (*L. casei*, *L. gasseri*, *L. johnsonii*) S-layers indicates that hemag1P does not bind to cells without an S-layer (**Figure 5.3**).

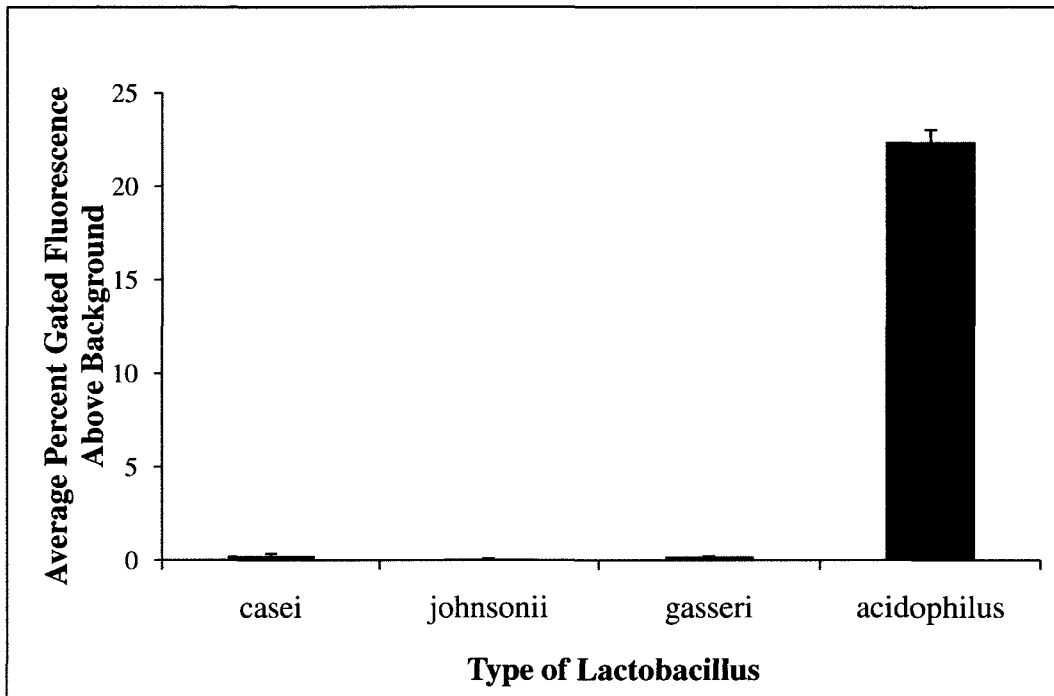


Figure 5.3. Binding of aptamer hemag1P to *Lactobacillus sp.* with and without an S-layer. Flow cytometry was carried out as previously on incubations of hemag1P with 10^7 cells. A total of 100 pmole of Hemag1P was incubated with each cell type for 45 minutes in binding buffer, washed, and then analysed. With the exception of *L. acidophilus*, all species tested above do not possess an S-layer.

Further evidence is provided by preliminary CE-LIF analysis of incubation mixtures of purified S-layer protein and fluorescently-labeled hemag1P. An SDS-PAGE gel of the LiCl extract obtained after purification of the S-layer protein shows the presence of a single band at around 43 KDa (**Figure 5.4**). Excision of this band followed by mass spectrometry analysis identified it as *L. acidophilus* 4356 S-layer protein. A decrease in the unbound hemag1P peak intensity was seen when incubated with S-layer protein, along with corresponding formation of an aptamer-protein complex peak, whereas incubation with BSA resulted in a slight shift in aptamer peak retention time and no complex peak formation (**Figure 5.5**). These preliminary results suggest that S-layer protein binds with sufficiently high affinity to hemag1P to form a stable complex, and is thus a likely target. However, while the height of the free aptamer peak decreased and the number and height of the complex peaks increased with increasing protein concentration, the heights and positions of these peaks were not consistent between triplicate runs of the same incubation or triplicate incubations (**Figures 5.6a-5.6c**). At high concentrations of S-layer protein (5 μ M) a number of irregular complex peaks sometimes formed and this pattern was not reproducible between runs (**Figure 5.7**). It is likely that purification of the S-layer protein from the cell surface alters protein conformation and hence aptamer-protein binding. In addition, the S-proteins may also be forming aggregates in the capillary.

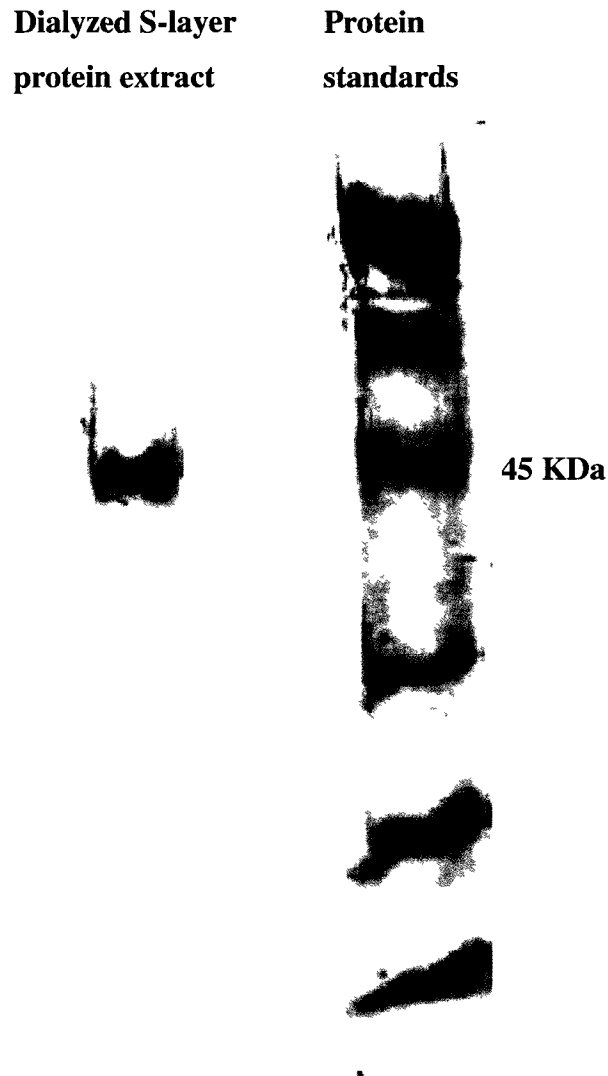


Figure 5.4. SDS-PAGE of S-protein purified via LiCl extraction. Dialyzed extracts were concentrated via freeze-drying, resuspended in 1XBB, and loaded on an 8% gel and run at 120 V. Gels were then Coomassie stained prior to excision of bands of interest for mass spectrometry analysis.

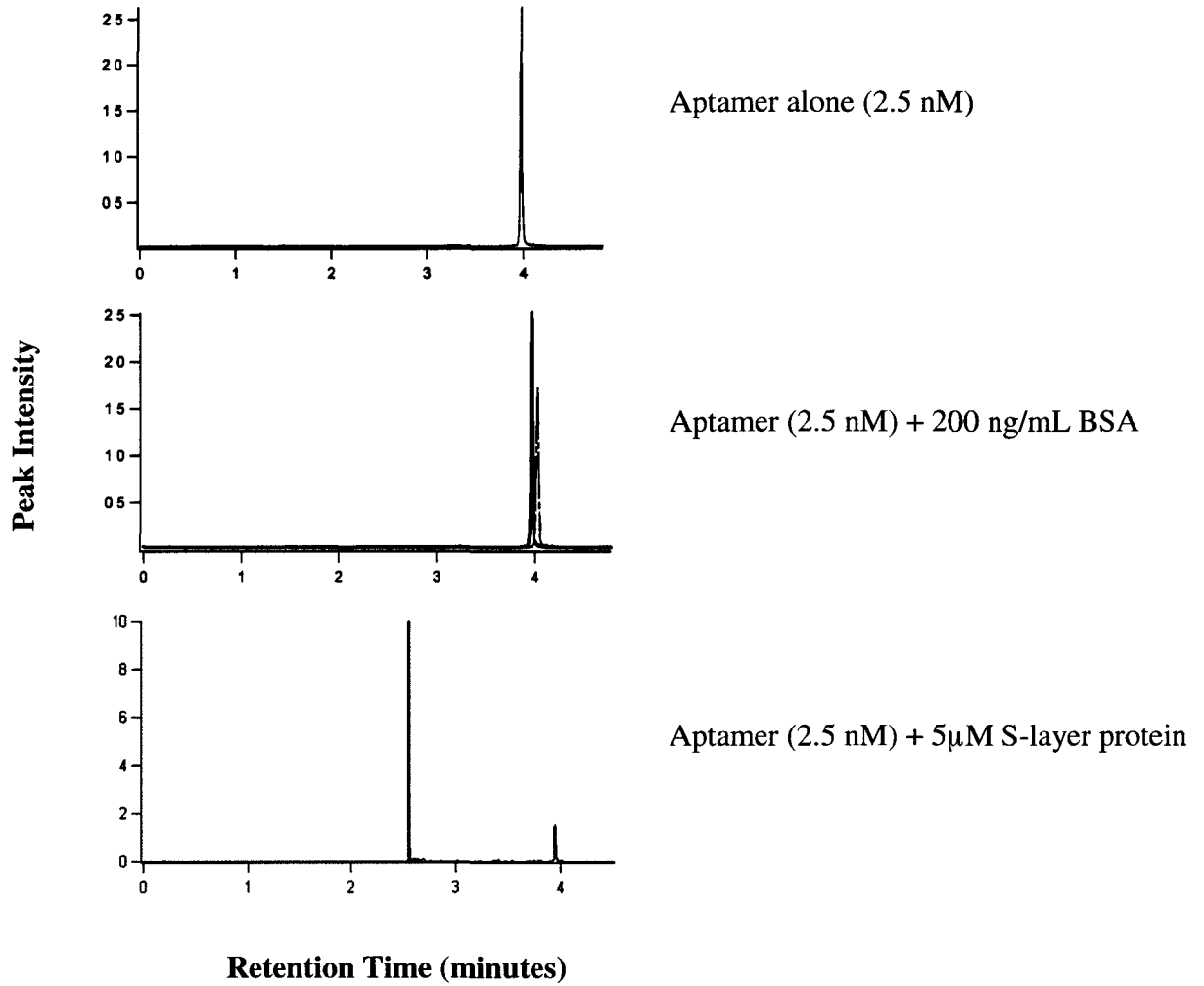


Figure 5.5. Capillary electrophoresis of fluorescently-labeled hemag1P incubated with BSA or with S-layer protein. The original aptamer peak in the middle figure is shown in black to illustrate the retention time shift.

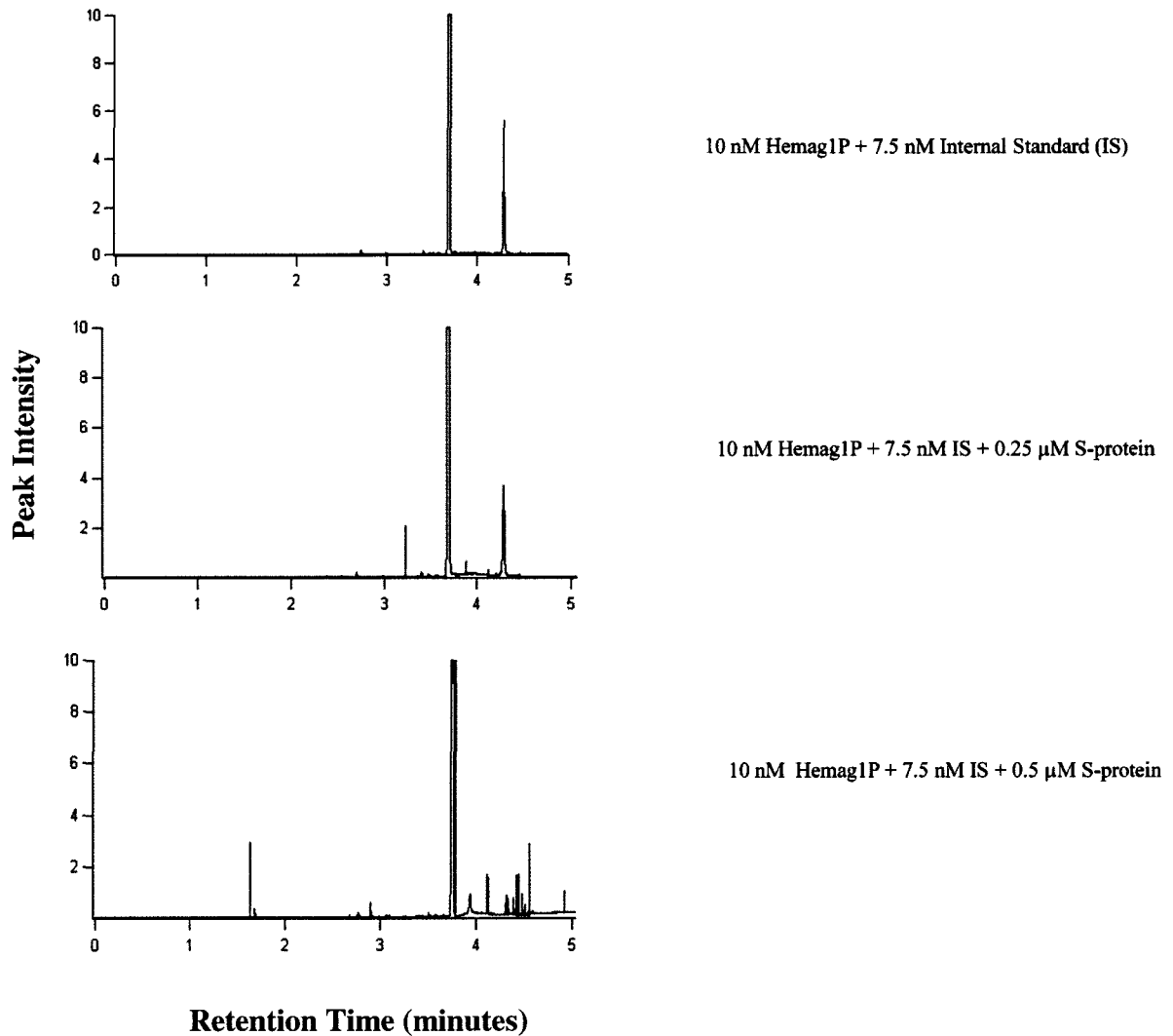


Figure 5.6a. CE-LIF chromatograms showing increased formation of complex peaks in incubations containing increasing amounts of S-protein and fixed amounts of hemag1P. Hemag1P was incubated at a concentration of 10 nM with either 0, 0.25, 0.5, 0.75, 1.0, 1.5, 2 or 5 μ M S-layer protein for 45 minutes in 1x BB prior to injection. A fluorescein internal standard was spiked into the sample at a concentration of 7.5 nM.

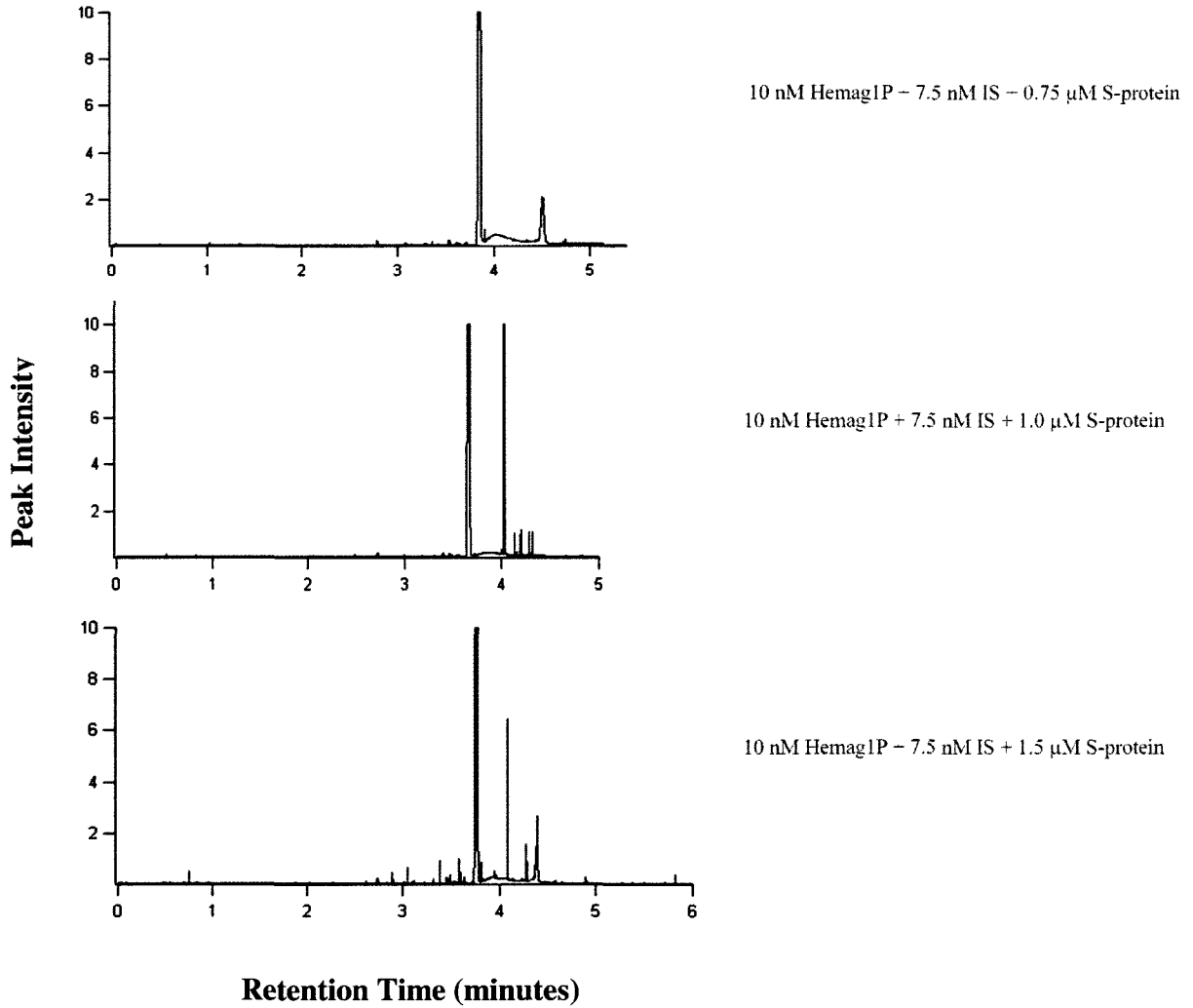


Figure 5.6b. CE-LIF chromatograms showing increased formation of complex peaks in incubations containing increasing amounts of S-protein and fixed amounts of hemag1P. Hemag1P was incubated at a concentration of 10 nM with either 0, 0.25, 0.5, 0.75, 1.0, 1.5, 2 or 5 μ M S-layer protein for 45 minutes in 1x BB prior to injection. A fluorescein internal standard was spiked into the sample at a concentration of 7.5 nM.

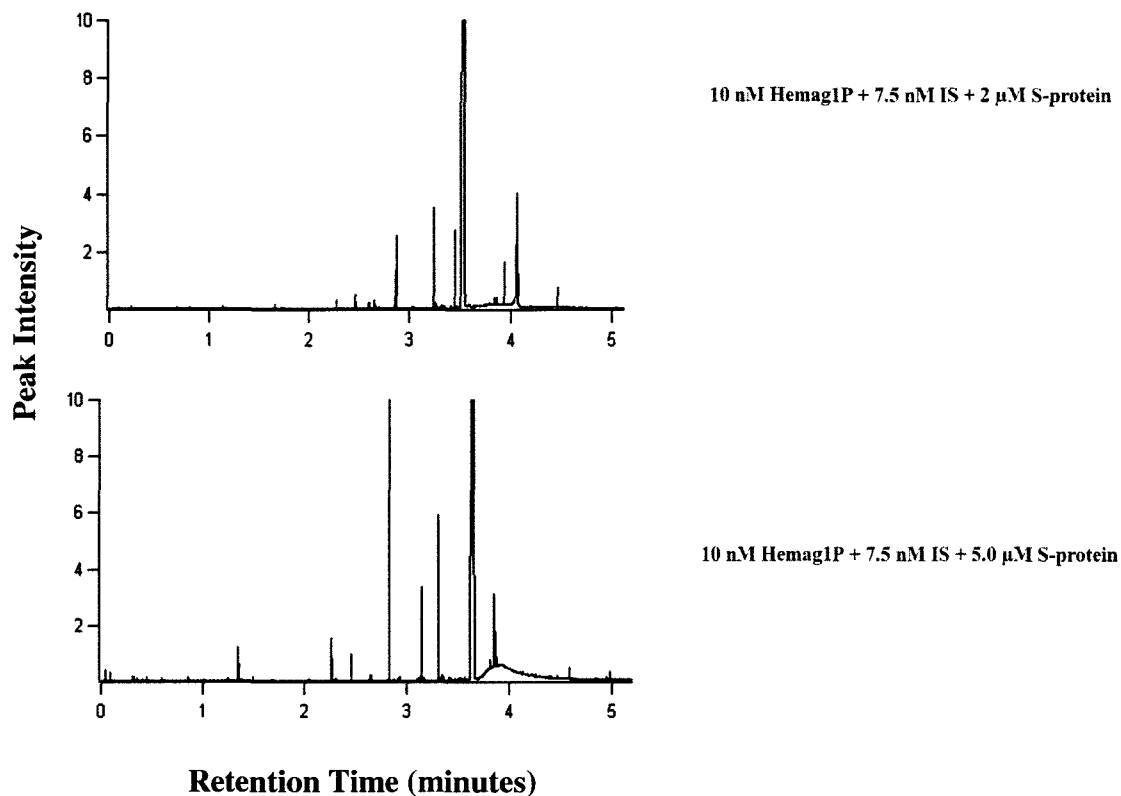


Figure 5.6c. CE-LIF chromatograms showing increased formation of complex peaks in incubations containing increasing amounts of S-protein and fixed amounts of hemag1P. Hemag1P was incubated at a concentration of 10 nM with either 0, 0.25, 0.5, 0.75, 1.0, 1.5, 2 or 5 μM S-layer protein for 45 minutes in 1x BB prior to injection. A fluorescein internal standard was spiked into the sample at a concentration of 7.5 nM.

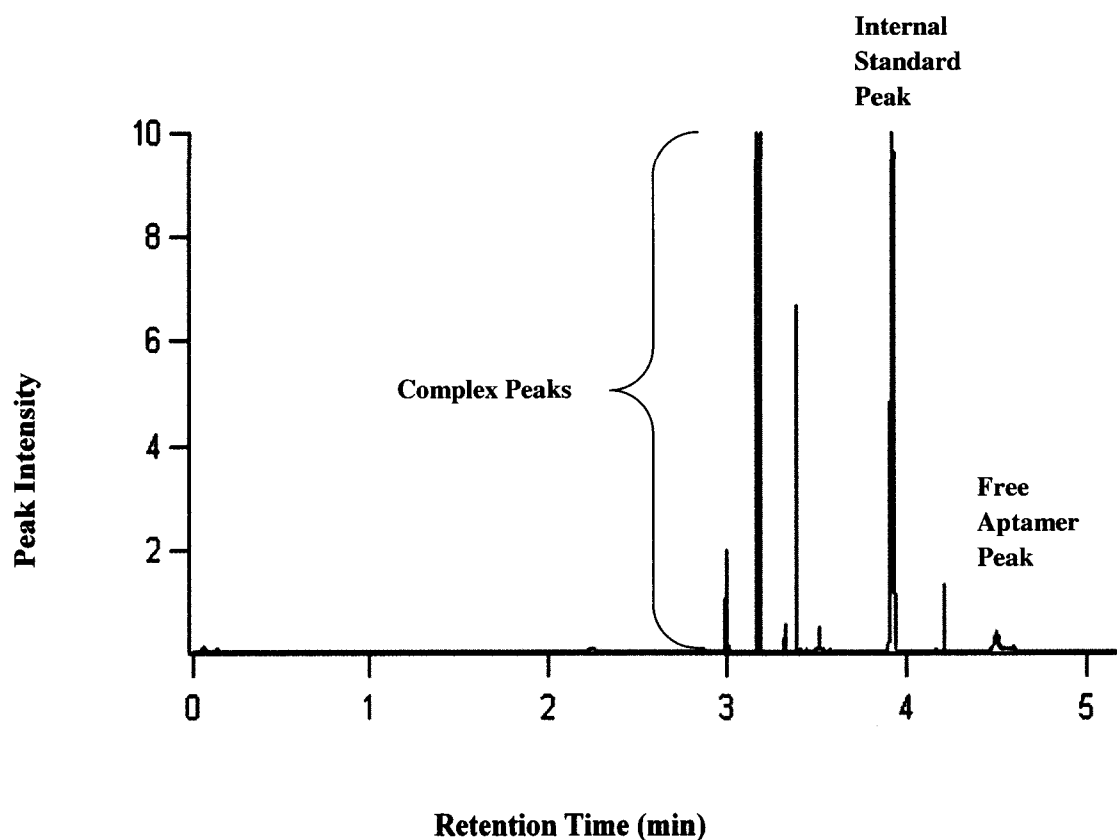


Figure 5.7. Irregular complex peak formation seen after CE-LIF of incubations containing high S-layer protein concentrations (5 μ M). Hemag1P was incubated at a concentration of 7.5 nM with S-layer protein in 1x BB for 45 minutes prior to capillary electrophoresis. A fluorescein internal standard was spiked into the sample at a concentration of 7.5 nM.

Further experiments were carried out in order to assess the affinity of hemag1P for the S-layer protein. Varying concentrations of protein were incubated with a fixed amount of aptamer (10 nM) and the incubations were analyzed via capillary electrophoresis. An internal standard, fluorescein (7.5 nM), was added to each incubation immediately prior to injection. The size of the

remaining free aptamer peak in comparison to the internal standard peak was measured, and a peak intensity ratio was calculated. Fluorescently-labeled randomized library was used as a negative control to assess non-specific adherence of DNA to the protein. A broad range of protein concentrations was examined (0–5 μ M) (**Figure 5.8**), and then further refined (0–1 μ M) (**Figure 5.9**). High concentrations of S-layer protein resulted in a decrease in free hemag1P peak intensity but not randomized library peak intensity. The average peak intensity ratio of unbound hemag1P to unbound internal standard decreases from a high of 0.2 at 0 nM protein to 0.05 at 5000 nM protein in **Figure 5.8**. A similar trend is seen in **Figure 5.9**, with a decrease from 0.6 at 0 nM protein to 0.3 at 1000 nM protein. This corresponds to a 4-fold and 2.3-fold difference, respectively. The average peak intensity ratio of randomized library to internal standards remains similar irregardless of protein concentration. However, the protein concentrations used in these experiments are very high. No decrease in hemag1P peak intensity ratio is seen when fewer than 500 nM S-layer protein is included in the incubation. This does not completely agree with the flow cytometry results seen in Figure 1.11 or with the predicted 13 nM K_d of hemag1P for *L. acidophilus*; hemag1P seems to have higher affinity for *L. acidophilus* 4356 cells than pure S-layer protein. Purification of the protein from the cell surface most likely results in a loss of conformation and hemag1P binding.

The results obtained with triplicate incubations of the randomized library were highly variable for the experiment in **Figure 5.8**, as can be seen by the large error bars. Most of this variability was not between incubations so much as it was

between injections of the same incubation, which could be explained by the formation of S-protein aggregates in the capillary. However, this problem was not observed in other experiments (**Figure 5.9**). At high S-layer protein concentrations, multiple peaks were present around the migration time of the free aptamer peak, making quantitation of this peak difficult. Further experiments are necessary. However, introduction of detergents to disrupt protein aggregation may affect aptamer-protein binding.

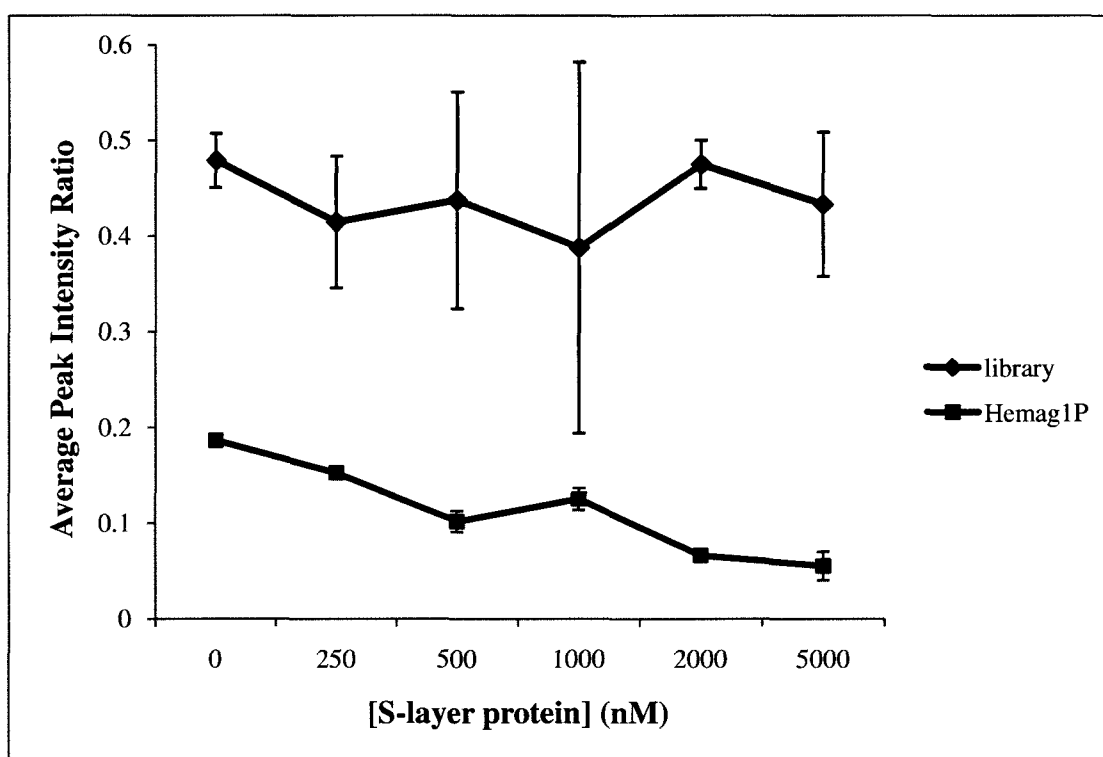


Figure 5.8. Change in unbound DNA peak intensity with increasing S-layer protein concentration. A broad range of protein concentrations (0–5000 nM) were incubated with a fixed amount of DNA (10 nM), either a fluorescently-labeled randomized oligonucleotide library or fluorescently-labeled aptamer Hemag1P. Incubations were carried out in 1 x BB for 45 minutes.

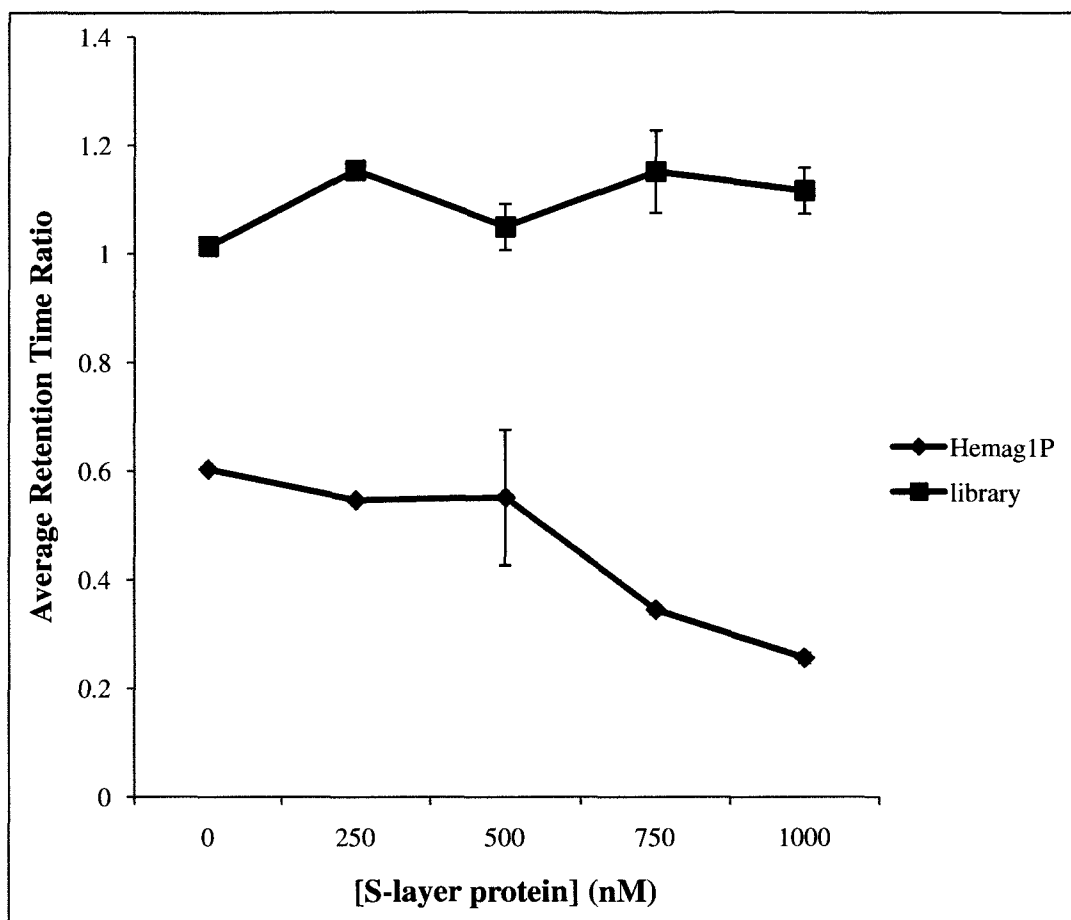
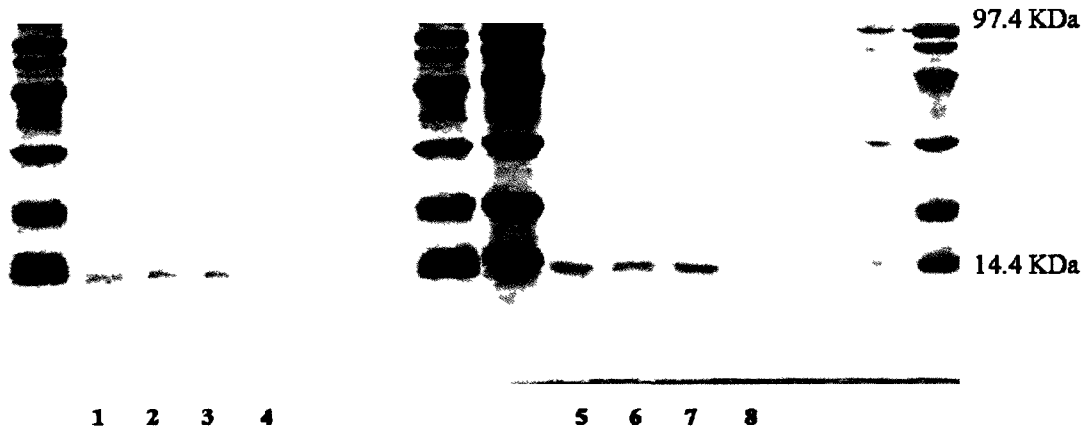


Figure 5.9. Change in unbound DNA peak intensity with increasing S-layer protein concentration. A range of protein concentrations (0–1000 nM) were incubated with a fixed amount of DNA (10 nM), either a fluorescently-labeled randomized oligonucleotide library or fluorescently-labeled aptamer Hemag1P. Incubations were carried out in 1 x BB for 45 minutes.

Aptamers can be conjugated to magnetic beads and the beads can then be mixed with cells or cell lysates to pull out target molecules. Hemag1P was conjugated via a 5'-Biotin to streptavidin-coated magnetic beads. Sufficient aptamer was used to saturate all the streptavidin sites on the bead surface. Cells were obtained from a logarithmic-phase liquid culture of *L. acidophilus* 4356 and

lysed in the presence of protease and nuclease inhibitors. The cell lysates and the cell pellets were then incubated separately with hemag1P-coated beads, the beads were washed and proteins were released from the bead surface via heating in SDS-PAGE loading buffer. Negative control incubations consisting of beads alone, and beads coated with randomized oligonucleotide library were prepared and run concurrently. Eluates from each set of beads were then loaded and run on an SDS-PAGE gel (**Figure 5.10**). The same 14 KDa band was seen in all lanes of the gels: beads alone (**lanes 1 and 5**), beads coated with library (lanes 2 and 6), and beads coated with hemag1P (**lanes 3 and 7**). Hence, cellular proteins seem to be interacting non-specifically with the beads. A blocking step will most likely be required prior to incubation of the beads and the *L. acidophilus* solutions.



1=beads alone + cell lysate; 2=library beads + cell lysate; 3= Hemag1P beads + cell lysate; 4=cell lysate alone; 5=beads alone + cell pellet; 6= library beads + cell pellet; 7= Hemag1P beads + cell pellet; 8= cell pellet alone

Figure 5.10. SDS-PAGE of eluates from aptamer-coated magnetic bead pulldowns.

5.3.2 Identification of a putative target of GAS aptamer pools

Following completion of SELEX A and B using an *S. pyogenes* mixture as a target, the aptamer pools found via flow cytometry to have the highest affinity for were cloned and sequenced. The pools all contained a large number of different sequences with minimal repetition. An alternate method of screening the pools, using aptamer blotting, was carried out in an attempt to identify specific sequence-target pairs. The aptamer pools were biotinylated by amplification with primers containing a 5' dual biotin, and used in place of primary antibodies during western blotting. The membranes were visualized via exposure of a chemiluminescence reaction to X-ray film. Although previous work on aptamer blotting has been carried out, notably by Noma et al. (2006), conditions were optimized using lysozyme and an anti-lysozyme aptamer as a control (**Figure 5.11**). An optimal ratio of aptamer:protein loaded on gel was determined in this fashion.

Upon optimization of conditions, two different types of *S. pyogenes* protein extracts were prepared. Logarithmic-phase cultures of each of the 10 M-types used in SELEX were pelleted and cells were either subjected to 1) pepsin cleavage of surface proteins or 2) repeated freeze-thawing. The two extracts were called the Pepsin Extract (PE) and the Whole Cell Extract (WC). The PE extract contained only proteins from the cell surface that contain aromatic amino acids including the M-protein. The WC extract contained all cellular proteins and was centrifuged and broken up into soluble and insoluble fractions. The insoluble fraction was used for aptamer blotting as it contains all cell surface molecules.

The extracts were loaded on SDS-PAGE gels, transferred to PVDF membranes, and then blotted with biotinylated aptamer pools followed by anti-biotin HRP. A BSA solution was used in the blocking step. A set of biotinylated protein standards was run in every gel.

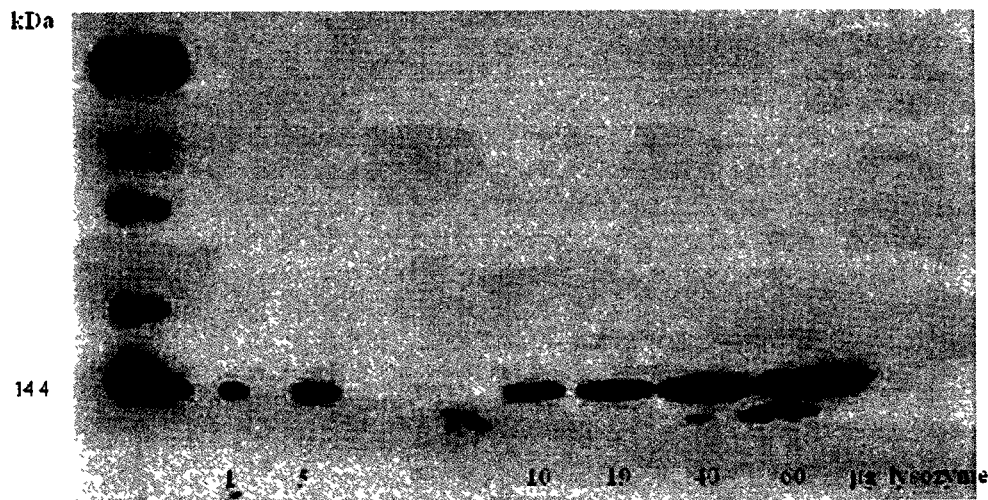


Figure 5.11. Blot of different amounts of lysozyme detected with a fixed amount of anti-lysozyme aptamer (180 nM).

As can be seen in **Figure 5.11**, blots were carried out by loading different amounts of lysozyme (0 to 60 μg) on a gel, running the gel and then transferring these proteins to a membrane, and incubating the membrane with 180 nM of anti-lysozyme aptamer. The binding dissociation constant (K_d) of the anti-lysozyme aptamer and lysozyme is 31 nM (344). All the protein amounts tested could be detected with anti-lysozyme aptamer at a concentration of 180 nM. No bands were detected below 20 μg protein when 60 nM aptamer was used (data not shown). Detection with 180 nM aptamer improved at amounts equal to or greater

than 10 μ g total protein. It is important to keep in mind that during these test incubations all of the aptamer sequences used are identical and all the protein on the membrane is the target protein lysozyme. In an aptamer pool, there are multiple sequences with different affinities for different targets. The sensitivity of aptamer pools for detection of target molecules may be less than that of a single sequence incubated with a known target. Also, the PE and WC extracts contain a wide array of potential target molecules. Hence, a higher amount of aptamer pool and total protein should be used when testing the aptamer pools and randomized library. The results of blots carried out with a randomized oligonucleotide library support this assumption (**Figures 5.12 and 5.13**). Bands could be detected on the blots when 270 nM randomized library was incubated with 20 μ g of total protein per lane. As expected, the randomized oligonucleotide library does have some affinity for molecules in both the PE and WC extracts (**Figures 5.12 and 5.13**). It appears to bind the pepsin band around 45 kDa in the PE fractions of M2, M3, and M4 (**Figure 5.12**). Binding of the randomized library is also observed for the WC extract insoluble fractions. For all M-types tested library consistently bound to low molecular weight molecules of 14kDa or less, and for most of the M-types it detected a band around 100 kDa (**Figure 5.13**). WC extracts of M-types M4, M6 and M11 did not produce 100 kDa bands when blotted with randomized library. There was no detectable binding of library to low molecular weight molecules in the M77 WC extract.

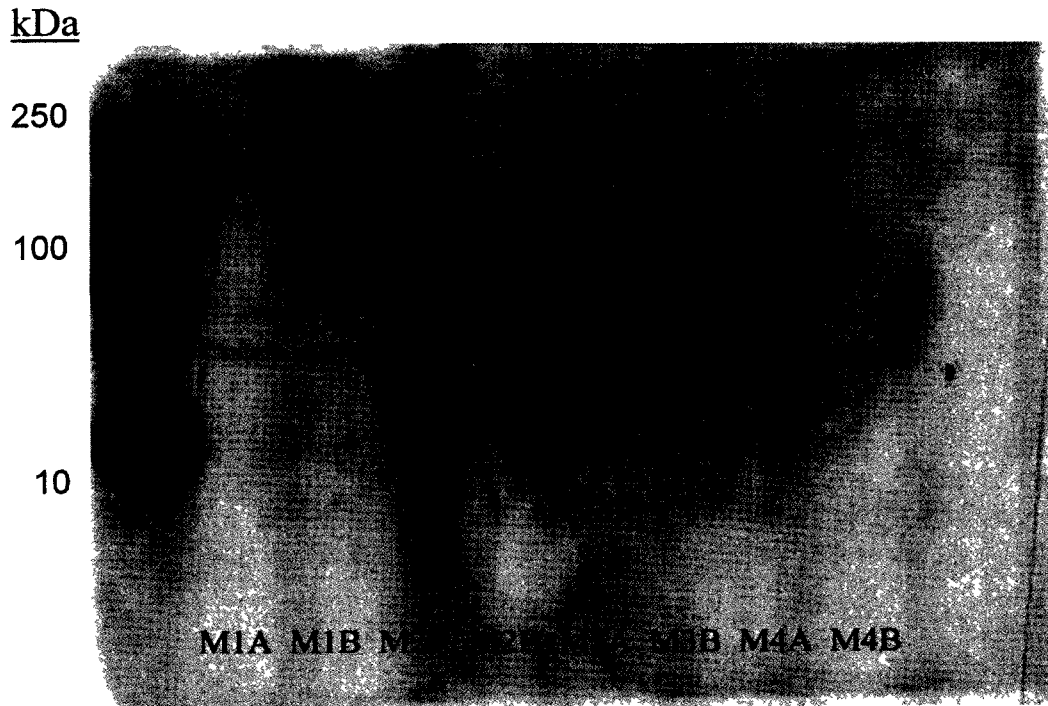


Figure 5.12. Aptamer blot of PE pepsin cell surface extracts using randomized oligonucleotide library (270 nM) and fixed amount of total protein per lane. Biotinylated library was detected with an anti-biotin horseradish peroxidase secondary antibody, and visualized chemiluminescently on X-ray film.

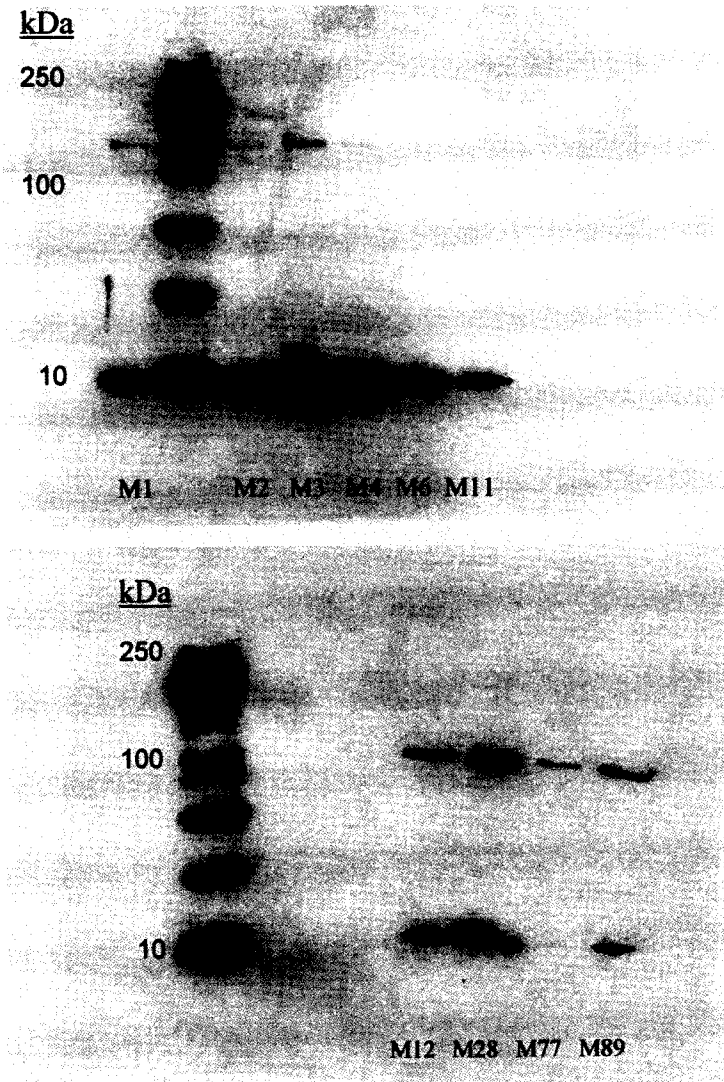


Figure 5.13. Aptamer blot of WC cell wall fractions using randomized oligonucleotide library (270 nM) and fixed amount of total protein per lane. Biotinylated library was detected with an anti-biotin horseradish peroxidase secondary antibody, and visualized chemiluminescently on X-ray film.

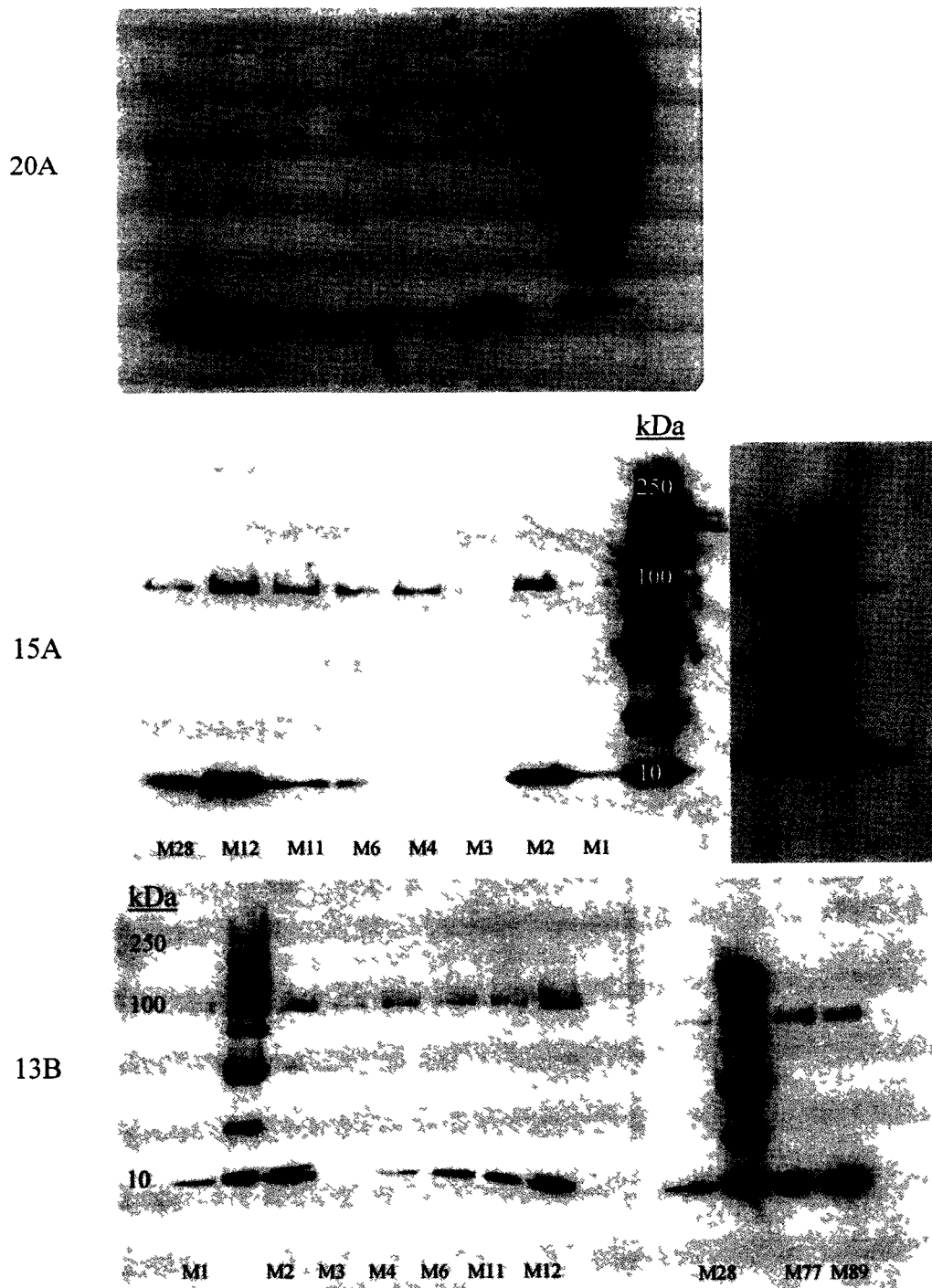


Figure 5.14. Aptamer blots of WC insoluble fractions using fixed amount of aptamer pool (270 nM) and fixed amount of total protein per lane.

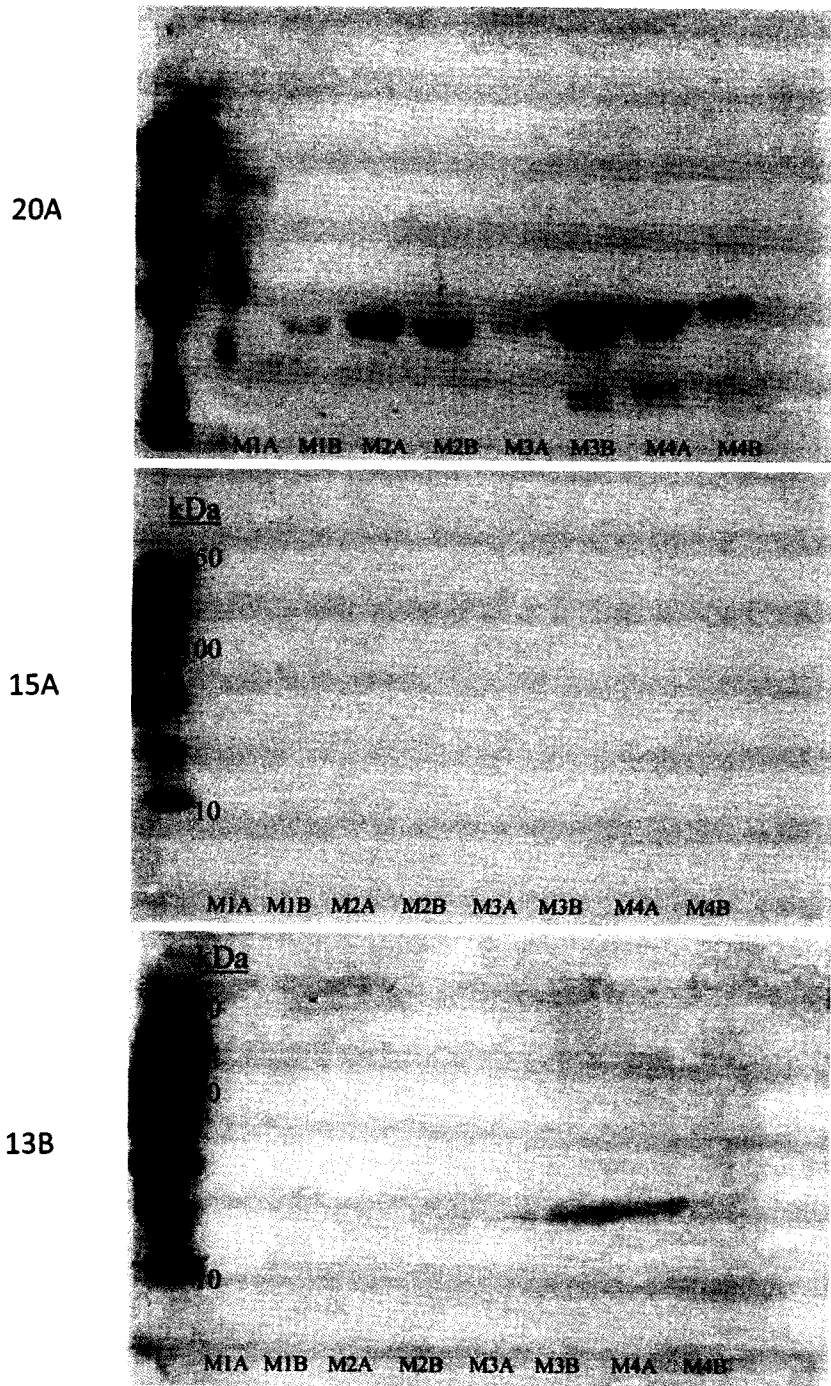


Figure 5.15. Aptamer blots of PE pepsin cell surface extracts using fixed amount of aptamer pool (270 nM) and fixed amount of total protein per lane.

The WC and PE extracts were then blotted with the aptamer pools 20A, 15A, and 13B. These pools were chosen because they seemed to demonstrate the most binding to the *S. pyogenes* target mixture when tested via flow cytometry (**Figure 4.5**). The aptamer pool 20A seemed to have affinity for most of the extracts tested. Like the randomized library, pool 20A detected bands at around 10 kDa and 100 kDa in WC extracts of all the different M-types (**Figure 5.14**). Higher molecular weight bands of around 225 kDa were detected in WC extracts M1, M3, M4, M11 and M12. A band of 150–175 kDa was detected by pool 20A in WC extract M1 (**Figure 5.14 Lane M1**). Pool 20A also detected bands in all the PE extracts tested except for M1A (**Figure 5.15**). The main bands detected in the PE extracts were the pepsin bands (about 45 kDa) but lower molecular weight bands were detected in M3 and M4 PE extracts. The aptamer pools seemed to bind preferentially to the M3B and M4a PE extracts.

Aptamer pools 15A and 13B seemed to have lower or more specific affinities for the pepsin extracts than pool 20A. Pools 15A and 13B only detected the same 10 kDa and 100 kDa bands also detected by the randomized library in the WC extracts (**Figure 5.14**). Pool 15A did not detect anything in the PE extracts and pool 13B only faintly detected pepsin in extracts M3B and M4a (**Figure 5.15**).

5.3.3 Removal of aptamer sequences from PVDF membrane

Randomized oligonucleotide library was incubated with WC extracts blotted on a membrane at the same time as the blots in **Figure 5.13**, except that this second set of blots was not visualized with chemiluminescence reagents.

Instead, the locations of the 10 kDa and 100 kDa bands were determined by overlaying the developed blot on the undeveloped PVDF membrane, and the protein bands were then sliced from the membrane. Proteins were extracted from the slices with phenol-chloroform, and the bound DNA was ethanol precipitated and PCR amplified. The results of this PCR amplification can be seen in **Figure 5.16**.

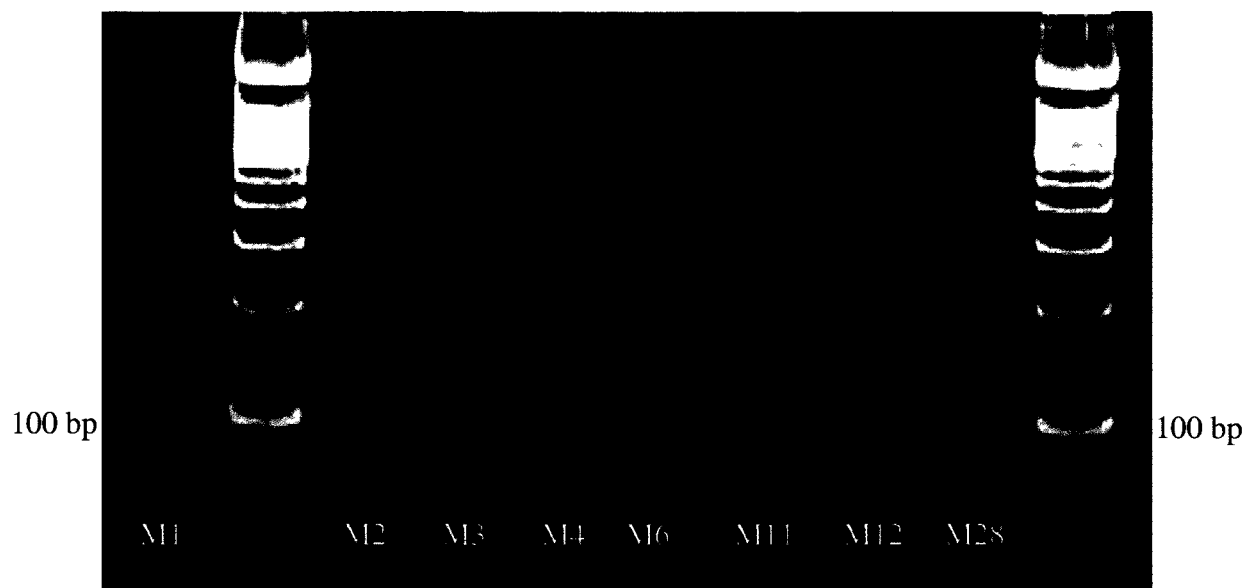


Figure 5.16. PAGE gel of aptamer sequences amplified from 100 KDa bands on a PVDF membrane. WC extracts from the indicated M-types were run on an SDS-PAGE gel and transferred to a PVDF membrane. Following incubation with randomized oligonucleotide library, the spots on the membrane corresponding to the 100 KDa band were excised and phenol extracted. DNA was then ethanol precipitated, resuspended in PCR reaction buffer, and amplified for 20 cycles at the same PCR conditions used in SELEX A and B. The 80 bp PCR products were visualized on a 7.5% PAGE gel with ethidium bromide staining.

5.4 References

1. Noma T, Ikebukuro K, Sode K, Ohkubo T, Sakasegawa Y, Hachiya N, et al. Screening of DNA aptamers against multiple proteins in tissue. *Nucleic Acids Symp Ser (Oxf)*. 2005;(49)(49):357-8.
2. Pavski V, Le XC. Detection of human immunodeficiency virus type 1 reverse transcriptase using aptamers as probes in affinity capillary electrophoresis. *Anal Chem*. 2001 Dec 15;73(24):6070-6.
3. Lortal S, Rouault A, Cesselin B, Sleytr UB. Paracrystalline surface layers of dairy propionibacteria. *Appl Environ Microbiol*. 1993 Aug;59(8):2369-74.
4. Beachey EH, Stollerman GH, Chiang EY, Chiang TM, Seyer JM, Kang AH. Purification and properties of M protein extracted from group A streptococci with pepsin: Covalent structure of the amino terminal region of type 24 M antigen. *J Exp Med*. 1977 Jun 1;145(6):1469-83.
5. Kirby R, Cho EJ, Gehrke B, Bayer T, Park YS, Neikirk DP, et al. Aptamer-based sensor arrays for the detection and quantitation of proteins. *Anal Chem*. 2004 Jul 15;76(14):4066-75.
6. Berezovski M, Drabovich A, Krylova SM, Musheev M, Okhonin V, Petrov A, et al. Nonequilibrium capillary electrophoresis of equilibrium mixtures: A universal tool for development of aptamers. *J Am Chem Soc*. 2005 Mar 9;127(9):3165-71.
7. Jensen KB, Atkinson BL, Willis MC, Koch TH, Gold L. Using in vitro selection to direct the covalent attachment of human immunodeficiency virus type 1 rev protein to high-affinity RNA ligands. *Proc Natl Acad Sci U S A*. 1995 Dec 19;92(26):12220-4.
8. Morris KN, Jensen KB, Julin CM, Weil M, Gold L. High affinity ligands from in vitro selection: Complex targets. *Proc Natl Acad Sci U S A*. 1998 Mar 17;95(6):2902-7.
9. Mendonsa SD, Bowser MT. In vitro selection of high-affinity DNA ligands for human IgE using capillary electrophoresis. *Anal Chem*. 2004 Sep 15;76(18):5387-92.
10. Boot HJ, Pouwels PH. Expression, secretion and antigenic variation of bacterial S-layer proteins. *Mol Microbiol*. 1996 Sep;21(6):1117-23.

Chapter 6

Comparison of Aptamer Pools From Different Sets of SELEX

6.1 Introduction

Seven aptamer pools were evolved using seven separate randomized libraries and two separate targets: *Lactobacillus acidophilus* or a mixture of 10 different *Streptococcus pyogenes* M-types. These pools have been named: Lacto heat, Lacto mag, GAS 15A, GAS 20A, GAS 13B, GAS 8D, and GAS 8E. The bacterial-cell SELEX methodology in **Figure 2.1** (1) formed the basis of the methodologies used for each pool. However, SELEX conditions were varied in order to determine which yield the best resultant aptamers. Conditions that were varied include 1) starting sequence diversity, 2) purification of PCR amplicons into single-stranded form, 3) introduction of a counterselection step, 4) collection of aptamers that remain bound to cells after heat elution, and 5) the incubation step ratio of target cells to DNA molecules. A detailed comparison of aptamers obtained from each pool enables a better understanding of how SELEX conditions affect outcome in bacterial cell-SELEX. Differences in the SELEX methodologies used for each pool are detailed below.

6.2 Reagents

6.2.1 Lacto heat pool

L. acidophilus 4356 cells were used as a target. A randomized oligonucleotide library was PCR amplified for 20 cycles prior to initiation of SELEX. Initially, 2 nmole of library representing around 10^{12} unique and 10^{15} total sequences was used. Aptamer pools obtained after each round of SELEX were also amplified for 20 cycles. It is 100 pmole of the amplified CA fraction that is used as an input in subsequent rounds of SELEX. Library and subsequent aptamer pools were rendered single-stranded via heat denaturation. A 10X molar excess (relative to DNA) of BSA and tRNA were included during incubation, and 0.05% BSA was included in each wash step. The Lacto heat pool was cloned and sequenced after 7 rounds of SELEX.

6.2.2 Lacto mag pool

The conditions used to generate the Lacto mag pool were the same as for the Lacto heat pool. The only difference is that the mag pool was rendered single-stranded by taking advantage of the biotin-streptavidin interaction. Streptavidin-coated magnetic beads were used to separate biotinylated from non-biotinylated strands of DNA amplified from the CA fractions. The forward strands were purified, and the CA fraction DNA was biotinylated via amplification with a reverse primer containing a 5'-Biotin. The Lacto mag pools were cloned and sequenced after 7 rounds of SELEX.

6.2.3 GAS 15A and 20A pools

Aptamers were generated against a mixture of 10 different M-types of *Streptococcus pyogenes*. The 10 most prevalent M-types in Canada were chosen: M1, M2, M3, M4, M6, M11, M12, M28, M77, M89 (2). Each M-type was grown in a separate culture, and an equal number of cells from each type was combined immediately prior to SELEX to reach a total of 10^8 cells. The GAS 15A pool was cloned and sequenced after 15 rounds of SELEX. The GAS 20A pool was cloned and sequenced after 20 rounds of SELEX. GAS 20A is a later pool from the same round of selection that generated GAS 15A.

6.2.4 GAS 13B pool

A set of selections was carried out against the same mixture of 10 *S. pyogenes* M-types as 15A and 20A. All conditions were kept the same except that the ratio of DNA to cells was altered in each round of selection in order to increase competition between sequences for target cells. The specific amounts of DNA and cells used are summarized in **Table 5**. The number of cells was decreased from 10^8 to 10^5 and the amount of DNA was held constant, and then increased in later rounds. The GAS 13B pool was cloned and sequenced after 13 rounds.

6.2.5 GAS 8D and 8E pools

A mixture of the 10 most prevalent *S. pyogenes* M-types was used as a target. The conditions for each round of selection are summarized in **Table 9**. A different number of unique starting library sequences were used; 10^{16} for SELEX D and 10^{14} for SELEX E. This discrepancy is due to the fact that the library for

SELEX E was amplified prior to the first round of selection whereas the library for SELEX D was used straight from the tube without further PCR amplification. Hence, SELEX E had fewer unique sequences and more copies of each sequence. Library for SELEX E and aptamer pools for both D and E were amplified and rendered single-stranded via gel purification. Hence, only the reverse strands were retained for use in the next round. The advantage over heat denaturation is that no sequences are lost due to reannealing. The same fractions were collected as in the methodology of Hamula et al., except that after heat-elution and removal of the CA fraction the cells were resuspended in PCR buffer and amplified as the Cells fraction. The Cells fraction contains high affinity aptamers that could not be released by heat and salt. The amplicons of the Cells and CA fractions were combined as inputs for the next round of selection. In addition, a round of counterselection was carried out at round 3 with *Streptococcus bovis* as a target.

6.3 Results

6.3.1 Amplification of DNA from different SELEX fractions

Following each round of selection, the various fractions collected were PCR amplified and run on PAGE gels. Gel photos for Round 1 fractions of Lacto heat and Lacto mag selections can be found in **Figure 2.1**; the remaining gel photos for those sets of SELEX can be found in the Appendix as **Figures A1 to A9**. Similarly, the fractions from the first round of SELEX A and B gel photo is **Figure 3.4**; rounds 2 through 20 of SELEX A and 2 through 13 of SELEX B can be found in Appendix **Figures A10 to A40**. For SELEX D and E, first round

fraction gel photos are **Figures 4.1 and 4.2**. Counterselection So and wash fractions are represented in **Figure 4.4**. Rounds 2 through 8 are Appendix **Figures A41 to A47**.

The DNA distribution between the fractions collected from different sets of SELEX varied as selection proceeded. The gels for the first round fractions were similar for all selections, with the majority of DNA remaining in the So fractions. Over the course of all the selections, the trend was for the amount of DNA to decrease in the supernatant and move into the wash and CA/cells fractions. In most rounds of selection, the CA fraction generated the highest amount of the target amplicon. This was also true for the Cells fractions of SELEX D and E. However, the distribution of DNA in the wash cycles was not consistent between sets of SELEX or even within a set of SELEX. Within a given set, there was an overall shift of DNA into later washes over the number of cycles, but there was a high degree of variation.

For example, in SELEX A there was no DNA detected in the wash fractions for some later rounds (rounds 14 and 15). However, rounds 16 through 20 saw a redistribution of DNA into the wash fractions. The presence of DNA in the wash fractions of rounds 16 through 20 may explain the lower binding of aptamer pools 16A through 20A relative to 15A for *S. pyogenes* cells, as seen in **Figure 3.5**. In contrast, during SELEX B some earlier rounds (rounds 4 and 5) had an absence of DNA in the wash fractions, and the trend was towards increasing DNA in the wash fractions of later rounds. The trend for SELEX D and E was for the amount of DNA in the supernatant to decrease dramatically in later

rounds, with increased DNA in the wash fractions. The Lacto heat and Lacto mag selections saw a movement of DNA out of the supernatant and wash fractions into the CA fraction with increasing rounds of SELEX.

6.3.2 Evolution of aptamer pool binding to target cells with increasing SELEX rounds

Following each round of SELEX, the amplified aptamer pools were fluorescently-labeled and their binding to target cells analyzed via flow cytometry. A typical flow cytometry output consists of a scatter plot, along with a fluorescence intensity histogram indicating the number of events counted at a given fluorescence intensity. With increased aptamer binding to cells, there is a peak shift towards the higher intensities on the histogram (indicated by a peak shift to the right). For aptamer pools from Lacto SELEX rounds (heat and mag), this shift was only a partial peak shift, as shown for the round 8_{heat} aptamer pool in **Figure 6.1**. In contrast, for the aptamer pools from GAS SELEX rounds (A,B,D,E) the entire peak shifted to the right as seen for the aptamer pool GAS 13B (**Figure 6.1**).

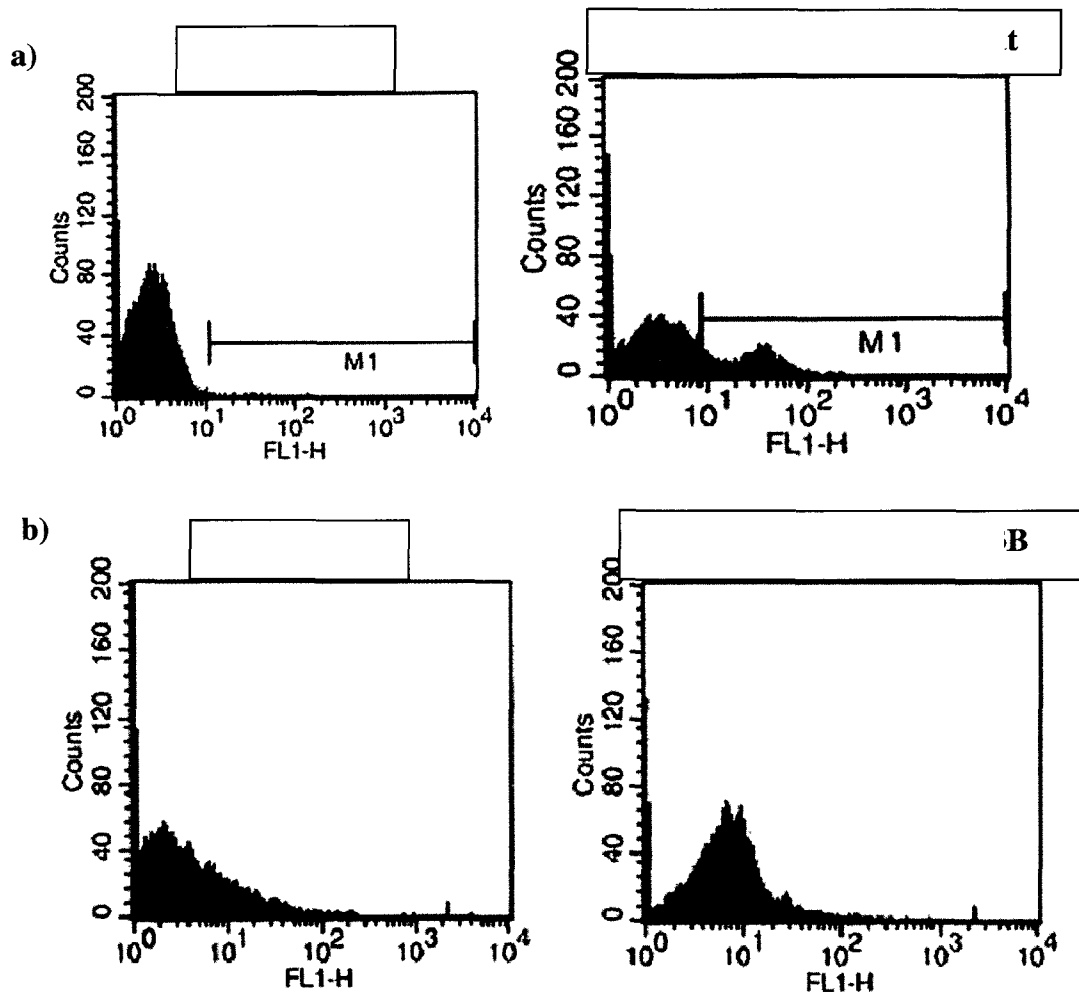


Figure 6.1. Typical fluorescence histograms from flow cytometry analysis of aptamer pool binding for (a) Lacto heat and (b) GAS B SELEX.

The peak shift is measured relative to a negative control of cells alone or cells incubated with fluorescently-labeled randomized library. This measurement is the percent gated fluorescence intensity over background, as indicated in **Figures 2.2, A11, and 4.5**. The percent gated fluorescence intensity over background can be plotted for each round of SELEX (**Figure 6.2**). Over the

course of selection, the extent of aptamer binding increased for all sets of SELEX; however the extent of binding was variable between sets. The results are described in detail in previous chapters 1 through 3. The aptamer pools from the Lacto rounds of SELEX evolved to have the highest values of percent gated fluorescence above background, climbing to 67 % in round 7heat and 49 % in round 6mag, respectively. The aptamer pools with the third highest evolved binding to target cells are the pools from GAS SELEX D, which have a maximum percent gated fluorescence intensity above background of 39% at round 8. The aptamer pools from GAS SELEX A, B, and E have lower evolved target cell binding with maximum percent gated fluorescence intensities of 14% for round 15A, 21% for round 7B, and 13% for round 7E. It appears from flow cytometry analysis of fluorescently-labeled aptamer pool binding to target cells that the SELEX sets Lacto heat, Lacto mag and GAS SELEX D worked the best in that they resulted in the highest affinity aptamer pools. The SELEX sets Lacto beads, Lacto heat, and GAS SELEX D also seemed to evolve high-binding aptamer pools faster than SELEX sets GAS A, B and E. A significant increase in percent gated fluorescence intensity above background was seen after the 4th round for these three sets of SELEX, whereas for SELEX A and B this increase was slight and started much later, and for SELEX E the increase started after round 2 but remained at the same level for all the remaining rounds. A fluorescently-labeled randomized oligonucleotide library control was subtracted from all the measurements in **Figure 6.2** except for the *Lactobacillus* selections. However, separate controls carried out using fluorescent aptamer pools alone and buffer

with BSA and tRNA alone did not yield any increase in gated fluorescence above background levels (data not shown).

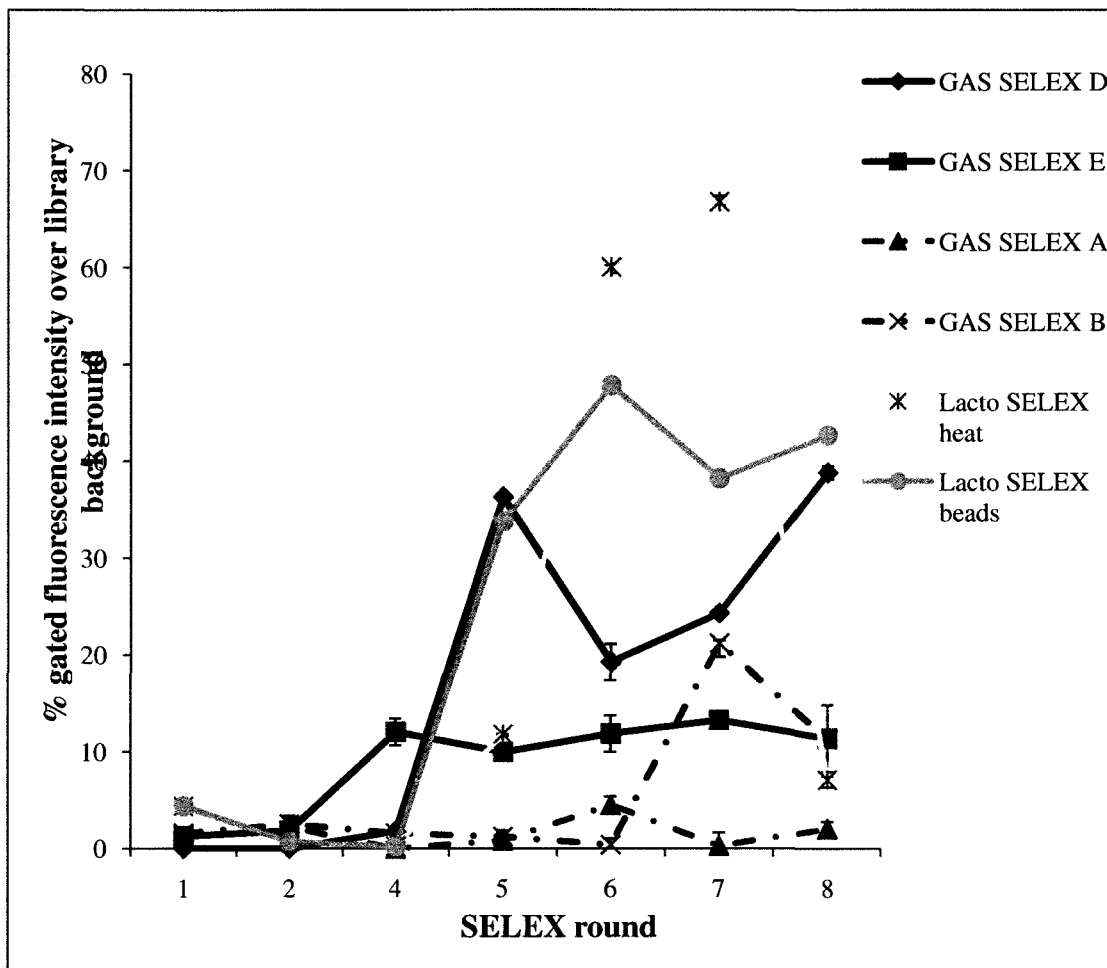


Figure 6.2. Comparison of change in gated fluorescence intensity over background with increasing cycle number for different sets of SELEX.

6.3.3 Aptamer pool sequence characteristics

Following flow cytometric screening, aptamer pools were cloned and sequenced. The aptamer pools chosen for sequencing were Lacto heat 7, Lacto mag 8, GAS 15A, GAS 20A, GAS 13B, GAS 8D and GAS 8E. A minimum of 15 sequences were obtained for each pool and these sequences are listed in Appendix **Tables A1** through **A6**. For all aptamer pools, many of the sequences had high GC content, including stretches of multiple C or G residues in a row. High amounts and large stretches of GC are conducive to the formation of secondary structures. Some of the pools also had more repetition of sequences within the pool than others. GAS SELEX pools A and B had no repetition; whereas in the Lacto pools the sequence hemag1P was repeated 6 times, another sequence was repeated 3 times. The GAS 8D and 8E pools had the highest amount of repetition, with large tracts of sequence repeated to form similar secondary structures for 13 of the SELEX D sequences and 7 of the SELEX E sequences.

6.3.4 Free energy distribution of each aptamer pool

Secondary structures with more negative free energy values are more likely to be stable at a given temperature. The average free energies of formation for the most likely secondary structures of each aptamer pool are listed in **Table 14**. The averages were calculated for all sequences within a pool, and separate averages were calculated for all sequences without primers, and all sequences with primers. For most aptamer sequences and predicted secondary structures, inclusion of the primers lowered the free energy of formation. Hence, the aptamer pools with the lowest average free energies are those with primers included in the

aptamer sequence. There is no significant difference in average free energy between any of the aptamer pools irregardless of whether primers are included or not. The free energies measured for all the predicted structures ranged from a low of -16.7 kcal/mole for a sequence in the Lacto heat pool to a high of 0.7 for a sequence in the 13B pool. The average free energies of the aptamer pools are also shown for the separate fractions of SELEX D and E (CA, Cells and CA Cells fractions) in **Table 15**. There is no significant difference in average free energy between any of the different fractions collected. The free energy distributions of each aptamer pool are roughly normal and are plotted in **Figures 6.3 to 6.9**. The distributions are shifted towards lower values when primer sequences are included.

Table 14. Mean free energies of likely predicted secondary structures of sequences cloned from different aptamer pools.

Aptamer pool	No Primers	Primers	Lowest ΔG (kcal/mole)	Overall Mean ΔG (kcal/mole)
Lacto heat	-3 ± 2	-9 ± 3	-16.7	-6 ± 4
Lacto beads	-3 ± 2	-10 ± 2	-12.7	-7 ± 4
GAS 15A	-4 ± 2	-10 ± 3	-12.6	-7 ± 3
GAS 20A	-2 ± 2	-7 ± 2	-12.6	-5 ± 3
GAS 13B	-4 ± 2	-10 ± 3	-14.2	-7 ± 4
GAS 8D	-2 ± 1	-7 ± 2	-11.6	-4 ± 3
GAS 8E	-2 ± 1	-7 ± 1	-11.2	-4 ± 3

Table 15. Mean free energies of predicted secondary structures of aptamer sequences cloned from CA (heat-eluted), cell-bound (cell), or pooled (CA cells) fractions in SELEX D and E.

Aptamer pool	Mean free energy (kcal/mole) CA fraction	Mean free energy (kcal/mole) Cells fraction	Mean free energy (kcal/mole) Pooled CA cells fraction
8D all	-5 ± 3	-4 ± 2	-5 ± 3
8E all	-5 ± 3	-4 ± 3	N/A
8D no P	-3 ± 2	-2 ± 1	-3 ± 1
8E no P	-2 ± 2	-1 ± 1	N/A
8D P	-8 ± 3	-7 ± 1	-7 ± 2
8E P	-8 ± 2	-7 ± 1	N/A

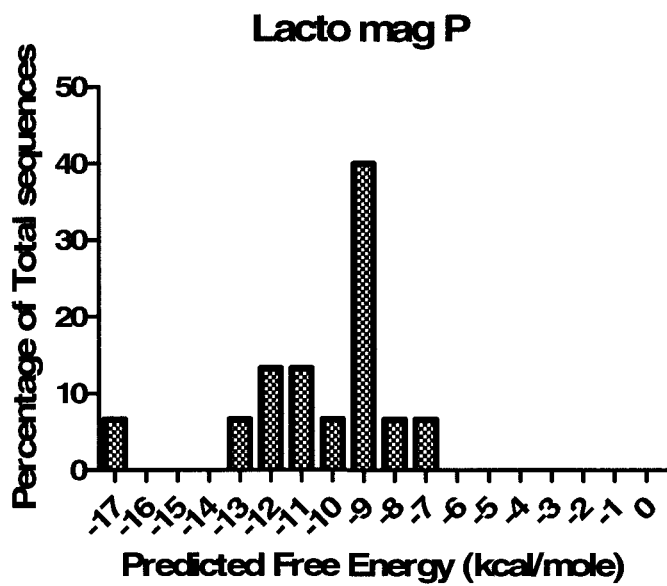
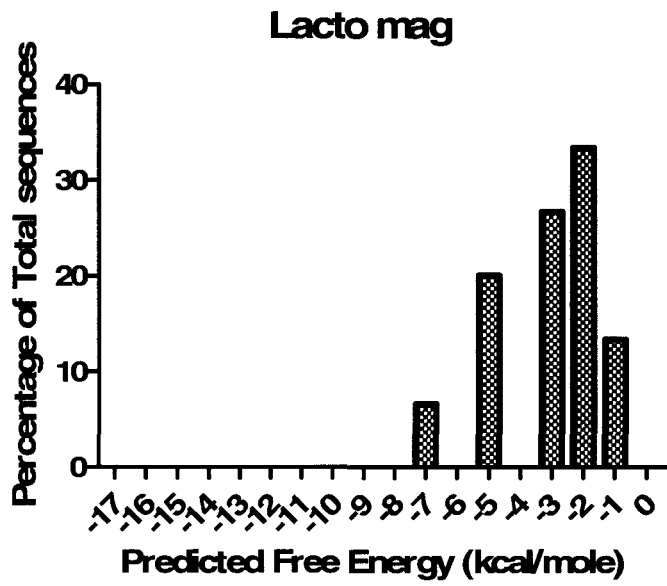


Figure 6.3. Free energy distribution of sequences from the Lacto mag (beads) aptamer pool, both without and with primers (P).

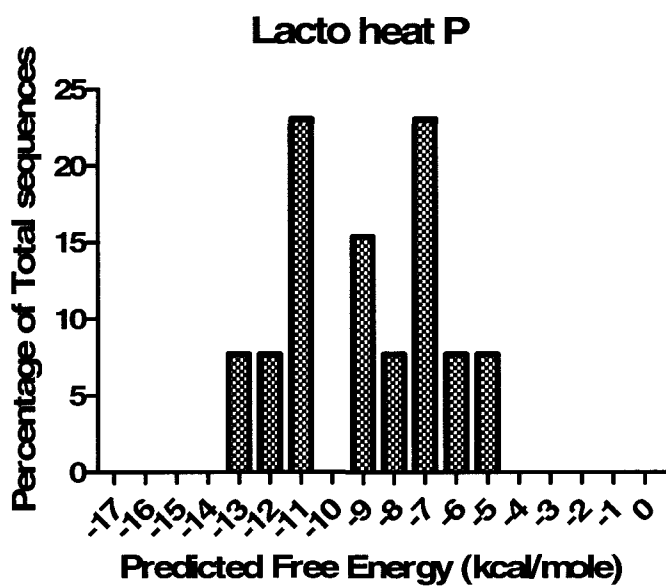
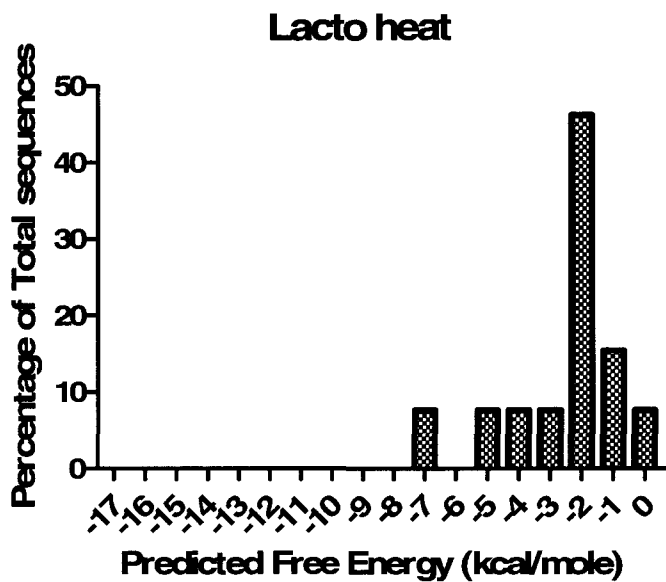


Figure 6.4. Free energy distribution of sequences from the Lacto heat aptamer pool, both without and with primers (P).

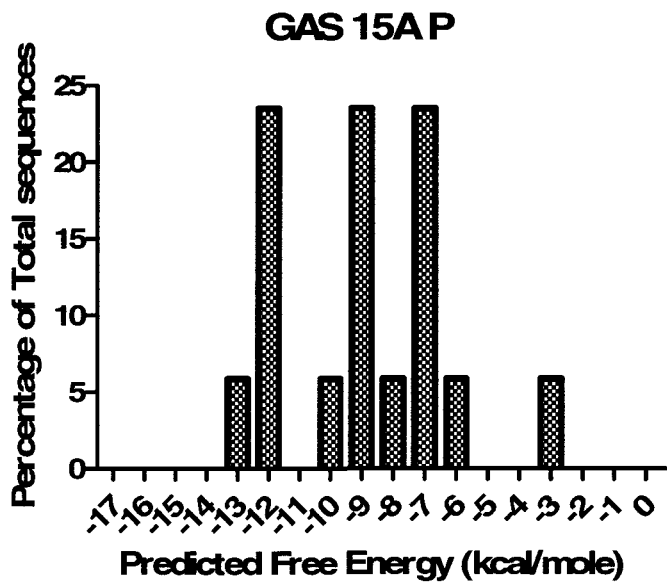
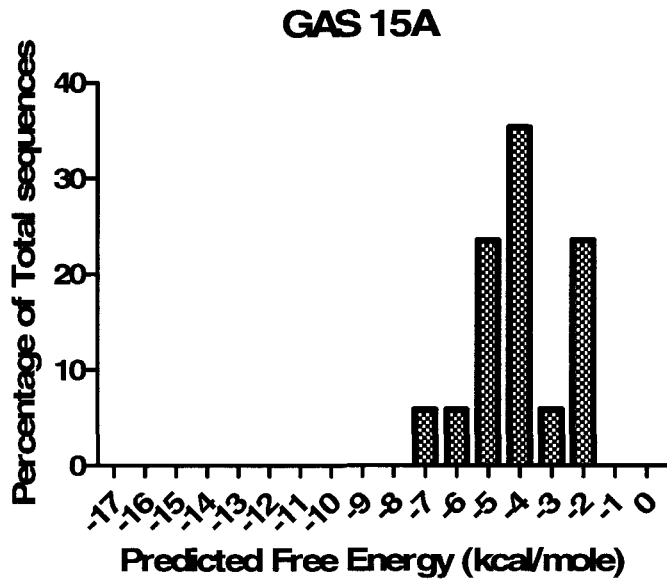


Figure 6.5. Free energy distribution of sequences from the GAS 15A aptamer pool, both without and with primers (P).

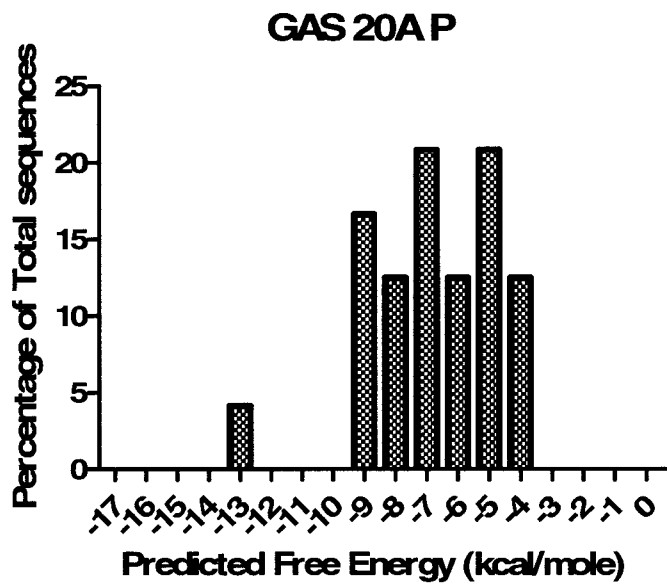
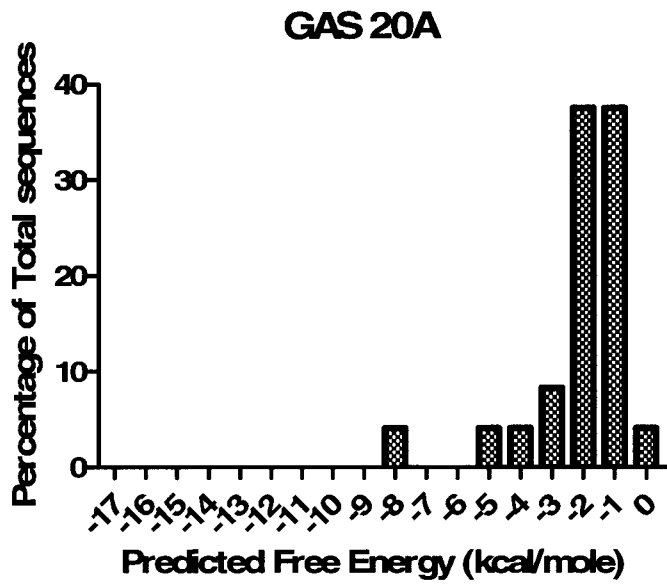


Figure 6.6. Free energy distribution of sequences from the GAS 20A aptamer pool, both without and with primers (P).

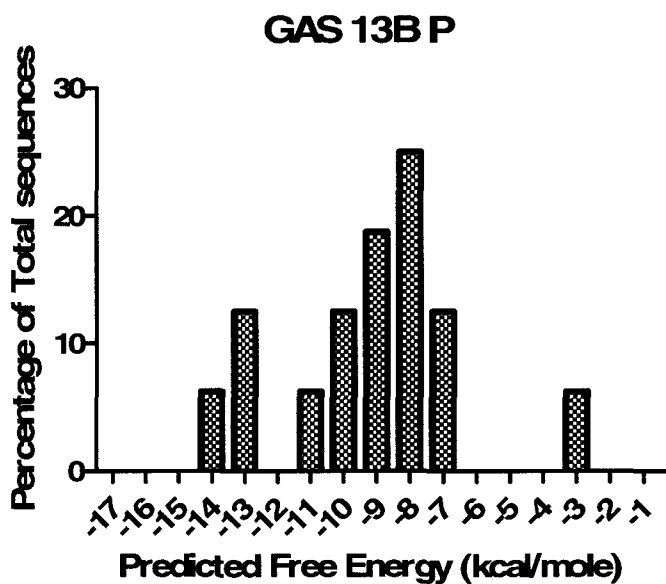
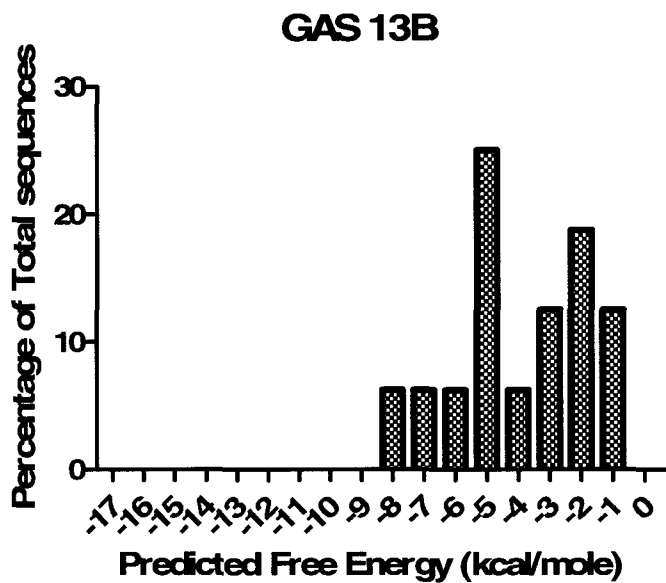


Figure 6.7. Free energy distribution of sequences from the GAS 13B aptamer pool, both without and with primers (P).

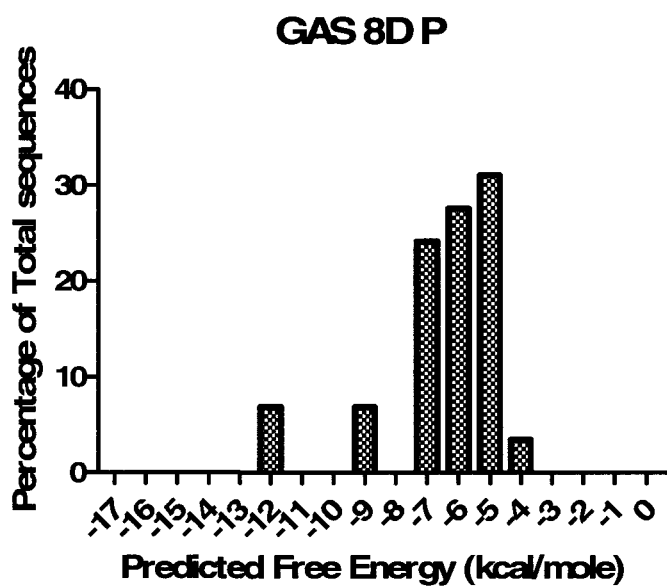
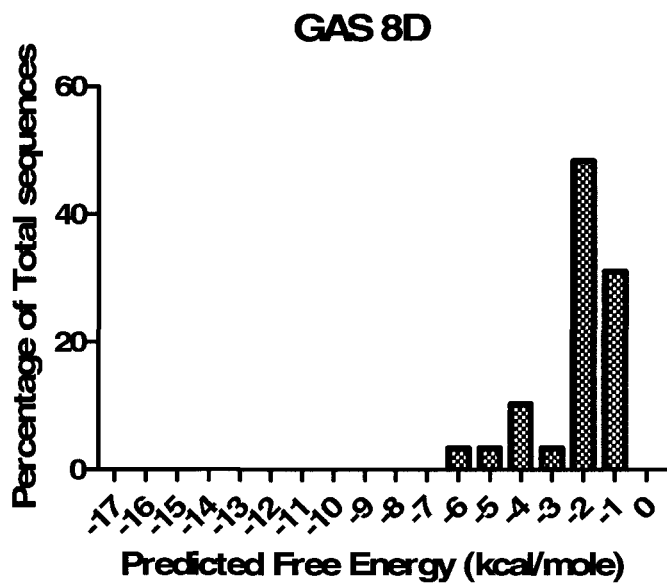


Figure 6.8. Free energy distribution of sequences from the GAS 8D aptamer pool, both without and with primers (P).

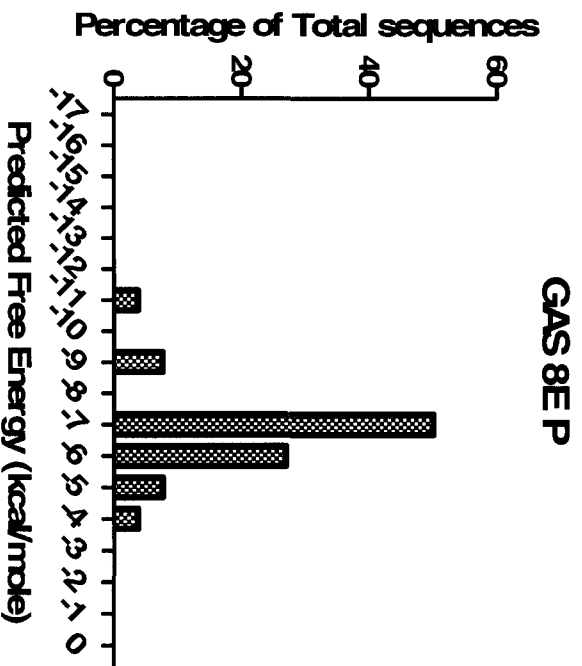
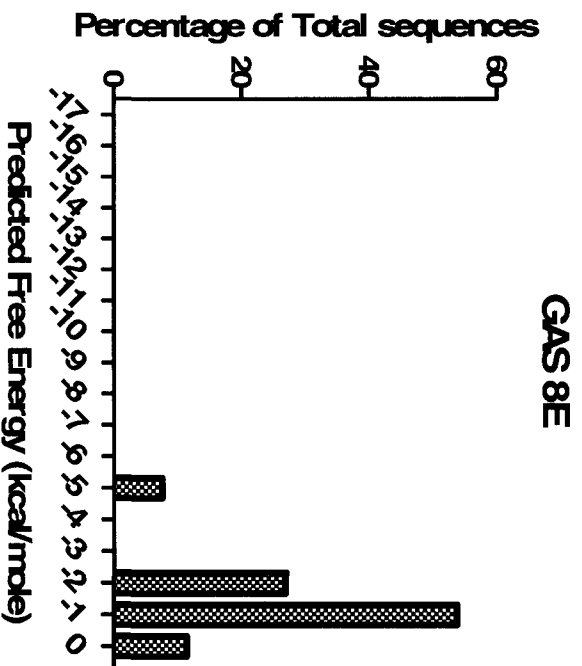


Figure 6.9. Free energy distribution of sequences from the GAS 8E aptamer pool, both without and with primers (P).

6.3.5 Secondary structural motif distribution of each aptamer pool

The most likely predicted secondary structure for each sequence was not evaluated merely on the basis of free energy of formation, but also on the type and shape of the secondary structure formed. The types of structures formed within an aptamer pool can be divided into three subcategories: 1) Hairpin-like structures, 2) Branched structures, and 3) Circular structures with minimal secondary structure formation. A summary of the types of secondary structures found in each aptamer pool, along with an example of each, is presented in **Table 16**.

The aptamer pools with the highest affinities for target cells, as demonstrated by flow cytometry, were Lacto heat, Lacto mag, and GAS 8D (**Figure 6.2**). These pools had a low proportion of circular sequences with minimal secondary structures, and a high proportion of hairpin and branched structures. Lacto heat, the aptamer pool with the highest binding, consisted of 31% hairpins, 50% branched and 19% circular structures. The Lacto mag pool had slightly lower binding than the Lacto heat pool and had a higher proportion of hairpins (53%), lower proportion of branched structures (33%), and similar proportion of circular structures (13%). The GAS 8D pool had a high proportion of hairpins (76%), some branched structures (19%) and very few circular structures (5%). The high proportion of hairpin structures in GAS 8D was partially due to the high amount of sequence repetition in this pool.

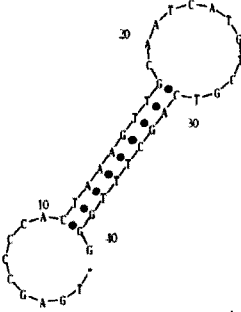
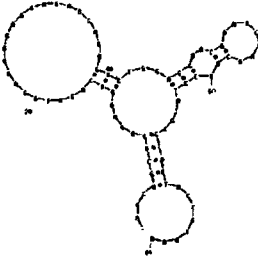
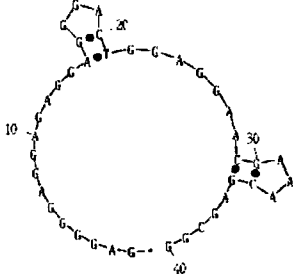
Other aptamer pools with low affinities for target cells when tested via flow cytometry were the pools GAS 15A, 20A, and 13B. The pools 15A and 20A had high proportions of open structures in comparison to the rest of the sequences,

29% and 42%, respectively, while the 13B pool had 12%. They also had high proportions of hairpins, 53%, 35%, and 66% for 15A, 20A, and 13B. The proportion of branched structures was somewhat lower than for the Lacto pools at 18% for 15A, 23% for 20A, and 22% for 13B.

The presence of a low proportion of circular structures does not necessarily guarantee a high affinity aptamer pool. Aptamer pool 8E had low affinity for the target *S. pyogenes* cells when tested via flow cytometry, and the highest proportion of hairpins of any pool (87%) and the second lowest proportion of circular structures (6%). GAS 8E had very few branched structures (7%).

Using *S. pyogenes* cells as a target increased the proportion of hairpin structures in the pool, with GAS 15A, 20A, 13B, 8D and 8E all having higher proportions of hairpins than any other sequence type (76% for 8D, 87% for 8E, 53% for 15A, 35% for 20A and 66% for 13B). Using *Lactobacillus* cells as a SELEX target seems to select for a higher proportion of branched structures than *S. pyogenes* (50% for Lacto heat and 33% for Lacto mag, versus 19% for 8D, 7% for 8E, 18% for 15A, 23% for 20A, and 22% for 13B).

Table 16. Distribution of different types of predicted secondary structures within aptamer pools for sequences both with and without primers.

Aptamer pool	Hairpin (%) 	Branched (%) 	Circular (%) 
Lacto mag	53	33	13
Lacto heat	31	50	19
GAS 15A	53	18	29
GAS 20A	35	23	42
GAS 13B	66	22	12
GAS 8D	76	19	5
GAS 8E	87	7	6

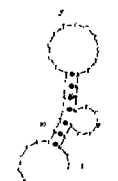
6.3.6 Sequences and secondary structures common to multiple aptamer pools

There were several sequences common to all the different aptamer pools generated against the same target cells. These are listed in **Table 17** along with their predicted secondary structures. Sequence Hemag1P was repeated 6 times between aptamer pools Lacto heat and Lacto mag. There was another sequence, Hemag2, repeated 3 times within the Lacto pools. The sequences found in both Lacto pools were unique to *L. acidophilus* as a target; none of them were shared with the aptamer pools evolved using *S. pyogenes*. The aptamer pools GAS 15A and 20A had only one sequence shared between them, A1 in **Table 17**. The sequences found in aptamer pool 13B were all unique. Two sequences shared extensively between the SELEX D and E pools were DE1 and ADE1 (**8D cells 9 and 8D cells 1 in Table 10**). These sequences share a similar secondary structure (**Figure 6.7**). Most significantly, the separate SELEX methodologies (A, D, and E) against *S. pyogenes* shared two identical aptamer sequences. Sequences 20A8 and 8D cells 1 are identical and are renamed ADE1 in **Table 17**. ADE1 is found once in aptamer pool 20A, 12 times in pool 8D, and 14 times in pool 8E. A second sequence, AD1, was found to be shared between the 15A and 8D pools. This sequence was found twice in aptamer pool 8D and once in 15A.

Despite minimal sequence repetition, there were multiple secondary structure motifs predicted to be formed by unique sequences and shared between pools Lacto heat and mag (**Figure 6.10**). Another unique set of secondary structural motifs was shared between unique sequences in aptamer pools 15A, 20A, and 13B (**Figure 6.11**). The number of times a given motif was predicted for

a unique sequence in one of the aptamer pools is indicated. Some of the unique sequences sharing a given motif also shared identical short tracts of nucleotides, while others did not. Some secondary structural motifs found in 13B, 15A, and 20A were also predicted for unique sequences in the other *S. pyogenes* aptamer pools from SELEX D and E (**Figure 6.12**). Two secondary structural motifs common to all *S. pyogenes* aptamer pools were each found twice in the *L. acidophilus* Lacto heat aptamer pool (**Figure 6.13**).

Table 17. Sequences shared between different aptamer pools.

Name	Sequence	Aptamer pools
Hemag1	5'-TAGCCCTTCAACATAGTAATATCTCTGCATTCTGTGATG-3' 	Lacto heat, mag
Hemag2	5'-TGAGCCCCAGTAAAGTTGCAATCATGTCGTCAGCTTTGGG-3' 	Lacto heat, mag
DE1	5'-GGGGAGGAGAAAAAAGGACCAGAGTAACGATTCGTGGGG-3' 	8D, 8E
ADE2	5'-CCCCACGAATCGTFACTCTGGTCTCTATTTCTCCTCCCC-3' 	20A, 8D, 8E
AD1	5'-GACGGTTCTTGATGGAGGGGACCTCAAGTGGGTTTCGGTG-3' 	15A, 8D
A1	5'-CCCACCCCGTCACTTCCTTCTCCGGTGTCTCCACGTC-3' 	20A, 15A

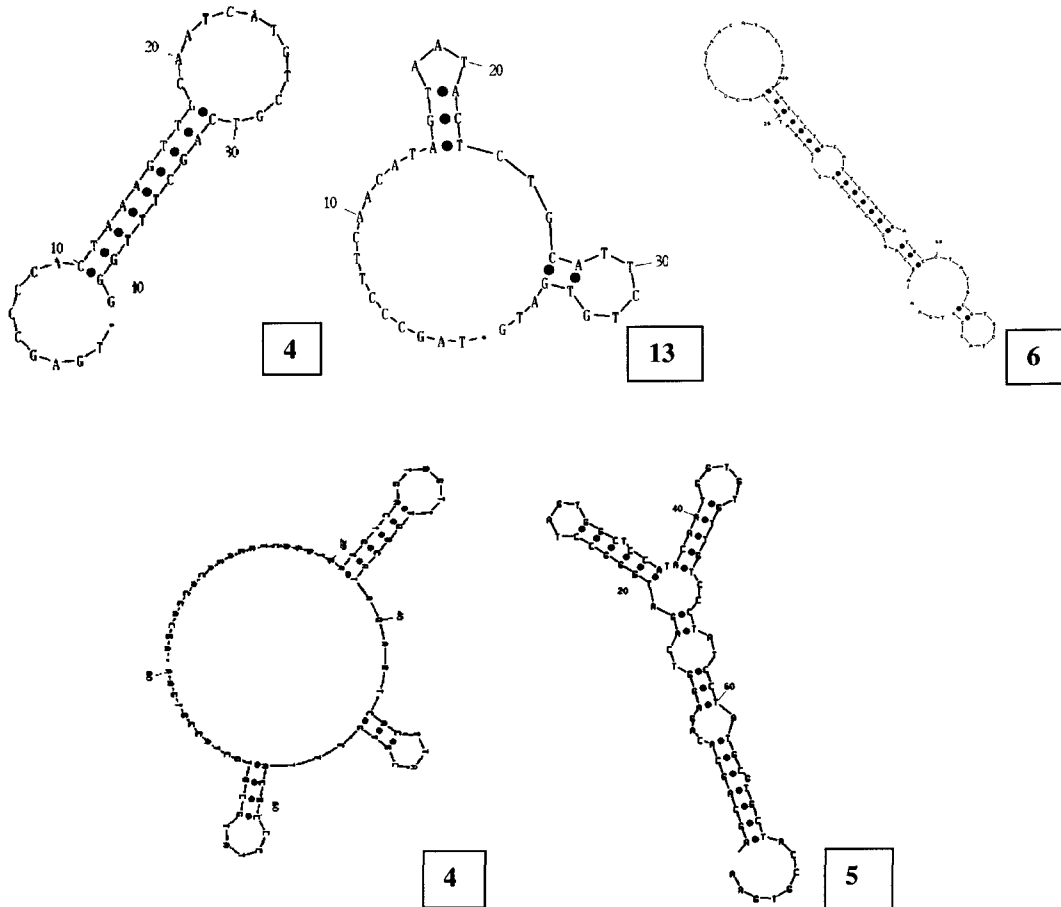


Figure 6.10. Secondary structure motifs repeated between unique sequences both with and without primers from Lacto heat and mag pools. The number of times each motif is repeated is indicated.

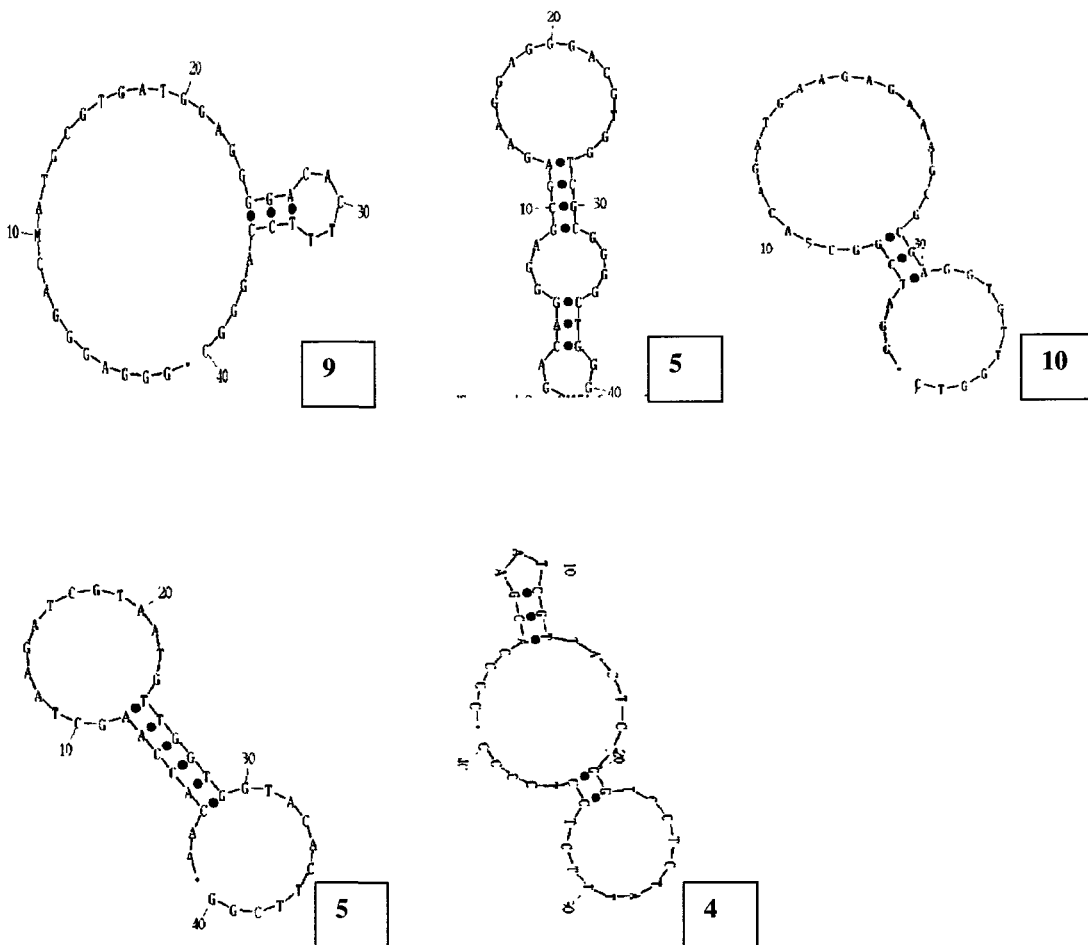


Figure 6.11. Secondary structure motifs repeated between unique sequences both with and without primers from different GAS A and B aptamer pools (15A, 20A, 13B). The number of times each motif is repeated is indicated.

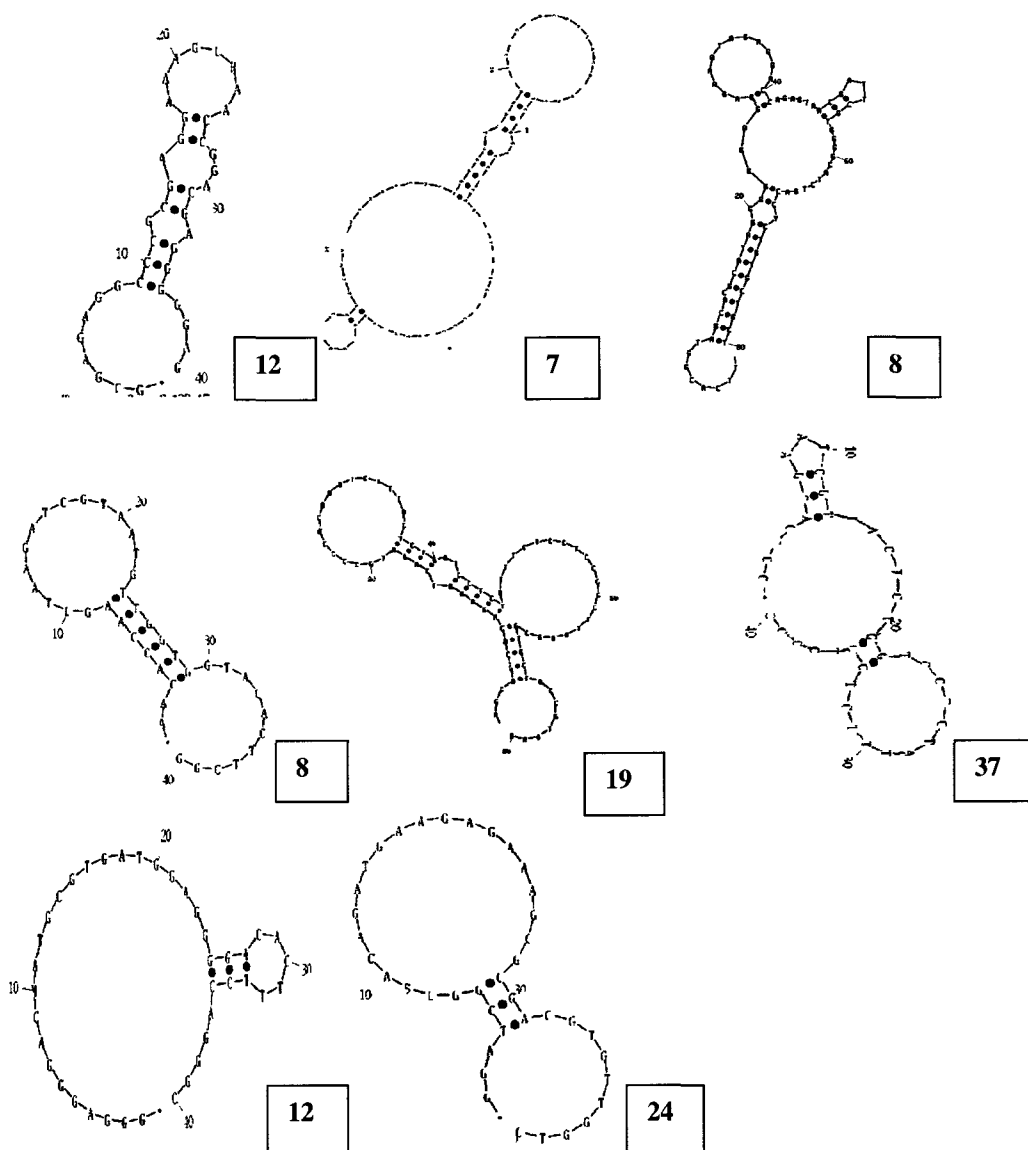


Figure 6.12. Secondary structure motifs shared between unique sequences from all *S. pyogenes* aptamer pools (13B, 15A, 20A, 8D, 8E). The number of times each motif is repeated is indicated. Motifs not present in **Figure 6.11** were found only once in one of aptamer pool 13B, 15A, or 20A.

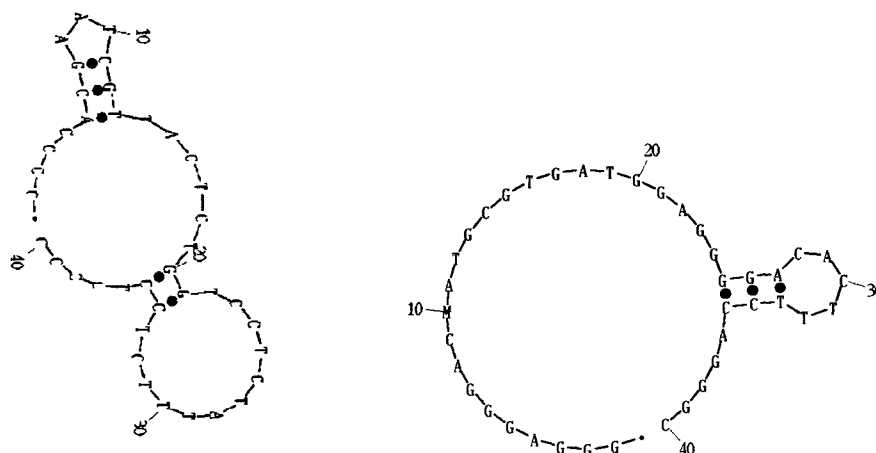


Figure 6.13. Secondary structure motifs shared between unique sequences from *S. pyogenes* and *L. acidophilus* aptamer pools.

6.3.7 Screening of individual sequences tested from each aptamer pool against target cells

A subset of sequences from each aptamer pool was selected for further testing based on predicted secondary structure, free energy of formation, and repetitiveness. The sequences were fluorescently-labeled and screened against the SELEX target cells via flow cytometry as described previously. Due to the high number of sequences obtained, not all of the sequences of a given aptamer pool were screened. Some of the sequences tested exhibited high binding to target cells whereas others did not, indicated by a high percent gated fluorescence over a randomized library background (**Figure 6.14**). A comparison of the number of high affinity sequences obtained from each aptamer pool indicates that SELEX A and D generated the most potentially useful aptamers and SELEX E the least. Furthermore, all of the high affinity sequences from SELEX D came from the

Cells fraction (**Figure 6.15**), indicating that many aptamers remain bound to the cell surface after heat elution into low salt. There was no difference in aptamer affinity distribution between the CA and Cells fractions of aptamer pool 8E.

Table 18 summarizes the number of sequences screened from each aptamer pool that had percent gated fluorescence intensities over background above 30%, as well as the sequences with the highest affinities.

The most high affinity aptamers were found in aptamer pool GAS 20A. However, SELEX D was the most successful methodology in generating high affinity aptamers since it only took 8 rounds to obtain aptamers of similarly high affinity as 20 rounds of SELEX A. The highest affinity aptamer obtained in 20A was 20A 1 with a percent gated fluorescence above background measurement of 73% when tested against the *S. pyogenes* target cell mixture. For 8D, the highest affinity aptamer was 8D cells 1 with a percent gated fluorescence above background of 75%. Since fewer 8D sequences were screened it is reasonable to assume that the end result of both sets of SELEX was a similar number of high affinity aptamers. Both of these pools also shared the same high affinity sequence, ADE1 (**Table 17**). This was sequence 20A 8 in the aptamer pool 20A and 8D cells 1 in the aptamer pool 8D. 20A 8 bound to the target cells with a percent gated fluorescence intensity above background of 72%, comparable to the 75% obtained for 8D cells 1.

SELEX D and A were both more successful than SELEX B in generating high affinity sequences; comparison of rounds 13B and 15A show that 15A sequences had higher percent gated fluorescence intensities above background.

Further evolution of the aptamer pool to round 20A further increased its affinity. Since aptamer pool 15A is taken from earlier in the same SELEX set as aptamer pool 20A, it is expected that 15A would have fewer high affinity sequences than 20A, as is seen in **Figure 6.14**. However, previous results of entire aptamer pools screened via flow cytometry show that 15A has slightly higher binding than 20A; 14% gated fluorescence versus 11% (**Figure 3.5**). This is most likely due to the fact that high affinity sequences were missed in the subsequent cloning and screening steps. It is also possible that increased competition and decreased pool complexity between sequences in the 20A pool over the 15A pool for a limited number of target cells or target cell surface molecules is responsible for the slightly lower 20A pool binding.

It is difficult to compare the efficiency of Lacto and GAS sets of SELEX in generating high affinity sequences since separate target cells are used. However, it appears from **Figure 6.14** that the aptamers generated against *L. acidophilus* bound less extensively to their target cells than the high affinity GAS aptamers bound to strep. The highest affinity sequence from the Lacto sets of SELEX, hemag1P, was common to both the Lacto heat and Lacto mag pool. Hemag1P had only 23% gated fluorescence intensity above background. However, when the same set of sequences is tested against *L. acidophilus* 4357 and 4355, two strains similar to the original target strain 4356, the measured affinities are higher. Hemag1P has 81% gated fluorescence intensity above background when tested with 4357 and 63% when tested with 4355. Another sequence, mag1, has 31% gated fluorescence intensity above background when

tested against 4357. These values are much more comparable to the values obtained for individual 20A and 8D sequences binding to GAS.

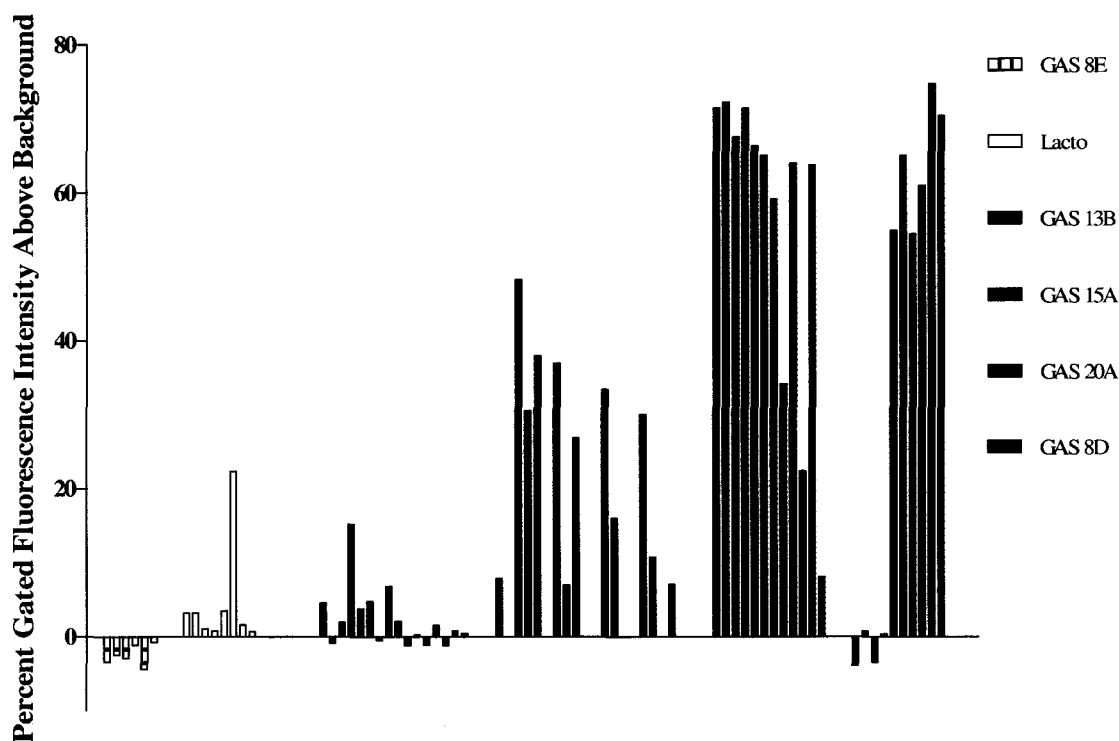


Figure 6.14. Affinities of different sequences for target cells as determined via flow cytometry, grouped by aptamer pool. Each bar represents a different tested sequence. Sequences from the same aptamer pool are all grouped together.

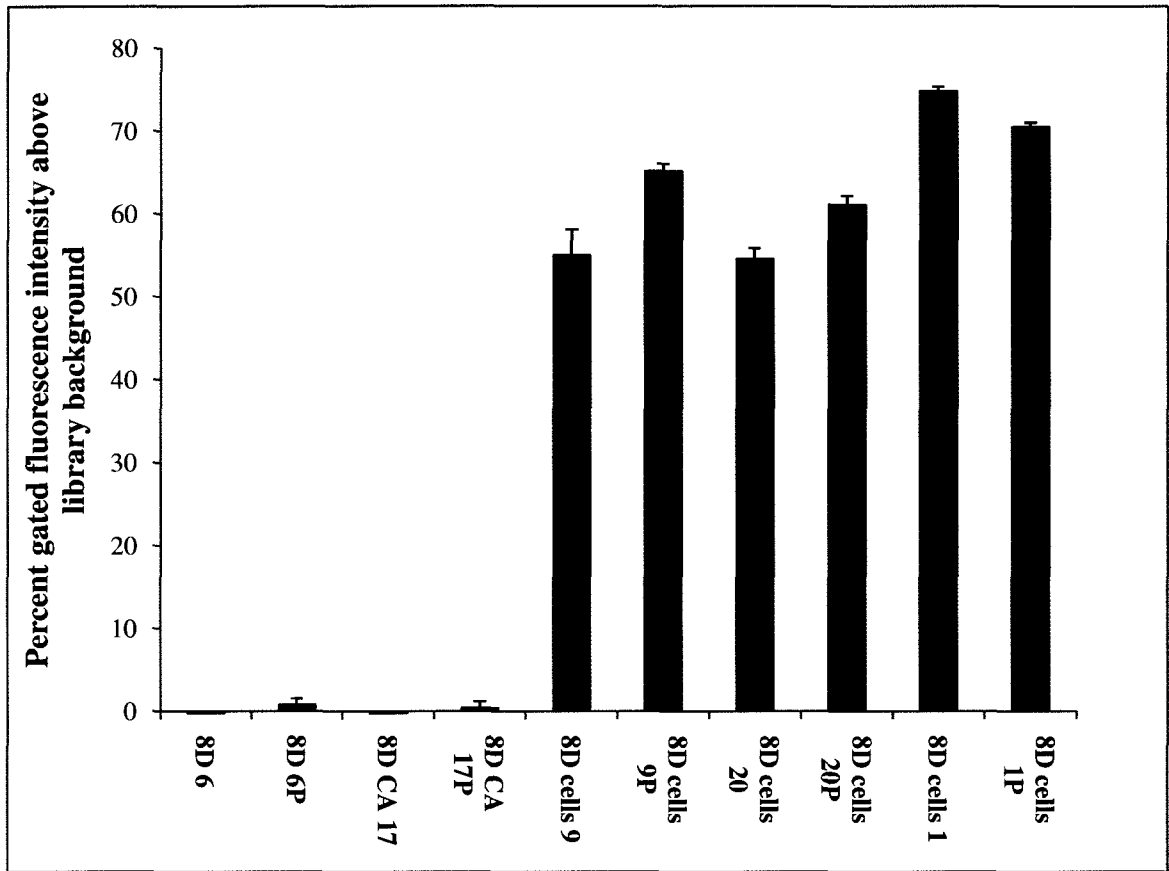


Figure 6.15. Affinities of sequences cloned from the heat-eluted (CA) and cell-bound (Cells) fractions of aptamer pool 8D, determined via flow cytometry.

Table 18. Summary of highest affinity sequences from each aptamer pool.

Aptamer pool	High affinity sequences	Total number of high affinity sequences (\geq 30% gated fluorescence above background)	Sequence with highest affinity	Highest % gated value measured
Lacto	None	0	Hemag1P	23%
GAS 13B	None	0	13B 5	15%
GAS 15A	15A3, 3P, 5P, 6P, 9, 15	6	15A3P	48%
GAS 20A	20A 1, 1P, 8, 8P, 9, 9P, 12, 12P, 14P, 24P	10	20A1	73%
GAS 8D	8D cells 1, 1P, 9, 9P, 20, 20P	6	8D cells 1	75%
GAS 8E	None	0	N/A	N/A

6.3.8 Screening of sequences from *S. pyogenes* aptamer pools against different M-types

After testing each individual sequence against the mixture of 10 different *S. pyogenes* M-types used as a target in SELEX A,B,D, and E, high affinity sequences were next screened against each M-type separately. As expected, different sequences exhibited different affinities for each of the M-types.

None of the sequences from the 13B, 15A, or 20A pools were M-type specific. As a rule of thumb, aptamer sequences that displayed high affinity towards the *S. pyogenes* mixture also displayed high overall affinity for each separate M-type. Conversely, those that displayed low affinity for the mixture usually displayed low overall affinity for the separate M-types. This trend is illustrated by comparing **Figures 6.16, 6.17, and 6.18**. The aptamer sequences 13B 5 and 13B 8 had low affinity for the M-type mixture and for each separate M-type; 13B 5 bound to the mixture with a percent gated fluorescence intensity over background value of 15%; aptamer sequence 13B 8 bound to the mixture with 7% gated fluorescence (**Figure 3.10**). For both sequences there was low level binding to many of the separate M-types with percent gated values ranging from 0 to 20% for 13B5 and 0 to 34% for 13B 8 (**Figure 6.16**). Similarly, aptamers 15A3, 15A 3P and 15A15 bound to the M-type mixture with percent gated values of 31%, 48% and 30%, respectively. They each bound to the majority of M-types with percent gated values ranging from 9 to 75% for 15A 3, 22 to 79% for 15A 3P, and 0 to 80% for 15A 15 (**Figure 6.17**). The highest binding for each of the 15A sequences was to M12; the three sequences did not

bind as strongly to any of the remaining M-types. Finally, aptamer sequences from the 20A pool seemed to bind strongly to most of the M-types (**Figure 6.18**) with a percent gated range of 31 to 79% for 20A8P and 26 to 80% for 20A8. For both sequences percent gated values were above 60% for seven out of the 10 M-types. This agrees with the respective percent gated values of 68% and 72% for 20A8P and 20A8 binding to the *S. pyogenes* mixture.

Since sequences 20A8 and 8D cells 1 are identical, it holds that they should have similar binding profiles for each of the separate M-types. When 8D cells 1 and 8D cells 1P were tested against the *S. pyogenes* mixture, they bound with percent gated fluorescence values of 75% and 71%, respectively (**Figure 4.8**). These values agree with the 68% and 72% values measured for 20A8P and 20A8. Likewise, 8D cells 1 and 8D cells 1P exhibited similar binding profiles as 20A8 and 20A 8P as they bound to most of the M-types when each M-type was tested separately (**Figure 6.19**). However, the measured percent gated fluorescence values were much lower for 8D cells 1 and 8D cells 1P (compare **Figures 6.19** and **6.18**); maximum percent gated fluorescence intensity for 8D cells 1 and 1P was only 18% and 14%, respectively. Controls carried out using randomized library for the 8D experiments had an average percent gated fluorescence intensity of 57% as opposed to 15% for the 20A experiments. This inconsistency in library binding accounts for the difference in percent gated fluorescence over background seen for 20A8/8P and 8D cells 1/1P when measured against separate M-types. The average percent gated fluorescence intensity of the library control for the flow cytometry experiment measuring

binding of 8D cells 1 and 8D cells 1P to the *S. pyogenes* mixture was 10%, consistent with the 20A experiments. Library inconsistencies will be discussed in more detail later. Unless specified, library average percent gated over background values for all experiments were below 15%.

A few of the sequences were specific for M11. The sequences 8D cells 9, 8E CA 20, 8E CA 20P, and 8E cells 1 all bound to only M11 with percent gated fluorescence intensity over background values of 15%, 6%, 16%, and 10%, respectively (**Figures 6.19** and **6.20**).

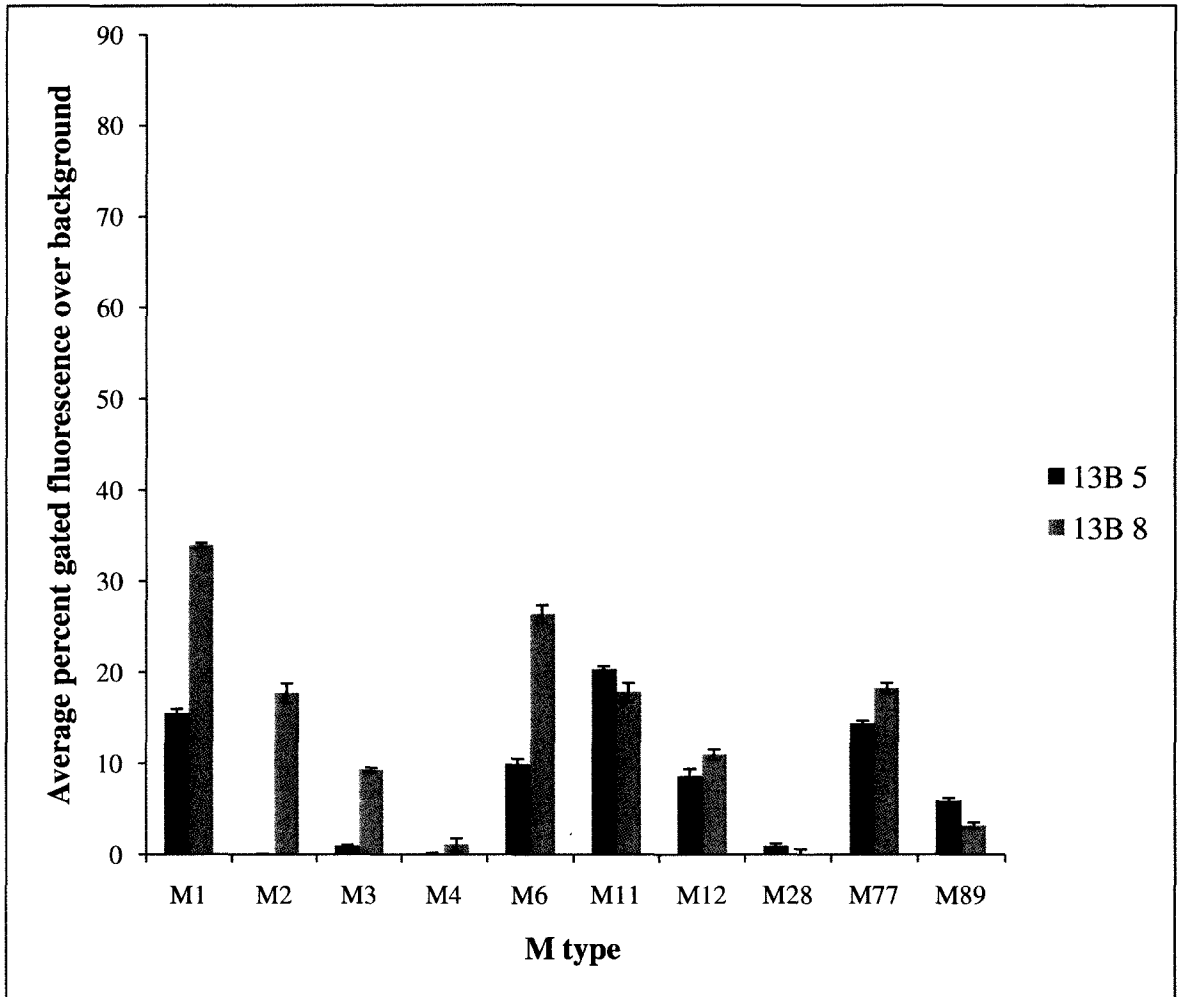


Figure 6.16. Binding of aptamer pool 13B sequences 13B 5 and 13B 8 to each of the 10 *S. pyogenes* M-types used in SELEX B.

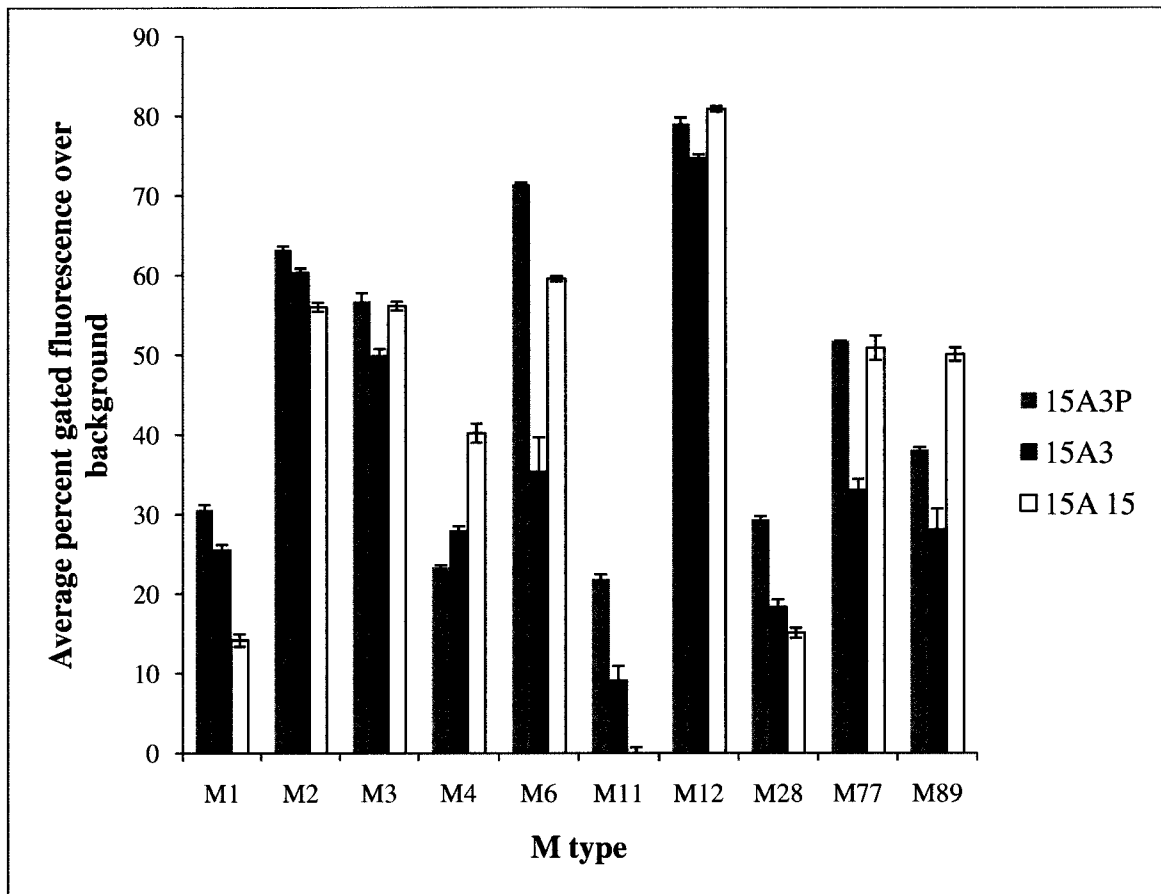


Figure 6.17. Binding of aptamer pool 15A sequences 15A3, 15A 3P, and 15A15 to each of the 10 *S. pyogenes* M-types used in SELEX A.

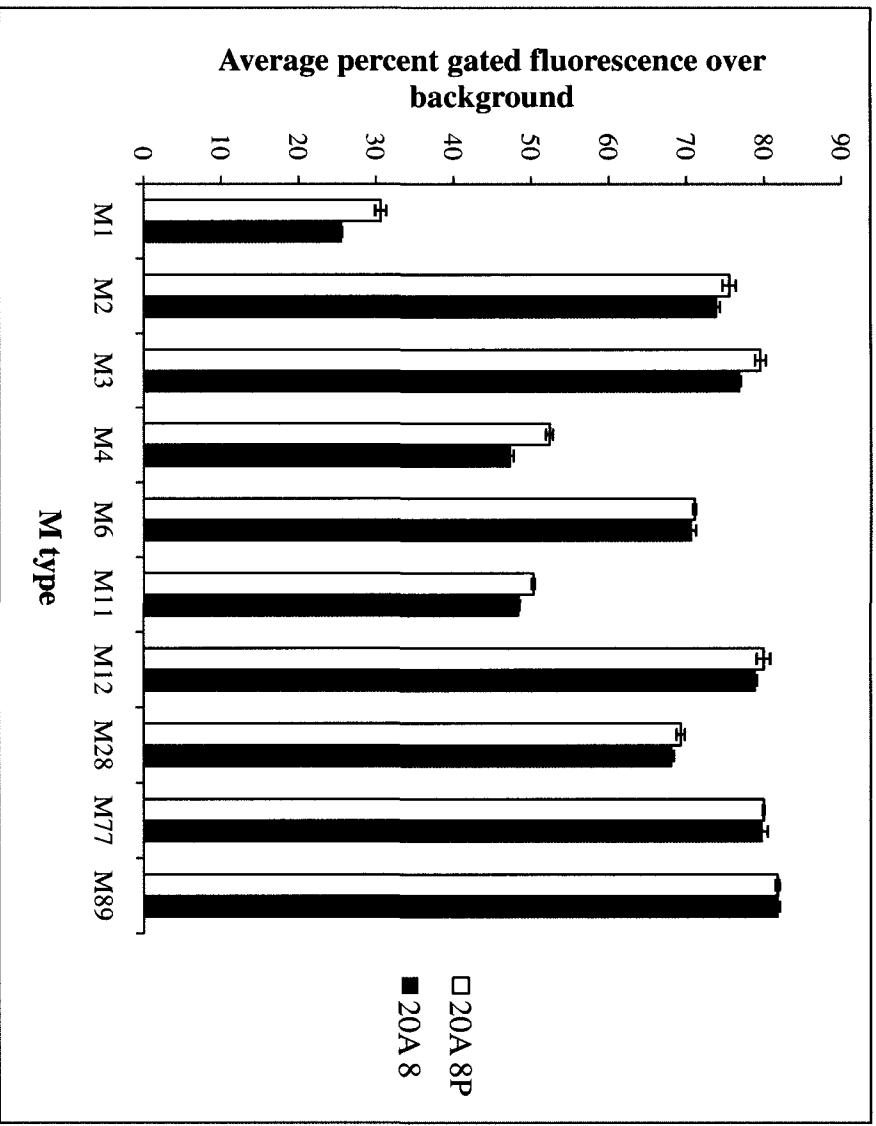


Figure 6.18. Binding of aptamer pool 20A sequences 20A8 and 20A8P to each of the 10 *S. pyogenes* M-types used in SELEX A.

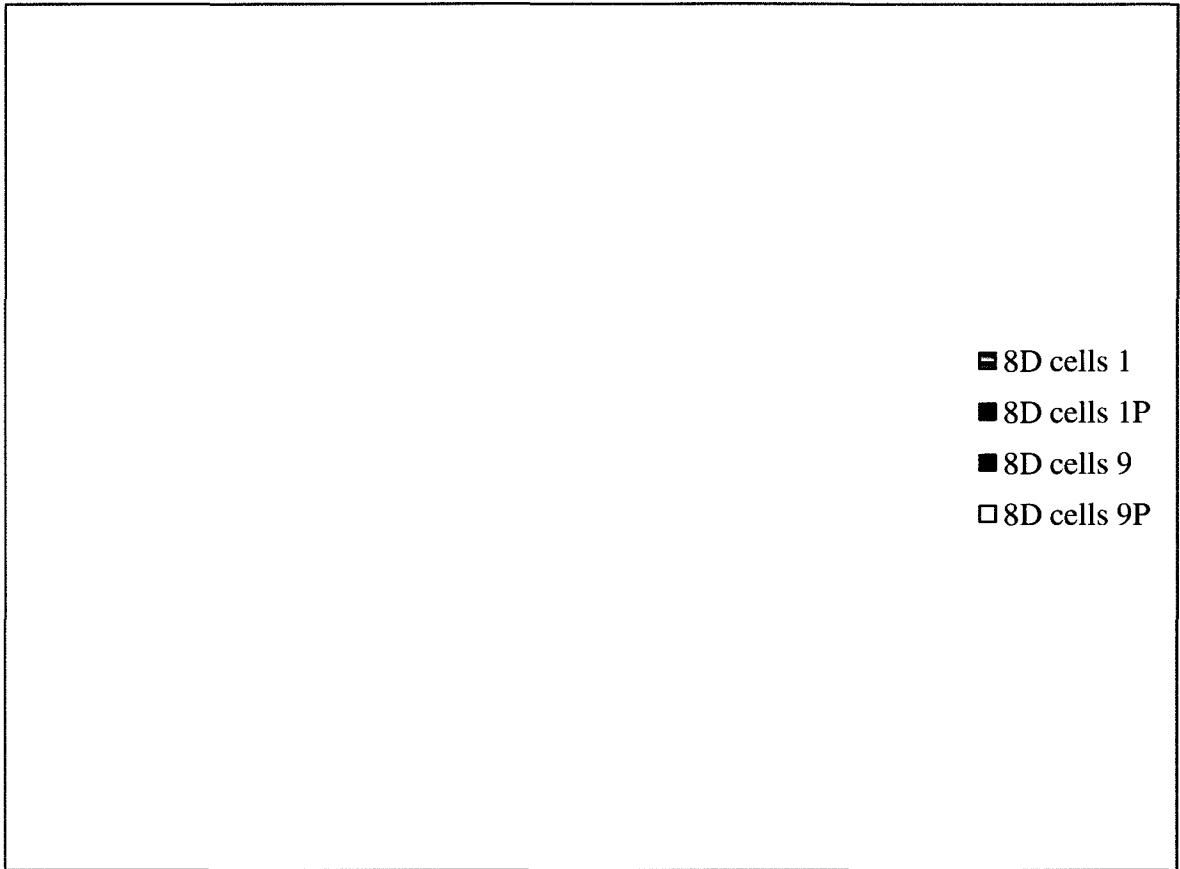


Figure 6.19. Binding of aptamer pool 8D sequences 8D cells 1, 8D cells 1P, 8D cells 9, and 8D cells 9P to each of the 10 *S. pyogenes* M-types used in SELEX

D.

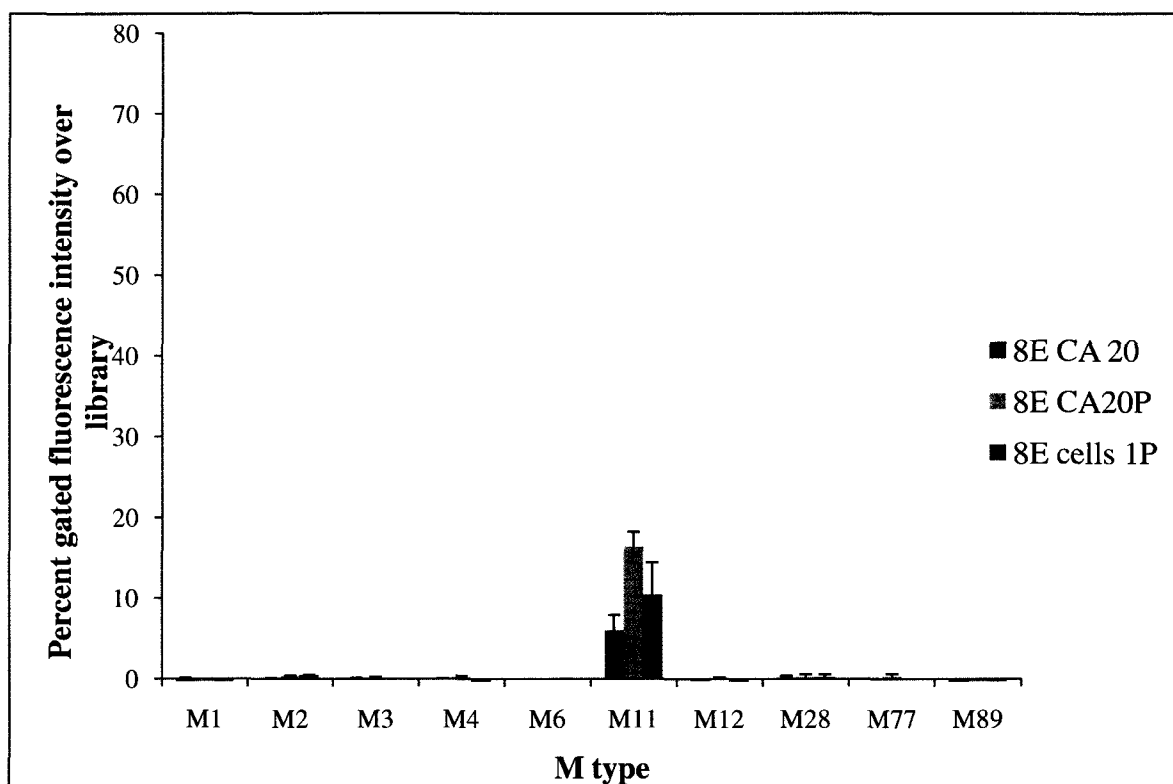


Figure 6.20. Binding of aptamer pool 8E sequences 8E CA20, 8E CA 20P, and 8E cells 1P to each of the 10 *S. pyogenes* M-types used in SELEX E.

6.3.9 Binding affinities of sequences from different aptamer pools for target cells

Different concentrations of each high affinity aptamer pool were incubated with a fixed number of the original target cell mixture. The target cells used were either *L. acidophilus* 4356 or the 10 M-type mixture of *S. pyogenes* used in SELEX A, B, D, and E. Incubations were subsequently analyzed via flow cytometry. A set of incubations using fluorescently-labeled randomized library was used to generate a negative control curve. Binding affinity curves were generated for each aptamer by plotting percent gated fluorescence over

background against aptamer concentration. GraphPad Prism 5.0 was used to fit curves to the data and estimate the binding dissociation constant for each sequence.

Binding curves for the high affinity aptamer sequences are listed separately in Chapters 1-3 as follows: **Figures 2.13** and **2.14** for Hemag1P; **Figures 3.16** to **3.21** for aptamer sequences from pools 13B, 15A, and 20A; **Figures 4.14** to **4.16** for aptamers from pools 8D and 8E. The curves for all sequences tested are shown together in **Figure 6.21**. Binding of aptamers to their target cells was found to increase exponentially at low aptamer concentrations and then level off as all aptamer binding sites on a cell surface were saturated. In all cases, the level of aptamer binding to target cells leveled off at or below 50 nM of aptamer. However, each curve leveled off at a different rate and hence different slope. This phenomenon is clearly illustrated by graphing all the curves up to 40 nM aptamer concentration (**Figure 6.22**). The curves with the highest slopes were those belonging to sequences 20A8 and 20A24P. The lowest slopes belonged to curves for aptamer sequences 8D cells 9 and 20A1. The higher the slope of a curve, the lower the predicted K_d of an aptamer and the higher its affinity. Accordingly, the aptamer sequences 20A8, 20A9P and 20A24P had low predicted K_d values (4 ± 1 nM, 9 ± 1 nM, 9 ± 1 nM, respectively) when compared to 8D cells 9 and 20A1 (17 ± 3 nM and 31 ± 4 nM, respectively). The predicted K_d values for all the aptamer sequences tested are summarized in **Table 19**. The predicted K_d values for all the aptamer sequences were in the nM range, from 4 ± 1 nM for sequence 8D cells 9P to 31 ± 4 nM for sequence 20A1. The predicted K_d

values of the sequence 20A8/8D cells 1 were similar when tested in separate experiments; 4 ± 1 nM for 20A8 and 14 ± 2 nM for 8D cells 1; 9 ± 1 nM for 8D cells 1P and 11 ± 1 nM for 20A8P.

The binding curves also leveled off at different values of percent gated fluorescence intensity, indicative of different theoretical maximum binding levels (B_{\max} values) and hence different points at which the cell surface became saturated. It stands to reason that the point of cell surface saturation of a given aptamer is proportional to the number of aptamer target molecules or the number of aptamer binding sites; aptamers specific for low abundance targets will not only saturate a cell surface much sooner than aptamers with high abundance targets but will also bind less extensively to the cell surface resulting in a lower B_{\max} value. Similarly, aptamers that bind to common structural motifs or binding sites on surface molecules will have a higher predicted B_{\max} than those that bind to rare or difficult to access motifs and binding sites. **Table 20** summarizes the B_{\max} values for all the aptamers tested. Aptamer Hemag1P has a markedly lower B_{\max} value than any of the *S. pyogenes* aptamers; 35 % versus the second lowest value of 69 % for sequence 8D cells 9P. The highest B_{\max} value of the *S.pyogenes* aptamers was 94% for 20A12P. The B_{\max} values of aptamers from pools A and B and pool D were similar. Aptamer 20A8/8D cells 1 had B_{\max} values of $86 \pm 1\%/90 \pm 3\%$.

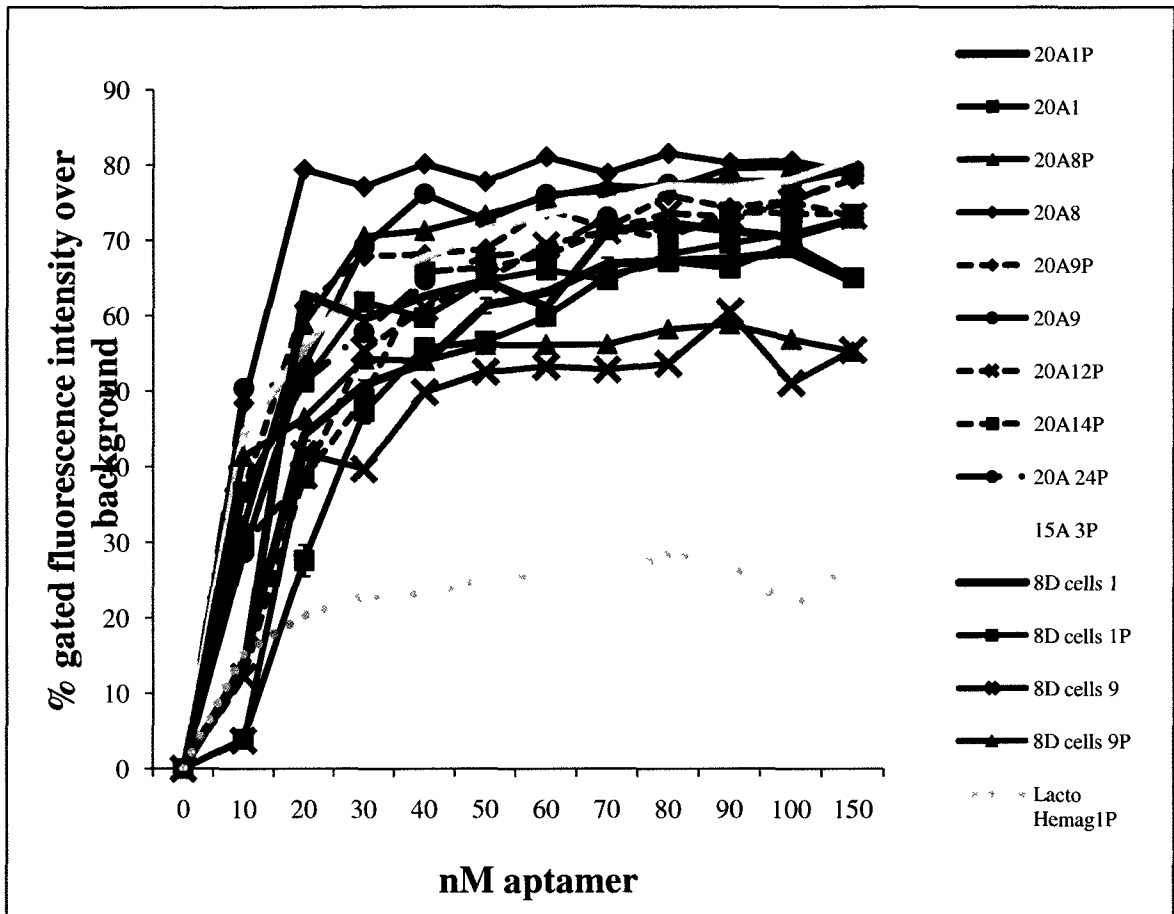


Figure 6.21. Binding curves for all high affinity aptamers tested and *S. pyogenes* target cell mixture.

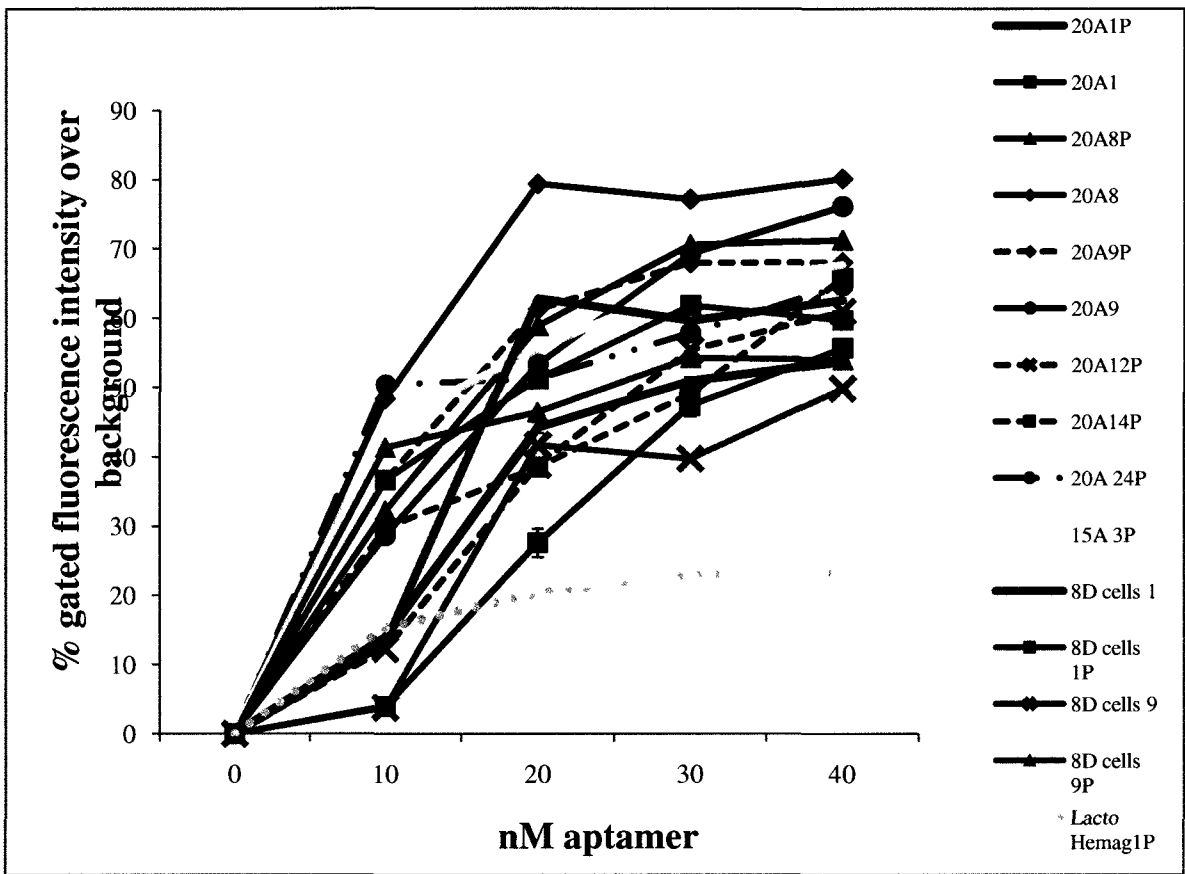


Figure 6.22. Binding curves for all high affinity aptamers tested and *S. pyogenes* target cell mixture.

Table 19. Binding dissociation constants (K_d s) of aptamer sequences evolved from all SELEX sets (Lacto SELEX heat and mag, GAS SELEX A, B, D, E).

SELEX set	Aptamer pool	Sequence name	K_d (nM)
Lacto heat and mag	7heat, 8mag	Hemag1P	13 ± 3
SELEX A	20A	20A 1	31 ± 4
	20A	20A 1P	20 ± 2
	20A	20A 8	4 ± 1
	20A	20A 8P	11 ± 1
	20A	20A 9	13 ± 1
	20A	20A 9P	9 ± 1
	20A	20A 12P	25 ± 3
	20A	20A 14P	17 ± 1
	20A	20A 24P	10 ± 1
	15A	15A 3P	9 ± 1
SELEX D	8D	8D cells 1	14 ± 2
	8D	8D cells 1P	9 ± 1
	8D	8D cells 9	17 ± 3
	8D	8D cells 9P	4 ± 1

Table 20. Theoretical maximum binding (B_{max}) values of aptamers derived from all SELEX sets (Lacto SELEX, GAS SELEX A,B,D,E).

SELEX set	Aptamer pool	Sequence name	B_{max} (%gated)
Lacto heat and mag	7heat, 8mag	Hemag1P	35
SELEX A	20A	20A 1	87
	20A	20A 1P	80
	20A	20A 8	86
	20A	20A 8P	89
	20A	20A 9	90
	20A	20A 9P	86
	20A	20A 12P	94
	20A	20A 14P	87
	20A	20A 24P	82
	15A	15A 3P	87
SELEX D	8D	8D cells 1	91
	8D	8D cells 1P	84
	8D	8D cells 9	77
	8D	8D cells 9P	69

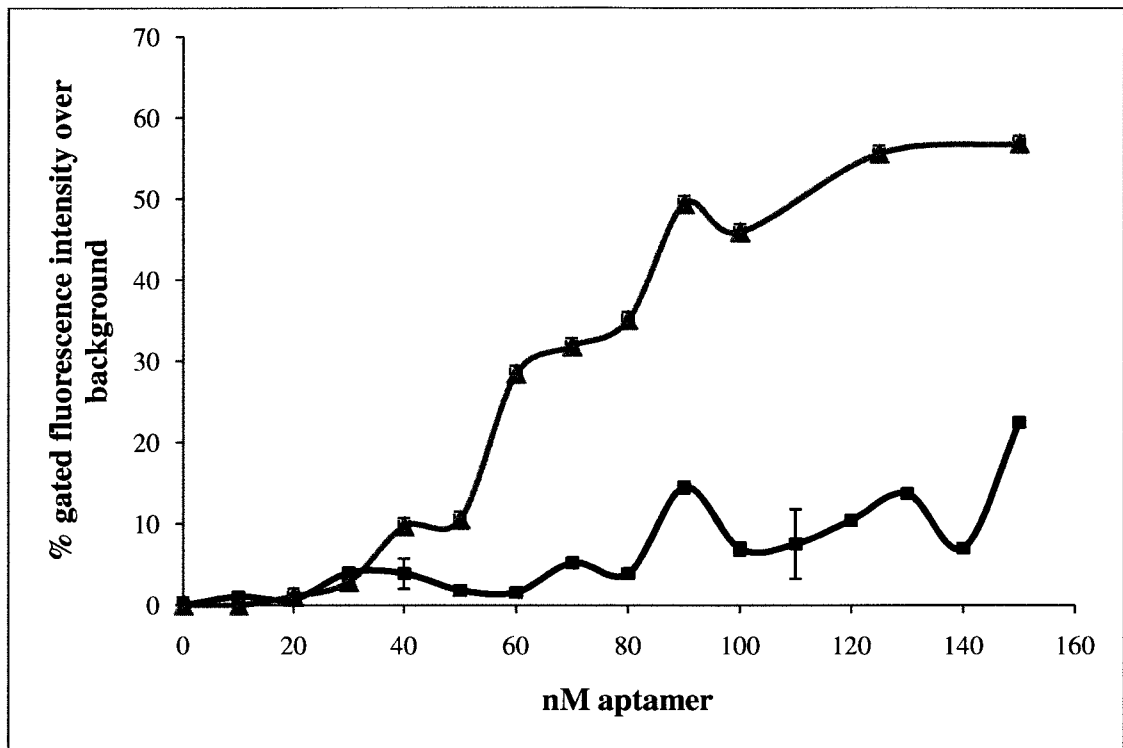


Figure 6.23. Binding of fluorescently-labeled randomized library to mixture of *S. pyogenes* cells. Two separate sets of libraries.

Binding of randomized library to cells was found to increase linearly with concentration, and remained lower than aptamer binding at all concentrations (Figure 6.23). There was a small discrepancy in library binding at high concentrations between two separate curves, each generated from triplicate incubations. Maximum binding in both cases was seen at 150 nM; values of 23 and 57% gated fluorescence were measured (Figure 6.23). The curves were run on the same instrument several months apart and each used separate commercial preparations of 5'-FAM fluorescently-labeled library. The differences observed in library binding are most likely due to differences in fluorescence intensity

between preparations. One of the library preparations may have incomplete labeling of all the oligonucleotides with 5'-FAM. It is also possible that with storage the fluorophore lost fluorescence due to photobleaching. Regardless, the level of library binding remained lower than that of the aptamers throughout the 0 to 150 nM concentration range and saturation binding kinetics were not observed. Predicted K_d values for the library curves were very high; in the micromolar range and above. Library binding was consistently low for all other experiments conducted; a detailed analysis of library variation is presented in **Section 6.3.12**.

6.3.10 Selectivities of sequences from each aptamer pool for target cells

The high affinity aptamer sequences tested and characterized were also tested against a variety of other cell types. Each fluorescently-labeled aptamer was incubated with a cell type, and the cells were washed and subsequently analyzed via flow cytometry. Fluorescently-labeled randomized oligonucleotide library was used as a negative control. The highest affinity *Lactobacillus* aptamers were also tested against *Streptococcus bovis*, *Escherichia coli*, and *Saccharomyces cerevisiae*. Aptamers with high affinity to *S. pyogenes* were tested against other cell types including *S. bovis*, mixtures of different *S. pneumoniae* serotypes, Group B Streptococcus (GBS), and *Enterococcus* species. The aptamer sequences with high affinities for their targets mostly had low affinities for all other cell types tested (**Figures 6.24** and **6.25**). The Lacto heat and mag pool aptamers demonstrated extremely low binding to other cell types, well below 5% gated fluorescence intensity above background in all cases (**Figure 6.24**). Aptamers tested from the GAS A, B, and D pools had low levels of binding to all

cell types tested (below 10% gated fluorescence over background) except for the sequence 20A8/8D cells 1 which bound to GBS with a percent gated fluorescence value around 22% (**Figure 6.25**). The level of 20A8/8D cells 1 binding to GBS may or may not interfere in the context of a diagnostic test.

Similarly, all of the high affinity aptamer sequences produced from SELEX using *S. pyogenes* as a target were screened against a mixture containing an equal number of 10 M-types not used in SELEX: M-types M5, M41, M49, M59, M75, M82, M83, M91, M92, and M114. The results of this screening are presented in **Figure 6.26**. All of the tested sequences bound to non-target *S. pyogenes* M-types with percent gated fluorescence values ranging from a low of 11% for 20A8P to a high of 35 % for sequence 8D cells 1P.

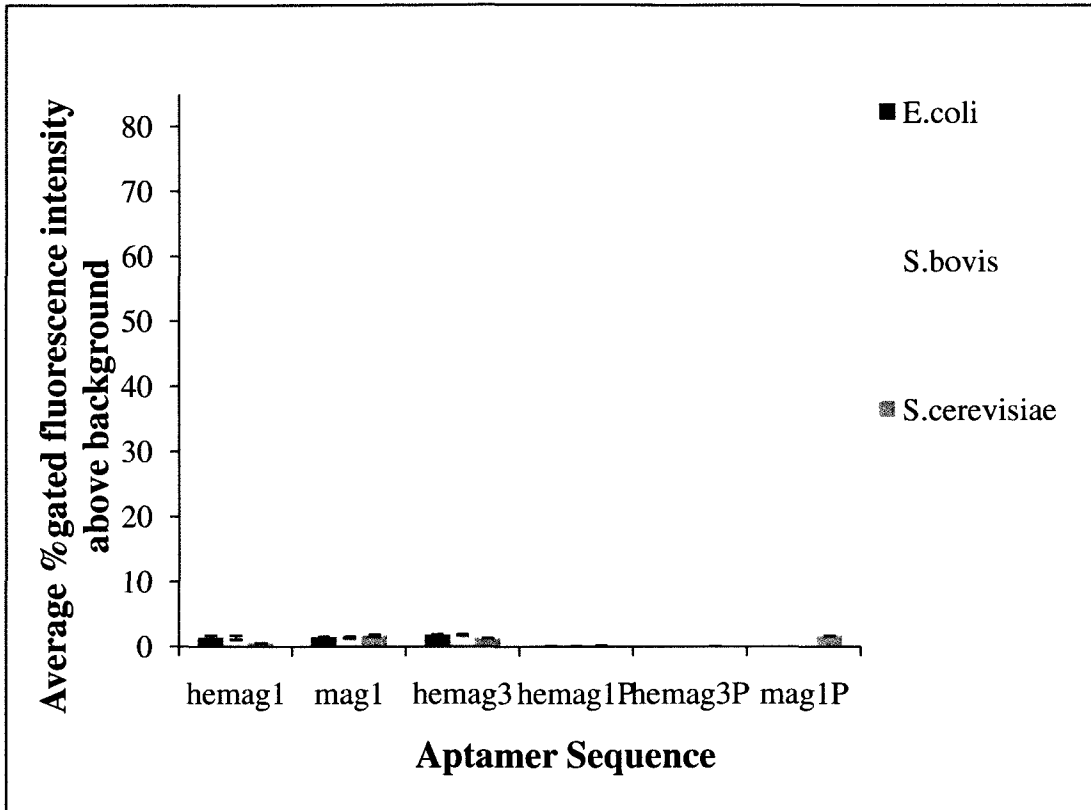


Figure 6.24. Selectivity of aptamer sequences from Lacto mag and heat pools for target cells *L. acidophilus* 4356.

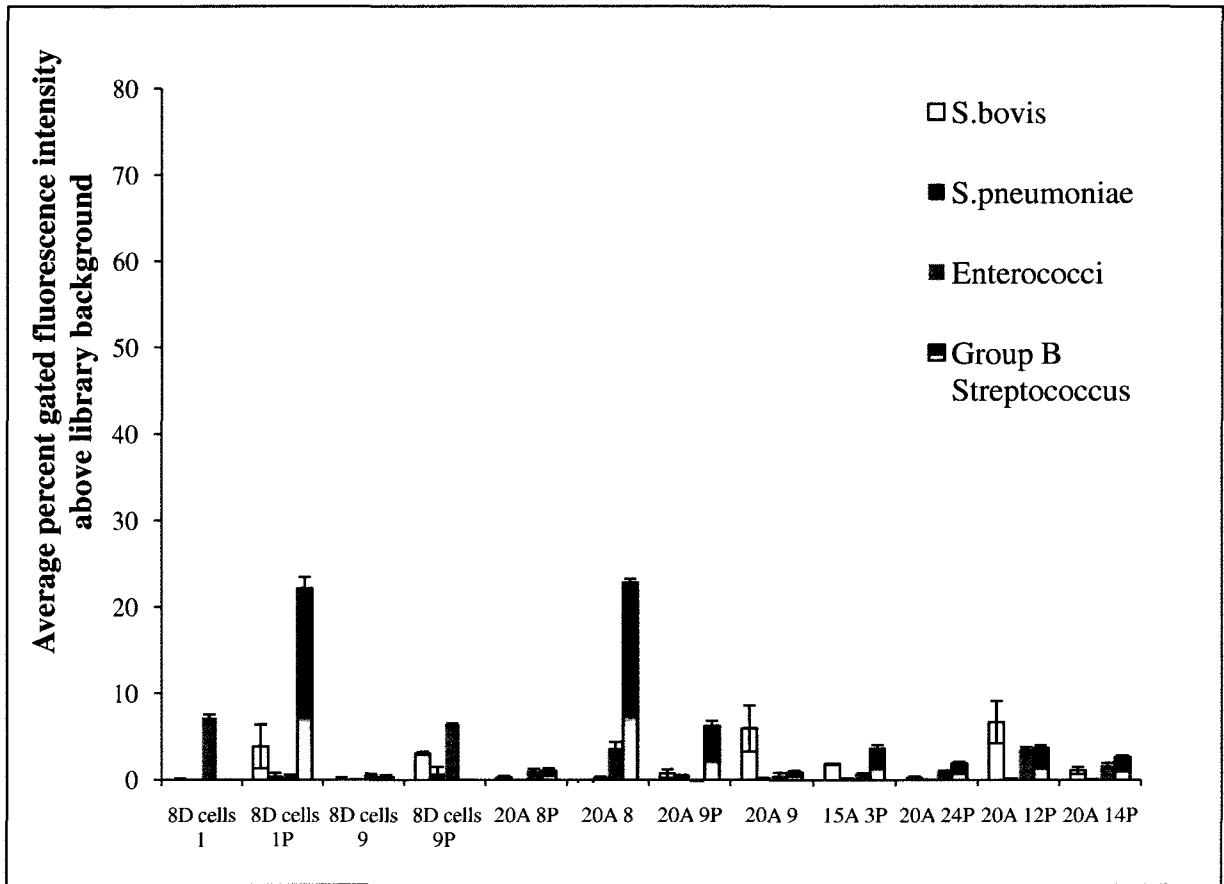


Figure 6.25. Affinity of aptamer sequences from 15A, 20A, and 8D pools for non-target cells.

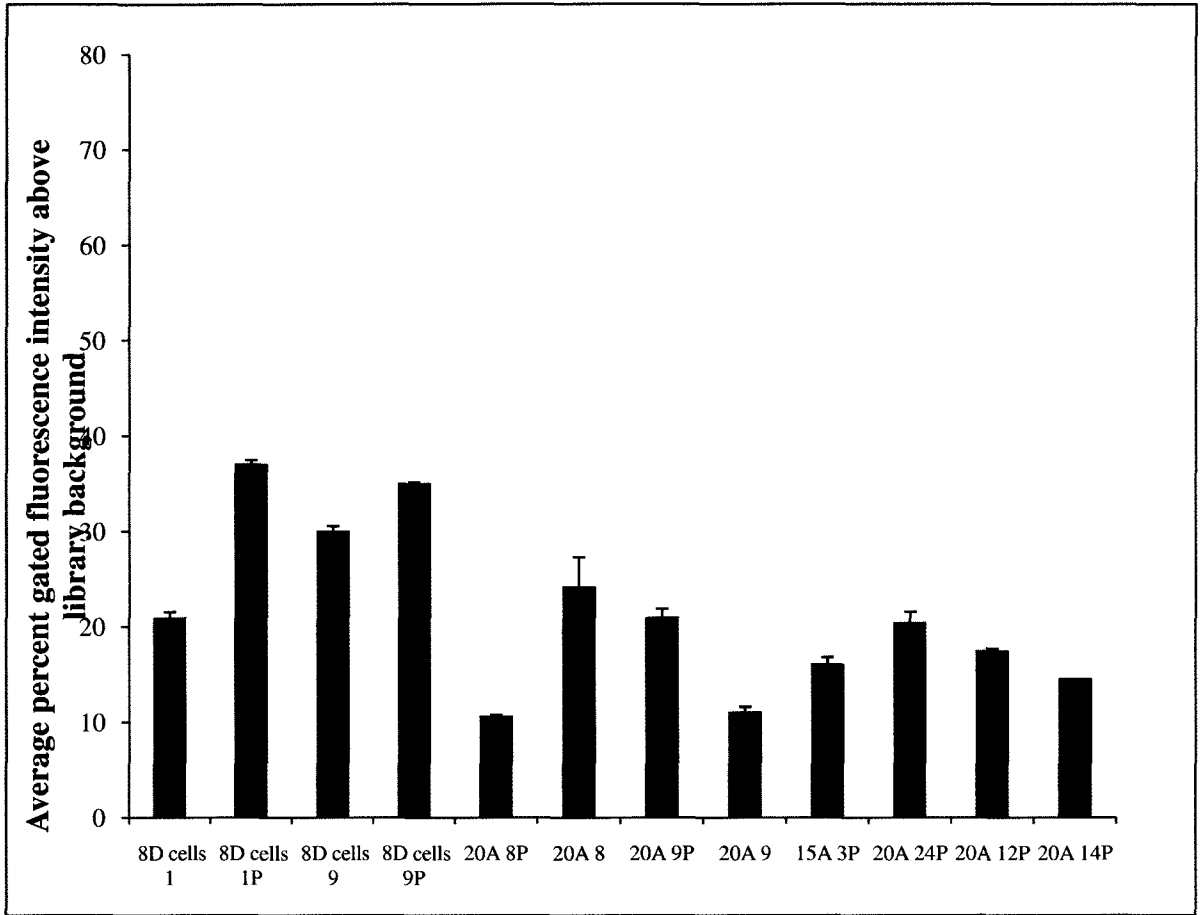
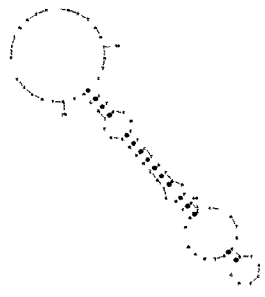
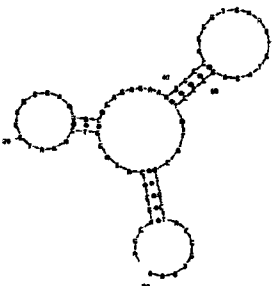
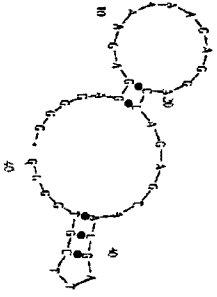


Figure 6.26. Affinity of aptamer sequences from 15A, 20A and 8D pools for a mixture of non-target *S. pyogenes* M-types.

6.3.11 Sequences with highest target cell affinity and selectivity from each aptamer pool

Following binding affinity and selectivity determination, the best sequence from each set of SELEX was identified. The criteria for identification as the “best sequence” were the lowest predicted K_d and the lowest binding to non-target cell types. **Table 21** summarizes the best sequences, their predicted secondary structures, and their predicted binding dissociation constants (K_d). From the Lacto heat and mag pools the sequence Hemag1P had the highest affinity and selectivity for the *L. acidophilus* target cells. The sequence with the highest affinity and selectivity from SELEX A was sequence 20A24P. From SELEX B, the best sequence was 15A 3P. The best sequence from SELEX D is sequence 8D cells 9, since this sequence had by far the highest selectivity of those tested from the 8D pool. None of the sequences tested from SELEX E had high affinity for the target cells.

Table 21. Sequences with highest target cell affinity and selectivity.

Sequence Name	Sequence	Secondary Structure	Predicted Kd (nM)
Hemag1P	5'- <u>AGCAGCACAGAGGTCAG</u> <u>ATGTAGCCCTTCAACATA</u> GTAATATCTCTGCATTCTG TGATGCCTATGCGTGCTA <u>CCGTGAA</u> -3'		13 ± 3
20A24P	5'- <u>AGCAGCACAGAG</u> <u>GTCAGATGGGGGA</u> AGACACAGAGAAAGG CCGGGGTGAAGTGTA GAGGCCTATGCGTGCT <u>ACCGTGAA</u> -3'		9 ± 1
15A3P	5'- <u>TTCACGGTAGCA</u> <u>CGCATAGG</u> GACAGC AAGCCCAAGCTGGGT GTGCAAGGTGAGGAG TGGGCATCTGACCTCT <u>GTGCTGCT</u> -3'		10 ± 1
8D cells 9	5'- GGGGAGGAGAAAAAGAG GACCAGAGTAACGATTCTG TGGGG-3'		17 ± 3

6.3.12 Comparison of library binding across all experiments

Separate binding curves using two sets of fluorescently-labeled random oligonucleotide libraries in the concentration range of 0 to 150 nM showed some variability, particularly at higher concentrations (**Figure 6.23**). In these curves, the library was incubated with the cells and directly run on the flow cytometer; there was no washing. Washing lowered the level of library binding substantially, and eliminated most of the variability. Controls carried out using an abundance of fluorescently-labeled library (200 pmole) and *L. acidophilus* cells showed average library binding was 9.22 ± 2.45 % gated fluorescence over background, and ranged from 6.6% to 12.1%. Similar controls carried out during flow cytometry screening of SELEX A, B, D and E aptamer pools and sequences showed low levels of library binding to the *S. pyogenes* target cell mixture. Average binding was 7.31 ± 9.34 % gated fluorescence and ranged from 0.7 to 44.2%. Most of the variability seen with GAS library binding is due to a couple of outliers; out of 28 experiments, only 2 had percent gated fluorescence values for the library control above 15%.

A potential source of library binding variability could be due to unequal fluorescent labeling between commercial library preparations. However, it is more likely that variability is due to variation in the number of cells of each M-type present in an *S. pyogenes* mixture. Library binding was not equal between all 10 M-types used (**Figure 6.27**). Binding to M1 and M11 was highest, an average of 41 and 40% gated fluorescence, respectively. Library binding was lowest to M12 and M77 with average values of 1 and 2% gated fluorescence. Differences in

library binding are most likely due to differences in DNA affinity between the M-types. M1 and M11 may have more positively charged surfaces than the other M-types resulting in increased retention of DNA. While every effort was made to ensure an equal number of cells of each M-type were added to a mixture, pipette error, loss of cells during centrifugation, and variation in the viability of each M-type most likely resulted in incongruity in the final target cell mixture.

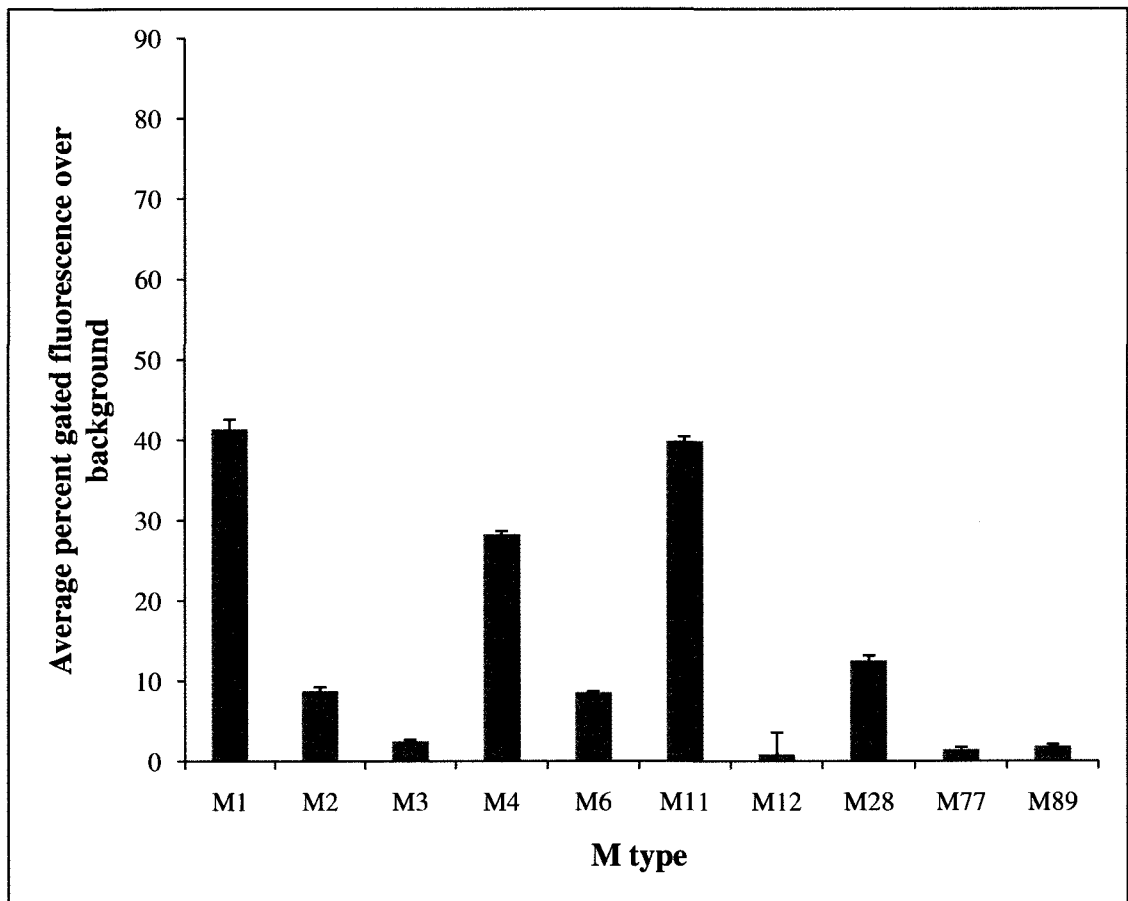


Figure 6.27. Binding of fluorescently-labeled randomized oligonucleotide library to each different target M-type of *S. pyogenes*. A total of 200 pmole of library were incubated with 10^8 cells. The cells were washed once and analyzed via flow cytometry as previously.

6.4 References

1. Hamula CL, Zhang H, Guan LL, Li XF, Le XC. Selection of aptamers against live bacterial cells. *Anal Chem.* 2008 Oct 15;80(20):7812-9.
2. Tyrrell GJ, Lovgren M, Forwick B, Hoe NP, Musser JM, Talbot JA. M types of group a streptococcal isolates submitted to the national centre for streptococcus (canada) from 1993 to 1999. *J Clin Microbiol.* 2002 Dec;40(12):4466-71.

Chapter 7

Conclusions and Synthesis

7.1 Introduction

Aptamers are an important emerging class of molecule; short, synthetic nucleic acids that bind to a target molecule with selectivity and affinity comparable to that of an antibody. Some aptamers inhibit the activity of the molecule to which they bind. Aptamers can be evolved against virtually any target molecule via a combinatorial chemistry technique known as Systematic Evolution of Ligands via Exponential Enrichment (SELEX). DNA aptamers possess a wide variety of advantageous properties over antibodies including increased temperature stability. DNA can be denatured and renatured; aptamer-based arrays and other technologies are hence potentially reuseable. Once an aptamer sequence is known, it is inexpensive and easy to synthesize. Variation between batches is low, animals are not needed for aptamer synthesis, and cross-reactivity is not as much of a problem as it is with antibodies. Aptamers are also open to a wide range of chemical modification.

Conventionally SELEX has been carried out using purified target molecules, particularly purified proteins. Aptamers exist that bind to smaller targets as well, including the alkaloid cocaine, nucleosides, amino acids, carbohydrates and amino acid mimics (1-4). More complex targets are becoming increasingly common including cell membrane fragments, spores, and viruses (5-

10). Aptamers are hence ideal ligands for cell surface molecules. In recent years, complex targets have been used with increasing frequency including cell membrane fragments, spores, and whole cells. Accordingly, aptamers have been developed against surface molecules on mammalian cells including cells engineered to over-express a specific protein and whole live cells without a pre-specified target molecule (11-15). Whole cell-SELEX work has primarily been limited to mammalian tissue culture cells with very little work on bacterial cells.

Aptamers are flexible reagents. They have been successfully employed in a variety of bioanalytical assays for target molecules and for cell detection. Included in these assays are Enzyme-Linked OligoNucleotide Assays (ELONA) and aptamer blotting (16, 17). Aptamer array devices, similar to microarrays, have been created for the detection of proteins including ricin, lysozyme, IgE, and thrombin (18, 19). Aptamers also make suitable fluorescence microscopy imaging reagents. Aptamers can not only replace antibodies in an established assay but are useful as novel sensors by themselves. Sequences can be engineered with a variety of labels and even enzymatic or signaling activities. Furthermore, nucleic acids can be chemically cross-linked to a target molecule using either ultraviolet light or customized bases. Introduction of modified bases and chemical groups to increase single-stranded DNA stability against degradation has broadened the application of aptamers as therapeutics and *in vivo* labels. Hence, aptamers that bind to the surface of live bacterial cells have a variety of potential applications.

7.2 Advancement of Knowledge

Chapter 2: Selection of Aptamers Against Live Bacterial Cells. Development of a novel SELEX technique capable of generating aptamers against whole, live bacterial cells eliminates the need to purify a specific cell surface target molecule ahead of time and then affix that purified molecule to a solid support. Instead, an aptamer can be developed and used to elucidate its specific cell surface target molecule post-selection. SELEX has not been applied to live bacterial cells until this thesis research. By developing a modified cell-based SELEX method, we have generated several ssDNA aptamers capable of binding to the bacterium *L. acidophilus*, without use of the purified target molecule during selection. Briefly, whole live bacterial cells in solution were used as a target matrix, and bound aptamers were separated from unbound via centrifugation and heat elution. Of the resultant aptamers, hemag1P displayed the highest and most specific binding with an estimated K_d of 13 ± 3 nM. Hemag1P most likely binds the highly abundant S-protein on the surface of *L. acidophilus* cells.

Developing a SELEX technique against whole, live bacterial cells versus purified components presents several key advantages. Foremost is the increased efficiency of this technique; since a specific target molecule does not need to be identified prior to selection, many troublesome purification steps are avoided. This technique could lead to discovery of novel cell surface molecules as well as the selection of aptamers against new disease and pathogenicity markers without the necessity of purifying them. Another advantage of these aptamers is that they are selected against the target in its native conformation, a particularly important

consideration for protein targets. A study by Pestourie et al. found that using mammalian cells as a matrix for an over-expressed target membrane protein, as opposed to selection against the protein on magnetic beads, was essential to evolving aptamers able to recognize the target protein in its native environment (13).

Aptamers that bind to bacterial cell surface molecules could be used in bacterial surveillance and typing, diagnosis of bacterial infections, and therapeutics. A variety of assays already developed for protein detection using aptamers could be extended towards bacterial detection, particularly aptamer-based ELISAs and microarrays. Similarly, aptamers could replace antibodies in bacterial typing. In addition to detecting cells expressing target molecules on their surface, aptamers could function as antimicrobials. In binding to a specific molecular target aptamers could inhibit the growth or pathogenesis of cells expressing that target molecule. Aptamers against mammalian cell surface molecules have been found to block cellular transformation and inhibit tumour growth; aptamer-siRNA chimeras show promise in targeting tumour cells for apoptosis through the RNA interference pathway (20, 21). Aptamers have also been used as escorts to target drugs to cancer cells over-expressing a target molecule.

Chapter 3: Selection of Aptamers for M-typing of *S. pyogenes*. We next applied the novel SELEX technique developed for *L. acidophilus* to a mixture of 10 different *Streptococcus pyogenes* M-types. *S. pyogenes* (Group A Streptococcus) is the causative agent of many infections including strep throat and

impetigo, as well as the invasive infections necrotizing fasciitis, streptococcal toxic shock, and sepsis. In addition to life-threatening infections GAS is responsible for a variety of post-infection sequelae including rheumatic fever, heart failure, and arthritis. GAS is typed using a protein-based system; the M protein. Conventional typing methodology employs serotyping, or sequencing of the M-protein gene (*emm*). These methodologies are laborious and require extensive comparison against myriad reference strains. In addition, the antisera are difficult to prepare and obtain, limiting M-typing to reference laboratories.

We selected aptamers against a mixture of the 10 most prevalent M-types in Canada: M1, M2, M3, M4, M6, M11, M12, M28, M77, and M89 (22). Of the resultant aptamers, several sequences were promising. The sequence 20A24P had the highest affinity and selectivity for *S. pyogenes*, with a predicted K_d of 9 ± 1 nM and very low levels of binding to other *Streptococcus* and *Enterococcus* species. Another promising sequence was 15A3P, with high selectivity for *S. pyogenes* and a predicted K_d of 10 ± 1 nM. None of the sequences from these sets of SELEX were M-type specific. However, they are potentially useful in a point-of-care diagnostic test for *S. pyogenes*. Current point-of-care testing methodology relies on antibody-based Rapid Antigen Detection (RAD), a 2-site sandwich immunoassay, to detect the Group A cell wall carbohydrate. RAD has poor sensitivity and negative results, which account for 70–80% of the results obtained, require a confirmatory culture step (23). Aptamers could negate the need for a culture step.

Chapter 4: Selection of Aptamers for M-typing of *S. pyogenes* Using a Second SELEX Technique. Since the first cell-SELEX methodology that we developed did not result in any *S. pyogenes* M-type specific aptamer sequences, a modified cell-SELEX method was employed. Two main objectives of the modified method were to increase starting library diversity and introduce a counterselection step using *S. bovis* cells to remove non-*S. pyogenes* specific sequences. In addition, loss of potential sequences was minimized at each step by increasing incubation time, volume, and mixing of cells and DNA, and also by using denaturing gel purification rather than heat denaturation to separate the single-stranded DNA. The previous sets of SELEX carried out against GAS, SELEX A and B, also took many rounds to generate high affinity sequences (20 and 13, respectively). Another aim of the modified novel cell-SELEX method (SELEX D and E) was to shorten the length of the selection process.

We selected aptamers against a mixture of the 10 most prevalent M-types in Canada, as with the previous sets of GAS SELEX. We obtained several promising sequences from SELEX D and E in only 8 SELEX rounds. Sequence 8D cells 9P was specific for *S. pyogenes* with a predicted K_d of 4 ± 1 nM. The sequence 8D cells 9 also had high affinity and selectivity for *S. pyogenes* with a predicted K_d of 17 ± 3 nM. This sequence was found to bind specifically to one M-type, M11. Several sequences isolated from the 8E aptamer pool, 8E CA 20, 8E CA 20P and 8E cells 1P, also bound specifically to M11. Most of the aptamers generated could bind to all M-types. M-type specific aptamers are still needed for the remaining M-types in order to achieve M-typing.

Chapter 5: Post-SELEX Elucidation of Aptamer Target Molecules. The aptamer sequences and aptamer pools with the highest binding affinities and selectivities were tested against different purified cell surface components. Aptamer Hemag1P was tested against the *L. acidophilus* 4356 S-layer protein (SLP). SLP is a highly abundant 43 kDa protein that forms a regular lattice covering the cell surface (24). Since SLP is so predominant on the *L. acidophilus* cell surface it is the likely target of Hemag1P. In order to test aptamer binding to this protein, aptamers were screened via flow cytometry against different species of *Lactobacillus*; those that possess S-layers and those that do not. Hemag1P did not bind to *Lactobacillus* sp. without an S-layer. SLP was next purified from the cell surface via detergent extraction and incubated with fluorescently-labeled Hemag1P. Following incubation, aptamer-protein binding was examined via capillary electrophoresis (CE). If an aptamer has high affinity for a given protein, a stable protein-aptamer complex will form and move faster through the capillary, resulting in a peak appearing at an earlier migration time on the electropherogram than the unbound (free) aptamer peak. When increasing concentrations of SLP (0-5 μ M) were tested against a fixed Hemag1P concentration, protein-aptamer complex peaks of increasing number and intensity were seen. The increased intensity of the peaks is expected with increasing protein concentration, but the increasing number of peaks at high SLP concentrations is not and is most likely due to formation of protein aggregates in solution. S-layer proteins of various species have been found to aggregate in aqueous solutions (25). Purification of

the SLP from the cell surface cannot be used to predict an accurate K_d of Hemag1P for SLP since the protein is no longer in its native conformation.

For the aptamer pools 13B, 15A, and 20A, evolved against *S. pyogenes*, aptamer blotting was used to identify aptamer target proteins. An aptamer blotting procedure was developed based on work by Noma et al. (17). Biotinylated aptamer pools were incubated with membranes containing different *S. pyogenes* protein extracts, including cell-surface protein extracts obtained with pepsin. The aptamer pool 20A seemed to have higher affinity for the pepsin extracts than pools 13B and 15A, and also than randomized library used as a control.

Other methods of post-SELEX target elucidation were unsuccessful. Using aptamer-coated magnetic beads to pull proteins out of cell lysates did not seem to work, proteins subsequently released from the beads were not aptamer-specific. Similarly, electrophoretic mobility shift assays (EMSAs) gave inconsistent and inconclusive results (data not shown).

Chapter 6: Comparison of Different Cell-SELEX Methodologies for Selection of Aptamers Against Live Bacterial Cells. The different SELEX methodologies used against *L. acidophilus* and *S. pyogenes* were compared in regards to their efficiencies, and the types and characteristics of sequences they produced. Aptamers from the Lacto pools seemed to have no sequence or structural overlap with those from the GAS pools. However, there was significant sequence and secondary structural motif overlap between all four GAS pools. The free energy distribution of sequences was similar between all of the pools, although the types of secondary structures found in each pool were not. Three of

the four SELEX methodologies used yielded some promising sequences. Most strikingly, two different SELEX methodologies against *S. pyogenes* yielded the same sequence: 20A8/8D cells 1. This sequence bound to *S. pyogenes* with high affinity (predicted K_d of $4 \pm 1/14 \pm 2$ nM) but low selectivity as it also bound to Group B Streptococcus. The presence of the same sequence in separately evolved aptamer pools indicated that both SELEX methodologies can be equally successful in generating aptamers against bacterial cell surface molecules. Introduction of a counter-selection step seems to result in more M-type specific sequences. Use of heat denaturation versus gel purification does not seem to be detrimental to the affinity of resultant aptamer sequences for a given target cell. However, use of magnetic beads to purify single-stranded sequences can be detrimental. We found that this method was not as effective as heat denaturation in generating aptamers against *L. acidophilus*. A subsequent study found that use of magnetic beads during cell-SELEX resulted in detachment of streptavidin moieties into the eluted aptamer pool and inhibition of aptamer binding due to aggregation of cells induced by the beads (26).

7.3 Conclusions

Aptamers were developed against two separate targets, *L. acidophilus* and *S. pyogenes*. The non-pathogenic *L. acidophilus* cells were used to demonstrate proof-of-principle in development of a novel cell-SELEX method for live bacterial cells. After demonstrating the feasibility of this method, we applied it to the pathogen *S. pyogenes* with the goal of creating *S. pyogenes* species or M-type specific aptamers. The first methodology was only successful in generating

aptamers that were species specific. We then developed a second cell-SELEX method for *S. pyogenes* that was successful in generating both species and M-type specific aptamers.

Comparison of the different SELEX methodologies indicates that the counterselection step is most important in conveying selectivity. However, the first methodology that we developed is just as successful when targeting an abundant cell-surface target molecule or a heterogeneous cell population. It is much more difficult to select aptamers against molecules of low abundance on the cell surface. Another problem associated with the selection and application of aptamers is the need for consistent cell expression of target molecules. Variability in levels of M-protein and the relative low abundance of M-protein on the cell surface have made selecting M-type specific aptamers difficult. We were able to select an aptamer specific for one M-type, M11.

7.4 Future Work

Much future work in the area of post-SELEX target elucidation using the *S. pyogenes* aptamer sequences can be done including testing of purified molecules via capillary electrophoresis, further optimization of aptamer-magnetic bead pulldowns, and aptamer blotting using single sequences rather than aptamer pools. In addition, conditions were optimized for removal and subsequent PCR amplification of bound aptamer sequences from a PVDF membrane. Such a procedure could be used either during or post-SELEX to isolate sequences from an aptamer pool that are specific for a single target molecule.

Aptamers specific for *S. pyogenes* can be used for a point-of-care diagnostic test. A simple way to do this would be to affix the aptamer sequence(s) to latex beads and develop an agglutination assay. The aptamer-coated beads would then clump in the presence of *S. pyogenes* cells but not in the presence of other types of cells. There are multiple candidate sequences for this type of assay from SELEX A, B, and D. These *S. pyogenes* specific aptamers could also be used in an array-like device for rapid identification of bacterial cells from unknown cultures. There are also a few M11 specific sequences from SELEX D. Further SELEX must be carried out in order to obtain aptamers specific for each of the 10 most prevalent M-types circulating in the Canadian population. Counterselection of the 8D aptamer pool against unwanted M-types, or more rounds of selection using the 8D pool and only a single M-type should be carried out to this end.

M-type specific aptamers can be affixed to a solid support to develop an aptamer array for high-throughput M-typing of clinical isolates. The support for the array device could take the form of a glass or silicon surface, electronic sensor array (silicon chip), or a silicon pin array. The aptamers on the array could be used in either a direct assay or a sandwich format assay to capture whole cells or the extracted M-proteins out of solution. The direct assay would involve using the array to capture GAS cells of a specific M-type out of solution, and then fixing and counting the number of cells captured. This array could be visualized using a light microscope. In the sandwich assay, the captured cells or protein could be visualized with a second fluorescently-labeled aptamer against the M protein or a

fluorescently-labeled antibody recognizing the non-variable M-protein C-terminus or a GAS cell wall component common to all M-types, such as the group A carbohydrate or peptidoglycan. These arrays could be analysed with a fluorescent microscope or a microarray reader. This is similar in principle to the ricin detection assay developed by Kirby et al. (18) and the multiple protein aptamer-based microarrays of Cho et al. (19). Also, all the aptamer sequences from the GAS mixture aptamer pool obtained could be attached to the same slide or chip. This approach would yield a different aptamer 'fingerprint' for each isolate. This 'fingerprint' would result from each aptamer in the pool having different affinity and selectivity for the surface molecules on each M-type. Alternatively, the aptamers could be arranged in a macroarray where each pin is covered in aptamers specific to one M-type. GAS isolates of unknown M-type could be screened using this pin array. The bacteria will be retained only on the pins covered by the aptamers specific to their M-type. The array can then be used to stamp agar plates and the specific pattern of bacterial growth on the plates used to determine M-type.

7.5 References

1. Stojanovic MN, de Prada P, Landry DW. Aptamer-based folding fluorescent sensor for cocaine. *J Am Chem Soc.* 2001 May 30;123(21):4928-31.
2. Huizenga DE, Szostak JW. A DNA aptamer that binds adenosine and ATP. *Biochemistry.* 1995 Jan 17;34(2):656-65.
3. Harada K, Frankel AD. Identification of two novel arginine binding DNAs. *EMBO J.* 1995 Dec 1;14(23):5798-811.
4. Vianini E, Palumbo M, Gatto B. In vitro selection of DNA aptamers that bind L-tyrosinamide. *Bioorg Med Chem.* 2001 Oct;9(10):2543-8.
5. Morris KN, Jensen KB, Julin CM, Weil M, Gold L. High affinity ligands from in vitro selection: Complex targets. *Proc Natl Acad Sci U S A.* 1998 Mar 17;95(6):2902-7.
6. Bruno JG, Kiel JL. In vitro selection of DNA aptamers to anthrax spores with electrochemiluminescence detection. *Biosens Bioelectron.* 1999 May 31;14(5):457-64.
7. Ikanovic M, Rudzinski WE, Bruno JG, Allman A, Carrillo MP, Dwarakanath S, et al. Fluorescence assay based on aptamer-quantum dot binding to bacillus thuringiensis spores. *J Fluoresc.* 2007 Mar;17(2):193-9.
8. Gopinath SC, Kawasaki K, Kumar PK. Selection of RNA-aptamer against human influenza B virus. *Nucleic Acids Symp Ser (Oxf).* 2005;(49)(49):85-6.
9. Gopinath SC, Sakamaki Y, Kawasaki K, Kumar PK. An efficient RNA aptamer against human influenza B virus hemagglutinin. *J Biochem.* 2006 May;139(5):837-46.
10. Nitsche A, Kurth A, Dunkhorst A, Panke O, Sielaff H, Junge W, et al. One-step selection of vaccinia virus-binding DNA aptamers by MonoLEX. *BMC Biotechnol.* 2007 Aug 15;7:48.
11. Daniels DA, Chen H, Hicke BJ, Swiderek KM, Gold L. A tenascin-C aptamer identified by tumor cell SELEX: Systematic evolution of ligands by exponential enrichment. *Proc Natl Acad Sci U S A.* 2003 Dec 23;100(26):15416-21.
12. Cerchia L, Duconge F, Pestourie C, Boulay J, Aissouni Y, Gombert K, et al. Neutralizing aptamers from whole-cell SELEX inhibit the RET receptor tyrosine kinase. *PLoS Biol.* 2005 Apr;3(4):e123.

13. Pestourie C, Cerchia L, Gombert K, Aissouni Y, Boulay J, De Franciscis V, et al. Comparison of different strategies to select aptamers against a transmembrane protein target. *Oligonucleotides*. 2006 Winter;16(4):323-35.
14. Shangguan D, Li Y, Tang Z, Cao ZC, Chen HW, Mallikaratchy P, et al. Aptamers evolved from live cells as effective molecular probes for cancer study. *Proc Natl Acad Sci U S A*. 2006 Aug 8;103(32):11838-43.
15. Mallikaratchy P, Tang Z, Kwame S, Meng L, Shangguan D, Tan W. Aptamer directly evolved from live cells recognizes membrane bound immunoglobulin heavy mu chain in burkitt's lymphoma cells. *Mol Cell Proteomics*. 2007 Dec;6(12):2230-8.
16. Drolet DW, Moon-McDermott L, Romig TS. An enzyme-linked oligonucleotide assay. *Nat Biotechnol*. 1996 Aug;14(8):1021-5.
17. Noma T, Ikebukuro K, Sode K, Ohkubo T, Sakasegawa Y, Hachiya N, et al. Screening of DNA aptamers against multiple proteins in tissue. *Nucleic Acids Symp Ser (Oxf)*. 2005;(49)(49):357-8.
18. Kirby R, Cho EJ, Gehrke B, Bayer T, Park YS, Neikirk DP, et al. Aptamer-based sensor arrays for the detection and quantitation of proteins. *Anal Chem*. 2004 Jul 15;76(14):4066-75.
19. Cho EJ, Collett JR, Szafranska AE, Ellington AD. Optimization of aptamer microarray technology for multiple protein targets. *Anal Chim Acta*. 2006 Mar 30;564(1):82-90.
20. Hicke BJ, Stephens AW, Gould T, Chang YF, Lynott CK, Heil J, et al. Tumor targeting by an aptamer. *J Nucl Med*. 2006 Apr;47(4):668-78.
21. McNamara JO, 2nd, Andrechek ER, Wang Y, Viles KD, Rempel RE, Gilboa E, et al. Cell type-specific delivery of siRNAs with aptamer-siRNA chimeras. *Nat Biotechnol*. 2006 Aug;24(8):1005-15.
22. Tyrrell GJ, Lovgren M, Forwick B, Hoe NP, Musser JM, Talbot JA. M types of group a streptococcal isolates submitted to the national centre for streptococcus (canada) from 1993 to 1999. *J Clin Microbiol*. 2002 Dec;40(12):4466-71.
23. Armengol CE, Schlager TA, Hendley JO. Sensitivity of a rapid antigen detection test for group A streptococci in a private pediatric office setting: Answering the red book's request for validation. *Pediatrics*. 2004 Apr;113(4):924-6.
24. Boot HJ, Kolen CP, Pouwels PH. Identification, cloning, and nucleotide sequence of a silent S-layer protein gene of *Lactobacillus acidophilus* ATCC 4356

which has extensive similarity with the S-layer protein gene of this species. *J Bacteriol.* 1995 Dec;177(24):7222-30.

25. Boot HJ, Pouwels PH. Expression, secretion and antigenic variation of bacterial S-layer proteins. *Mol Microbiol.* 1996 Sep;21(6):1117-23.

26. Paul A, Avci-Adali M, Ziemer G, Wendel HP. Streptavidin-coated magnetic beads for DNA strand separation implicate a multitude of problems during cell-SELEX. *Oligonucleotides.* 2009 Sep;19(3):243-54.

Appendix



Figure A1. Native PAGE of PCR-amplified oligonucleotide fractions after the first round of SELEX using streptavidin-coated bead purification. SELEX was carried out similarly as in **Figure 2.1**. A randomized, biotinylated single-stranded DNA library was incubated with *L. acidophilus* cells in the presence of tRNA and BSA. Duplicate incubations were carried out for this round. The different fractions collected during SELEX (So, W1-W3, CA) and the parallel negative control were PCR amplified and analysed via PAGE. Unlabeled lanes on the gel contain the DNA ladder (100-2072 bp) and lanes 1-5 contain the supernatant fractions (order: neg So x 2, So x 2). Lanes 6-17 contain the wash fractions (in order: neg W1, W1, neg W2, W2, neg W3, W3). Lanes 18 and 19 contain the neg CA fractions and lanes 20 and 21 contain the duplicate CA fractions.

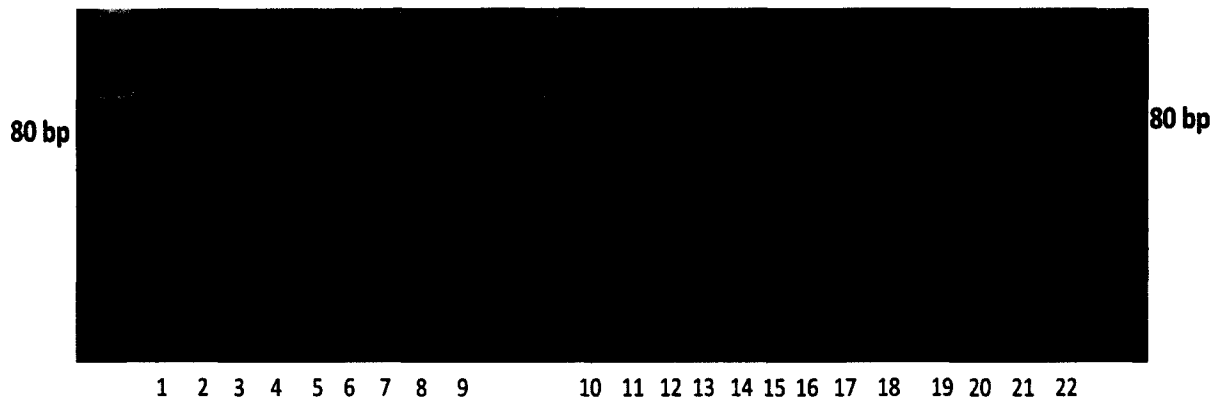


Figure A2. Native PAGE of PCR-amplified oligonucleotide fractions after the second round of SELEX using heat denaturation. SELEX was carried out as previously (Figure 1.1a) except that the aptamer CA pool from round 1 was used in place of single-stranded randomized library. Duplicate incubations were carried out for this round. The different fractions collected during SELEX (So, W1-W3, CA) and the negative control were PCR amplified and analysed via PAGE. Unlabeled lanes on the gel contain the DNA ladder (100-2072 bp) and lane 1 contains the PCR negative control. Lanes 2-5 contain the supernatant fractions (order: neg So x 2, So x 2) and lanes 6-18 the duplicate wash fractions (in order: neg W1, W1, neg W2, W2, neg W3, W3). Lanes 19, 20 contain the neg CA fractions and 21 and 22 contain the duplicate CA fractions.



Figure A3. Native PAGE of PCR-amplified oligonucleotide fractions after the third round of SELEX using heat denaturation and second round using streptavidin bead purification. SELEX was carried out as previously (**Figure 1.1a**) except that the aptamer CA pool from rounds 2 heat (**Figure 1.1c lanes 21-22**) and 1 beads (**Figure 1.1b lanes 20 and 21**) was used in place of single-stranded randomized library. Duplicate incubations were carried out for each round. The different fractions collected during SELEX (So, W1-W3, CA) and the negative control were PCR amplified and analysed via PAGE. Unlabeled lanes on the gel contain the DNA ladder (100-2072 bp). Lanes 1-6 contain the supernatant fractions (neg So, So 3heat, So 2beads). Lanes 7-24 contain the wash fractions (in order: neg W1, W1, neg W2, W2, neg W3, W3) and lanes 25 and 26 contain the neg CA fractions. Lanes 27-30 contain the CA fractions in order: 3 heat x2 and 2 beads x 2. For each type of fraction duplicate lanes are loaded in the order: neg, heat, beads.

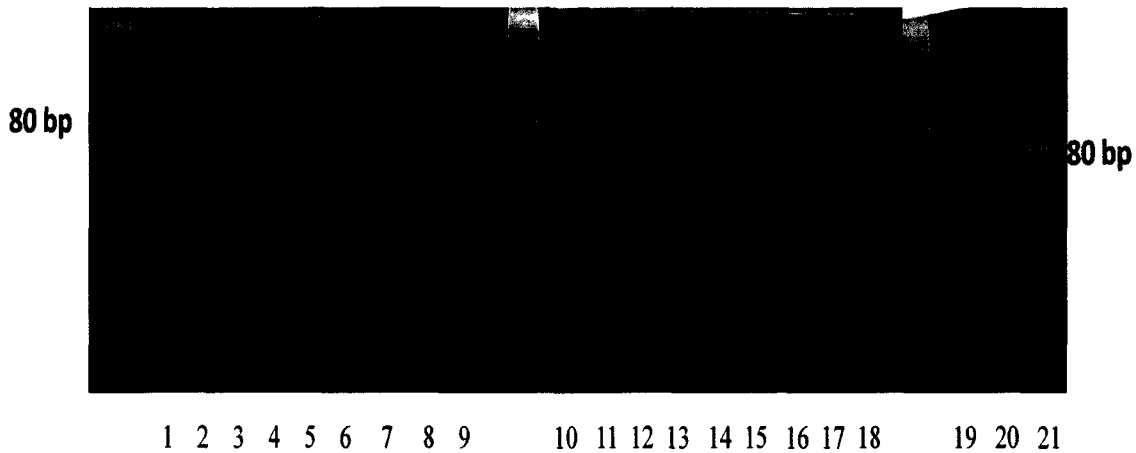


Figure A4. Native PAGE of PCR-amplified oligonucleotide fractions after the fourth round of SELEX using heat denaturation and the third round of SELEX using streptavidin bead purification. SELEX was carried out as previously (**Figure 1.1a**) except that the CA aptamer pool from rounds 3 heat and 2 beads (**Figure 1.1d, lanes 27-30**) were used in place of single-stranded randomized library. The different fractions collected during SELEX (So, W1-W3, CA) and the negative control were PCR amplified and analysed via PAGE. Unlabeled lanes on the gel contain the DNA ladder (100-2072 bp) and lane 1 contains the PCR negative control. Lanes 2-5 contain the supernatant fractions (neg So, So 4heat, So 3beads). Lanes 6-18 contain the wash fractions (in order: neg W1, W1, neg W2, W2, neg W3, W3) and lanes 18 and 19 contain the neg CA fractions. Lanes 20 and 21 contain the CA fractions 4 heat and 3 beads, respectively. For each type of fraction lanes are loaded in the order: neg, heat, beads.

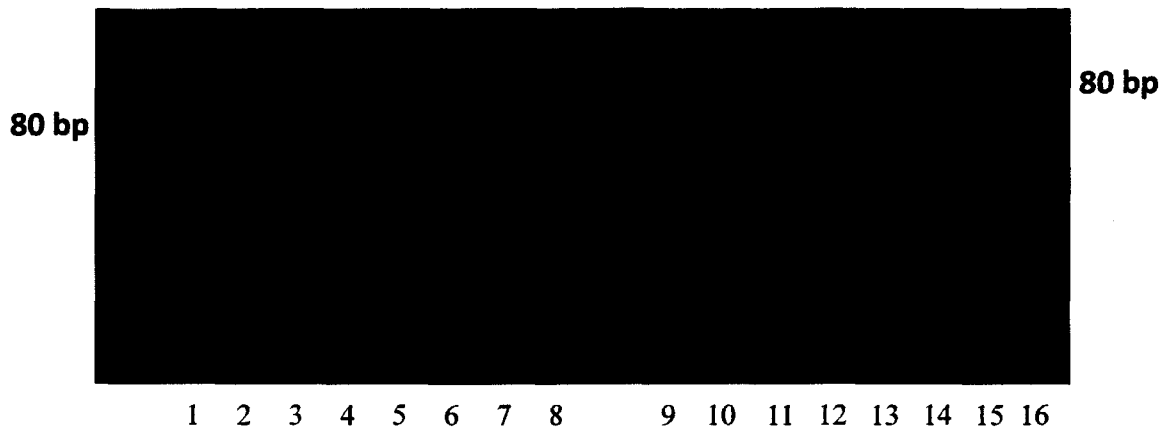


Figure A5. Native PAGE of PCR-amplified oligonucleotide fractions after the fourth round of SELEX using streptavidin bead purification. SELEX was carried out as previously (**Figure A1**) except that the CA aptamer pool from rounds 3 beads (**Figure 1.1e, lane 21**) was used in place of single-stranded randomized library. The different fractions collected during SELEX (So, W1-W3, CA) and the negative control were PCR amplified and analysed via PAGE. Unlabeled lanes on the gel contain the DNA ladder (100-2072 bp) and lane 1 contains the PCR negative control. Lanes 2-3 contain the supernatant fractions (neg So, So 4beads). Lanes 4-9 contain the wash fractions (in order: neg W1, W1, neg W2, W2, neg W3, W3) and lanes 10 and 11 contain the neg CA and CA 4beads fractions, respectively.

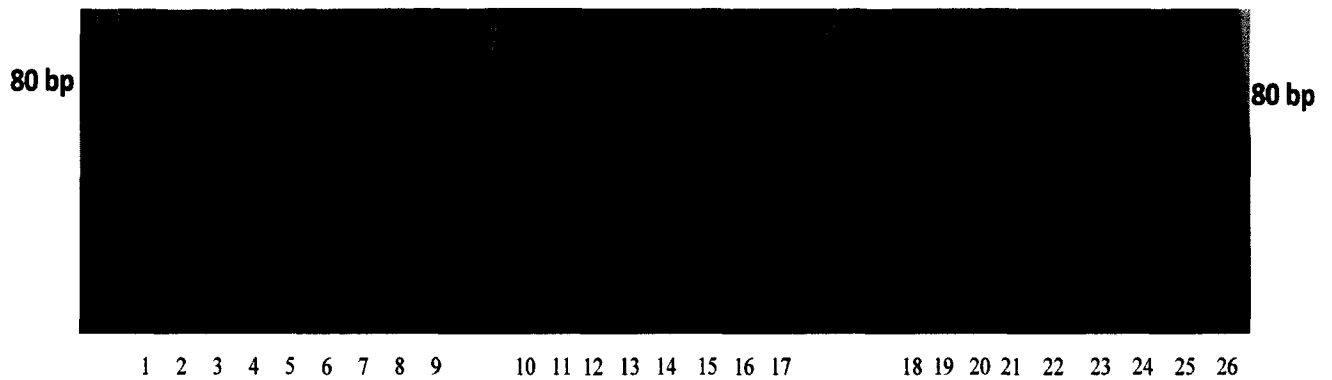


Figure A6. Native PAGE of PCR-amplified oligonucleotide fractions after the fifth round of SELEX using both heat denaturation and streptavidin bead purification. SELEX was carried out as previously (**Figure A1**) except that the CA aptamer pool from rounds 4 heat and beads (**Figure A4 lane 20 and A5 lane 11, respectively**) was used in place of single-stranded randomized library. Duplicate incubations were carried out for each round of SELEX. The different fractions collected during SELEX (So, W1-W3, CA) and the negative control were PCR amplified and analysed via PAGE. Unlabeled lanes on the gel contain the DNA ladder (100-2072 bp) and lane 1 contains the PCR negative control. Lanes 2-6 contain the supernatant fractions (neg So, So 5heat, So 5beads). Lanes 7-20 contain the wash fractions (in order: neg W1, W1, neg W2, W2, neg W3, W3) and lanes 21 and 22 contain the neg CA fractions. Lanes 23-26 contain the duplicate CA fractions 5 heat and 5 beads. For each type of fraction lanes are loaded in the order: neg, heat, beads.

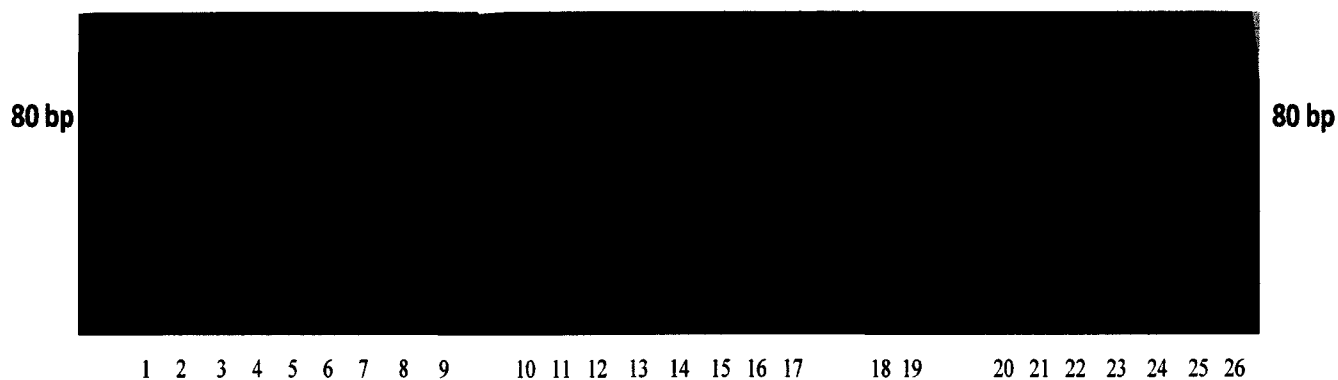


Figure A7. Native PAGE of PCR-amplified oligonucleotide fractions after the sixth round of SELEX using both heat denaturation and streptavidin bead purification. SELEX was carried out as previously (**Figure A1**) except that the CA aptamer pools from rounds 5 heat (**Figure A6 lanes 23, 24**) and 5 beads (**Figure A6 lanes 25, 26**) were used in place of single-stranded randomized library. Duplicate incubations were carried out for each round of SELEX. The different fractions collected during SELEX (So, W1-W3, CA) and the negative control were PCR amplified and analysed via PAGE. Unlabeled lanes on the gel contain the DNA ladder (100-2072 bp) and lane 1 contains the PCR negative control. Lanes 2-6 contain the supernatant fractions (neg So, So 6heat, So 6beads). Lanes 7-20 contain the wash fractions (in order: neg W1, W1, neg W2, W2, neg W3, W3) and lanes 21 and 22 contain the neg CA fractions. Lanes 23-26 contain the duplicate CA fractions 6 heat and 6 beads. For each type of fraction lanes are loaded in the order: neg, heat, beads.

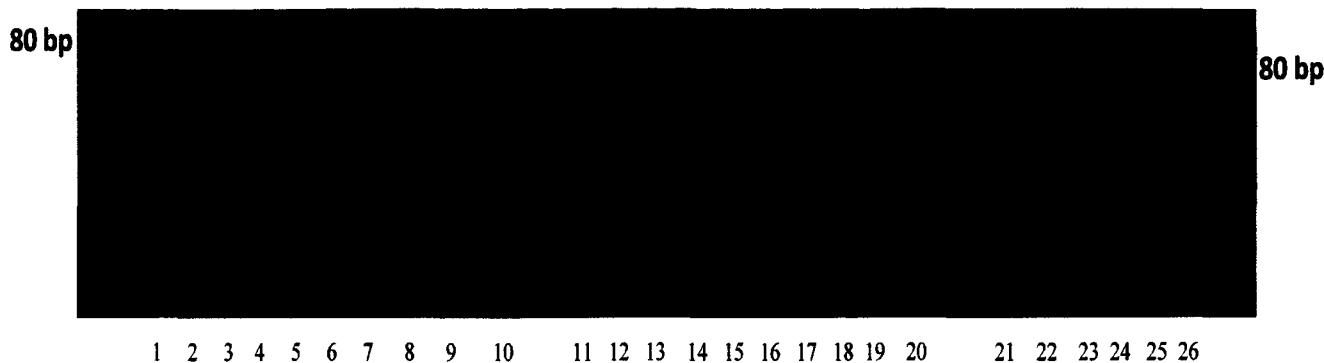
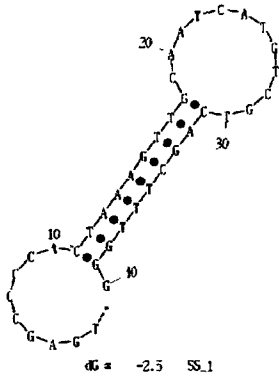
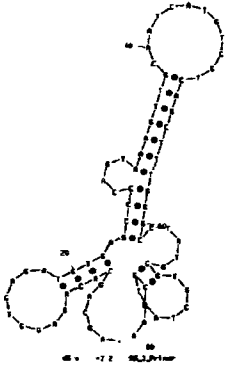


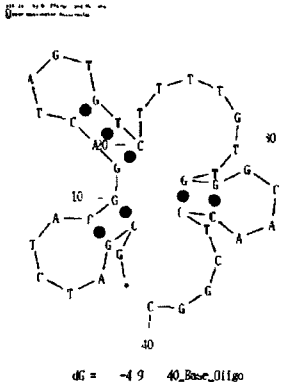
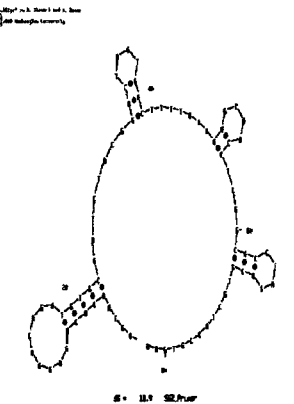
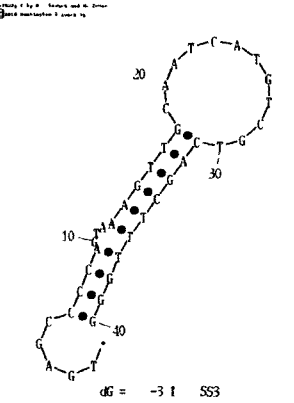
Figure A8. Native PAGE of PCR-amplified oligonucleotide fractions after the seventh round of SELEX using both heat denaturation and streptavidin bead purification. SELEX was carried out as previously (**Figure 1.1a**) except that the CA aptamer pools from rounds 6 heat (**Figure A7 lanes 23, 24**) and 6 beads (**Figure A7 lanes 25, 26**) were used in place of single-stranded randomized library. Duplicate incubations were carried out for each round of SELEX. The different fractions collected during SELEX (So, W1-W3, CA) and the negative control were PCR amplified and analysed via PAGE. Unlabeled lanes on the gel contain the DNA ladder (100-2072 bp) and lane 1 contains the PCR negative control. Lanes 2-6 contain the supernatant fractions (neg So, So 7heat, So 7beads). Lanes 7-20 contain the wash fractions (in order: neg W1, W1, neg W2, W2, neg W3, W3) and lanes 21 and 22 contain the neg CA fractions. Lanes 23-26 contain the duplicate CA fractions 7 heat and 7 beads. For each type of fraction lanes are loaded in the order: neg, heat, beads.

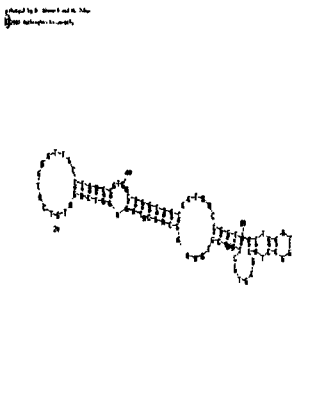
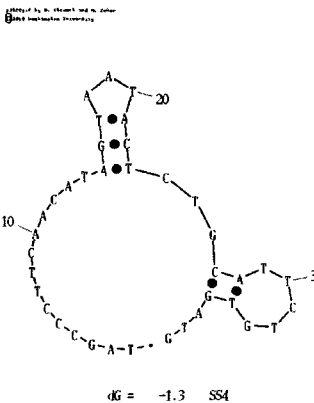
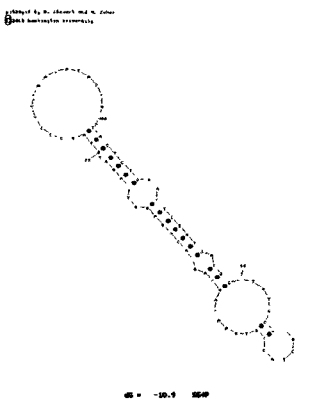


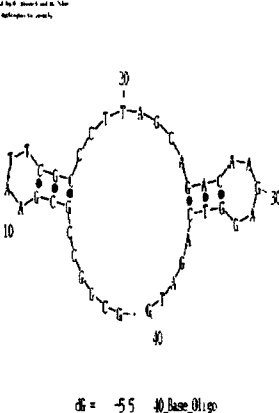
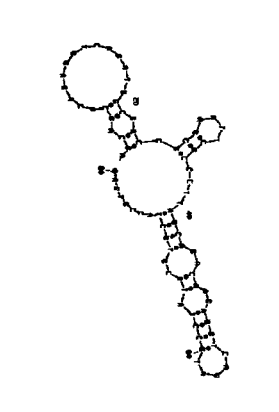
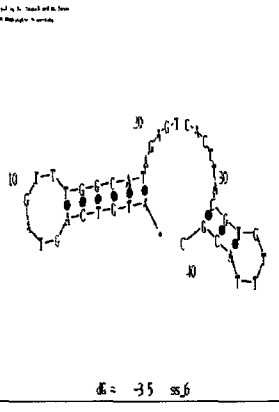
Figure A9. Native PAGE of PCR-amplified oligonucleotide fractions after the eighth round of SELEX using both heat denaturation and streptavidin bead purification. SELEX was carried out as previously (**Figure A1**) except that the CA aptamer pools from rounds 7 heat (**Figure A8 lanes 23, 24**) and 7 beads (**Figure A8 lanes 25, 26**) were used in place of single-stranded randomized library. Duplicate incubations were carried out for each round of SELEX. The different fractions collected during SELEX (So, W1-W3, CA) and the negative control were PCR amplified and analysed via PAGE. Unlabeled lanes on the gel contain the DNA ladder (100-2072 bp). Lanes 1-5 contain the supernatant fractions (neg So, So 8heat, So 8beads). Lanes 6-19 contain the wash fractions (in order: neg W1, W1, neg W2, W2, neg W3, W3) and lanes 20 and 21 contain the neg CA fractions. Lanes 22-25 contain the duplicate CA fractions 7 heat and 7 beads. For each type of fraction lanes are loaded in the order: neg, heat, beads.

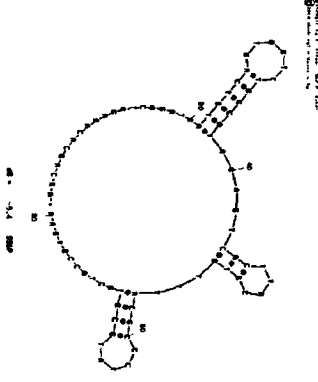
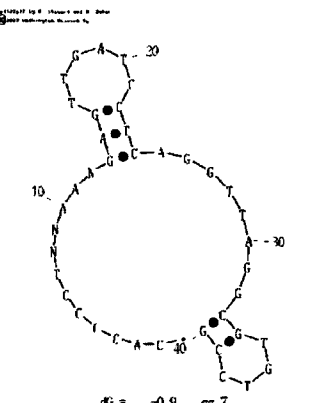
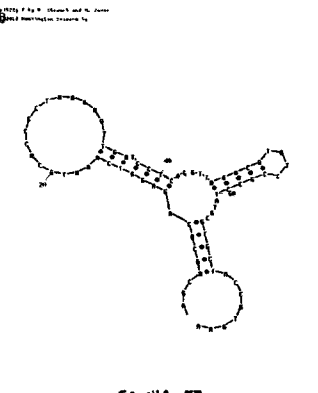
Table A1: Sequences, most likely secondary structures, and free energy of formation obtained from cloning round 7 heat denatured and round 8 bead purified aptamer pools.

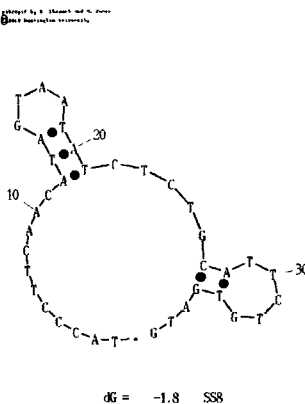
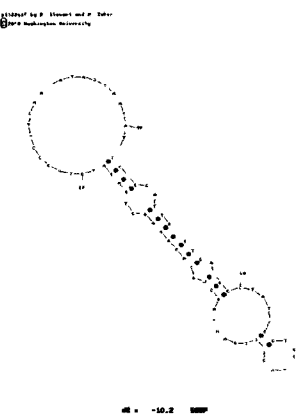
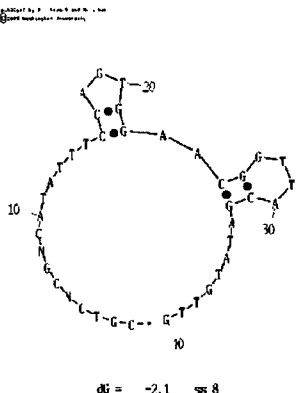
Name	Sequence	Structure	ΔG (kcal/mol)
mag1	5'- TAGCCCTTCAACAT AGTAATATCTCTGC ATTCTGTGATG-3'		-2.5
mag1P	5'- AGCAGCACAGAGGT CAGATG TAGCCCTTCAACAT AGTAATATCTCTGC ATTCTGTGATGCCT ATGCGTGCTACCGT GAA-3'		-7.2

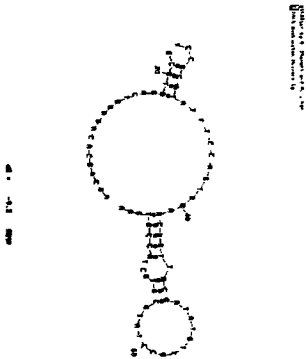
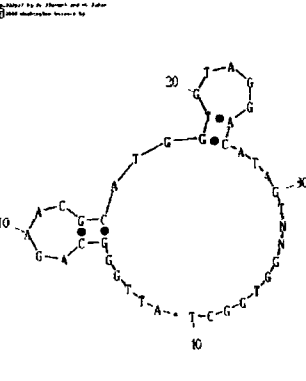
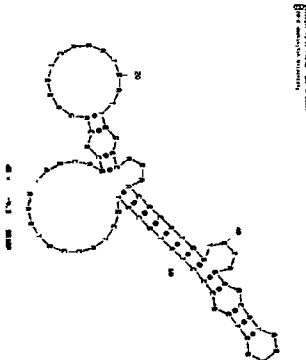
Name	Sequence	Structure	ΔG (kcal/mol)
mag2	5'- GCGATCTACGGAC TAGTGTCTTTTGT GGGCAACCTCGGC- 3'	 <p>$\Delta G = -4.9$ 40_Base_Oligo</p>	-4.9
mag2P	5'- AGCAGCACAGAGGT CAGATG TAGCCCTTCAACAT AGTAATATCTCTGC ATTCTGTGATG CCTATGCGTGCTAC CGTGAA-3'	 <p>$\Delta G = -11.9$ 527bp</p>	-11.9
mag3	5'- TGAGCCCCAGTAA AGTTGCAATCATG TCGTCAGCTTTGG G-3'	 <p>$\Delta G = -3.1$ 553</p>	-3.1

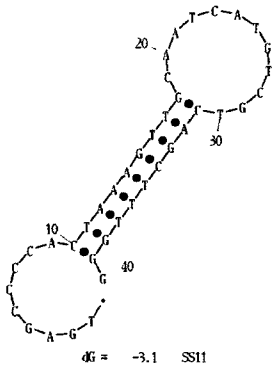
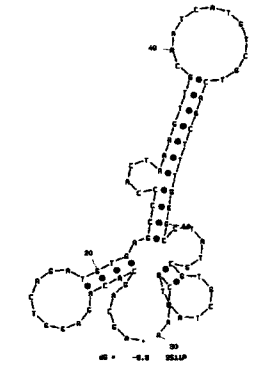
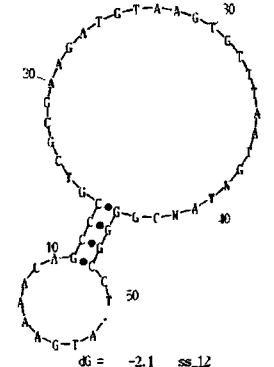
Name	Sequence	Structure	ΔG (kcal/mol)
mag3P	5'- AGCAGCACAGAGGT CAGATG TGAGCCCCAGTAA AGTTGCAATCATG TCGTCAGCTTTGG GCCTATGCGTGCTA CCGTGAA-3'	 <p>44 - 42.9 kcal/mol</p>	-12.9
mag4	5'- TAGCCCTTCAACAT AGTAATACTCTGC ATTCTGTGATG-3'	 <p>46 - -1.3 kcal/mol</p>	-1.3
mag4P	5'- AGCAGCACAGAGGT CAGATG TAGCCCTTCAACAT AGTAATACTCTGC ATTCTGTGATGCCT ATGCGTGCTACCGT GAA-3'	 <p>46 - -10.9 kcal/mol</p>	-10.9

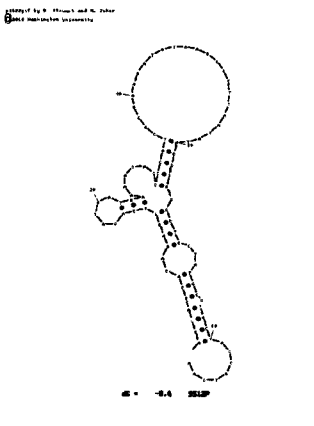
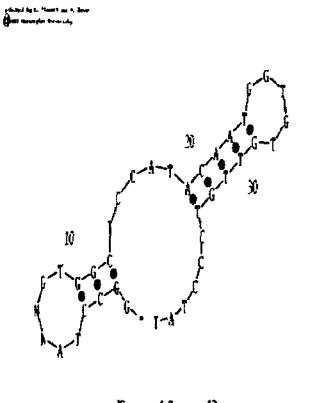
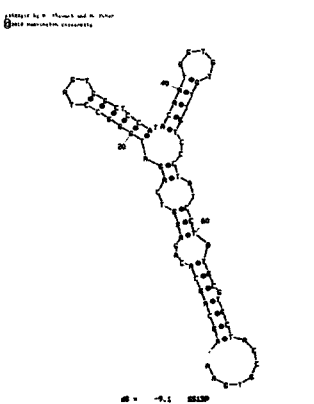
Name	Sequence	Structure	ΔG (kcal/mol)
mag5	5'- GCGGCCGCGAATT CGCCCTTAGCAGA CAAGAGGTCAGAT G-3'		-5.5
mag5P	5'- AGCAGCACAGAGGT CAGATG GCGGCCGCGAATT CGCCCTTAGCAGA CAAGAGGTCAGAT GCCTATGCGTGCTA CCGTGAA-3'		-11.3
mag6	5'- ATGTCAGTAGTTT GGCATAGAGTCAC TTACGTGTTTACGC -3'		-3.5

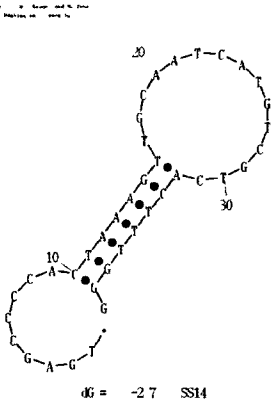
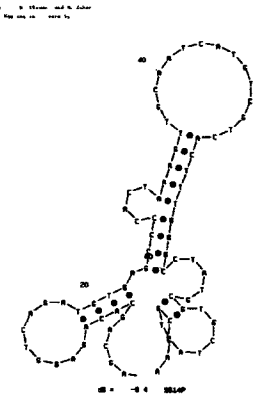
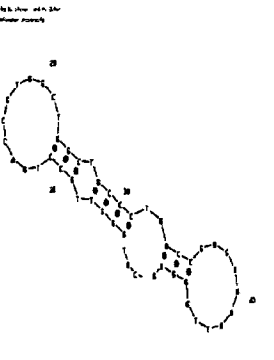
Name	Sequence	Structure	ΔG (kcal/mol)
mag6P	5'- AGCAGCACAGAGGT CAGATG ATGTCAGTAGTTT GGCATAGAGTCAC TTACGTGTTTACGC CCTATGCGTGCTAC CGTGAA-3'		-9.4
mag7	5'- CACCCCTAAGAGT TGATCCTCAGGT AGGCGTGTCCG-3'		-0.9
mag7P	5'- AGCAGCACAGAGGT CAGATG CACCCCTAAGAGT TGATCCTCAGGT AGGCGTGTCCGCC TATGCGTGCTACCG TGAA-3'		-11.9

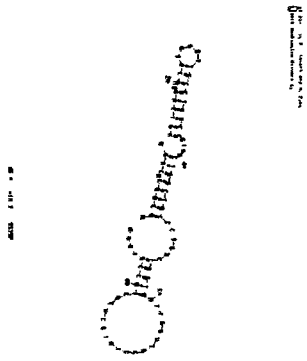
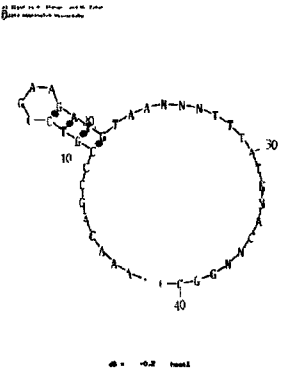
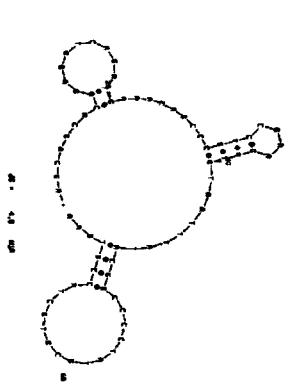
Name	Sequence	Structure	ΔG (kcal/mol)
mag8	5'- TACCCTTCAACATA GTAATATCTCTGCA TTCTGTGATG-3'	 <p style="text-align: center;">dG = -1.8 SS8</p>	-1.8
mag8P	5'- AGCAGCACAGAGGT CAGATG TACCCTTCAACATA GTAATATCTCTGCA TTCTGTGATGCCTA TGCGTGCTACCGTG AA-3'	 <p style="text-align: center;">dG = -10.2 SS8</p>	-10.2
mag9	5'- CGTCCGCATAT TTC CAGTGGAACGGTT ACGATATGTTG-3'	 <p style="text-align: center;">dG = -2.1 SS8</p>	-2.1

Name	Sequence	Structure	ΔG (kcal/mol)
mag9P	5'- AGCAGCACAGAGGT CAGATG CGTCCGCATAT TTC CAGTGG AACGGTT ACGATATGTTGCCT ATGCGTGCTACCGT GAA-3'		-9.2
mag10	5'- ATTGGGCAGAACG CATGGTGTAGGAC ATAGTGGTGGCT-3'		-1.9
mag10P	5'- AGCAGCACAGAGGT CAGATG ATTGGGCAGAACG CATGGTGTAGGAC ATAGTGGTGGCCC TATGCGTGCTACCG TGAA-3'		-9.3

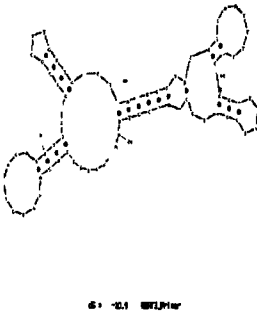
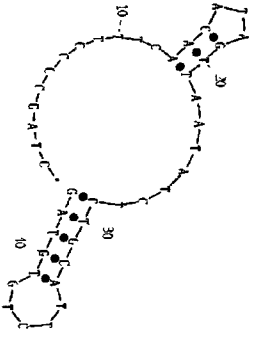
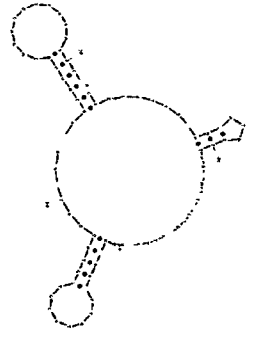
Name	Sequence	Structure	ΔG (kcal/mol)
mag11	5'- TGAGCCCCACTAA AGTTGCAATCATG TCGTCAGCTTTGG G-3'		-3.1
mag11P	5'- AGCAGCACAGAGGT CAGATG TGAGCCCCACTAA AGTTGCAATCATG TCGTCAGCTTTGG GCCTATGCGTGCTA CCGTGAA-3'		-8.8
mag12	5'- ATGAAAACAGCCC GTCGCGAAGATGT AAGTGTTTAATGTA CGGGGCCT-3'		-2.1

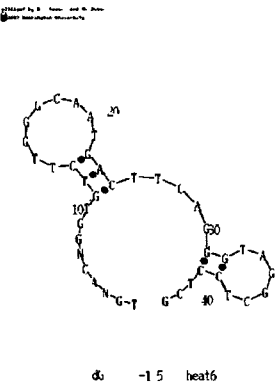
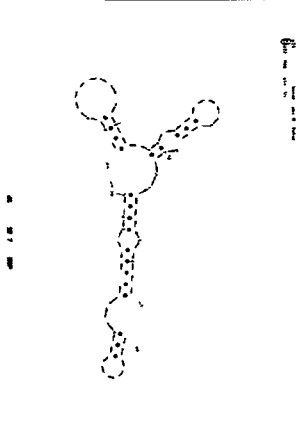
Name	Sequence	Structure	ΔG (kcal/mol)
mag12P	5'- AGCAGCACAGAGGT CAGATG ATGAAAACAGCCC GTCGCGAAGATGT AAGTGTTTAATGTA CGGGGCCTCCTATG CGTGCTACCGTGAA- 3'		-8.6
mag13	5'- GGCCTAGTGGCTC CATACAATGGTGT GTTGTCCCTAT-3'		-4.8
mag13P	5'- AGCAGCACAGAGGT CAGATG GGCCTAGTGGCTC CATACAATGGTGT GTTGTCCCTATCCT ATGCGTGCTACCGT GAA-3'		-9.1

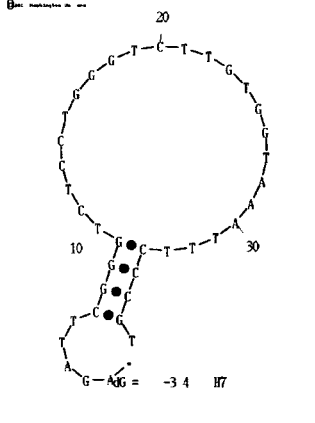
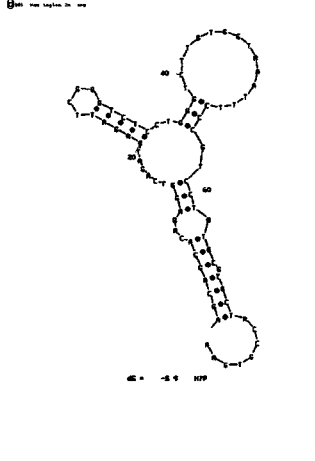
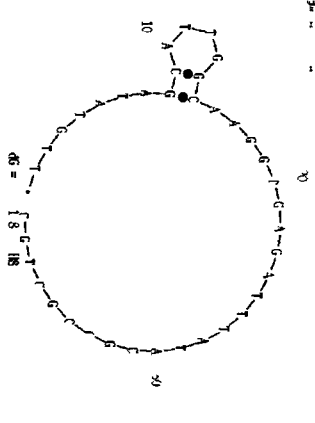
Name	Sequence	Structure	ΔG (kcal/mol)
mag14	5'- TGAGCCCCACTAA AGTTGCAATCATG TCGTCAC TTTGGG- 3'		-2.7
mag14P	5'- AGCAGCACAGAGGT CAGATG TGAGCCCCACTAA AGTTGCAATCATG TCGTCAC TTTGGG CCTATGCGTGCTAC CGTGAA-3'		-8.4
mag15	5'- CATGGGTTGCCTG ACCGTGGCTGGCT GCCCTGACCGGTA ATTGGGTG-3'		-6.8

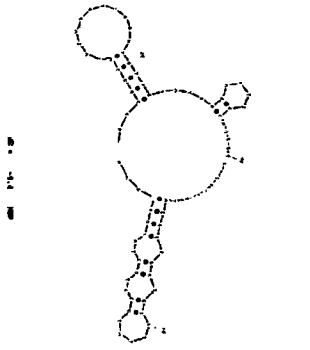
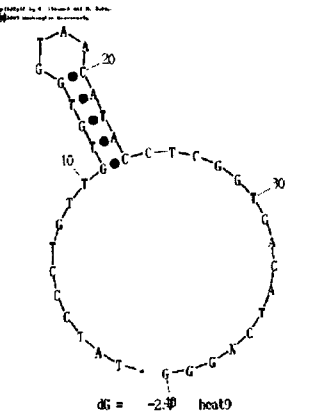
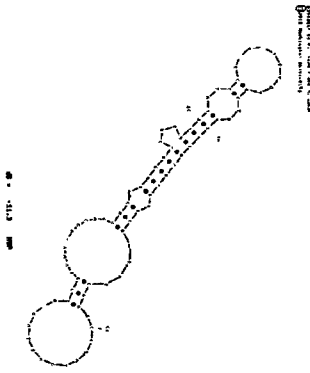
Name	Sequence	Structure	ΔG (kcal/mol)
mag15P	5'- AGCAGCACAGAGGT CAGATG CATGGGTTGCCTG ACCGTGGCTGGCT GCCCTGACCGGTA ATTGGGTGCCTATG CGTGCTACCGTGAA- 3'		-16.7
heat 1	5'- AAACAGCCCGTCC GAAGATGTAATT ATACGGCC-3'		-0.2
heat 1P	5'- AGCAGCACAGAGGT CAGATG AAACAGCCCGTCC GAAGATGTAATT ATACGGCCCCTATG CGTGCTACCGTGAA- 3'		-4.8

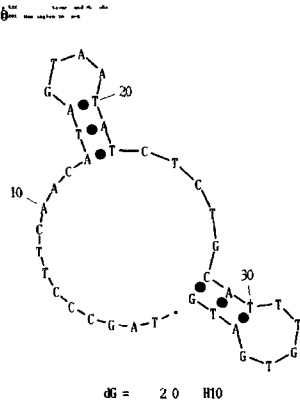
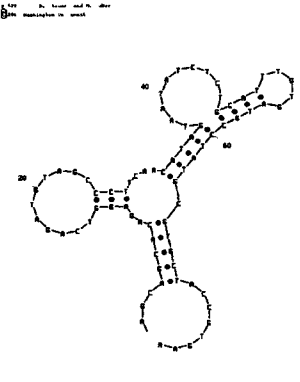
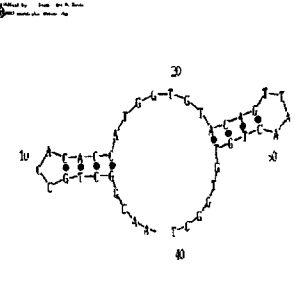
Name	Sequence	Structure	ΔG (kcal/mol)
heat 2	5'- TGCCCTTCAACATA GTAATATCTCTGCA TTCTGTGATG-3'	<p>$\Delta G = -1.8$ H2</p>	-1.8
heat 2P	5'- AGCAGCACAGAGGT CAGATG TGCCCTTCAACATA GTAATATCTCTGCA TTCTGTGATGCCTA TGCCGTGCTACCGTG AA-3'	<p>$\Delta G = -7.4$ H2</p>	-7.4
heat 3	5'- CGTCCGCGTTATA TTTAGAGTGGAAC GGTCAC-3'	<p>$\Delta G = -2.3$ kcal3</p>	-2.3

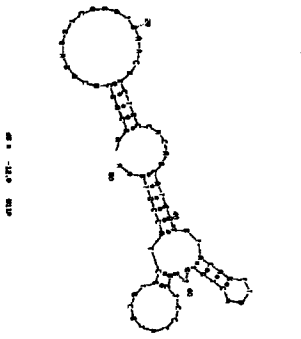
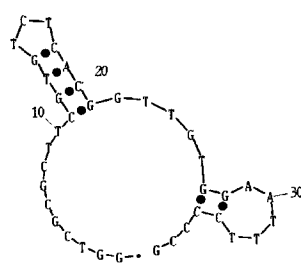
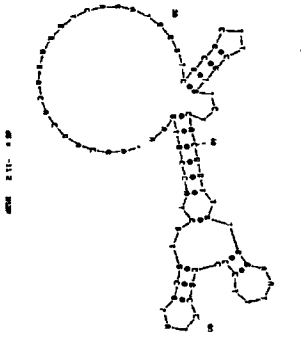
Name	Sequence	Structure	ΔG (kcal/mol)
heat 3P	5'- AGCAGCACAGAGGT CAGATG CGTCCGCGTTATA TTAGAGTGGAAC GGTCACCCTATGCG TGCTACCGTGAA-3'		-10.9
heat 4	5'- CTAGCCCCTTTCAA CATAGTTAATATCT CTGCATTCTGTGTA G-3'		-1.3
heat 4P	5'- AGCAGCACAGAGGT CAGATG CTAGCCCCTTTCAA CATAGTTAATATCT CTGCATTCTGTGTA GCCTATGCGTGCTA CCGTGAA-3'		-7.2

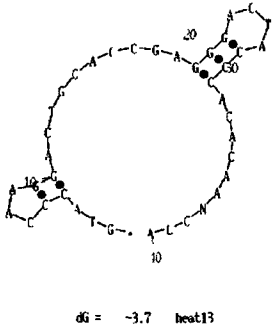
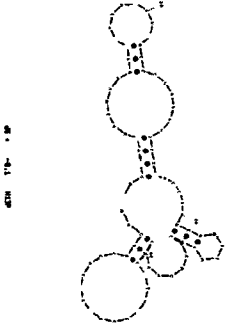
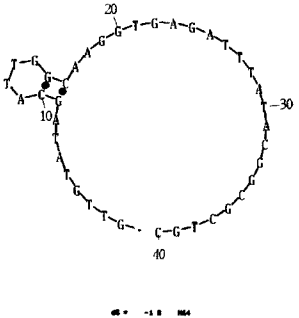
Name	Sequence	Structure	ΔG (kcal/mol)
heat 5	5'- NGNNTCNNNNGGC GGNATTNANGCA GCGGGTTACNCG A-3'	Sequence of low quality	N/A
heat 5P	5'- AGCAGCACAGAGGT CAGATG NGNNTCNNNNGGC GGNATTNANGCA GCGGGTTACNCG ACCTATGCGTGCTA CCGTGAA-3'	Sequence of low quality	N/A
heat 6	5'- TGACGGTGTCTTG GGCAATGACTTCA GGGTAGGCTCCTC G-3'		-1.5
heat 6P	5'- AGCAGCACAGAGGT CAGATG TGACGGTGTCTTG GGCAATGACTTCA GGGTAGGCTCCTC GCCTATGCGTGCTA CCGTGAA-3'		-12.7

Name	Sequence	Structure	ΔG (kcal/mol)
heat 7	5'- AGATTCGGGTCTC CTGGGTCTTGTGG TAAATTTCCCGT-3'		-3.4
heat 7P	5'- AGCAGCACAGAGGT CAGATG AGATTCGGGTCTC CTGGGTCTTGTGG TAAATTTCCCGTCC TATGCGTGCTACCG TGAA-3'		-5.9
heat 8	5'- TTGTATAGCATTG GCAAGGTGAGATT TATACGGCGCTGC- 3'		-1.8

Name	Sequence	Structure	ΔG (kcal/mol)
heat 8P	5'- AGCAGCACAGAGGT CAGATG TTGTATAGCATTG GCAAGGTGAGATT TATACGGCGCTGC CCTATGCGTGCTAC CGTGAA-3'		-9.4
heat 9	5'- TATCCCTGTTGTGT GGTAACATACCTC GGTGACATCGGG- 3'		-2.4
heat 9P	5'- AGCAGCACAGAGGT CAGATG TATCCCTGTTGTGT GGTAACATACCTC GGTGACATCGGGC CTATGCGTGCTACC GTGAA-3'		-11.3

Name	Sequence	Structure	ΔG (kcal/mol)
heat 10	5'- TAGCCCTTCAACAT AGTAATATCTCTGC ATTTGTGATG-3'		-2.0
heat 10P	5'- AGCAGCACAGAGGT CAGATG TAGCCCTTCAACAT AGTAATATCTCTGC ATTTGTGATGCCTA TGCGTGCTACCGTG AA-3'		-7.3
heat 11	5'- AACGGCTGCCACA GCATGGTGTACAG TAACTGTGTGGC T-3'		-6.9

Name	Sequence	Structure	ΔG (kcal/mol)
heat 11P	5'- AGCAGCACAGAGGT CAGATG AACGGCTGCCACA GCATGGTGTACAG TTAAGTGTGTGGC TCCTATGCGTGCTA CCGTGAA-3'		-12.0
heat 12	5'- GGTCGCGCTTCGT GTCTCACGGTTGT GGAATTTCCCCG-3'	 <p>dG = -4.8 H12</p>	-4.8
heat 12P	5'- AGCAGCACAGAGGT CAGATG GGTCGCGCTTCGT GTCTCACGGTTGT GGAATTTCCCCGC CTATGCGTGCTACC GTGAA-3'		-11.2

Name	Sequence	Structure	ΔG (kcal/mol)
heat 13	5'- GTACCCAAGGACT GCACCGAGGGACT ACCCACACAACCA- 3'		-3.7
heat 13P	5'- AGCAGCACAGAGGT CAGATG GTACCCAAGGACT GCACCGAGGGACT ACCCACACAACCA CCTATGCGTGCTAC CGTGAA-3'		-8.1
heat 14	5'- GTTGTATAGCATT GGCAAGGTGAGAT TTATACGGCGCTG C-3'		-1.8

Name	Sequence	Structure	ΔG (kcal/mol)
heat 14P	5'- AGCAGCACAGAGGT CAGATG GTTGTATAGCATT GGCAAGGTGAGAT TTATACGGCGCTG CCCTATGCGTGCTA CCGTGAA-3'		-8.6

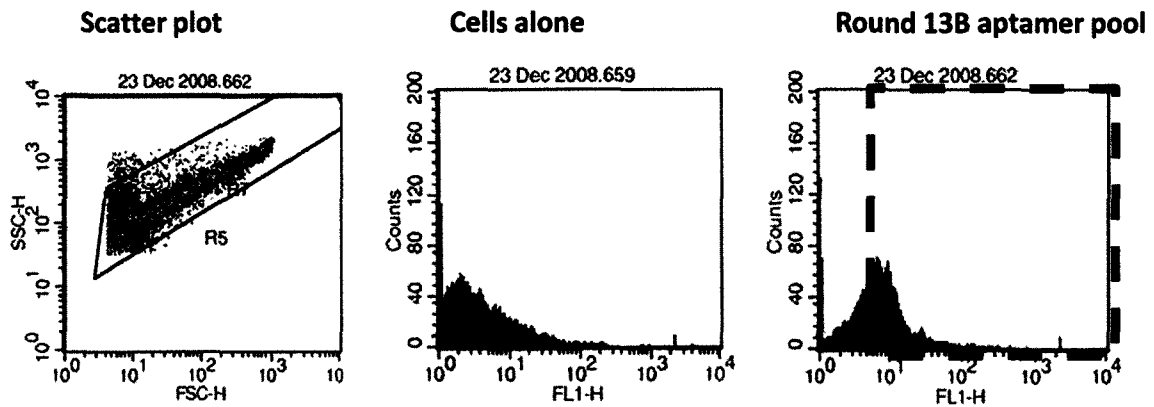


Figure A10. Typical flow cytometry outputs from screening of aptamer pools following each round of selection, showing increase in gated fluorescence intensity above background (boxed area) following incubation with round 13B aptamer pool.



Figure A11- PCR amplification and PAGE of GAS SELEX round 2A

fractions. Aptamers and cell mixtures were incubated and fractions collected as in **Figure 3.4**. Lane 1=neg PCR control; Lane 2=neg So; Lane 3=So; Lane 4=neg W1; Lane 5=W1, Lane 6=neg W2, Lane 7=W2, Lane 8=neg W3, Lane 9=W3, Lane 10=neg W4, Lane 11=W4; Lane 12=neg CA, Lane 13=CA.

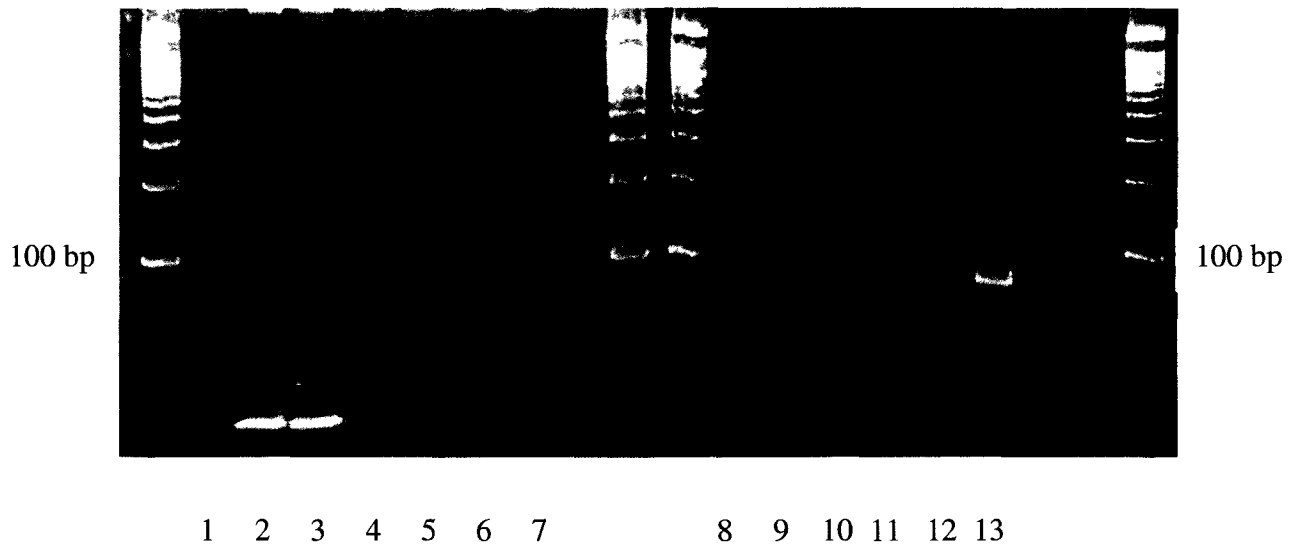


Figure A12- PCR amplification and PAGE of GAS SELEX round 3A

fractions. Aptamers and cell mixtures were incubated and fractions collected as in **Figure 3.4**. Lane 1=neg PCR control; Lane 2=neg So; Lane 3=So; Lane 4=neg W1; Lane 5=W1, Lane 6=neg W2, Lane 7=W2, Lane 8=neg W3, Lane 9=W3, Lane 10=neg W4, Lane 11=W4; Lane 12=neg CA, Lane 13=CA.

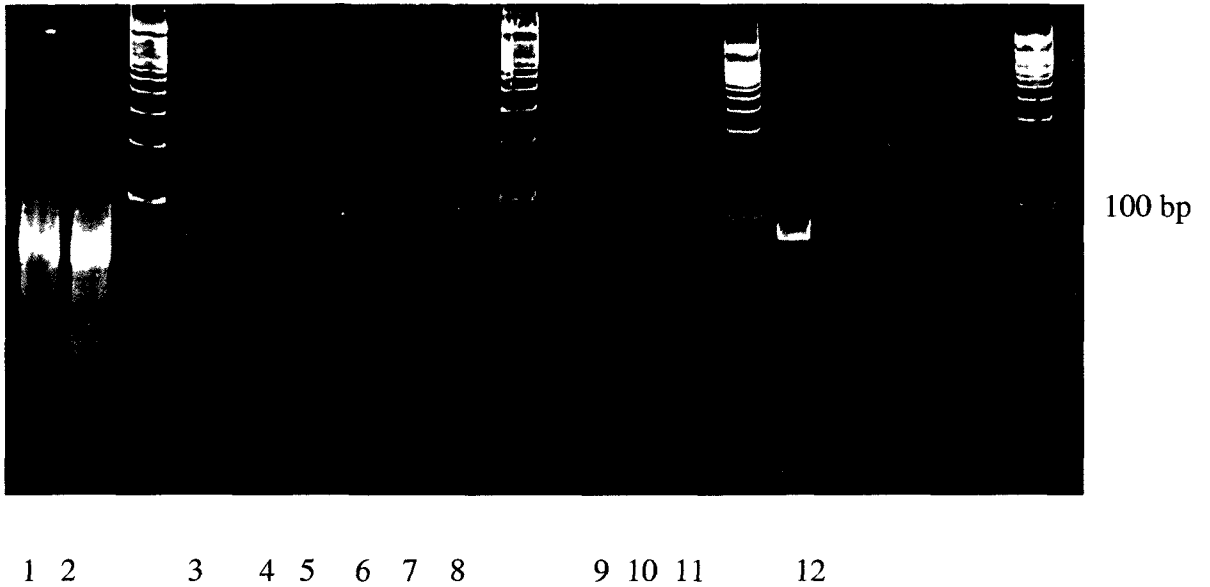


Figure A13- PCR amplification and PAGE of GAS SELEX round 3B

fractions. Aptamers and cell mixtures were incubated and fractions collected as in **Figure 3.4**. Lane 1= neg So; Lane 2=So; Lane 3=W1; Lane 4=neg W1, Lane 5=neg W2, Lane 6=W2, Lane 7=neg W3, Lane 8=W3, Lane 9=neg W4, Lane 10=W4; Lane 11=neg CA, Lane 12=CA.

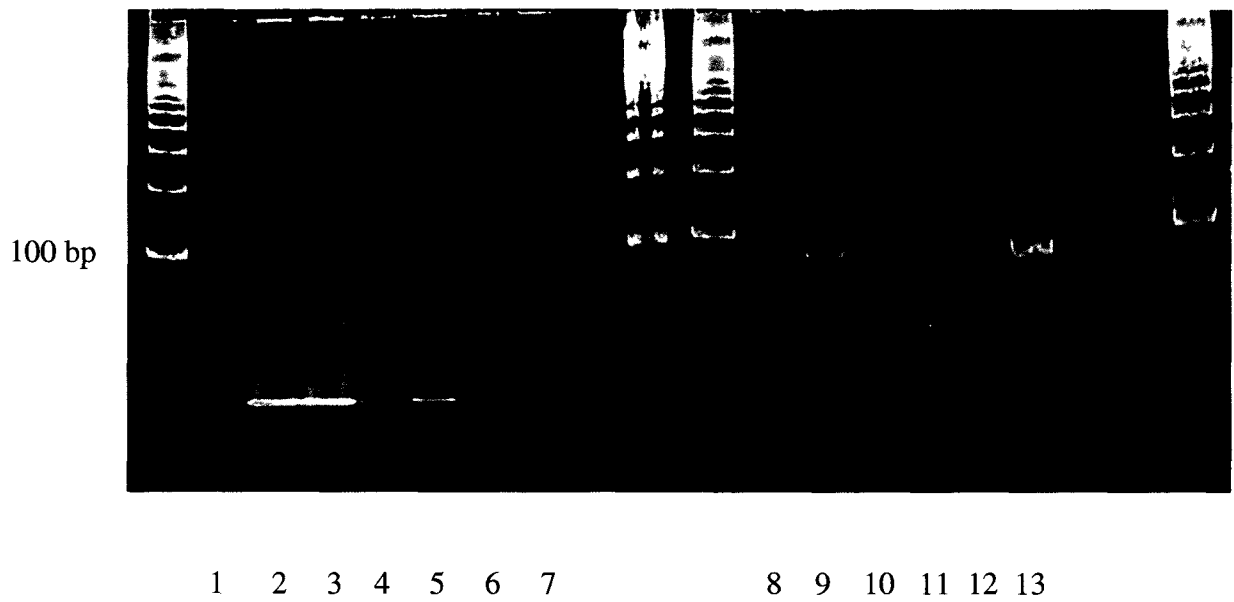


Figure A14- PCR amplification and PAGE of GAS SELEX round 4A

fractions. Aptamers and cell mixtures were incubated and fractions collected as in **Figure 3.4**. Lane 1=neg PCR control; Lane 2=neg So; Lane 3=So; Lane 4=neg W1; Lane 5=W1, Lane 6=neg W2, Lane 7=W2, Lane 8=neg W3, Lane 9=W3, Lane 10=neg W4, Lane 11=W4; Lane 12=neg CA, Lane 13=CA.

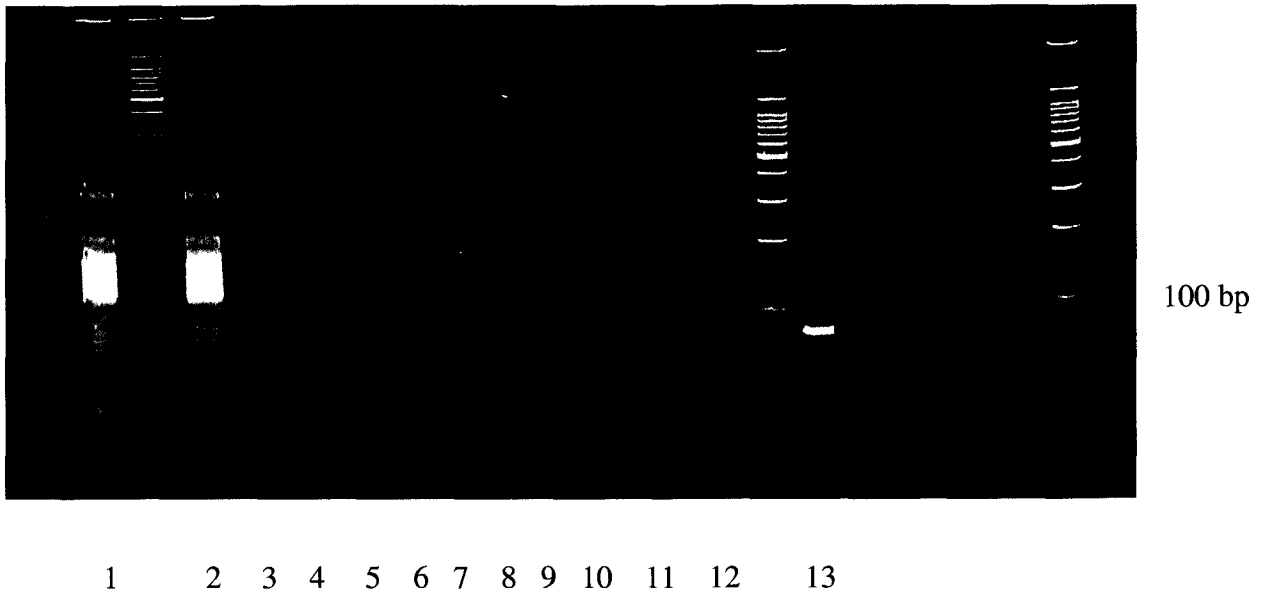


Figure A15- PCR amplification and PAGE of GAS SELEX round 4B

fractions. Aptamers and cell mixtures were incubated and fractions collected as in **Figure 3.4**. Lane 1=neg PCR control; Lane 2=neg So; Lane 3=So; Lane 4=neg W1; Lane 5=W1, Lane 6=neg W2, Lane 7=W2, Lane 8=neg W3, Lane 9=W3, Lane 10=neg W4, Lane 11=W4; Lane 12=neg CA, Lane 13=CA.

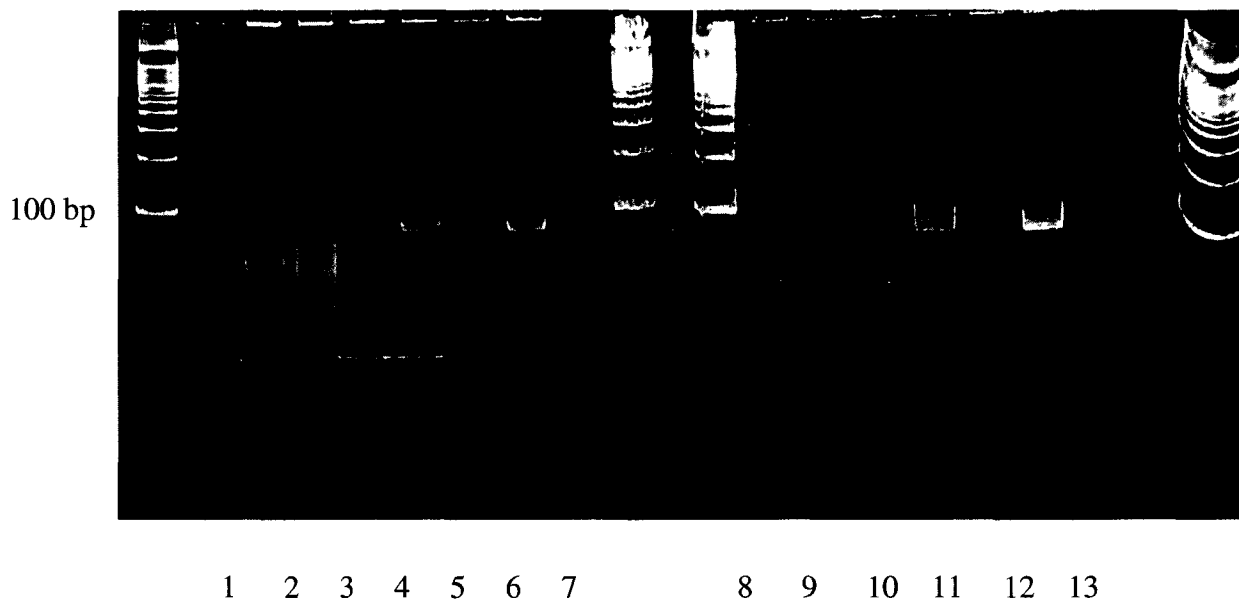


Figure A16- PCR amplification and PAGE of GAS SELEX round 5A

fractions. Aptamers and cell mixtures were incubated and fractions collected as in **Figure 3.4**. Lane 1=neg PCR control; Lane 2=neg So; Lane 3=So; Lane 4=neg W1; Lane 5=W1, Lane 6=neg W2, Lane 7=W2, Lane 8=neg W3, Lane 9=W3, Lane 10=neg W4, Lane 11=W4; Lane 12=neg CA, Lane 13=CA.

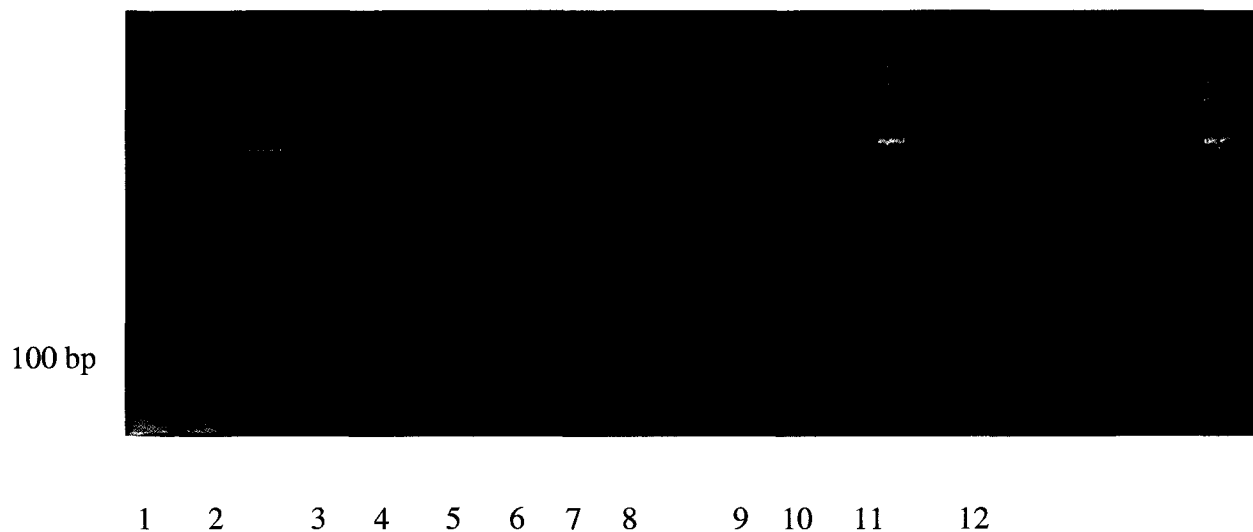


Figure A17- PCR amplification and PAGE of GAS SELEX round 5B

fractions. Aptamers and cell mixtures were incubated and fractions collected as in **Figure 3.4**. Lane 1=neg So; Lane 2=So; Lane 3=neg W1; Lane 4=W1, Lane 5=neg W2, Lane 6=W2, Lane 7=neg W3, Lane 8=W3, Lane 9=neg W4, Lane 10=W4; Lane 11=neg CA, Lane 12=CA.

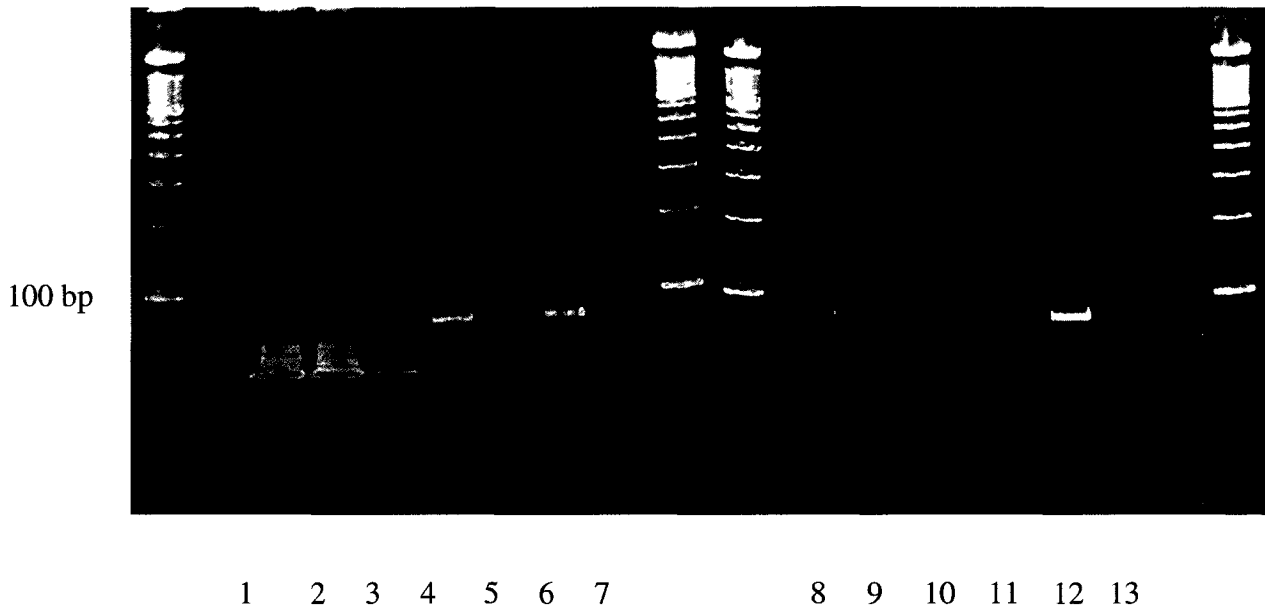


Figure A18- PCR amplification and PAGE of GAS SELEX round 6A

fractions. Aptamers and cell mixtures were incubated and fractions collected as in **Figure 3.4**. Lane 1=neg PCR control; Lane 2=neg So; Lane 3=So; Lane 4=neg W1; Lane 5=W1, Lane 6=neg W2, Lane 7=W2, Lane 8=neg W3, Lane 9=W3, Lane 10=neg W4, Lane 11=W4; Lane 12=neg CA, Lane 13=CA.

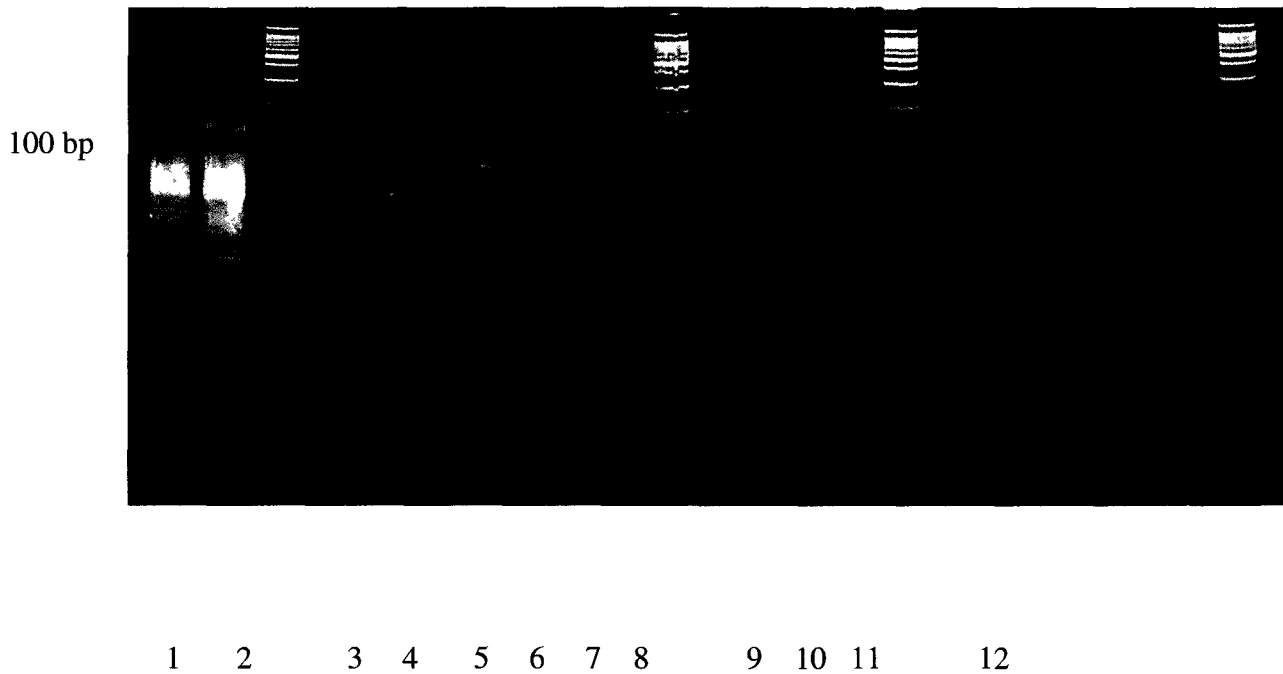


Figure A19- PCR amplification and PAGE of GAS SELEX round 6B

fractions. Aptamers and cell mixtures were incubated and fractions collected as in **Figure 3.4**. Lane 1=neg So; Lane 2=So; Lane 3=neg W1; Lane 4=W1, Lane 5=neg W2, Lane 6=W2, Lane 7=neg W3, Lane 8=W3, Lane 9=neg W4, Lane 10=W4; Lane 11=neg CA, Lane 12=CA.

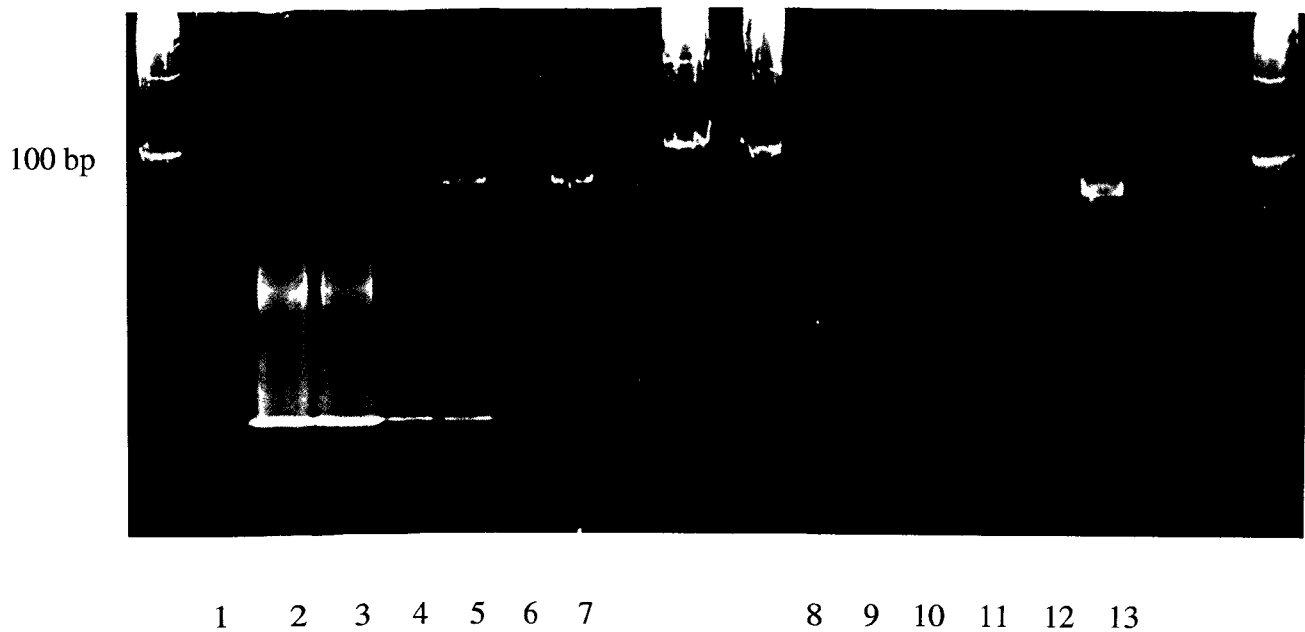


Figure A20- PCR amplification and PAGE of GAS SELEX round 7A fractions. Aptamers and cell mixtures were incubated and fractions collected as in **Figure 3.4**. Lane 1=neg PCR control; Lane 2=neg So; Lane 3=So; Lane 4=neg W1; Lane 5=W1, Lane 6=neg W2, Lane 7=W2, Lane 8=neg W3, Lane 9=W3, Lane 10=neg W4, Lane 11=W4; Lane 12=neg CA, Lane 13=CA.

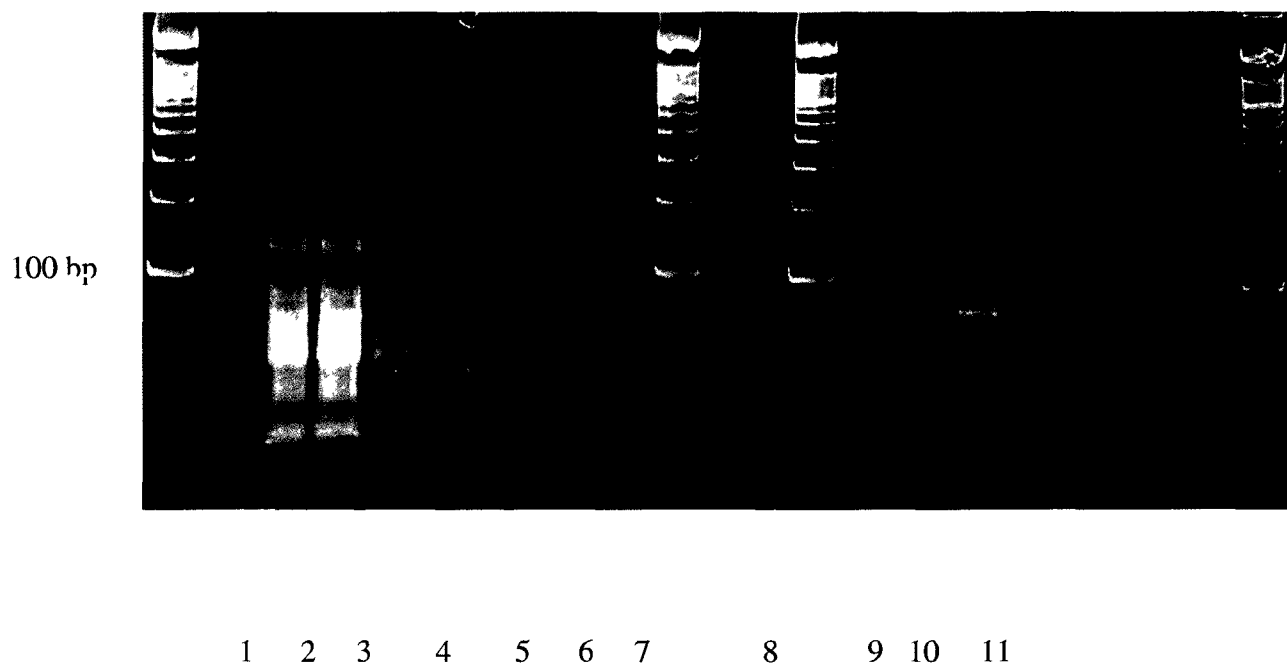


Figure A21- PCR amplification and PAGE of GAS SELEX round 7B

fractions. Aptamers and cell mixtures were incubated and fractions collected as in **Figure 3.4**. Lane 1=neg PCR control; Lane 2=neg So; Lane 3=So; Lane 4=neg W1; Lane 5=W1, Lane 6=neg W2, Lane 7=W2, Lane 8=neg W3, Lane 9=W3; Lane 10=neg CA, Lane 11=CA.

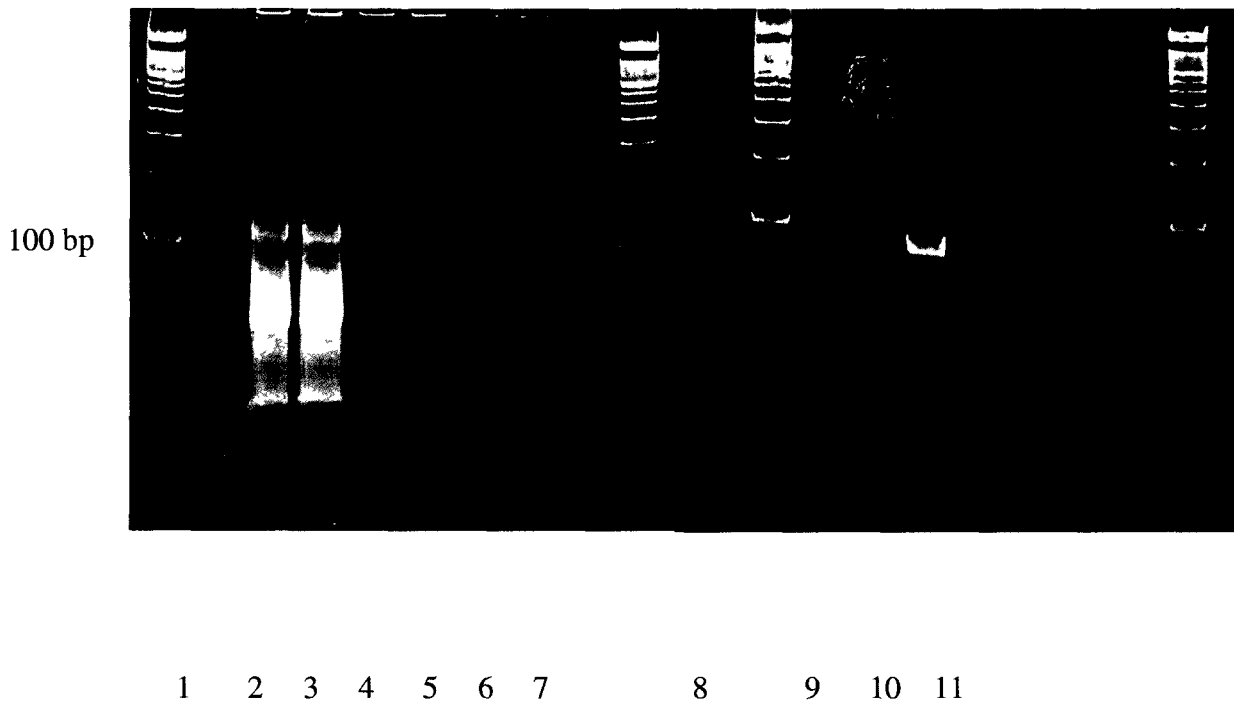


Figure A22- PCR amplification and PAGE of GAS SELEX round 8A

100 bp s. Aptamers and cell mixtures were incubated and fractions collected as in **Figure 3.4**. Lane 1=neg PCR control; Lane 2=neg So; Lane 3=So; Lane 4=neg W1; Lane 5=W1, Lane 6=neg W2, Lane 7=W2, Lane 8=neg W3, Lane 9=W3; Lane 10=neg CA, Lane 11=CA.

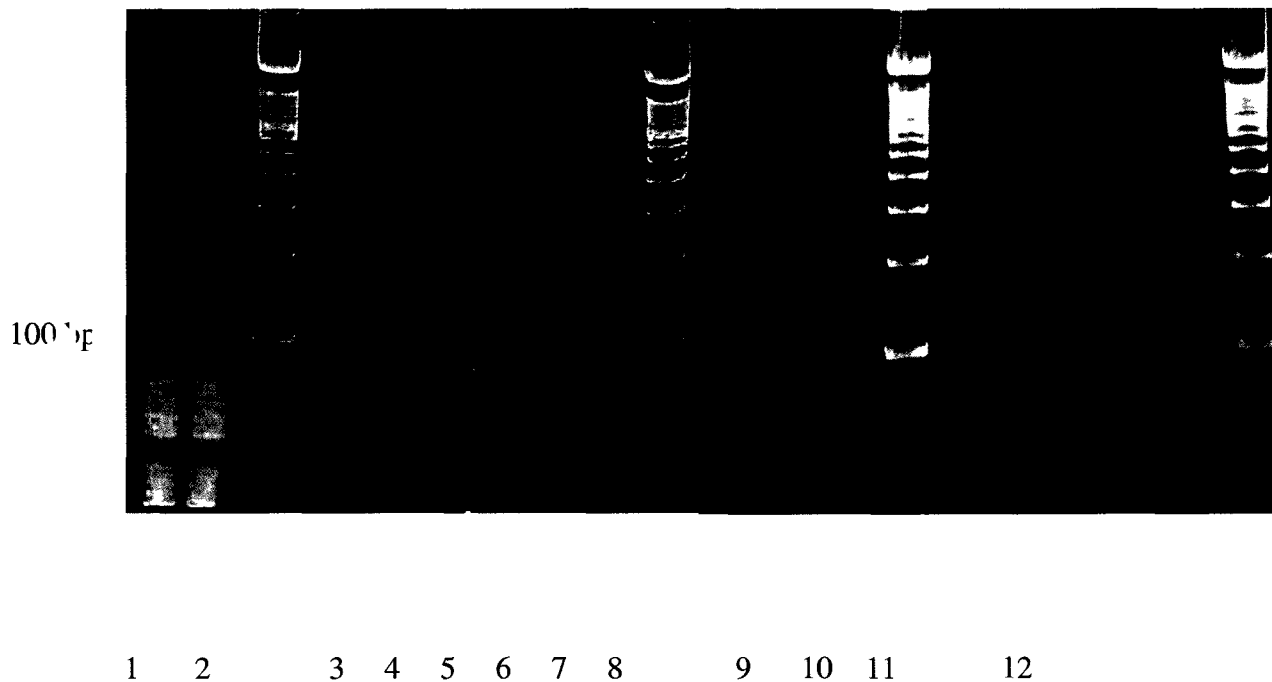


Figure A23- PCR amplification and PAGE of GAS SELEX round 8B

fractions. Aptamers and cell mixtures were incubated and fractions collected as in **Figure 3.4**. Lane 1=neg So; Lane 2=So; Lane 3=neg W1; Lane 4=W1, Lane 5=neg W2, Lane 6=W2, Lane 7=neg W3, Lane 8=W3, Lane 9=neg W4, Lane 10=W4; Lane 11=neg CA, Lane 12=CA.

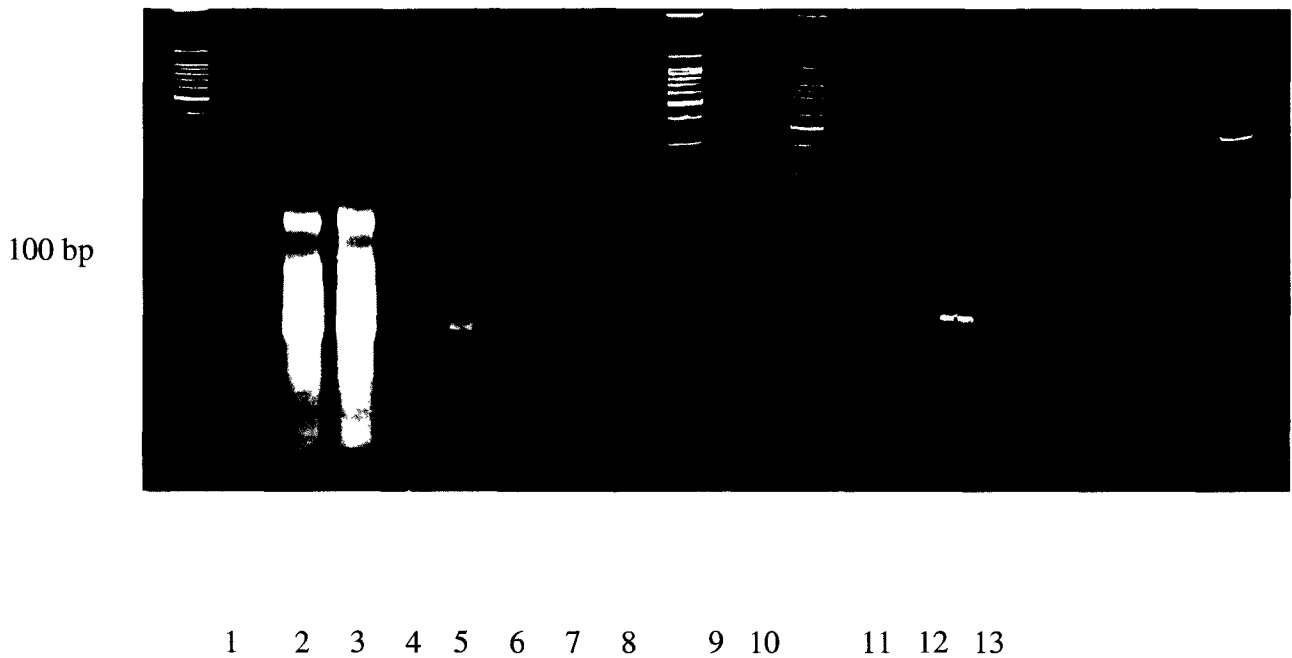


Figure A24- PCR amplification and PAGE of GAS SELEX round 9A

100 bp is. Aptamers and cell mixtures were incubated and fractions collected as in **Figure 3.4**. Lane 1=neg PCR control; Lane 2=neg So; Lane 3=So; Lane 4=neg W1; Lane 5=W1, Lane 6=neg W2, Lane 7=W2, Lane 8=neg W3, Lane 9=W3, Lane 10=neg W4, Lane 11=W4; Lane 12=neg CA, Lane 13=CA.

100 bp

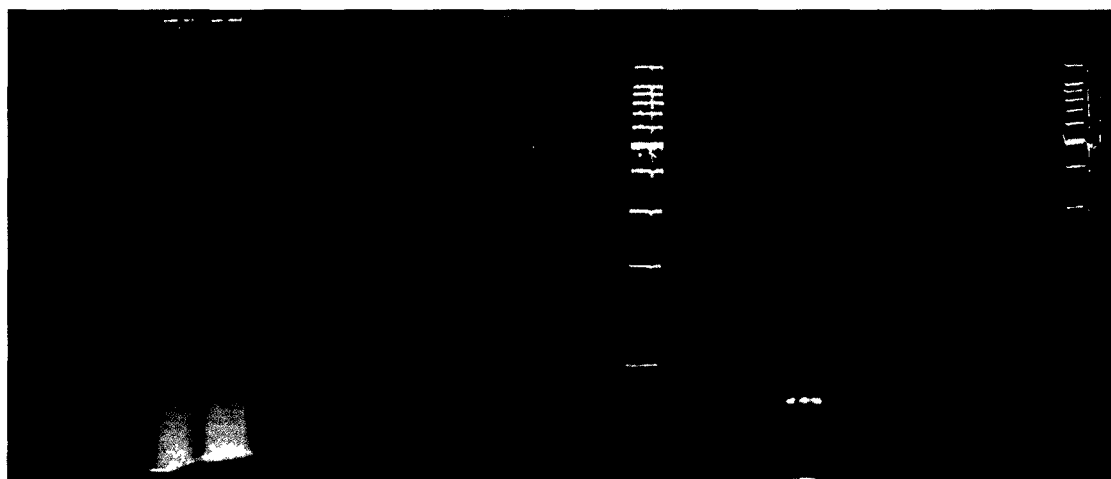


1 2 3 4 5 6 7 8 9 10 11 12 13

Figure A25- PCR amplification and PAGE of GAS SELEX round 9B

fractions. Aptamers and cell mixtures were incubated and fractions collected as in **Figure 3.4**. Lane 1=neg PCR control; Lane 2=neg So; Lane 3=So; Lane 4=neg W1; Lane 5=W1, Lane 6=neg W2, Lane 7=W2, Lane 8=neg W3, Lane 9=W3, Lane 10=neg W4, Lane 11=W4; Lane 12=neg CA, Lane 13=CA.

100 bp



1 2 3 4 5 6 7 8 9 10 11

Figure A26- PCR amplification and PAGE of GAS SELEX round 10A

fractions. Aptamers and cell mixtures were incubated and fractions collected as in **Figure 3.4**. Lane 1=neg PCR control; Lane 2=neg So; Lane 3=So; Lane 4=neg W1; Lane 5=W1, Lane 6=neg W2, Lane 7=W2, Lane 8=neg W3, Lane 9=W3; Lane 10=neg CA, Lane 11=CA.

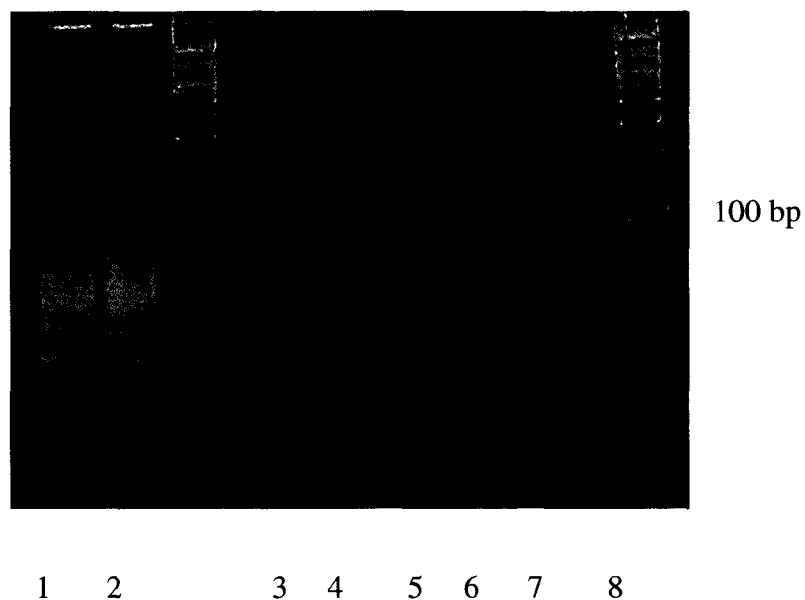


Figure A27- PCR amplification and PAGE of GAS SELEX round 10B

fractions. Aptamers and cell mixtures were incubated and fractions collected as in **Figure 3.4**. Lane 1=neg So; Lane 2=So; Lane 3=neg W1; Lane 4=W1, Lane 5=neg W2, Lane 6=W2, Lane 7=neg CA, Lane 8=CA.

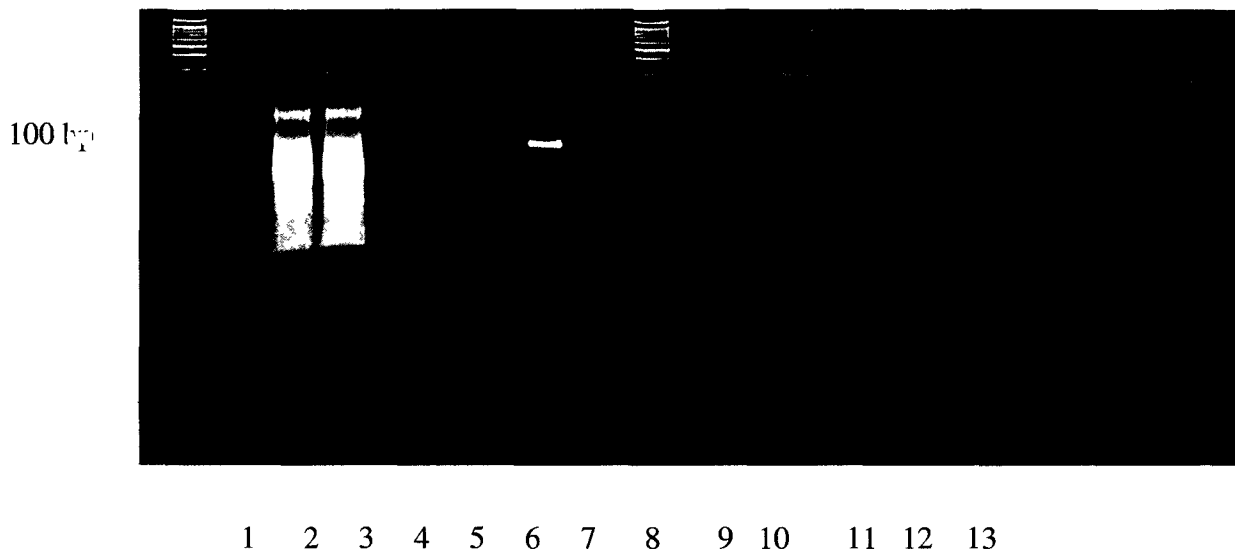


Figure A28- PCR amplification and PAGE of GAS SELEX round 11A

fractions. Aptamers and cell mixtures were incubated and fractions collected as in **Figure 3.4**. Lane 1=neg PCR control; Lane 2=neg So; Lane 3=So; Lane 4=neg W1; Lane 5=W1, Lane 6=neg W2, Lane 7=W2, Lane 8=neg W3, Lane 9=W3, Lane 10=neg W4, Lane 11=W4; Lane 12=neg CA, Lane 13=CA.

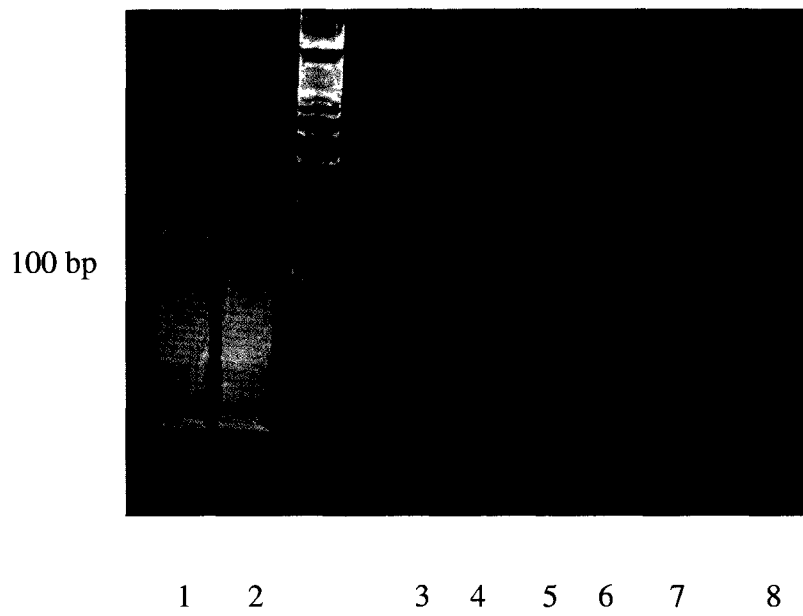


Figure A29- PCR amplification and PAGE of GAS SELEX round 11B

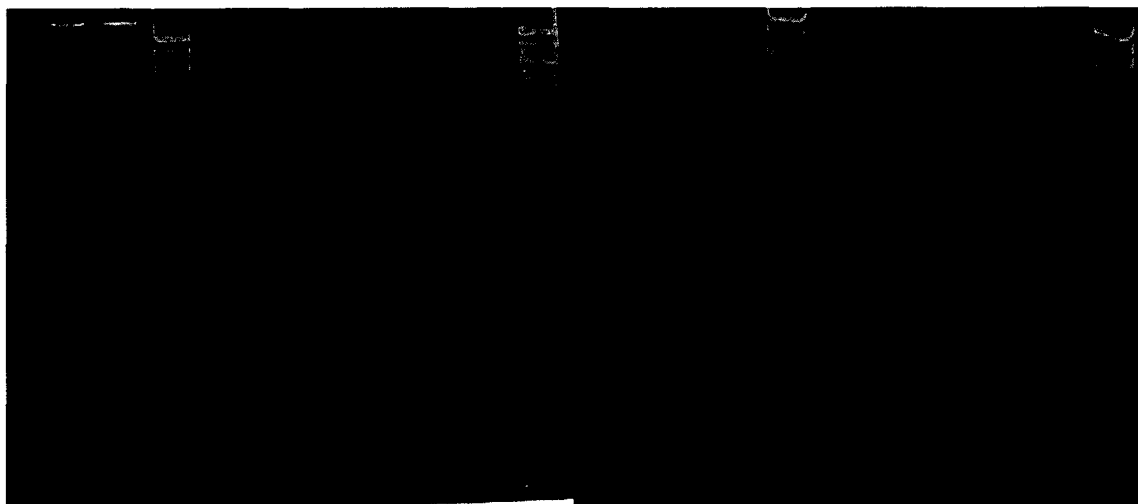
fractions. Aptamers and cell mixtures were incubated and fractions collected as in **Figure 3.4**. Lane 1=neg So; Lane 2=So; Lane 3=neg W1; Lane 4=W1, Lane 5=neg W2, Lane 6=W2; Lane 7=neg CA; Lane 8=CA.



Figure A30-PCR amplification and PAGE of GAS SELEX round 12A

fractions. Aptamers and cell mixtures were incubated and fractions collected as in **Figure 3.4**. Lane 1=neg PCR control; Lane 2=neg So; Lane 3=So; Lane 4=neg W1; Lane 5=W1, Lane 6=neg W2, Lane 7=W2, Lane 8=neg W3, Lane 9=W3, Lane 10=neg W4, Lane 11=W4; Lane 12=neg CA, Lane 13=CA.

100 bp



1 2 3 4 5 6 7 8 9 10 11 12

Figure A31- PCR amplification and PAGE of GAS SELEX round 12B

fractions. Aptamers and cell mixtures were incubated and fractions collected as in **Figure 3.4**. Lane 1=neg So; Lane 2=So; Lane 3=neg W1; Lane 4=W1, Lane 5=neg W2, Lane 6=W2, Lane 7=neg W3, Lane 8=W3, Lane 9=neg W4, Lane 10=W4; Lane 11=neg CA, Lane 12=CA.

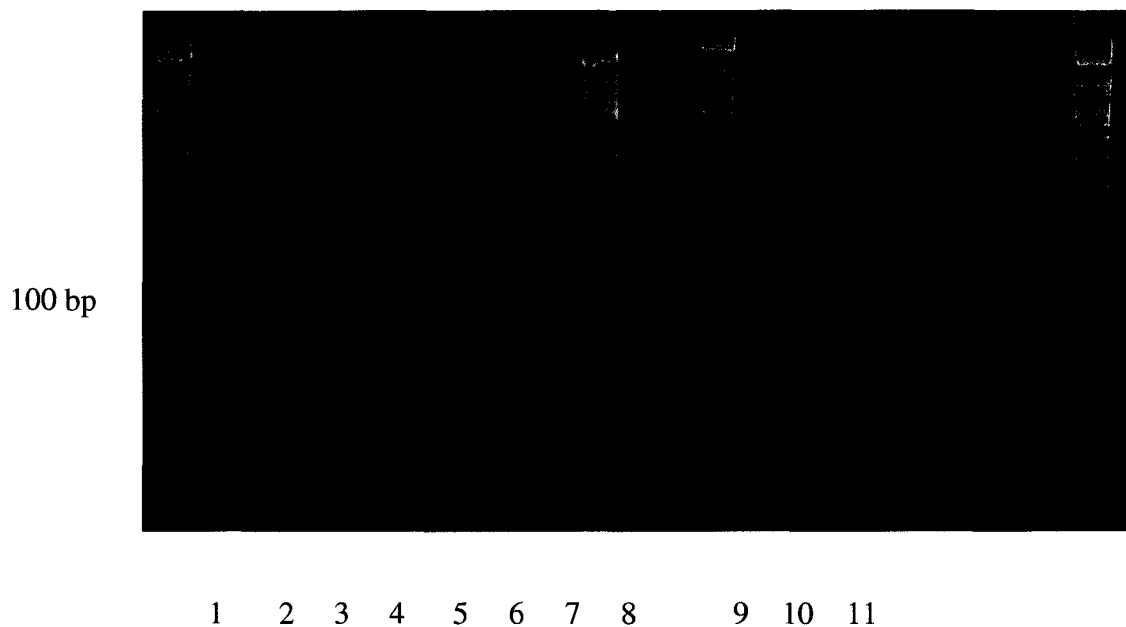


Figure A32- PCR amplification and PAGE of GAS SELEX round 13A

fractions. Aptamers and cell mixtures were incubated and fractions collected as in **Figure 3.4**. Lane 1=neg PCR control; Lane 2=neg So; Lane 3=So; Lane 4=neg W1; Lane 5=W1, Lane 6=neg W2, Lane 7=W2, Lane 8=neg W3, Lane 9=W3; Lane 10=neg CA; Lane 11=CA.

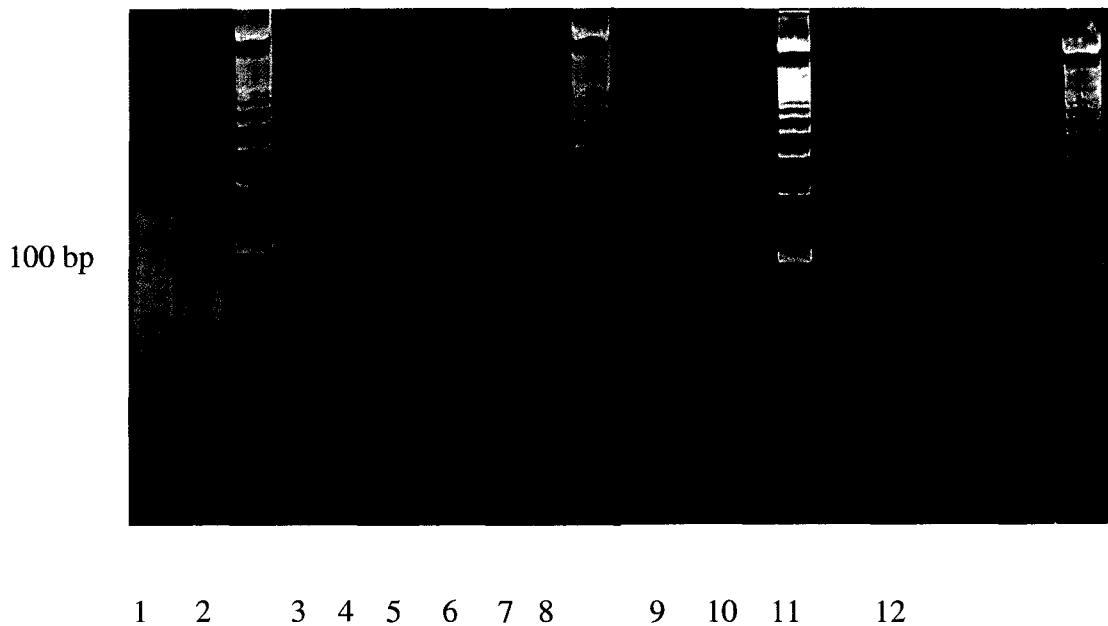
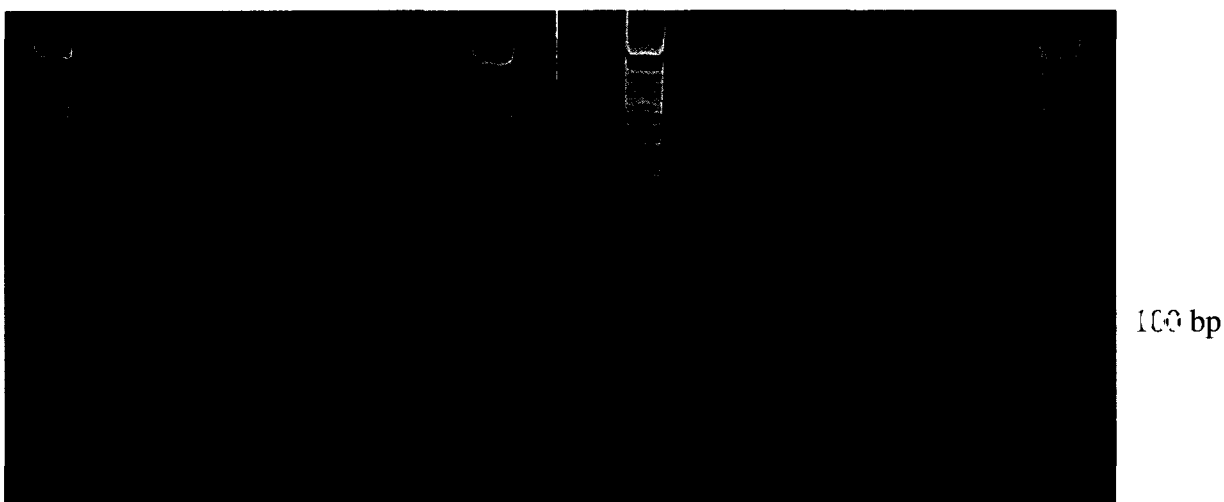


Figure A33- PCR amplification and PAGE of GAS SELEX round 13B

fractions. Aptamers and cell mixtures were incubated and fractions collected as in **Figure 3.4**. Lane 1=neg So; Lane 2=So; Lane 3=neg W1; Lane 4=W1, Lane 5=neg W2, Lane 6=W2, Lane 7=neg W3, Lane 8=W3, Lane 9=neg W4, Lane 10=W4; Lane 11=neg CA, Lane 12=CA.

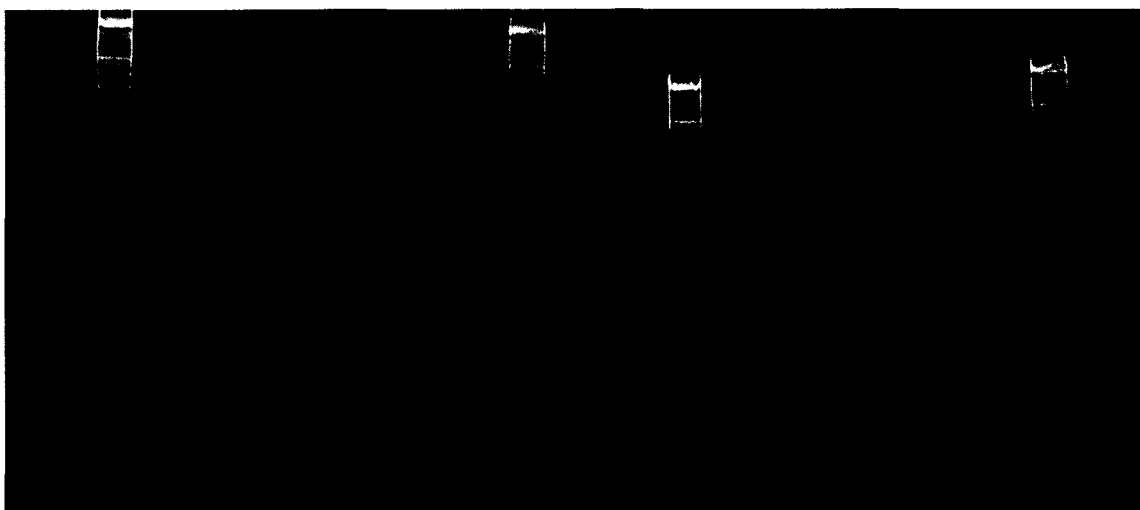


1 2 3 4 5 6 7 8 9 10 11 12 13

Figure A34- PCR amplification and PAGE of GAS SELEX round 14A

fractions. Aptamers and cell mixtures were incubated and fractions collected as in **Figure 3.4**. Lane 1=neg PCR control; Lane 2=neg So; Lane 3=So; Lane 4=neg W1; Lane 5=W1, Lane 6=neg W2, Lane 7=W2, Lane 8=neg W3, Lane 9=W3, Lane 10=neg W4, Lane 11=W4; Lane 12=neg CA, Lane 13=CA.

100 bp

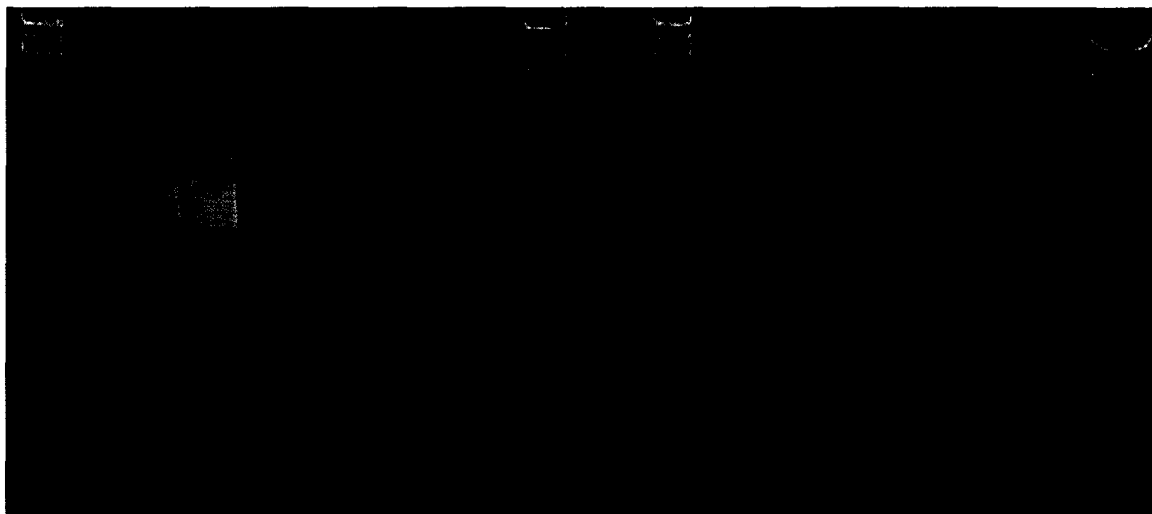


1 2 3 4 5 6 7 8 9 10 11

Figure A35- PCR amplification and PAGE of GAS SELEX round 15A

fractions. Aptamers and cell mixtures were incubated and fractions collected as in **Figure 3.4**. Lane 1=neg PCR control; Lane 2=neg So; Lane 3=So; Lane 4=neg W1; Lane 5=W1, Lane 6=neg W2, Lane 7=W2, Lane 8=neg W3, Lane 9=W3; Lane 10=neg CA, Lane 11=CA.

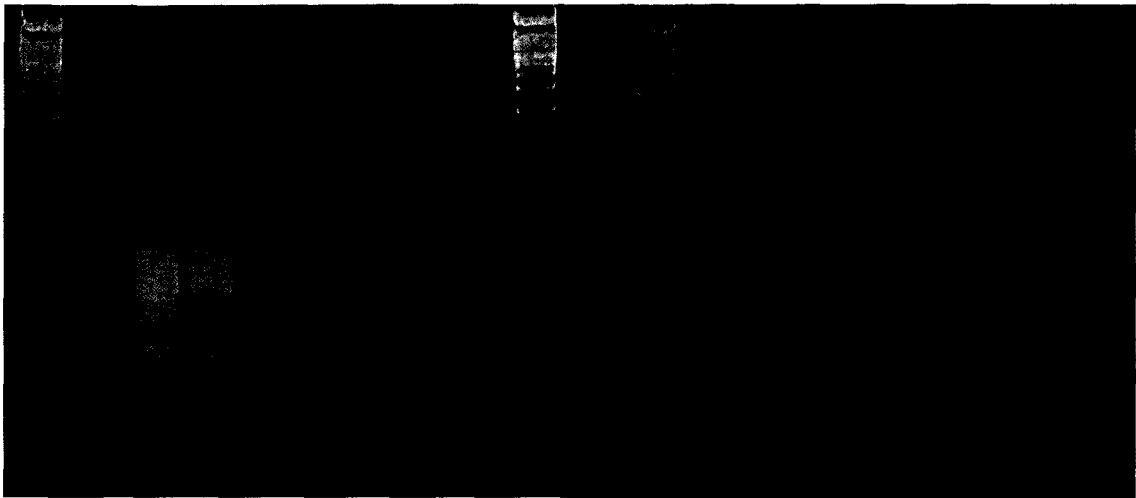
100 bp



1 2 3 4 5 6 7 8 9 10 11

Figure A36- PCR amplification and PAGE of GAS SELEX round 16A

fractions. Aptamers and cell mixtures were incubated and fractions collected as in **Figure 3.4**. Lane 1=neg PCR control; Lane 2=neg So; Lane 3=So; Lane 4=neg W1; Lane 5=W1, Lane 6=neg W2, Lane 7=W2, Lane 8=neg W3, Lane 9=W3; Lane 10=neg CA, Lane 11=CA.

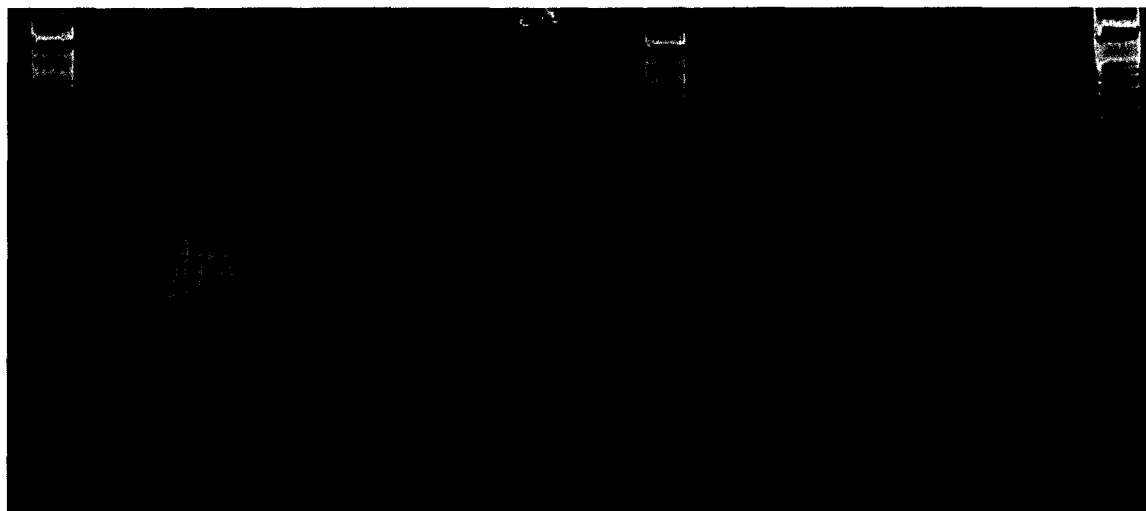


1 2 3 4 5 6 7 8 9 10 11

Figure A37- PCR amplification and PAGE of GAS SELEX round 17A

fractions. Aptamers and cell mixtures were incubated and fractions collected as in **Figure 3.4**. Lane 1=neg PCR control; Lane 2=neg So; Lane 3=So; Lane 4=neg W1; Lane 5=W1, Lane 6=neg W2, Lane 7=W2, Lane 8=neg W3, Lane 9=W3; Lane 10=neg CA, Lane 11=CA.

100 bp



1 2 3 4 5 6 7 8 9 10 11

Figure A38- PCR amplification and PAGE of GAS SELEX round 18A

fractions. Aptamers and cell mixtures were incubated and fractions collected as in **Figure 3.4**. Lane 1=neg PCR control; Lane 2=neg So; Lane 3=So; Lane 4=neg W1; Lane 5=W1, Lane 6=neg W2, Lane 7=W2, Lane 8=neg W3, Lane 9=W3; Lane 10=neg CA, Lane 11=CA.

100 bp

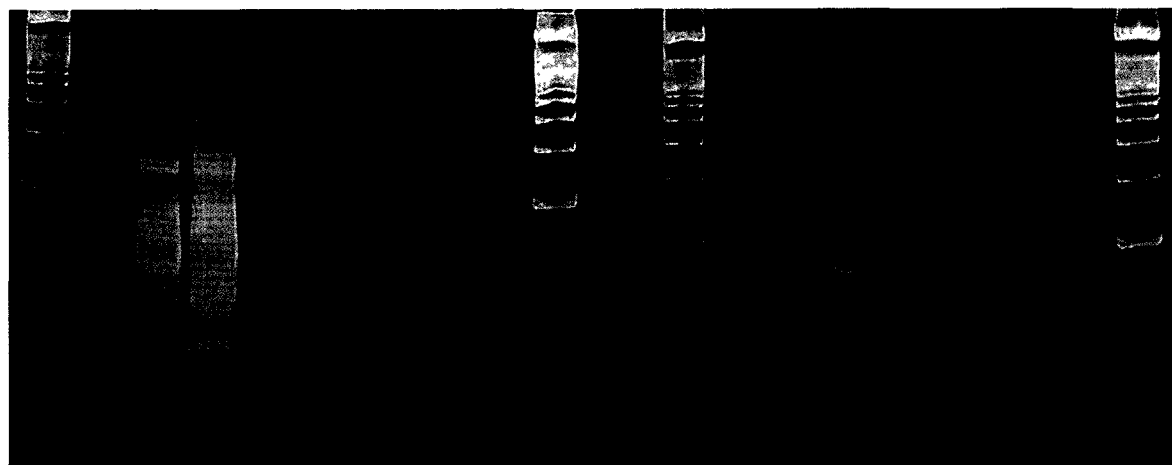


1 2 3 4 5 6 7 8 9 10 11

Figure A39- PCR amplification and PAGE of GAS SELEX round 19A

fractions. Aptamers and cell mixtures were incubated and fractions collected as in **Figure 3.4**. Lane 1=neg PCR control; Lane 2=neg So; Lane 3=So; Lane 4=neg W1; Lane 5=W1, Lane 6=neg W2, Lane 7=W2, Lane 8=neg W3, Lane 9=W3; Lane 10=neg CA, Lane 11=CA.

100 bp

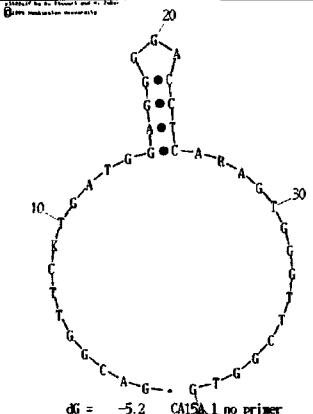
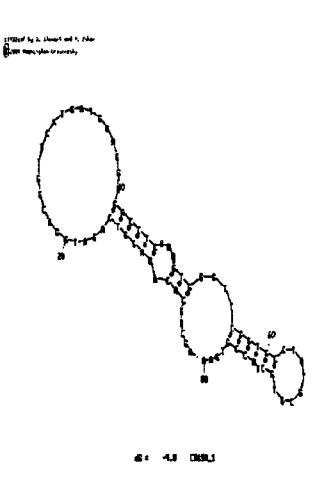
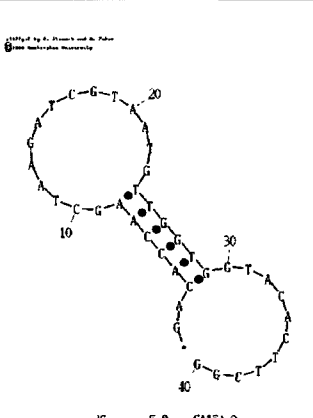


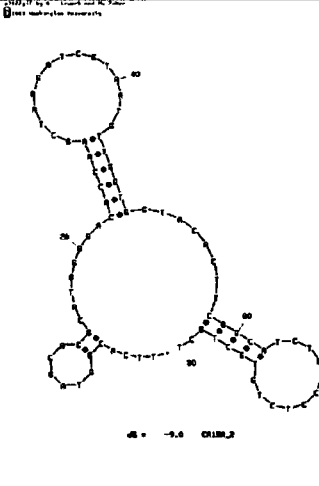
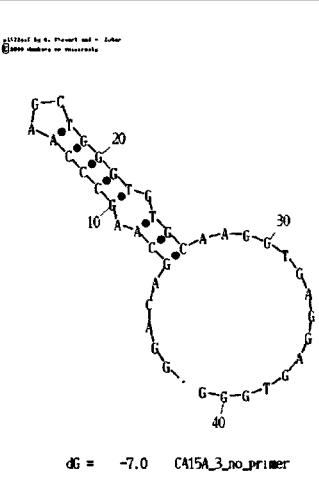
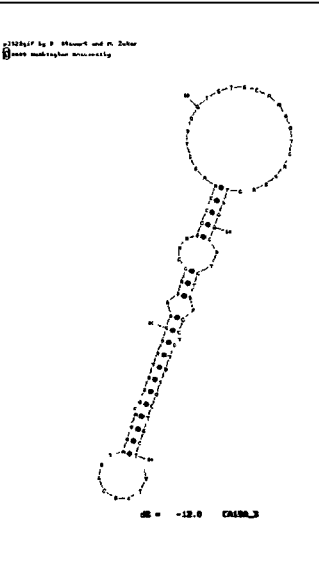
1 2 3 4 5 6 7 8 9 10 11

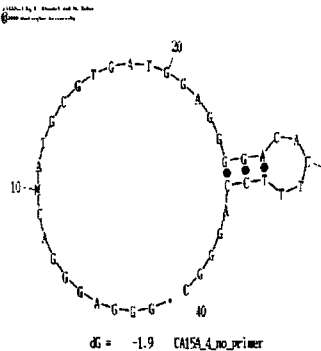
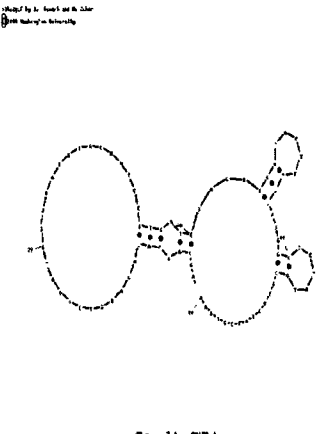
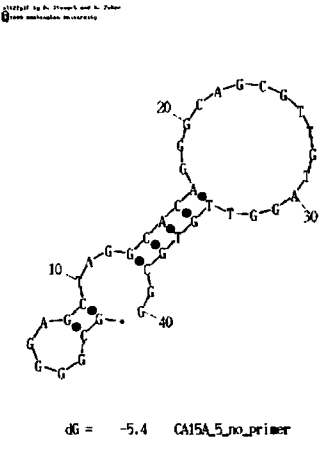
Figure A40-PCR amplification and PAGE of GAS SELEX round 20A

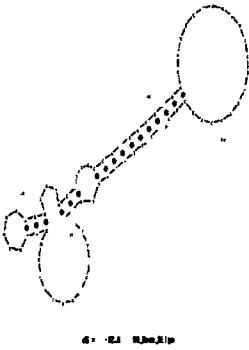
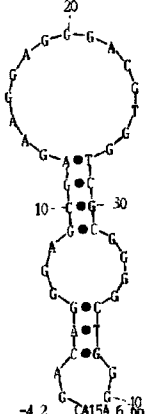
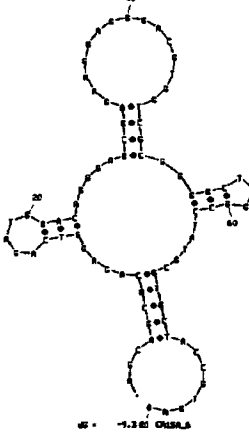
fractions. Aptamers and cell mixtures were incubated and fractions collected as in **Figure 3.4**. Lane 1=neg PCR control; Lane 2=neg So; Lane 3=So; Lane 4=neg W1; Lane 5=W1, Lane 6=neg W2, Lane 7=W2, Lane 8=neg W3, Lane 9=W3; Lane 10=neg CA, Lane 11=CA.

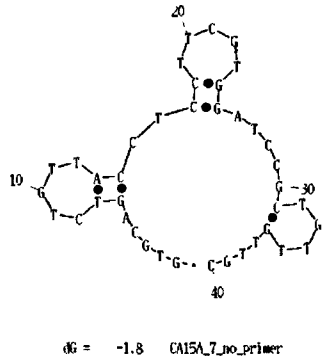
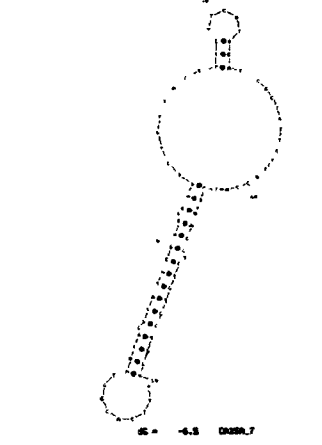
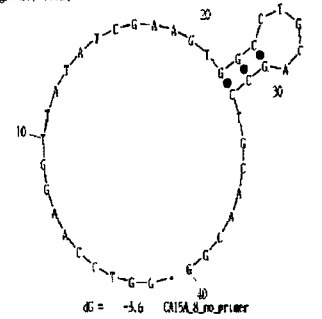
Table A2. Sequences and most likely secondary structures of aptamers from SELEX 15A.

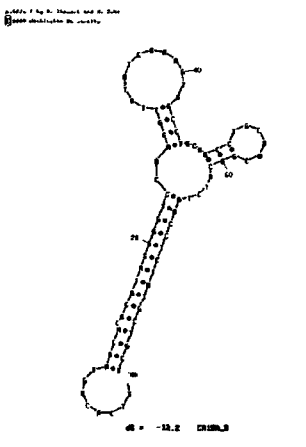
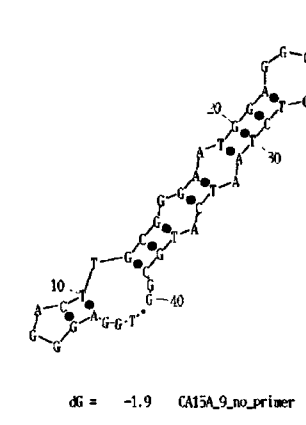
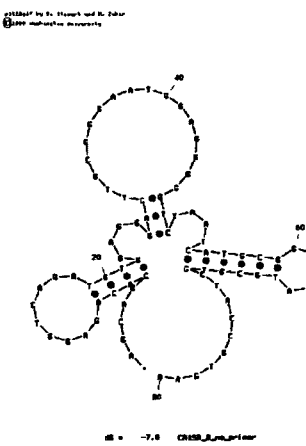
Name	Sequence	Structure	ΔG (kcal/mol)
15A 1	<p>5'-GAC GGT TCK TGA TGG AGG GGA CCT CAR AGT GGG TTC GGT G -3'</p>		-5.2
15A1P	<p>5'-AGC AGC ACA GAG GTC AGA TG GAC GGT TCK TGA TGG AGG GGA CCT CAR AGT GGG TTC GGT G CCT ATG CGT GCT ACC GTG AA-3'</p>		-9.8
15A2	<p>5'-GAC ACC AAG CTA AGA TCG TAA TGT TGG TGG TAC ACT TCG G -3'</p>		-5.2

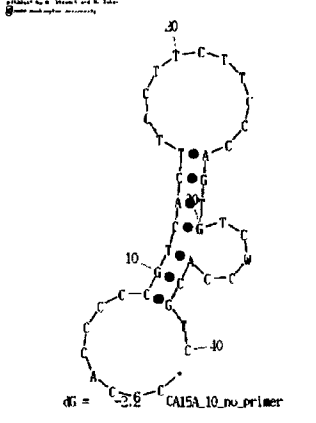
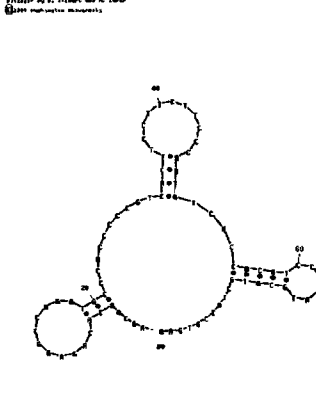
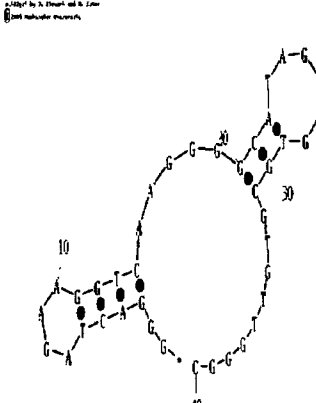
Name	Sequence	Structure	ΔG (kcal/mol)
15A2P	5'-TTC ACG GTA GCA CGC ATA GG GAC ACC AAG CTA AGA TCG TAA TGT TGG TGG TAC ACT TCG G CAT CTG ACC TCT GTG CTG CT-3'		-9.0
15A3	5'- GAC AGC AAG CCC AAG CTG GGT GTG CAA GGT GAG GAG TGG G -3'		-7.0
15A3P	5'-TTC ACG GTA GCA CGC ATA GG GAC AGC AAG CCC AAG CTG GGT GTG CAA GGT GAG GAG TGG G CAT CTG ACC TCT GTG CTG CT-3'		-12.0

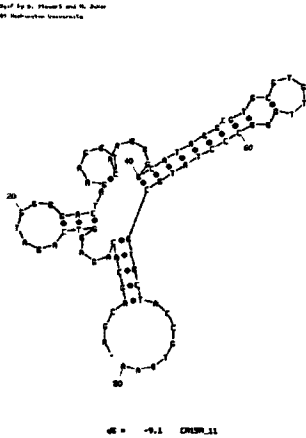
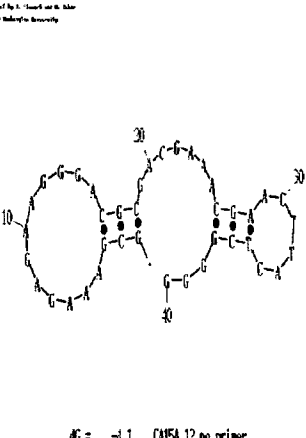
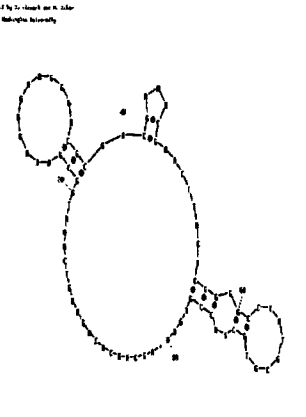
Name	Sequence	Structure	ΔG (kcal/mol)
15A4	<p>5'- GGG AGG GAC MAT GCG TGA TGG AGG GGA CAC TTT CCA GGG C -3'</p>	 <p>$\Delta G = -1.9$ CA15A_4_no_primer</p>	-1.9
15A4P	<p>5'-AGC AGC ACA GAG GTC AGA TG GGG AGG GAC MAT GCG TGA TGG AGG GGA CAC TTT CCA GGG C CCT ATG CGT GCT ACC GTG AA-3'</p>	 <p>$\Delta G = -3.1$ ORU4</p>	-3.1
15A5	<p>5'- GCG GGG AGC TAG GCA CAG GGC AGC GTT GTA GGT TGT GCG G -3'</p>	 <p>$\Delta G = -5.4$ CA15A_5_no_primer</p>	-5.4

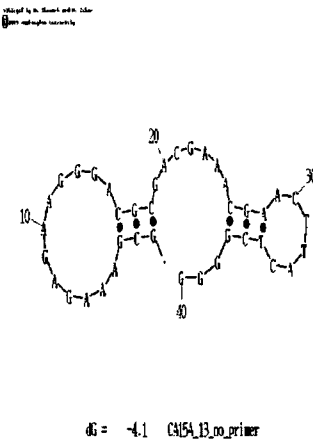
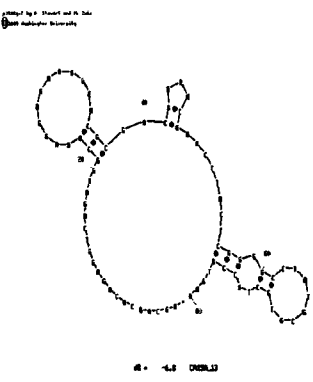
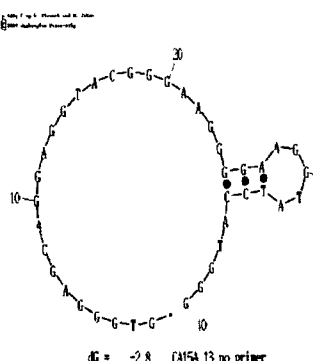
Name	Sequence	Structure	ΔG (kcal/mol)
15A5P	5'-TTC ACG GTA GCA CGC ATA GG GCG GGG AGC TAG GCA CAG GGC AGC GTT GTA GGT TGT GCG G CAT CTG ACC TCT GTG CTG CT-3'		-12.6
15A6	5'- GAC AGG GAG CGA GAA GGA GGG ACG TGG TCG CGG GGC TGG G -3'		-4.6
15A6P	5'-AGC AGC ACA GAG GTC AGA TG GAC AGG GAG CGA GAA GGA GGG ACG TGG TCG CGG GGC TGG G CCT ATG CGT GCT ACC GTG AA-3'		-9.3

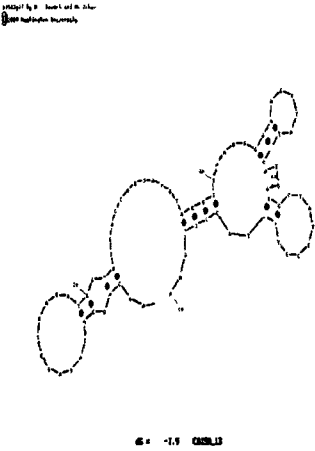
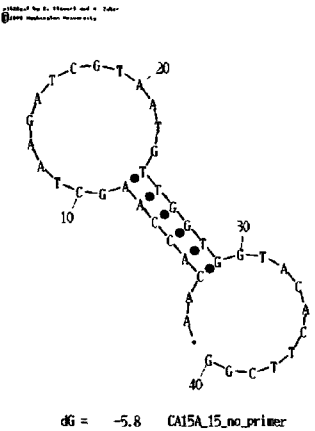
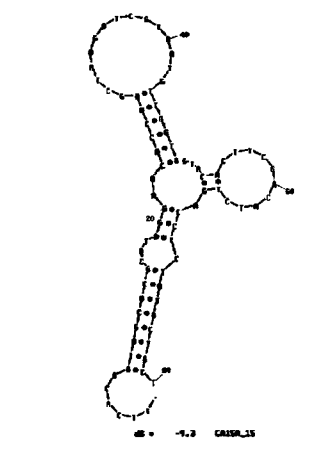
Name	Sequence	Structure	ΔG (kcal/mol)
15A7	5'- GTG CAG TCT GTT ACC TCC TTC GTG GAT CCG CTG TTG TTG C -3'		-1.8
15A7P	5'-TTC ACG GTA GCA CGC ATA GG GTG CAG TCT GTT ACC TCC TTC GTG GAT CCG CTG TTG TTG C CAT CTG ACC TCT GTG CTG CT-3'		-6.5
15A8	5'- GGT CCA AGG TTA TAT CGA AGT GGC CTG CAG CCT GCA ACG G -3'		-3.6

Name	Sequence	Structure	ΔG (kcal/mol)
15A8P	5'-TTC ACG GTA GCA CGC ATA GG GGT CCA AGG TTA TAT CGA AGT GGC CTG CAG CCT GCA ACG G CAT CTG ACC TCT GTG CTG CT-3'		-12.2
15A9	5'- TGG AGG GAC TTG CGG GAA TGG AGG GGG TCT AAT CAT GCG G -3'		-1.9
15A9P	5'-AGC AGC ACA GAG GTC AGA TG TGG AGG GAC TTG CGG GAA TGG AGG GGG TCT AAT CAT GCG G CCT ATG CGT GCT ACC GTG AA-3'		-7.0

Name	Sequence	Structure	ΔG (kcal/mol)
15A10	5'- CCC ACC CCC GTC ACT TCC TTC TTC CCA GTG TCW CCA CGT C-3'		-2.2
15A10P	5'-AGC AGC ACA GAG GTC AGA TG CCC ACC CCC GTC ACT TCC TTC TTC CCA GTG TCW CCA CGT C CCT ATG CGT GCT ACC GTG AA-3'		-7.1
15A11	5'-GCC AGT ATG TAT CTC AGT CCC CCC CCC CAC CTT CTC TG-3'		-3.9

Name	Sequence	Structure	ΔG (kcal/mol)
15A11P	5'-AGC AGC ACA GAG GTC AGA TG GCC AGT ATG TAT CTC AGT CCC CCC CCC CAC CTT CTC TG CCT ATG CGT GCT ACC GTG AA-3'		-9.1
15A12	5'- GGG ACT AGA AGG TCA AGG GGC ATA GGC GTG CGT GTT GGG C -3'		-4.1
15A12P	5'-AGC AGC ACA GAG GTC AGA TG GGG ACT AGA AGG TCA AGG GGC ATA GGC GTG CGT GTT GGG C CCT ATG CGT GCT ACC GTG AA-3'		-6.8

Name	Sequence	Structure	ΔG (kcal/mol)
15A13	<p>5'- GCG AAA GAG AAG GGA CGC GAC GAA ACG AAC TTA CTC GGG G -3'</p>		-4.1
15A13P	<p>5'-AGC AGC ACA GAG GTC AGA TG GCG AAA GAG AAG GGA CGC GAC GAA ACG AAC TTA CTC GGG G CCT ATG CGT GCT ACC GTG AA-3'</p>		-6.8
15A14	<p>5'- GTG GGA GCA GGA GGT ACG GGA AGG GGA AGG TAT CCA TGG G -3'</p>		-2.8

Name	Sequence	Structure	ΔG (kcal/mol)
15A14P	5'-AGC AGC ACA GAG GTC AGA TG GTG GGA GCA GGA GGT ACG GGA AGG GGA AGG TAT CCA TGG G CCT ATG CGT GCT ACC GTG AA-3'		-7.9
15A15	5'- AAC ACC AAG CTA AGA TCG TAA TGT TGG TGG TAC ACT TCG G -3'		-5.8
15A15P	5'-TTC ACG GTA GCA CGC ATA GG AAC ACC AAG CTA AGA TCG TAA TGT TGG TGG TAC ACT TCG G CAT CTG ACC TCT GTG CTG CT-3'		-9.3

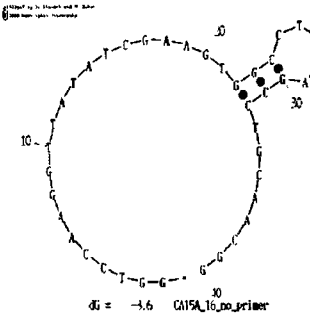
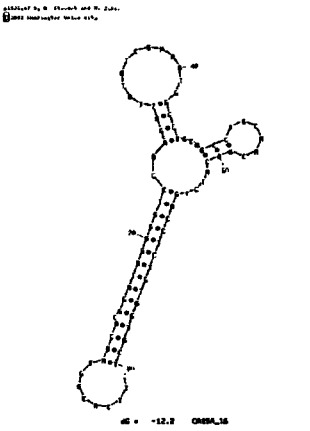
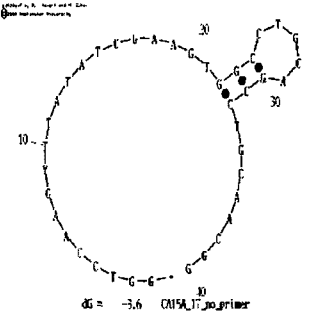
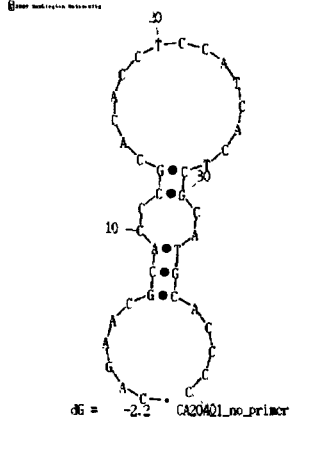
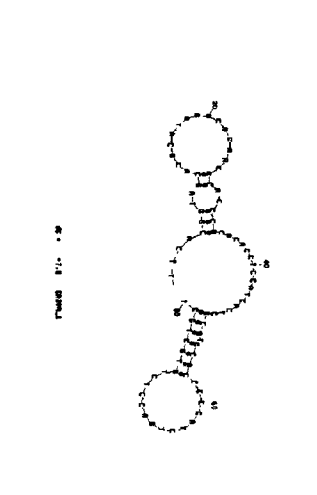
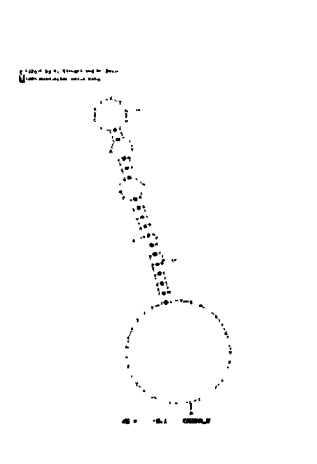
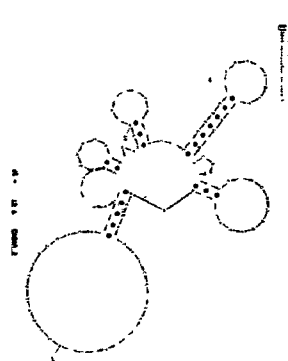
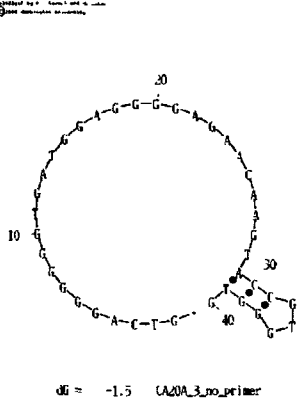
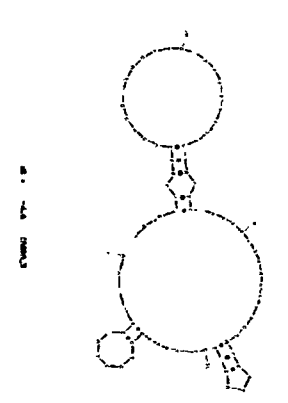
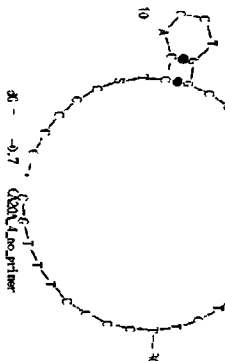
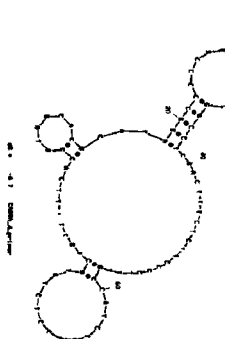
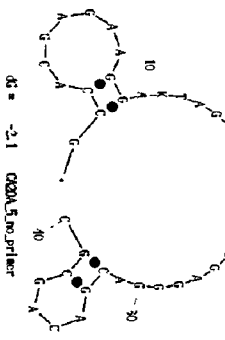
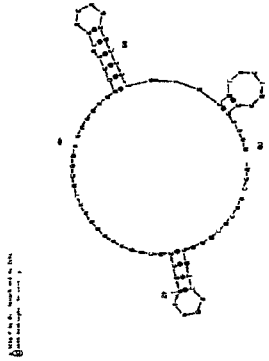
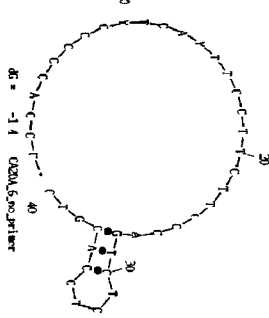
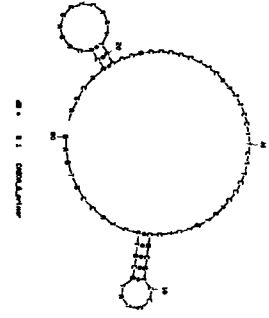
Name	Sequence	Structure	ΔG (kcal/mol)
15A16	<p>5'- GGT CCA AGG TTA TAT CGA AGT GGC CTG CAG CCT GCA ACG G -3'</p>		-3.6
15A16P	<p>5'-TTC ACG GTA GCA CGC ATA GG GGT CCA AGG TTA TAT CGA AGT GGC CTG CAG CCT GCA ACG G CAT CTG ACC TCT GTG CTG CT-3'</p>		-12.2
15A17	<p>5'- GGT CCA AGY TTA TAT CGA AGT GGC CTG CAG CCT GCA ACG G -3'</p>		-3.6

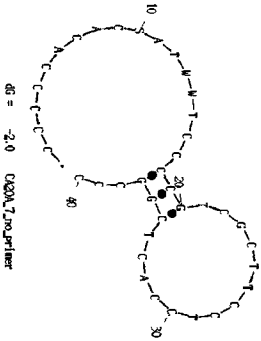
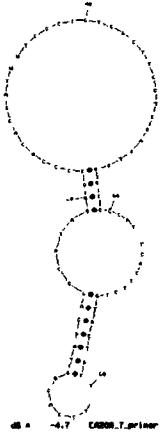
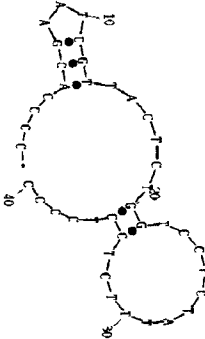
Table A3. Sequences and predicted structures of aptamers from SELEX 20A pool.

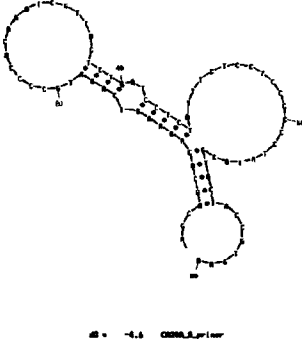
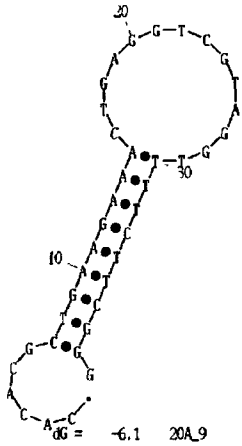
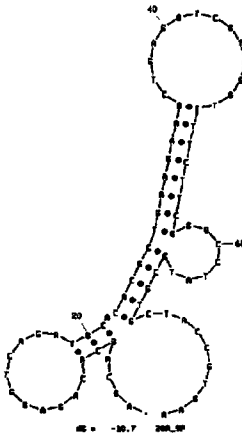
Name	Sequence	Structure	ΔG (kcal/mol)
20A 1	<p>5'-CAG AAC GCA CCC GCA CAC CTC CAT CAC TCG CAT GCA CCC C -3'</p>		-2.2
20A1P	<p>5'-TTC ACG GTA GCA CGC ATA GG CAG AAC GCA CCC GCA CAC CTC CAT CAC TCG CAT GCA CCC C CAT CTG ACC TCT GTG CTG CT-3'</p>		-7.8
20A2	<p>5'-CAT CTG ACC TCT GTG CTG CTA GTT CAC GGT AGC ACG CAT AGG CCC ACC AAA CTA CGC CAA GCA CTC ACC CCC TTC TCC CGC C -3'</p>		-8.1

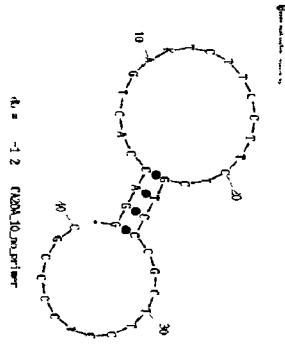
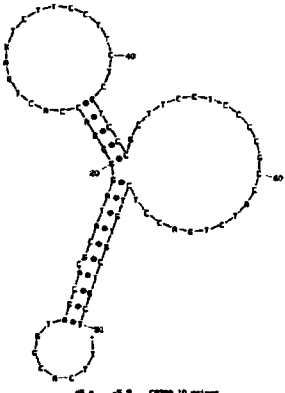
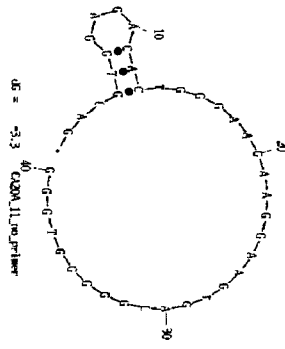
Name	Sequence	Structure	ΔG (kcal/mol)
20A2P	5'-TTC ACG GTA GCA CGC ATA GG CAT CTG ACC TCT GTG CTG CTA GTT CAC GGT AGC ACG CAT AGG CCC ACC AAA CTA CGC CAA GCA CTC ACC CCC TTC TCC CGC C CAT CTG ACC TCT GTG CTG CT-3'		-12.6
20A3	5'-GTC AGG GGG GTG ATG GAG GGG AGA ACA AGT ACC GTG GGT G -3'		-1.5
20A3P	5'-AGC AGC ACA GAG GTC AGA TG GTC AGG GGG GTG ATG GAG GGG AGA ACA AGT ACC GTG GGT G CCT ATG CGT GCT ACC GTG AA-3'		-4.6

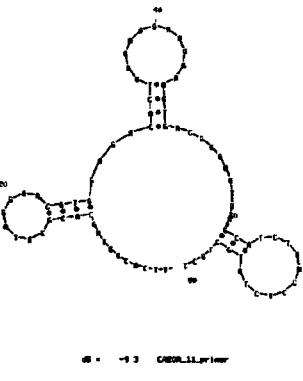
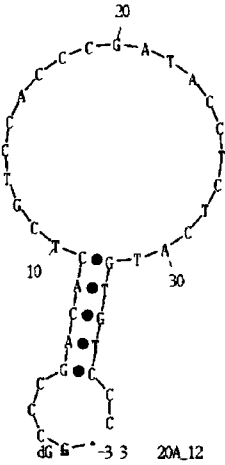
Name	Sequence	Structure	ΔG (kcal/mol)
20A4	5'- CCC CCS TCC ACC TGG CCT CGA CTT TCT CTT CCC CTT TGC -3'		-0.7
20A4P	5'-TTC ACG GTA GCA CGC ATA GG CCC CCS TCC ACC TGG CCT CGA CTT TCT CTT CCC CTT TGC CAT CTG ACC TCT GTG CTG CT-3'		-6.7
20A5	5'- GCC ACG AGA AGG AKT AGG AAG AGA GGA GGG ACG ACA GCG C -3'		-2.1

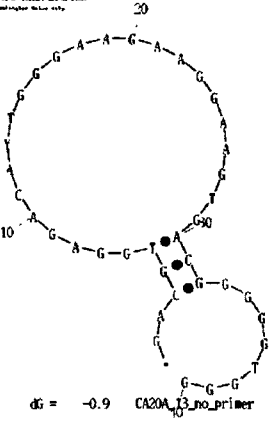
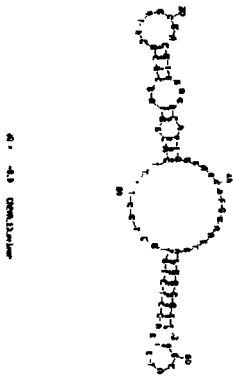
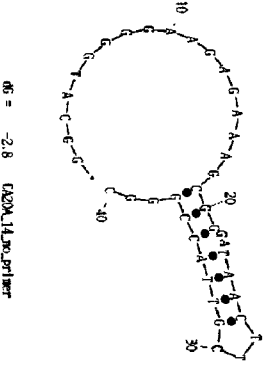
Name	Sequence	Structure	ΔG (kcal/mol)
20A5P	5'-AGC AGC ACA GAG GTC AGA TG GCC ACG AGA AGG AKT AGG AAG AGA GGA GGG ACG ACA GCG C CCT ATG CGT GCT ACC GTG AA-3'		-7.1
20A6	5'- CCC ACC CCC YTC AYT TCC TTC TTC CCA GTG TCT CCA CGT C -3'		-1.4
20A6P	5'-AGC AGC ACA GAG GTC AGA TG CCC ACC CCC YTC AYT TCC TTC TTC CCA GTG TCT CCA CGT C CCT ATG CGT GCT ACC GTG AA-3'		-5.1

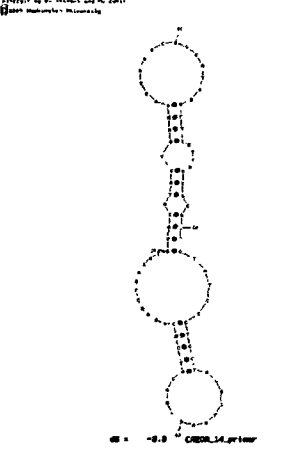
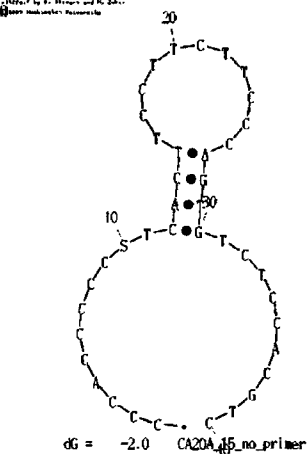
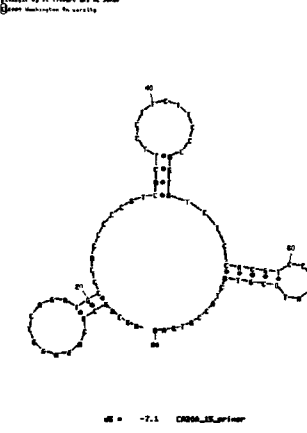
Name	Sequence	Structure	ΔG (kcal/mol)
20A7	5'- CCC CCA CAC SAT WWT CCC CGT CGC TTC CTC CAC TCG GCC C -3'		-2.0
20A7P	5'-TTC ACG GTA GCA CGC ATA GG CCC CCA CAC SAT WWT CCC CGT CGC TTC CTC CAC TCG GCC C CAT CTG ACC TCT GTG CTG CT-3'		-4.7
20A8	5'- CCC CAC GAA TCG TTA CTC TGG TCC TCT ATT TCT CCT CCC C -3'		-1.2

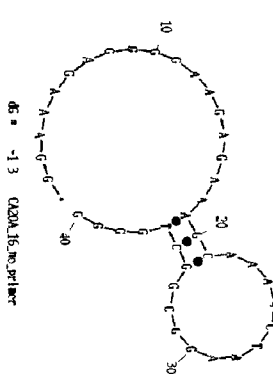
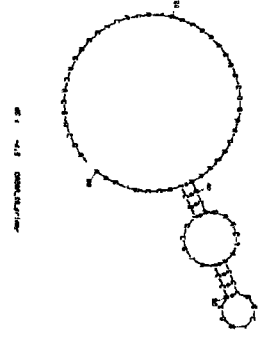
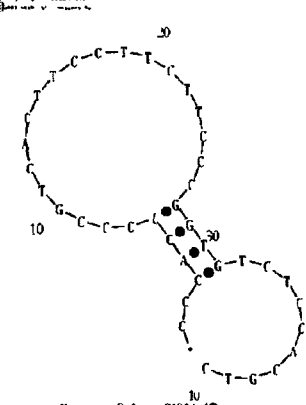
Name	Sequence	Structure	ΔG (kcal/mol)
20A8P	5'-AGC AGC ACA GAG GTC AGA TG CCC CAC GAA TCG TTA CTC TGG TCC TCT ATT TCT CCT CCC C CCT ATG CGT GCT ACC GTG AA-3'		-6.6
20A9	5'- CAC ACG CT GAA GAA ACT GAG GTC GTA GGT TTT CTT CGG G -3'		-6.1
20A9P	5'-AGC AGC ACA GAG GTC AGA TG CAC ACG CT GAA GAA ACT GAG GTC GTA GGT TTT CTT CGG G CCT ATG CGT GCT ACC GTG AA-3'		-10.7

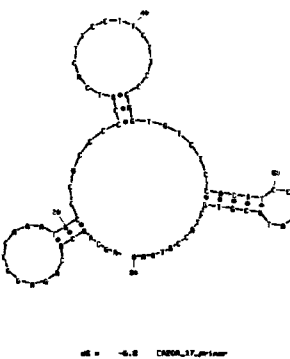
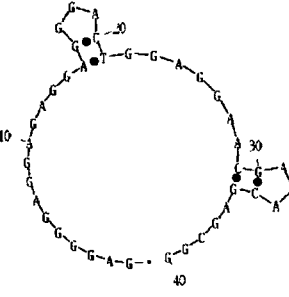
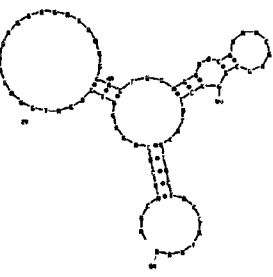
Name	Sequence	Structure	ΔG (kcal/mol)
20A10	<p>5'-GGA CCA CTG AKT CTT CCT TCT CGT CCC GCT TCC TCC CCG C -3'</p>		-1.2
20A10P	<p>5'-TTC ACG GTA GCA CGC ATA GG GGA CCA CTG AKT CTT CCT TCT CGT CCC GCT TCC TCC CCG C CAT CTG ACC TCT GTG CTG CT-3'</p>		-5.9
20A11	<p>5'-GAC GTG GAG ACA CTG GGA AGA AGG AAG TGA CGG GGG TGG G -3'</p>		-3.3

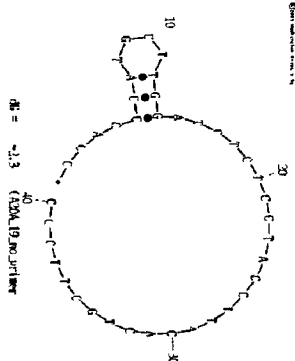
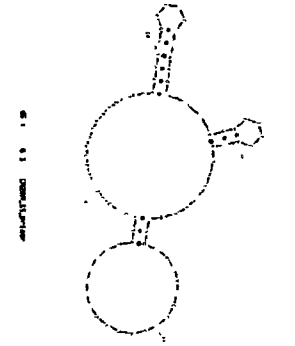
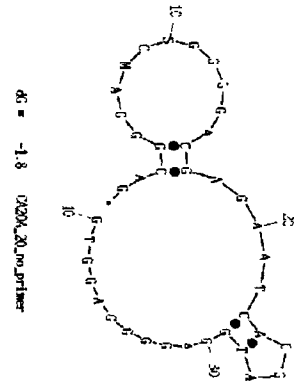
Name	Sequence	Structure	ΔG (kcal/mol)
20A11P	5'-TTC ACG GTA GCA CGC ATA GG GAC GTG GAG ACA CTG GGA AGA AGG AAG TGA CGG GGG TGG G CAT CTG ACC TCT GTG CTG CT-3'		-9.3
20A12	5'-GCC CGA CAC TC GT CCA CCC GAT ACC TCT CAT GTG TCC C-3'		-3.3
20A12P	5'-TTC ACG GTA GCA CGC ATA GG GCC CGA CAC TC GT CCA CCC GAT ACC TCT CAT GTG TCC C CAT CTG ACC TCT GTG CTG CT-3'		-7.2

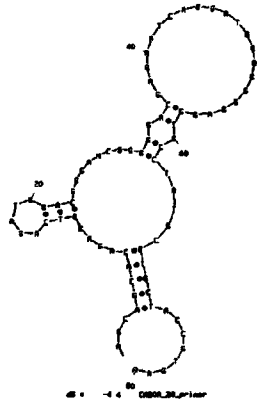
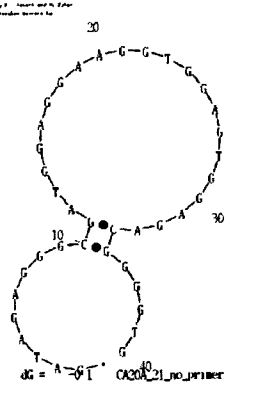
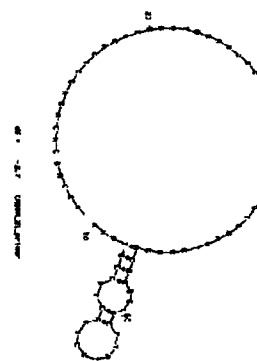
Name	Sequence	Structure	ΔG (kcal/mol)
20A13	5'- GAC GTG GAG ACA YTG GGA AGA AGG AAG TGA CGG GGG TGG G -3'		-0.9
20A13P	5'-TTC ACG GTA GCA CGC ATA GG GAC GTG GAG ACA YTG GGA AGA AGG AAG TGA CGG GGG TGG G CAT CTG ACC TCT GTG CTG CT-3'		-8.9
20A14	5'-GGC ATG GGG AAG AGA AAG CGG GAT AAC TTC GTT ACC GGG C -3'		-2.8

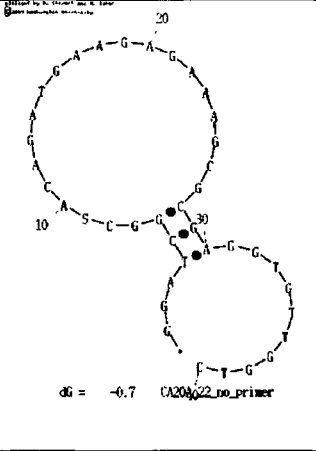
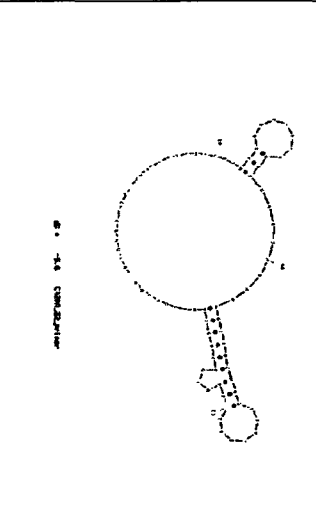
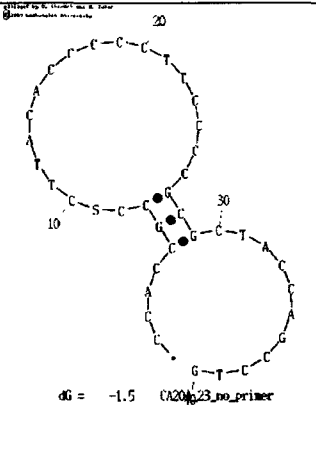
Name	Sequence	Structure	ΔG (kcal/mol)
20A14P	5'-AGC AGC ACA GAG GTC AGA TG GGC ATG GGG AAG AGA AAG CGG GAT AAC TTC GTT ACC GGG C CCT ATG CGT GCT ACC GTG AA-3'		-8.8
20A15	5'-CCC ACC CCC STC ACT TCC TTC TTC CCA GTG TCT CCA CGT C-3'		-2.0
20A15P	5'-AGC AGC ACA GAG GTC AGA TG CCC ACC CCC STC ACT TCC TTC TTC CCA GTG TCT CCA CGT C CCT ATG CGT GCT ACC GTG AA-3'		-7.1

Name	Sequence	Structure	ΔG (kcal/mol)
20A16	<p>5'- GGA AAG AGG GGA AGA GAA AGC AAA ACT AAG GCG GCT GGG G-3'</p>		-1.3
20A16P	<p>5'-AGC AGC ACA GAG GTC AGA TG GGA AAG AGG GGA AGA GAA AGC AAA ACT AAG GCG GCT GGG G CCT ATG CGT GCT ACC GTG AA-3'</p>		-4.5
20A17	<p>5'-CCC ACC CCC GTC ACT TCC TTC TTC CCG GTG TCT CCA CGT C-3'</p>		-2.1

Name	Sequence	Structure	ΔG (kcal/mol)
20A17P	5'-AGC AGC ACA GAG GTC AGA TG CCC ACC CCC GTC ACT TCC TTC TTC CCG GTG TCT CCA CGT C CCT ATG CGT GCT ACC GTG AA-3'	 <p style="text-align: center;">dG = -6.8 20A17P_primer</p>	-6.8
20A18	5'-GAG GGG AGG AGA GGA GGG ACT GGA GGA ACG AAA CGA GCG G-3'	 <p style="text-align: center;">dG = -2.2 20A18_primer</p>	-2.2
20A18P	5'-AGC AGC ACA GAG GTC AGA TG GAG GGG AGG AGA GGA GGG ACT GGA GGA ACG AAA CGA GCG G CCT ATG CGT GCT ACC GTG AA-3'	 <p style="text-align: center;">dG = -5.1 20A18P_primer</p>	-5.1

Name	Sequence	Structure	ΔG (kcal/mol)
20A19	<p>5'-CCA CCC ATG CTT GGA TCT CTC CTA CCT TAC ACT GCT TCC C -3'</p>		-2.3
20A19P	<p>5'-TTC ACG GTA GCA CGC ATA GG CCA CCC ATG CTT GGA TCT CTC CTA CCT TAC ACT GCT TCC C CAT CTG ACC TCT GTG CTG CT-3'</p>		-6.1
20A20	<p>5'-GAC GGG AMC SGG GGA CGA GAA TCA GGA TGG AGG GGA GGT G-3'</p>		-1.8

Name	Sequence	Structure	ΔG (kcal/mol)
20A20P	5'-AGC AGC ACA GAG GTC AGA TG GAC GGG AMC SGG GGA CGA GAA TCA GGA TGG AGG GGA GGT G CCT ATG CGT GCT ACC GTG AA-3'		-4.4
20A21	5'-GAT AGA GGG CGA TGG AGG AAG GTG GAG TGG AGA CGG GGT G -3'		-0.1
20A21P	5'-AGC AGC ACA GAG GTC AGA TG GAT AGA GGG CGA TGG AGG AAG GTG GAG TGG AGA CGG GGT G CCT ATG CGT GCT ACC GTG AA-3'		-3.7

Name	Sequence	Structure	ΔG (kcal/mol)
20A22	<p>5'-GGA TCG GCS ACA GAT GAA GAG AAA GCG CGA GGT GTT GGT-3'</p>		-0.7
20A22P	<p>5'-AGC AGC ACA GAG GTC AGA TG GGA TCG GCS ACA GAT GAA GAG AAA GCG CGA GGT GTT GGT CCT ATG CGT GCT ACC GTG AA-3'</p>		-5.6
20A23	<p>5'-CCA CCG CCS CTT ACA CCC CCT TCC CCG CGC TAC CAG CCT G -3'</p>		-1.5

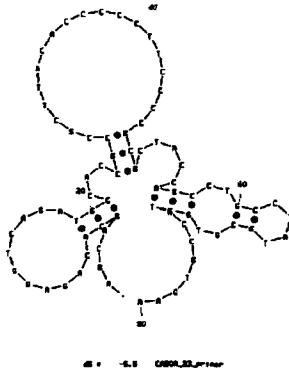
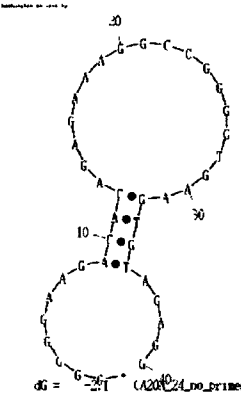
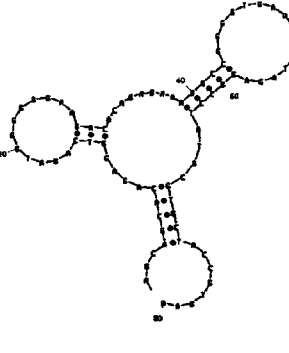
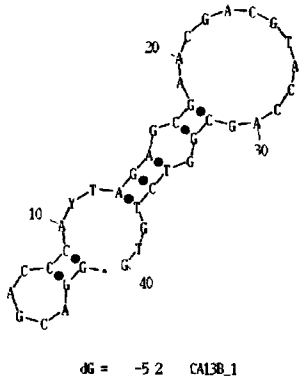
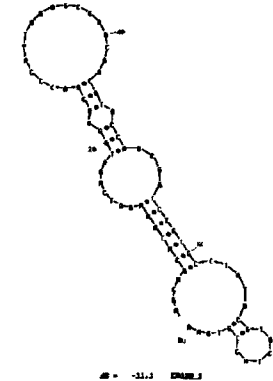
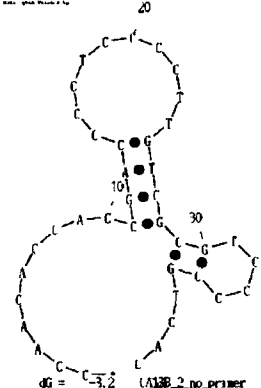
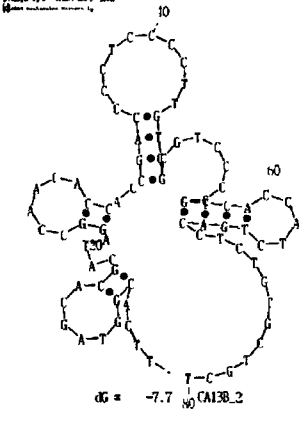
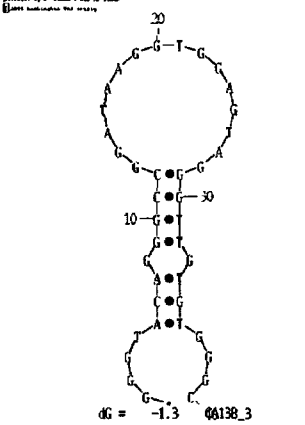
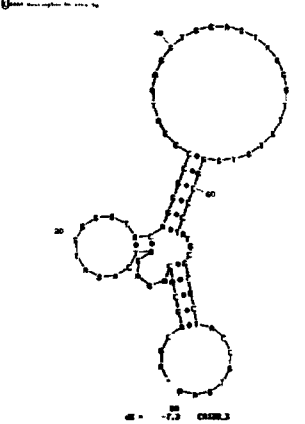
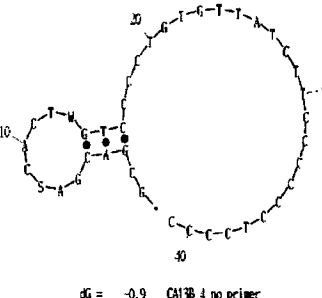
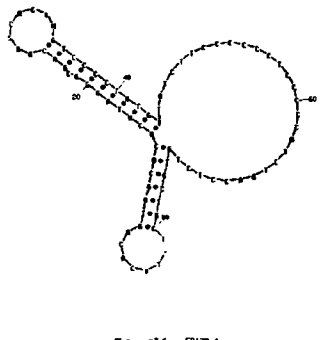
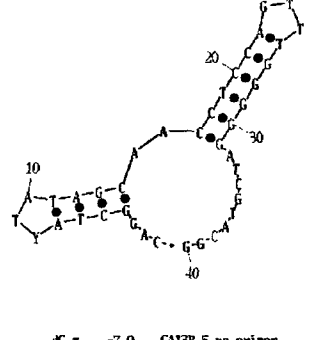
Name	Sequence	Structure	ΔG (kcal/mol)
20A23P	5'-AGC AGC ACA GAG GTC AGA TG CCA CCG CCS CTT ACA CCC CCT TCC CCG CGC TAC CAG CCT G CCT ATG CGT GCT ACC GTG AA-3'		-5.5
20A24	5'-GGG GGA AGA CAC AGA GAA AGG CCG GGG TGA AGT GTA GAG G -3'		-2.1
20A24P	5'-AGC AGC ACA GAG GTC AGA TG GGG GGA AGA CAC AGA GAA AGG CCG GGG TGA AGT GTA GAG GCCT ATG CGT GCT ACC GTG AA-3'		-8.1

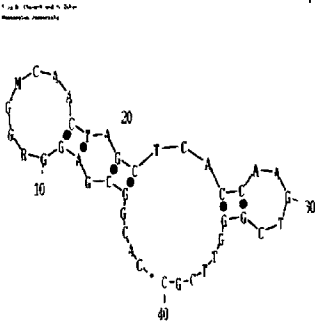
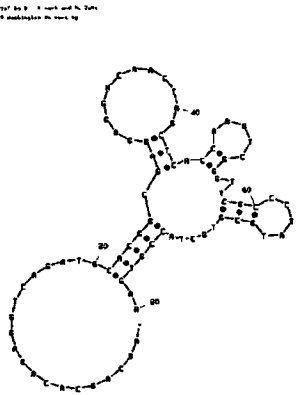
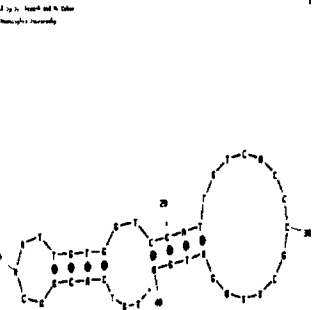
Table A4. Sequences and predicted structures of aptamers from the SELEX

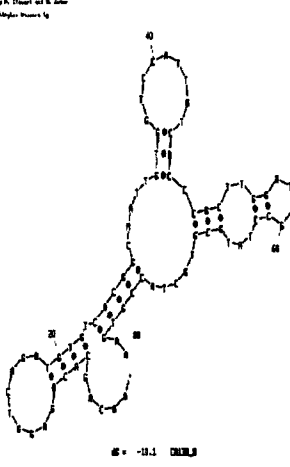
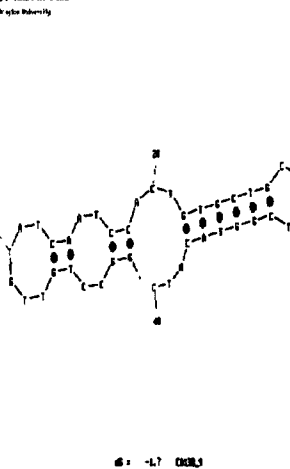
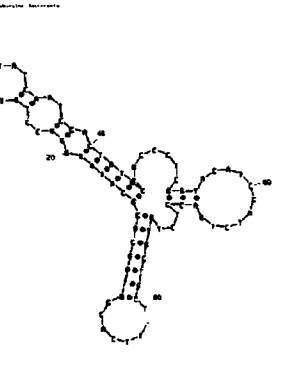
13B pool.

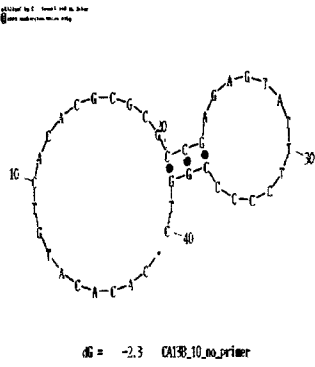
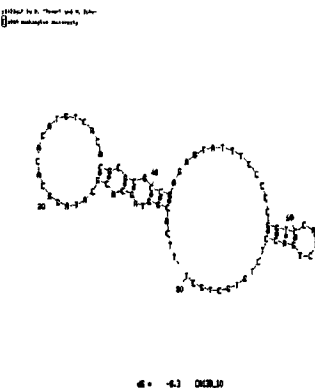
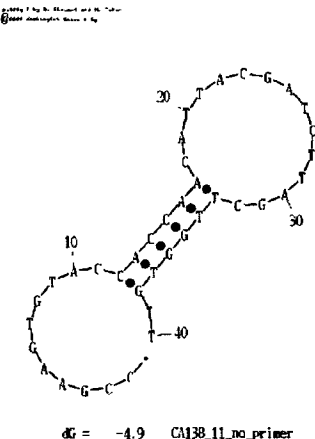
Name	Sequence	Structure	ΔG (kcal/mol)
13B 1	<p>5'-GGA CGA CCC AYT AGA GCG AAC GAC GTA CCA GCG GTC TGTG-3'</p>		-5.2
13B 1P	<p>5'-AGC AGC ACA GAG GTC AGA TG GGA CGA CCC AYT AGA GCG AAC GAC GTA CCA GCG GTC TGTG CCT ATG CGT GCT ACC GTG AA-3'</p>		-11.1
13B 2	<p>5'-CCA ACA CCA CCG ACC CCT CCC CTT GTC GCG TCC CCG TCA C-3'</p>		-3.2

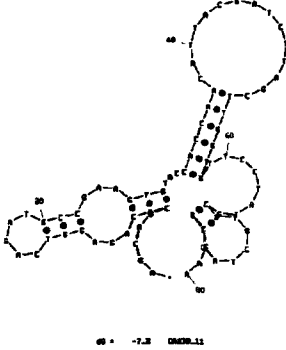
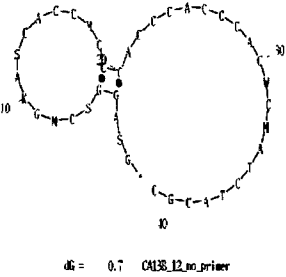
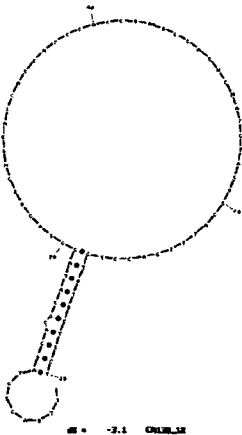
Name	Sequence	Structure	ΔG (kcal/mol)
13B 2P	5'-TTC ACG GTA GCA CGC ATA GG CCA ACA CCA CCG ACC CCT CCC CTT GTC GCG TCC CCG TCA C CAT CTG ACC TCT GTG CTG CT-3'		-7.7
13B 3	5'-GGG TAC AGG GCC GGA TAA GGT GGA GTA GGG TTG TGT GGGC -3'		-1.3
13B 3P	5'- AGC AGC ACA GAG GTC AGA TG GGG TAC AGG GCC GGA TAA GGT GGA GTA GGG TTG TGT GGGC CCT ATG CGT GCT ACC GTG AA-3'		-7.3

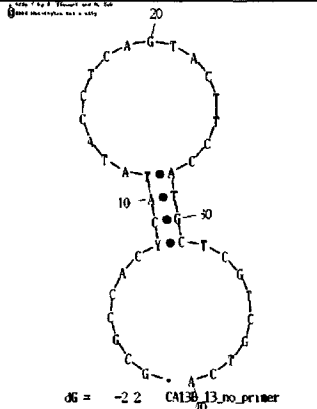
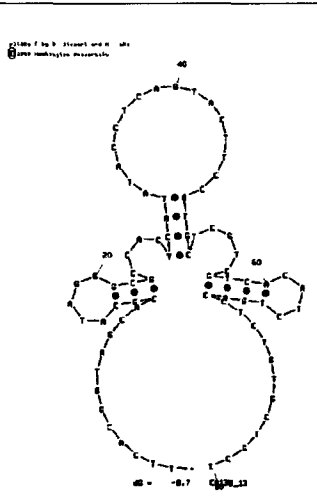
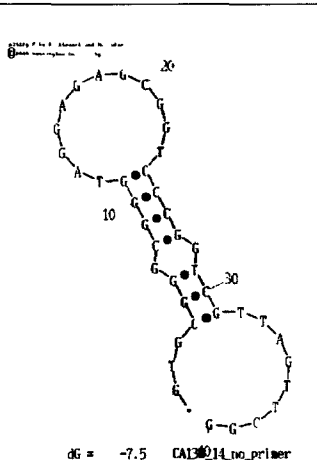
Name	Sequence	Structure	ΔG (kcal/mol)
13B 4	<p>5'-GCG ACG ASC ACT WGT CCC CTG TGT TAT CTT CCC CCC TCCCC-3'</p>		-0.9
13B 4P	<p>5'-TTC ACG GTA GCA CGC ATA GG GCG ACG ASC ACT WGT CCC CTG TGT TAT CTT CCC CCC TCCCC CAT CTG ACC TCT GTG CTG CT-3'</p>		-7.6
13B 5	<p>5'- CAG GCT AYT ATA GCA ACC TCC AGT TTG GGG GAT CGT ACG G-3'</p>		-7.9

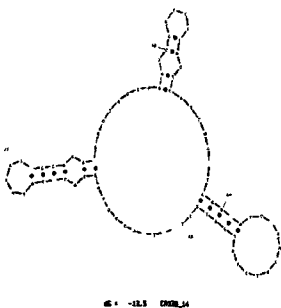
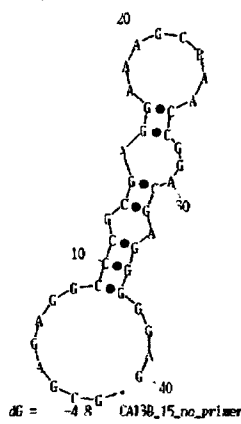
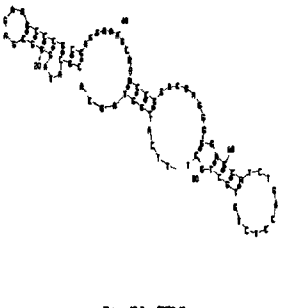
Name	Sequence	Structure	ΔG (kcal/mol)
13B 7	5'-CAC GGC GAG GRG GMC AAC TAG CTC ACC AAG TCG GGT TCG C-3'	 <p>$\Delta G = -3.0$ 13B_7_01_01_01_01_01_01</p>	-3.0
13B 7P	5'-AGC AGC ACA GAG GTC AGA TG CAC GGC GAG GRG GMC AAC TAG CTC ACC AAG TCG GGT TCG C CCT ATG CGT GCT ACC GTG AA-3'	 <p>$\Delta G = -9.1$ 13B_7P_01_01_01_01_01_01</p>	-9.1
13B 8	5'-TGT CAC GGC MAT TGT GGT CCA TTG TCA CCC GCT TGG ATG G-3'	 <p>$\Delta G = -4.1$ 13B_8_01_01_01_01_01_01</p>	-4.1

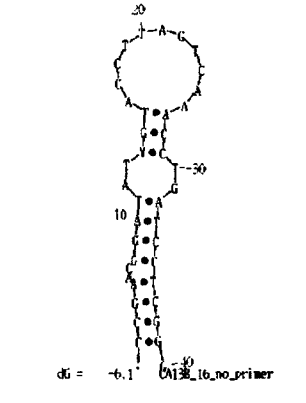
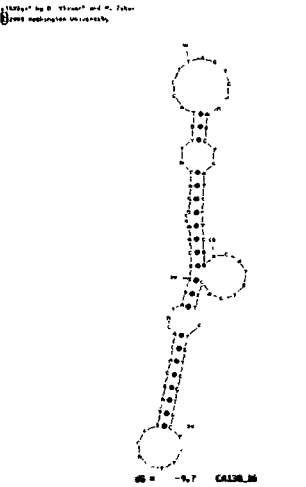
Name	Sequence	Structure	ΔG (kcal/mol)
13B 8P	<p>5'-AGC AGC ACA GAG GTC AGA TG TGT CAC GGC MAT TGT GGT CCA TTG TCA CCC GCT TGG ATG G CCT ATG CGT GCT ACC GTG AA-3'</p>		-10.1
13B 9	<p>5'-GGC CTG TTG TAT CAA TCC ACT GTG CTG CCC TCG GTA CAT C-3'</p>		-1.7
13B 9P	<p>5'-TTC ACG GTA GCA CGC ATA GG GGC CTG TTG TAT CAA TCC ACT GTG CTG CCC TCG GTA CAT C CAT CTG ACC TCT GTG CTG CT-3'</p>		-8.4

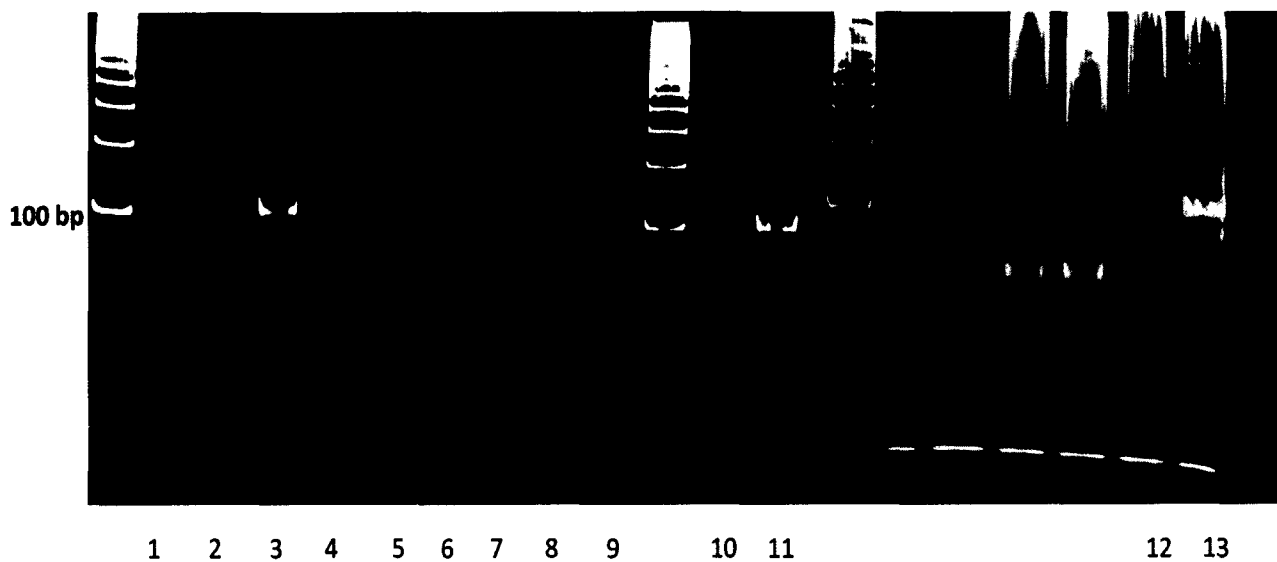
Name	Sequence	Structure	ΔG (kcal/mol)
13B 10	<p>5'-CAC ACA TGT CAC ACG CGC GCC GAG AGT ATT TCC CCC GGT C-3'</p>		-2.3
13B 10P	<p>5'-TTC ACG GTA GCA CGC ATA GG CAC ACA TGT CAC ACG CGC GCC GAG AGT ATT TCC CCC GGT C CAT CTG ACC TCT GTG CTG CT-3'</p>		-8.3
13B 11	<p>5'- CCG AAG TGT ACC ACC AAC ATT ACG ATC TTA GCT TGG TGT T -3'</p>		-4.9

Name	Sequence	Structure	ΔG (kcal/mol)
13B 11P	5'-AGC AGC ACA GAG GTC AGA TG CCG AAG TGT ACC ACC AAC ATT ACG ATC TTA GCT TGG TGT T CCT ATG CGT GCT ACC GTG AA-3'		-7.3
13B 12	5'- SAG GSC MGK ASC ACC MCC CAC CCA CCC ACW CMA TCT ACG C-3'		0.7
13B 12P	5'-TTC ACG GTA GCA CGC ATA GG SAG GSC MGK ASC ACC MCC CAC CCA CCC ACW CMA TCT ACG C CAT CTG ACC TCT GTG CTG CT-3'		-3.1

Name	Sequence	Structure	ΔG (kcal/mol)
13B 13	<p>5'- GCG CCA CYC ATA TAC CTC AGT ACT TCC ATG CTC GTC GTC A-3'</p>		-2.2
13B 13P	<p>5'-TTC ACG GTA GCA CGC ATA GG GCG CCA CYC ATA TAC CTC AGT ACT TCC ATG CTC GTC GTC A CAT CTG ACC TCT GTG CTG CT-3'</p>		-8.7
13B 14	<p>5'-GTG CGG GCG GGT AGG AGA GCG GTC CCG GTC GTT AGT TCG G-3'</p>		-7.5

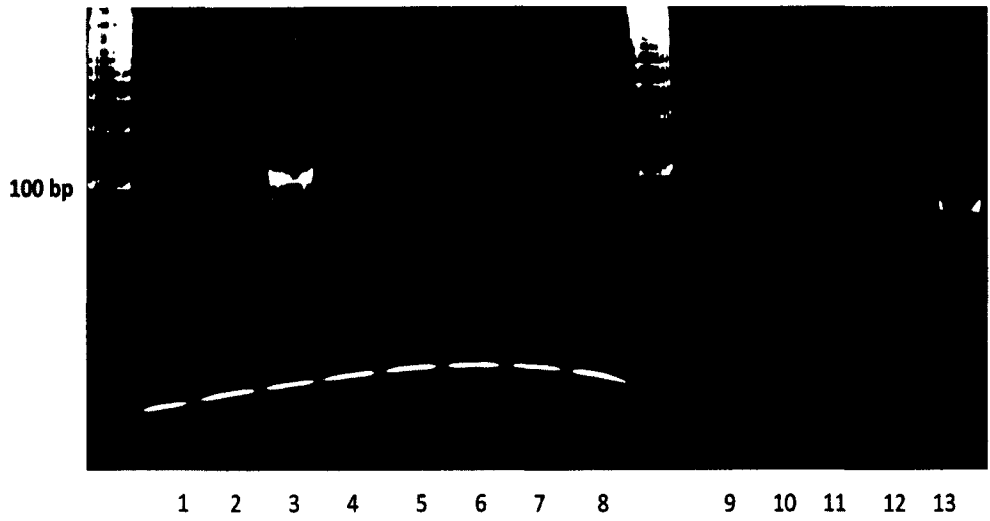
Name	Sequence	Structure	ΔG (kcal/mol)
13B 14P	5'-TTC ACG GTA GCA CGC ATA GG GTG CGG GCG GGT AGG AGA GCG GTC CCG GTC GTT AGT TCG G CAT CTG ACC TCT GTG CTG CT-3'		-13.5
13B 15	5'- GCG AGA GGC CCG CGA GGA AAG CRA ACC GGA CGA GGG GGA G-3'		-4.8
13B 15P	5'-TTC ACG GTA GCA CGC ATA GG GCG AGA GGC CCG CGA GGA AAG CRA ACC GGA CGA GGG GGA G CAT CTG ACC TCT GTG CTG CT-3'		-12.9

Name	Sequence	Structure	ΔG (kcal/mol)
13B 16	5'- CCG AAC GGA TAT YGT ACC TTA GTC AAA CCT GAT CCT CGG G-3'		-6.1
13B 16P	5'-TTC ACG GTA GCA CGC ATA GG CCG AAC GGA TAT YGT ACC TTA GTC AAA CCT GAT CCT CGG G CAT CTG ACC TCT GTG CTG CT-3'		-9.7



1=neg control PCR; 2=neg So; 3= library So; 4=neg W1; 5=W1; 6=neg W2; 7=W2; 8=neg W3; 9=W3; 10=neg CA; 11=CA fraction; 12=neg cells; 13=cell fraction

Figure A41- PCR amplification and native PAGE of GAS SELEX round 2D fractions.



1=neg control PCR; 2=neg So; 3= library So; 4=neg W1; 5=W1; 6=neg W2; 7=W2; 8=neg W3; 9=W3; 10=neg CA; 11=CA fraction; 12=neg cells; 13=cell fraction

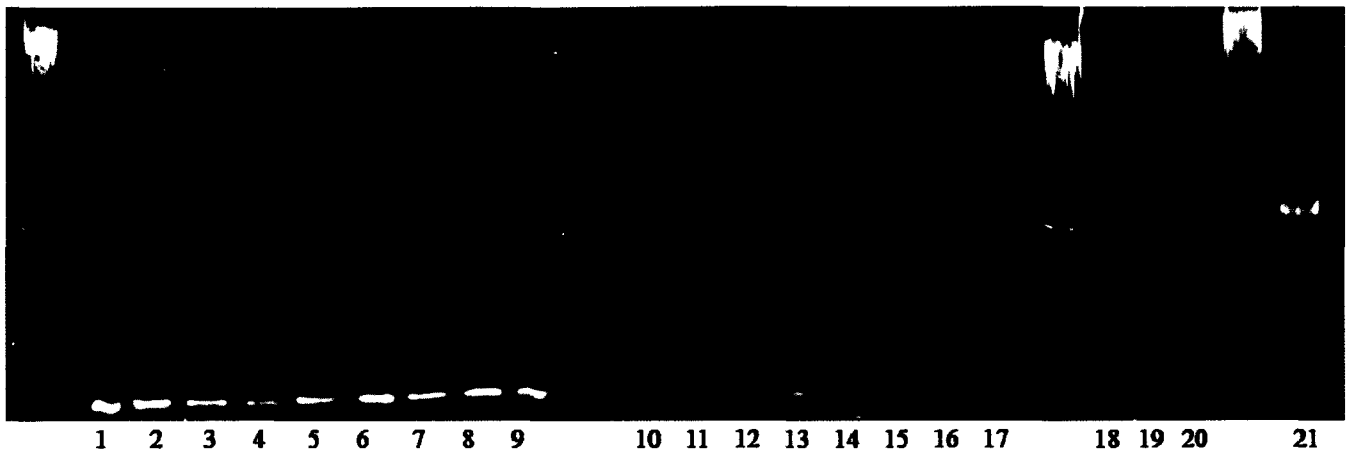
Figure A42- PCR amplification and native PAGE of GAS SELEX round 2E fractions.



1 2 3 4 5 6 7 8 9 10 11 12 13 14 15 16 17 18

1=neg So; 2= So 4D; 3= So 4E; 4= neg W1; 5=W1 4D; 6=W1 4E; 7=neg W2; 8=W2 4D; 9=W2 4E; 10=neg W3; 11= W3 4D; 12=W3 4E; 13=neg CA 4; 14=CA4D; 15=CA 4E; 16=neg cells; 17=cells 4D; 18= cells 4E

Figure A43- PCR amplification and native PAGE of GAS SELEX round 4D and 4E fractions.



1=neg So; 2= So 6D; 3= So 6E; 4= neg W1; 5=W1 6D; 6=W1 6E; 7=neg W2; 8=W2 6D; 9=W2 6E; 10=neg W3; 11= W3 6D; 12=W3 6E; 13=neg W4; 14=W4 6D; 15=W4 6E; 16=neg CA; 17=CA 6D; 18= CA 6E; 19= neg cells; 20= cells 6D; 21=cells 6E.

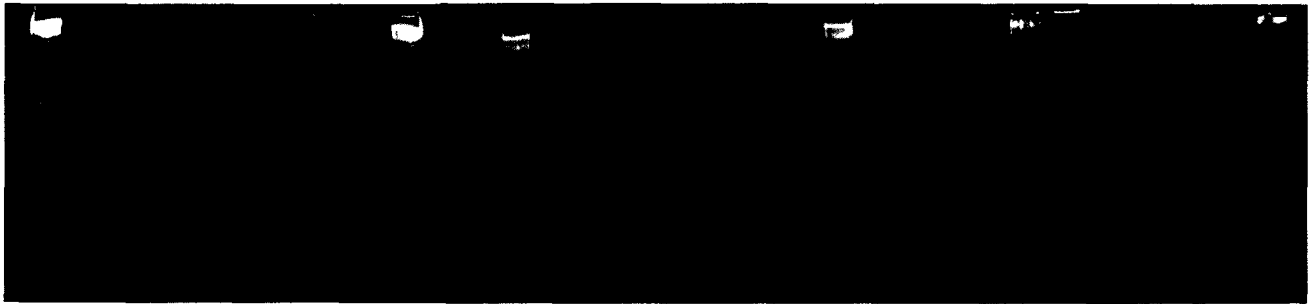
Figure A44- PCR amplification and native PAGE of GAS SELEX round 5D and 5E fractions.



1 2 3 4 5 6 7 8 9 10 11 12 13 14 15 16 17 18 19 20 21

1=neg So; 2= So 5D; 3= So 5E; 4= neg W1; 5=W1 5D; 6=W1 5E; 7=neg W2; 8=W2 5D;
9=W2 5E; 10=neg W3; 11= W3 5D; 12=W3 5E; 13=neg W4; 14=W4 5D; 15=W4 5E; 16=neg
CA; 17=CA 5D; 18= CA 5E; 19= neg cells; 20= cells 5D; 21=cells 5E.

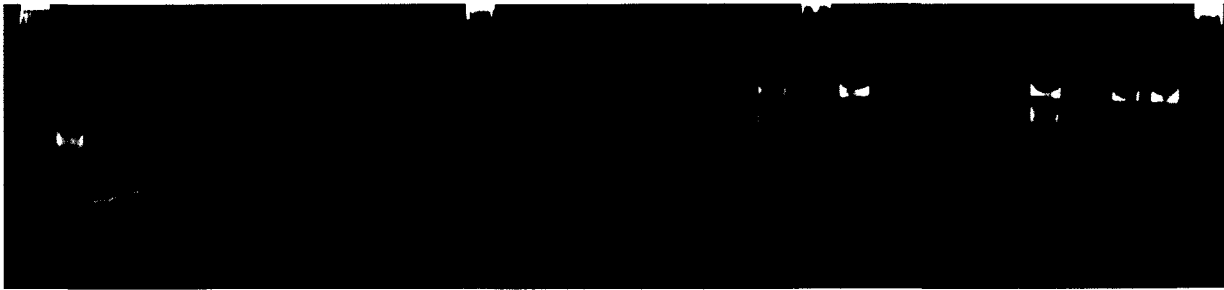
**Figure A45- PCR amplification and native PAGE of GAS SELEX round 6D
and 6E fractions.**



1 2 3 4 5 6 7 8 9 10 11 12 13 14 15 16 17 18 19 20 21

1-neg So; 2- So 7D; 3- So 7E; 4-neg W1; 5-W1 7D; 6-W1 7E; 7-neg W2; 8-W2 7D; 9-W2 7E; 10-neg W3; 11-W3 7D; 12-W3 7E; 13-neg W4; 14-W4 7D; 15-W4 7E; 16-neg CA; 17-CA 7D; 18- CA 7E; 19- neg cells; 20- cells 7D; 21=cells 7E.

Figure A46- PCR amplification and native PAGE of GAS SELEX round 7D and 7E fractions.

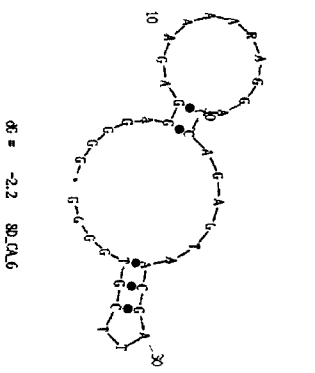
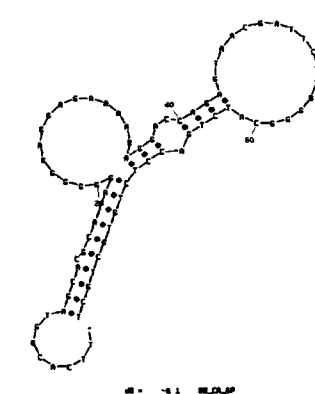
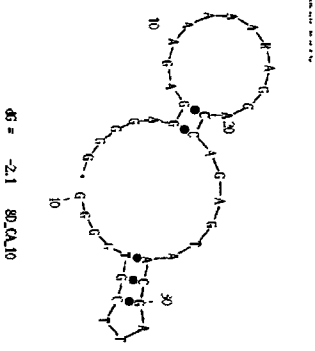


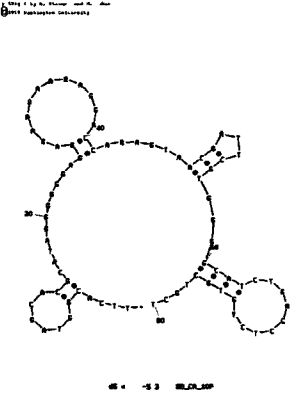
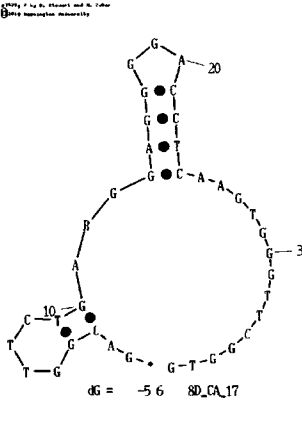
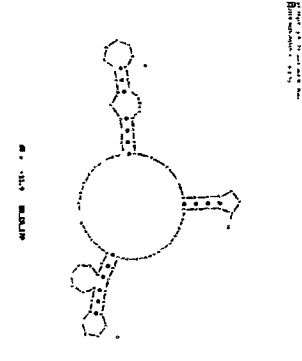
1 2 3 4 5 6 7 8 9 10 11 12 13 14 15 16 17 18 19 20 21 22 23 24 25

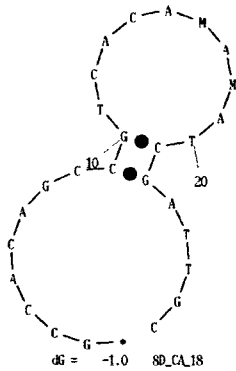
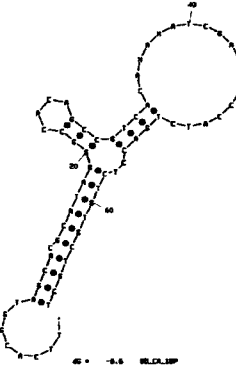
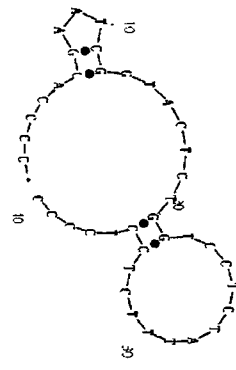
1=neg So; 2= So 8D; 3= So 8E; 4= neg W1; 5=W1 8D; 6=W1 8E; 7=neg W2; 8=W2 8D; 9=W2 8E; 10=neg W3; 11=W3 8D; 12=W3 8E; 13=neg W4; 14=W4 8D; 15=W4 8E; 16=neg CA; 17=CA 8D; 18= CA 8E; 19= neg cells; 20= cells 8D; 21=cells 8E; 22= cells 8D amplification 2; 23= cells 8D reamplification 3; 24= cells 8E amplification 2; 25= cells 8E amplification 3.

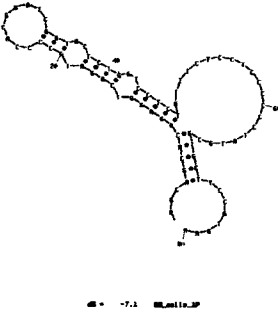
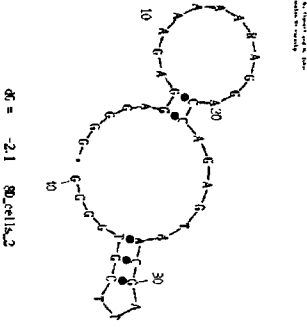
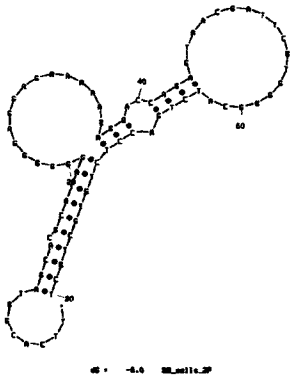
Figure A47-PCR amplification and native PAGE of GAS SELEX round 8D and 8E fractions.

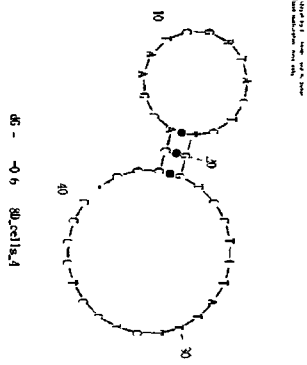
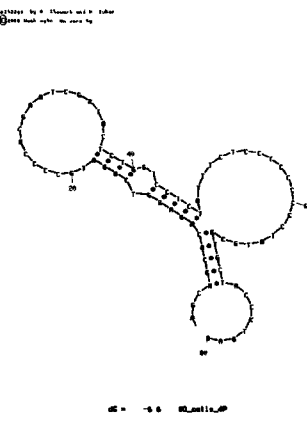
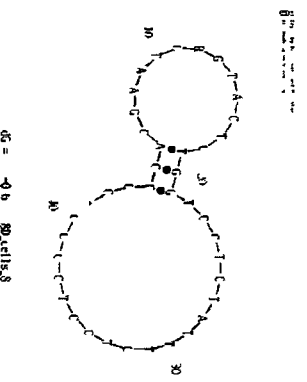
Table A5. Sequences and most likely secondary structures of aptamers from SELEX D.

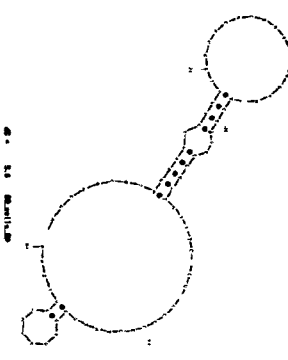
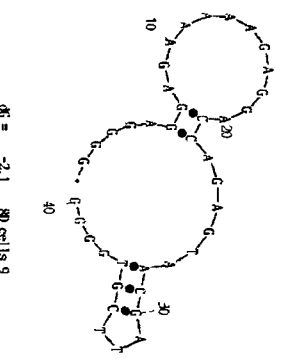
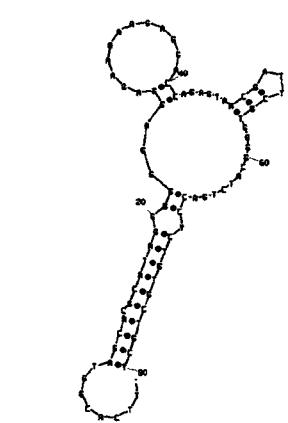
Name	Sequence	Structure	ΔG (kcal/mol)
8D CA 6	5'- GGGGAGGAGAAAA RAGGACCAGAGTA ACGATTCGTGGGG- 3'		-2.2
8D CA 6P	5'- TTCACGGTAGCACG CATAGGGGGGAGG AGAAAARAGGACC AGAGTAACGATTC GTGGGGCATCTGAC CTCTGTGCTGCT-3'		-6.11
8D CA 10	5'- GGGGAGGAGAAAA ARAGGACCAGAGT AACGATTCGTGGG G-3'		-2.1

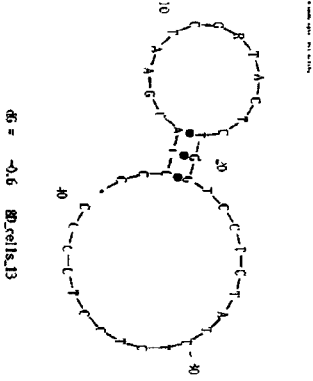
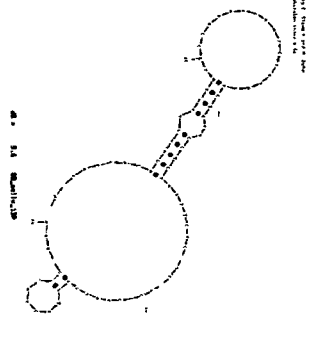
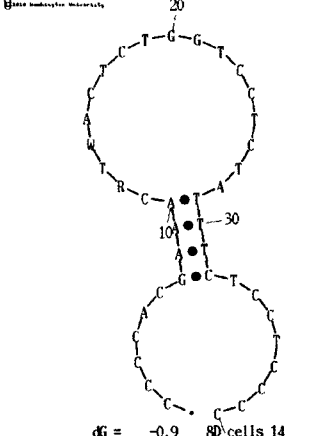
Name	Sequence	Structure	ΔG (kcal/mol)
8D CA 10P	5'- TTCACGGTAGCACG CATAGGGGGGAGG AGAAAAARAGGAC CAGAGTAACGATT CGTGGGGGCATCTG ACCTCYGTGCTGCT- 3'		-5.8 (same structure as 6P has ΔG of -4.08)
8D CA 17	5'- GACGGTTCTGARG GAGGGGACCTCAA GTGGGTTTCGGTG- 3'		-5.6
8D CA 17P	5'- AGCAGCACAGAGGT CAGATGGACGGTT CTGARGGAGGGGA CCTCAAGTGGGTT CGGTGCCTATGCGT GCTMCCGTGAA-3'		-11.6

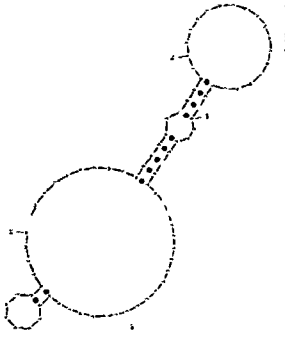
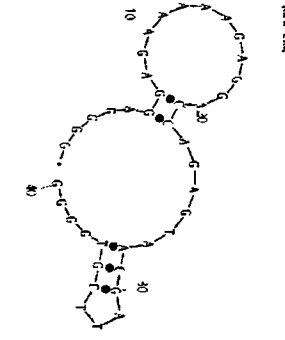
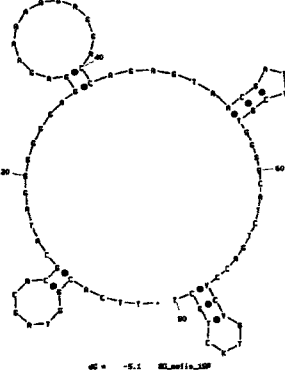
Name	Sequence	Structure	ΔG (kcal/mol)
8D CA 18	5'- GCCACAGCCGTCA CAMAMATCGATTG C-3'		-1.05
8D CA 18P	5'- TTCACGGTAGCACG CATAGGGCCACAG CCGTCACAMAMAT CGATTGCCATCTGA CCTCTGTGCTGCT-3'		-6.6
8D cells 1	5'- CCCCACGAATCGG TACTCTGGTCCTCT ATTTCTCCTCCCC- 3'		-1.1

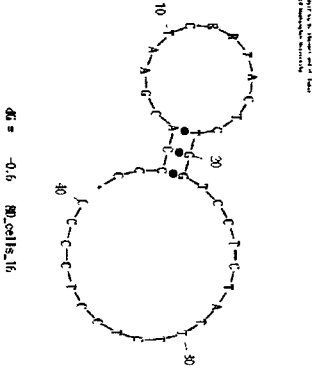
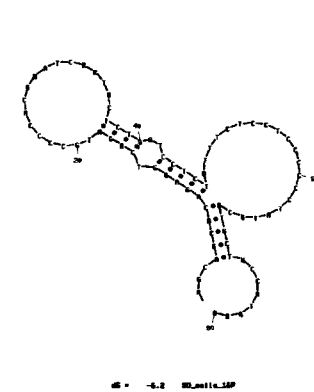
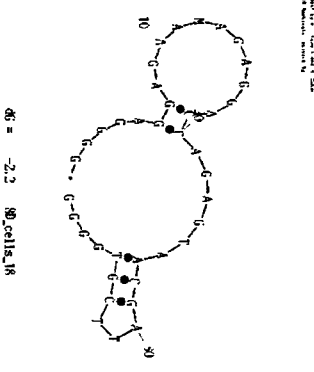
Name	Sequence	Structure	ΔG (kcal/mol)
8D cells 1P	5'- AGCAGCACAGAGGT CAGATGCCCCACG AATCGGTA CTCTG GTCCTCTATTTCTC CTCCCCCTATGCG TGCTYCCGTGAA-3'		-7.1
8D cells 2	5'- GGGGAGGAGAAAA ARAGGACCAGAGT AACGATTCGTGGG G-3'		-2.1
8D cells 2P	5'- TTCACGGTAGCACG CATAGGGGGGAGG AGAAAAARAGGAC CAGAGTAACGATT CGTGGGGCATCTG ACCTCTGTGCTGCT- 3'		-6.0

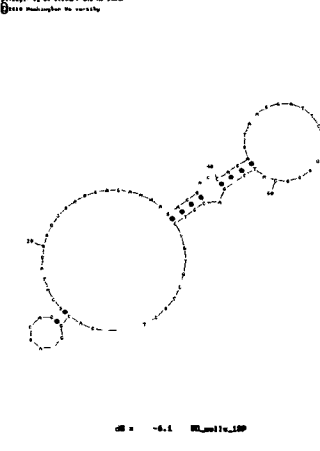
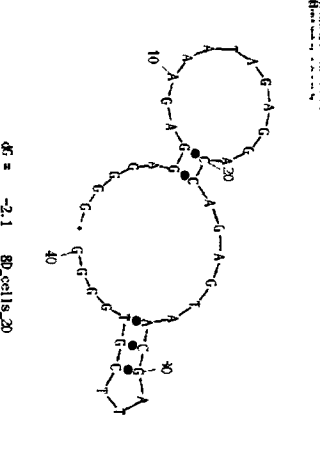
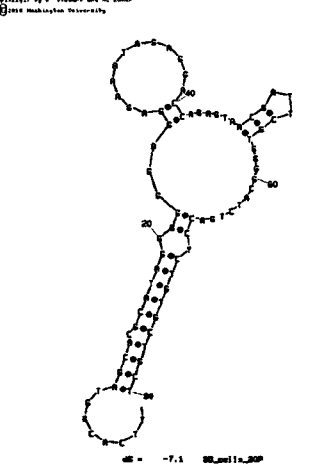
Name	Sequence	Structure	ΔG (kcal/mol)
8D cells 4	5'- CCCCACGAATCGR TACTCTGGTCCTCT ATTCTCCTCCCC- 3'		-0.6
8D cells 4P	5'- AGCAGCACAGAGGT CAGATGCCCCACG AATCGRTACTCTG GTCCTCTATTTCTC CTCCCCCCTATGCG TGCTACCKTGAA-3'		-6.6
8D cells 8	5'- CCCCACGAATCRG TACTCTGGTCCTCT ATTCTCCTCCCC- 3'		-0.6

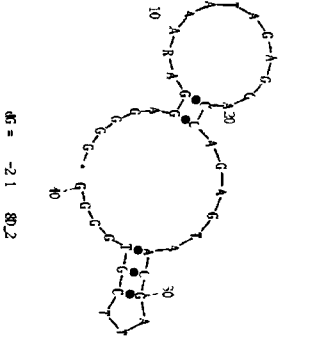
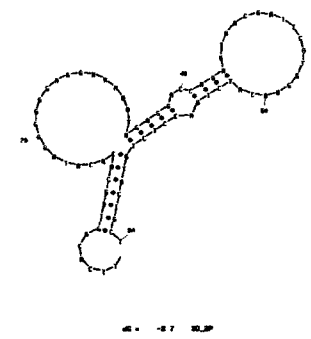
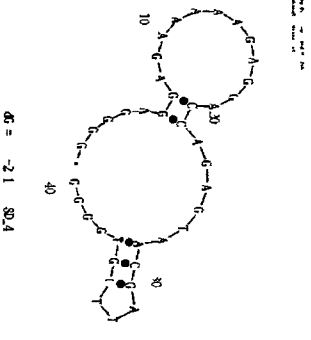
Name	Sequence	Structure	ΔG (kcal/mol)
8D cells 8P	5'- AGCAGCACAGAGGT CAGATGCCCCACG AATCRGTA CTCTG GTCCTCTATTTCTC CTCCCCCTATGCG TGCYACCGTGAA-3'		-5.6
8D cells 9	5'- GGGGAGGAGAAAA AGAGGACCAGAGT AACGATTCGTGGG G-3'		-2.1
8D cells 9P	5'- TTCACGGTAGCACG CATAGGGGGGAGG AGAAAAAGAGGAC CAGAGTAACGATT CGTGGGGCATCTG ACCYCTGTGCTGCT- 3'		-7.06

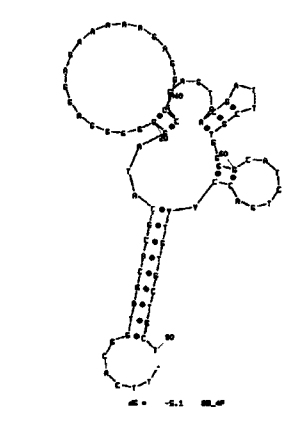
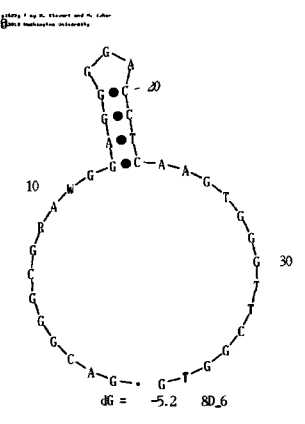
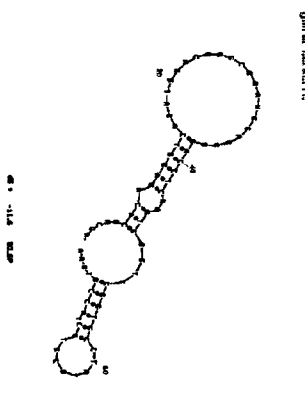
Name	Sequence	Structure	ΔG (kcal/mol)
8D cells 13	5'- CCCCACGAATCGR TACTCTGGTCCTCT ATTCTCCTCCCC- 3'		-0.6
8D cells 13P	5'- AGCAGCACAGAGGT CAGATGCCCCACG AATCGRTACTCTG GTCCTCTATTTCTC CTCCCCCTATGCG TGCYACCGTGAA-3'		-5.6
8D cells 14	5'- CCCCACGAAACRT WACTCTGGTCCTC TATTTCTCCTCCCC -3'		-0.9

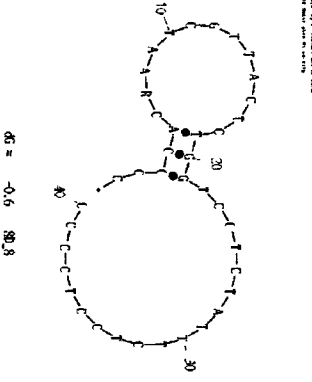
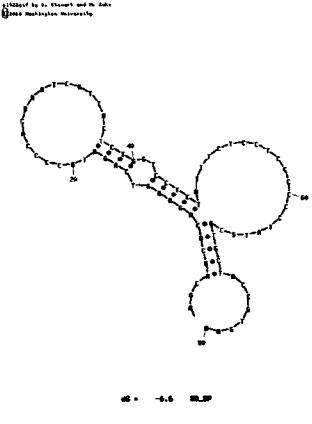
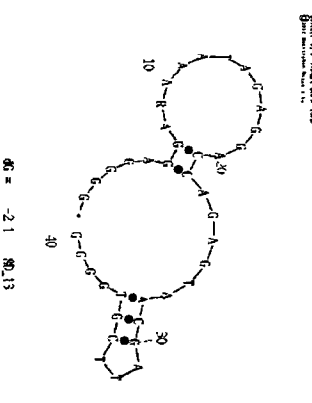
Name	Sequence	Structure	ΔG (kcal/mol)
8D cells 14P	5'- AGCAGCACAGAGGT CAGATGCCCCACG AAACRTWACTCTG GTCCTCTATTTCTC CTCCCCCTATGCG TGCYACCGTGAA-3'		-5.6
8D cells 15	5'- GGGGAGGAGAAAA AGAGGACCAGAGT AACGATTCGTGGG G-3'		-2.1
8D cells 15P	5'- TTCACGGTAGCACG CATAGGGGGGAGG AGAAAAAGAGGAC CAGAGTAACGATT CGTGGGGCATCTG ACCYCYGTKCTGCT- 3'		-5.1

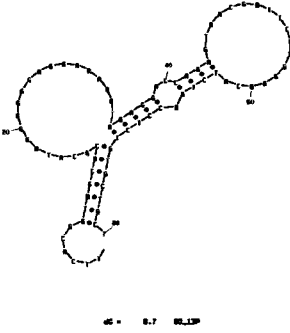
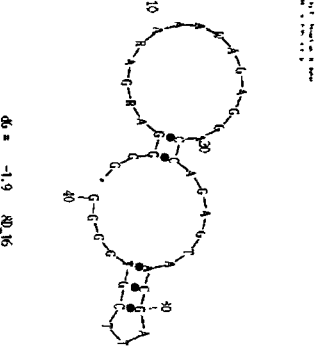
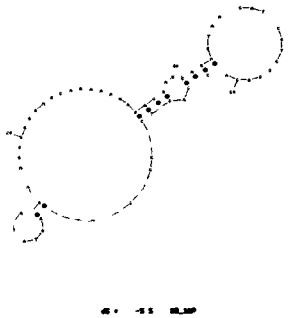
Name	Sequence	Structure	ΔG (kcal/mol)
8D cells 16	5'- CCCCACGAATCRR TACTCTGGTCCTCT ATTTCTCCTCCCC- 3'		-0.6
8D cells 16P	5'- AGCAGCACAGAGGT CAGATGCCCCACG AATCRRTACTCTG GTCCTCTATTTCTC CTCCCCCCTATGCG TGCTWCCGTGAA-3'		-6.2
8D cells 18	5'- GGGGAGGAGAAM AGAGGACCAGAGT AACGATTCGTGGG G-3'		-2.2

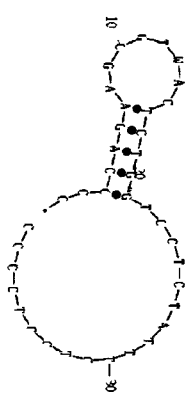
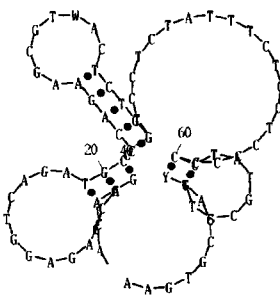
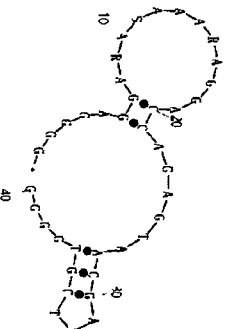
Name	Sequence	Structure	ΔG (kcal/mol)
8D cells 18P	5'- TTCACGGTAGCACG CATAGGGGGGAGG AGAAMAGAGGACC AGAGTAACGATTC GTGGGGCATCTGAC CTCYGTGCTGCT-3'		-6.1
8D cells 20	5'- GGGGAGGAGAAAT AGAGGACCAGAGT AACGATTCGTGGG G-3'		-2.1
8D cells 20P	5'- TTCACGGTAGCACG CATAGGGGGGAGG AGAAATAGAGGAC CAGAGTAACGATT CGTGGGGCATCTG ACCYCTGTGCTGCT- 3'		-7.1

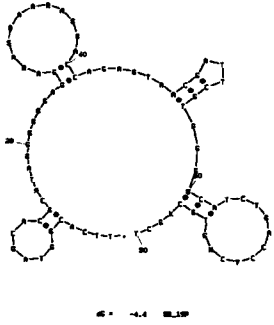
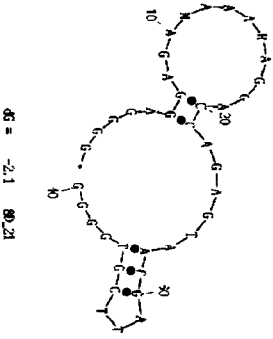
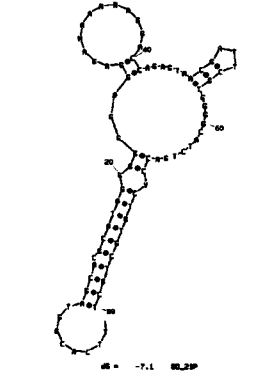
Name	Sequence	Structure	ΔG (kcal/mol)
8D 2	5'- GGGGAGGAAAAAT AGAGGACCAGAGT AACGATTCGTGGG G-3'	 <p>$\Delta G = -2.1$ kcal/mol</p>	-2.1
8D 2P	5'- TTCACGGTAGCACG CATAGGGGGGAGG AAAAATAGAGGAC CAGAGTAACGATT CGTGGGGCATCTG ACCTCTGTGCTGCT- 3'	 <p>$\Delta G = -8.7$ kcal/mol</p>	-8.7
8D 4	5'- GGGGAGGAGAAAA AGAGGACCAGAGTA ACGATTCGTGGGG- 3'	 <p>$\Delta G = -2.1$ kcal/mol</p>	-2.1

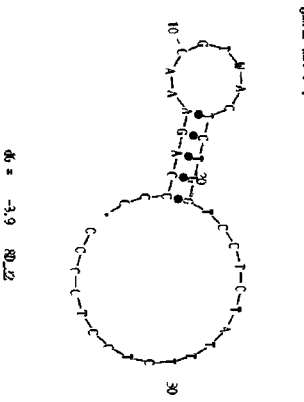
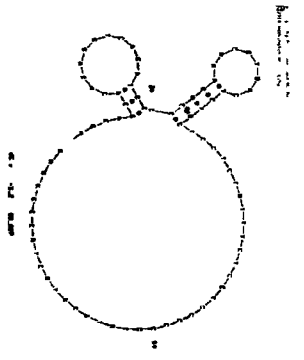
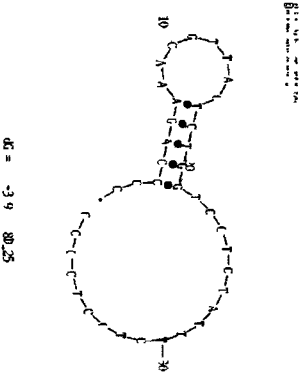
Name	Sequence	Structure	ΔG (kcal/mol)
8D 4P	5'- TTCACGGTAGCACG CATAGGGGGGAGG AGAAAAAGAGGAC CAGAGTAACGATT CGTGGGGCATCTG ACCYYTGTGCTGCT- 3'		-5.1
8D 6	5'- GACGGGCRAWG GAGGGGACCTCAA GTGGGTTCGGTG- 3'		-5.2
8D 6P	5'- AGCAGCACAGAGGT CAGATGGACGGGC GRAWGGAGGGGA CCTCAAGTGGGTT CGGTGCCTATGCST GCTACCGTGAA-3'		-11.6

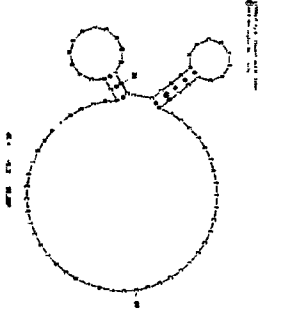
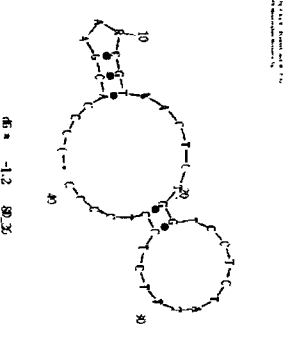
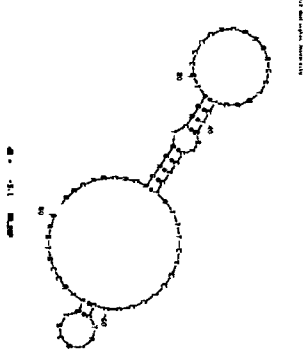
Name	Sequence	Structure	ΔG (kcal/mol)
8D 8	5'- CCCCACRAATCGT TACTCTGGTCCTCT ATTTCTCCTCCCC- 3'	 <p>$\Delta G = -0.6$ $\Delta G_{13} = 80.8$</p>	-0.6
8D 8P	5'- AGCAGCACAGAGGT CAGATGCCCCACRA ATCGTTACTCTGGT CCTCTATTTCTCCT CCCCCCTATSCGTG CTACCGTGAA-3'	 <p>$\Delta G = -6.6$ $\Delta G_{13} = 82.8$</p>	-6.6
8D 13	5'- GGGGAGGARAAT AGAGGACCAGAGT AACGATTCGTGGG G-3'	 <p>$\Delta G = -2.1$ $\Delta G_{13} = 80.13$</p>	-2.1

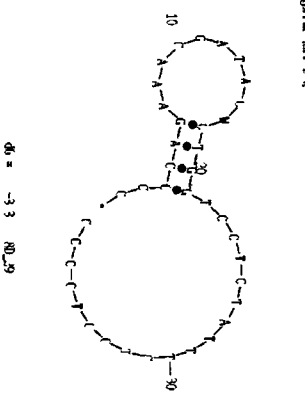
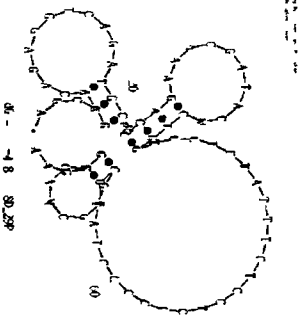
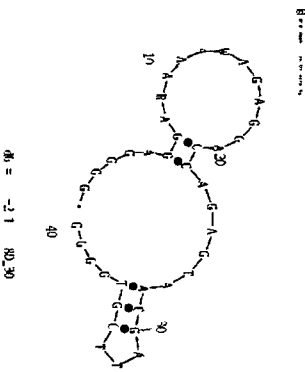
Name	Sequence	Structure	ΔG (kcal/mol)
8D 13P	5'- TTCACGGTAGCACG CATAGGGGGGAGG ARAAATAGAGGAC CAGAGTAACGATT CGTGGGGGCATCTG ACCTCTGTGCTGCT- 3'		-8.7
8D 16	5'- GGGGARGARAAAW AGAGGACCAGAGT AACGATTCGTGGG G-3'		-1.9
8D 16P	5'- TTCCGGTAGCACGC ATAGGGGGGARGA RAAAWAGAGGACC AGAGTAACGATTC GTGGGGGCATCTGAC CTCKGKGCTGCT-3'		-5.5

Name	Sequence	Structure	ΔG (kcal/mol)
8D 17	5'- CCCCAGAAGCGTW ACTCTGGTCCTCTA TTTCTCCTCCCC-3'	 <p>$\Delta G = -3.9$ 8D_17</p>	-3.9
8D 17P	5'- AGCAGCACAGAGGT CAGATGCCCCAGA AGCGTWACTCTGG TCCTCTATTTCTCC TCCCCCTATGCST GYTACCGTGAA-3'	 <p>$\Delta G = -5.3$ 8D_17P</p>	-5.3
8D 19	5'- GGGGAGGARASAA ARAGGACCAGAGT AACGATTCGTGGG G-3'	 <p>$\Delta G = -2.1$ 8D_19</p>	-2.1

Name	Sequence	Structure	ΔG (kcal/mol)
8D 19P	5'- TTCACGGTAGCACG CATAGGGGGGAGG ARASAAARAGGAC CAGAGTAACGATT CGTGGGGCATCTG ACCYCMGTGCKGCT -3'		-4.4
8D 21	5'- GGGGAGGAGAMA AARAGGACCAGAG TAACGATTCGTGG GG-3'		-2.1
8D 21P	5'- TTCACGGTAGCACG CATAGGGGGGAGG AGAMAAARAGGAC CAGAGTAACGATT CGTGGGGCATCTG ACCYCTGTGCTGCT- 3'		-7.1

Name	Sequence	Structure	ΔG (kcal/mol)
8D 22	5'- CCCCAGAAACGTW ACTCTGGTCCTCTA TTTCTCCTCCCC-3'		-3.9
8D 22P	5'- AGCAGCACAGAGGT CAGATGCCCCAGA AACGTWACTCTGG TCCTCTATTTCTCC TCCCCCCTATGCSY GCTACCGKGAA-3'		-5.2
8D 25	5'- CCCCAGAAACGTT ACTCTGGTCCTCTA TTTCTCCTCCCC-3'		-3.9

Name	Sequence	Structure	ΔG (kcal/mol)
8D 25P	5'- AGCAGCACAGAGGT CAGATGCCCCAGA AACGTTACTCTGG TCCTCTATTTCTCC TCCCCCTATGCST GCTACCGTGAA-3'		-5.2
8D 26	5'- CCCACGAARCGT WACTCTGGTCCTC TATTTCTCCTCCCC -3'		-1.2
8D 26P	5'- AGCAGCACAGAGGT CAGATGCCCCACG AARCGTWACTCTG GTCCTCTATTTCTC CTCCCCCTATGCS TGYTACCGTGAA-3'		-5.1

Name	Sequence	Structure	ΔG (kcal/mol)
8D 29	5'- CCCCAGAAACGAT ACWCTGGTCCTCT ATTTCTCCTCCCC- 3'		-3.3
8D 29P	5'- AGCAGCACAGAGGT CAGATGCCCCAGA AACGATACWCTGG TCCTCTATTTCTCC TCCCCCCTATGCGT GCMACCGKGAA-3'		-4.8
8D 30	5'- GGGGAGGARAAA WAGAGGACCAGAG TAACGATTCGTGG GG-3'		-2.1

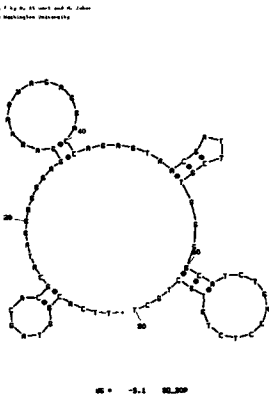
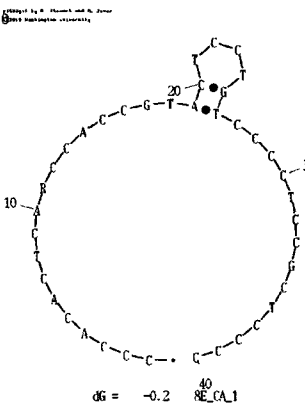
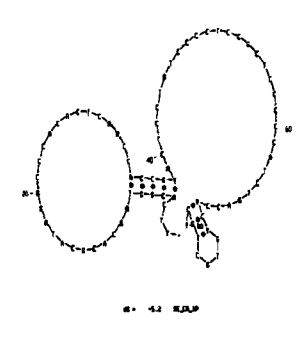
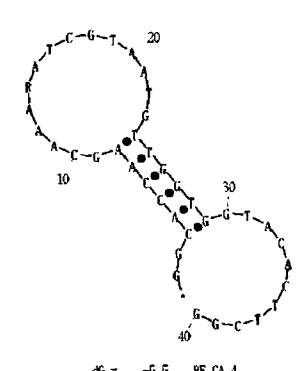
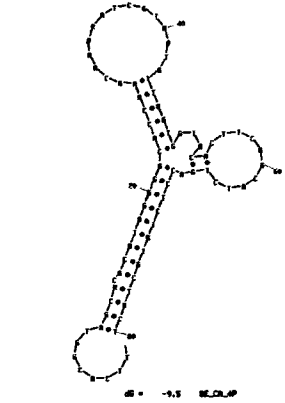
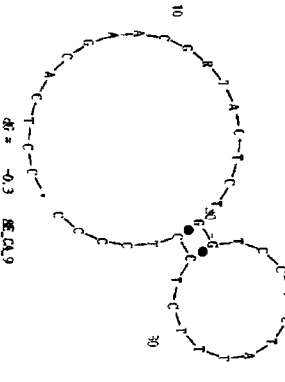
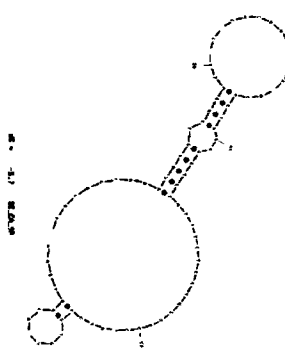
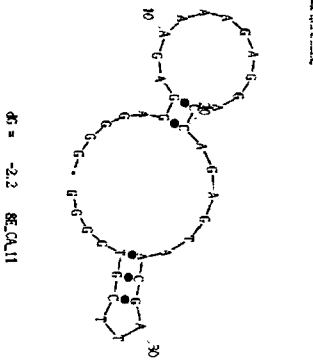
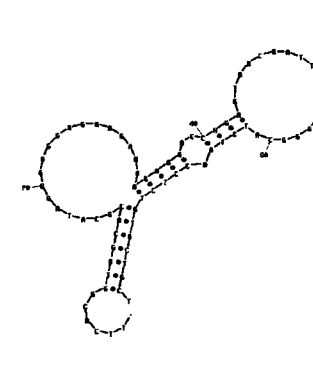
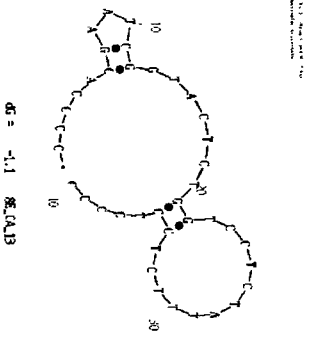
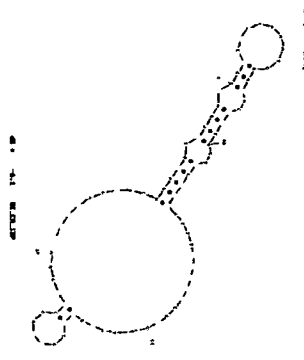
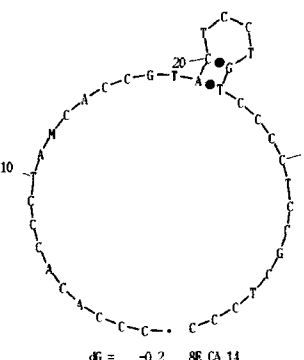
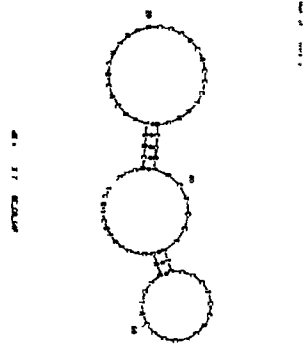
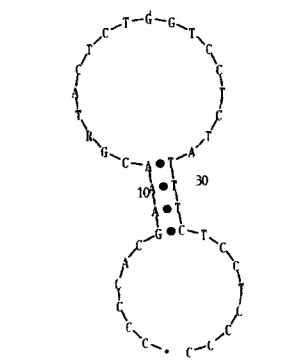
Name	Sequence	Structure	ΔG (kcal/mol)
8D 30P	5'- TTCACGGTAGCACG CATAGGGGGGAGG ARAAWAGAGGAC CAGAGTAACGATT CGTGGGGGCATCTG MCCTCTGTGCTGCT- 3'		-5.1

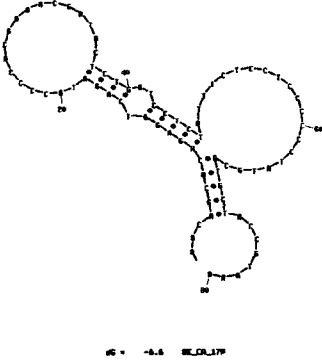
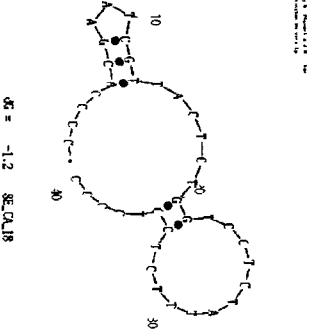
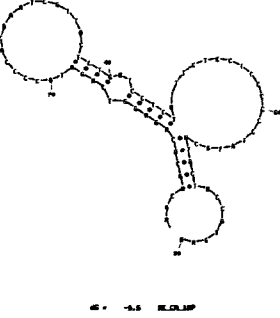
Table A6. Sequences and most likely secondary structures of aptamers from SELEX E.

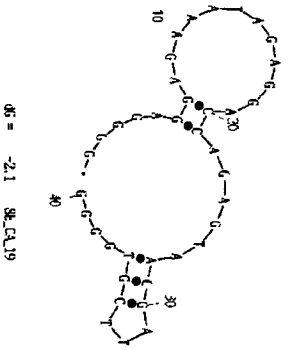
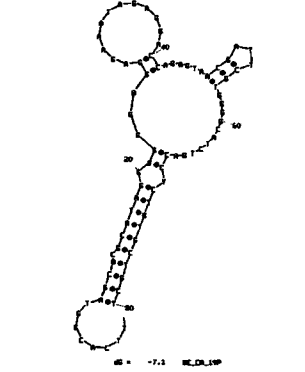
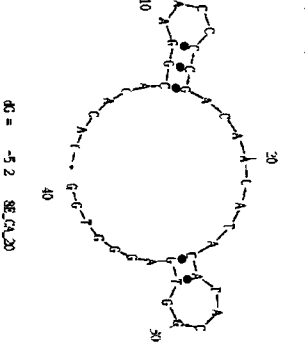
Name	Sequence	Structure	ΔG (kcal/mol)
8E CA 1	5'- CCCACACTCARCC ACCGTACTCCTGT CCCCTCCGCTCCC C-3'		-0.2
8E CA 1P	5'- TTCACGGTAGCACG CATAGGCCACACT CARCCACCGTACT CCTGTCCCCTCCG CTCCCCATCTGAC CYCYGTGCTGCT-3'		-5.22
8E CA 4	5'- GGCACCAAGCAAA RATCGTAATGTTG GTGGTACACTTCG G-3'		-5.5

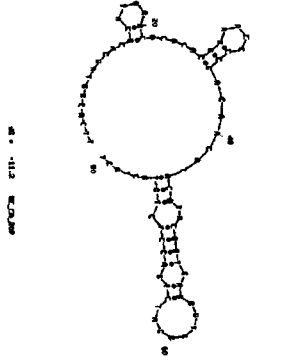
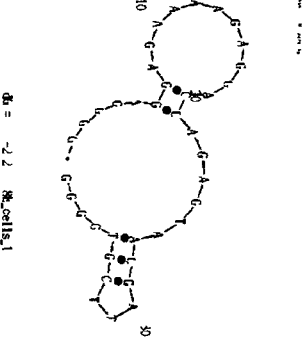
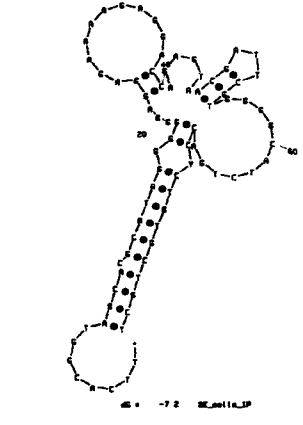
Name	Sequence	Structure	ΔG (kcal/mol)
8E CA 4P	5'- TTCACGGTAGCACG CATAGGGGCACCA AGCAAARATCGTA ATGTTGGTGGTAC ACTTCGGCATCTGA CCTCTGTGCTGCT-3'		-9.5
8E CA 9	5'- CCTCACGAACGRT ACTCTGGTCCTCTA TTTCTCCTCCCC-3'		-0.3
8E CA 9P	5'- AGCAGCACAGAGGT CAGATGCCTCACGA ACGRTACTCTGGT CCTCTATTTCTCCT CCCCCCTATGCGTG YTACCGTGAA-3'		-5.7

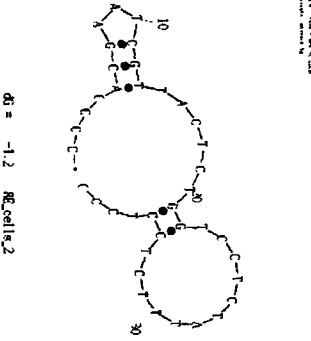
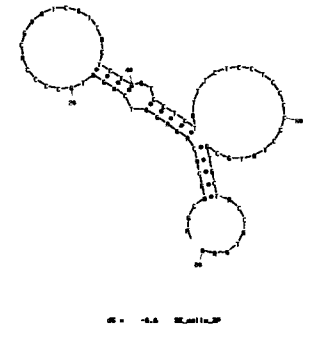
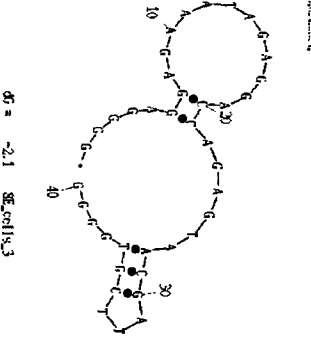
Name	Sequence	Structure	ΔG (kcal/mol)
8E CA 11	5'- GGGGAGGAGAAAA GAGGACCAGAGTA ACGATTCGTGGGG- 3'		-2.2
8E CA 11P	5'- TTCACGGTAGCACG CATAGGGGGGAGG AGAAAAGAGGACC AGAGTAACGATTC GTGGGGCATCTGAC CTCTGTGCTGCT-3'		-8.7
8E CA 13	5'- CCCCACGAATCGG TACTCTGGTCCTCT ATTTCTCCTCCCC- 3'		-1.1

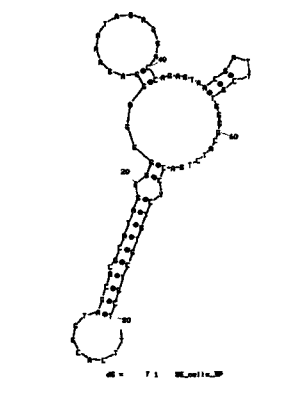
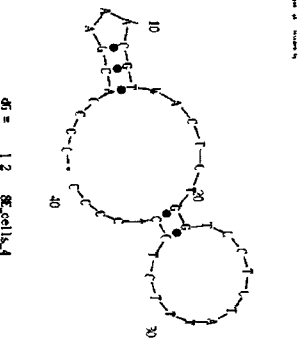
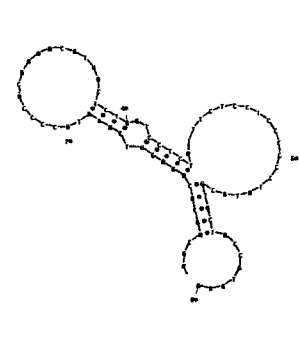
Name	Sequence	Structure	ΔG (kcal/mol)
8E CA13P	5'- AGCAGCACAGAGGT CAGATGCCCCACG AATCGGTA CTCTG GTCCTCTATTTCTC CTCCCCCTATGCG TGCYACCGTGAA-3'		-6.1
8E CA 14	5'- CCCACACCCTAMC ACCGTACTCCTGT CCCCTCCGCTCCC- 3'	 <p style="text-align: center;">dg = -0.2 8E_CA14</p>	-0.2
8E CA 14P	5'- TTCACGGTAGCACG CATAGGCCACACC CTAMCACCGTACT CCTGTCCCCTCCG CTCCCCATCTGACC TCTGTGCTGCT-3'		-3.7
8E CA17	5'- CCCACGAAACGR TACTCTGGTCCTCT ATTTCTCCTCCCC- 3'	 <p style="text-align: center;">dg = -0.9 8E_CA17</p>	-0.9

Name	Sequence	Structure	ΔG (kcal/mol)
8E CA17P	5'- AGCAGCACAGAGGT CAGATGCCCCACG AAACGRTACTCTG GTCCTCTATTTCTC CTCCCCCCTATGCG TGCTACCGTGAA-3'		-6.6
8E CA18	5'- CCCACGAATCGT TACTCTGGTCCTCT ATTTCTCCTCCCC- 3'		-1.2
8E CA18P	5'- AGCAGCACAGAGGT CAGATGCCCCACG AATCGTTACTCTG GTCCTCTATTTCTC CTCCCCCCTATGCG TGCTACCGTGAA-3'		-6.6

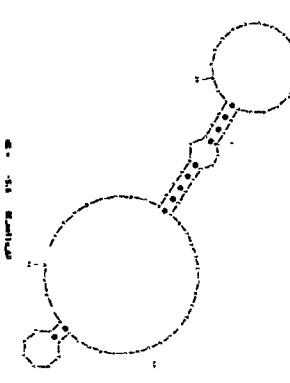
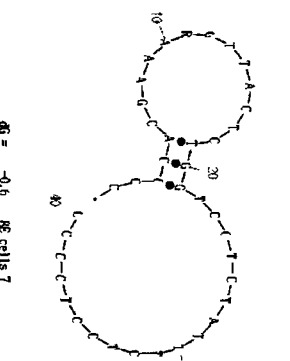
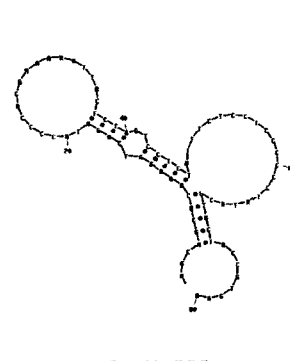
Name	Sequence	Structure	ΔG (kcal/mol)
8E CA19	5'- GGGGAGGAGAAAT AGAGGACCAGAGT AACGATTCGTGGG G-3'	 <p>$\Delta G = -2.1$ kcal/mol</p>	-2.1
8E CA19P	5'- TTCACGGTAGCACG CATAGGGGGGAGG AGAAATAGAGGAC CAGAGTAACGATT CGTGGGGCATCTG ACCYCTGTGCTGCT- 3'	 <p>$\Delta G = -7.1$ kcal/mol</p>	-7.1
8E CA20	5'- CACACACGGAACC CCGACAACATACA TACGGTGAGGGTG G-3'	 <p>$\Delta G = -5.2$ kcal/mol</p>	-5.2

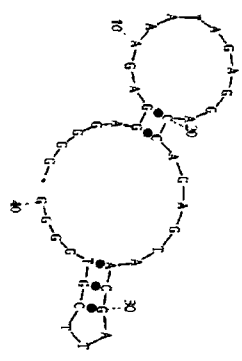
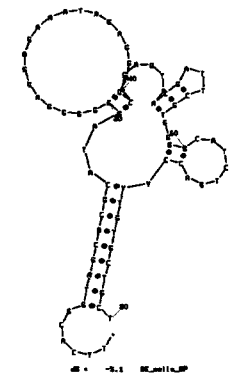
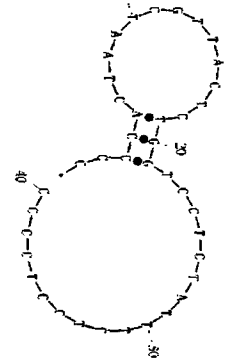
Name	Sequence	Structure	ΔG (kcal/mol)
8E CA20P	5'- TTCACGGTAGCACG CATAGGCACACAC GGAACCCCGACAA CATACATACGGTG AGGGTGGCATCTG ACCYCTGTGCTGCT- 3'		-11.2
8E cells 1	5'- GGGGAGGAGAAAA GAGGACCAGAGTA ACGATTCGTGGGG- 3'		-2.2
8E cells 1P	5'- TTCACGGTAGCACG CATAGGGGGGAGG AGAAAAGAGGACC AGAGTAACGATTC GTGGGGCATCTGAC CYCTGTGCTGCT-3'		-7.2

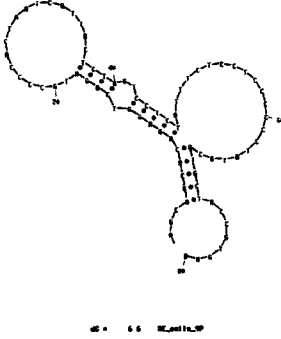
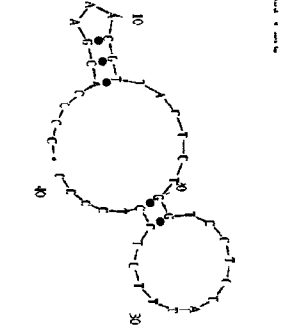
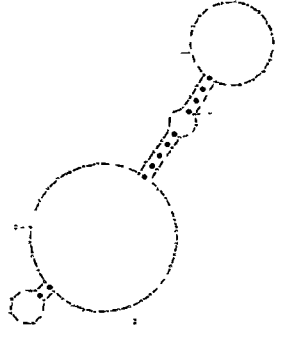
Name	Sequence	Structure	ΔG (kcal/mol)
8E cells 2	5'- CCCCACGAATCGT TACTCTGGTCCTCT ATTCTCCTCCC-3'		-1.2
8E cells 2P	5'- AGCAGCACAGAGGT CAGATGCCCCACG AATCGTTACTCTG GTCCTCTATTTCTC CTCCCCCTATGCG TGCTACCGTGAA-3'		-6.6
8E cells 3	5'- GGGGAGGAGAAAT AGAGGACCAGAGT AACGATTCGTGGG G-3'		-2.1

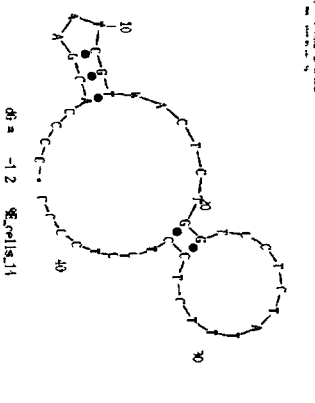
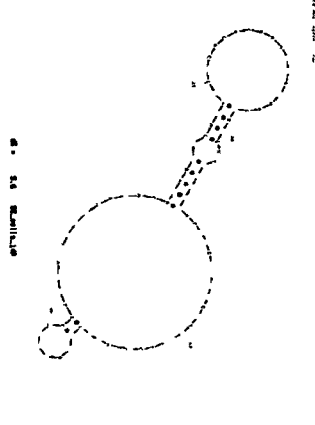
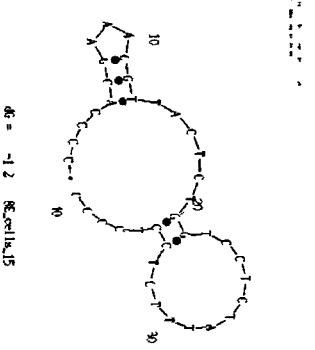
Name	Sequence	Structure	ΔG (kcal/mol)
8E cells 3P	5'- TTCACGGTAGCACG CATAGGGGGGAGG AGAAATAGAGGAC CAGAGTAACGATT CGTGGGGGCATCTG ACCYCTGTGCTGCT- 3'		-7.1
8E cells 4	5'- CCCACGAAACGT WACTCTGGTCCTC TATTTCTCCTCCCC -3'		-1.2
8E cells 4P	5'- AGCAGCACAGAGGT CAGATGCCCCACG AAACGTWACTCTG GTCCTCTATTTCTC CTCCCCCCTATGCG TGCTACCGTGAA-3'		-6.6

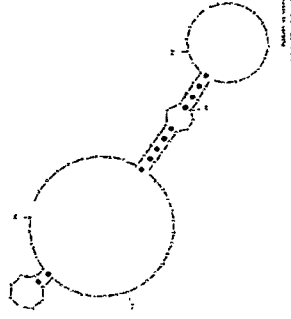
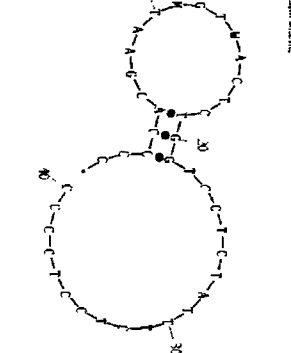
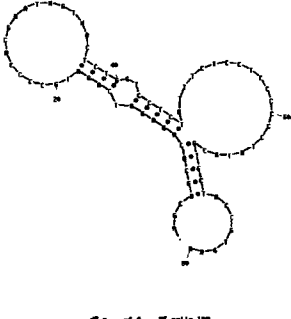
Name	Sequence	Structure	ΔG (kcal/mol)
8E cells 5	5'- CCCCACGAAACGT WACTCTGGTCCTC TATTCTCCTCCCC -3'		-1.2
8E cells 5P	5'- AGCAGCACAGAGGT CAGATGCCCCACG AAACGTWACTCTG GTCCTCTATTTCTC CTCCCCCTATGCG TGYTACCGTGAA-3'		-5.6
8E cells 6	5'- CCCCACGAAACGT TACTCTGGTCCTCT ATTCTCCTCCCC- 3'		-1.2

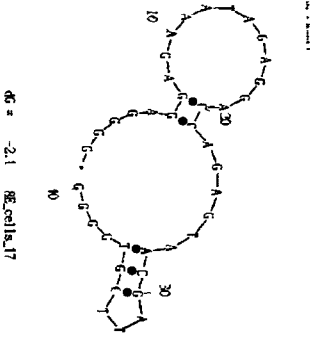
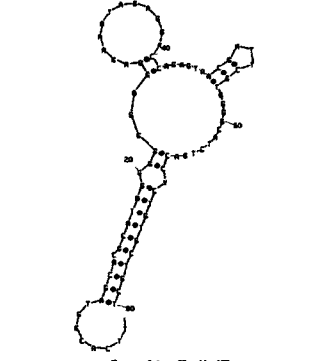
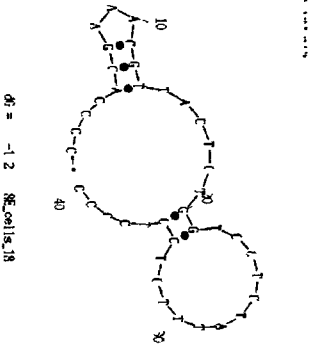
Name	Sequence	Structure	ΔG (kcal/mol)
8E cells 6P	5'- AGCAGCACAGAGGT CAGATGCCCCACG AACGTTACTCTG GTCCTCTATTTCTC CTCCCCCTATGCG TGYTACCGTGAA-3'		-5.6
8E cells 7	5'- CCCCACGAAARGT TACTCTGGTCCTCT ATTTCTCCTCCCC- 3'		-0.6
8E cells 7P	5'- AGCAGCACAGAGGT CAGATGCCCCACG AAARGTTACTCTG GTCCTCTATTTCTC CTCCCCCTATGCG TGCTACCGTGAA-3'		-6.6

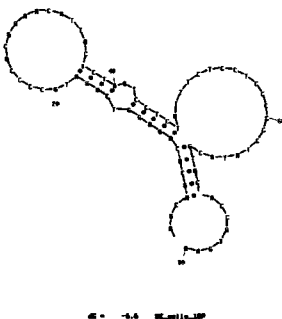
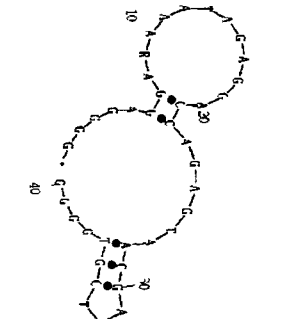
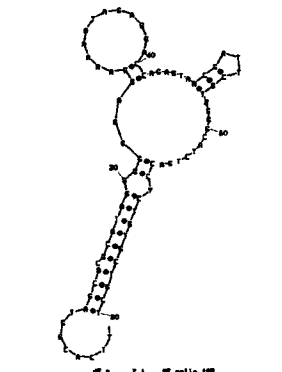
Name	Sequence	Structure	ΔG (kcal/mol)
8E cells 8	5'- GGGGAGGAGAAAT AGAGGACCAGAGT AACGATTCGTGGG G-3'		-2.2
8E cells 8P	5'- TTCACGGTAGCACG CATAGGGGGGAGG AGAAATAGAGGAC CAGAGTAACGATT CGTGGGGCATCTG ACCYYTGTGCTGCT- 3'		-5.1
8E cells 9	5'- CCCCACTAATCGTT ACTCTGGTCCTCTA TTTCTCCTCCCC-3'		-0.6

Name	Sequence	Structure	ΔG (kcal/mol)
8E cells 9P	5'- AGCAGCACAGAGGT CAGATGCCCCACTA ATCGTTACTCTGGT CCTCTATTTCTCCT CCCCCCTATGCGTG CTACCGTGAA-3'		-6.6
8E cells 12	5'- CCCACGAAACGT TACTCTGGTCCTCT ATTTCTCCTCCCC- 3'		-1.2
8E cells 12P	5'- AGCAGCACAGAGGT CAGATGCCCCACG AAACGTTACTCTG GTCCTCTATTTCTC CTCCCCCTATGCG TGYTWCCGTGAA-3'		-5.6

Name	Sequence	Structure	ΔG (kcal/mol)
8E cells 14	5'- CCCCACGAATCGT WACTCTGGTCCTC TATTTCTCCTCCTC CCC-3'		-1.2
8E cells 14P	5'- AGCAGCACAGAGGT CAGATGCCCCACG AATCGTWACTCTG GTCCTCTATTTCTC CTCCTCCCCCCTAT GCYTGYTACCGTGA A-3'		-5.6
8E cells 15	5'- CCCCACGAAACGT TACTCTGGTCCTCT ATTTCTCCTCCCC- 3'		-1.2

Name	Sequence	Structure	ΔG (kcal/mol)
8E cells 15P	5'- AGCAGCACAGAGGT CAGATGCCCCACG AAACGTTACTCTG GTCCTCTATTTCTC CTCCCCCCTATGCG TYYTACCGTGAA-3'		-5.6
8E cells 16	5'- CCCCACGAATMGT WACTCTGGTCCTC TATTTCTCCTCCCC -3'		-0.6
8E cells 16P	5'- AGCAGCACAGAGGT CAGATGCCCCACG AATMGTWACTCTG GTCCTCTATTTCTC CTCCCCCCTATGCG TGCTACCGTGAA-3'		-6.6

Name	Sequence	Structure	ΔG (kcal/mol)
8E cells 17	5'- GGGGAGGAGAAAT AGAGGACCAGAGT AACGATTCGTGGG G-3'	 <p>$\Delta G = -2.1$ kcal/mol</p>	-2.1
8E cells 17P	5'- TTCACGGTAGCACG CATAGGGGGGAGG AGAAATAGAGGAC CAGAGTAACGATT CGTGGGGGCATCTG ACCYCTGTGCTGCT- 3'	 <p>$\Delta G = -7.1$ kcal/mol</p>	-7.1
8E cells 18	5'- CCCCACGAAACGT TACTCTGGTCCTCT ATTCTCCTCCCC- 3'	 <p>$\Delta G = -1.2$ kcal/mol</p>	-1.2

Name	Sequence	Structure	ΔG (kcal/mol)
8E cells 18P	5'- AGCAGCACAGAGGT CAGATGCCCCACG AAACGTTACTCTG GTCCTCTATTTCTC CTCCCCCTATGCG TGCTACCGTGAA-3'		-6.6
8E cells 19	5'- GGGGAGGARAAT AGAGGACCAGAGT AACGATTCGTGGG G-3'		-2.1
8E cells 19P	5'- TTCACGGTAGCACG CATAGGGGGGAGG ARAAATAGAGGAC CAGAGTAACGATT CGTGGGGCATCTG ACCYCTGTGCTGCT- 3'		-7.1